# Diverse Applications of Flow Technology in Discovery Chemistry

by

Jennifer L. Poole
B.S., University of Pittsburgh, 2006

Submitted to the Department of Medicinal Chemistry and the Faculty of the Graduate School of the University of Kansas in partial fulfillment of the requirements for the degree of Doctor of Philosophy.

Thesis Committee

_____
Dr. Jeffrey Aubé (Chairperson)

_____
Dr. Blake Peterson

_____
Dr. Stevan Djuric

_____
Dr. Jon Tunge

_____
Dr. Michael Rubin

Date defended: _____

The Dissertation Committee for Jennifer L. Poole certifies that
this is the approved version of the following dissertation:

**Diverse Applications of Flow Technology in Discovery Chemistry**

Thesis Committee

_____
Dr. Jeffrey Aubé (Chairperson)

_____
Dr. Blake Peterson

_____
Dr. Stevan Djuric

_____
Dr. Jon Tunge

_____
Dr. Michael Rubin

Date defended: _____

## Abstract

The research presented herein describes the development of methods and applications of flow technology in discovery chemistry. The first two chapters highlight the use of several beneficial features offered by flow technology to increase the throughput, safety, and convenience of organic synthesis. The last two chapters describe the use of microfluidic technology as a platform for rapid reaction discovery.

Working with researchers at Abbott Laboratories, a droplet-based library method was developed. This approach allowed for the preparation of a theoretically unlimited number of compounds in a single run using minimal amounts of material. The universal nature of this approach was subsequently demonstrated in the preparation of two 20-membered libraries based around thiazole and pyrazole cores.

A second methodology study, also completed with researchers at Abbott Laboratories, took advantage of the intrinsic closed environment of flow systems which enabled the creation, reaction, and removal of noxious chemicals *in situ*. Using these features an *in situ* synthesis of isocyanides, reagents notorious for their unpleasant smell, was developed. Coupling this method to the Ugi four-component reaction, a series of medicinally relevant amides was synthesized. Reactions performed in the flow system experienced an overall reduction in transformation time from two-days to two-hours and gave yields that were generally higher than those for the same reactions performed on the benchtop or in the microwave.

Expanding the application of this technology toward the discovery and development of new synthetic methodologies we partnered with the laboratory of Dr. John A. Porco, Jr. at Boston University to explore transformations of multifunctional substrates. Given the variant nature of these reactions, both a simple iminium ether and a densely functionalized iminium ether derived from a bicyclo[3.2.1]octanoid scaffold were explored. Multidimensional reaction screening on an automated microfluidic platform was employed to facilitate the simultaneous investigation of multiple reaction variables. While the majority of products obtained from the study resulted from expected modes of *O*- and *N*- alkylation, several interesting transformations were uncovered. These included the pseudo-dimerization of homophthalic anhydride, an unusual integration of the van Leusen sulfone, and an unexpected carbon-carbon bond forming event of ethyl diazoacetate and acetonitrile.

Finally, in a follow-up study, collaboration with Boston University was continued to explore additional reactivity of the bicyclo[3.2.1]octanoid scaffold. Preliminary reaction screens uncovered the synthesis of a series of densely functionalized donor-acceptor cyclopropanes which resulted from the photochemical rearrangement of the bicyclic scaffolds. Expansion of the photochemical screening to a polycyclic iminium ether led to the first example of an aza-di-π reaction of a charged iminium species. Subjection of the new cyclopropane scaffolds to a variety of reaction conditions led to the discovery of additional rearrangement reactions affording several structurally diverse chemotypes including a fused dihydropyran, a fused pyrrole, a bicyclic imide, and a complex cyclic imine.

**Acknowledgements**

I would like to express my sincere appreciation to my graduate advisor, Professor Jeffrey Aubé. It is through his guidance, motivation and unwavering support that I have grown both professionally and personally. I am truly grateful for the opportunities he has given me to gain experience and perspective.

I would like to thank Professors Paul Hanson, Thomas Prisinzano and all those involved in the University of Kansas Dynamic Aspects Of Chemical Biology Training Grant. The experience, knowledge, and friendships I have gained through participation in this grant have been invaluable to me, thank you.

I would like to extend special thanks to Professor John A. Porco, Jr. and Dr. Stevan Djuric for their kindness, mentorship, and inspiration. To Dr. John Goodell and Dr. Christina Thompson, I am deeply grateful for your guidance and the integral roles you have played in my graduate career.

I would like to thank all my colleagues in the Aubé group with whom I have had the opportunity to work. In particular, I would like to thank Dr. Thomas Coombs and Angelica Meyer for their stimulating scientific discussions, constant motivation, and support. It has been a wonderful experience to be a part of the Aubé group over these years.

I am grateful to all my family and friends for their loving encouragement and unwavering faith.

To my husband Eric, I am eternally thankful for your love. I could never have completed this program without you. You are my best friend, the love of my life, and an endless source of support.

Finally, I would like to extend my deepest thanks to my mom, the most amazing woman I know. You have been the rock of my life. Thank you for always encouraging me to reach for the stars, be the best that I can be, and never give up.

"I'll love you forever, I'll love you for always,

as long as I'm living my Mommy you'll be."

– Robert Munsch

This dissertation is dedicated in her honor.

## Table of Contents

## List of Figures

## List of Tables

# Chapter 1

## Introduction

Reaction discovery has historically been guided by problems in total synthesis, interest in developing specific chemical transformations, or an underlying biological need. An emerging area that has recently gained momentum is the development of novel and diverse sets of transformations and chemotypes which can be used to access unique chemical entities and probe new chemical space.[1] Traditionally, the pursuit of innovative reactivity through reaction discovery and development has been expensive and time consuming, generating substantial quantities of waste with little return on the investment. Standard techniques still rely upon the tedious systematic evaluation of individual reaction parameters such as stoichiometry, solvent, temperature, and additives. Advances in instrumentation and automation over the past 20 years have greatly streamlined these processes such that chemical exploration and technology now regularly go hand-in-hand. Now, in addition to the discovery of unique reactions and chemotypes, an equally beneficial side product of the search for new reactivity is the development of innovative tools that aim to expand the scope and reduce the waste of rapid chemical synthesis.

Much of the technology used today in discovery chemistry is derived from advancements in efficiency of high-throughput biological screening and in the advent of combinatorial synthetic chemistry. Automated screening approaches allow many reaction parameters to be assessed simultaneously in an array format, producing

exponentially large amounts of data detailing the ideal conditions per reaction. Using these technologies, reactions can be performed faster, in fewer numbers, and on an ultra-small scale, reducing both the overall cost and waste of these processes.

While many different platforms have been designed for reaction discovery, flow technology has flourished particularly well in this area. The popularity of flow technology arises primarily from the versatility of the platform, being capable of performing many different kinds of tasks across a number of fields, from biology to chemistry to material science. In this chapter the general strategies and challenges of reaction discovery and development will be discussed alongside fundamental considerations for performing reactions in flow.

**Reaction discovery and high-throughput technology.** From the ancient days of alchemy to the modern synthetic lab, scientists have continually searched for new and better methods to synthesize molecules. Chemists continue to refine the conventions on how chemical entities react together to form new molecules. A number of criteria have been developed to evaluate the ideality of each transformation including complexity, efficiency, generality, chemo-, regio- or enantioselectively and diversity potential.[2] While many different strategies may be envisioned to uncover new transformations,[3] most approaches fall into two naturally broad categories:

- Intelligent design
    - Building from known reactivity
    - Combining known reactions
- Serendipity

Intelligent reaction design is often the most difficult method by which to develop new reactions. This technique requires an acute knowledge of molecular reactivity. For even the most experienced chemist, it can be difficult to predict how particular components will behave in combination or under given conditions. More likely, upon finding new reactions, the product and order of events are speculated upon and verified retrospectively.

Two common sub-types of intelligent design are building from known reactivity and combining known reactions. Both of these concepts build on knowledge derived from previous work to form a successful approach toward discovery. As implied by the name, "building from known reactivity" involves considering the most productive pairing of known functionality. On the other hand, "combining known reactions" generates additional complexity by bringing together two previously separate transformations. In both techniques, the reactivity and compatibility of various components must be assessed to determine the likelihood of a reaction being viable. Nevertheless a period of trial and error is common in the successful application of these approaches.

In an elegant example of reactivity-based discovery, Kelly et. al. designed a one-pot synthesis of complex pyridines by merging a previously identified Knoevenagel route to pyridines with known enolate chemistry (Scheme 1).[4] Overall, this three-component reaction (3-CR) offers a straightforward method for the assembly of pyridine cores with up to five different substituents and full regiocontrol in a single operation.

**Scheme 1**

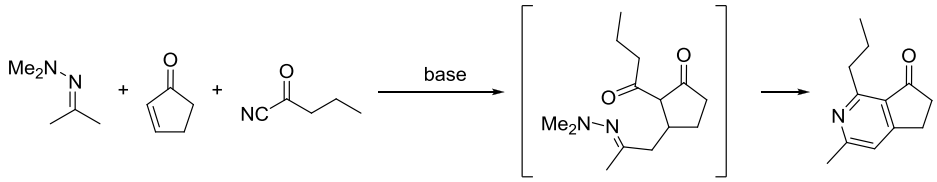


An example of intelligent design through combining known reactions was demonstrated by Grieco et. al. in the design of a 3-CR for the synthesis of tetrahydroquinolines from aromatic amines, aldehydes, and electron-rich dienophiles (Scheme 2).[5] The sequence entails the initial formation of an imine through the combination of an aldehyde and an amine. Following imine formation an aza-Diels-Alder cycloaddition occurs between the imine intermediate and dienophile to form a tetrahydroquinoline product. Both phases of the 3-CR were known as individual reactions prior to the reported transformation; however, the recognition that the dienophile was inert prior to imine formation was required to successfully complete such a synthesis.[3]

**Scheme 2**

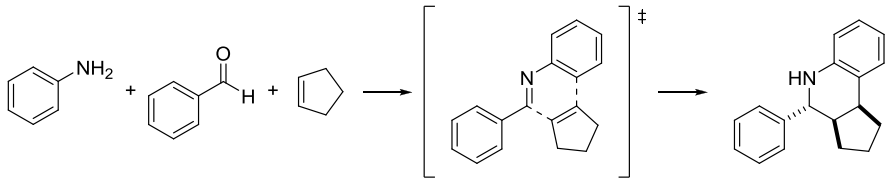

Perhaps the most famous example of combining two or more known reactions is the Robinson annulation.[6] In this reaction two fundamental organic transformations, the Michael addition and the aldol reaction, are joined for the preparation of substituted six-membered cyclic ketones. Certain variants of this reaction have proven so useful in synthesis that the products themselves have common names. For example, reaction of 1,3-cyclohexadione with methyl vinyl ketone yields the Wieland-Miescher ketone (Scheme 3)[7] and reaction of 1,3-cyclopentadione with methyl vinyl ketone yields the Hajos-Parrish ketone.[8] Both products are widely available and popular starting points in total synthesis.

**Scheme 3**

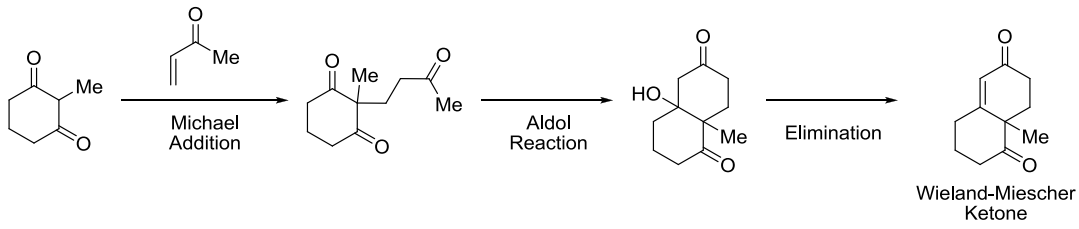


Considering the difficulty associated with intelligent reaction design, computational methods have been created to facilitate the conception of reactions.[3,9] These programs are commonly fashioned to search databases of reaction prototypes that describe the reactivity of atomic arrangements. The proposed reactions are then computationally assessed in terms of their calculated thermodynamics to determine the likelihood of observing the predicted product.

One such program, designed for computational reaction discovery, is the Daylight reaction toolkit program suite.[10] Among the numerous reactions proposed using this program was a Lewis-acid catalyzed hetero-Diels-Alder reaction between an imine and a silylenol ether diene for the formation of α,β-unsaturated piperidinones (Scheme 4). Although a version of this reaction was originally reported by Danishefsky in the 1980's, Gálves et. al. demonstrated the validity of the proposed reaction and applied the transformation to the synthesis of piperidine cores.[11]

**Scheme 4**

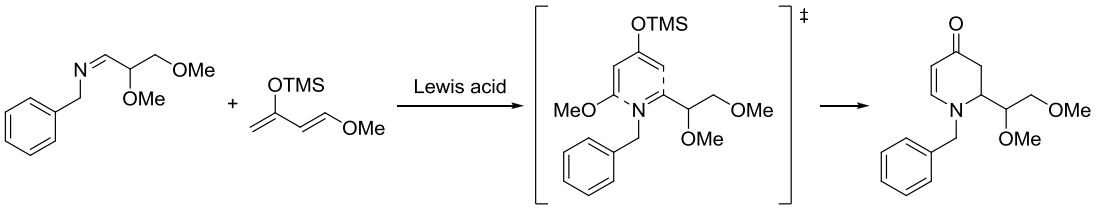


Serendipitous reaction discovery is a common event in many labs. A frequent by-product of target-oriented synthesis is the discovery of an unexpected, if not always entirely unknown, transformation. In this way, reactions have been repeatedly discovered and rediscovered throughout history. These transformations are often considered novelties and of limited utility, since they give alternatives to the targeted product. However, these side reactions can often be manipulated into valuable transformations with broad application. Serendipitous reaction discovery is particularly valuable for the creation of scaffold diversity and producing new chemotypes, desirable traits for researchers who aim to patent their work.

Weber et. al. demonstrated a thorough approach to serendipitous reaction discovery using a high-throughput combinatorial method (Figure 1).[12] Starting from ten reagents varying in functionality, all of the possible multi-component reaction combinations were studied systematically. Mathematically, the total count of reactions possible for any given number of components can be determined using the equation in figure 1. Given the ten predefined components, the equation directs that only one 10-CR is possible, only ten 9-CR are possible, and so on. Summing the entire set from 10-CR to 2-CR a total of 1013 reactions are possible![13] Using automated parallel synthesis techniques Weber et. al. tested all 1013 reaction combinations. So doing, the team discovered two new transformations, one of which provided the 4-CR product seen in the center of the circle (Figure 1). In addition, they uncovered several previously identified MCRs of isocyanides and aldehydes.[12]

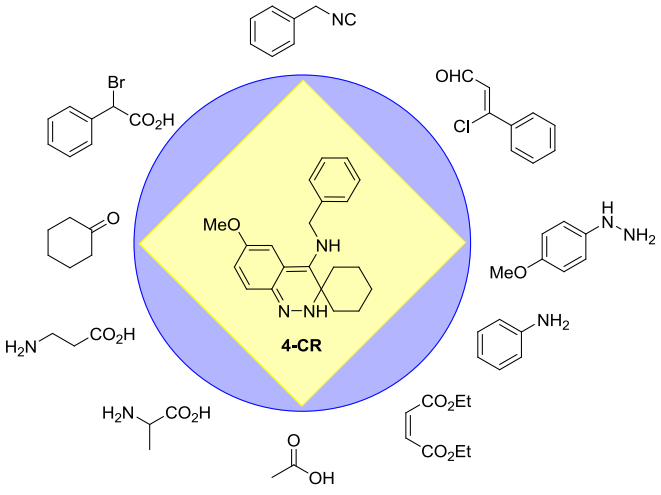


$$ {}_{x}C_{n} = \sum_{n=2}^{10} \frac{x!}{n!\,(x-n)!} $$

| Components in MCR | Reactions *(statistically)* |
|---|---|
| 10 | 1 |
| 9 | 10 |
| 8 | 45 |
| 7 | 120 |
| 6 | 210 |
| 5 | 252 |
| 4 | 210 |
| 3 | 120 |
| 2 | 45 |
| | Tota (C) = 1013 |

**Figure 1.** Combinatorial multicomponent reactions.[9,13]

When constructing new transformations, a combination of approaches is typically used, and trial and error is natural. When conducting searches for new reactions or chemotypes with traditional benchtop techniques, a range of spectroscopic methods are available to assess and characterize the progress of transformations. Reaction discovery performed in this manner is low-throughput and can take weeks, months, or even years to produce an interesting result. For such cases, implementing a high-throughput screening approach of small-scale reactions has proven most successful in accessing new reactivity in a time-efficient manner.

Many techniques used in combinatorial and high-throughput reaction discovery are simple variations of those used in combinatorial and high-throughput synthesis. Similarly these methods are derived from advances and automation of high-throughput biological screening. The technology used for performing high-throughput reactions encompasses a variety of solid-phase and solution-phase chemistry methods.[14] To date, discovery efforts have been reported using polymer-supported beads,[15] homogenous solution-phase polymer-supported scaffolds,[16] automated synthesizers,[17] microchips,[18] and DNA-tethered supports.[19] The option of manual versus automated reaction platforms also gives the user control over the development of discovery and productivity.[3]

The choice of reaction platform is often limited by the techniques available for analysis and identification of transformations. While many methods exist to gauge the productivity and identify the products of a reaction, the high-throughput nature of

discovery chemistry necessitates that key features be present in a desirable analysis method. The ideal analysis method includes:[20]

- Minimal sample preparation
- Programmable automobility
- Short analysis time for high sample throughput
- High sensitivity for the analysis of small quantities of compounds
- A nondestructive measurement method to minimize compound loss

Few methods exist which can meet all of these requirements so multiple analysis techniques are usually coupled together or used in parallel.[21] Instrumentation regularly used for chemical identification include chromatographic methods (HPLC, UPLC, GC, or TLC),[22] mass spectrometry (MS),[22c] one-dimensional and multi-dimensional nuclear magnetic resonance spectroscopy (NMR),[22a,23] infrared (IR) thermography,[24] calorimetric methods, colorimetric methods,[25] capillary electrophoresis,[26] fluorescence spectroscopy[24a,27] and fluorescence resonance energy transfer (FRET).[28] In the case of standard solid- and solution-phase syntheses, the most common analysis methods are traditionally HPLC, GC, MS, NMR and IR.

Researchers in the field of catalysis were among the first to embrace combinatorial and high-throughput techniques for the discovery of new transformations.[22-29] The vast majority of effective metal-based catalysts are complexes bearing ligands that direct the outcome of the reaction through control of the steric and electronic properties of the metal center. The nature of the interactions between metal and coordination environment is often poorly understood, making it

difficult to predict the optimal combination of metal and ligand for a given reaction. The lack of understanding necessary for the intelligent design of these catalysts make a serendipitous screening approach an attractive way to address this problem.

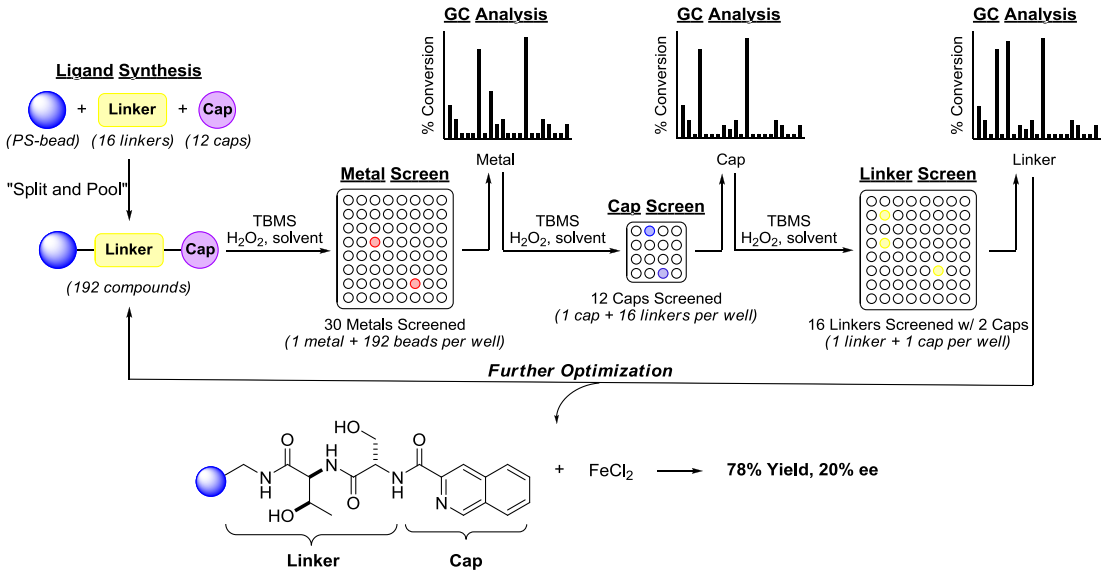


**Figure 2.** High-throughput oxidative catalyst discovery.[30]

Jacobsen and coworkers reported one of the earliest applications of this type of screening approach in the discovery of a catalyst to promote olefin epoxidation reactions using hydrogen peroxide (Figure 2).[30] Their efforts were divided into two phases: lead discovery, screening a wide variety of metal complexes, and lead optimization, with systematic variation of ligand components and reaction conditions. The ligands were first synthesized using solid phase synthesis and split-and-pool techniques to achieve a pool of beads containing 192 different ligands. The ligand pool was then divided and subjected to reaction with 30 different metals for oxidation

of *trans*-β-methylstyrene (TBMS). The crude solution from reaction with each metal was analyzed by GC which demonstrated productive reactions with $VOSO_4$ and $FeCl_2$. The latter was chosen for subsequent follow-up experiments.[30]

Upon identification of productive reaction conditions, the group set out to deconvolute the optimal ligand combination. A screen was set-up to investigate the optimal ligand "cap" and the beads were reacted in pools according to cap identity. GC analysis of the crude reaction solution showed two optimal caps, both pyridine derivatives. Finally, using the two pyridine-derived caps, each linker-cap combination was subjected to the reaction conditions individually and the crude solutions were again analyzed by GC. Identification of three productive linker-cap combinations provided insight into the optimal metal-ligand interactions for the desired reaction. This information was then used to repeat the sequence of discovery and further optimize the transformation.[30]

When the use of more high-throughput analysis methods are desired, special synthetic techniques must be used. Visualization of productive reactions by fluorescence requires the immobilization of one set of reaction partners and the presence of a fluorophore in the second set of reaction partners. Similarly, while FRET can be completed in solution it also requires that a donor and acceptor fluorophore pair be present in the molecular pair prior to the reaction discovery event. While these analysis methods are very efficient, the complication of incorporating bulky fluorophores or immobilizing reagents may hinder some reactions that would otherwise be productive, leading to an increase in false

negatives. The incorporation of these moieties may also limit the available reaction conditions compatible with the platform, as seen in the next example.

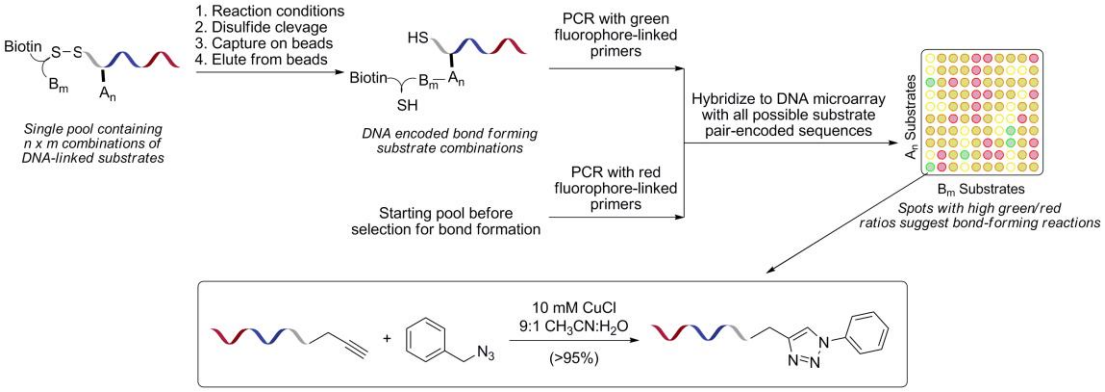


**Figure 3.** DNA-Encoded reaction discovery.[19]

Liu and coworkers recently reported a novel approach to reaction discovery using DNA-templated organic synthesis and *in vitro* selection to simultaneously evaluate numerous potential reactions in a single solution (Figure 3).[19] The stoichiometry of each reaction was controlled by Watson-Crick base pairing of the DNA tethered substrates. Bond-forming combinations were uncovered by *in vitro* selection using chromatographic methods, followed by PCR amplification, and DNA microarray analysis. Positive reactions were identified colorimetrically using a combination of two colored fluorophores. While this technique is limited to conditions and catalysts that are compatible with DNA, the versatility and efficiency of the method is evident by the discovery of reactions between a wide range of substrates. Included in these transformations were the Huisgen 1,3-dipolar

cycloaddition shown above and a novel palladium-mediated synthesis of α,β-unsaturated macrocyclic ketones.[19c]

A major limiting factor of many high-throughput methods is the necessity of deconvolution.[31] When performing multiple reactions in a single pot the presence of a successful transformation may be observed quickly, but an involved follow-up process must be completed to identify the components and products of the positive result. Alternatively, parallel synthesis techniques can be used to take advantage of the efficiency of combinatorial methods while bypassing the disadvantages of deconvolution and compound identification.[20] While it is not possible to synthesize as many compounds by parallel technology as with other high-throughput techniques, parallel methods are particularly useful for reaction optimization and small-scale discovery efforts.

When using various parallel synthesis techniques, compounds are separated by space or time. Typical parallel platforms include multi-welled block reactors, automated chemical synthesizers and flow reactors. While each of these platforms exhibits its own unique set of benefits and drawbacks, an area of major growth over the last few decades has focused around flow-based technologies.

**Discovery chemistry and flow technology.** Fundamentally, flow technology encompasses the ability to perform a task within a continuously moving stream of solution in a network of interconnecting tubes or channels (Figure 4).[32] The most elementary flow process simply involves the combination of reagents in a "reactor"

and flowing the solution until the transformation is complete, at which time the solution exits the instrument. A basic application of this technology was demonstrated by Ley and coworkers in the synthesis of amides from carboxylic acids via the Curtius rearrangement (Figure 4).[33]

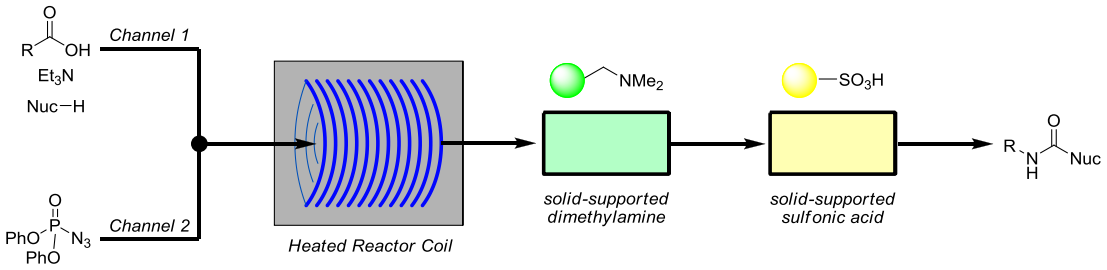


**Figure 4.** Curtius rearrangement as performed in continuous flow.[33]

Flow technology has been prevalent in many industrial processes for decades with some of the most visible applications in the practices of oil refineries and the large-scale synthesis of pharmaceuticals.[34] Over the past twenty years flow technology has begun to expand beyond its limited scope and has found new applications across the fields of chemistry, biology, and pharmacology. With such vast potential for multidisciplinary use, flow techniques have found value at almost every stage of the drug development process (Figure 5).[35] In addition to various synthetic applications; biological assays,[36] formulation studies, and pharmacologic profiling are among the assortment of operations that have been developed for flow.[18c,37]

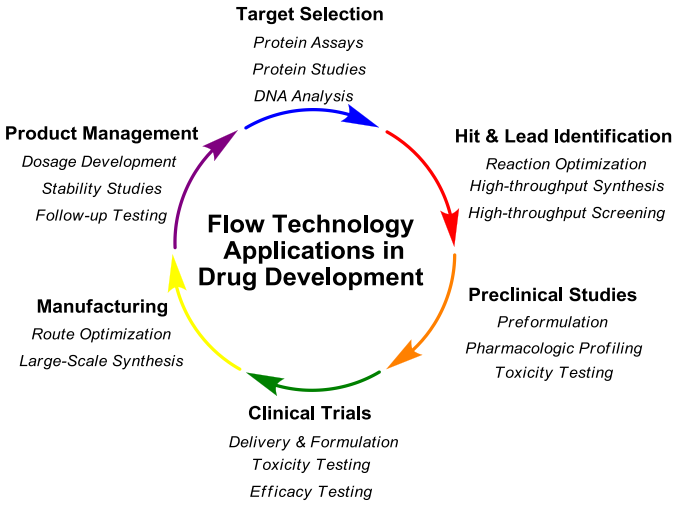


**Figure 5.** Applications of flow technology in drug development.

Flow platforms may be constructed using a wide assortment of materials and can be designed for a range of volumes, from microliter to multi-liter scale.[18a,18b] Typically, microreactors perform reactions on chips consisting of a network of miniature channels embedded in a flat surface, handling volume on the micro- to milliliter scale. Alternatively, mesoflow reactors typically perform reactions in tubes or coils and handle larger volumes ranging from milliliter to multi-liter.[39] A variety of materials can be used to construct the reactor chip and coils including glass, quartz, silicon, stainless steel, metals, and polymers.[18b,38,40] The optimal choice of material depends on the type of chemistry for which the platform is intended.[35] With the recent popularity of flow chemistry, a number of standardized flow platforms are now commercially available (Figure 6). Some of the more versatile systems include the H-cube,[41] FlowSyn,[42] Vapourtec,[43] Africa, FRX,[44] and CYTOS.[45] While each system boasts its own unique set-up and features, the basic aspects of each platform remain

the same: an operating system, a pumping mode, a liquid handler, a reactor (chip, coil, or column) and a collection unit.

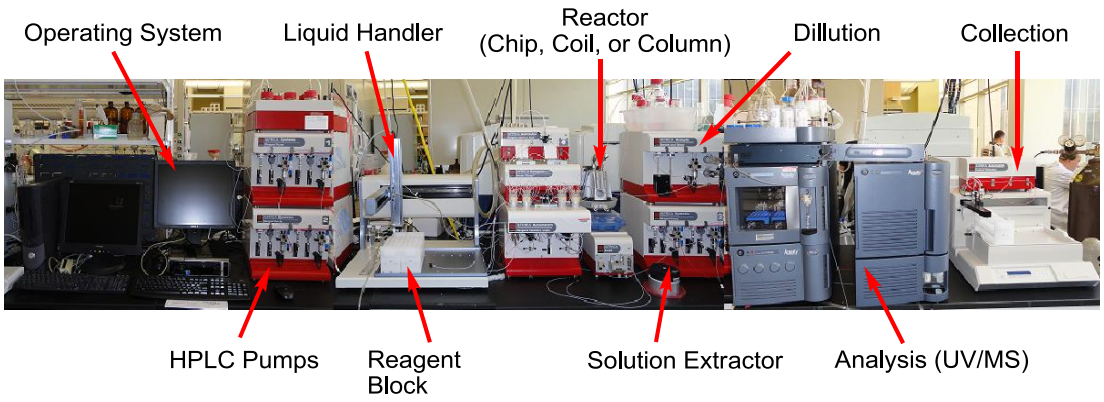


**Figure 6.** Africa flow platform manufactured by Syrris.[44]

Fluid can be moved through the reactor using a number of different methods including hydrodynamic pumping, electrokinetic pumping, and capillary flow.[18b] The most straightforward and commonly used method is hydrodynamic pumping either by syringe or HPLC pump. Although less often used, electroosmotic flow (EOF) can be advantageous since it involves no moving parts, is easily miniaturized, and computer controlled. Capillary flow is the least versatile as it is limited to very small volumes and is not easily manipulated. Regardless of the mode of pumping, mixing in the channels is laminar and occurs by diffusion and convection.[18b] Additional mixing regions, comprised of twists and turns in channels, can also be used early in the flow process to increase the turbulent integration of components.

**Table 1.** Reactions developed for use in flow platforms.

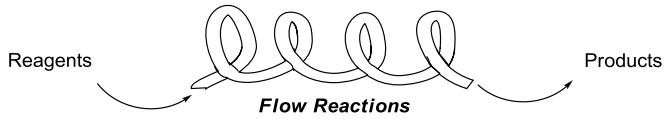


| | | |
|---|---|---|
| Paal-Knorr Pyrrole | Decarboxylation | Nucleophilic Substitution |
| Knorr Pyrazole Synthesis | Williamson Ether | Finkelstein Reaction |
| Benzimidazole Synthesis | Curtius Rearrangement | Grignard Reaction |
| Newman-Kwart Reaction | Knoevenagel Reaction | 1,2-Additions |
| Fischer Indole Synthesis | Claisen Rearrangement | Eliminations |
| Bohlmann-Rahtz Pyridine | Diels-Alder Reaction | Amidation |
| Hantzsch Pyridine Synthesis | Suzuki-Miyaura Coupling | Enamine Formation |
| Passerini Multicomponent | Kumada Coupling | Azide Reduction |
| Biginelli Multicomponent | Sonogashira Coupling | Bromination |
| Hoffmann Degradation | Heck Coupling | Fluorination |
| Baylis-Hillman Reaction | Ullman Coupling | Nitration Reaction |
| Mannich Reaction | Swern-Moffatt Oxidation | Nitro Reduction |
| Michael Addition | TPAP Oxidation | Diazo Synthesis |
| Aldol Condensation | Hydrogenation | Photocyanation |
| Ester Formation | Protection | Phosphonium Ylide Prep. |
| Ester Hydrolysis | Deprotection | Wittig Reaction |
| Carbamate Formation | $S_NAr$ | Aza-Wittig Reaction |

The growing versatility in the set-up of flow platforms has enabled these systems to become amenable to many different types of reactions (Table 1).[32,38,46] Combining flow technology with other modern high-throughput synthesis techniques, reactions can be performed in liquid phase, liquid-solid phase, liquid-gas phase, and liquid-solid-gas phase.[18b,39] Although chemical transformations involving solid reagents or intermediates are difficult to conduct in flow due to potential clogging of the channels, a number of alternative means for introducing solids in flow are available. For example, solution can be passed through columns of solid-supported

reagents or through channels coated with the solid reagent, as is commonly done for metal catalysts. Transformations using toxic gases are actually made safer using flow systems since the flow of the gas can be precisely controlled and integrated gas-liquid separators can be used to separate the gaseous phase at the end of the reaction.[18b]

While direct in-line reaction monitoring is still in the early stages of development, most common analytical and purification techniques are easily amenable to flow processes upon completion. Aligning these techniques in flow provides a direct connection of these instruments to in-line reaction synthesis and increases the overall efficiency of discovery operations.[39] Analytical detection methods currently available for flow include electrochemical methods, mass spectrometry, optical methods such as absorption[40] infrared, and fluorescence spectroscopy, chromatographic methods (HPLC, UPLC, GC), and NMR spectroscopy.[18c] Connecting the synthetic steps directly to purification and analysis enables an exponential enhancement in the throughput of chemical screening. This concept can be extended to also include high-throughput biological assays. Computational systems have also been developed which are capable of automatically interpreting analytical data. This information can then be used to direct which compounds should be synthesized next, creating an automatic intelligence feedback loop to direct discovery efforts (Figure 7).[38]

Reactions performed in flow can benefit greatly from many features unique to flow technology. For instance, the small dimensions and increased surface-to-volume ratio of flow reactors make mass and heat transport significantly more efficient than

in batch reactors. At these small scales, the mixing of reagents can be very fast and heat exchange between the reaction and the environment is highly efficient. These features allow reactions performed in flow to be precisely controlled and have increased homogeneity, leading to a decrease in unwanted side-reactions and by-products to afford cleaner reactions.[18b] This precise control also enables the completion of reactions with unstable intermediates with increased efficiency.[47]

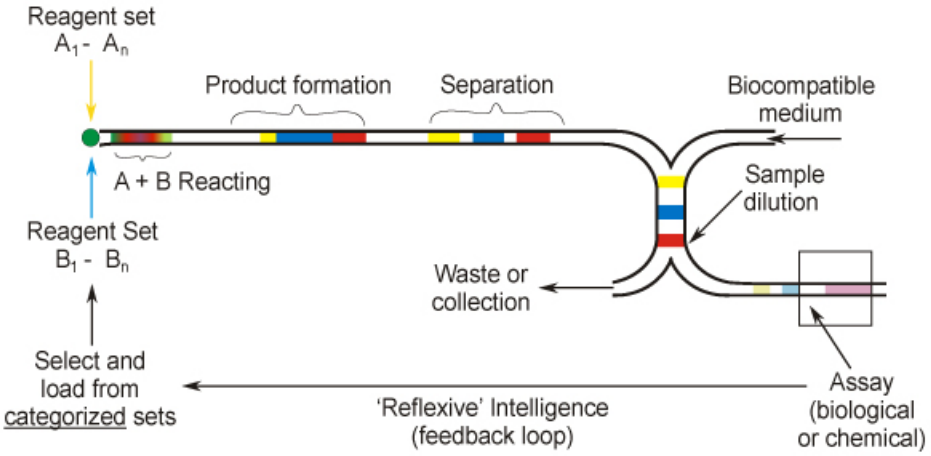


**Figure 7.** Integrated flow model for rapid chemical discovery and optimization.[38]

Despite the relatively small volumes used in micro- and mesoflow techniques scale-up options are available. Reactions performed in flow can provide large amounts of material simply by flowing longer, "scaling-out", or by connecting several reactors in parallel, "numbering-up" (Figure 8).[46] Use of these techniques help avoid the problem of reoptimization of a transformation during scale-up. Continuous flow processes can also address problems commonly related to the scale-up of batch

reactions such as accurate control of the reaction time and continuity of mixing. Problematic, hazardous, and runaway reactions are made safer and easier by allowing the chemist this precise control at critical points within the reaction.[32,47]

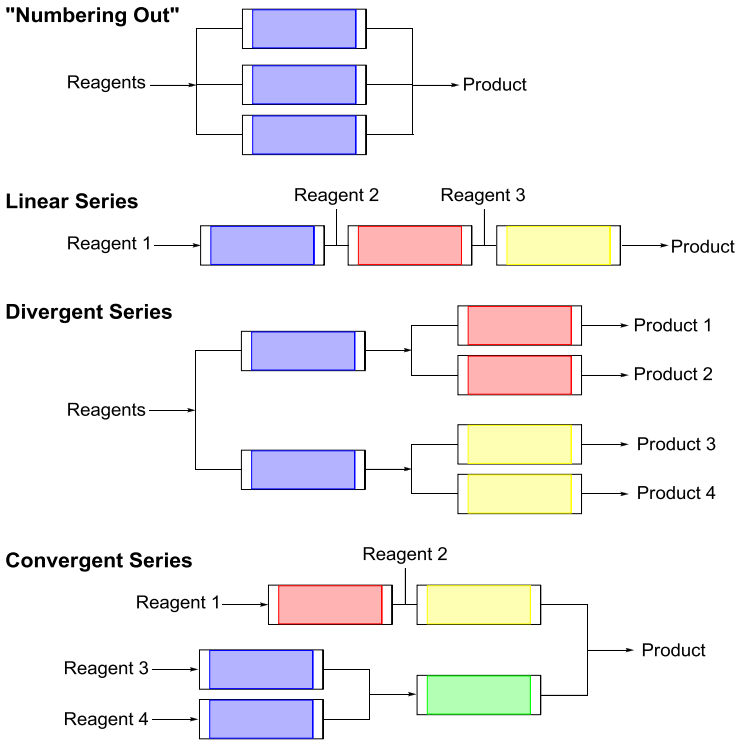


**Figure 8.** Arrangements available for combined flow processes.[46]

The complexity of a synthetic scheme can be increased by combining the lines of multiple flow reactors to complete linear, divergent, or convergent multi-step syntheses (Figure 8). When performing multi-step syntheses in flow, all steps must be compatible with one another concerning the solvent, by-products, and reaction time.[48] If the reactions are not well-matched in these respects, break points can be inserted into the synthetic scheme to allow for a solvent switch, purification, or change in the

flow rate.[46] Reactions performed in flow also typically have shorter reaction times. The closed nature of the flow system enable the reactor to pressurize and achieve solvent temperatures beyond the boiling point of the solvent (superheating),[35] resulting in an increase in the overall rate of reaction.

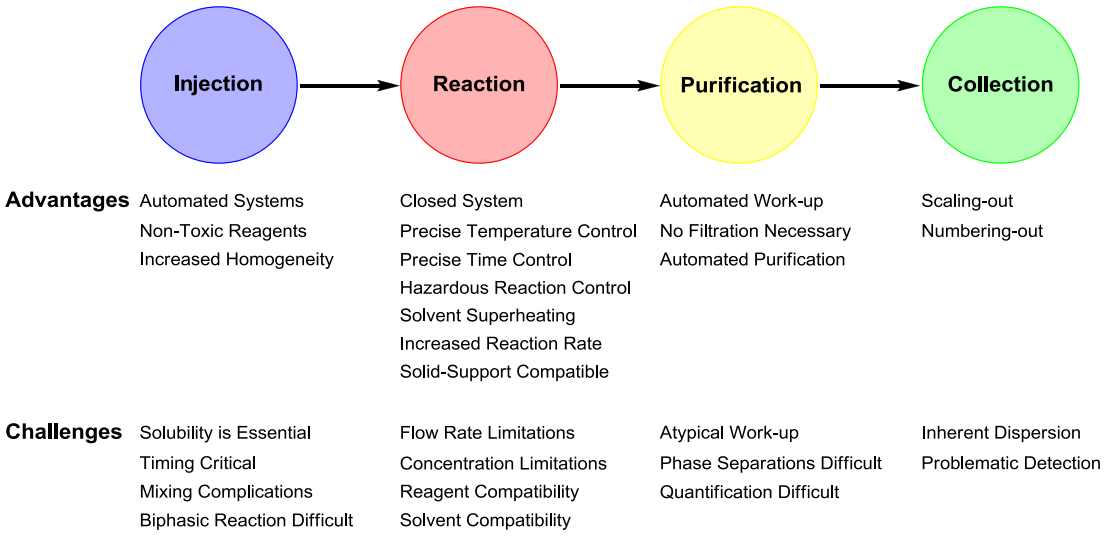


**Figure 9**. Advantages and challenges of flow-based reaction technology.

Alongside the many benefits of flow technology is an equally long list of challenges and limitations (Figure 9).[49] When completing several reactions in series, the compatibility of reagents, solvents, and possible by-products for each transformation must be considered. A simple process using benchtop chemistry, such as changing solvent, can prove difficult in flow reactors. Although reactions performed using flow technology tend to be of high purity, by-products can gradually accumulate across multiple steps and make late-sequence transformation less

efficient. Problems such as these often limit the maximum number of sequential steps that are feasible before purification is necessary. Upon completion of a sequence in a flow reactor, a number of techniques have been devised to quench and work-up reactions in-line.[32,39] Unfortunately, these methods are far fewer in number and less convenient than those available for reactions in batch. Common work-up procedures typically include using one or more of the following approaches: addition of water or aqueous solutions, passing reactions through columns of solid supported reagents or scavengers, or complex separation techniques.[39] All things considered, these manipulations add length and complexity to the overall process. When performing multiple reactions in a continuous flowing solvent stream using segmented flow, dispersion of the reaction into the spacer solvent typically occurs.[50] The extent of dispersion is dependent upon the flow rate and path length, with slower, longer reactions experiencing greater mixing. Dispersion of reactions can complicate many aspects of an otherwise straightforward sequence, including the addition of reagents, timing of the run, and material collection from the instrument.

As is evident from the discussion above, flow technology possesses many attributes which make chemical discovery faster, more cost effective, and less wasteful. Yet, despite all of the advantages flow technology currently offers there are still many challenges to overcome for each experiment performed on this platform. Further investigations using flow technologies can instruct not only about the chemical transformations being performed but also about the capabilities of this valuable technology.

Throughout this dissertation flow technology will be used in various ways to enhance reaction throughput, reaction development, and reaction discovery. In the first chapter, the separation of reactions by space and time in a flow reactor was used to produce a library of biologically relevant heterocycles. In the second chapter, the closed nature of the flow reactor was used to create a safe and efficient protocol for the *in situ* synthesis and use of isocyanide reagents in synthetic protocols. Finally, the last two chapters describe the use of flow technology as a platform for reaction discovery.

## Chapter 2

## Heterocycle Synthesis in Droplets

In conjunction with researchers at Abbott Laboratories a droplet based library synthesis method was developed which allowed for the preparation of a theoretically unlimited number of compounds using a single Teflon loop and very minimal amounts of solvent. This method exploited the ability of flow technology to spatially separate library members along the length of a tube by employing immiscible solvents as spacers. The utility of the droplet-based library method was demonstrated through the synthesis of two 20-membered libraries derived from heterocyclic cores.

**Heterocycles in medicinal chemistry.** Heterocycles are cyclic organic molecules wherein at least one atom within the ring is a heteroatom (not carbon). From this broad definition, it is found that more than half of all known organic compounds are heterocyclic.[51] These molecules play an essential biological role in the basis of life, being key components of fundamental processes such as provision of energy, transmission of nerve impulses, sight, metabolism, and the transfer of hereditary information.[52]

Much of the interest in heterocycles surrounds their ability to mimic biologically important functional groups such as amides and peptide ligands. Heterocycles often exhibit a type of stability that natural ligands lack, making them more resistant to degradation *in vivo*, allowing them to be biologically useful.[52] This

class of molecules can be involved in an extraordinarily large range of reaction types and depending on the reagents, conditions, and reaction medium, heterocycles can act as nucleophiles, electrophiles, oxidizers, reductants or can be exceptionally inert. They are known to participate in all different types of bonding including covalent, ionic, hydrogen bonding, and van der Waals interactions. It is the moderate nature of heterocycles that makes them particularly useful as components in current drug therapies.[51] In fact, the vast majority of existing small molecule-based drugs are either built around a heterocyclic core or contain a heterocyclic appendage (Figure 10).[53]

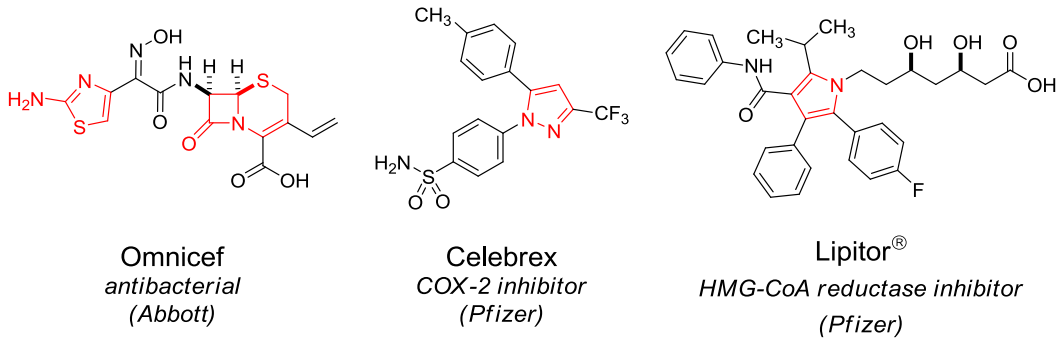


**Figure 10.** Heterocycles in modern drugs.

With such a large variety of heterocycles available, the choice of which to introduce in an experimental agent is primarily determined by key medicinal evidence. Considering the pharmacological impact of varying the ring size and heteroatom placement, the ultimate goal is to maintain or enhance the biological activity of the agent while optimizing its ADMET (absorption, metabolic stability, toxicity) properties.[54]

In almost all cases, before the optimal agent is found, a variety of different heterocyclic types are investigated in a high-throughput format. Companies, institutions, and federal agencies amass large collections of diverse heterocycles in an effort to expedite this bottleneck in the discovery process. New compounds are continually added to these collections to try and obtain the most optimal compounds early in the drug discovery process. A quick and efficient method, by which, numerous types of heterocycles could be synthesized would greatly facilitate this practice.

**Heterocycle library synthesis in flow.** Flow platforms offer many key advantages for performing rapid heterocyclic library synthesis. Reactions performed in flow have precise timing and temperature control which leads to increased homogeneity and ultimately cleaner reactions requiring less purification. Segmented flow enables a single-reaction flow platform to be transformed into a multi-reaction system through the introduction of an immiscible solvent which spatially separates different reactions across the length of the channel, thus creating individual reaction droplets. This ability to separate reactions in time and space along the length of a continuous flow path allows a theoretically unlimited number of reactions to be performed continuously. The ability to perform multiple, unrelated reactions in a single run permits this type of method to have an extremely high throughput, which is ideal when the goal is to make small quantities of many different compounds as quickly and efficiently as possible.[37b,50] Reactions performed in flow are part of a

closed system so solvents may be superheated, using high temperatures and pressures to enhance the rate of the reactions and shortening the overall time of the process. If a larger quantity of a compound originally synthesized in flow is desired more material may be accessed simply by scaling out, making further optimization unnecessary.

In the development of such a method some challenges exist which must be addressed. Heterocycles are inherently polar, a property which can create problems when trying to perform reactions in typical organic solvents. Often, the insoluble nature of either the reagents or the heterocyclic products, leads to precipitation and sluggish reactions, which are obstacles for processes completed in flow. First, both the reagents and products must remain soluble throughout the reaction. Precipitation of any component within the flow apparatus can cause a blockage leading to a break in the flow line or instrument failure. Second, a minimum flow rate must be maintained within the apparatus to ensure that reaction droplet integrity is maintained. This requires reactions to be completed in a short amount of time.

With the above limitations in mind, we set out to find transformations that met the optimal properties for performing successful heterocycle syntheses in flow. The desired features included:

- Single step transformations
- Solubility of both reagents and products
- Reaction completion in less than 10 minutes

To begin, a number of known heterocycle-forming transformations were investigated in the microwave under superheating conditions to gauge their potential

for use in flow. Reactions found to be successful in the microwave were then pursued further to gauge if the synthetic method would be viable in a continuous flow library setting. The syntheses targeted for investigation focused on various routes to 5- and 6-membered heterocyclic rings containing oxygen, nitrogen, and sulfur in assorted placements. The first heterocycle-forming reaction that showed promise from the scouting efforts was the synthesis of thiazole from *N*-alkylthioureas and 2-bromo-1-arylpropan-1-ones (Table 2).[55]

**Table 2.** Solubility studies for the synthesis of thiazoles.

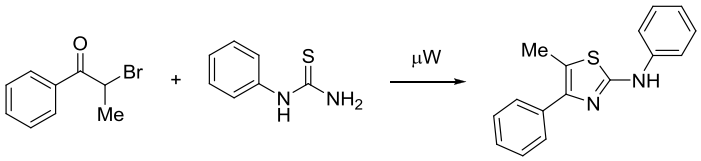


| entry | solvent | additive | temp. (°C) | time (min.) | outcome[a] |
|---|---|---|---|---|---|
| 1 | MeCN | – | 60 | 15 | precipitate |
| 2 | MeCN | – | 80 | 15 | precipitate |
| 3 | MeCN | $Et_3N$ | 60 | 15 | precipitate |
| 4 | DMSO | $Et_3N$ | 80 | 15 | no reaction |
| 5 | DMF:MeCN (1:3) | $Et_3N$ | 60 | 15 | soluble |
| 6 | DMF:MeCN (1:1) | $Et_3N$ | 60 | 15 | soluble |
| 7 | DMF:MeCN (3:1) | $Et_3N$ | 60 | 15 | soluble |
| 8 | DMF | $Et_3N$ | 60 | 15 | soluble |

[a]Outcome based on visual observation.

Early attempts to perform this transformation in the microwave in acetonitrile led to low conversions and precipitation of the starting thiourea (Table 2, entries 1-3). Changing the solvent to from acetonitrile to dimethyl sulfoxide greatly increased the solubility of the reagents; however, no reaction was observed upon heating (Table 2,

entry 4). Use of a *N*,*N*-dimethylformamide:acetonitrile mixture led to both the desired increase in reagent solubility and an increase in the efficiency of conversion to the desired product as observed by LCMS/ELSD (Table 2, entries 5-8).

**Scheme 5**

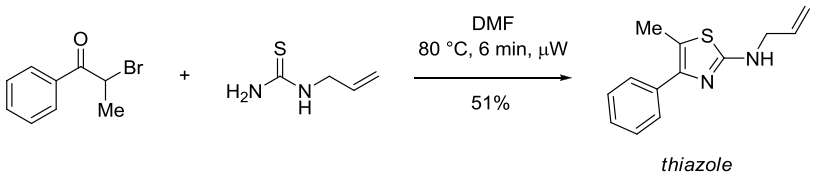


After optimization it was determined that *N*,*N*-dimethylformamide was the best solvent for the reaction to be performed in flow since it maintained reagent and product solubility in addition to exhibiting an acceptable reactivity profile. Using similar bromoketone and thiourea components reaction in the microwave, heating the components in *N*,*N*-dimethylformamide at 80 ºC for 6 minutes, gave a 51% yield of the desired thiazole (Scheme 5).

**Scheme 6**

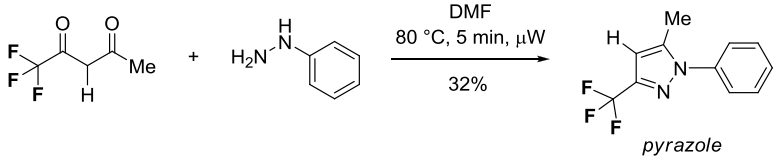


Similar solubility and condition studies were performed using 3,4-methylpentane-2,4-dione and phenylhydrazine for the synthesis of pyrazoles (Scheme

6), and hexane-2,5-dione and allyl amine for the synthesis of pyrroles (Scheme 7). In the first case, the conditions used for the thiazole synthesis also were found amenable to the synthesis of pyrazoles. Initial investigations of the pyrrole syntheses showed that product formation was possible using the conditions listed above (DMF, μW 80 ºC, 6 min). However, the limited commercial availability of 1,4-diketones and narrow substrate scope prevented the use of this reaction in a library setting.

**Scheme 7**

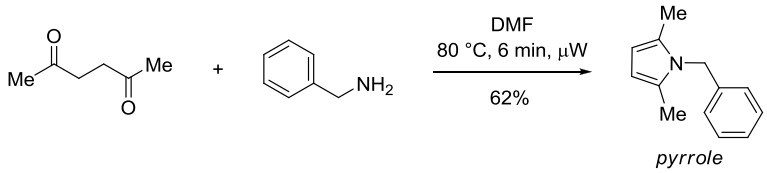

*pyrrole*

After a small survey of catalysts, it was found that the synthesis of triazoles was also amenable to the common reaction conditions (DMF, 80 ºC, 6 min) when a copper (I) source was added to the solution (Scheme 8). Preliminary tests using copper iodide showed only slight insolubility due to the addition of the catalyst. Upon heating in the microwave the copper became completely soluble and gave quantitative conversion to the triazole by LCMS. Efforts to transfer this sequence to the flow setting, however, showed that the initial insolubility of the catalyst was a problem. Designs to increase solubility of the copper catalyst by pre-heating, pre-mixing with the reagents, and switching to other copper(I) sources were unsuccessful.

In light of these complications the triazole synthesis was also abandoned and the library was not completed in flow.

**Scheme 8**

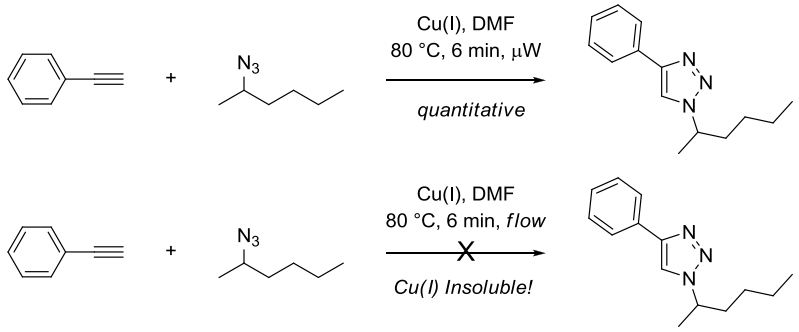


In addition to the four syntheses mentioned above, routes toward a number of alternative heterocycle-forming reactions were investigated, including imidazoles,[56] furans,[57] thiophenes, oxazoles, isoxazoles, pyridines, and indoles.[58] For many of these attempts a central limitation was the short reaction time. Even a high reaction temperature and pressurized environment in the microwave could not compensate for the abridged reaction time. Under these conditions most transformations gave less than 10% conversion to the desired product by LCMS, if product was observed at all.

Using the successful heterocycle syntheses described above (thiazole and pyrazole), two 20-membered libraries were synthesized in flow. Because both reactions required the same flow rate, temperature, and solvent; synthesis of both heterocycles could be performed in a single run without changing any setting on the flow instrument.

**Flow instrument design and droplet technique.** The commercially available Uniqsis FlowSyn continuous flow apparatus[42] was used to perform the synthesis of heterocycles in droplets. The standard instrument included two injection ports, two HPLC pumps, a variant temperature flow coil (Teflon or metal), a variant temperature solid-support reagent column, and two solvent storage bottles (Figure 11). The apparatus could be controlled in automatic or manual mode through a computerized control panel at the base of the instrument. The control panel was used for programming the flow rate, temperature, injection, and collection. The operating system also continually monitored the system pressure to ensure user safety and an automatic system shut-down was triggered if the internal pressure reached an unsafe level.

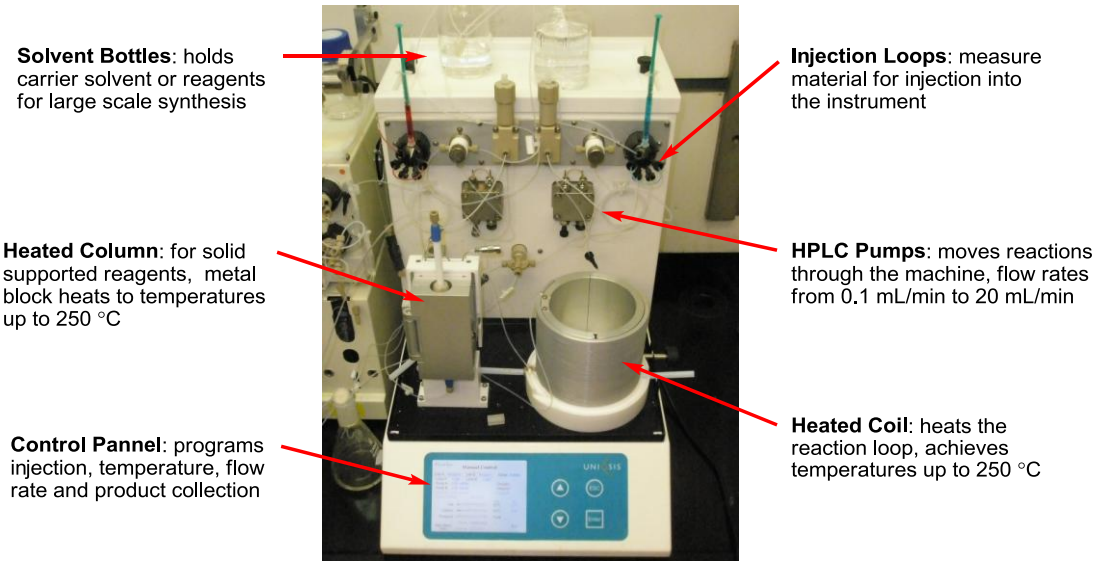


**Figure 11.** FlowSyn mesoscale continuous flow platform.[42]

Taking advantage of the ability to separate reactions by time and space in flow, it was possible to perform multiple reactions in a single sitting using a continuously flowing stream of solvent. Fluorous solvent was used as the carrier stream since it is immiscible with most organic solvents, which enables the fluorous solvent to form a physical spacer between reaction plugs. Manual injection of pre-made reagent component solutions into the fluorous solvent stream formed reaction droplets in the flow coil. Substitution of the reaction components with colored dye enabled visualization of the droplets and showed the efficiency of droplet separation using fluorous solvent (Figure 12). The separation meniscus between the reaction droplet and solvent spacer was observable even for colorless organic reactions. The integrity of the droplets was best when a highly viscous solvent (DMF or DMSO) was used in the reaction. If a less viscous solvent (MeCN, THF, $CH_2Cl_2$) was used the droplets tended to break apart and exhibit variable flow rates inconsistent with the instrument settings.

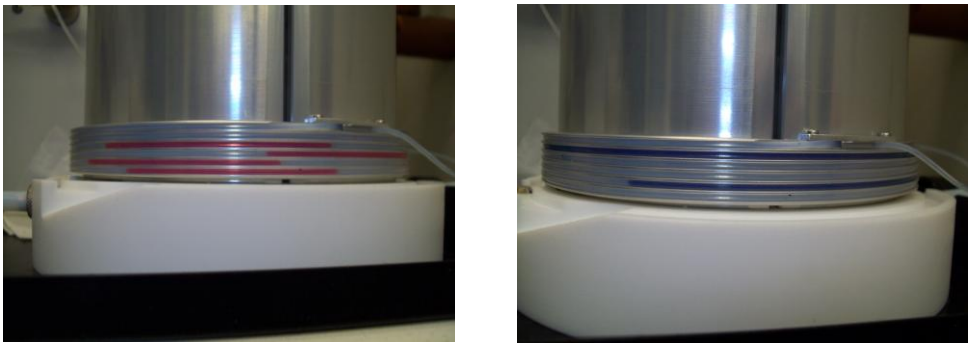

**Figure 12.** Droplet formation in continuous flow.[59]

Library reactions completed in the continuous flow apparatus were performed using stock solutions of library reaction partners prepared by dissolving 2.0 mmol of each component in 2.0 mL of anhydrous DMF. Each solution was sufficient to perform up to 10 reactions in flow with each component injection at a volume of 0.1 mL of solution. The concentrations of component solutions were elevated to maximize the amount of material synthesized within each plug for each library product (35 – 75 mg expected material). Insolubility of the reaction partners at these elevated concentrations was a limiting factor since it occasionally caused reagent or product precipitation and clogged the instrument. Many viable reaction partners were dropped or substituted as a result of this reoccurring problem.

Each reaction droplet was injected into the FlowSyn using the manual injection feature and pre-measured injection loops. The loops were filled in between injections using pre-filled syringes of each reaction component solution. Each loop injected 0.1 mL of reaction partner stock solution into the fluorous stream to give a total droplet volume of 0.2 mL. The flow rate was set to 1.3 mL/min to achieve a reaction time of 5.0 min within the instrument. Droplet injection occurred every 1.0 minute with a wash droplet of anhydrous *N*,*N*-dimethylformamide injected in between each droplet. Therefore library members were injected on odd minutes (1,3,5, *etc*.) and washes on even minutes (2,4,6, *etc*.). The inclusion of washes increased the overall recovery of library material and limited contamination between adjacent droplets. Each run took a total of 45 minutes to complete reaction of all 20 library members.

Upon completion of each library member the droplets exiting the reactor were collected manually in tubes (by visualization). The crude material was then extracted from the excess fluorous solvent directly. Although the fluorous solvent was largely immiscible with the *N*,*N*-dimethylformamide-based reaction droplets, some dispersion of reaction material into the fluorous spacer was observed. To address this problem the adjacent fluorous spacer solvent for each library member was extracted at least three times with equal parts of *N*,*N*-dimethylformamide and the combined extracts were reduced to obtain the final products. Failure to complete this extraction process resulted in very poor product recovery. After product extraction, the fluorous solvent was recycled and reused in multiple libraries. The crude material collected from the reactions was often of very high quality and required little purification. Purification was completed using an automated HPLC/MS MDF system. On a few occasions, the purity of the material was so high that it spontaneously crystallized, either directly in the instrument, upon cooling or collection. This was particularly problematic since it created a blockage within the flow tubing and caused the instrument to shutdown.

**Heterocycle synthesis in flow.** Based on the preliminary investigations mentioned above, two 20-membered heterocycle libraries were completed in flow to generate thiazoles and pyrazoles. Stock solutions from each reagent measuring 0.10 mL were used per reaction. Concentrations of the stock solutions were set as to aim for a minimum of 35 mg of material for each library member.

Thiazoles were synthesized by the combination of various α-bromoketone and thiourea reaction components (Table 3). The reactions were performed in *N*,*N*-dimethylformamide at 80 ºC with a reaction time of 5 minutes (1.3 mL/min flow rate). Yields from the library were moderate, ranging from 12% to 63%, with most compounds achieving yields around 50%.

**Table 3.** Thiazole library.

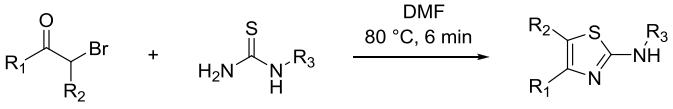


| entry | $R_1$ | $R_2$ | $R_3$ | product | yield (%)[a] |
|---|---|---|---|---|---|
| 1 | Ph | $CH_3$ | $CH_3$ | **1** | 61 |
| 2 | Ph | $CH_3$ | Ph | **2** | 40 |
| 3 | Ph | $CH_3$ | *m*-$FC_6H_4$ | **3** | 31 |
| 4 | Ph | $CH_3$ | allyl | **4** | 41 |
| 5 | -$C_6H_4$-2-$CH_2$- | | $CH_3$ | **5** | 53 |
| 6 | -$C_6H_4$-2-$CH_2$- | | Ph | **6** | 34 |
| 7 | -$C_6H_4$-2-$CH_2$- | | *m*-$FC_6H_4$ | **7** | 24 |
| 8 | -$C_6H_4$-2-$CH_2$- | | allyl | **8** | 12 |
| 9 | *t*-Bu | H | $CH_3$ | **9** | 36 |
| 10 | *t*-Bu | H | Ph | **10** | 40 |
| 11 | *t*-Bu | H | *m*-$FC_6H_4$ | **11** | 49 |
| 12 | *t*-Bu | H | allyl | **12** | 50 |
| 13 | *p*-$CNC_6H_4$ | H | $CH_3$ | **13** | 48 |
| 14 | *p*-$CNC_6H_4$ | H | Ph | **14** | 48 |
| 15 | *p*-$CNC_6H_4$ | H | *m*-$FC_6H_4$ | **15** | 49 |
| 16 | *p*-$CNC_6H_4$ | H | allyl | **16** | 42 |
| 17 | *p*-$FC_6H_4$ | H | $CH_3$ | **17** | 55 |
| 18 | *p*-$FC_6H_4$ | H | Ph | **18** | 31 |
| 19 | *p*-$FC_6H_4$ | H | *m*-$FC_6H_4$ | **19** | 46 |
| 20 | *p*-$FC_6H_4$ | H | allyl | **20** | 63 |

[a]Isolated yield after MDF.

Pyrazoles were synthesized by the combination of various 1,3-diketone and hydrazine reaction components (Table 4). The reactions were performed in *N*,*N*-dimethylformamide at 80 ºC with a reaction time of 5 minutes (1.3 mL/min flow rate). Yields from the library were moderate and ranged from 9% to 79%, with most compounds achieving yields around 30%.

**Table 4.** Pyrazole library results.

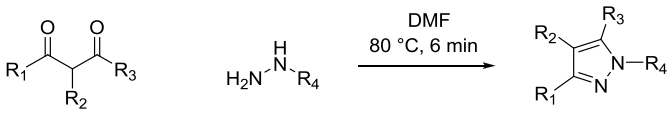


| entry | $R_1$ | $R_2$ | $R_3$ | $R_4$ | product | yield (%)[a] |
|---|---|---|---|---|---|---|
| 1 | $CH_3$ | $CH_3$ | $CH_3$ | Ph | **21** | 33 |
| 2 | $CH_3$ | $CH_3$ | $CH_3$ | *m*,*m*-$Cl_2C_6H_4$ | **22** | 26 |
| 3 | $CH_3$ | $CH_3$ | $CH_3$ | $CH_3$ | **23** | 44 |
| 4 | $CH_3$ | $CH_3$ | $CH_3$ | $(CH_2)_2OH$ | **24** | 37 |
| 5 | $CH_3$ | $CH_3$ | $CH_3$ | Cy | **25** | 34 |
| 6 | $CF_3$ | H | $CH_3$ | Ph | **26** | 38 |
| 7 | $CF_3$ | H | $CH_3$ | *m*,*m*-$Cl_2C_6H_4$ | **27** | 15 |
| 8 | $CF_3$ | H | $CH_3$ | $CH_3$ | **28** | 0 |
| 9 | $CF_3$ | H | $CH_3$ | $(CH_2)_2OH$ | **29** | 17 |
| 10 | $CF_3$ | H | $CH_3$ | Cy | **30** | 23 |
| 11 | $CH_3$ | H | Ph | Ph | **31** | 29 |
| 12 | $CH_3$ | H | Ph | *m*,*m*-$Cl_2C_6H_4$ | **32**[b] | 23 |
| 13 | $CH_3$ | H | Ph | $CH_3$ | **33**[b] | 21 |
| 14 | $CH_3$ | H | Ph | $(CH_2)_2OH$ | **34**[b] | 79 |
| 15 | $CH_3$ | H | Ph | Cy | **35** | 26 |
| 16 | $CH_3$ | -$(CH_2)_3$- | | Ph | **36** | 32 |
| 17 | $CH_3$ | -$(CH_2)_3$- | | *m*,*m*-$Cl_2C_6H_4$ | **37**[b] | 9 |
| 18 | $CH_3$ | -$(CH_2)_3$- | | $CH_3$ | **38** | 43 |
| 19 | $CH_3$ | -$(CH_2)_3$- | | $(CH_2)_2OH$ | **39**[b] | 50 |
| 20 | $CH_3$ | -$(CH_2)_3$- | | Cy | **40**[b] | 40 |

[a]Isolated yield after MDF. [b]Isolated as a mixture of regioisomers.

**Summary.** A continuous flow method was developed using a segmented flow approach to perform the synthesis of a theoretically unlimited number of heterocycle libraries in droplets. It was demonstrated that different types of heterocycles could be interchangeably synthesized in a single run without stopping the flow of the instrument or altering the condition settings (temperature, carrier solvent and flow rate). The technique was applied for library synthesis around two heterocyclic cores, each containing 20 members. While overall yields from the libraries were moderate, each reaction afforded greater than 35 mg of material in high purity and produced very minimal waste. When considered together these features reveal the utility a droplet-based library approach can exhibit for the rapid and efficient synthesis of drug-like molecules.

## Chapter 3

## In situ Reagent Generation with Continuous Flow

A second methodology study, completed in conjunction with researchers at Abbott Laboratories, aimed to take advantage of the unique closed environment inherently maintained by flow platforms. The intrinsic closed nature of flow systems enables the creation, reaction, and removal of noxious chemicals *in situ*, making the overall process safer by limiting chemical exposure of the user and allowing for only small quantities of the noxious chemical to be present at any one time. Aimed at this purpose an *in situ* synthesis of isocyanides, reagents notorious for their unpleasant smell, was developed. In a demonstration of the applicability of this method, the *in situ* isocyanide preparation was coupled to the Ugi four-component reaction for the synthesis of a series of complex amines, eliminating exposure of the user to isocyanides and their odor.

**Isocyanides and the Ugi reaction.** The field of isocyanide chemistry began in 1859 when Lieke reported the first synthesis of allyl isocyanide from allyl iodide and silver cyanide.[60] Following this discovery came the development of two classical isocyanide syntheses from Gautier[61] and Hoffmann[62] in the late 1800s. For the remainder of the century only 12 isocyanides were prepared due to the unreliability of the synthetic methods[63] and their universally unpleasant odor. Even in this period of limited availability, exploration and expansion of the chemistry of this small

functional group had begun. The first important uses of isocyanides were for the synthesis of tetrazoles from hydrazoic acid and in the Passerini three-component reaction (Passerini 3-CR) (Figure 13).[64a]

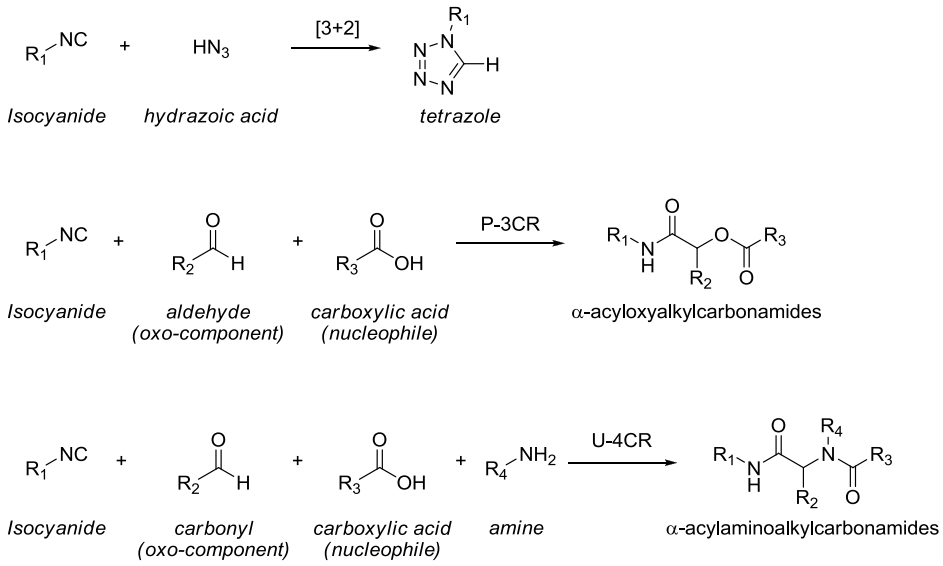


**Figure 13.** Isocyanides in tetrazole synthesis, Passerini, and Ugi reaction.

The next notable advancement in this field did not occur until the 1950s when the naturally derived isocyanide-containing antibiotic *O,O'*-dimethylxanthocillin was prepared through the dehydration of the diformylamine with benzenesulfonyl chloride and pyridine.[64] The applicability of this dehydration method to a wide range of substrates for the first time demonstrated a general, high-yielding approach for the synthesis of isocyanides. (Figure 14).[64a] With the development of a reliable synthetic method and increasing commercial availability, isocyanides found use in numerous synthetic applications for the formation of amides and various heterocycles. They

have been known to participate in a variety of reactions including free radical additions, organometallic reactions, polymerizations, and multicomponent reactions.[65]

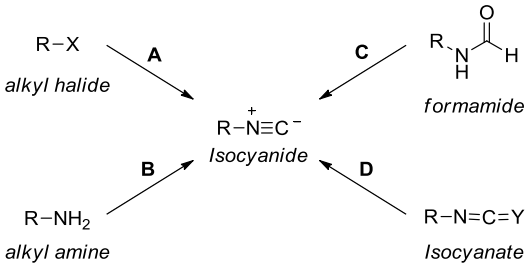


**A**: AgCN, KCN, or HCN, $\Delta E_{el}$
**B**: $CCl_2$, KOH
**C**: acylating agent, base
*acylating agents*: $COCl_2$, $SOCl_2$, $PhSO_2Cl$, $CH_3PhSO_2Cl$, $PBr_3$, $PCl_3$, $PCl_5$, $Cl_3PO$, $PO_5$
*bases*: $R_3N$, $R_2NH$, pyridine, quinoline, $K_2CO_3$, t-BuOK
**D**: Y = O, $PO_3Et_3$, $\Delta$, or Y = S, $Et_3P$, $\Delta$, or $Ph_3SnH$, or $h\nu$

**Figure 14.** General routes to isocyanides.[63]

In 1961 Ivar Karl Ugi introduced perhaps the most popular application of isocyanides in a four-component coupling reaction, which later became known as the Ugi four-component reaction (Ugi 4-CR) (Figure 13).[64a] The scope of the four components makes this reaction particularly dynamic since the products can not only differ in substituent but also in structure. The components of the Ugi 4-CR are isocyanides, amines (ammonia, mono- and disubstituted amines, hydroxylamine, and suitable derivatives), carbonyl compounds (aldehydes and ketones), and acid components or related compounds (water, thiosulfates, hydrogen selenide, hydrazoic acid, hydrogen cyanate and thiocyanate, aminocyanic acid, carboxylic acids, and thioacids, alkoxycarboxylic acids and amines) (Figure 15).[64a] Considering the

commercially available permutations of carboxylic acids, amines, aldehydes, ketones, and isocyanides alone, the theoretical combinations of Ugi 4-CRs span a chemical space greater than $10^{14}$ small molecules.[64a] Such implicit potential makes this transformation a powerful tool for the rapid construction of organic molecules.[66]

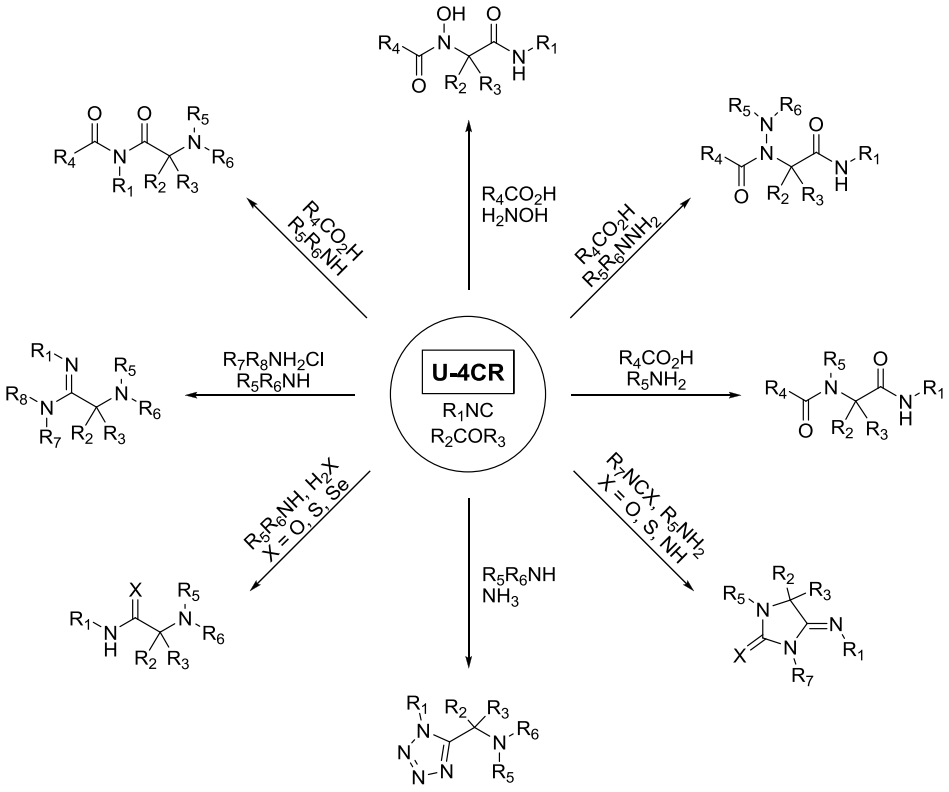


**Figure 15.** Variability of the Ugi 4-CR products.

Use of the isocyanide-based multicomponent reactions (IMCR) was popularized in the early 1990s as combinatorial chemistry became a major focus in both industry and academia. Performing the Ugi 4-CR in a semi-automatic liquid- or solid-phase format enabled chemists to exponentially increase their productivity and

facilitated the investigation of millions of compounds annually.[67] Products derived from the Ugi 4-CR or Passerini 3-CR have found medicinal application across a wide range of disease states including antibacterial, antiviral, anticancer, ion channel blockers and GPCR modulators (Figure 16).[67] These transformations have also proved useful for rapid access to the medicinally privileged structures of benzodiazopines and spiropiperidines.[67] The breadth of scope of the IMCR and efficient access to these structures have greatly facilitated the study of these popular agents.

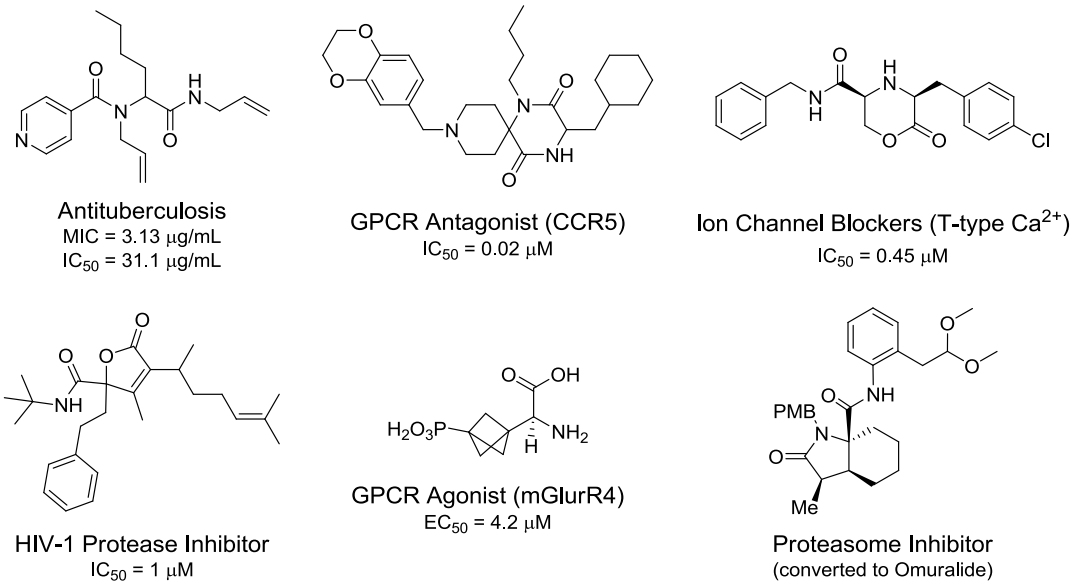


**Figure 16.** Medicinally relevant compounds derived from IMCRs.[67]

The increase in availability of IMCR chemotypes initially generated concerns surrounding the peptidic nature of the products because such compounds typically exhibit short half-lives and are quickly metabolized in biological systems. Fortunately

further transformations of these scaffolds can give compounds with good pharmacokinetic properties.[67]

**Isocyanides in a multi-step flow process.** Isocyanides are among the most versatile functional groups, however their intense offensive odor has greatly discouraged their use. Ugi himself stated, "The development of the chemistry of isonitriles has probably suffered through the characteristic odor of volatile isonitriles, which has been described by Hofmann and Gautier as 'highly specific, almost overpowering', 'horrible', and 'extremely distressing'".[62,65,68,69] This characteristic has been known to cause migraines upon sensitization and even prompted their investigation as non-lethal weapons.[65,70]

While isocyanides with high molecular weights are commonly solid and odorless the majority of commercially available isocyanides are of low molecular weight and volatile.[66] One method to embrace the versatility of the isocyanide without dealing with the problems of direct handling (*i.e.* volatility) is to devise a procedure wherein the isocyanide is made *in situ* and quenched at the end of the sequence, prior to exposure of the user. For this purpose, the inherent closed nature of a flow system makes it the ideal platform for the development of such a method (Figure 17).

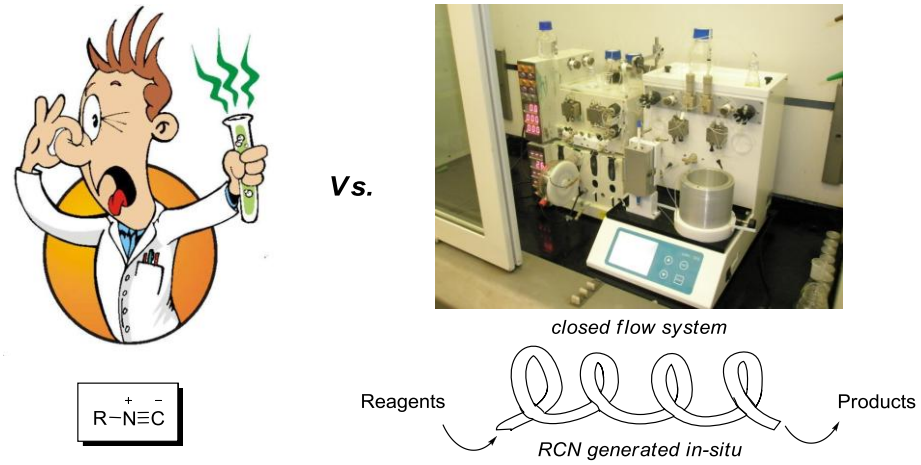


**Figure 17.** Isocyanides in traditional settings vs. flow settings.

Flow reactors have been used previously to generate noxious, toxic, unstable, explosive, or dangerous chemical *in situ*, with removal of these agents before the reaction exits the instrument. In this way the user is never directly exposed to the offending agent and the scale of the instrument is such that only a small amount of the problematic material is present at any given time during the reaction. These benefits make difficult or dangerous reactions safer and more convenient. In addition, flow reactors have many of the same advantages as microwaves, namely the ability to pressurize and superheat reactions causing an increase in rate. Flow reactors also have the added benefit of scalability where essentially endless amounts of material may be made simply by flowing continuously.

Performing these reactions in flow does present challenges which must be considered. Isocyanides are typically synthesized using harsh condition and the chosen method of formation must be compatible with the flow apparatus components

(pump, injectors, tubing, connectors, *etc*.). In addition, any excess reagents or by-products must not interfere with any succeeding reactions performed on the isocyanide. Isocyanide formation and subsequent reactions also must be fast since the flow rates accessible through the system impose a limitation on the maximum reaction time.

**Development of a two-step Ugi sequence**. As the Ugi 4-CR is a versatile reaction and creates products of medicinal relevance, we set out to exhibit the utility of a flow isocyanide synthesis through the creation of a two-step Ugi sequence. The Ugi 4-CR was specifically chosen for its close tie to relevant medicinal applications, as shown above. The envisioned sequence consisted of the *in situ* generation of isocyanides followed by their immediate use in the Ugi 4-CR, and ultimately hydrolysis of the isocyanide prior to the product exiting the instrument.

The first challenge in the development of the two-step Ugi 4-CR sequence was to choose the optimal method for isocyanide synthesis in flow. Traditional methods for the preparation of isocyanides from alkylhalides and alkylamines are known to be unreliable, low-yielding, and harsh (Figure 15). In addition, these methods use salt-based forms of cyanide (AgCN, KCN), which would create solubility problems in the flow reactor. The most reliable method of isocyanide preparation, as discussed previously, is the dehydration of formamides (Figure 18).

Many reagents have been used to promote the dehydration of formamides for the synthesis of isocyanides. By far the most consistent and widely used reagent has

been phosgene;[63] however for our purposes a less toxic and less reactive reagent was needed to carry through the multistep sequence.

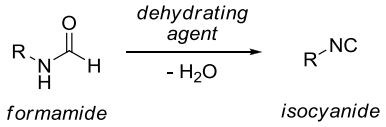


**Figure 18.** Isocyanide synthesis through formamide dehydration.

The optimal conditions for dehydration in flow were determined by gauging reactions using traditional benchtop techniques. From there, successful reagent combinations were tested in the microwave under superheating temperatures to simulate conditions in flow. With this plan in place, a number of reagents were investigated including, but not limited to, Burgess reagent,[71] oxalyl chloride,[72] and polymer-supported triphenylphosphine.[73] Three formamides (cyclohexyl, *p*-bromophenyl, *o*-chlorophenyl) were subjected to these dehydration conditions using various reaction times, temperatures, solvents, and additives. Initial attempts to follow the dehydrations using LMCS/ELSD/MS were unsuccessful as the isocyanide products exhibited little to no UV activity and showed poor mass response. As a result, it was determined that the most reliable method to test the efficiency of isocyanide formation was by performing a standard Ugi 4-CR using the crude isocyanide mixture and subsequently comparing the outcome of the two-step procedures directly.

**Scheme 9**

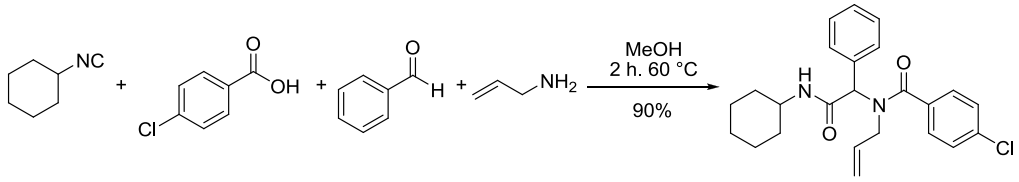


The Ugi 4-CR of cyclohexyl formamide, *p*-chlorobenzoic acid, benzaldehyde, and allylamine was chosen as the model reaction from which to establish the optimal dehydration conditions. As a benchmark, the Ugi 4-CR was performed using cyclohexyl isocyanide purchased from commercial sources (Scheme 9). For this reaction, all four-components were combined in equal equivalents at the start of the reaction. Heating in an oil bath at 60 ºC for two hours afforded 90% of the desired Ugi 4-CR product.

Using this result, the transformation was investigated starting from the dehydration of cyclohexyl formamide and a limited survey of dehydration conditions was performed (Table 5). The reactions were completed according to their optimized literature procedures.[71-73] Ultimately Burgess reagent gave the most promising result (Table 5, entry 4), yielding 50% of the desired product. However, to achieve this yield the two-step sequence required continual stirring at room temperature for three days. For any flow-based technique to be viable a much shorter reaction time was needed. The minimum flow rate of the HPLC pumps required reactions to be completed on the order of hours rather than days.

**Table 5.** benchtop survey of the two-step dehydration–Ugi 4-CR sequence.

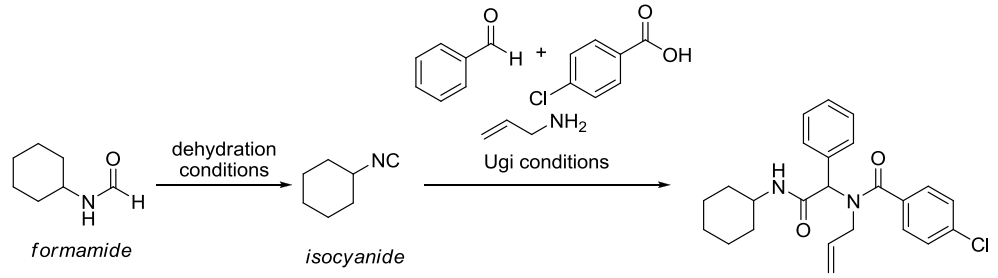


| | Dehydration | | | | Ugi | | |
|---|---|---|---|---|---|---|---|
| entry | reagents | time (min) | temp. (ºC) | solvent | time (h) | solvent | yield (%)[a] |
| 3 | oxalyl chloride | 60 | 40 | $CH_2Cl_2$ | 24 | $MeOH/CH_2Cl_2$ | – |
| 1 | PS-$PPh_3$, $Et_3N$ | 15 | 80 | $CCl_4$ | 24 | $MeOH/CCl_4$ | – |
| 2 | PS-$PPh_3$, $Et_3N$ | 15 | 80 | $CCl_4$ | 72 | $MeOH/CCl_4$ | 20 |
| 4 | Burgess salt | 24 | rt | $CH_2Cl_2$ | 72 | $MeOH/CH_2Cl_2$ | 50 |

[a]Isolated yield.

To determine the effect of superheating conditions on the rate, and potentially decrease the overall transformation time, a series of microwave reactions were completed simulating prospective scenarios in flow. The two-step process involving formamide dehydration with Burgess reagent followed by Ugi 4-CR of the preformed isocyanide was completed using variations of the component ratio, temperature, time, and solvent for both the dehydration and Ugi steps. Starting at 90 ºC and using a five minute reaction time for each step (Table 6, entry 1 and 2), a drop in the conversion was observed when methanol was used as the only solvent. A gradual increase in the reaction time lead to a jump (up to 75%) in the overall conversion (Table 6, entries 2 and 3). With this result the two-step process became feasible for flow applications, achieving adequate conversions in fewer than two hours.

The optimal microwave-based procedure was found to use two equivalents of both Burgess reagent and formamide in dichloromethane heating at 65 ºC for 2 hours. This was followed by addition of a premixed solution of aldehyde, amine, and acid in methanol, and heating at 90 ºC for an additional hour. The overall process gave 95% conversion to the desired product (Table 6, entry 5). Use of a single equivalent of Burgess reagent and formamide under these conditions gave very little conversion (Table 6, entry 6), demonstrating that the reaction outcome had a strong dependence on the component stoichiometry.

**Table 6.** Microwave survey of the two-step dehydration–Ugi 4-CR sequence.

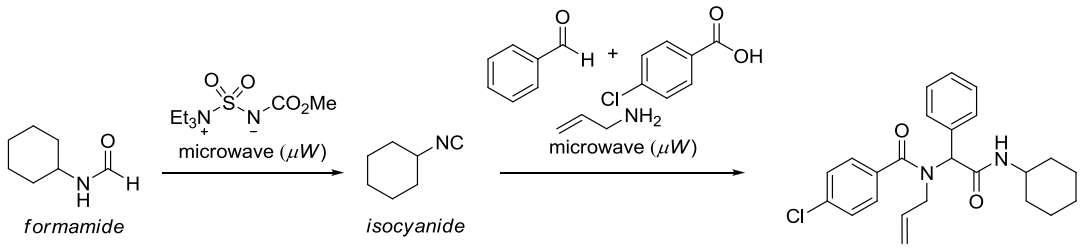


| | Dehydration | | | | Ugi | | | |
|---|---|---|---|---|---|---|---|---|
| entry | amide (equiv.) | temp. (ºC) | time (min.) | solvent | temp (ºC) | time (min.) | solvent | conversion (%)[a] |
| 1 | 2 | 90 | 5 | $CH_2Cl_2$ | 90 | 5 | MeOH/$CH_2Cl_2$ | 30 |
| 2 | 2 | 90 | 5 | MeOH | 90 | 5 | MeOH | 15 |
| 3 | 2 | 90 | 30 | $CH_2Cl_2$ | 90 | 60 | MeOH/$CH_2Cl_2$ | 75 |
| 4 | 2 | 90 | 60 | $CH_2Cl_2$ | 90 | 60 | MeOH/$CH_2Cl_2$ | 75 |
| 5 | 2 | 65 | 120 | $CH_2Cl_2$ | 90 | 60 | MeOH/$CH_2Cl_2$ | 95 |
| 6 | 1 | 65 | 120 | $CH_2Cl_2$ | 90 | 60 | MeOH/$CH_2Cl_2$ | 10 |

[a]Conversion estimated by LMCS/ELSD

Using the optimized microwave conditions a small subset of formamides were subjected to the two-step procedure to gauge the scope of the sequence (Table 7).

Overall the isolated yields were much lower than predicted by LCMS. This discrepancy was initially attributed to problems encountered during purification. The highly lipophilic nature of the Ugi 4-CR products complicated purification and made isolation of the pure material difficult. In addition, an unknown by-product co-eluted with the desired Ugi 4-CR products, further complicating isolation.

**Table 7.** Formamide scope in the dehydration–Ugi 4-CR microwave sequence.

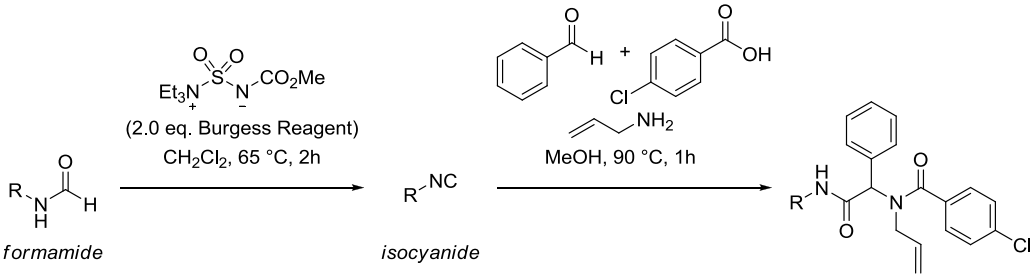


| entry | R | conversion (% by LCMS)[a] | yield (% by isolation) |
|---|---|---|---|
| 1 | Cy | 95 | 61 |
| 2 | *t*-Bu | 75 | 66 |
| 3 | $C_5H_{11}$ | 75 | 68 |
| 4 | Bn | 30 | – |
| 5 | Ph | 10 | – |

[a]Estimated according to LCMS data of crude reaction.

Despite the unexpected low yields, the reaction appeared to work best for alkyl formamides (Table 7, entries 1-3). Benzyl and phenyl formamides performed poorly and gave no isolated product despite some conversion observed by the LCMS/ELSD/MS (Table 7, entries 4 and 5). In addition to those listed in Table 6, four other formamides were tested using the optimized microwave two-step sequence

but, for reasons such as poor solubility and polymerization, these substrates failed to yield the desired product (Figure 19).

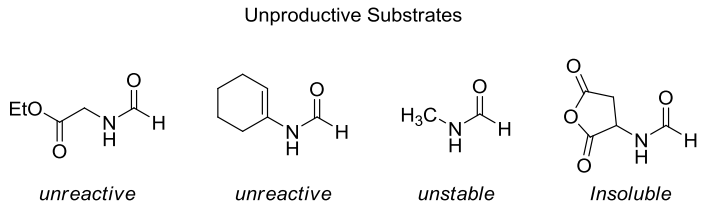


**Figure 19**. Formamides not viable in the two-step microwave sequence.

While the vast majority of organic transformations benefit from the advantages of microwave heating, previous studies focused on the use of isocyanides in microwaves suggest that these conditions may actually exhibit a detrimental effect on isocyanide-based reactions.[66] Often the use of microwaves in IMCRs leads to different, unexpected, or unwanted products. Several classes of isocyanides are known to be highly prone to polymerization; the concentrated conditions and high temperatures used in microwave synthesis can enhance this process leading to a larger quantity of unwanted side products. In addition, a number of reactive intermediates generated during the course of the MCR can react with unintended partners present in solution (solvent, intramolecular reactions, *etc.*) to promote polymerization, oligomerization and other unwanted side products. It was speculated that these difficulties contributed to the low yields and conversion for some of the formamides investigated in the microwave study. Also, it was initially unknown if these problems would carry over to transformations performed in a flow setting. Even so, we hoped

that the use of dilute conditions and precise heating in flow could diminish the potential for these problems.

**Flow apparatus design.** The continuous flow apparatus employed for *in situ* isocyanide formation and Ugi 4-CR was created by combining two commercially available flow units, the Uniqsis FlowSyn and the Vapourtec R Series (Figure 20).[42,43] In the design of the instrument, the FlowSyn heating coil was used to synthesize the isocyanides by mixing formamide and Burgess reagent. Upon exiting the FlowSyn heating coil the newly formed isocyanide was combined with a premixed solution of aldehyde, amine, and acid. The two solutions were united using a T-joint. The mixture was then passed through the Vapourtec heating coil which was used to complete the Ugi 4-CR. Finally, upon exiting the Vapourtec coil the solution was passed through a column filled with solid-supported *p*-toluenesulfonic acid located on the FlowSyn base. Upon passing through the column the excess isocyanide was hydrolyzed back to formamide before the solution exited the instrument.[74]

Although the individual reaction platforms were both automated, the timing of each reaction had to be dictated to each machine individually and accompanied by a physical switch between solvent and reaction solution. Therefore, system injection of both the initial dehydration reaction and the subsequent Ugi 4-CR was controlled manually. To determine the injection time for the Ugi 4-CR components, a plug of colored dye was sent through the instrument to measure the path length (length of tubing) and residence time at various flow rates. Injection was completed by

continuous flow using standard HPLC pumps equipped on both the FlowSyn and Vapourtec instruments.

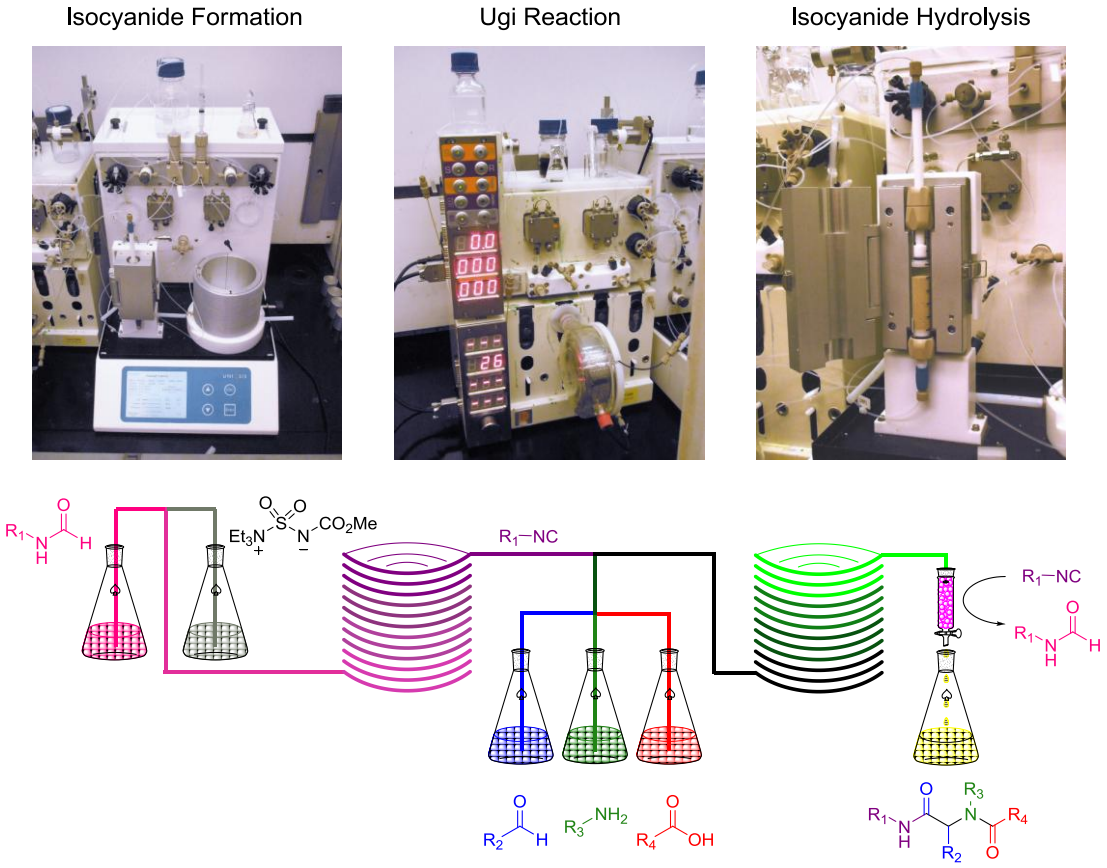


**Figure 20.** Diagram of the continuous flow platform for the two-step Ugi 4-CR.

Reactions completed in the continuous flow apparatus were performed by combining 0.750 mmol (101 mg, 2 equiv.) of formamide with 1.50 mmol (206 mg, 2 equiv.) of Burgess reagent in 1.5 mL of anhydrous dichloromethane in a sealed conical-tipped vial. An injector tube was inserted through a hole in the vial cap and extended until it touched the bottom of the vial. The solution was allowed to flow

continuously into the reactor at a flow rate of 0.1 mL/min (equivalent to one hour reaction time), the maximum reproducible reaction time which could be achieved using the FlowSyn. The total injection time for the dehydration step of the sequence was approximately one hour, after which point the primary injection line was switched to anhydrous dichloromethane to move the remaining reaction solution through the instrument. The flushing solvent injection required one additional hour.

During this time, a solution of the remaining Ugi 4-CR components was prepared by combining 0.375 mmol (1 equiv.) of acid, 0.375 mmol (1 equiv.) of aldehyde, and 0.375 mmol (1 equiv.) of amine in 1.5 mL of anhydrous methanol in a sealed conical-tipped vial. The combined solution was allowed to sit for 1-2 hours prior to injection into the instrument. Prior to the start of the Ugi 4-CR component injection, a solution of anhydrous methanol was pumped through the instrument to maintain the appropriate backpressure. As the newly-formed isocyanide reached the T-joint merge point an injector tube was inserted through a hole in the vial cap of the Ugi 4-CR component solution and extended until it touched the bottom of the vial. The solution was allowed to flow continuously into the Vapourtec reactor at a rate of 0.1 mL/min (equivalent to one hour reaction time), which was the longest reaction time which could be achieved reproducibly by the instrument. The total injection time for the Ugi 4-CR step of the sequence equaled approximately one hour, after which point the second injection line was switched to anhydrous methanol to move the remaining reacting solution through the instrument. Flushing of the Ugi 4-CR took approximately one additional hour. The time from the start of the dehydration

injection to the exit of all reaction material from the instrument measured a total of three hours.

**Study of Ugi reaction scope in flow.** During the initial investigation of the optimal dehydration conditions using the microwave, it was observed that the overall yield of the two-step sequence fluctuated in response to variation in the stoichiometry (Table 6, entry 5 vs. entry 6). To address this phenomenon and determine the optimal stoichiometric ratio of reactants, the relationship between the Burgess reagent, formamide, and the remaining Ugi 4-CR components was briefly investigated in flow (Table 8). Reactions were performed in both the microwave and in continuous flow for direct comparison. In most cases, reactions performed in flow had yields equivalent to or slightly better than those performed in the microwave.

**Table 8**. Study of the two-step Ugi 4-CR stoichiometry in flow.

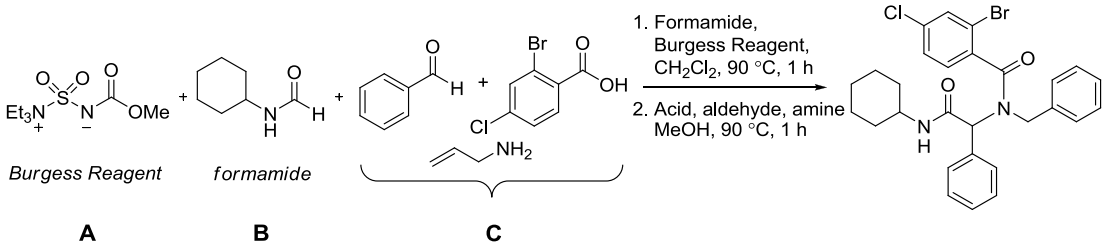


| entry | **A** (equiv.) | **B** (equiv.) | **C** (equiv.) | microwave (% yield)[a] | flow (% yield)[b] |
|---|---|---|---|---|---|
| 1 | 3 | 2 | 1 | 46 | 41 |
| 2 | 2 | 2 | 1 | 76 | 79 |
| 3 | 2 | 1 | 1 | 26 | 37 |
| 4 | 1 | 1 | 1 | 40 | 48 |

[a]Both dehydration and Ugi reactions completed in microwave at 90 ºC for 1 h.
[b]Both dehydration and Ugi reactions completed in continuous flow at 90 ºC for 1h.

The optimal stoichiometry was found as two equivalents of Burgess reagent and formamide for each equivalent of the remaining three components (aldehyde, amine, and acid). This combination gave the highest isolated yield for reactions completed both in the microwave (76%) and in flow (79%) (Table 8, entry 2). In all other cases, different stoichiometric combinations gave lower yields (40-50% overall). With a general understanding of the stoichiometry, the substrate scope of the two-step flow sequence was then investigated (Table 9).

**Table 9.** Study of the two-step Ugi 4-CR substrate scope.

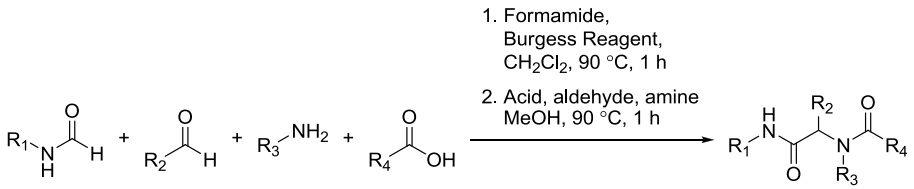


| entry | $R_1$ | $R_2$ | $R_3$ | $R_4$ | product | μW (%)[a,b] | flow (%)[a,b] |
|---|---|---|---|---|---|---|---|
| 1 | Bn | Ph | Bn | 2-Br,4-Cl$C_6H_3$ | **41** | 14 | 79 |
| 2 | Cy | Ph | Bn | 2-Br,4-Cl$C_6H_3$ | **42** | 47 | 75 |
| 3 | *t*-Bu | Ph | Bn | 2-Br,4-Cl$C_6H_3$ | **43** | 20 | 60 |
| 4 | *p*-Cl$C_6H_4$ | Ph | Bn | 2-Br,4-Cl$C_6H_3$ | **44** | 14 | 52 |
| 5 | Ph | Ph | Bn | 2-Br,4-Cl$C_6H_3$ | **45** | 18 | 48 |
| 6 | EtOCOCH | Ph | Bn | 2-Br,4-Cl$C_6H_3$ | **46** | 17 | 46 |
| 7 | Bn | H | Bn | Ph | **47** | 52 | 83 |
| 8 | Bn | *p*-Cl$C_6H_4$ | Bn | Ph | **48** | 42 | 78 |
| 9 | Bn | Ph | Bn | Ph | **49** | 53 | 72 |
| 10 | Bn | *n*Pr | Bn | Ph | **50** | 6 | 28 |
| 11 | Ph | Ph | Bn | Ph | **51** | 33 | 43 |
| 12 | Ph | Ph | *p*-Cl$C_6H_4$ | Ph | **52** | 13 | 28 |
| 13 | Cy | Ph | Bn | Ph | **53** | 64 | 83 |
| 14 | Cy | Ph | Bn | *p*-Cl$C_6H_4$ | **54** | 43 | 79 |
| 15 | Cy | Ph | Bn | *n*Pr | **55** | 77 | 57 |
| 16 | Cy | Ph | Bn | $CH_3$ | **56** | 51 | 54 |

[a]Both dehydration and Ugi reactions completed at 90 ºC for 1 h. [b]Isolated yield.

Once again, reactions were performed both in continuous flow and in the microwave, under identical heating and reaction time, for comparison purposes. The majority of the reactions gave good to excellent yields across the two-step process. Yields from the microwave transformations were overall lower than those for reactions completed using the flow process. The decrease in product observed from the microwave reaction may be attributed to a number of factors. One consideration is that in order to directly compare the two reaction techniques the optimized flow parameters were used for both the microwave and flow-based reactions. As a result, microwave-based experiments were shortened and run under increased temperatures. This decrease in time and increase in temperature may have contributed to an increase in unwanted by-products and an overall decrease in yield of the desired product.

**Summary.** Overall, the good yields and large substrate scope demonstrate the general and robust nature of the continuous flow two-step method. In addition, the sequence was completed in only three hours using the continuous flow method, a vast improvement over the benchtop method which required reaction times greater than three days. While reactions performed in the microwave were also completed in a matter of hours, the sequence still required exposure to isocyanides during the addition of the Ugi 4-CR components and extensive purification. The flow methodology enabled reactions to be completed rapidly while eliminating direct exposure of the user to isocyanides, increasing the safety and convenience of these reactions.

# Chapter 4

## Reaction Discovery Using Microfluidic-Based Screening of Polycyclic Iminium Ethers

In cooperation with the laboratory of Dr. John A. Porco, Jr. at Boston University (BU) we aimed to extend the use of flow technology to include applications of reaction discovery and development of synthetic methodologies. Starting from two iminium ether substrates, a simple bicyclic iminium ether and a densely functionalized bicyclo[3.2.1]octanoid derived iminium ether, a high-throughput flow-based method was designed to probe the variety of chemotypes that are accessible from these intermediates. The highly condition-dependent nature of iminium ether transformations makes them particularly excellent candidates for multidimensional reaction screening on a microfluidic platform. Accordingly, systematic screening of substrates, reaction partners, additives, and conditions in an array format was completed to access the greatest breadth of substrate reactivity. Moreover, use of an automated microfluidics reaction screening platform allowed for the reactions to be completed on an analytical scale in continuous succession, resulting in considerable savings of both time and material. This chapter details the development of a multidimensional reaction screen for polycyclic iminium ethers the resulting chemotypes derived from those experiments.

**Synthesis and reactivity of cyclic iminium ethers.** Cyclic iminium ethers are ambident electrophilic intermediates that react with a range of nucleophiles in a highly condition-dependent manner. Iminium ether stability, nucleophile identity, solvent, reaction time, and temperature, among other factors, have all been shown to influence the course of iminium ether reactions.[75] Nevertheless, these reactive intermediate have demonstrated particular utility in the synthesis of densely functionalized heterocycles.[76] Acyclic iminium ethers are typically formed through the *O*-alkylation of amides, while cyclic and bicyclic versions can be formed through the direct *N*-alkylation of oxazolines and dihydrooxazines (Figure 21)[77] or by reaction of ketones with hydroxyalkyl azides (Figure 22).[78] The ambident electrophilic nature of these species gives access to different reaction pathways (path *a*-*c*) within a single substrate (Figure 21).[75,79]

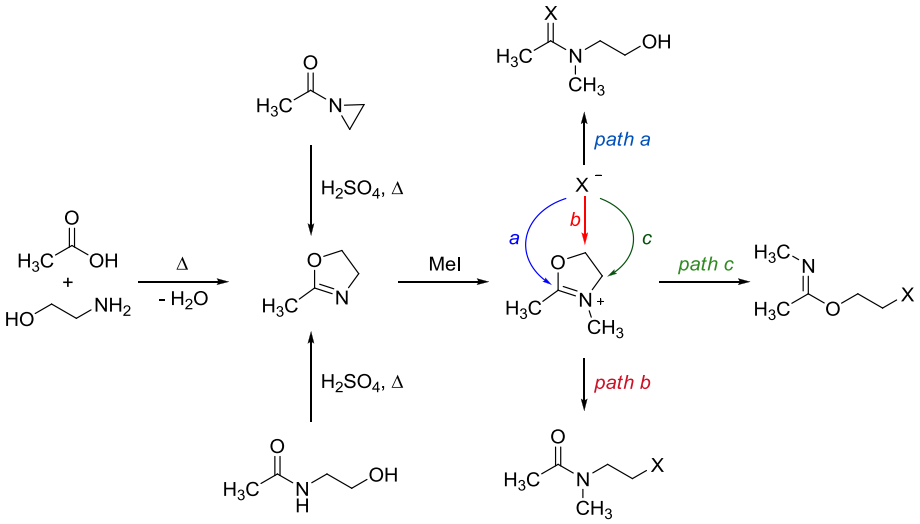


**Figure 21**. Synthesis and reactivity of cyclic iminium ethers.

While multiple products are possible, in practice most substrate combinations give rise to a single dominate species. These features make iminium ethers particularly attractive substrates for reaction screening, as there is the possibility for multiple chemotypes to arise from a single substrate while one path is typically favored to afford acceptable conversion to a major product. In addition, a wide range of structurally diverse iminium ethers are available and their capacity to react with a wide selection of nucleophiles further increases the potential for these substrates to generate a unique set of functionalized products.

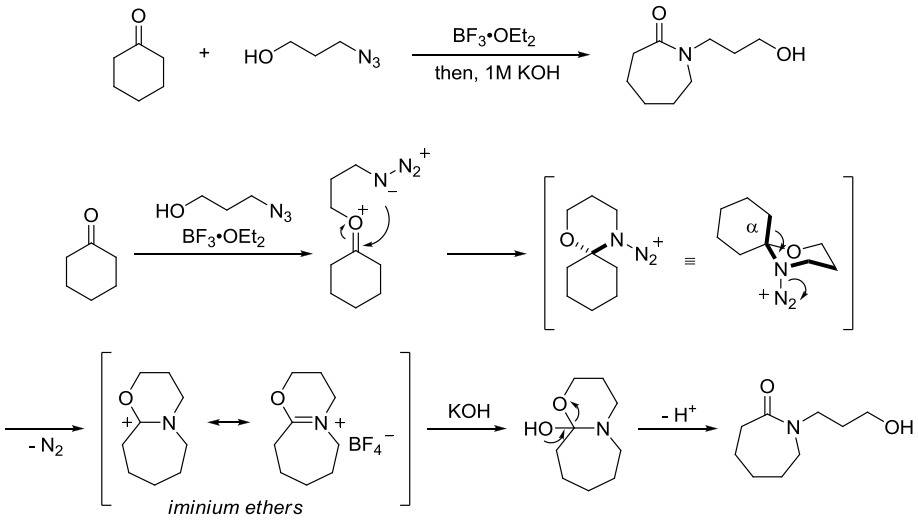


**Figure 22.** Mechanism of the azido-Schmidt reaction with hydroxyalkyl azides.

Previous studies conducted within the Aubé group, based on early work by Hünig, revealed two predominate modes of addition for 5,7-bicyclic iminium ethers (Table 10).[78] It was found that while path a was kinetically favored it was also often reversible, which led to a greater percentage of product isolated from path b. Path a

products resulted from instances where the initial nucleophile addition was either irreversible or where iminium ether ring opening successfully competed with nucleophile ejection (Table 10, entries 1-4). Path b products arose when nucleophiles were able to undergo elimination from the initial-formed adduct and ultimately underwent addition at the carbon adjacent to the imine center (Table 10, entries 5-8). A small group of stabilized carbon-based nucleophiles were also investigated but the mode of addition was found to differ according to the nature of the stabilizing anion and the nucleophile size (Table 10, entries 9-11).[78]

**Table 10**. Nucleophilic addition reactions of iminium ethers.[78]

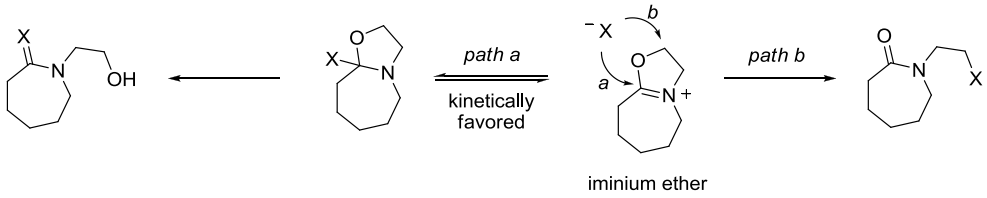


| entry | nucleophile | X | path | yield (%)[a] |
|---|---|---|---|---|
| 1 | $H_2$ | –H,H | a | 87 |
| 2 | $Na_2S$ | –S | a | 57 |
| 3 | $H_2NBn$ | –NBn | a | 88 |
| 4 | $H_2NNMe_2$ | $–NNMe_2$ | a | 88 |
| 5 | NaSPh | –SPh | b | 95 |
| 6 | NaOPh | –OPh | b | 74 |
| 7 | $NaN_3$ | $–N_3$ | b | 85 |
| 8 | NaCN | –CN | b | 82 |
| 9 | $NaCH(CO_2Me)_2$ | $–OCOCH_2CO_2Me$ | b | 34 |
| 10 | $NaCH(SO_2Ph)_2$ | $–CH(SO_2Ph)_2$ | b | 54 |
| 11 | $NaCH(CN)_2$ | $–C(CN)_2$ | a | 71 |

[a]Isolated yield as reported.

Based on these findings, it was initially unclear how the majority of carbon-based nucleophiles would behave with these systems. Given that a key aim in organic chemistry is the pursuit of carbon-carbon bond forming reactions, this was an important question to address. In addition, previous studies of these systems were limited and did not examine differences in reaction conditions or substrate identity. In order to gain a greater understanding of iminium ether reactivity the plan was to:

- Investigate more complex and functionalized cyclic iminium ethers
- Explore a broad range of carbon-based nucleophiles
- Expand the breadth of reaction conditions

In order to complete these aims in a time and material efficient manner a microfluidic-based multidimensional screening approach was employed.

**Microfluidic-based multidimensional reaction screening.** Inspired by advances in the miniaturization and automation of biological screening, applications of this technology to the realm of chemical synthesis and reaction discovery have been an active field of research in recent years. The development of similar small-scale automated techniques using microfluidic technologies has enabled high-throughput reaction screening using only small quantities of material.[80]

A multidimensional screening workflow[82] was developed based on the use of an automated microfluidics platform (Figure 23).[80] Reactions performed in the microfluidic reactor could be completed in a time-efficient manner and on an analytical scale (2 μmol). Upon recovery from the instrument, the crude reaction

solution was analyzed by UPLC/MS/ELSD to determine each reaction outcome. Reactions affording greater than 20% conversion to a single product were deemed "productive" and suitable for follow-up studies. All productive reactions were repeated using traditional benchtop techniques. Isolation of the products was completed using either silica gel column chromatography or preparative HPLC. Traditional structure elucidation techniques such as NMR, IR, and MS were then used to determine the identity of the reaction product. If the newly discovered transformation was deemed interesting, additional optimization of the reaction was completed.

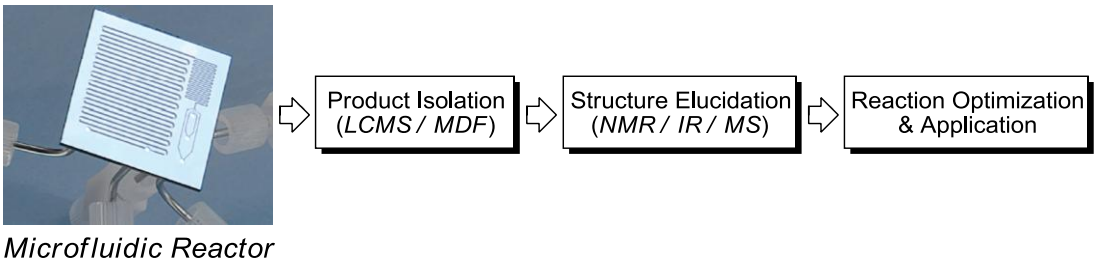


**Figure 23.** Multidimensional reaction screening workflow.[81]

An automated microfluidic reaction screening platform, previously developed at the BU-CMLD, was used for the multidimensional screen.[80] The microfluidic platform consisted of a multi-head syringe pump, liquid handler, a microreactor, and a UV-triggered fraction collector (Figure 24). The platform was controlled using a Trilution® operating system and was capable of combining specified reagents in a sequential format. The liquid handler systematically injected pulses of reactants into a

continuously flowing solvent stream driven by the multi-head syringe pump. The three reagent pulses converged in the microreactor to undergo mixing and become a single reaction pulse. The reactions were quenched upon exiting the reactor with a continuously flowing stream of quenching solution, giving each reaction a finite endpoint. UV triggered collection allowed for the isolation of the most concentrated region of the reaction pulse by setting an acceptable absorbance, thus selectively extracting individual reaction mixtures form the pulse stream.

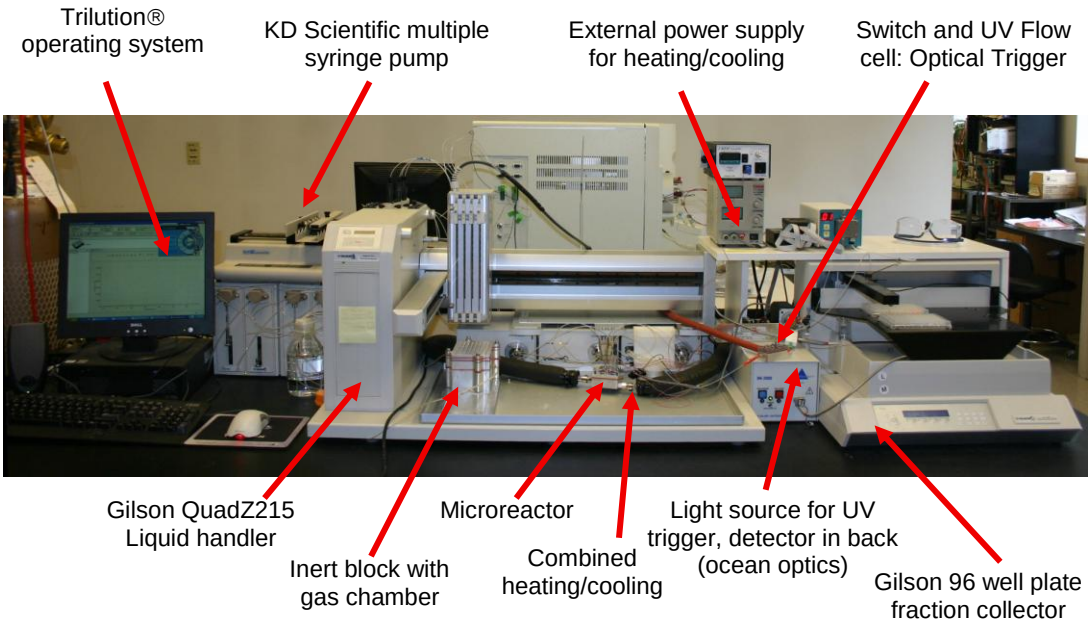


**Figure 24.** Microfluidic reaction screening platform.[80]

**Iminium ether substrate selection.** At the outset, a complex scaffold was sought which could be used to examine iminium ether reactivity. To this end, a small benchtop multidimensional reactivity screen was set systematically reacting five

multifunctional ketones **79**–**83**[80,83] with two hydroxyalkyl azides (2-azido-1-ethanol **77**, 3-azido-1-propanol **78**) and four additives ($BF_3{\cdot}OEt_2$, TfOH, $PPh_3$, *t*-BuOK) (Figure 25). Due to the inherent hydrolytic instability of iminium ethers, upon completion each reaction was hydrolyzed with saturated aqueous $NaHCO_3$ to ease product identification.[78] The outcome of each reaction was determined by LCMS analysis of the crude sample. The majority of reaction attempts resulted in dehydration, decomposition, or no observable reaction. Of these, only bicyclo[3.2.1]octanoid **63** led to an appreciable quantity of novel products.

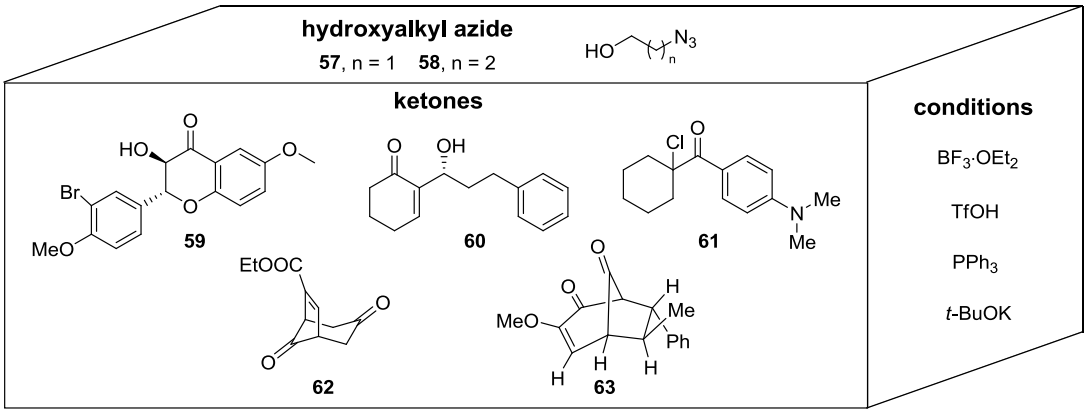


**Figure 25**. Multidimensional screening parameters for substrate selection.

Further investigation of the reaction of bicyclo[3.2.1]octanoid **63** with hydroxyalkyl azides **57** and **58** in the presence of acid revealed three identifiable products, a ketal, an iminium ether, and a lactam (Table 11). In all cases, isolation of ketal was only possible in reactions of 2-azido-1-propanol and $BF_3{\cdot}OEt_2$. All attempts to induce further reaction from the ketal by treatment with strong acid lead only to

recovered starting material. Lactam product was recovered in small quantities from reactions of both $BF_3 \cdot OEt_2$ and TfOH; however, when TfOH was used the iminium ether became the major product but the still contained minor contamination from the lactam. Changing the work-up procedure from saturated aqueous $NaHCO_3$ to a quick deionized water wash afforded the desired iminium ether as the exclusive product in excellent yield.

**Table 11.** Survey of bicyclo[3.2.1]octanoid **63** in reaction with hydroxyalkyl azides.

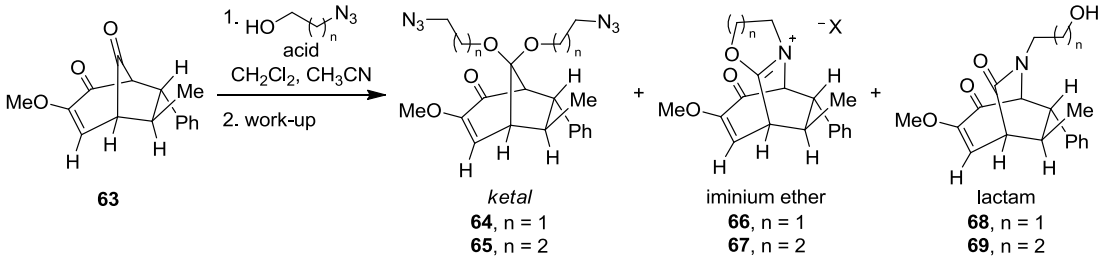


| entry | acid (equiv.) | azide (n) (equiv.) | work-up (aqueous) | ketal (%)[a] | iminium ether (%)[a] | lactam (%)[a,b] |
|---|---|---|---|---|---|---|
| 1 | $BF_3 \cdot OEt_2$ (2.0) | **57** (1.5) | $NaHCO_3$ | 23 | – | – |
| 2 | $BF_3 \cdot OEt_2$ | **57** (1.5) | $NaHCO_3$ | – | – | 13 |
| 3 | $BF_3 \cdot OEt_2$ (2.0) | **57** (excess) | $NaHCO_3$ | 45 | – | 13 |
| 4 | TfOH (1.0) | **57** (1.0) | $NaHCO_3$ | – | – | – |
| 5 | $TiCl_4$ (5.0) | **57** (1.5) | $NaHCO_3$ | – | – | – |
| 6 | $BF_3 \cdot OEt_2$ (2.0) | **58** (1.5) | $NaHCO_3$ | – | – | – |
| 7 | TfOH (3.0) | **58** (1.5) | $NaHCO_3$ | – | 54 | 15 |
| 8 | $BF_3 \cdot OEt_2$ (3.0) | **58** (1.5) | $H_2O$ | – | – | – |
| 9 | TfOH (3.0) | **58** (1.5) | $H_2O$ | – | 87 | – |
| 10 | $HBF_4$ (4.0) | **58** (1.5) | $H_2O$ | – | – | – |

[a]Isolated yield. [b] Isolated as a mixture of regioisomers.

Characterization of the resulting iminium ether and lactam revealed the formation of a mixture of regioisomeric products arising from differential migration

of the carbon centers adjacent to the bridgehead ketone. At this point it was also found that the hydrolytic instability of the iminium ether prevented traditional normal and reverse phase chromatographic purification techniques from being used. Efforts to purify the iminium ethers in this manner led to the recovery of a large percentage of lactam hydrolysis product. In addition, the soft triflate counter ion gave the iminium ether salt an amorphous appearance, thereby preventing purification by recrystallization. Modification of the work-up allowed for isolation of the iminium ether intermediates as a mixture of regioisomers. Ultimately, the iminium ethers derived from **63** were deemed suitably complex substrates for the present study.

**Scheme 10**

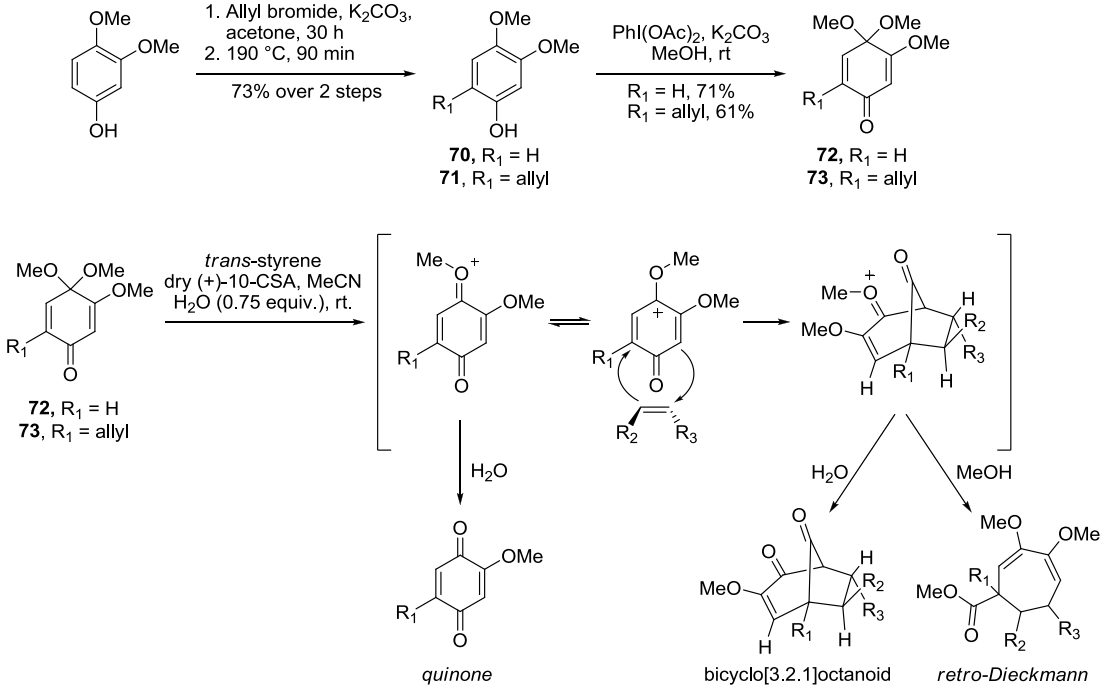

Bicyclo[3.2.1]octanoid **63** was derived from a [5+2] cycloaddition between quinone monoketal **72** and *trans*-β-methylstyrene (Scheme 10).[80,84] Use of this methodology allowed for the synthesis of four additional bicyclo[3.2.1]octanoid ketone scaffolds **74**-**77** (Table 12).

**Table 12.** Bicyclo[3.2.1]octanoid ketone substrates.

| entry | monoketal | alkene | bicyclo[3.2.1]octanoid | product (yield, %)[a] |
|---|---|---|---|---|
| 1 | 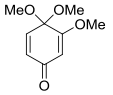 | 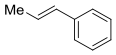 | 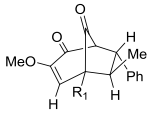 | **63** (50) |
| 2 | 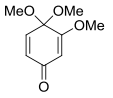 |  | 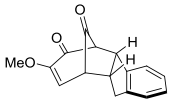 | **74** (38) |
| 3 | 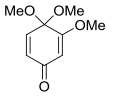 | 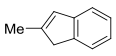 | 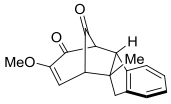 | **75** (75) |
| 4 | 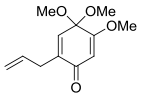 |  | 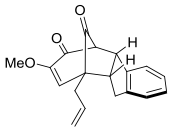 | **76** (54) |
| 5 | 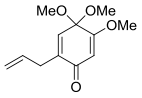 | 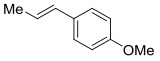 | 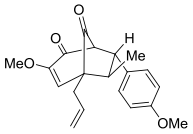 | **77** (56) |

[a]Isolated yield.[80]

All bicycles were synthesized starting from 3,4-dimethoxyphenol. Direct oxidation with phenyl iododiacetate afforded the quinone monoketal. In cases where $R_1$ of the bicyclo[3.2.1]octanoids is equal to allyl, the allyl group was installed prior to oxidation through a sequence of phenolic *O*-allylation followed by Claisen rearrangement. An acid-catalyzed [5+2] cycloaddition was then used to couple the

quinone monoketals with various styrenes. This reaction yielded three major products, the ratio of which depended on the concentration of water within the solution. An excess or shortage of water within the reaction afforded either a quinone or a 7-membered cyclic diene as the major product, respectively. Using the optimized amount of water (0.75 equiv.), bicyclo[3.2.1]octanoids were isolated as the major component of the product mixture (Table 12).[80] Each of the five bicyclo[3.2.1]octanoid scaffolds was then evaluated for its performance in the azido-Schmidt reaction with 3-azido-1-propanol (Table 13).

**Table 13.** Bicyclo[3.2.1]octanoid ketones in the azido-Schmidt reaction.

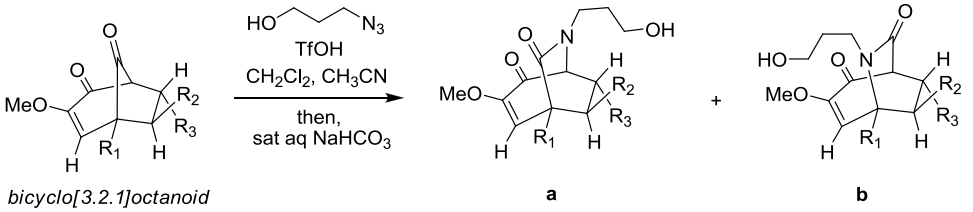


*bicyclo[3.2.1]octanoid* **a** **b**

| entry | $R_1$ | bicyclo[3.2.1]octanoid | product (yield %)[a] | **a:b** ratio[b] |
|---|---|---|---|---|
| 1 | H | **63** | **69** (88) | 3:1 |
| 2 | H | **74** | **78** (49) | 2:1 |
| 3 | H | **75** | **79** (40) | 2:1 |
| 4 | allyl | **76** | **80** (–) | – |
| 5 | allyl | **77** | **81** (–) | – |

[a]Isolated yield of regioisomeric mixture. [b]Ratio estimated by crude $^1$H NMR

Bicyclo[3.2.1]octanoid scaffolds bearing an allyl group in the $R_1$ position failed to react under typical azido-Schmidt conditions (Table 13, entries 4 and 5). However, when $R_1$ was hydrogen a mixture of regioisomeric lactams was isolated (Table 13, entries 1-3).[80] Substrate **63**, synthesized from *trans-β*-methylstyrene, gave

both the greatest overall yield (88%) and the best regioselectivity (3:1) in this study. Therefore, substrate **63** was chosen as the scaffold for multidimensional screening studies and additional optimization.

**Table 14.** Acid survey of bicyclo[3.2.1]octanoid **63** in the azido-Schmidt reaction.

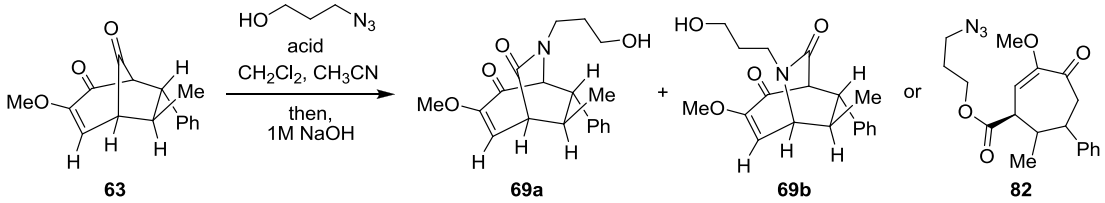


| entry | acid | equiv. | outcome | product (conversion %) |
|---|---|---|---|---|
| 1 | $Sc(OTf)_3$ | 0.20 | ester | **82** (94)[a] |
| 2 | $La(OTf)_3$ | 0.20 | no reaction | – |
| 3 | $Zn(OTf)_2$ | 0.20 | no reaction | – |
| 4 | $Yb(OTf)_3/PhCO_2H$ | 0.02/1.0 | no reaction | – |
| 5 | $La(OTf)_3/PhCO_2H$ | 0.02/1.0 | no reaction | – |
| 6 | $Zn(OTf)_2/PhCO_2H$ | 0.02/1.0 | no reaction | – |
| 7 | PTSA | 3.0 | no reaction | – |
| 8 | CSA (+) | 3.0 | no reaction | – |
| 9 | TFA | 3.0 | no reaction | – |
| 10 | $BF_3 \cdot OEt_2$ | 3.0 | lactam | **69a,b** (trace) |
| 11 | $HBF_4$ | 3.0 | lactam | **69a,b** (trace) |
| 12 | $Tf_2NH_2$ | 3.0 | lactam | **69a,b** (51)[b] |
| 13 | TMSOTf | 3.0 | lactam | **69a,b** (65)[b] |
| 14 | TfOH | 3.0 | lactam | **69a,b** (100)[b] |

[a]Isolated yield. [b]Estimated conversion by UPLC.

The azido-Schmidt reaction of **63** was further explored to determine the effect of the acid promoter, hydroxyalkyl azide, solvent, and temperature on the yield and regioselectivity of the transformation. A series of protic, Brønsted, lanthanide, and mixed acid conditions were examined (Table 14). Of the acids tested, only those in

which triflic acid was present or produced gave significant amounts of product; triflic acid itself afforded full conversion. The majority of acids investigated gave no observable reaction and resulted in the recovery of the starting bicyclic ketone. Interestingly, despite previous reports of $Sc(OTf)_3$ use as a promoter in the azido-Schmidt reaction, the only product isolated from this reaction was the retro-Dieckmann azidoester **82**. Notably, none of the remaining lanthanides used in the study gave either of these products.

**Table 15.** Condition survey for the azido-Schmidt reaction bicyclo[3.2.1]octanoid **63**.

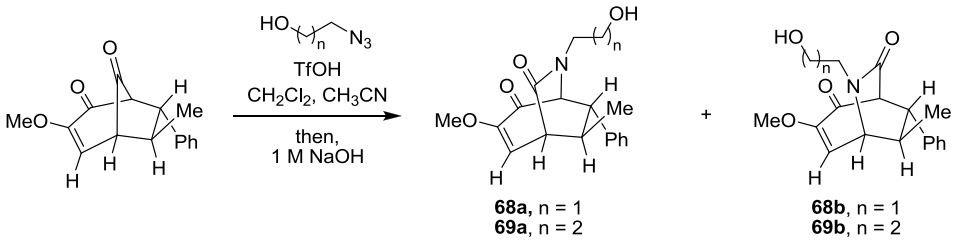


| entry | azide (n) | solvent | temp. (ºC) | time (h.) | **a:b** ratio[a] |
|---|---|---|---|---|---|
| 1 | 1 | $CH_3CN$ | -20 | 7 | 6.5:1[b] |
| 2 | 1 | $CH_3CN$ | -20 | 12 | 7.3:1 |
| 3 | 1 | (1:1) $CH_3CN$:$CH_2Cl_2$ | -20 | 7 | 5.9:1[b] |
| 4 | 1 | (1:1) $CH_3CN$:$CH_2Cl_2$ | -20 | 12 | 7.6:1 |
| 5 | 1 | $CH_2Cl_2$ | -20 | 7 | 6.7:1[b] |
| 6 | 1 | $CH_2Cl_2$ | -20 | 12 | 7.6:1 |
| 7 | 1 | $CH_3CN$ | 0 → rt | 12 | 6.1:1 |
| 8 | 1 | (1:1) $CH_3CN$:$CH_2Cl_2$ | 0 → rt | 12 | 5.8:1 |
| 9 | 1 | $CH_2Cl_2$ | 0 → rt | 12 | 4.8:1 |
| 10 | 2 | $CH_3CN$ | -20 | 12 | 2.8:1 |
| 11 | 2 | (1:1) $CH_3CN$:$CH_2Cl_2$ | -20 | 12 | 3.1:1 |
| 12 | 2 | $CH_2Cl_2$ | -20 | 12 | 3.2:1 |
| 13 | 2 | $CH_3CN$ | 0 → rt | 12 | 2.4:1 |
| 14 | 2 | (1:1) $CH_3CN$:$CH_2Cl_2$ | 0 → rt | 12 | 2.2:1 |
| 15 | 2 | $CH_2Cl_2$ | 0 → rt | 12 | 3.1:1 |

[a]Regioisomeric ratio based on crude $^1$H NMR. [b]Full conversion was not obtained.

Next, the effects of hydroxylalkyl azide, solvent, and temperature on the regioselectivity of the reaction were investigated (Table 15). A marked increase in regioselectivity was observed when 2-azido-1-ethanol was substituted for 3-azido-1-propanol. The regioselectivity also showed significant temperature dependence when 2-azido-1-ethanol was employed. Conversely, this effect was not observed in reactions using 3-azido-1-propanol. Changes in solvent appeared to have little effect on the regioselectivity.

**Scheme 11**

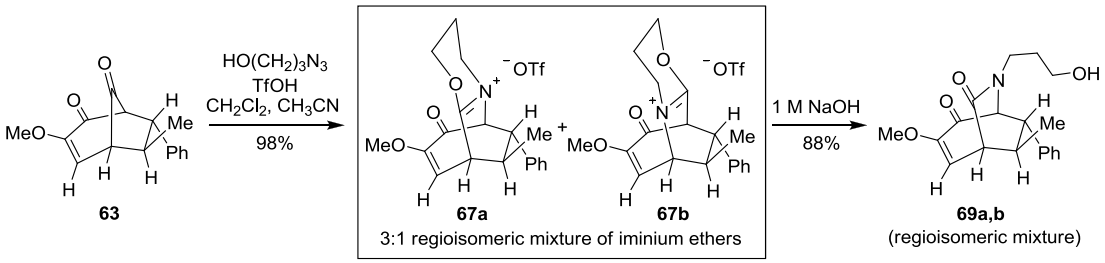


Iminium ethers **67a** and **67b** were obtained as a 3:1 mixture of regioisomers by carrying out the hydroxyalkyl azide addition step according to the conditions noted above (Table 15, entry 15) followed by a water wash (Scheme 11). It was previously reported that some iminium ethers can be purified by column chromatography, but the compounds under investigation proved unstable to silica gel chromatography. Therefore, the regioisomeric mixture of **67a/67b** was used without further purification in multidimensional screening experiments. The regioisomeric ratio was determined by spectroscopic analysis and by its conversion to **69a/69b** upon

treatment with mild aqueous base (Scheme 11). In all but a few cases, the products from the **67a**/**67b** mixture were separable by silica gel chromatography. In contrast, the iminium ethers arising from the reaction of **63** and 2-azido-1-ethanol (Table 15, entry 1-9) proved unstable when isolated and were not further used in the study.

Previous work has shown that the regiochemical outcome of ring expansion reactions of hydroxyalkyl azides and α-substituted cyclic ketones is dependent both on the influence of the steric environment and the electronic nature of the migrating centers.[85] Thus, while reactions of methyl and ethyl α-substituted ketones were generally nonselective, migration of the more highly substituted carbon was favored when bulkier substituents were used. In contrast, when inductively electron-withdrawing substituents were placed α to the ketone, selective (up to 9:1) migration was observed for the less-substituted carbon. However, there are no obvious steric differences in the two potentially migrating carbons of bicyclo[3.2.1]octanoid (**63**), leaving open the question of what forces are responsible for the modest but systematic regioselectivity of its reactions with hydroxyalkyl azides. Assuming antiperiplanar migration relative to the $N_2^+$ leaving group, two mechanistic scenarios arising from the intermediate oxonium ion are possible (Figure 26). Thus, addition of azide can occur from either face of the oxonium ion species (paths a and b as depicted), in each case leading to a mixture of *N*-diazoniumoxazinane intermediates.

In this scenario, it is conceivable that path a would be favored due to the presence of steric interactions arising from the methyl group in path b. Prior reports suggest that azide adducts formed in this way can equilibrate via chair–chair

interconversion prior to loss of $N_2$ and formation of the iminium ether[85] at which point the reaction trajectory is determined and regiochemistry is fully established. Given the relatively low energy differences leading to **69a** over **69b** and lack of obvious preference between the two chair forms of the oxazinanes shown to the left of the diagram in Figure 26, it was not possible to speculate further on the cause of the preference for **69a**.

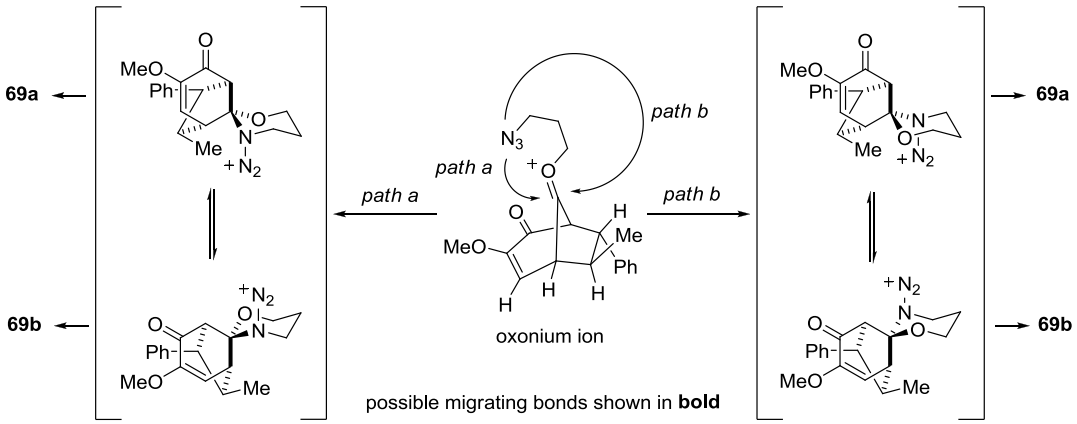


**Figure 26**. Regioselectivity analysis for the reaction of bicyclo[3.2.1]octanoids.

The proficiency of these multifunctional iminium ethers in ring-opening screens was validated by treatment of **67a,b** with nucleophilic reagents previously shown to react with 5,7-bicyclic iminium ethers (Table 16). Products resulting from reactions at both the cationic center (path a) and the *O*-alkyl portion of the iminium ether (path b) were observed in accordance with previously reported examples.[78]

**Table 16.** Heteroatom nucleophile addition to iminium ethers **67a,b**.

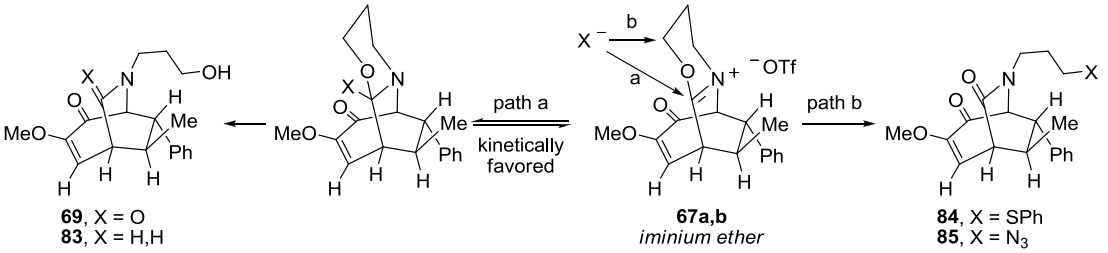


| entry | reagent | X | path | product | yield (%)[a] |
|---|---|---|---|---|---|
| 1 | sat. aq. $NaHCO_3$ | –O | a | **69** | 89 |
| 2 | $NaBH_4$ | –H,H | a | **83** | 59[b] |
| 3 | NaSPh | –SPh | b | **84** | 62 |
| 4 | $NaN_3$ | $–N_3$ | b | **85** | 70 |

[a]Isolated yield corresponds to major regioisomer. [b]Enone reduced to allylic alcohol.

Iminium ether **87** was also selected for screening and prepared according to the previously reported protocol (Scheme 12).[78] This compound was selected based on its simplicity, similarity to previously studied examples,[78] and the presence of a phenyl substituent, which provided a chromophore to aid in product detection and analysis. As usual, this iminium ether could be subjected to base hydrolysis to afford lactam **88**.

**Scheme 12**

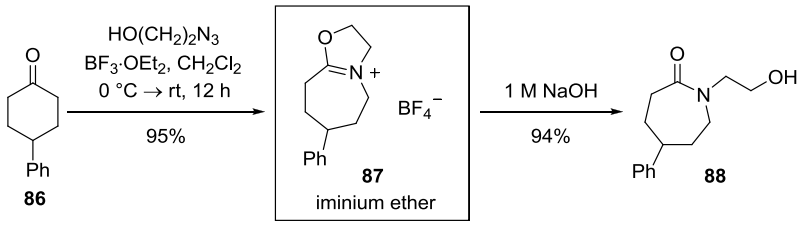

**Multidimensional screening of iminium ether substrates.** Using the microfluidic-based multidimensional screening platform depicted in Figure 24,[80] scaffolds **67a**,**b** and **87** were evaluated using 23 nucleophilic reaction partners and two non-nucleophilic bases (Figure 27).

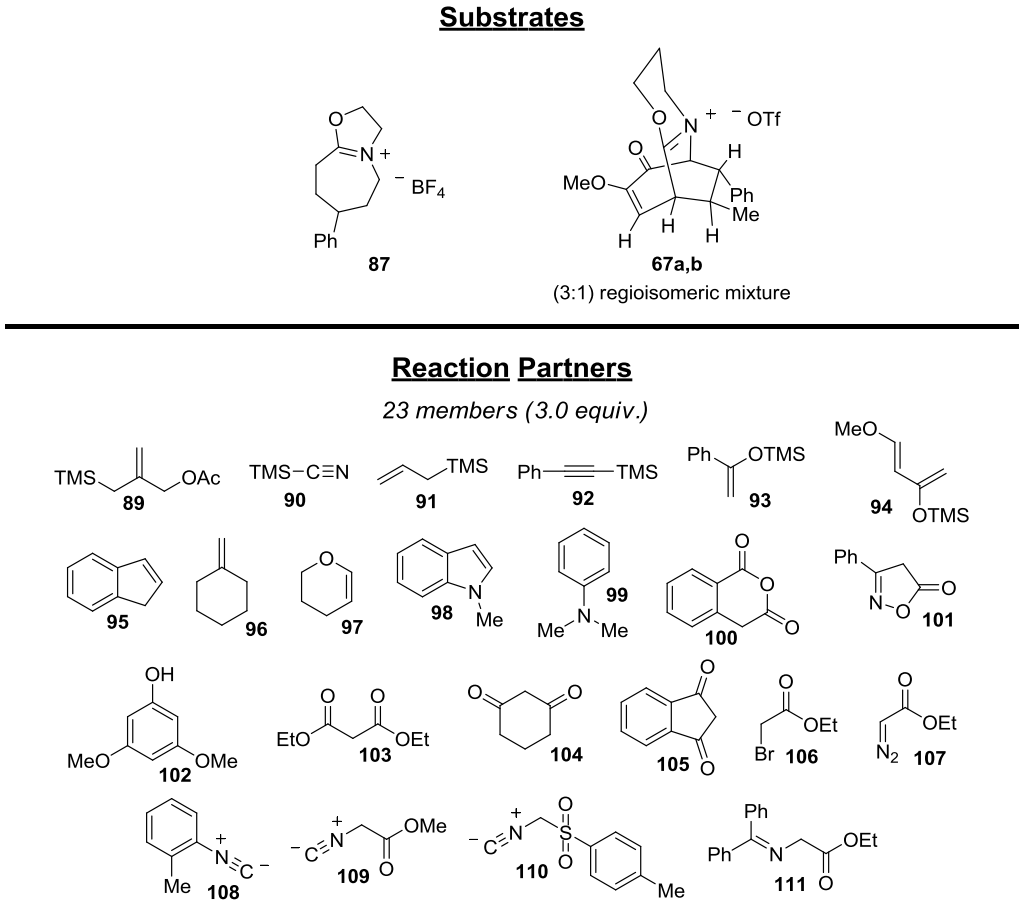


**Figure 27**. Multidimensional reaction screening substrates, partners, and conditions.

Reaction partners were chosen for their potential to participate in both condensations and cycloadditions. Since there are only a few examples of carbon-carbon bond-forming reactions of iminium ethers, particular attention was focused on the expansion of carbon-based nucleophilic reaction partners. The reactions were screened under neutral conditions as well as in the presence of non-nucleophilic bases *N,N*-diisopropylethylamine (DIEA, $pK_a$ = 9.5) and 1,8-diazabicyclo[5.4.0]-undec-7-ene (DBU, $pK_a$ = 12) in order to generate reactive nucleophilic species.

Reactions completed in the microfluidic system were performed using 2 μmol (ca. 1 mg of **67** or 0.6 mg of **87**) of substrate with 3.0 equiv. of reaction partner and 3.0 equiv. of base (if used). Reagents were prepared as stock solutions in dimethyl sulfoxide (ca. 0.25 M for **67** and **87**, 0.75 M for reaction partners and bases) with minimal exposure to air and stored in oven-dried glass sleeves housed in the inert reagent storage block. Each reaction used 8 μL from each desired stock solution for a total reaction volume of 24 μL (reaction concentration 1.75 M). Flow rates for the system were set at either 4.5 μL/min or 1.2 μL/min to achieve reaction times of 5 min or 20 min, respectively.

To ensure comparable reaction times for each addition, reactions were quenched by the addition of water (excess) prior to exiting the microreactor. The resulting solutions were analyzed in 96 well-plates without further treatment using UPLC/MS/ELSD (Figure 28).[86]

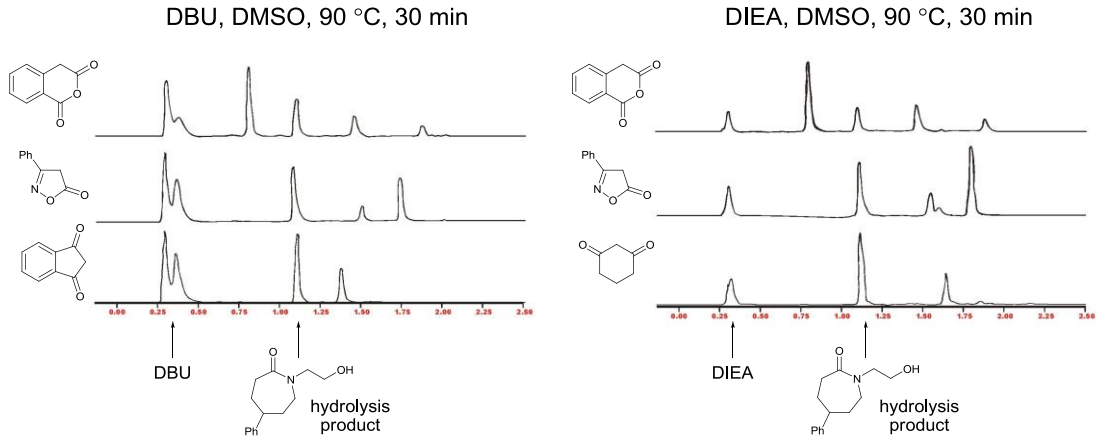


**Figure 28**. Representative UPLC/ELSD traces of crude screening products.

Previous reports showed that nucleophilic additions to iminium ethers, such as those attempted within this screen, may require longer reaction times than may be achieved using the microfluidic platform.[78] To ensure that no productive reactions were overlooked due to insufficient reaction time, reactions were also completed under similar conditions using capped glass sleeves in an orbital shaker. After 24 hours the reactions were quenched with excess water, transferred to 96 well plates, and analyzed by UPLC/MS/ELSD.

In general, the reactions performed at 90 ºC were far more productive than those performed at 30 ºC (Table 17). After eliminating the redundant positive results across the three condition sets, five reaction partners were identified with positive outcomes for iminium ether **87** and ten reaction partners were identified for iminium ether **67**. These reactions were subsequently scaled up, the products were isolated and structures elucidated using traditional bench methods. For comparison purposes, the

scale-up reactions of both **87** and **67** were carried out on all of the reaction partners that were found to be productive in the initial screens. Additionally, scale-up reactions were carried out in acetonitrile instead of dimethyl sulfoxide to increase the ease of product isolation and overall yield. *N*,*N*-Diisopropylethylamine was selected as the only base for the scale-up studies, since 1,8-diazabicyclo[5.4.0]undec-7-ene was found to react with the iminium ether substrates which led to adduct formation and results from the original screen suggested this switch would not greatly influence the outcome of the reactions.

**Table 17**. Productive reactions tabulated from the crude UPLC/ELSD analysis.

| iminium | | | microfluidics[a] | | orbital shaker[a] |
|---|---|---|---|---|---|
| entry | ether | base | 5 min, 30 ºC | 30 min, 90 ºC | 24 h, 90 ºC |
| 1 | **87** | blank | – | 1 | 1 |
| 2 | **87** | DIEA | 2 | 3 | 3 |
| 3 | **87** | DBU | 2 | 3 | 3 |
| 4 | **67a**,**b** | blank | – | – | 1 |
| 5 | **67a**,**b** | DIEA | – | 7 | 5 |
| 6 | **67a**,**b** | DBU | – | 7 | 5 |

[a]All positive reactions shown. Redundant results are not excluded.

**Iminium ether reaction discovery products and mechanisms.** All products isolated from the scale-up process were the result of nucleophilic addition to the iminium ethers at the position adjacent to the imine center, distal to the nitrogen (Tables 18 and 19) *via* path b (Table 16). The preference for product formation *via* one path over another, as mentioned earlier, is dependent upon several reaction variables, including nucleophile size and the nature of the anion-stabilizing group.[78]

Since all of the reaction partners used in this study were larger than those previously observed to result in path a products, it was not surprising that the observed outcome was the less hindered mode of addition.[78]

**Table 18.** Products resulting from reaction with iminium ether **87**.

| entry | nucleophile | product[a] | yield (%) | entry | nucleophile | product[a] | yield (%) |
|---|---|---|---|---|---|---|---|
| 1 | 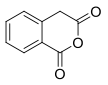 **100** | 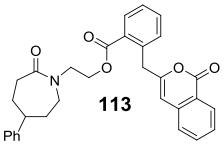 **113** | 43 | 6 | 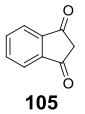 **105** | 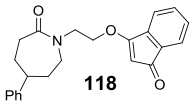 **118** | 25 |
| 2 |  **101** | 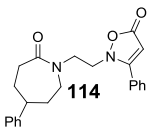 **114** | 87 | 7 |  **106** | 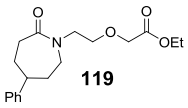 **119** | 7 |
| 3 | 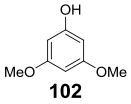 **102** | 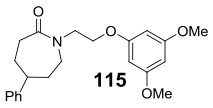 **115** | 29 | 8 |  **107** | 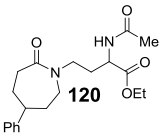 **120** | 13[c] |
| 4 | 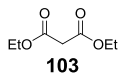 **103** | 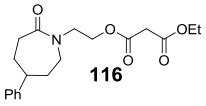 **116** | 23 | 9 | 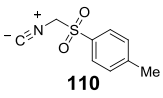 **110** | 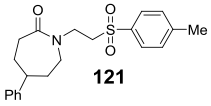 **121** | 40 |
| 5 |  **104** | 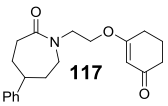 **117** | 58 | 10 |  **112** | 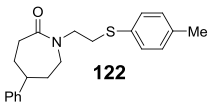 **122** | 94[b] |

[a]Reaction Conditions: Nucleophile (3.0 equiv.), DIEA (3.0 equiv.), MeCN, 80 °C, 24h. [b]Reaction conditions: Nucleophile (3.0 equiv.), KH (3.0 equiv.), DMF, 80 °C, 24h. [c]Reaction Conditions: Nucleophile (3.0 equiv.), MeCN, 80 °C, 24 h.

Previous cases involving the addition of carbon nucleophiles to iminium ethers included the use of pre-formed sodium salts of stabilized carbon species.[78] In these instances, elimination followed the initial reversible addition *via* path a to provide products irreversibly. Since the reaction partners employed in this screen

were not used as stabilized anions, and the basic additives may not have been capable of inducing the irreversible elimination required to stabilize the products resulting from path a. Even if products derived from other pathways were formed, they were neither observed nor isolated.

**Table 19.** Products resulting from reaction with iminium ethers **67a,b**.

| entry | nucleophile | product[a] | yield (%)[b] | entry | nucleophile | product[a] | yield (%)[b] |
|---|---|---|---|---|---|---|---|
| 1 | 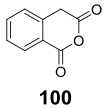 **100** | 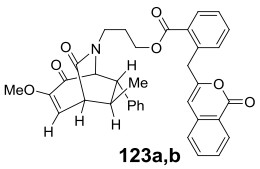 **123a,b** | 25[c] | 4 | 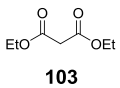 **103** | 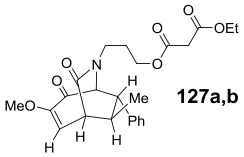 **127a,b** | 21[c] |
| 2 |  **101** | 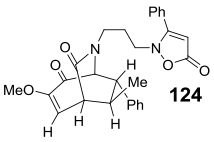 **124** | 26 | 5 |  **104** | 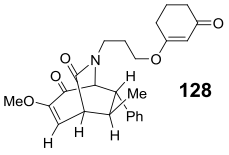 **128** | 58 |
| | | 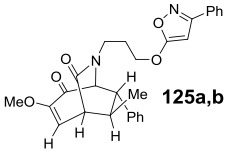 **125a,b** | 28[c] | 6 |  **106** | 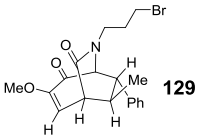 **129** | 64 |
| 3 | 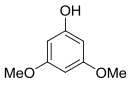 **102** | 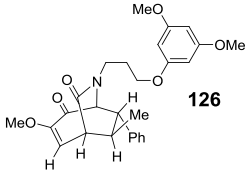 **126** | 57 | 7 | 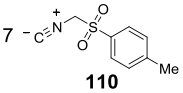 **110** | 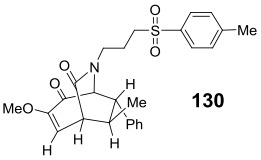 **130** | 48 |

[a]Reaction Conditions: Nucleophile (3.0 equiv.), DIEA (3.0 equiv.), MeCN, 80 °C, 24h. [b]Isolated yield corresponding to single major regioisomer. [c]Isolated yield corresponding to a mixture of regioisomers. Only major regioisomer is shown.

Products resulting from enolate formation frequently favored *O*-alkylation, including compounds **113**, **116**, **117**, and **118** originating from substrate **87**, as well as

compounds **123**, **125**, **127** and **128** derived from substrate **67a,b**. This type of addition was described above in the case where dimethylmalonate sodium salt was used as the nucleophile (Table 10, entry 9).[78] Interestingly, the reaction between 3-phenyl-5-isoxazolone **101** and substrate **87** gave exclusive *N*-alkylation whereas the reaction with substrate **67a,b** produced a mixture (approx. 1:1) of both *N*-alkylation (**124**) and *O*-alkylation (**125**) products. The lack of regioselectivity may have been a result of the increased steric bulk present in **67a,b** as compared to the relatively unhindered **87**.

Esters **113** and **123** may also be derived from a form of *O*-alkylation on the iminium ether which was preceded by the pseudo-dimerization of homophthalic anhydride to first produce acid **131** (Scheme 13).

**Scheme 13**

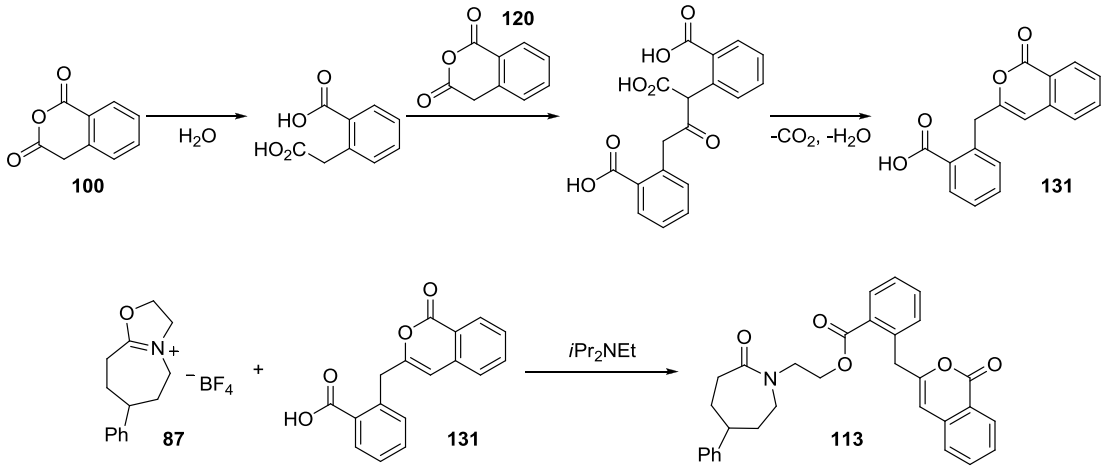


Similar dimerization processes, where one or both of the anhydride molecules were replaced by the corresponding free acid, have been previously reported.[87] Since

this process is only catalytic in water, a trace amount of water would be sufficient to initiate the dimerization of this reaction partner. Once dimerization is complete, the resulting acid may then open the iminium ether under the basic reaction conditions to provide the observed products. An alternative mechanism may also be feasible in which the homophthalic anhydride first opens the iminium ether, then subsequent dimerization and hydrolysis occurs upon work-up. Further mechanistic investigation would be required to differentiate between these two possibilities.

Treatment of the densely functionalized iminium ether **67** with ethyl bromoacetate **106** afforded a ring-opened alkyl bromide **129**. The synthesis of **129** is likely the result of bromide addition via path b. Formation of a bromide anion under the reaction conditions could be attributed to the long reaction times and higher temperatures under which these reactions were completed. Such conditions may induce displacement or elimination of bromide anion, which may then re-add to the iminium ether to give the observed $\gamma$-bromolactam. Interestingly, when iminium ether **107** was treated with ethyl bromoacetate **106** under the same conditions, the same reactivity was not observed. In this case, the only product isolated was lactam **119**, albeit in low yield. Lactam **119** may arise from initial iminium ether hydrolysis followed by displacement of $\alpha$-halogenated **106**. It is unclear as to why ethyl bromoacetate gave bromination in decent yield upon reaction with **67**, yet gave little to no reaction with **107**. In this instance, the stabilizing ability of the counter ion may have a notable influence on the reaction. The formation of **87** as a tetrafluoroborate salt imparts greater stability to the complex as compared to the triflate salt of **67**.

Attempts made to exchange the triflate anion of **67** for the tetrafluoroborate anion were unsuccessful.

**Scheme 14**

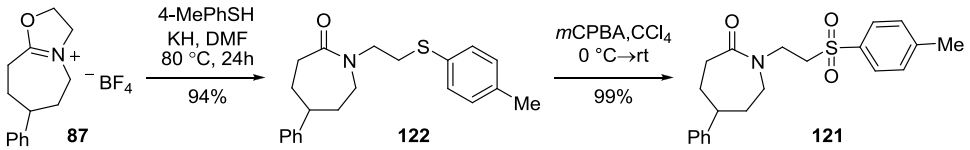


Reactions using isonitrile **110** (TosMIC) afforded lactams **121** and **130** from **87** and **67** respectively (Tables 18 and 19). The structural assignment of **121** was verified by the spectroscopic comparison of the identical product synthesized through an alternative route (Scheme 14). TosMIC (**110**) is commonly used to prepare a variety of heterocycles.[88] Often, in this purpose, *p*-toluenesulfonate (tosyl) **132** serves as a leaving group to enable product aromatization, giving a positive driving force to the overall sequence. In the absence of an adequate cyclization partner, however, decomposition of TosMIC is known to occur.[89] Early reports proposed that the tosyl group may be released by direct substitution of the TosMIC anion.[90] However, more recent studies suggest a more complex decomposition route is responsible for tosyl release.[89a] Rather than direct substitution, solvent participation[89a] or the self-cyclization of TosMIC may result in the release of tosyl (**132**) along with a complex mixture of by-products (Scheme 15). The instability of the resulting by-products, in turn make the isolation and identification of these species difficult.

**Scheme 15**

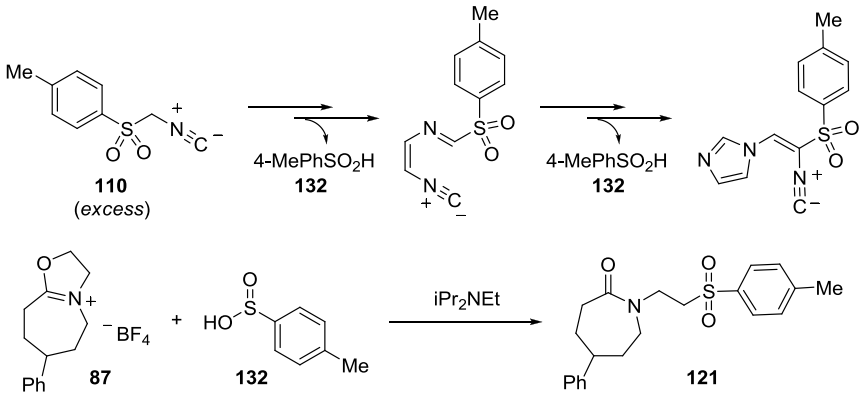


Once free in solution, anion (**132**) may directly add to the electrophilic iminium ethers **87** and **67** to produce sulfones **121** and **130**, respectively. While the stabilized tosyl anion is commonly used in the preparation of sulfones,[89c,90] the reaction of tosyl with an electrophile following ejection from TosMIC was not previously reported.

Ethyl diazoacetate (**107**) was the only reaction partner of the set found to form a new carbon-carbon bond upon addition to the iminium ether, albeit in low yield. Interestingly, the product isolated from the scale-up reaction did not correspond to the product observed in the original screen. This was apparent as the structure obtained from the scale-up study incorporated one equivalent of acetonitrile which was not present in the original reaction screen. Efforts made to reproduce the original reaction in dimethyl sulfoxide were unsuccessful. The proposed mechanism of this transformation involves the initial decomposition of ethyl diazoacetate in the presence of excess acetonitrile to furnish nitrilium ion **133**.[91] Nucleophilic addition of **133** to

iminium ether **87** completes the carbon-carbon bond formation to generate amide **134**. Hydrolysis upon work-up provides the observed product **120** (Scheme 16, Table 18). It is likely that iminium ether **87** solely participated in this reaction due to the presence of residual $BF_3$ contaminating substrate **87** present from the initial iminium ether formation. This residual promoter would not have been present in substrate **67,** which used TfOH in iminium ether formation (Scheme 11).

**Scheme 16**

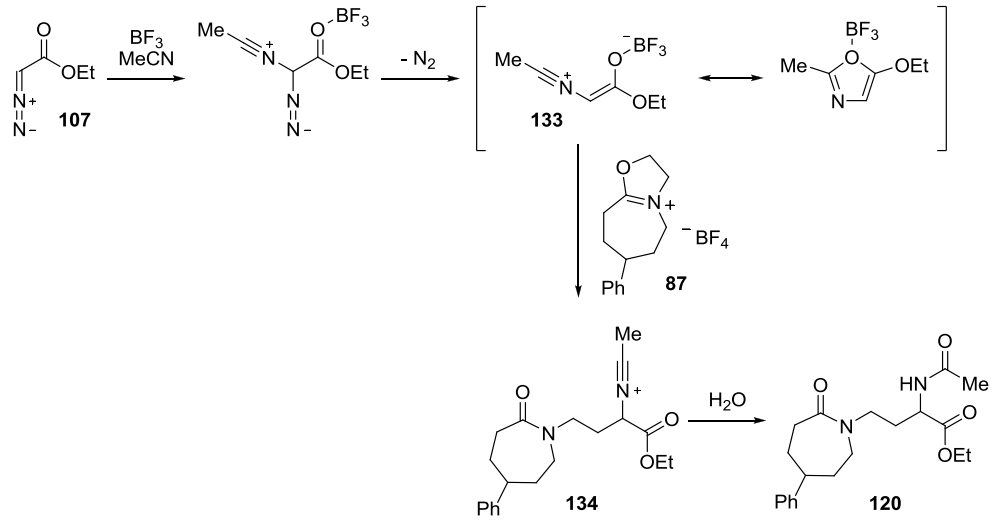


Although reaction partners **97** and **109** were also classified as productive in the original reaction screen, scaled up reactions with these nucleophiles afforded complex mixtures of products which could not be identified or isolated. All attempts to favor successful recovery through modification of the reaction conditions, such as use of alternative solvents, times, and temperatures, were unsuccessful.

**Summary.** This work exemplifies the benefits of using microfluidics technology for the discovery of new reactions of bicyclic iminium ethers. The regioselective addition of various carbon nucleophiles was examined under several reaction conditions in an array format to multidimensionally screen the condition-dependent nature of these transformations. Over 400 reactions were completed and analyzed on an analytical scale resulting in the discovery of both interesting reagent behavior (e.g. homophthalic anhydride *pseudo*-dimerization prior to iminium ether addition) and new reaction products (e.g. sulfone formation from reactions with TosMIC).

## Chapter 5

## Reaction Discovery of Donor-Acceptor Cyclopropanes

Reaction discovery presents an effective means for the development of new synthetic methodologies affording complex chemotypes.[80,82,92] Previous reaction screening efforts utilizing bicyclo[3.2.1]octanoids led to the discovery of a number of diverse scaffolds,[80,92b] some of which were described in the previous chapter.[92a] In this follow-up study, collaboration with the laboratory of Dr. John A. Porco, Jr. at Boston University was continued to explore additional reactivity of the bicyclo[3.2.1]octanoid scaffold. Preliminary reaction screens performed by researchers at Boston University uncovered the synthesis of a densely functionalized donor-acceptor cyclopropane resulting from the photochemical rearrangement of such bicyclic scaffolds. Subjection of the new cyclopropane scaffold to a variety of reaction conditions enabled the discovery of additional rearrangement reactions to access further sets of structurally diverse chemotypes which will be discussed.

**Synthesis and reactivity of donor-acceptor cyclopropanes.** Donor-acceptor (D-A) cyclopropanes possess great potential as versatile building blocks for organic synthesis.[93] Activation of the ring system through the addition of electron-donating or -accepting substituents is often necessary to make these polar processes more favorable. Geminally substituted D-A cyclopropanes are significantly less reactive than vicinally substituted D-A cyclopropanes since the substituents do not act in a

synergistic manner. Vicinally substituted D-A cyclopropanes, on the other hand, are properly substituted for synergistic activation and are highly useful for a number of valuable transformations. Formally, vicinally substituted D-A cyclopropanes behave analogous to a 1,3-dipolar synthon (Figure 29).

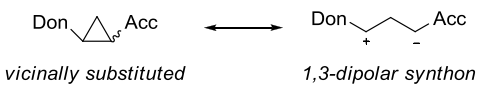


**Figure 29.** Reactivity of vicinally substituted donor-acceptor cyclopropanes.

The formal 1,3-charge relationship in the D-A cyclopropane synthon means that many reactions involving these substrates may be regarded as involving a formal umpolung of reactivity, and therefore afford unique products that are not easily accessible by alternate methods. The majority of D-A cyclopropane reactions utilize carbonyl functionality as the acceptor group whereas the most common donor groups are various forms of oxygen- and nitrogen-based groups. A wide variety of reactions can be derived from these multifunctional substrates to quickly generate diversity and complexity (Figure 30).[93]

Many synthetically useful methods are known for the synthesis of D-A cyclopropanes. The most common syntheses of simple D-A cyclopropanes involve the formal [2+1] cycloaddition of carbenes to alkenes, additions to cyclopropanes, and intramolecular cyclization reactions.[93] These methods are particularly useful for the synthesis of monocyclic D-A cyclopropanes, however low conversion and side reactions may result when more complex substrates are used.

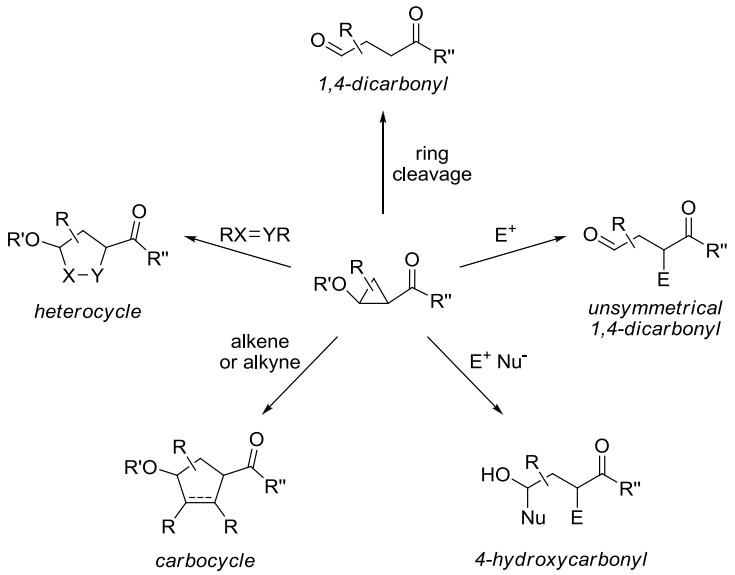


**Figure 30.** Reaction modes of donor-acceptor cyclopropanes.

One mild and highly selective method for the synthesis of D-A cyclopropanes in complex systems is the di-π-methane rearrangement. Generally described, the di-π-methane rearrangement involves the photolysis of substrates containing two π moieties connected to an $sp^3$-hybridized carbon leading to the formation of a π-substituted cyclopropane (Figure 31).[94] The ease of preparation of the di-π substrates in comparison to the cyclopropyl products make this transformation of particular use synthetically. It is often the case that the resulting photoadducts are not accessible through alternative synthetic routes.

Common variants of the di-π-methane rearrangement involve substitution of one alkene for a ketone (oxa-di-π) or imine (aza-di-π). Oxa-di-π transformations result in the formation of α-cyclopropyl carbonyl compounds, like those seen in the D-A cyclopropane scaffolds. Depending on the position of the imine nitrogen, aza-di-

π transformations produce either α-cyclopropyl imines or *N*-cyclopropyl imines. Hydrolysis of the resulting imines can afford α-cyclopropyl carbonyl compounds, as obtained in the oxa-di-π rearrangement, or *N*-cyclopropyl amines, respectively.[94]

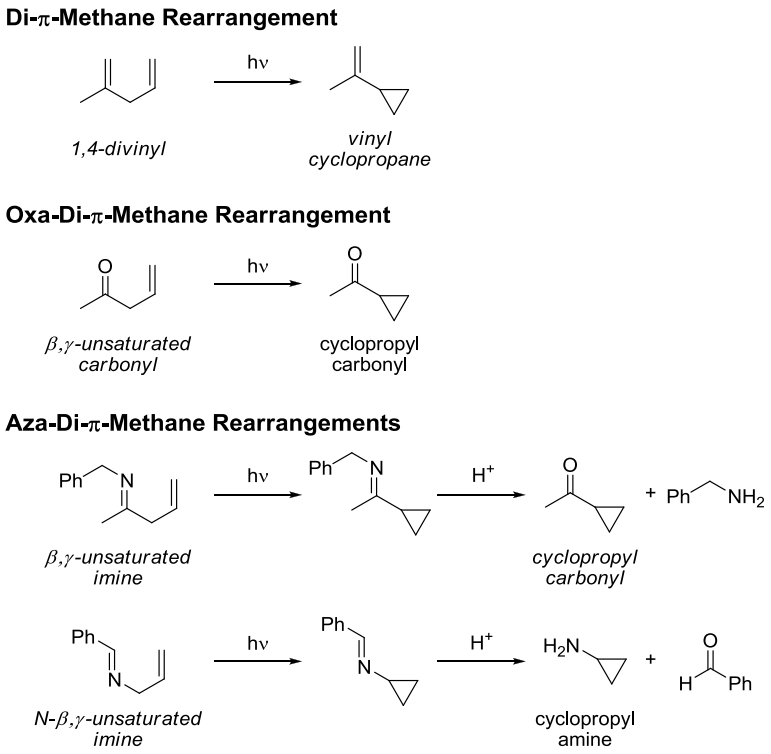


**Figure 31.** Variants of the di-π-methane rearrangement.

Since di-π-methane rearrangements are promoted by photo-excitation, the efficiency of the reaction is enhanced as substrates become increasingly strained (Figure 32). Non-cyclic substrates exhibit low efficiency since the numerous rotational modes are able to dissipate the excitation energy before productive rearrangement can occur. Because of this, substrates whose rotation and vibration are

constrained by a bridged, bicyclic, or polycyclic scaffold exhibit highly efficient and often fast reactivity in the di-π-methane rearrangement to afford extremely complex scaffolds in excellent yields.[94]

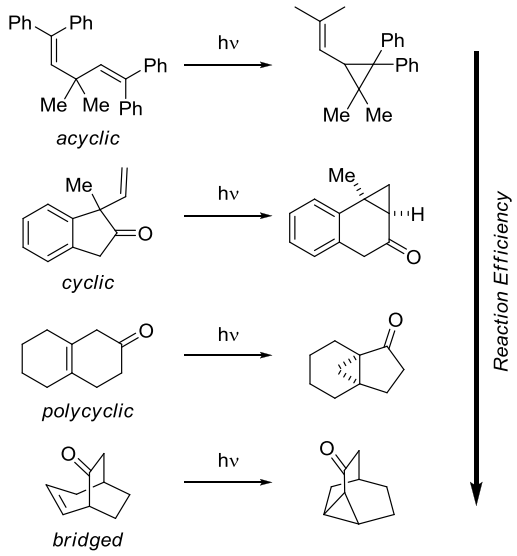


**Figure 32**. Reactivity trends of the di-π-methane rearrangement.

The prearranged β,γ-unsaturated carbonyl and constricted rotation of the bicyclo[3.2.1]octanoid scaffold introduced in the previous chapter,[80] make it a particularly attractive candidate for the oxa-di-π rearrangement. Successful rearrangement of this substrate would provide a highly functionalized polycyclic donor-acceptor scaffold ideal for reaction discovery experiments.

**Oxa-di-π rearrangement of bicyclo[3.2.1]octanoids.** Multidimensional reaction screening of a range of scaffolds was initially completed by researches at

Boston University using a high-throughput photoflow platform (Figure 33). This apparatus was created through modification of the microfluidic platform described in the previous chapter.[80,92a] Various aspects of each photo reaction were investigated in series, including the choice of solvent, sensitizer, and light source.

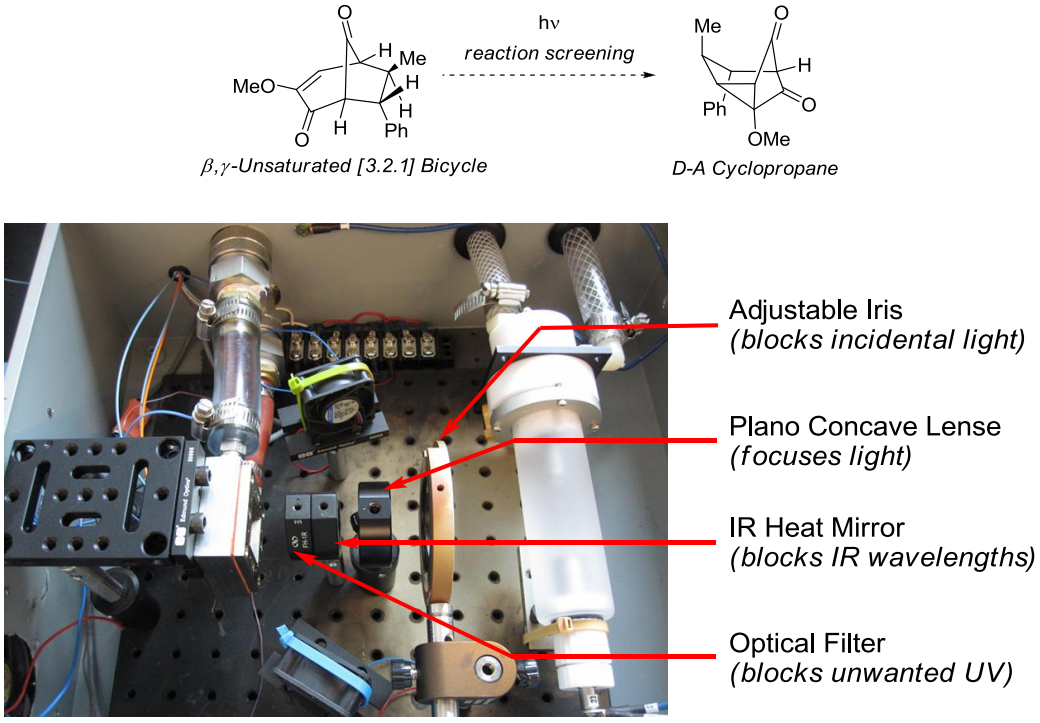


**Figure 33.** Photoflow apparatus used in reaction discovery.[81]

Examination of products resulting from the screen revealed that bicyclo[3.2.1]octanoid scaffold **63** readily underwent an oxa-di-π-methane rearrangement (Scheme 17). UV irradiation of bicyclo[3.2.1]octanoid **63** for four hours, in the absence of a triplet sensitizer, afforded the polycyclic cyclopropane product **155** in quantitative yield. The cleanest versions of this transformation resulted

from reaction in acetonitrile. However, this reaction was also viable in acetone and afforded acceptable yields of the desired product.

**Scheme 17**

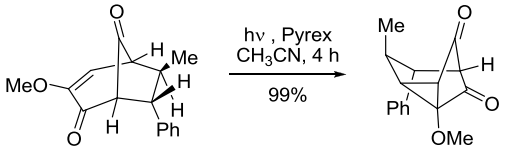


In order to unequivocally assign the structure of the newly formed polycycle, researchers at Boston University further derivatized donor-acceptor cyclopropane **135** using a retro-Dieckmann-type fragmentation.[80] Based on previously reported methodology, cyclopropane **135** was treated with *p*-bromobenzylamine in the presence of base to afford hemiaminal **136** as a crystalline solid (Scheme 18). X-ray crystallographic analysis of the resulting hemiaminal **136** confirmed the expected structure[94] and by analogy the structure of cyclopropane **135**.

**Scheme 18**

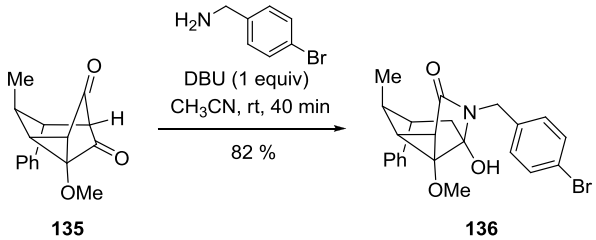

While oxa-di-π-methane rearrangements often require triplet sensitization,[95] in the case of the bicyclo[3.2.1]octanoid scaffolds it is possible that the enone functionality is able to undergo singlet excitation followed by intersystem crossing to achieve the required triplet state. The proposed mechanism of the transformation begins with photo-excitation of either the ketone or the enone to form a diradical (Figure 34). The carbon-based radical then attacks the adjacent unsaturated moiety to form the first bond. From this species, homolytic bond cleavage of the intermediary cyclopropane leads to reformation of the ketone and produces the observed polycyclic cyclopropane product.

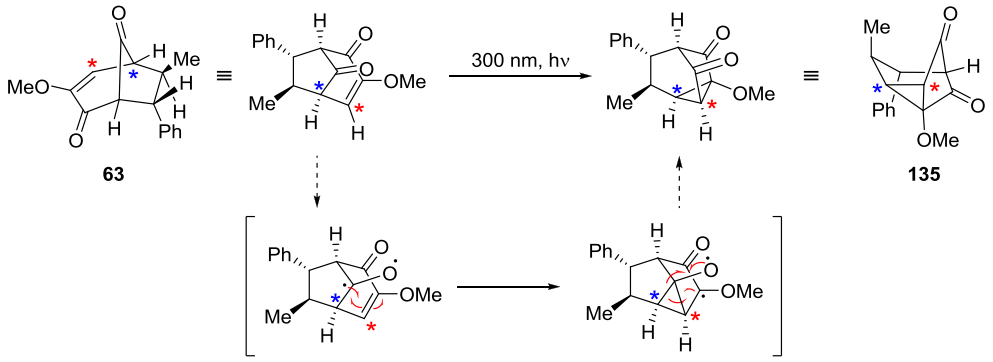


**Figure 34.** Mechanism of the oxa-di-π rearrangement of bicyclo[3.2.1]octanoids.

To evaluate the scope and limitations of the rearrangement analogous reactions were carried out on several bicyclo[3.2.1]octanoid scaffolds. From this study it was found that the oxa-di-π-methane rearrangement was limited to bicyclo[3.2.1]octanoids **63**, **75**, **77**, and **137**, each containing an β,γ-unsaturated ketone (Table 20). Tertiary alcohol 1**38** failed to undergo rearrangement.

Surprisingly, cycloheptenone **139** also failed to react using either direct irradiation or triplet sensitization with benzoquinone.

**Table 20.** Substrate scope of the oxa-di-π rearrangement.

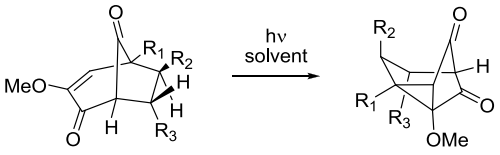


| entry | substrate | ketone | solvent | cyclopropane | product | yield[b] |
|---|---|---|---|---|---|---|
| 1 | 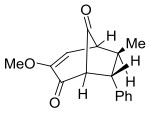 | **63** | MeCN | 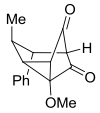 | **135** | 99 |
| 2 | 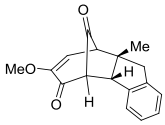 | **75** | acetone | 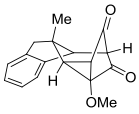 | **140** | 96 |
| 3 | 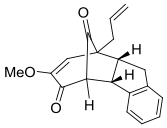 | **137**[a] | acetone | 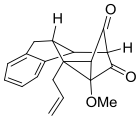 | **141** | 99 |
| 4 | 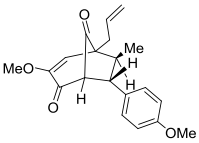 | **77** | acetone | 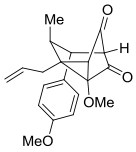 | **142** | 97 |
| 5 | 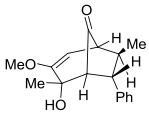 | **138**[a] | benzoquinone | 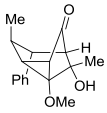 | **143** | 0[c] |
| 6 | 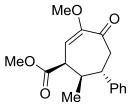 | **139**[a] | benzoquinone | 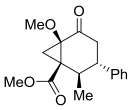 | **144** | 0[c] |

[a]Synthesized using a route analogous to that seen in Scheme 10.[80]
[b]Isolated yield given as percentage. [c]No reaction observed.

With this set of densely functionalized donor-acceptor cyclopropanes readily available, work began to probe the reactivity of these unique scaffolds for reactions leading to new chemotypes. Using the previously observed reactivity of donor-acceptor cyclopropanes as a model, a diverse array of reaction types were investigated including nucleophilic additions, cycloadditions, fragmentations, and rearrangements.

**Grignard reactions of polycyclic donor-acceptor cyclopropanes.** To probe the reactivity of the polycyclic donor-acceptor cyclopropanes in the presence of nucleophiles, cyclopropanes **135** and **141** were subjected to a series of Grignard reactions. Treatment of cyclopropane **135** with methylmagnesium bromide at 0 ºC resulted in facially selective addition of the Grignard reagent to the bridgehead ketone, affording tertiary alcohol **145** (Scheme 19 and Table 21, entry 1). This was in contrast to the similar reaction of the bicyclo[3.2.1]octanoid scaffold **63,** which favored selective addition to the α-methoxy carbonyl affording tertiary alcohol **146**.[80]

**Scheme 19**

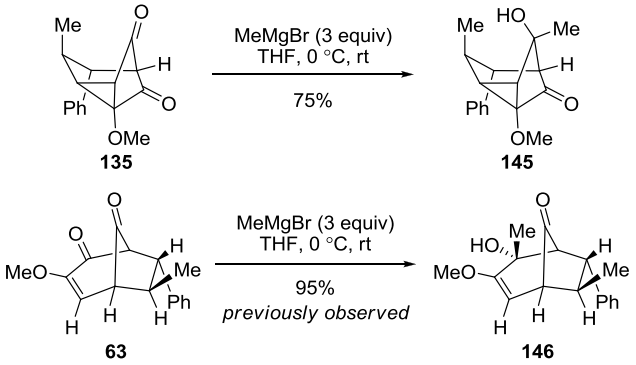


135 145 63 146

Interestingly, when the reaction of cyclopropane **135** and methylmagnesium bromide was warmed to room temperature, further rearrangement occurred to yield dihydrofuran **147** (Table 21, entry 2). A similar rearrangement was observed upon treatment of **135** with the bulkier 3-methoxyphenylmagnesium bromide. Reactions performed with this Grignard reagent at 0 ºC and at room temperature both afforded exclusively dihydrofuran **148** as a single product (Table 21, entry 3).

**Table 21.** Grignard additions of cyclopropane **135**.

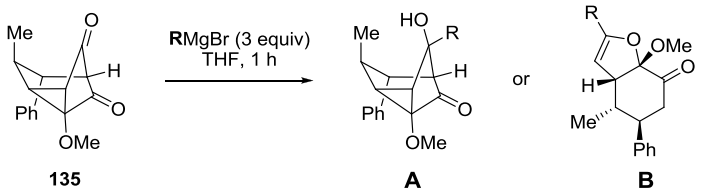


135 A B

| entry | R | temp. | product | **A** (% yield)[a] | **B** (% yield)[a] |
|---|---|---|---|---|---|
| 1 | $CH_3$ | 0 ºC | **145** | 75 | – |
| 2 | $CH_3$ | 0 ºC→rt | **147** | – | 82 |
| 3 | *m*-$OCH_3C_6H_4$ | 0 ºC | **148** | – | 77 |

[a]Isolated yield.

The proposed mechanism of rearrangement to dihydrofuran begins with methyl Grignard addition to the exo-face of the bicyclo[3.2.1]octanoid ketone. At this point, warming of the solution causes a retro-Dieckmann fragmentation to form a fused 3,6-ring system. Rearrangement of the cyclopropane and cyclization completes formation of the dihydrofuran (Figure 35).

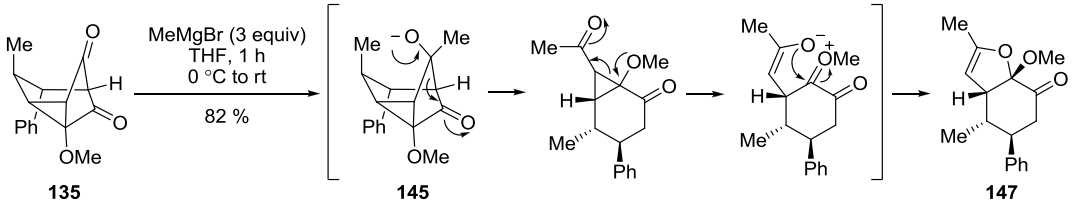


**Figure 35.** Mechanism of Grignard addition and rearrangement of **135**.

Performing similar Grignard reactions using cyclopropane **141** afforded only tertiary alcohols **149** and **150** (Table 22, entries 1 and 2). All efforts to obtain a dihydrofuran product from either cyclopropane **141** or tertiary alcohol **149** using 3-methoxyphenylmagnesium bromide failed to give the desired dihydrofuran. Efforts to favor the rearrangement by warming the reactions to room temperature resulted only in epimerization of the tertiary alcohol (Table 22, entry 3).

**Table 22.** Grignard additions of cyclopropane **141**.

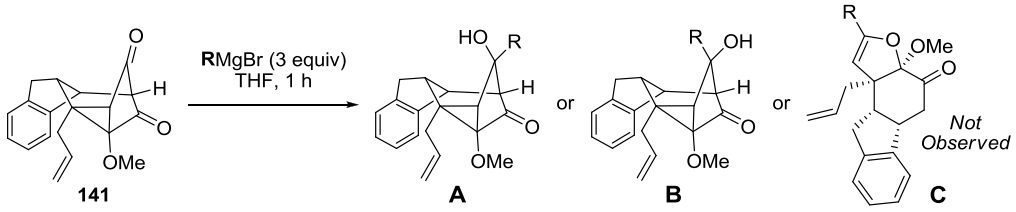


| entry | R | temp. | product | **A** (%)[a] | **B** (%)[a] | **C** (%)[a] |
|---|---|---|---|---|---|---|
| 1 | $CH_3$ | 0 ºC | **149** | 83 | – | – |
| 2 | *m*-$OCH_3C_6H_4$ | 0 ºC | **150** | 82 | – | – |
| 3 | *m*-$OCH_3C_6H_4$ | rt | **151** | – | 88 | – |

[a]Isolated yield.

Applying the same analysis to the reaction of cyclopropane **135,** it is suspected that upon warming the bicyclic scaffold **A** undergoes a retro-Dieckmann fragmentation (Figure 36); however, in this slightly more complex structure, the rate of recyclization to the tertiary alcohol must be greater than the rate of rearrangement to the dihydrofuran. Furthermore, it is suspected that there may be poor orbital alignment between the fragmenting bond for tertiary alcohol **B**, this would make re-fragmentation of alcohol **B** slightly more difficult than alcohol **A** and explain why **B** is ultimately the major product observed.

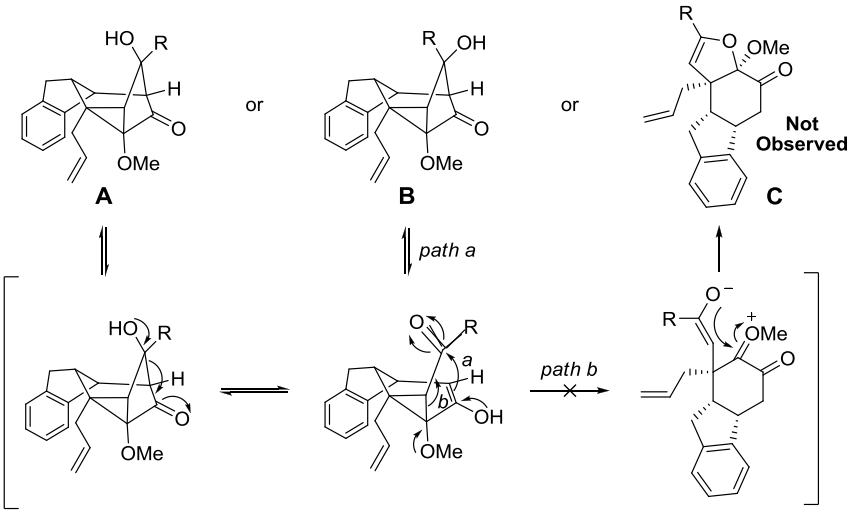


**Figure 36.** Mechanism of rearrangement and epimerization of **141**.

Cyclopropanes **140** and **142** reacted similarly to cyclopropane **141**, suggesting that the greater structural rigidity and functionality in these scaffolds, as compared to cyclopropane **135**, may also hinder rearrangement to the dihydrofuran.

**Azido-Schmidt reactions of polycyclic donor-acceptor cyclopropanes.** To investigate the behavior of donor-acceptor cyclopropanes in the presence of conditions that typically induce rearrangement, tertiary alcohols **145**, **150**, and **151** were subjected to a series of azido-Schmidt reactions.[78,96] Alcohol **145** was combined with 3-azido-1-propanol and the resulting solution was treated with super-stoichiometric amounts of triflic acid. Unexpectedly, bicyclic imide **152** was the lone product isolated from the reaction, albeit in poor yield. Imides had not been previously reported as products from an azido-Schmidt reaction (Scheme 20). To confirm the structure of **152,** the γ-hydroxyl of the imide was derivatized by reaction with *p*-bromobenzoyl chloride in the presence of pyridine to produce the *p*-bromobenzoyl ester **153** (Scheme 20). The structure of **153** was confirmed by X-ray crystallographic analysis. [94]

**Scheme 20**

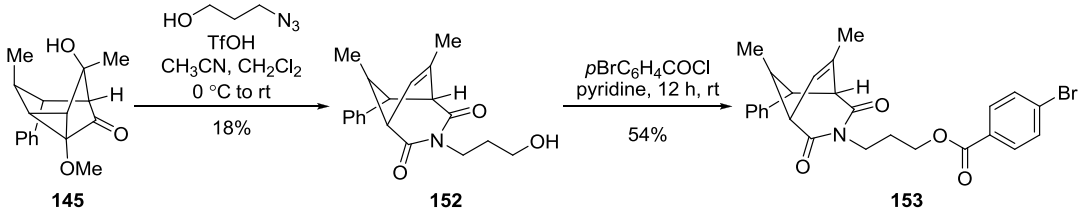


It is proposed that under strong Brønsted acid conditions, a Grob-type fragmentation occurs through the elimination of water leading to the formation of diketone intermediate **155**. Comparable fragmentations have been previously observed for similar ring systems upon treatment with strong acids.[97] A subsequent

azido-Schmidt ring expansion on the intermediary diketone then produces the intermediary iminium ether which, upon work-up with base, affords the corresponding imido alcohol **152** (Figure 37). An attempt was made to verify this mechanism through the isolation of the intermediate diketone or iminium ether but these experiments were ultimately unsuccessful. Treatment of alcohol **145** with triflic acid in the absence of hydroxyalkyl azide led only to the formation of an unidentifiable by-product and not the anticipated diketone.

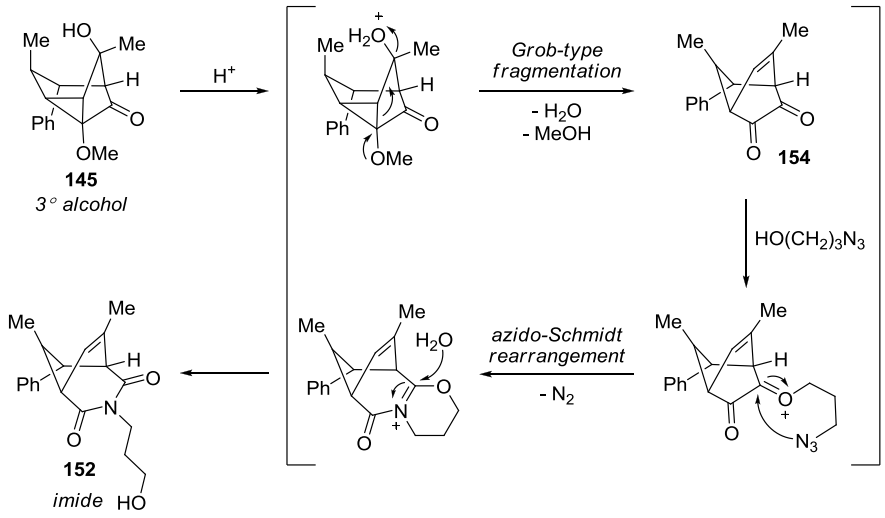


**Figure 37.** Mechanism for the fragmentation and azido-Schmidt reaction of **145**.

An alternative mechanism could be suggested proceeding with the azido-Schmidt reaction first and the Grob-type fragmentation second, however there are two pieces of evidence that contest this order of events. First, as demonstrated above in the Grignard additions, nucleophilic addition to the α-methoxy ketone is hindered such that methylmagnesium bromide adds to the less electrophilic ketone to avoid

interactions upon addition. If a small nucleophile such as methylmagnesium bromide does not add to this center, it is unlikely that the hydroxyalkyl azide would be able to add to this ketone and form the oxonium ion necessary to initiate the Schmidt rearrangement. Second, even if addition of the hydroxyalkyl azide to this hindered ketone were possible, and the Schmidt reaction were to take place, previous study of α-methoxy ketone substrates shows preferential migration of the bond not adjacent to the methoxy group. Therefore, if this mechanism were occurring, the opposite regiochemistry would be expected, resulting in an α-keto amide rather than an imide. Ultimately, however, the possibility of alternative mechanisms cannot be fully discredited in the absence of additional work.

Analogous treatment of alcohols **150** and **151** with 3-azido-1-propanol afforded a mixture of imide **155** and ester **156** in varying ratios (Scheme 21). Upon performing this reaction multiple times it was found that the ratio of imide to ester varied slightly in response to differing work-up conditions.[85,98]

**Scheme 21**

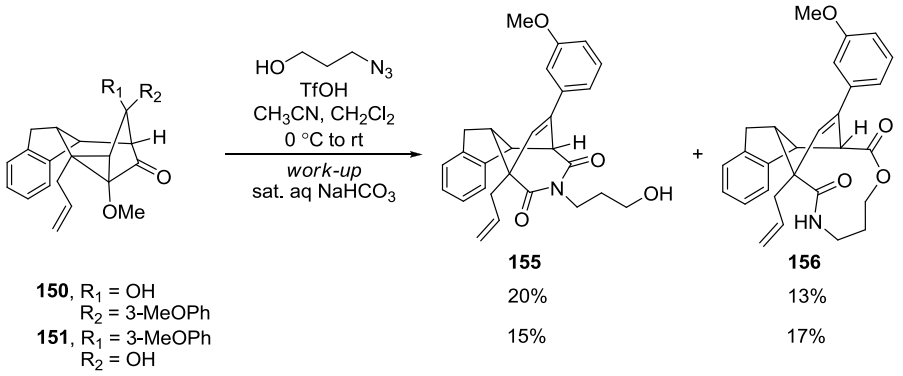


**150**, $R_1$ = OH, $R_2$ = 3-MeOPh
**151**, $R_1$ = 3-MeOPh, $R_2$ = OH

| | **155** | **156** |
|---|---|---|
| | 20% | 13% |
| | 15% | 17% |

Both the imide and ester product can arise from a common iminium ether intermediate (Figure 38). Upon hydrolysis, two routes are available for fragmentation of the aminal. Heterolytic division of the C–O bond (path a) leads to the γ-hydroxy imide product **155**, while heterolytic division of the C–N bond (path b) leads to the ester product **156**. Previous studies of simple iminium ethers described a similar dependence between the nature of the quenching reagent and the preferred mode of iminium ether intermediate ring opening. These studies suggest that the product ratio between **155** and **156** may be ultimately controlled by altering the work-up protocol.[85,98] In addition, the increased skeletal rigidity of carbocycle **166** as compared to carbocycles **150** and **151**, as seen for the Grignard reactivity, may influence the overall strain of the system leading to the observed differences in iminium ether reactivity between alcohols **145**, **150**, and **151**.

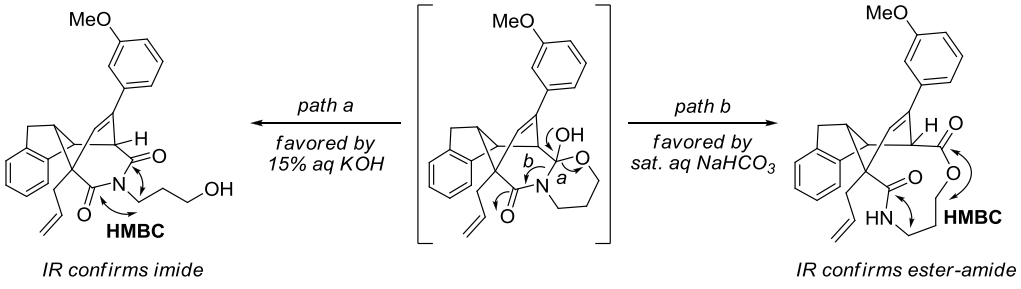


**Figure 38.** Iminium ether expansion pathways.

**Cycloadditions of polycyclic donor-acceptor cyclopropanes.** A number of elegant examples have been reported in the literature of donor-acceptor cyclopropanes undergoing ionization upon treatment with TMSOTf.[99] The resulting

zwitterions are known to participate in cycloaddition reactions in the presence of a wide variety of dipolarophiles. Accordingly, cyclopropane **135** was investigated for reaction with various dipolarophiles upon treatment with TMSOTf (Table 23).

**Table 23.** Cycloadditions of cyclopropane substrates.

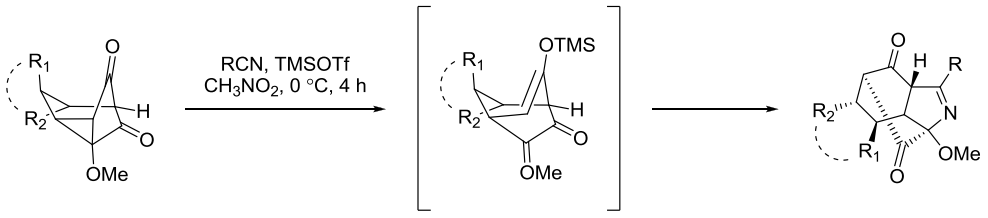


| entry | substrate | dipolarophile | imine | product | yield (%)[a] |
|---|---|---|---|---|---|
| 1 | **135** | Me−CN | 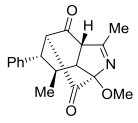 | **157** | 51 |
| 2 | **135** |  | 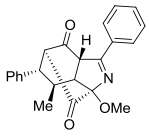 | **158** | 90 |
| 3 | **135** | 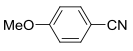 | 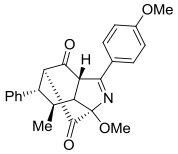 | **159** | 90 |
| 4 | **135** | 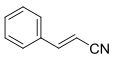 | 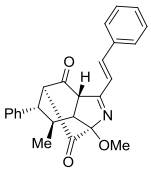 | **160** | 44 |
| 5 | **141** | 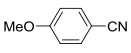 | 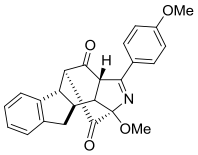 | **161** | 54 |

[a]Isolated yield.

Subjection of cyclopropane **135** to a series of nitriles in the presence of TMSOTf afforded polycyclic imines **157-161** (Table 23, entries 1-4). The structural identity of **159** was confirmed through X-ray crystallographic analysis;[94] additional structures in the series were then assigned by analogy. Extension of this reaction using cyclopropane **141** and *p*-methoxybenzonitrile was also successful and afforded the desired tetracyclic imine in acceptable yield (Table 23, entry 5).

Further investigations of the polycyclic imine scaffolds resulted in the discovery of an interesting retro-Dieckmann fragmentation of imine **159** (Scheme 22). Heating polycyclic imine **159** in anhydrous methanol at 100 ºC for 24 hours resulted in formation of pyrrole **162**. As there were two potential regiochemical outcomes possible from this rearrangement, further structural confirmation was required. Methylation of the pyrrole nitrogen was achieved by reaction of **162** with methyliodide and potassium carbonate in acetonitrile, heating at reflux for 12 hours. Two-dimensional NMR analysis of methylated pyrrole **163** was used to confirm the regiochemical outcome, and by analogy, the identity of pyrrole **162** (Scheme 22).

**Scheme 22**

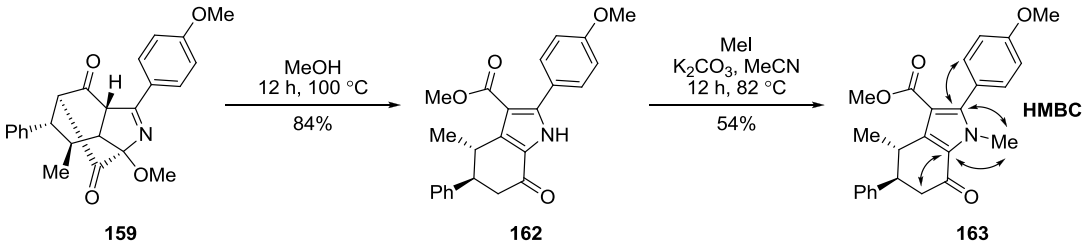

The mechanism of the rearrangement presumably begins with addition of methanol to the less hindered ketone (Figure 39). Next, fragmentation of the bond α to the ketone occurs through a retro-Dieckmann process which opens the bridged bicycle to produce a new fused 5,6-ring system. This process is facilitated through the resonance stabilization available within the adjacent α-methoxy ketone moiety. Next, a series of proton exchanges and loss of the α-methoxy group as methanol finally produces the observed pyrrole product.

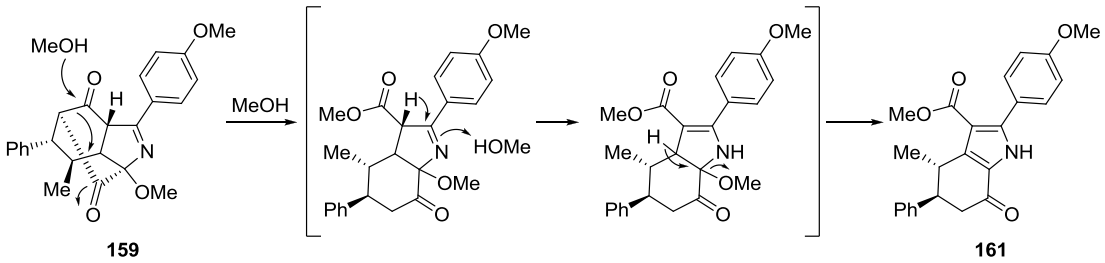


**Figure 39.** Fragmentation mechanism of polycyclic imine **159**.

As is evident from the immediate discussion, cycloadditions to donor-acceptor cyclopropanes hold a great wealth of potential for creating new and interesting chemotypes. Inspired by the success of nitriles in undergoing cycloadditions with the donor-acceptor cyclopropanes, the scope of available dipolarophiles was investigated.

In this study, donor-acceptor cyclopropane **135** was subjected to reactions with alkenes, alkynes, ketones, enol ethers, cyanopyridines, and indoles (Table 24). If successful, reaction with these partners would have provided access to a diverse and interesting array of polycyclic products and involve the formation of C–C, C–O, and

C–N bonds. Unfortunately, however, none of the dipolarophiles tested gave any appreciable amount of desired product.

**Table 24.** Cycloadditions investigated using cyclopropane substrate **135**.

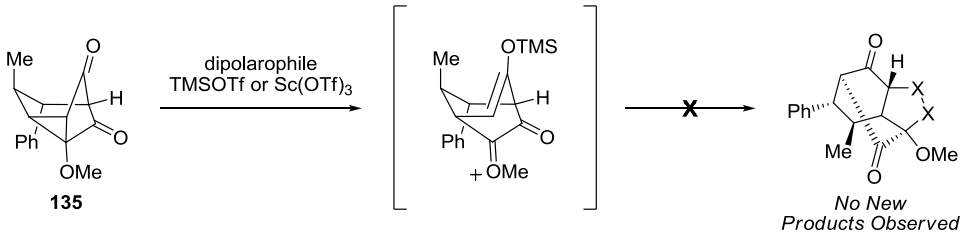


| entry | dipolarophile | anticipated product | entry | dipolarophile | anticipated product |
|---|---|---|---|---|---|
| 1 |  | 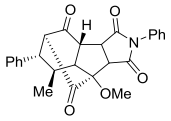 | 4 |  | 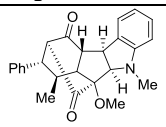 |
| 2 |  | 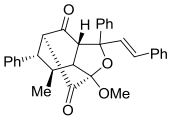 | 5 |  | 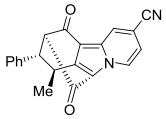 |
| 3 | 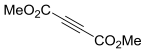 | 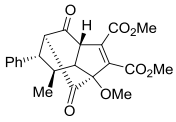 | 6 |  | 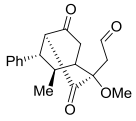 |

**Aza-di-π rearrangement of polycyclic iminium ethers.** As described above, imines are the primary substrates known to participate in the typical aza-di-π methane rearrangement.[93,100] Charged iminium ions typically exhibit reactivity different from that of imines upon photochemical irradiation (Figure 40).[101] In cases where a single iminium ion is the only π moiety within the molecule, intermolecular addition reactions can occur with alkenes, alkynes and other radical acceptors free in

solution.[102] When additional centers of unsaturation are present within the iminium substrate, intramolecular cyclization reactions typically occur prior to any intermolecular additions.[101,103]

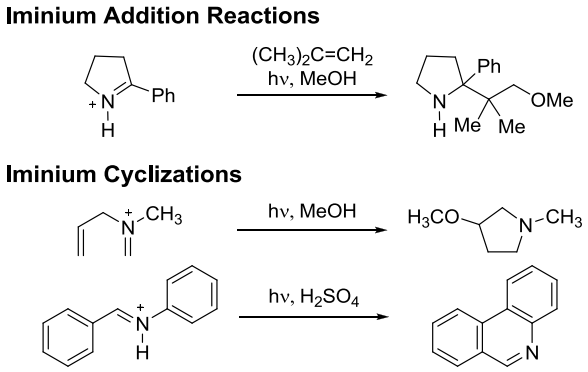


**Figure 40.** Photochemical iminium reactivity.

Iminium ethers exhibit reactivity patterns distinctive from both imines and iminium ions. While iminium ethers are charged species, the products resulting from their reaction are not always the result of direct addition to the imine center. Given this unique reactivity profile, it was initially unknown how an iminium ether would act upon photoirradiation (Figure 41). It was feasible that the iminium ether may behave like an iminium ion and cyclize to give a compound like **164**. It was also possible that it may behave as an imine, undergoing an aza-di-π rearrangement to give a compound like **165**. Alternatively, both reaction pathways could be viable, resulting in a mixture of products.

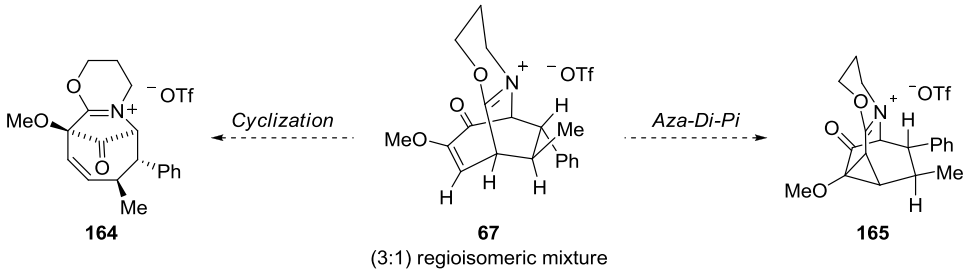


**Figure 41.** Photochemical reaction pathways of polycyclic iminium ether **67a,b**.

The photochemical reactivity of iminium ethers **67a,b** was investigated. The regioisomeric mixture of iminium ethers was derived from bicyclo[3.2.1]octanoid **63** using the azido-Schmidt reaction conditions described in the previous chapter (Chapter 4, Scheme 11).[80,92a] Photoirradiation of the iminium ether mixture **67a**,**b** (>300 nm) in acetone afforded cyclopropane **165** as a single product (Scheme 23).

**Scheme 23**

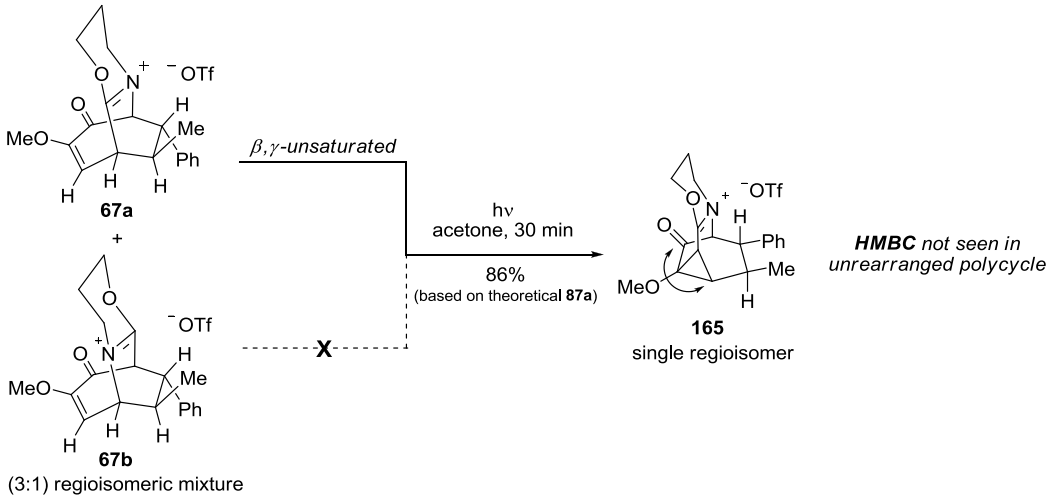

The assigned structure was confirmed using 1D and 2D NMR techniques. The reaction is presumed to proceed through an analogous aza-di-π methane rearrangement. This result shows that despite their charged nature, these iminium ethers behaved more like imines than iminium ions upon photochemical irradiation. Examining the structures of iminium ethers **67a** and **67b**, it is evident that polycycle **67a**, containing a prearranged β,γ-unsaturated system, is properly aligned to favor the aza-di-π rearrangement. Alternatively, iminium ether **67b**, which lacks this prearranged β,γ-unsaturated system, is unable to undergo a similar transformation. As a result only a single regioisomeric product was isolated from the reaction which arose from the major component of the iminium ether mixture. The minor iminium ether decomposed upon irradiation and was not observed in the crude product material.

As observed with previous iminium ethers,[78] α-cyclopropyl iminium ether **165** underwent ring opening transformations with various nucleophilic reagents (Table 25). A small series of heteroatom nucleophiles were used in the study to demonstrate addition to both the imine center (sat. aq. $NaHCO_3$) and the center adjacent to the oxygen (NaSPh and $NaN_3$). The ring-opening transformations were completed using the crude α-cyclopropyl iminium ether since the compound proved unstable to silica gel chromatography. Yields of the lactam product were good to excellent and similar to those previously observed for heteroatom nucleophilic additions to iminium ethers.[78]

**Table 25**. Nucleophilic ring-opening reactions of α-cyclopropyl iminium ether **165**.

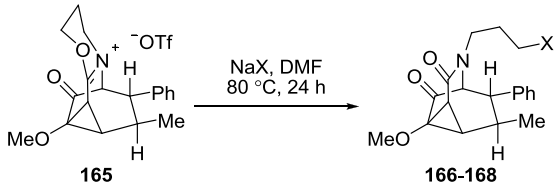


165 166-168

| entry | nucleophile | X | product | yield (%)[a] |
|---|---|---|---|---|
| 1 | NaSPh | SPh | **166** | 99 |
| 2 | $NaN_3$ | $N_3$ | **167** | 91 |
| 3 | sat. aq $NaHCO_3$ | OH | **168** | 68 |

[a]Isolated yield calculated according to major regioisomer.

Additional investigations geared toward probing the reactivity of both the α-cyclopropyl iminium ether and the α-cyclopropyl lactam were completed in a manner analogous that for the α-cyclopropyl polycyclic donor-acceptor ketone described above. Nucleophilic addition reactions to these scaffolds were explored using lithium reagents. Treatment of lactam **168** with methyl lithium resulted in the selective addition of methyl to the α-methoxy ketone on the exo-face, to yield tertiary alcohol **169** (Scheme 24).

**Scheme 24**

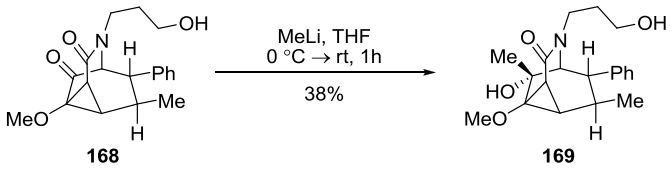


168 169

The reactivity of the lactam and iminium ether scaffolds was further probed for their utility in cycloaddition, fragmentation, and rearrangement reactions. However, despite extensive condition screening no additional reactivity was observed from these substrates.

**Summary.** Photochemical reaction screening of a series of bicyclo[3.2.1]octanoid scaffolds resulted in the formation of a set of donor-acceptor cyclopropanes via an oxa-di-π methane rearrangement. Exposure of the newly synthesized donor-acceptor cyclopropanes to various conditions led to the discovery of new and distinctive chemotypes, each arising from a single common starting point (Figure 42).

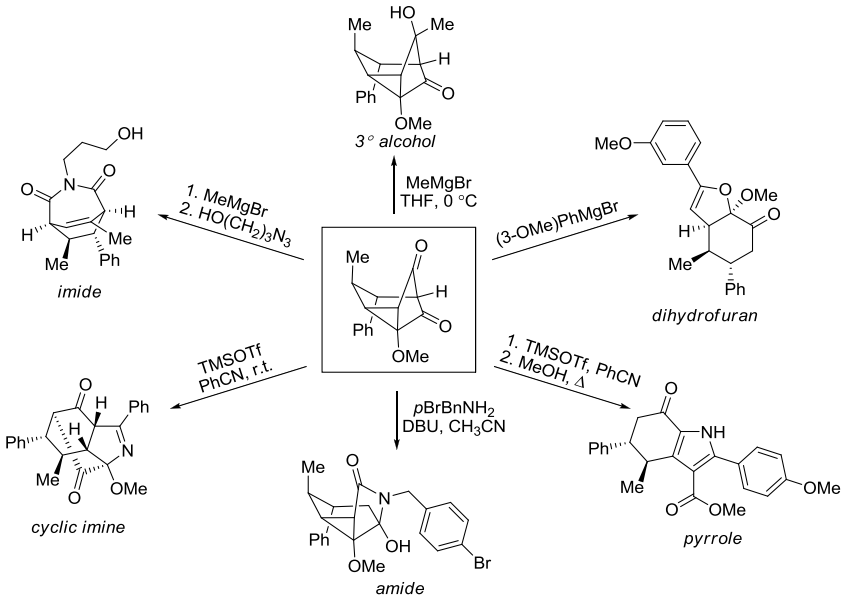


**Figure 42.** New chemotypes derived from donor-acceptor cyclopropane **135**.

In conjunction, investigation of similar photochemical reaction screens led to the first known example of an aza-di-π methane rearrangement of a β,γ-unsaturated iminium ether. The breadth of chemotypes accessed in this study demonstrates the vast potential reaction screening of multifunctional substrates possesses for the rapid discovery of new and unique compounds.

# Chapter 6

## Experimental Section

**General Information:** All reactions were performed under an argon atmosphere in flame-dried glassware. The stainless steel needles used for handling anhydrous solvents and reagents were oven dried, cooled in a desiccator, and flushed with dry argon prior to use. Plastic syringes were flushed with dry argon before use. Methylene chloride and acetonitrile were purified using a solvent purification system.[104] Acetonitrile for the iminium ether project was further purified by drying over 4 Å molecular sieves, as was methanol and *N*,*N*-dimethylformamide. The hydroxyalkyl azides were prepared from the corresponding hydroxyalkyl bromides according to previously published procedures.[78] *N*,*N*-Diisopropylethylamine (DIEA) was purified by distillation. All other reagents were purchased from commercial sources and used without further purification. All nuclear magnetic resonance spectra were recorded on either a Varian or Bruker spectrometer. All NMR samples were recorded in deuterochloroform unless otherwise noted. Chemical shifts are reported in parts per million (ppm) and are referenced to the deuterosolvent centerline of deuterochloroform (δ 7.26 ppm $^{1}$H NMR, 77.0 ppm $^{13}$C NMR), deuterodimethyl sulfoxide (δ 2.50 ppm $^{1}$H NMR, 39.52 ppm $^{13}$C NMR), or deuteroacetone (δ 2.05 ppm $^{1}$H NMR, 30.8 ppm $^{13}$C NMR). Data for $^{1}$H NMR are reported as follows: chemical shift, integration, multiplicity (br = broad, ovrlp = overlapping, s = singlet, d = doublet, t = triplet, q = quartet, qt = quintuplet, m = multiplet) and coupling

constants are reported as values in hertz (Hz). All $^{13}C$ NMR spectra were recorded with complete proton decoupling. Where discernible, rotamers and inseparable minor regioisomers are denoted with (*). When regioisomers were not completely separable the major rotamer peaks are denoted with ($^{\Phi}$). Infrared spectra were recorded on either a Nicolet Nexus 670 FT-IR, Shimadzu FTIR-8400S, or a Perkin Elmer Spectrum 100 FT-IR spectrophotometer. Melting points were recorded on either a Mel-Temp (Laboratory Devices), SRS OptiMelt, or Thomas-Hoover melting point apparatus and are uncorrected. High-resolution mass spectra were obtained in the Boston University Chemical Instrumentation Center using a Waters Q-TOF mass spectrometer or at Kansas University using a Waters LCT Premier Micromass from MS Technologies. Analytical LC was performed on a Waters Acquity UPLC with PDA, ELS and SQ detectors. An Acquity UPLC BEH 2.1 x 50 mm 1.7 μM C18 column was used for analytical LC. All chromatograms shown were generated using MassLynx 4.1. Analytical thin□ layer chromatography was performed using 0.25 mm silica gel 60-F plates. Analytical HPLC-MS analysis was completed using a Waters Alliance 2795 HPLC, a Waters LCT Premier TOF mass spectrometer, the Waters XBridge C-18 column (5 μM, 4.6 x 150 mm w/ 20 mm guard column), and a Waters 2996 Photodiode Array at 214 nm for sample detection. A gradient elution of 5% $CH_3CN$ to 95% $CH_3CN$ over 8.6 minutes was used, where the second mobile phase was water for neutral compounds, 0.05% formic acid in water for acidic compounds, or pH 9.8 ammonium formate in water for basic compounds. Preparative mass-directed fractionation was preformed using a Waters Mass Directed Fractionation

HPLC with a 2767 sample manager, a 2525 binary pump and a 515 make-up pump. A Waters XBridge C-18 column was used (5 μM, 19 x 150 mm w/ 10 mm guard column). The Waters ZQ quadrapole mass spectrometer and the Waters 2487 Dual Wavelength UV spectrometer were used for sample detection as a dual UV/MS fraction trigger. The same gradient elution and mobile phases were invoked as for the analytical run and the flow rate was set to 18 mL/min. Otherwise, flash chromatography was performed using 200-400 mesh silica gel (Scientific Absorbent Incorporated). Yields refer to chromatographically and spectroscopically pure materials, unless otherwise stated. Acetonitrile, DCM,[S1] THF, and toluene were purified by passing through two packed columns of neutral alumina (Innovative Technologies, MA). Chemical names were generated using MDL AutoNom 2000. All structural assignments were made based on correlation of the proposed structure with HRMS and IR data.

**KEY**

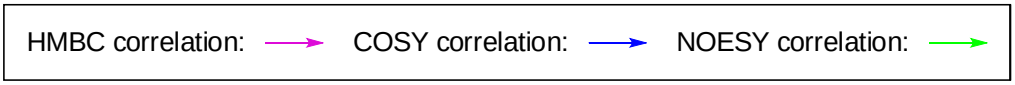

## Heterocycle Synthesis in Droplets

**General procedure for the synthesis of thiazoles in droplets.** (Synthesis of thiazoles **1**-**20**). Stock solutions of each bromoketone and thiourea starting material were first created by adding 2 mmol of a given starting material to a 20 mL scintillation vial. To each of these vials was then added 2 mLs of dry DMF, and the vials were then sonicated to form clear solutions. For each library member, 100 uL of stock solution from each of the required building blocks was loaded into a metering loop of known volume on a Uniqsis flow system. The machine then injected both metering loops to form a single cohesive droplet that was then flowed at 1.3 mL/min through an 80 °C heated coil, giving a final reaction time of 5 minutes. One minute after the library member was injected, a blank plug of 200 mL of DMF was added to the machine, and both the library droplet and the wash droplet were collected into culture tubes. The DMF layer was then removed, the fluorous layer was extracted with DMF, and the collective DMF solution was evaporated under warm nitrogen. The resulting residue was purified by preparative HPLC on a Waters Symmetry C8 column (25 mm x 100 mm, 7 μm particle size) using a gradient of 10% to 100% acetonitrile:0.1% aqueous TFA over 8 min (10 min run time) at a flow rate of 40 ml/min to give the desired compound.

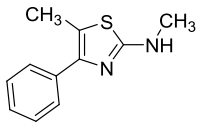

***N*,5-Dimethyl-4-phenylthiazol-2-amine (1).** 2-Bromo-1-phenylpropan-1-one (66.5 mg, 0.314 mmol) and 1-methylthiourea (28.2 mg, 0.314 mmol) afford thiazole **1** (39.3 mg, 0.192 mmol, 61%). $^{1}$H NMR (500 MHz, DMSO-d6) $\delta_H$ 7.55 (d, *J* = 7.5 Hz, 1H), 7.49 (t, *J* = 7.6 Hz, 1H), 7.43 (t, *J* = 7.2 Hz, 1H), 2.96 (d, *J* = 13.9 Hz, 2H), 2.27 (d, *J* = 23.5 Hz, 2H); $^{13}$C NMR (101 MHz, DMSO-d6) $\delta_c$ 166.8, 134.0, 129.4, 128.9, 128.7, 128.2, 114.5, 31.9, 11.6; MS (DCI+) *m/z* calcd for $C_{11}H_{13}N_2S$ ($M+H^+$): 205.0, found 205.2.

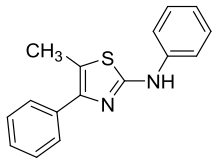


**5-Methyl-*N*,4-diphenylthiazol-2-amine (2).** 2-Bromo-1-phenylpropan-1-one (64.0 mg, 0.302 mmol) and 1-phenylthiourea (45.9 mg, 0.302 mmol) afford thiazole **2** (32.2 mg, 0.108 mmol, 40%). $^{1}$H NMR (500 MHz, DMSO-d6) $\delta_H$ 10.05 (s, 1H), 7.66 (dd, *J* = 12.6, 8.3 Hz, 4H), 7.46 (t, *J* = 7.6 Hz, 2H), 7.37-7.26 (m, 3H), 6.92 (td, *J* = 7.4, 0.9 Hz, 1H), 2.43 (s, 3H); $^{13}$C NMR (101 MHz, DMSO-d6) $\delta_c$ 159.5, 144.8, 141.2, 134.8, 129.0, 128.3, 128.0, 121.2, 116.9, 116.3, 11.9; MS (DCI+) *m/z* calcd for $C_{16}H_{15}N_2S$ ($M+H^+$): 267.0, found 267.2.

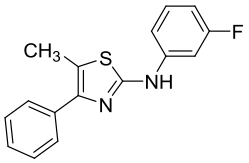

***N*-(3-Fluorophenyl)-5-methyl-4-phenylthiazol-2-amine (3).** 2-Bromo-1-phenylpropan-1-one (81.4 mg, 0.384 mmol) and 1-(3-fluorophenyl)thiourea (65.2 mg, 0.384 mmol) afford thiazole **3** (33.9 mg, 0.119 mmol, 31%). $^{1}$H NMR (500 MHz, DMSO-d6) $\delta_H$ 10.30 (s, 1H), 7.74 (d, *J* = 12.2 Hz, 1H), 7.67 (d, *J* = 8.0 Hz, 2H), 7.47 (t, *J* = 7.6 Hz, 2H), 7.40-7.24 (m, 3H), 6.82-6.65 (m, 1H), 2.44 (s, 3H); $^{13}$C NMR (101 MHz, DMSO-d6) $\delta_c$ 163.4, 161.5, 158.7, 145.3, 142.9, 142.8, 134.9, 130.4, 130.3, 128.3, 127.9, 127.1, 117.0, 112.5, 107.1, 106.9, 103.3, 103.1, 11.9; MS (DCI+) *m/z* calcd for $C_{16}H_{14}FN_2S$ ($M+H^+$): 285.0, found 285.4.

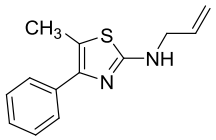


***N*-Allyl-5-methyl-4-phenylthiazol-2-amine (4).** 2-Bromo-1-phenylpropan-1-one (80.5 mg, 0.380 mmol) and 1-allylthiourea (44.0 mg, 0.380 mmol) afford thiazole **4** (35.9 mg, 0.156 mmol, 41%). $^{1}$H NMR (500 MHz, DMSO-d6) $\delta_H$ 7.55 (d, *J* = 8.1 Hz, 2H), 7.46 (t, *J* = 7.6 Hz, 2H), 7.38 (t, *J* = 7.3 Hz, 1H), 5.91 (dtd, *J* = 15.8, 10.5, 5.3 Hz, 1H), 5.30 (d, *J* = 10.2 Hz, 1H), 5.18 (d, *J* = 10.3 Hz, 1H), 3.95 (s, 2H), 2.31 (s, 3H); $^{13}$C NMR (101 MHz, DMSO-d6) $\delta_c$ 166.5, 136.8, 132.6, 129.9, 128.8, 128.6, 128.6, 117.3, 114.5, 47.4, 11.6; MS (DCI+) *m/z* calcd for $C_{13}H_{15}N_2S$ ($M+H^+$): 231.0, found 231.2.

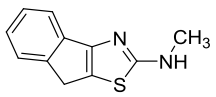

***N*-Methyl-8*H*-indeno[1,2-*d*]thiazol-2-amine (5).** 2-Bromo-2,3-dihydro-1*H*-inden-1-one (66.0 mg, 0.314 mmol) and 1-methylthiourea (28.2 mg, 0.314 mmol) afford thiazole **5** (33.7 mg, 0.166 mmol, 53%). $^{1}$H NMR (500 MHz, DMSO-d6) $\delta_H$ 7.51-7.44 (m, 2H), 7.32 (t, *J* = 7.5 Hz, 1H), 7.19 (t, *J* = 7.5 Hz, 1H), 3.72 (s, *J* = 18.8 Hz, 2H), 2.96 (s, *J* = 5.4 Hz, 3H); $^{13}$C NMR (101 MHz, DMSO-d6) $\delta_c$ 173.8, 145.3, 136.3, 126.6, 124.7, 124.4, 122.0, 117.7, 32.6, 31.1; MS (DCI+) *m/z* calcd for $C_{11}H_{11}N_2S$ ($M+H^+$): 203.0, found 203.3.

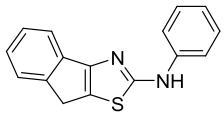


***N*-Phenyl-8*H*-indeno[1,2-*d*]thiazol-2-amine (6).** 2-Bromo-2,3-dihydro-1*H*-inden-1-one (55.6 mg, 0.265 mmol) and 1-phenylthiourea (40.2 mg, 0.265 mmol) afford thiazole **6** (23.8 mg, 0.0901 mmol, 34%). $^{1}$H NMR (500 MHz, DMSO-d6) $\delta_H$ 10.33 (s, 1H), 7.73 (d, *J* = 7.9 Hz, 2H), 7.54 (dd, *J* = 17.7, 7.4 Hz, 2H), 7.37-7.31 (m, *J* = 7.5, 3.9 Hz, 3H), 7.21 (t, *J* = 9.5, 5.4 Hz, 1H), 6.97 (t, *J* = 7.3 Hz, 1H), 3.81 (s, 2H); $^{13}$C NMR (101 MHz, DMSO-d6) $\delta_c$ 167.4, 156.1, 145.4, 141.0, 137.3, 129.0, 126.7, 124.7, 124.4, 121.2, 117.7, 116.9, 32.2; MS (DCI+) *m/z* calcd for $C_{16}H_{13}N_2S$ ($M+H^+$): 265.0, found 265.1.

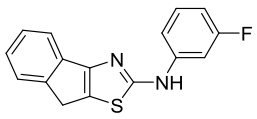

***N*-(3-Fluorophenyl)-8*H*-indeno[1,2-*d*]thiazol-2-amine (7).** 2-Bromo-2,3-dihydro-1*H*-inden-1-one (45.8 mg, 0.218 mmol) and 1-(3-fluorophenyl)thiourea (37.0 mg, 0.218 mmol) afford thiazole **7** (14.8 mg, 0.0524 mmol, 24%). $^{1}$H NMR (500 MHz, DMSO-d6) $\delta_H$ 7.81 (d, *J* = 7.3 Hz, 1H), 7.58 (d, *J* = 7.5 Hz, 1H), 7.53 (d, *J* = 7.4 Hz, 1H), 7.38-7.32 (m, 3H), 7.22 (t, *J* = 7.5 Hz, 1H), 6.81-6.75 (m, 1H), 3.83 (s, 2H); $^{13}$C NMR (101 MHz, DMSO-d6) $\delta_c$ 166.9, 163.8, 161.4, 156.1, 145.3, 142.6, 137.2, 130.4, 126.7, 125.1, 124.8, 124.5, 117.8, 112.7, 107.5, 107.3, 103.7, 103.4, 32.3; MS (DCI+) *m/z* calcd for $C_{16}H_{12}FN_2S$ ($M+H^+$): 283.0, found 283.3.

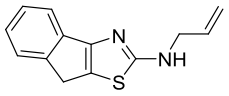


***N*-Allyl-8*H*-indeno[1,2-*d*]thiazol-2-amine (8).** 2-Bromo-1-phenylpropan-1-one (56.6 mg, 0.270 mmol) and 1-allylthiourea (31.3 mg, 0.270 mmol) afford thiazole **8** (7.4 mg, 0.0324 mmol, 12%). $^{1}$H NMR (500 MHz, DMSO-d6) $\delta_H$ 7.47 (dd, *J* = 13.3, 7.4 Hz, 2H), 7.31 (t, *J* = 7.5 Hz, 1H), 7.18 (t, *J* = 7.4 Hz, 1H), 5.95 (ddt, *J* = 17.0, 10.4, 5.3 Hz, 1H), 5.41-5.22 (m, 1H), 5.17 (dd, *J* = 10.2, 1.4 Hz, 1H), 4.02 (s, 1H); $^{13}$C NMR (101 MHz, DMSO-d6) $\delta_c$ 173.0, 145.4, 136.7, 134.3, 126.6, 124.7, 124.3, 122.5, 117.6, 46.7, 32.4; MS (DCI+) *m/z* calcd for $C_{13}H_{13}N_2S$ ($M+H^+$): 229.0, found 229.1.

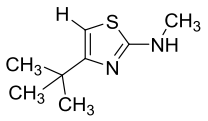

**4-*tert*-Butyl-*N*-mthythiazol-2-amine (9).** 1-Bromo-3,3-dimethylbutan-2-one (59.0 mg, 0.332 mmol) and 1-methylthiourea (29.9 mg, 0.332 mmol) afford thiazole **9** (20.4 mg, 0.119 mmol, 36%). $^{1}$H NMR (500 MHz, DMSO-d6) δ 6.50 (s, 1H), 2.97 (s, 3H), 1.32 (s, 9H); $^{13}$C NMR (101 MHz, DMSO-d6) $\delta_c$ 170.2, 162.2, 148.8, 100.1, 35.9, 33.1, 32.9, 28.3; MS (DCI+) *m/z* calcd for $C_8H_{15}N_2S$ ($M+H^+$): 171.0, found 171.3.

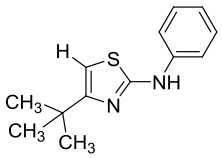


**4-*tert*-Butyl-*N*-phenylthiazol-2-amine (10).** 1-Bromo-3,3-dimethylbutan-2-one (58.0 mg, 0.326 mmol) and 1-phenylthiourea (49.6 mg, 0.326 mmol) afford thiazole **10** (30.3 mg, 0.130 mmol, 40%). $^{1}$H NMR (500 MHz, DMSO-d6) $\delta_H$ 10.08 (s, 1H), 7.68-7.54 (m, 2H), 7.30 (t, *J* = 7.7 Hz, 2H), 6.92 (t, *J* = 7.3 Hz, 1H), 6.41 (s, 1H), 1.31 (s, 9H); $^{13}$C NMR (101 MHz, DMSO-d6) $\delta_c$ 162.9, 160.8, 141.2, 128.9, 121.1, 116.8, 99.2, 34.3, 29.5; MS (DCI+) *m/z* calcd for $C_{13}H_{17}N_2S$ ($M+H^+$): 233.1, found 233.2.

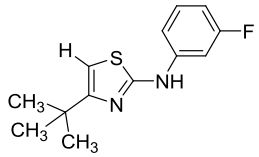


**4-*tert*-Butyl-*N*-(3-fluorophenyl)thiazol-2-amine (11).** 1-Bromo-3,3-dimethylbutan-2-one (49.5 mg, 0.278 mmol) and 1-(3-fluorophenyl)thiourea (47.2

mg, 0.278 mmol) afford thiazole **11** (34.1 mg, 0.136 mmol, 49%). $^{1}$H NMR (500 MHz, DMSO-d6) $\delta_H$ 10.33 (s, 1H), 7.82-7.65 (m, 1H), 7.41-7.16 (m, 2H), 6.71-6.65 (m, 1H), 6.57-6.38 (m, 1H), 1.27 (s, 9H); $^{13}$C NMR (101 MHz, DMSO-d6) $\delta_c$ 163.5, 162.0, 161.6, 161.5, 143.1, 130.4, 130.3, 112.4, 107.0, 106.8, 103.3, 103.1, 99.9, 34.3, 29.5; MS (DCI+) *m/z* calcd for $C_{13}H_{16}FN_2S$ ($M+H^+$): 251.1, found 251.1.

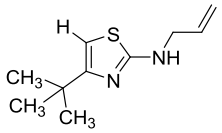


***N*-Allyl-4-*tert*-butylthiazol-2-amine (12).** 1-Bromo-3,3-dimethylbutan-2-one (58.9 mg, 0.331 mmol) and 1-allylthiourea (38.4 mg, 0.331 mmol) afford thiazole **12** (32.5 mg, 0.165 mmol, 50%). $^{1}$H NMR (500 MHz, DMSO-d6) $\delta_H$ 6.46 (s, 1H), 5.88 (m, 1H), 5.31 (d, *J* = 17.2 Hz, 1H), 5.23 (d, *J* = 10.3 Hz, 1H), 3.96 (s, *J* = 4.1 Hz, 2H), 1.24 (s, 9H); $^{13}$C NMR (101 MHz, DMSO-d6) $\delta_c$ 169.7, 149.3, 131.7, 117.9, 100.0, 48.1, 33.2, 28.3; MS (DCI+) *m/z* calcd for $C_{10}H_{17}N_2S$ ($M+H^+$): 197.1, found 197.1.

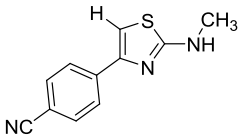


**4-(2-(Methylamino)thiazol-4-yl)benzonitrile (13).** 4-(2-Bromoacetyl)benzonitrile (63.7 mg, 0.286 mmol) and 1-methylthiourea (25.8 mg, 0.286 mmol) afford thiazole **13** (29.6 mg, 0.137 mmol, 48%). $^{1}$H NMR (500 MHz, DMSO-d6) $\delta_H$ 8.01 (d, *J* = 8.2 Hz, 2H), 7.90 (d, *J* = 8.2 Hz, 2H), 7.39 (s, 1H), 3.15 (s,

3H); $^{13}$C NMR (101 MHz, DMSO-d6) $\delta_c$ 169.4, 147.7, 138.6, 132.5, 126.2, 119.0, 109.3, 104.8, 31.0; MS (DCI+) *m/z* calcd for $C_{11}H_{10}N_3S$ ($M+H^+$): 216.0, found 216.3.

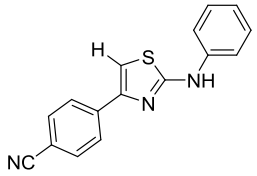


**4-(2-(Phenylamino)thiazol-4-yl)benzonitrile (14).** 4-(2-Bromoacetyl)benzonitrile (61.9 mg, 0.278 mmol) and 1-phenylthiourea (42.4 mg, 0.278 mmol) afford thiazole **14** (37.1 mg, 0.133 mmol, 48%). $^1$H NMR (500 MHz, DMSO-d6) $\delta_H$ 10.36 (s, 1H), 8.11 (d, *J* = 8.4 Hz, 2H), 7.90 (d, *J* = 8.4 Hz, 2H), 7.72 (d, *J* = 7.9 Hz, 2H), 7.66 (s, 1H), 7.36 (t, *J* = 7.9 Hz, 2H), 6.99 (t, *J* = 7.3 Hz, 1H); $^{13}$C NMR (126 MHz, DMSO-d6) $\delta_C$ 163.3, 148.3, 140.9, 138.5, 132.7, 129.0, 126.2, 121.4, 119.0, 116.9, 109.5, 106.8; MS (DCI+) *m/z* calcd for $C_{16}H_{12}N_3S$ ($M+H^+$): 278.0, found 278.3.

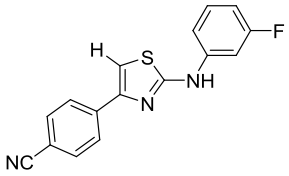


**4-(2-(3-Fluorophenylamino)thiazol-4-yl)benzonitrile (15).** 4-(2-Bromoacetyl)benzonitrile (56.2 mg, 0.252 mmol) and 1-(3-fluorophenyl)thiourea (42.8 mg, 0.252 mmol) afford thiazole **15** (36.5 mg, 0.123 mmol, 49%). $^1$H NMR (500 MHz, DMSO-d6) $\delta_H$ 10.61 (s, 1H), 8.10 (d, *J* = 8.3 Hz, 2H), 7.92 (d, *J* = 8.3 Hz,

2H), 7.78 (d, *J* = 11.8 Hz, 1H), 7.72 (s, 1H), 7.44-7.27 (m, 3H), 6.80 (m, 1H); $^{13}$C NMR (101 MHz, DMSO-d6) $\delta_c$ 162.9, 163.5, 161.5,148.3, 142.5, 138.3, 132.7, 130.6, 126.2, 118.9, 112.8, 109.7, 107.7, 107.5, 103.6, 103.4; MS (DCI+) *m/z* calcd for $C_{16}H_{11}FN_3S$ ($M+H^+$): 296.0, found 296.3.

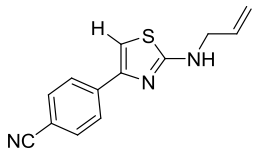


**4-(2-(Allylamino)thiazol-4-yl)benzonitrile (16).** 4-(2-Bromoacetyl)benzonitrile (62.5 mg, 0.280 mmol) and 1-allylthiourea (32.5 mg, 0.280 mmol) afford thiazole **16** (28.4 mg, 0.117 mmol, 42%). $^1$H NMR (500 MHz, DMSO-d6) $\delta_H$ 8.00 (d, *J* = 8.4 Hz, 3H), 7.83 (d, *J* = 8.3 Hz, 2H), 7.41 (s, 1H), 5.94 (ddd, *J* = 22.5, 10.5, 5.4 Hz, 1H), 5.28 (d, *J* = 17.2 Hz, 1H), 5.14 (d, *J* = 10.2 Hz, 1H), 3.93 (d, *J* = 19.5 Hz, 2H); $^{13}$C NMR (101 MHz, DMSO-d6) $\delta_C$ 168.3, 147.9, 138.8, 134.7, 132.4, 126.1, 119.0, 115.9, 109.3, 105.0, 46.6; MS (DCI+) *m/z* calcd for $C_{13}H_{12}N_3S$ ($M+H^+$): 242.0, found 242.1.

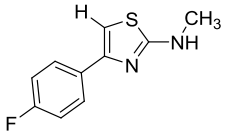


**4-(4-Fluorophenyl)-*N*-methylthiazol-2-amine (17).** 2-Bromo-1-(4-fluorophenyl)ethanone (60.2 mg, 0.278 mmol) and 1-methylthiourea (25.0 mg, 0.278 mmol) afford thiazole **17** (31.9 mg, 0.153 mmol, 55%). $^1$H NMR (500 MHz, DMSO-

d6) $\delta_H$ 7.90-7.80 (m, 2H), 7.28-7.18 (m, 2H), 7.23 (s, 1H), 2.91 (s, 3H); $^{13}$C NMR (101 MHz, DMSO-d6) $\delta_c$ 169.4, 162.4, 160.5, 130.9, 127.6, 127.6, 115.3, 115.1, 100.7; MS (DCI+) *m/z* calcd for $C_{10}H_{10}FN_2S$ ($M+H^+$): 209.0, found 209.2.

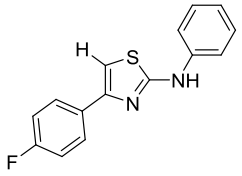


**4-(4-Fluorophenyl)-*N*-phenylthiazol-2-amine (18).** 2-Bromo-1-(4-fluorophenyl)ethanone (51.8 mg, 0.240 mmol) and 1-phenylthiourea (36.4 mg, 0.240 mmol) afford thiazole **18** (20.1 mg, 0.0744 mmol, 31%). $^1$H NMR (500 MHz, DMSO-d6) $\delta_H$ 10.27 (s, 1H), 8.03-7.89 (m, 2H), 7.72 (d, *J* = 8.3 Hz, 2H), 7.42-7.30 (m, 2H), 7.24-7.30 (t, *J* = 7.2 Hz, 2H), 6.98 (t, *J* = 6.9 Hz, 1H); $^{13}$C NMR (101 MHz, DMSO-d6) $\delta_C$ 163.1, 162.8, 160.3, 149.0, 141.1, 131.1-131.1 (d, *J* = 3.0 Hz, 1C), 129.0, 127.6-127.5 (d, *J* = 8.0 Hz, 1C), 121.2, 116.8, 115.5, 115.3, 102.6; MS (DCI+) *m/z* calcd for $C_{15}H_{12}FN_2S$ ($M+H^+$): 271.0, found 271.3.

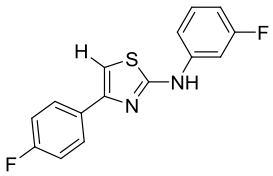


***N*-(3-Fluorophenyl)-4-(4-fluorophenyl)thiazol-2-amine (19).** 2-Bromo-1-(4-fluorophenyl)ethanone (58.5 mg, 0.270 mmol) and 1-(3-fluorophenyl)thiourea (45.9 mg, 0.270 mmol) afford thiazole **19** (35.9 mg, 0.124 mmol, 46%). $^1$H NMR

(500 MHz, DMSO-d6) $\delta_H$ 10.52 (s, 1H), 7.95 (dd, *J* = 8.4, 5.7 Hz, 2H), 7.79 (d, *J* = 11.0 Hz, 1H), 7.42-7.32 (m, 3H), 7.29 (t, *J* = 8.8 Hz, 2H), 6.78 (m, 1H); $^{13}$C NMR (101 MHz, DMSO-d6) $\delta_c$ 162.7, 163.5, 162.6, 161.5, 160.1, 149.0, 142.7, 142.6, 130.9, 130.9, 130.5, 130.4, 127.6, 127.5, 115.6, 115.4, 112.7, 112.6, 107.5, 107.3, 103.5, 103.3; MS (DCI+) *m/z* calcd for $C_{15}H_{11}F_2N_2S$ ($M+H^+$): 289.0, found 289.4.

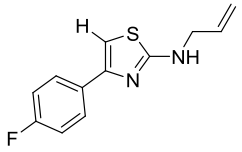


***N*-Allyl-4-(4-fluorophenyl)thiazol-2-amine (20).** 2-Bromo-1-(4-fluorophenyl)ethanone (68.6 mg, 0.318 mmol) and 1-allylthiourea (36.9 mg, 0.318 mmol) afford thiazole **20** (46.9 mg, 0.200 mmol, 63%). $^1$H NMR (500 MHz, DMSO-d6) $\delta_H$ 7.90-7.74 (m, 2H), 7.21 (t, *J* = 8.8 Hz, 2H), 7.06 (s, 1H), 5.93-5.85 (m, 1H), 5.28 (d, *J* = 8.8 Hz, 2H), 5.15 (d, *J* = 10.3 Hz, 2H), 3.95 (d, *J* = 5.2 Hz, 1H); $^{13}$C NMR (101 MHz, DMSO-d6) $\delta_C$ 168.3, 147.9, 138.8, 134.7, 126.1, 119.0, 115.9, 109.3, 109.1, 105.0, 46.6; MS (DCI+) *m/z* calcd for $C_{12}H_{12}FN_2S$ ($M+H^+$): 235.0, found 235.2.

**General procedure for the synthesis of pyrazoles in droplets.** (Synthesis of pyrazoles **21**-**40**). Stock solutions of each diketone and hydrazine starting material were first created by adding 2.0 mmol of a given starting material to a 20 mL scintillation vial. To each of these vials was then added 2 mLs of dry DMF, and the

vials were then sonicated to form clear solutions. For each library member, 100 μL of stock solution from each of the required building blocks was loaded into a metering loop of known volume on a Uniqsis flow system. The machine then injected both metering loops to form a single cohesive droplet that was then flowed at 1.3 mL/min through an 80 °C heated coil, giving a final reaction time of 5 minutes. One minute after the library member was injected, a blank plug of 200 mL of DMF was added to the machine, and both the library droplet and the wash droplet were collected into culture tubes. The DMF layer was then removed, the fluorous layer was extracted with DMF, and the collective DMF solution was evaporated under warm nitrogen. The resulting residue was purified by preparative HPLC on a Waters Symmetry C8 column (25 mm x 100 mm, 7 μm particle size) using a gradient of 10% to 100% acetonitrile:0.1% aqueous TFA over 8 min (10 min run time) at a flow rate of 40 ml/min to give the desired compound.

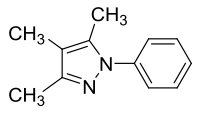


**3,4,5-Trimethyl-1-phenyl-1*H*-pyrazole (21).** 3-Methylpentane-2,4-dione (23.2 mg, 0.203 mmol) and phenylhydrazine (21.9 mg, 0.203 mmol) afford pyrazole **21** (12.5 mg, 0.0671 mmol, 33%). $^{1}$H NMR (400 MHz, DMSO-d6) $\delta_H$ 7.53-7.40 (m, 4H), 7.40-7.26 (m, 1H), 2.20 (s, 3H), 2.13 (s, 3H), 1.93 (m, 3H); $^{13}$C NMR (101 MHz, DMSO-d6) $\delta_c$ 147.0, 139.7, 135.8, 129.0, 126.7, 124.0, 112.8, 11.6, 10.7, 7.90; MS (DCI+) *m/z* calcd for $C_{12}H_{15}N_2$ ($M+H^+$): 187.1, found 187.3.

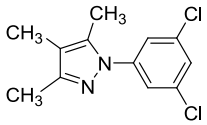

**1-(3,5-Dichlorophenyl)-3,4,5-trimethyl-1*H*-pyrazole (22).** 3-Methylpentane-2,4-dione (22.4 mg, 0.196 mmol) and (3,5-dichlorophenyl)hydrazine (34.4 mg, 0.196 mmol) afford pyrazole **22** (13.0 mg, 0.0511 mmol, 26%). $^{1}$H NMR (400 MHz, DMSO-d6) $\delta_H$ 7.67-7.43 (m, 3H), 2.27 (s, 3H), 2.12 (s, 3H), 1.92 (s, 3H); $^{13}$C NMR (101 MHz, DMSO-d6) $\delta_C$ 148.6, 141.8, 136.2, 134.3, 125.6, 121.7, 114.1, 11.6, 10.8, 7.8; $^{13}$C NMR (101 MHz, DMSO-d6) $\delta_c$ 148.6, 141.8, 136.3, 134.3, 125.8, 121.8, 114.1, 11.7, 10.8, 7.87; MS (DCI+) *m/z* calcd for $C_{12}H_{13}Cl_2N_2$ ($M+H^+$): 255.0, found 255.1.

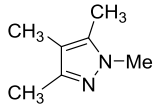

**1,3,4,5-Tetramethyl-1*H*-pyrazole (23).** 3-Methylpentane-2,4-dione (24.4 mg, 0.214 mmol) and methylhydrazine (9.86 mg, 0.214 mmol) afford pyrazole **23** (11.7 mg, 0.0942 mmol, 44%). $^{1}$H NMR (400 MHz, DMSO-d6) $\delta_H$ 3.57 (s, 3H), 2.08 (s, 3H), 1.99 (s, 3H), 1.82 (s, 3H); $^{13}$C NMR (101 MHz, DMSO-d6) $\delta_c$ 143.9, 135.3, 110.0, 35.4, 11.5, 9.05, 7.85; MS (DCI+) *m/z* calcd for $C_7H_{13}N_2$ ($M+H^+$): 125.1, found 125.2.

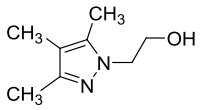

**2-(3,4,5-Trimethyl-1*H*-pyrazol-1-yl)ethanol (24).** 3-Methylpentane-2,4-dione (23.0 mg, 0.201 mmol) and 2-hydrazinylethanol (15.3 mg, 0.201 mmol) afford pyrazole **24** (11.5 mg, 0.0746 mmol, 37%). $^{1}$H NMR (400 MHz, DMSO-d6) $\delta_H$ 4.06 (t, *J* = 5.6 Hz, 2H), 3.64 (t, *J* = 5.6 Hz, 2H), 2.18 (s, 3H), 2.11 (s, 3H), 1.90-1.82 (s, 3H); $^{13}$C NMR (101 MHz, DMSO-d6) $\delta_c$ 143.4, 139.3, 111.5, 59.8, 50.6, 10.5, 9.19, 7.44; MS (DCI+) *m/z* calcd for $C_{11}H_8Cl_2F_3N_2$ ($M+H^+$): 155.1, found 155.1.

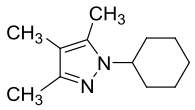

**1-Cyclohexyl-3,4,5-trimethyl-1*H*-pyrazole (25).** 3-Methylpentane-2,4-dione (23.0 mg, 0.202 mmol) and cyclohexylhydrazine (23.0 mg, 0.202 mmol) afford pyrazole **25** (13.2 mg, 0.0686 mmol, 34%). $^{1}$H NMR (400 MHz, DMSO-d6) $\delta_H$ 4.11-3.86 (m, 1H), 2.16 (s, 3H), 2.08 (s, 3H), 1.85 (s, 3H), 1.82-1.57 (m, 7H), 1.50-1.27 (m, 2H), 1.26-1.02 (m, 1H); $^{13}$C NMR (101 MHz, DMSO-d6) $\delta_c$ 143.5, 137.5, 111.2, 56.6, 32.0, 25.0, 24.8, 10.8, 9.05, 7.43; MS (DCI+) *m/z* calcd for $C_{12}H_{21}N_2$ ($M+H^+$): 193.1, found 193.2.

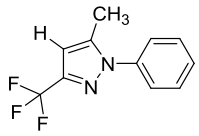

**5-Methyl-1-phenyl-3-(trifuloromethyl)-1*H*-pyrazole (26).** 1,1,1-Trifluoropentane-2,5-dione (30.3 mg, 0.197 mmol) and phenylhydrazine (21.3 mg, 0.197 mmol) afford pyrazole **26** (17.0 mg, 0.0751 mmol, 38%). $^{1}$H NMR (400 MHz, DMSO-d6) $\delta_H$ 7.55 (m, 5H), 6.76 (s, 1H), 2.36 (s, 3H); $^{13}$C NMR (101 MHz, DMSO-d6) $\delta_c$ 141.5, 138.4, 129.3, 129.2, 128.7, 125.5, 125.0, 104.8, 11.8; MS (DCI+) *m/z* calcd for $C_{11}H_{10}F_3N_2$ ($M+H^+$): 227.0, found 227.2.

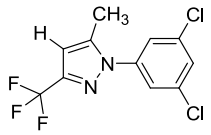


**1-(3,5-Dichlorophenyl)-5-methyl-3-(trifuloromethyl-1*H*-pyrazole (27).** 1,1,1-Trifluoropentane-2,5-dione (30.7 mg, 0.199 mmol) and (3,5-dichlorophenyl)hydrazine (35.0 mg, 0.199 mmol) afford pyrazole **27** (8.80 mg, 0.0299 mmol, 15%). $^{1}$H NMR (400 MHz, DMSO-d6) $\delta_H$ 7.84 (dt, *J* = 16.5, 1.8 Hz, 1H), 7.76 (d, *J* = 1.8 Hz, 2H), 6.81 (s, 1H), 2.40 (s, 3H); $^{13}$C NMR (101 MHz, DMSO-d6) $\delta_c$ 151.3, 144.7, 133.8, 127.3, 125.3, 125.0, 120.0, 119.1, 114.4, 92.6, 92.3, 92.1, 91.8, 47.7, 15.3; MS (DCI+) *m/z* calcd for $C_{11}H_8Cl_2F_3N_2$ ($M+H^+$): 295.0, found 295.1

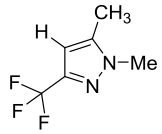

**1,5-Dimethyl-3-(trifuloromethyl)-1*H*-pyrazole (28).** 1,1,1-Trifluoropentane-2,5-dione (31.3 mg, 0.203 mmol) and methylhydrazine (9.38 mg, 0.203 mmol) afford pyrazole **28** (0.00 mg, 0.00 mmol, 0.0%).

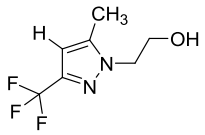


**2-(5-Methyl-3-(trifuloromethyl)-1*H*-pyrazole-1-yl)ethanol (29).** 1,1,1-Trifluoropentane-2,5-dione (30.8 mg, 0.200 mmol) and 2-hydrazinylethanol (15.2 mg, 0.200 mmol) afford pyrazole **29** (6.60 mg, 0.0340 mmol, 17%). $^{1}$H NMR (400 MHz, DMSO-d6) $\delta_H$ 6.45 (s, 1H), 4.92 (t, *J* = 5.4 Hz, 1H), 4.21-4.08 (m, 2H), 3.71 (q, *J* = 5.5 Hz, 2H), 2.30 (dd, *J* = 17.1, 10.9 Hz, 3H); MS (DCI+) *m/z* calcd for $C_7H_{10}F_3N_2O$ ($M+H^+$): 195.0, found 195.1.

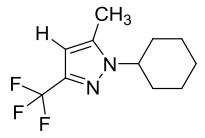


**1-Cyclohexyl-5-methyl-3-(trifuloromethyl)-1*H*-pyrazole (30).** 1,1,1-Trifluoropentane-2,5-dione (30.5 mg, 0.198 mmol) and cyclohexylhydrazine (22.6 mg, 0.198 mmol) afford pyrazole **30** (10.6 mg, 0.0456 mmol, 23%). $^{1}$H NMR (400 MHz, DMSO-d6) $\delta_H$ 6.43 (s, 1H), 4.18 (tt, *J* = 11.5, 3.9 Hz, 1H), 2.32 (s, 3H), 1.85-1.60. (m, 8H), 1.48-1.34 (m, 2H), 1.28-1.14 (m, 1H); $^{13}$C NMR (101 MHz, DMSO-d6) $\delta_c$ 139.6, 139.5, 139.1, 138.8, 138.4, 125.8, 123.1, 120.4, 117.8, 103.0, 57.0, 32.2, 24.8, 10.3; MS (DCI+) *m/z* calcd for $C_{11}H_{16}F_3N_2$ ($M+H^+$): 233.1 found 233.3.

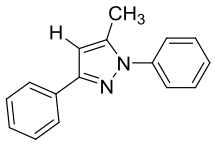


**5-Methyl-1,3-diphenyl-1*H*-pyrazole (31).** 1-Phenylbutane-1,3-dione (32.4 mg, 0.200 mmol) and phenylhydrazine (21.6 mg, 0.200 mmol) afford pyrazole **31** (13.6 mg, 0.0580 mmol, 29%). $^{1}$H NMR (400 MHz, DMSO-d6) $\delta_H$ 7.46-7.26 (m, 6H), 7.27-7.13 (m, 3H), 6.45 (s, 1H), 2.25 (s, 3H); $^{13}$C NMR (101 MHz, DMSO-d6) $\delta_c$ 148.5, 143.1, 139.8, 130.2, 128.9, 128.5, 128.3, 128.9, 127.3, 124.9, 107.8, 13.2; MS (DCI+) *m/z* calcd for $C_{16}H_{15}N_2$ ($M+H^+$): 235.1, found 235.3.

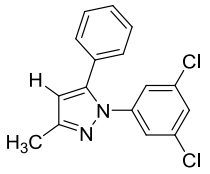


**1-(3,5-Dichlorophenyl)-3-methyl-5-phenyl-1*H*-pyrazole (32a).** 1-Phenylbutane-1,3-dione (32.7 mg, 0.202 mmol) and (3,5-dichlorophenyl)hydrazine (35.5 mg, 0.202 mmol) afford a mixture of regioisomeric pyrazoles (14.1 mg, 0.0466 mmol, 23%). Regioisomer **32a** (5.60 mg, 0.0185 mmol, 10%). $^{1}$H NMR (400 MHz, DMSO-d6) $\delta_H$ 7.57 (t, *J* = 1.9 Hz, 1H), 7.47-7.36 (m, 3H), 7.32-7.25 (m, 3H), 7.26 (d, *J* = 0.6 Hz, 1H), 6.48 (s, 1H), 2.24 (d, *J* = 34.1 Hz, 3H); MS (DCI+) *m/z* calcd for $C_{16}H_{13}Cl_2N_2$ ($M+H^+$): 303.0, found 303.2.

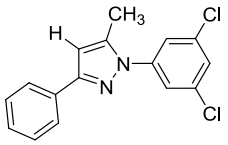


**1-(3,5-Dichlorophenyl)-5-methyl-3-phenyl-1*H*-pyrazole (32b).** 1-Phenylbutane-1,3-dione (32.7 mg, 0.202 mmol) and (3,5-dichlorophenyl)hydrazine (35.5 mg, 0.202 mmol) afford a mixture of regioisomeric pyrazoles (14.1 mg, 0.0466 mmol, 23%). Regioisomer **32b (**8.10 mg, 0.0268 mmol, 13%). $^{1}$H NMR (400 MHz, DMSO-d6) $\delta_H$ 7.85 (dt, *J* = 8.2, 1.7 Hz, 2H), 7.75 (d, *J* = 1.8 Hz, 2H), 7.70 (t, *J* = 1.8 Hz, 1H), 7.38-7.32 (m, 2H), 6.81 (d, *J* = 0.8 Hz, 1H), 2.45 (d, *J* = 0.5 Hz, 3H); $^{13}$C NMR (101 MHz, DMSO-d6) $\delta_c$ 149.7, 143.5, 141.4, 134.0, 129.6, 128.7, 128.7, 128.5, 126.3, 122.9, 109.0, 13.2; MS (DCI+) *m/z* calcd for $C_{16}H_{13}Cl_2N_2$ ($M+H^+$): 303.0, found 303.2.

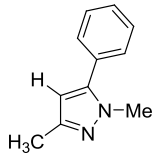


**1,3-Dimethyl-5-phenyl-1*H*-pyrazole (33a).** 1-Phenylbutane-1,3-dione (9.32.2 mg, 0.199 mmol) and methylhydrazine (9.17 mg, 0.199 mmol) afford a mixture of regioisomeric pyrazoles (7.20 mg, 0.0418 mmol, 21%). Regioisomer **33a** (1.90 mg, 0.0110 mmol, 6%). $^{1}$H NMR (400 MHz, DMSO-d6) $\delta_H$ 7.61-7.27 (m, 5H), 6.18 (s, 1H), 3.76 (s, 3H), 2.20 (s, 3H); MS (DCI+) *m/z* calcd for $C_{11}H_{13}N_2$ ($M+H^+$): 173.1, found 173.1.

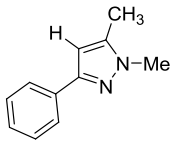


**1,5-Dimethyl-3-phenyl-1*H*-pyrazole (33b).** 1-Phenylbutane-1,3-dione (32.2 mg, 0.199 mmol) and methylhydrazine (9.17 mg, 0.199 mmol) afford a mixture of regioisomeric pyrazoles (7.20 mg, 0.0418 mmol, 21%). Regioisomer **33b** (5.30 mg, 0.0307 mmol, 15%). $^{1}$H NMR (400 MHz, DMSO-d6) $\delta_H$ 7.72 (dt, *J* = 8.1, 1.6 Hz, 2H), 7.41-7.31 (m, 2H), 7.31-7.17 (m, 1H), 6.46 (s, 1H), 3.75 (s, 3H), 2.25 (s, 3H); $^{13}$C NMR (101 MHz, DMSO-d6) $\delta_c$ 146.0, 148.5, 130.1, 128.7, 128.3, 128.3, 105.2, 37.0, 13.1; MS (DCI+) *m/z* calcd for $C_{11}H_{13}N_2$ ($M+H^+$): 173.1, found 173.1.

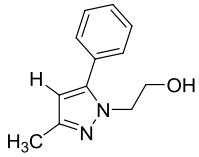


**2-(3-Methyl-5-phenyl-1*H*-pyrazol-1-yl)ethanol (34a).** 1-Phenylbutane-1,3-dione (32.4 mg, 0.200 mmol) and 2-hydrazinylethanol (15.2 mg, 0.200 mmol) afford a mixture of regioisomeric pyrazoles (32.0 mg, 0.158 mmol, 79%). Regioisomer **34a** (8.90 mg, 0.0440 mmol, 22%). $^{1}$H NMR (400 MHz, DMSO-d6) δ 7.64-7.27 (m, 5H), 6.15 (s, 1H), 4.03 (t, *J* = 5.9 Hz, 2H), 3.75 (t, *J* = 5.9 Hz, 2H), 2.20 (s, 3H); MS (DCI+) *m/z* calcd for $C_{12}H_{15}N_2O$ ($M+H^+$): 203.1, found 203.1.

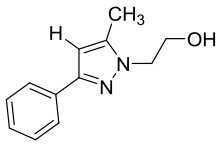

**2-(5-Methyl-3-phenyl-1*H*-pyrazol-1-yl)ethanol (34b).** 1-Phenylbutane-1,3-dione (32.4 mg, 0.200 mmol) and 2-hydrazinylethanol (15.2 mg, 0.200 mmol) afford a mixture of regioisomeric pyrazoles (32.0 mg, 0.158 mmol, 79%). Regioisomer **34b** (23.1 mg, 0.114 mmol, 57%). $^{1}$H NMR (400 MHz, DMSO-d6) $\delta_H$ 7.73 (dd, *J* = 8.3, 1.2 Hz, 2H), 7.44-7.31 (m, 2H), 7.25 (ddd, *J* = 8.6, 2.6, 1.3 Hz, 1H), 6.44 (s, 1H), 4.09 (t, *J* = 5.8 Hz, 2H), 3.72 (t, *J* = 5.8 Hz, 2H), 2.30 (s, 3H); $^{13}$C NMR (101 MHz, DMSO-d6) $\delta_c$ 146.6, 144.4, 130.4, 128.8, 128.7, 128.3, 105.3, 59.9, 50.8, 13.2; MS (DCI+) *m/z* calcd for $C_{12}H_{15}N_2O$ ($M+H^+$): 203.1, found 203.1.

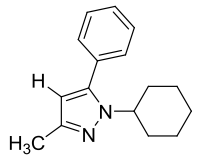


**1-Cyclohexyl-5-methyl-3-phenyl-1*H*-pyrazole (35).** 1-Phenylbutane-1,3-dione (32.5 mg, 0.201 mmol) and cyclohexylhydrazine (23.0 mg, 0.201 mmol) afford pyrazole **35** (12.6 mg, 0.0524 mmol, 26%). $^{1}$H NMR (400 MHz, DMSO-d6) δ 7.57-7.27 (m, 5H), 6.06 (s, 1H), 3.98 (tt, *J* = 11.2, 4.2 Hz, 1H), 2.19 (s, 3H), 2.00-1.68 (m, 6H), 1.52-1.50 (m, 1H), 1.36-1.01 (m, 3H); $^{13}$C NMR (101 MHz, DMSO-d6) $\delta_c$ 146.1, 142.9, 130.6, 128.8, 128.6, 128.4, 105.2, 56.8, 33.0, 25.1, 24.8, 13.4; MS (DCI+) *m/z* calcd for $C_{16}H_{20}N_2$ ($M+H^+$): 241.1, found 241.2.

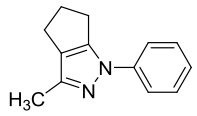

**3-Methyl-1-phenyl-1,4,5,6-tetrahydrocyclopenta[*c*]pyrazole (36).** 2-Acetylcyclopentanone (24.8 mg, 0.197 mmol) and phenylhydrazine (21.3 mg, 0.197 mmol) afford pyrazole **36** (12.5 mg, 0.0630 mmol, 32%). $^{1}$H NMR (400 MHz, DMSO-d6) $\delta_H$ 7.59 (d, *J* = 8.8 Hz, 2H), 7.51-7.34 (m, 2H), 7.31-7.14 (m, 1H), 3.10-2.91 (m, 2H), 2.15 (s, 3H); $^{13}$C NMR (101 MHz, DMSO-d6) $\delta_c$ 148.6, 143.0, 139.9, 129.4, 127.9, 125.0, 118.0, 30.5, 26.2, 21.7, 12.5; MS (DCI+) *m/z* calcd for $C_{13}H_{15}N_2$ ($M+H^+$): 199.1, found 199.2.

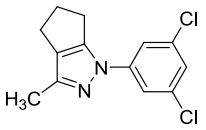


**2-(3,5-Dichlorophenyl)-3-methyl-2,4,5,6-tetrahydrocyclopenta[*c*]pyrazole (37a).** 2-Acetylcyclopentanone (22.1 mg, 0.175 mmol) and (3,5-dichlorophenyl)hydrazine (30.6 mg, 0.175 mmol) afford a mixture of regioisomeric pyrazoles (4.70 mg, 0.0176 mmol, 9%). Regioisomer **37a** (0.50 mg, 0.00187 mmol, 1%). $^{1}$H NMR (400 MHz, DMSO-d6) $\delta_H$ 7.59 (m, 3H), 2.63 (t, *J* = 7.4 Hz, 2H), 2.56 (t, *J* = 7.1 Hz, 2H), 2.39-2.33 (m, 2H), 2.33 (s, 3H); MS (DCI+) *m/z* calcd for $C_{13}H_{12}Cl_2N_2$ ($M+H^+$): 267.0, found 267.1.

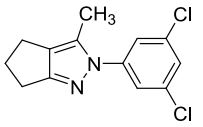


**1-(3,5-Dichlorophenyl)-3-methyl-1,4,5,6-tetrahydrocyclopenta[*c*]pyrazole (37b).** 2-Acetylcyclopentanone (22.1 mg, 0.175 mmol) and (3,5-dichlorophenyl)hydrazine

(30.6 mg, 0.175 mmol) afford a mixture of regioisomeric pyrazoles (4.70 mg, 0.0176 mmol, 9%). Regioisomer **37b** (4.20 mg, 0.0176 mmol, 8%). $^{1}$H NMR (400 MHz, DMSO-d6) $\delta_H$ 7.57 (d, *J* = 1.8 Hz, 2H), 7.45 (t, *J* = 1.8 Hz, 1H), 3.05 (m, 2H), 2.59-2.49 (m, 4H), 2.16 (s, 3H); $^{13}$C NMR (101 MHz, DMSO-d6) $\delta_c$ 149.3, 144.7, 141.6, 134.8, 129.2, 124.1, 116.2, 30.3, 26.1, 21.6, 12.5; MS (DCI+) *m/z* calcd for $C_{13}H_{12}Cl_2N_2$ ($M+H^+$): 267.0, found 267.1.

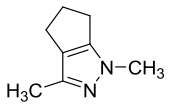


**1,3-Dimethyl-1,4,5,6-tetrahydrocyclopenta[*c*]pyrazole (38).** 2-Acetylcyclopentanone (29.2 mg, 0.232 mmol) and methylhydrazine (10.7 mg, 0.232 mmol) afford pyrazole **38** (13.6 mg, 0.0999 mmol, 43%). $^{1}$H NMR (400 MHz, DMSO-d6) $\delta_H$ 3.57 (s, 1H), 2.59 (m, 1H), 2.42 (m, 1H), 1.98 (m, 1H); $^{13}$C NMR (101 MHz, DMSO-d6) $\delta_c$ 150.1, 139.7, 123.9, 36.2, 30.6, 23.1, 22.5, 12.3; MS (DCI+) *m/z* calcd for $C_8H_{13}N_2$ ($M+H^+$): 137.1, found 137.1.

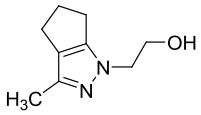


**2-(3-Methyl-5,6-dihydrocyclopenta[*c*]pyrazol-1(4*H*)-yl)ethanol (39).** 2-Acetylcyclopentanone (25.0 mg, 0.199 mmol) and 2-hydrazinylethanol (15.2 mg, 0.199 mmol) afford a mixture of regioisomeric pyrazoles (16.6 mg, 0.0999 mmol, 50%). $^{1}$H NMR (400 MHz, DMSO-d6) $\delta_H$ 3.94 (t, *J* = 5.6 Hz, 2H), 3.63 (t, *J* = 5.6

Hz, 2H), 2.70-2.65 (m, 2H), 2.48-2.40 (m, 4H), 2.07 (s, 3H); $^{13}$C NMR (101 MHz, DMSO-d6) $\delta_c$ 158.6*, 158.4*, 153.9, 139.1, 124.9, 60.4*, 59.4, 52.4*, 51.0, 29.8, 29.4*, 24.2*, 23.7, 22.0, 11.0, 10.1*; MS (DCI+) *m/z* calcd for $C_9H_{15}N_2O$ ($M+H^+$): 167.1, found 167.2.

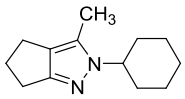


**2-Cyclohexyl-3-methyl-2,4,5,6-tetrahydrocyclopenta[*c*]pyrazole (40).** 2-Acetylcyclopentanone (25.4 mg, 0.201 mmol) and cyclohexylhydrazine (22.9 mg, 0.201 mmol) afford a mixture of regioisomeric pyrazoles (16.5 mg, 0.0.807 mmol, 40%). $^1$H NMR (400 MHz, DMSO-d6) $\delta_H$ 4.04 (ddd, *J* = 11.9, 8.1, 3.9 Hz, 1H), 2.88-2.69 (m, 2H), 2.49-2.35 (m, 4H), 2.15 (s, 3H), 2.01-1.89 (m, 2H), 1.85-1.74 (m, 2H), 1.74-1.57 (m, 3H), 1.35 (qd, *J* = 13.0, 9.7 Hz, 2H), 1.27-1.09 (m, 1H); $^{13}$C NMR (101 MHz, DMSO-d6) $\delta_c$ 151.4, 138.8, 125.1, 59.7, 31.8, 29.8, 24.8, 24.6, 24.4, 21.6, 11.1; MS (DCI+) *m/z* calcd for $C_{13}H_{21}N_2$ ($M+H^+$): 205.2, found 205.3.

## In situ Reagent Generation with Continuous Flow

**General procedure for two-step dehydration–Ugi 4-CR in continuous flow.** (Continuous flow synthesis of amides **41**-**56**). Reactions completed in the continuous flow apparatus were performed by combining 0.750 mmol (101 mg, 2 equiv.) of formamide with 1.50 mmol (206 mg, 2 equiv.) of Burgess reagent in 1.5 mL of anhydrous dichloromethane in a sealed conical-tipped vial. An injector tube was inserted through a hole in the vial cap and extended until it touched the bottom of the vial. The solution was allowed to flow continuously into the reactor at a flow rate of 0.1 mL/min (equivalent to one hour reaction time), which was the maximum reproducible reaction time achievable using the FlowSyn. The total injection time for the dehydration step of the sequence was approximately one hour, after which point the first injection line was switched to anhydrous dichloromethane to move the remaining reacting solution through the instrument. The final solvent injection required one additional hour. During this time, a solution of the remaining Ugi 4-CR components was prepared by combining 0.375 mmol (1 equiv.) of acid, 0.375 mmol (1 equiv.) of aldehyde, and 0.375 mmol (1 equiv.) of amine in 1.5 mL of anhydrous methanol in a sealed conical-tipped vial. The combined solution was allowed to sit for 1-2 hours prior to injection into the instrument. Prior to the start of the Ugi 4-CR component injection, a solution of anhydrous methanol was pumped through the instrument to maintain the appropriate backpressure. As the newly-formed isocyanide reached the T-joint merge point an injector tube was inserted through a hole in the

vial cap of the Ugi 4-CR component solution and extended until it touched the bottom of the vial. The solution was allowed to flow continuously into the flow reactor at a rate of 0.1 mL/min (equivalent to one hour reaction time), which was the maximum reproducible reaction time achievable using the Vapourtec. The total injection time for the Ugi 4-CR step of the sequence equaled approximately one hour, after which point the second injection line was switched to anhydrous methanol to move the remaining reacting solution through the instrument, which took approximately one additional hour. From the start of the dehydration injection to the exit of all reaction material from the instrument took a total of 3 hours. The reaction solution collected from the flow instrument was concentrated and the crude material was purified by silica gel chromatography.

**General procedure for two-step dehydration–Ugi 4-CR in the microwave.** (Microwave synthesis of amides **41**-**56**). A solution of formamide (0.839 mmol) and Burgess reagent (0.839 mmol) in anhydrous $CH_2Cl_2$ (2.0 mL) were mixed in a microwave vial, the vial was sealed, and heated at 90 ºC in the microwave for 1 h. While dehydrating the formamide, a solution of aldehyde (0.419 mmol), amine (0.419 mmol), and acid (0.419 mmol) in MeOH (2.0 mL) was prepared and stirred for 1 h at rt Upon completion of isocyanide synthesis the Ugi component solution was added to the isocyanide solution in one portion. The microwave vial was resealed and again heated at 90 ºC in the microwave for 1 h. The final solution was then concentrated and the crude material was purified by mass directed fractionation. Characterization

data was collected using microwave produced samples. All compounds used for characterization had purity >90% according to final LCMS analysis. Where appropriate, NMR spectrum were taken at -30 ºC in order to enhance resolution of the rotamers.

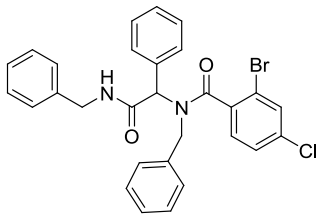


***N*-Benzyl-*N*-(2-(benzylamino)-2-oxo-1-phenylethyl)-2-bromo-4-chlorobenzamide (41).** *N*-Benzylformamide (113 mg, 0.839 mmol), Burgess reagent (200 mg, 0.839 mmol), benzaldehyde (44.4 mg, 0.419 mmol), benzylamine (44.8 mg, 0.419 mmol), and 2-bromo-4-chlorobenzoic acid (98.6 mg, 0.419 mmol) afforded Ugi product **41** (33.1 mg, 0.0606 mmol, 14%) as a white solid. The product appeared as a mixture of three rotamers while in solution. The major rotamer is denoted by ($^{\Phi}$) where discernable. $R_f$ = 0.25 (25% EtOAc/Hex); mp 152.4-155.0 ºC; $^1$H NMR at -30 ºC (500 MHz, $CDCl_3$) $\delta_H$ 7.60-6.82 (m, 18H), 6.02-6.01 (m, 1H), 5.30-5.13 (m, 1H), 4.62-4.09 (m, 3H); $^{13}$C NMR at -30 ºC (125 MHz, $CDCl_3$) $\delta_C$ 169.8, 169.3, 169.2$^{\Phi}$, 169.0, 168.8, 168.1$^{\Phi}$, 137.7, 137.5$^{\Phi}$, 137.4, 137.2, 136.1, 135.8, 135.6, 135.5$^{\Phi}$, 135.2$^{\Phi}$, 135.2$^{\Phi}$, 135.1, 134.0$^{\Phi}$, 133.7, 132.3, 132.2, 132.1, 132.0$^{\Phi}$, 130.1, 129.7$^{\Phi}$, 129.1$^{\Phi}$, 129.1$^{\Phi}$, 128.8, 128.8, 128.7, 128.5, 128.5, 128.5$^{\Phi}$, 128.4$^{\Phi}$, 128.4$^{\Phi}$, 128.0, 127.9, 127.8$^{\Phi}$, 127.8$^{\Phi}$, 127.5$^{\Phi}$, 127.5$^{\Phi}$, 127.4, 127.4, 127.3, 127.2, 127.2$^{\Phi}$, 127.1$^{\Phi}$,

127.1, 127.0, 126.7$^{\Phi}$, 126.0, 119.6, 119.4$^{\Phi}$, 118.7, 66.2, 64.0$^{\Phi}$, 63.0, 51.8$^{\Phi}$, 51.6, 47.6, 43.3, 43.3$^{\Phi}$, 43.2; IR (neat) 1671, 1624, 1412, 907 cm$^{-1}$; MS (ES+) m/z 547.0 (M+H$^{+}$); HRMS calcd for $C_{29}H_{25}BrClN_2O_2$ (M+H$^{+}$): 547.0788, found 547.0775.

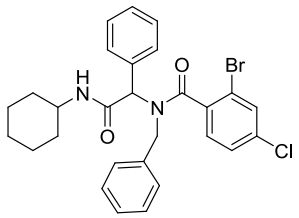


***N*-Benzyl-2-bromo-4-chloro-*N*-(2-(cyclohexylamino)-2-oxo-1-phenylethyl)benzamide (42).** *N*-Cyclohexyl formamide (106.6 mg, 0.839 mmol), Burgess reagent (200 mg, 0.839 mmol), benzaldehyde (44.4 mg, 0.419 mmol), benzylamine (44.8 mg, 0.419 mmol), and 2-bromo-4-chlorobenzoic acid (98.6 mg, 0.419 mmol) afforded Ugi product **42** (105.5 mg, 0.196 mmol, 47%) as a white solid. The major rotamer is denoted by ($^{\Phi}$) where discernable. $R_f$ = 0.33 (25% EtOAc/Hex); mp 144.0-147.4 ºC; $^{1}$H NMR at -30 ºC (500 MHz, $CDCl_3$) $\delta_H$ 7.68-6.80 (m, 13H), 6.04-4.93 (m, 2H), 4.55-4.25 (m, 1H), 3.82 (brs, 1H), 2.23-0.57 (m, 10H); $^{13}$C NMR -30 ºC (125 MHz, $CDCl_3$) $\delta_C$ 169.9, 169.5, 169.2$^{\Phi}$, 168.0, 167.8, 167.2$^{\Phi}$, 137.9, 136.3, 136.0, 135.8, 135.6$^{\Phi}$, 135.5, 135.4$^{\Phi}$, 135.2$^{\Phi}$, 135.0, 134.2, 134.1, 132.6, 132.5, 132.1, 132.0$^{\Phi}$, 130.0, 129.6, 129.5$^{\Phi}$, 129.1$^{\Phi}$, 128.9, 128.8, 128.7, 128.7, 128.5, 128.4$^{\Phi}$, 128.2, 128.0, 128.0, 127.9$^{\Phi}$, 127.7, 127.5, 127.4, 127.3$^{\Phi}$, 127.3, 127.0, 126.6$^{\Phi}$, 126.5, 119.6, 119.4$^{\Phi}$, 119.0, 66.6$^{\Phi}$, 64.0$^{\Phi}$, 62.8, 51.7$^{\Phi}$, 48.8 (br), 47.2, 32.6 (br), 25.1$^{\Phi}$, 24.8

(br); IR (neat) 2930, 1670, 1619, 1584, 1416 $cm^{-1}$; MS (ES+) m/z 539.1 ($M+H^+$); HRMS calcd for $C_{28}H_{29}BrClN_2O_2$ ($M+H^+$): 539.1101, found 539.1075.

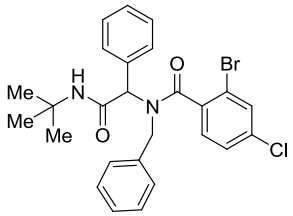


***N*-Benzyl-2-bromo-*N*-(2-(*tert*-butylamino)-2-oxo-1-phenylethyl-4-chlorobenzamide (43).** *N-tert*-Butylformamide (84.8 mg, 0.839 mmol), Burgess reagent (200 mg, 0.839 mmol), benzaldehyde (44.4 mg, 0.419 mmol), benzylamine (44.8 mg, 0.419 mmol), and 2-bromo-4-chlorobenzoic acid (98.6 mg, 0.419 mmol) afforded Ugi product **43** (42.4 mg, 0.0827 mmol, 20%) as a white solid. The major rotamer is denoted by ($^{\Phi}$) where discernable. $R_f$ = 0.37 (25% EtOAc/Hex); mp 156.0-157.5 ºC; $^1$H NMR at -30 ºC (500 MHz, $CDCl_3$) $\delta_H$ 7.65-6.70 (m, 13H), 6.03-5.20 (m, 1H), 4.60-4.26 (m, 2H), 1.36-1.25 (m, 9H); $^{13}$C NMR -30 ºC (125 MHz, $CDCl_3$) $\delta_C$ 169.8, 169.3$^{\Phi}$, 168.2, 167.1$^{\Phi}$, 136.4, 135.7, 135.7$^{\Phi}$, 135.1, 135.0, 134.4$^{\Phi}$, 134.3, 132.2, 132.0$^{\Phi}$, 129.5, 129.4$^{\Phi}$, 129.0$^{\Phi}$, 128.8$^{\Phi}$, 128.6$^{\Phi}$, 128.5, 128.3$^{\Phi}$, 127.9$^{\Phi}$, 127.6$^{\Phi}$, 127.3, 127.2$^{\Phi}$, 127.1$^{\Phi}$, 126.9, 126.5$^{\Phi}$, 119.8, 119.3$^{\Phi}$, 64.1$^{\Phi}$, 62.8, 51.7, 51.6, 51.5$^{\Phi}$, 51.4, 51.3, 40.5$^{\Phi}$, 28.3, 28.1$^{\Phi}$; IR (neat) 1673, 1618, 1416, 729 $cm^{-1}$; MS (ES+) m/z 513.0 ($M+H^+$); HRMS calcd for $C_{26}H_{27}BrClN_2O_2$ ($M+H^+$): 513.0944, found 513.0956.

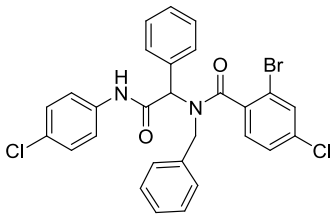


***N*-Benzyl-2-bromo-4-chloro-*N*-(2-(4-chlorophenylamino)-2-oxo-1-phenylethyl)benzamide (44).** 4-Chloro-*N*-phenylformamide (130 mg, 0.839 mmol), Burgess reagent (200 mg, 0.839 mmol), benzaldehyde (44.4 mg, 0.419 mmol), benzylamine (44.8 mg, 0.419 mmol), and 2-bromo-4-chlorobenzoic acid (98.6 mg, 0.419 mmol) afforded Ugi product **44** (32.6 mg, 0.0575 mmol, 14%) as a dark yellow solid. The major rotamer is denoted by ($^{\Phi}$) where discernable. $R_f$ = 0.37 (25% EtOAc/Hex); mp 143.4-146.7 ºC; $^{1}$H NMR at -30 ºC (500 MHz, $CDCl_3$) $\delta_H$ 7.62-6.84 (m, 17H), 6.43-5.30 (m, 1H), 4.64-4.33 (m, 2H); $^{13}$C NMR -30 ºC (125 MHz, $CDCl_3$) $\delta_C$ 170.4$^{\Phi}$, 169.8, 169.6, 167.8, 167.6, 166.7$^{\Phi}$, 136.3, 136.1, 135.8, 135.6, 135.6, 135.4$^{\Phi}$, 135.3, 135.2, 135.0, 133.4, 133.1$^{\Phi}$, 132.4, 132.1$^{\Phi}$, 132.1$^{\Phi}$, 132.0, 130.1, 129.8$^{\Phi}$, 129.6$^{\Phi}$, 129.4, 129.3$^{\Phi}$, 129.2$^{\Phi}$, 128.9, 128.9, 128.8, 128.7, 128.7$^{\Phi}$, 128.6, 128.4$^{\Phi}$, 128.4$^{\Phi}$, 128.3$^{\Phi}$, 128.0$^{\Phi}$, 127.7, 127.5, 127.5, 127.5, 127.1, 127.1$^{\Phi}$, 127.0, 126.5$^{\Phi}$, 121.2$^{\Phi}$, 121.0, 120.6$^{\Phi}$, 119.4, 119.4, 66.7, 66.0, 63.5$^{\Phi}$, 51.3, 51.2$^{\Phi}$; IR (neat) 1697, 1619, 1491, 1399, 827 cm$^{-1}$; MS (ES+) m/z 567.0 (M+H$^{+}$); HRMS calcd for $C_{28}H_{23}BrCl_2N_2O_2$ (M+H$^{+}$): 567.0242, found 567.0222.

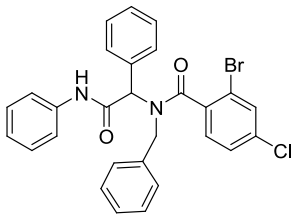


***N*-Benzyl-2-bromo-4-chloro-*N*-(2-oxo-1-phenyl-2-(phenylamino)ethyl)benzamide (45).** *N*-Phenylformamide (101 mg, 0.839 mmol), Burgess reagent (200 mg, 0.839 mmol), benzaldehyde (44.4 mg, 0.419 mmol), benzylamine (44.8 mg, 0.419 mmol), and 2-bromo-4-chlorobenzoic acid (98.6 mg, 0.419 mmol) afforded Ugi product **45** (40.1 mg, 0.0752 mmol, 18%) as a pale yellow solid. The major rotamer is denoted by ($^{\Phi}$) where discernable. $R_f$ = 0.33 (25% EtOAc/Hex); mp 84.9-88.8 ºC; $^1$H NMR at -30 ºC (500 MHz, $CDCl_3$) $\delta_H$ 7.65-6.56 (m, 18H), 5.87-5.34 (m, 0.5H), 4.69-4.29 (m, 1H), 3.51-3.49 (m, 1H), 2.63-2.21 (m, 0.5H); $^{13}$C NMR -30 ºC (125 MHz, $CDCl_3$) $\delta_C$ 170.3$^{\Phi}$, 169.7, 169.6, 168.6, 167.8, 167.6, 166.7$^{\Phi}$, 137.7, 137.4$^{\Phi}$, 137.0$^{\Phi}$, 136.5, 136.4, 135.9, 135.7, 135.4, 135.4, 135.2, 135.1, 134.5, 133.7, 133.6, 132.7, 132.4, 132.2, 132.0$^{\Phi}$, 130.3$^{\Phi}$, 130.1, 129.8$^{\Phi}$, 129.5$^{\Phi}$, 129.1, 129.1$^{\Phi}$, 129.0, 128.9, 128.8, 128.7, 128.7$^{\Phi}$, 128.6, 128.6$^{\Phi}$, 128.5, 128.4, 128.4, 128.3, 128.2$^{\Phi}$, 128.1, 128.1, 128.0, 127.9$^{\Phi}$, 127.8, 127.7, 127.4, 127.3, 127.2$^{\Phi}$, 127.1$^{\Phi}$, 127.0, 126.9, 126.8, 126.4$^{\Phi}$, 126.2, 124.6, 124.2$^{\Phi}$, 123.9, 123.9$^{\Phi}$, 66.7, 65.9$^{\Phi}$, 63.4, 63.3, 55.0, 54.0, 51.3$^{\Phi}$, 47.8; IR (neat) 1692, 1625, 1599, 1584, 1548, 1494, 1442, 906 cm$^{-1}$; MS (ES+) m/z 533.0 (M+H$^+$); HRMS calcd for $C_{28}H_{24}BrClN_2O_2$ (M+H$^+$): 533.0631, found 533.0642.

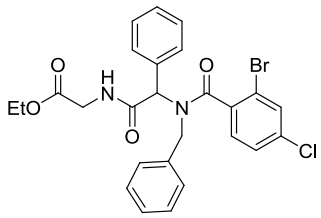


**Ethyl-2-(2-(*N*-benzyl-2-bromo-4-chlorobenzamido)-2-phenylacetamido)acetate (46).** *N*-Formylglycine ethyl ester (109 mg, 0.839 mmol), Burgess reagent (200 mg, 0.839 mmol), benzaldehyde (44.4 mg, 0.419 mmol), benzylamine (44.8 mg, 0.419 mmol), and 2-bromo-4-chlorobenzoic acid (98.6 mg, 0.419 mmol) afforded Ugi product **46** (38.6 mg, 0.0712 mmol, 17%) as a pale yellow solid. The major rotamer is denoted by ($^{\Phi}$) where discernable. $R_f$ = 0.17 (25% EtOAc/Hex); mp 61.7-73.2 ºC; $^1$H NMR at -30 ºC (500 MHz, $CDCl_3$) $\delta_H$ 7.67-6.16 (m, 13H), 5.37-5.19 (m, 1H), 4.55-4.20 (m, 2H), 4.22-4.09 (m, 3H), 3.99-3.86 (m, 1H), 1.30-1.23 (m, 3H); $^{13}$C NMR -30 ºC (125 MHz, $CDCl_3$) $\delta_C$ 169.8$^{\Phi}$, 169.5, 169.4, 169.4, 169.2, 169.2$^{\Phi}$, 168.2$^{\Phi}$, 136.0, 135.7, 135.6, 135.5, 135.4$^{\Phi}$, 135.3$^{\Phi}$, 135.2$^{\Phi}$, 135.1, 133.7$^{\Phi}$, 133.4, 132.4, 132.3, 132.3, 132.1, 132.1$^{\Phi}$, 130.2$^{\Phi}$, 130.0$^{\Phi}$, 129.6$^{\Phi}$, 129.2$^{\Phi}$, 129.1$^{\Phi}$, 128.9, 128.8, 128.8$^{\Phi}$, 128.6, 128.5$^{\Phi}$, 128.4, 128.3$^{\Phi}$, 128.2, 127.9$^{\Phi}$, 127.7$^{\Phi}$, 127.4$^{\Phi}$, 127.3$^{\Phi}$, 127.0, 126.9, 126.6$^{\Phi}$, 126.0, 119.6, 119.5$^{\Phi}$, 119.3, 119.0, 66.4, 65.9, 64.8, 63.6$^{\Phi}$, 62.3, 61.6, 61.5$^{\Phi}$, 51.0$^{\Phi}$, 51.3, 47.7, 41.3$^{\Phi}$, 41.0, 40.4, 15.2, 14.0, 13.9$^{\Phi}$; IR (neat) 1747, 1683, 1630, 1584, 1409, 1197 cm$^{-1}$; MS (ES+) m/z 543.0 ($M+H^+$); HRMS calcd for $C_{26}H_{25}BrClN_2O_4$ ($M+H^+$): 543.0686, found 543.0698.

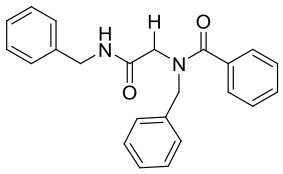

***N*-Benzyl-*N*-(2-(benzylamino)-2-oxoethyl)benzamide (47).** *N*-Benzylformamide (113 mg, 0.839 mmol), Burgess reagent (200 mg, 0.839 mmol), 37% formaldehyde in $H_2O$ (33.7 mg, 0.419 mmol), benzylamine (44.8 mg, 0.419 mmol), and benzoic acid (51.1 mg, 0.419 mmol) afforded Ugi product **47** (78.3 mg, 0.218 mmol, 52%) as a white solid. The major rotamer is denoted by ($^{\Phi}$) where discernable. $R_f$ = 0.33 (25% EtOAc/Hex); mp 108.0-109.9 ºC; $^1$H NMR at -30 ºC (500 MHz, $CDCl_3$) $\delta_H$ 7.45-7.17 (m, 15H), 4.72-4.61 (m, 2H), 4.38-4.37 (m, 2H), 4.09-3.77 (m, 2H); $^{13}$C NMR -30 ºC (125 MHz, $CDCl_3$) $\delta_C$ 172.8$^{\Phi}$, 172.4, 168.4$^{\Phi}$, 168.0, 137.8, 137.7$^{\Phi}$, 135.5, 135.4$^{\Phi}$, 134.4, 134.2$^{\Phi}$, 130.2$^{\Phi}$, 130.0, 128.7$^{\Phi}$, 128.6, 128.4$^{\Phi}$, 128.3$^{\Phi}$, 127.9, 127.6$^{\Phi}$, 127.6, 127.4$^{\Phi}$, 127.5, 127.1, 126.5, 126.5$^{\Phi}$, 126.5, 53.8$^{\Phi}$, 51.3, 48.9, 48.2$^{\Phi}$, 43.0, 42.9$^{\Phi}$; IR (neat) 1665, 1628, 1453, 1427, 1241 cm$^{-1}$; MS (ES+) m/z 359.1 (M+H$^+$); HRMS calcd for $C_{23}H_{23}N_2O_2$ (M+H$^+$): 359.1760, found 359.1768.

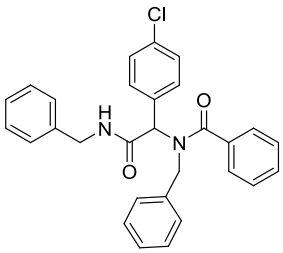

***N*-Benzyl-*N*-(2-(benzylamino)-1-(4-chlorophenyl)2-oxoethyl)benzamide (48).** *N*-Benzylformamide (113 mg, 0.839 mmol), Burgess reagent (200 mg, 0.839 mmol), 4-chlorobenzaldehyde (58.6 mg, 0.419 mmol), benzylamine (44.8 mg, 0.419 mmol), and benzoic acid (51.1 mg, 0.419 mmol) afforded Ugi product **48** (82.7 mg, 0.176 mmol, 42%) as a white solid. The major rotamer is denoted by ($^{\Phi}$) where discernable. $R_f$ = 0.13 (25% EtOAc/Hex); mp 159.6-162.0 ºC; $^1$H NMR at -30 ºC (500 MHz, $CDCl_3$) $\delta_H$ 7.52-6.77 (m, 19H), 5.56-5.48 (m, 1H), 5.05-4.81 (m, 1H), 4.49-4.18 (m, 3H); $^{13}$C NMR -30 ºC (125 MHz, $CDCl_3$) $\delta_C$ 172.9$^{\Phi}$, 172.6, 168.7$^{\Phi}$, 168.5, 137.6$^{\Phi}$, 137.5, 137.4, 136.3$^{\Phi}$, 135.2, 134.9$^{\Phi}$, 134.2$^{\Phi}$, 133.9, 132.6$^{\Phi}$, 132.5, 130.9$^{\Phi}$, 130.6, 129.9$^{\Phi}$, 129.7, 128.6, 128.6$^{\Phi}$, 128.4, 128.3$^{\Phi}$, 128.2$^{\Phi}$, 128.2$^{\Phi}$, 128.1, 127.7, 127.6, 127.2, 127.1$^{\Phi}$, 126.9$^{\Phi}$, 126.9$^{\Phi}$, 126.7, 126.4$^{\Phi}$, 126.3, 126.3$^{\Phi}$, 125.8, 65.6, 63.0$^{\Phi}$, 52.3$^{\Phi}$, 47.5, 43.0$^{\Phi}$, 40.1; IR (neat) 1670, 1623, 1492, 1408, 906 cm$^{-1}$; MS (ES+) m/z 469.1 (M+H$^+$); HRMS calcd for $C_{29}H_{26}ClN_2O_2$ (M+H$^+$): 469.1683, found 469.1686.

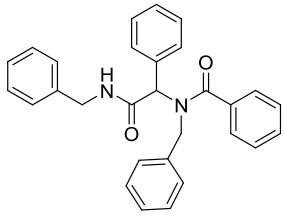


***N*-Benzyl-*N*-(2-(benzylamino)-2-oxo-1-phenylethyl)benzamide (49).** *N*-Benzylformamide (113 mg, 0.839 mmol), Burgess reagent (200 mg, 0.839 mmol), benzaldehyde (44.4 mg, 0.419 mmol), benzylamine (44.8 mg, 0.419 mmol), and

benzoic acid (51.1 mg, 0.419 mmol) afforded Ugi product **49** (97.3 mg, 0.224 mmol, 53%) as a white solid. The major rotamer is denoted by ($^{\Phi}$) where discernable. $R_f$ = 0.11 (25% EtOAc/Hex); mp 114.4-118.0 ºC; $^{1}$H NMR at -30 ºC (500 MHz, $CDCl_3$) $\delta_H$ 7.57-6.99 (m, 20H), 5.64-5.40 (m, 1H), 4.99-4.84 (m, 1H), 4.53-4.37 (m, 3H); $^{13}$C NMR -30 ºC (125 MHz, $CDCl_3$) $\delta_C$ 172.8$^{\Phi}$, 172.7, 168.9$^{\Phi}$, 168.8, 137.7$^{\Phi}$, 137.6, 137.4, 136.4$^{\Phi}$, 135.5, 135.0$^{\Phi}$, 134.0$^{\Phi}$, 134.0, 129.9$^{\Phi}$, 129.6, 129.4$^{\Phi}$, 129.2, 128.7$^{\Phi}$, 128.6$^{\Phi}$, 128.4, 128.3, 128.3$^{\Phi}$, 128.2$^{\Phi}$, 128.2$^{\Phi}$, 127.7, 127.6, 127.2, 127.1$^{\Phi}$, 126.9$^{\Phi}$, 126.8$^{\Phi}$, 126.5$^{\Phi}$, 126.3$^{\Phi}$, 126.1, 126.0, 66.5, 65.8, 64.1$^{\Phi}$, 52.4$^{\Phi}$, 47.5, 43.0$^{\Phi}$; IR (neat) 1666, 1623, 1495, 1453, 1408, 907 cm$^{-1}$; MS (ES+) m/z 435.2 (M+H$^{+}$); HRMS calcd for $C_{29}H_{27}N_2O_2$ (M+H$^{+}$): 435.2073, found 435.2063.

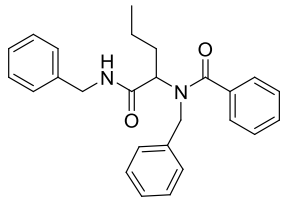


***N*-Benzyl-*N*-(1-benzylamino)-1-oxopentan-2-yl)benzamide (50).** *N*-Benzylformamide (113 mg, 0.839 mmol), Burgess reagent (200 mg, 0.839 mmol), butyraldehyde (30.1 mg, 0.419 mmol), benzylamine (44.8 mg, 0.419 mmol), and benzoic acid (51.1 mg, 0.419 mmol) afforded Ugi product **50** (10.6 mg, 0.0264 mmol, 6.2%) as a yellow oil. The major rotamer is denoted by ($^{\Phi}$) where discernable. $R_f$ = 0.28 (25% EtOAc/Hex); $^{1}$H NMR at -30 ºC (500 MHz, $CDCl_3$) $\delta_H$ 7.59-7.04 (m, 15H), 6.13-5.26 (m, 1H), 5.04-3.97 (m, 4H), 2.22-0.59 (m, 7H); $^{13}$C NMR -30 ºC (125 MHz, $CDCl_3$) $\delta_C$ 177.0, 173.9$^{\Phi}$, 173.8, 172.8$^{\Phi}$, 170.5$^{\Phi}$, 169.8, 168.9$^{\Phi}$, 161.3,

137.9$^{\Phi}$, 137.8, 137.7$^{\Phi}$, 137.3, 136.4, 136.3, 135.3$^{\Phi}$, 135.0, 134.1, 130.1, 130.0, 129.8, 129.5$^{\Phi}$, 129.3, 129.0$^{\Phi}$, 128.8, 128.7, 128.5, 128.5$^{\Phi}$, 128.3$^{\Phi}$, 128.2$^{\Phi}$, 127.9, 127.9, 127.8, 127.7, 127.6, 127.6, 127.4, 127.4$^{\Phi}$, 127.3, 127.2$^{\Phi}$, 127.1, 127.1, 127.0, 126.9$^{\Phi}$, 126.6$^{\Phi}$, 126.5$^{\Phi}$, 126.4$^{\Phi}$, 126.1, 126.1, 64.5$^{\Phi}$, 63.6, 58.8, 54.2, 52.7$^{\Phi}$, 51.1, 47.1, 46.2, 45.6, 43.4, 43.3$^{\Phi}$, 43.1, 42.9$^{\Phi}$, 41.7, 34.4, 30.8, 30.0$^{\Phi}$, 26.7, 20.6, 19.5$^{\Phi}$, 19.3, 13.9$^{\Phi}$, 13.4; IR (neat) 1666, 1621, 1495, 1453, 1412 cm$^{-1}$; MS (ES+) m/z 401.2 (M+H$^{+}$); HRMS calcd for $C_{26}H_{29}N_2O_2$ (M+H$^{+}$): 401.2229, found 401.2232.

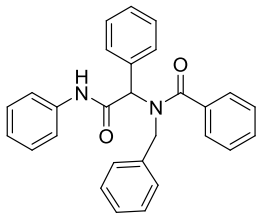


***N*-Benzyl-*N*-(2-oxo-1-phenyl-2-(phenylamino)ethyl)benzamide (51).** *N*-Phenylformamide (101 mg, 0.839 mmol), Burgess reagent (200 mg, 0.839 mmol), benzaldehyde (44.4 mg, 0.419 mmol), benzylamine (44.8 mg, 0.419 mmol), and benzoic acid (51.1 mg, 0.419 mmol) afforded Ugi product **51** (58.0 mg, 0.138 mmol, 33%) as a light yellow solid. The major rotamer is denoted by ($^{\Phi}$) where discernable. $R_f$ = 0.22 (25% EtOAc/Hex); mp 64.7-70.4 ºC; $^{1}$H NMR at -30 ºC (500 MHz, $CDCl_3$) $\delta_H$ 7.48-6.98 (m, 20H), 6.18 (s, 1H), 4.75 (m, 2H); $^{13}$C NMR -30 ºC (125 MHz, $CDCl_3$) $\delta_C$ 173.4$^{\Phi}$, 173.1, 171.3, 168.1$^{\Phi}$, 167.5, 162.3, 137.5$^{\Phi}$, 137.0$^{\Phi}$, 135.1$^{\Phi}$, 133.6$^{\Phi}$, 130.7, 130.2, 129.9$^{\Phi}$, 129.6$^{\Phi}$, 129.3, 128.8, 128.7, 128.7, 128.6, 128.5$^{\Phi}$, 128.4$^{\Phi}$, 128.3, 128.2$^{\Phi}$, 128.1, 128.0, 127.9$^{\Phi}$, 127.8, 127.4, 127.1, 126.9, 126.8,

126.5$^{\Phi}$, 126.5$^{\Phi}$, 126.2$^{\Phi}$, 123.7, 119.5$^{\Phi}$, 119.2, 119.0, 67.4, 65.9, 64.9, 63.8$^{\Phi}$, 51.9$^{\Phi}$; IR (neat) 1691, 1618, 1599, 1548, 1495, 1443, 906 cm$^{-1}$; MS (ES+) m/z 421.1 (M+H$^{+}$); HRMS calcd for $C_{28}H_{25}N_2O_2$ (M+H$^{+}$): 421.1916, found 421.1925.

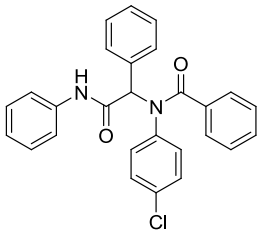


***N*-(4-Chlorophenyl)-*N*-(oxo-1-phenyl-2-(phenylamino)ethyl)benzamide (52).** *N*-Phenylformamide (101 mg, 0.839 mmol), Burgess reagent (200 mg, 0.839 mmol), benzaldehyde (44.4 mg, 0.419 mmol), 4-chloroaniline (53.2 mg, 0.419 mmol), and benzoic acid (51.1 mg, 0.419 mmol) afforded Ugi product **52** (24.2 mg, 0.0549 mmol, 13%) as a white solid. $R_f$ = 0.28 (25% EtOAc/Hex); mp 193.0-197.7 $^{o}$C; $^{1}$H NMR (500 MHz, $CDCl_3$) $\delta_H$ 8.16 (s, NH), 7.39-6.85 (m, 19H), 6.42 (s, 1H); $^{13}$C NMR (125 MHz, $CDCl_3$) $\delta_C$ 171.4, 168.0, 139.2, 137.6, 135.4, 133.7, 133.0, 131.9, 130.3, 129.7, 128.8, 128.6, 128.4, 128.4, 127.7, 124.2, 119.9, 66.5; IR (neat) 1693, 1625, 1600, 1549, 1490, 1443, 1376, 906 cm$^{-1}$; MS (ES+) m/z 441.1 (M+H$^{+}$); HRMS calcd for $C_{27}H_{22}ClN_2O_2$ (M+H$^{+}$): 441.1370, found 441.1365.

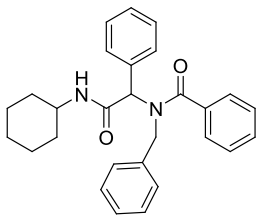

***N*-Benzyl-*N*-(2-(cyclohexylamino)-2-oxo-1-phenylethyl)benzamide (53).** *N*-Cyclohexyl formamide (106 mg, 0.839 mmol), Burgess reagent (200 mg, 0.839 mmol), benzaldehyde (44.4 mg, 0.419 mmol), benzylamine (44.8 mg, 0.419 mmol), and benzoic acid (51.1 mg, 0.419 mmol) afforded Ugi product **53** (114 mg, 0.267 mmol, 64%) as a white solid. The major rotamer is denoted by ($^{\Phi}$) where discernable. $R_f$ = 0.17 (25% EtOAc/Hex); mp 133.3-136.7 ºC; $^1$H NMR at -30 ºC (500 MHz, $CDCl_3$) $\delta_H$ 7.53-7.13 (m, 15H), 5.81-5.61 (m, 1H), 5.29 (s, 1H), 4.84-4.29 (m, 2H), 3.81 (brs, 1H) 2.00-0.64 (m, 10H); $^{13}$C NMR -30 ºC (125 MHz, $CDCl_3$) $\delta_C$ 173.1, 172.7$^{\Phi}$, 167.8, 167.8$^{\Phi}$, 137.9, 136.5$^{\Phi}$, 135.5, 135.0$^{\Phi}$, 134.2$^{\Phi}$, 129.8$^{\Phi}$, 129.8, 129.2$^{\Phi}$, 129.1, 128.8$^{\Phi}$, 128.7, 128.6, 128.5$^{\Phi}$, 128.4, 128.3$^{\Phi}$, 128.2, 128.1$^{\Phi}$, 127.3, 126.8$^{\Phi}$, 126.7, 126.4$^{\Phi}$, 126.3$^{\Phi}$, 125.9, 67.0, 65.8, 64.1$^{\Phi}$, 52.3$^{\Phi}$, 48.5 (br)$^{\Phi}$, 46.9, 40.3$^{\Phi}$, 32.4$^{\Phi}$, 25.0$^{\Phi}$, 24.8 (br) $^{\Phi}$; IR (neat) 2929, 1622, 1601, 1542, 1495, 1449, 1408 cm$^{-1}$; MS (ES+) m/z 427.2 (M+H$^+$); HRMS calcd for $C_{28}H_{31}N_2O_2$ (M+H$^+$): 427.2386, found 427.2379.

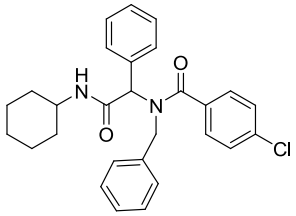


***N*-Benzyl-4-chloro-*N*-(2-cyclohexylamino)-2-oxo-1-phenylethyl)benzamide (54).** *N*-Cyclohexyl formamide (106 mg, 0.839 mmol), Burgess reagent (200 mg, 0.839 mmol), benzaldehyde (44.4 mg, 0.419 mmol),

benzylamine (44.8 mg, 0.419 mmol), and 4-chlorobenzoic acid (65.3 mg, 0.419 mmol) afforded Ugi product **54** (82.3 mg, 0.178 mmol, 43%) as a white solid. $R_f$ = 0.33 (25% EtOAc/Hex); mp 142.4-145.4 ºC; $^1$H NMR (500 MHz, $CDCl_3$) $\delta_H$ 7.40-7.03 (m, 14H), 5.72 (s, 1H), 5.55 (s, 1H), 4.72-4.43 (m, 2H), 3.84-3.46 (m, 2H) 1.90-1.05 (m, 10H); $^{13}$C NMR (125 MHz, $CDCl_3$) $\delta_C$ 172.0, 167.9, 135.6, 134.5, 129.5, 128.7, 128.6, 128.2, 128.0, 126.9, 64.1 (br), 52.6 (br), 48.5, 32.5, 25.2, 24.5 15.1; IR (neat) 2929, 1622, 1601, 1542, 1495, 1449, 1408 cm$^{-1}$; MS (ES+) m/z 461.1 (M+H$^+$); HRMS calcd for $C_{28}H_{30}ClN_2O_2$ (M+H$^+$): 461.1996, found 461.1992.

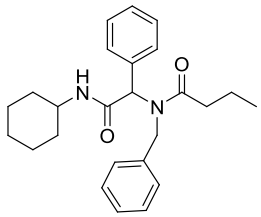


***N*-Benzyl-*N*-(2-(cyclohexylamino)-2-oxo-1-phenylethyl)butyramide (55).** *N*-Cyclohexyl formamide (106 mg, 0.839 mmol), Burgess reagent (200 mg, 0.839 mmol), benzaldehyde (44.4 mg, 0.419 mmol), benzylamine (44.8 mg, 0.419 mmol), and butyric acid (36.8 mg, 0.419 mmol) afforded Ugi product **55** (127 mg, 0.323 mmol, 77%) as a white solid. $R_f$ = 0.35 (25% EtOAc/Hex); mp 131.0-134.1 ºC; $^1$H NMR (500 MHz, $CDCl_3$) $\delta_H$ 7.35-6.98 (m, 10H), 6.00-5.90 (m, 1H), 4.77-4.54 (m, 2H), 3.79-3.77 (m, 1H), 2.59-0.84 (m, 17H); $^{13}$C NMR (125 MHz, $CDCl_3$) $\delta_C$ 174.8, 168.6, 137.6, 135.2, 129.5, 128.6, 128.2, 128.1, 126.6, 125.9, 62.5, 49.8, 48.3, 35.7, 32.6, 25.3, 24.6, 18.5, 13.6; IR (neat) 1628, 1542, 1451, 1412, 1200, 908 cm$^{-1}$; MS

(ES+) m/z 393.2 ($M+H^+$); HRMS calcd for $C_{25}H_{33}N_2O_2$ ($M+H^+$): 393.2542, found 393.2532.

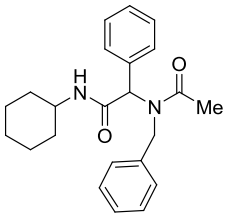


**2-(*N*-Benzylacetamido)-*N*-cyclohexyl-2-phenylacetamide (56).** *N*-Cyclohexyl formamide (106 mg, 0.839 mmol), Burgess reagent (200 mg, 0.839 mmol), benzaldehyde (44.4 mg, 0.419 mmol), benzylamine (44.8 mg, 0.419 mmol), and acetic acid (25.1 mg, 0.419 mmol) afforded Ugi product **56** (77.7 mg, 0.213 mmol, 51%) as a white solid. $R_f$ = 0.17 (25% EtOAc/Hex); mp 166.0-168.5 ºC; $^1$H NMR (500 MHz, $CDCl_3$) $\delta_H$ 7.35-6.97 (m, 10H), 6.03-5.94 (m, 1H), 4.75-4.56 (m, 2H), 3.79-3.78 (m, 1H), 2.59-1.03 (m, 10H), 2.04 (s, 3H); $^{13}$C NMR (125 MHz, $CDCl_3$) $\delta_C$ 172.6, 168.7, 137.6, 135.4, 129.6, 128.6, 128.4, 128.3, 126.8, 126.0, 62.4, 50.7, 48.5, 32.7, 25.5, 24.7, 22.5; IR (neat) 1628, 1543, 1450, 1409, 907 $cm^{-1}$; MS (ES+) m/z 365.2 ($M+H^+$); HRMS calcd for $C_{23}H_{29}N_2O_2$ ($M+H^+$): 365.2229, found 365.2237.

**Reaction Discovery Using Microfluidic-Based Screening of Polycyclic Iminium Ethers**

**General procedure for reaction screening and profiling with the microfluidics system**. Stock solutions of iminium ether substrate (0.25 M), reaction partner (0.70 M), and base (0.70 M) were prepared in DMSO and placed in oven-dried glass sleeves that were fitted into a custom-designed 96-well aluminum holding block. The holding block was sealed with a cover containing a continuous flow inert gas chamber and attached to the microfluidics platform. System parameters were set to perform reactions by mixing 8 μL of each reagent at 30 °C for 5 min or at 90 °C for 20 min. The reactions were quenched in the microreactor by flowing water into the quench port. Individual reactions were colleted according to a UV trigger into 96-well plates and analyzed by UPLC/MS/ELSD (10-90% $CH_3CN$), 2 min.

**General procedure for reaction screening and profiling with orbital shaker.** Stock solutions of substrate (0.25 M), reaction partner (0.70 M), and base (0.70 M) were prepared in DMSO. Individual reactions were prepared in oven-dried glass sleeves under inert atmosphere by combining 0.50 mL of each stock solution. The glass sleeves were individually capped and placed in a 96-well holding bock. Reaction blocks were mixed in an orbital mixer for 24 h at 90 °C. The reactions were quenched by the addition of water and analyzed by UPLC/MS/ELSD (10-90% $CH_3CN$), 2min.

**Synthesis of bicyclo[3.2.1]octanoid scaffold.**

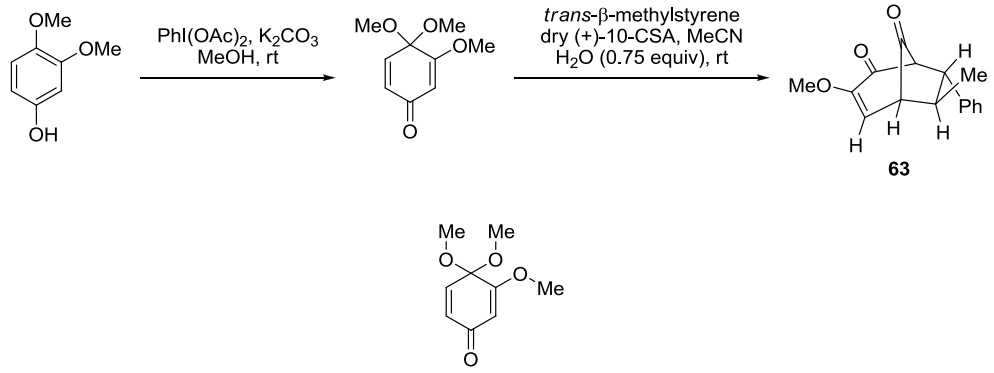


**3,4,4-Trimethoxycyclohexa-2,5-dienone (72).** To a flame-dried flask was added dry MeOH (90 mL) followed by iodobenzene diacetate (6.26 g, 19.4 mmol) and potassium carbonate (5.89 g, 42.6 mmol). In a second flame-dried flask 3,4-dimethoxyphenol (3.00 g, 29.4 mmol) was dissolved in dry MeOH (10 mL). The phenol solution was added to the first flask dropwise over 5 min and the reaction was stirred at rt for 2.5 h. The reaction was quenched with sat. aq. $NaHCO_3$ solution, extracted with $CH_2Cl_2$ (3 × 50 mL), washed with brine, dried over anhydrous $Na_2SO_4$ and reduced to give a thick yellow oil. The crude oil was purified by silica gel column chromatography (66% EtOAc/Hex) to afford 2.54 g (71%) as a white solid. $R_f$ = 0.22, (66% EtOAc/Hex); mp 61.0-63.0 °C; $^1$H NMR (400 MHz, $CDCl_3$) $\delta_H$ 6.59 (d, $J$ = 10.0 Hz, 1H), 6.32 (dd, $J$ = 10.0, 1.6 Hz, 1H), 5.64 (d, $J$ = 2.0 Hz, 1H), 3.82 (s, 3H), 3.32 (s, 6H); $^{13}$C NMR (100 MHz, $CDCl_3$) $\delta_c$ 186.1, 169.1, 140.2, 131.2, 104.1, 94.1, 55.9, 51.4; IR (neat) 2945, 1666, 1633, 1604, 1460, 1367, 1097, 856 cm$^{-1}$; MS (ES+) m/z 185.1 (M+H$^+$); HRMS calcd for $C_9H_{12}O_4$ (M+H$^+$): 185.0814, found 185.0816.

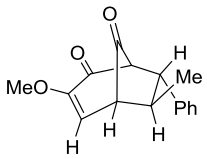


**(1*R*,5*R*,6*R*,7*R*)-3-Methoxy-6-methyl-7-phenylbicyclo[3.2.1]oct-3-ene-2,8-dione (63).** To a flame dried flask was added acetonitrile (20 mL) followed by dry (+)-10-camphorsulfonic acid (568 mg, 2.44 mmol) and *β*-trans-methylstyrene (0.633 mL, 2.44 mmol). The solution was stirred until homogeneous. In a second flame dried flask 3,4,4-trimethoxycyclohexa-2,5-dienone (**70**) (450 mg, 2.44 mmol) was dissolved in acetonitrile (10 mL) and the dienone was added to the first flask. Acetonitrile (5 mL) was used to wash the dienone flask and the washings were also added to the first flask. Water (32.9 μL, 1.83 mmol) was added to the reaction and the solution became dark while it stirred at rt for 1.5 h. The reaction was quenched with triethylamine (0.342 mL, 2.44 mmol) and stirred for 15 min. The solution was washed with sat. aq. $NaHCO_3$ and extracted with $Et_2O$ (3 × 20 mL). The organic extracts were combined, washed with brine, dried over anhydrous $Na_2SO_4$, and reduced. The resulting black oil was purified by silica gel column chromatography (20% EtOAc/Hex). The product appeared as a yellow solid and was then recrystallized by dissolving the residue in minimal EtOAc followed by adding hexanes carefully as to produce 2 layers. The mixture was placed in the freezer and as the two layers mixed, crystals formed. The supernanent was removed; the crystals were washed with cold hexanes and dried to afford 314.9 mg (50%) of **63** as flat clear needles. $R_f$ = 0.55, (66% Hex/EtOAc); mp 129.5-130.0 °C; $^1$H NMR (500 MHz,

$CDCl_3$) $\delta_H$ 7.29-7.32 (m, 2H), 7.25 (m, 1H), 7.08 (d, *J* = 7.5 Hz, 2H), 6.51 (d, *J* = 8.5 Hz, 1H), 3.83 (d, *J* = 7.0 Hz, 1H), 3.74 (s, 3H), 3.23 (t, *J* = 6.5 Hz, 1H), 3.08 (d, *J* = 8.5 Hz, 1H), 2.58 (p, *J* = 6.5 Hz, 1H), 1.28 (d, *J* = 7.0 Hz, 3H); $^{13}$C NMR (125 MHz, $CDCl_3$) $\delta_c$ 199.9, 190.0, 154.4, 137.7, 128.8, 128.3, 127.6, 117.7, 70.8, 55.8, 53.8, 49.3, 42.9, 21.5; IR (neat) 2358, 1760, 1685, 1606, 1151, 1103 $cm^{-1}$; MS (ES+) m/z 257.1 ($M+H^+$); HRMS calcd for $C_{16}H_{17}O_3$ ($M+H^+$): 257.1178, found 257.1171.

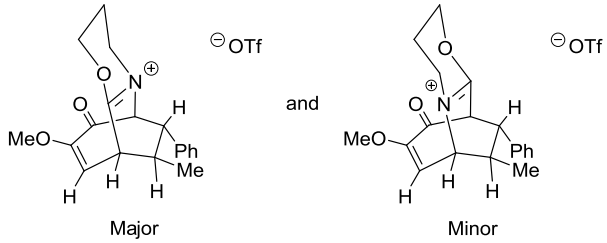


**Bicyclic iminium ether mixture (67a,b)**. To a solution of racemic 3-methoxy-6-methyl-7-phenylbicyclo[3.2.1]oct-3-ene-2,8-dione (300 mg, 1.17 mmol), and 3-azido-1-propanol (118 mg, 1.17 mmol) in $CH_2Cl_2$ (15 mL) at 0 °C was added a 1.17 M stock solution of TfOH (3.11 mL, 3.51 mmol) dropwise over 5 min. The acid stock solution was freshly prepared by the addition of TfOH (0.40 mL, 4.51 mmol) to a mixture of $CH_3CN$ (0.7 mL) and $CH_2Cl_2$ (2.9 mL). After 1 h at 0 °C the reaction was warmed to rt and stirred for 12 h. Upon dilution with water (10 mL) the solution was extracted with $CH_2Cl_2$ (3 × 20 mL), the organic extracts were combined, washed with brine, dried over anhydrous $Na_2SO_4$, and reduced to afford 527 mg (98%) of **67a,b** as a fluffy yellow solid and a mixture of regioisomers (3.5:1.0 regioisomeric ratio determined by $^1$NMR). Mp 88.5-91.0 °C; $^1$NMR (400 MHz, $CDCl_3$) $\delta_H$ 7.19-

7.32 (m, 3.9H), 7.13-7.15 (m, 2H), 7.05-7.07 (m, 0.6H), 6.70 (d, *J* = 9.0 Hz, 0.3H), 6.38 (d, *J* = 10.0 Hz, 1H), 4.85-4.94 (m, 1.3H), 4.72-4.78 (m, 1.3H), 4.66 (m, 0.3H), 4.45, (d, *J* = 5.0 Hz, 1H), 4.31 (m, 1H), 4.06-4.12 (m, 0.6H), 3.89 (m, 0.3H), 3.80 (m, 1H), 3.70 (s, 3H), 3.69 (s, 0.9H), 3.64 (d, *J* = 11.0 Hz, 1H), 3.61 (m, 1H), 3.43 (m, 0.3H), 2.74-2.80 (m, 1.3H), 2.39-2.43 (m, 1.3H), 2.16-2.30 (m, 1.3H), 1.30 (d, *J* = 7.0 Hz, 0.9H), 1.25 (d, *J* = 7.0 Hz, 3H); $^{13}$C NMR (100 MHz, $CDCl_3$) $\delta_C$ 183.7, 181.3*, 177.4, 171.9*, 154.2*, 153.1, 135.9*, 135.0, 129.2*, 129.1, 128.7, 128.4, 128.3*, 127.3*, 117.2*, 114.1, 76.3, 71.0, 70.8*, 64.8*, 63.0*, 55.9*, 55.8, 48.8, 47.6*, 46.7, 46.5*, 45.1, 42.0, 41.9*, 21.5, 20.5*, 19.7, 19.7*; IR (neat) 3055, 1700, 1662, 1265, 1031, 738, 703, 639 cm$^{-1}$; MS (ES+) m/z 312.1 ($M^+$); HRMS calcd for $C_{19}H_{22}NO_3$ ($M^+$): 312.1600, found 312.1582.

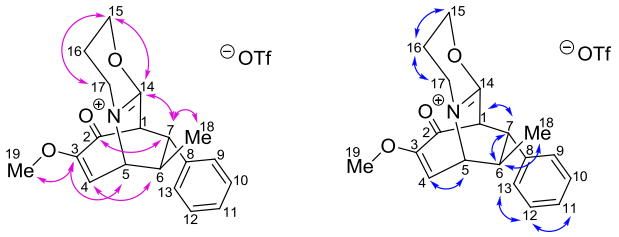


**Bicyclic iminium ether, minor regioisomer (67b).** Compound **67b** was proposed based on the distinctive $^1$H and $^{13}$C chemical shift of C1, C5, C14, and C15 in addition to connectivity data derived from HMBC and COSY. C1 appears at 63.0 ppm in the $^{13}$C and the $^1$H shows a doublet around 4.06 ppm, consistent with a bridgehead methylene between electron withdrawing groups such as an α-methoxy ketone and an iminium ether. C5 appears at 64.8 ppm in the $^{13}$C and the $^1$H shows a

multiplet around 4.75 ppm, consistent with the assignment of C5 as the bridgehead position between two electron withdrawing groups such as nitrogen and an olefin. C14 appears at 171.9 ppm in the $^{13}C$, supporting the presence of the iminium ether which typically exists slightly downfield from the corresponding lactam $^{13}C$ value. C15 appears at 70.8 ppm in the $^{13}C$ and the $^{1}H$ shows a pair of multiplets around 4.98 ppm and 4.66 ppm, suggesting C15 to be a methylene with diastereotopic hydrogens adjacent to a heteroatom, such as oxygen. The HMBC supports the retention of the major bicyclic structure though the 3-bond correlations between C2 and C7, C3 and C19, C3 and C5, C4 and C6, and C7 and C18. In addition, the HMBC supports the assigned regioisomer of nitrogen insertion with the 3-bond correlations between C7 and C14, C14 and C15, and C15 and C17. The COSY reaffirms this conclusion by showing the retention of the carbon connectivity throughout the bicycle with correlations between C1, C4, C5, C6, C7, and C18, as well as between C11, C12, and C13. COSY data also showed the retention of the carbon connectivity in the heterocycle of the iminium ether with correlations between C15, C16, and C17.

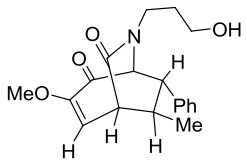


**(*E*)-6-(3-Hydroxypropyl)-3-methoxy-8-methyl-9-phenyl-6-azabicyclo[3.2.2]non-2-ene-4,7-dione (69a)**. Sat. aq $NaHCO_3$ solution (5 mL) was added to a solution of bicyclic iminium ether **67** (100 mg, 2.17 mmol) in $CH_2Cl_2$ (5 mL) and the biphasic mixture was stirred at rt for 2 h. The reaction was diluted with

water (5 mL), and was extracted with $CH_2Cl_2$ (3 × 10 mL). The organic extracts were combined, washed with brine, dried over anhydrous $Na_2SO_4$, and reduced to give a yellow oil. The crude material was purified by silica gel preparative thin layer chromatography (5% MeOH/$CH_2Cl_2$) to afford 33.1 mg (67%) of **69a** as a yellow oil. $R_f$ = 0.76 (10% MeOH/$CH_2Cl_2$); $^1$H NMR (400 MHz, $CDCl_3$) $\delta_H$ 7.22-7.31 (m, 3H), 7.07-7.10 (m, 2H), 6.34 (d, *J* = 10.4 Hz, 1H), 4.10 (d, *J* = 5.6 Hz, 1H), 3.69 (s, 3H), 3.47-3.66 (m, 4H), 3.33 (dd, *J* = 10.0, 1.2 Hz, 1H), 3.10 (t, *J* = 6.0 Hz, 1H), 2.61 (t, *J* = 6.8 Hz, 1H), 1.68 (m, 2H), 1.22 (d, *J* = 6.8 Hz, 3H); $^{13}$C NMR (100 MHz, $CDCl_3$) $\delta_C$ 188.9, 172.9, 153.3, 137.4, 129.0, 128.3, 127.9, 116.9, 73.0, 58.3, 55.5, 52.7, 48.9, 43.4, 41.2, 30.5, 22.9; IR (neat) 3421, 2958, 1650, 1623, 1456, 1126 cm$^{-1}$; MS (ES+) m/z 330.1 (M+H$^+$); HRMS calcd for $C_{19}H_{24}NO_4$ (M+H$^+$): 330.1705, found 330.1378.

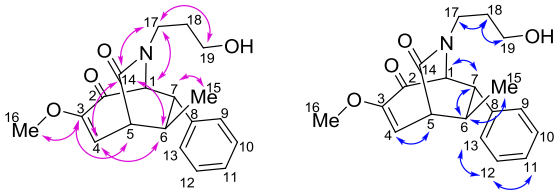


**(*E*)-6-(3-Hydroxypropyl)-3-methoxy-8-methyl-9-phenyl-6-azabicyclo[3.2.2]non-2-ene-4,7-dione (69a)**. Compound **69a** was proposed based on the distinctive $^1$H and $^{13}$C chemical shift of C1, C5, C14, C17, and C19 in addition to connectivity data derived from HMBC and COSY. C1 appears at 73.0 ppm in the $^{13}$C and the $^1$H shows a doublet at 4.10 ppm with an integration of 1.0, consistent with the assignment of C1 as the bridgehead position between two electron withdrawing groups such as nitrogen and an α-methoxy ketone. C5 appears at 48.9 ppm in the $^{13}$C

and the $^{1}H$ shows a doublet at 3.10 ppm, consistent with a bridgehead methylene between slight electron withdrawing groups such as an olefin and an amide. C14 appears at 172.9 ppm in the $^{13}C$, typical of a lactam. C17 and C19 appear at 43.4 ppm and 58.3 ppm respectively in the $^{13}C$ and the $^{1}H$ shows a multiplet at 3.47-3.66 ppm, suggesting C17 and C19 to be methylenes with diastereotopic hydrogens adjacent to heteroatoms such as nitrogen and oxygen. The HMBC supports the retention of the major bicyclic structure through the 3-bond correlations between C3 and C16, C3 and C5, C4 and C6, and C7 and C15. In addition, the HMBC supports the assigned regioisomer of nitrogen insertion with the 3-bond correlations between C4 and C14, C6 and C14, C14 and C17, and C17 and C19. The COSY reaffirms this conclusion by showing the retention of the carbon connectivity throughout the bicycle with correlations between C1, C4, C5, C6, C7, and C15, as well as between C11, C12, and C13. COSY data also shows the retention of the carbon connectivity between C15, C16, and C17.

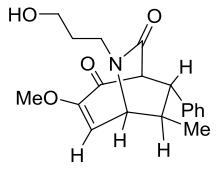


**(*E*)-6-(3-Hydroxypropyl)-3-methoxy-9-methyl-8-phenyl-6-azabicyclo[3.2.2]non-3-ene-2,7-dione (69b).** Sat. aq $NaHCO_3$ solution (5 mL) was added to a solution of bicyclic iminium ether **67** (100 mg, 2.17 mmol) in $CH_2Cl_2$ (5 mL) and the biphasic mixture was stirred at rt for 2 h. The reaction was diluted with

water (5 mL), and was extracted with $CH_2Cl_2$ (3 × 10 mL). The organic extracts were combined, washed with brine, dried over anhydrous $Na_2SO_4$, and reduced to give a yellow oil. The crude material was purified by silica gel preparative thin layer chromatography (5% MeOH/$CH_2Cl_2$) to afford 11.0 mg (22%) of **69b** as a yellow oil. $R_f$ = 0.72 (10% MeOH/$CH_2Cl_2$); $^1$H NMR (400 MHz, $CDCl_3$) $\delta_H$ 7.21-7.30 (m, 3H), 7.02-7.04 (m, 2H), 6.37 (d, *J* = 9.2 Hz, 1H), 3.95 (d, *J* = 4.8 Hz, 1H), 3.89 (dd, *J* = 9.2, 0.8 Hz, 1H), 3.82 (m, 1H), 3.67 (s, 3H), 3.59 (m, 1H), 3.41-3.51 (m, 2H), 3.24 (m, 1H), 2.98 (dd, *J* = 6.4, 4.8 Hz, 1H), 2.64 (p, *J* = 6.8 Hz, 1H), 1.70-1.82 (m, 2H), 1.23 (d, *J* = 6.8 Hz, 3H); $^{13}$C NMR (100 MHz, $CDCl_3$) $\delta_C$ 186.3, 169.5, 154.9, 138.4, 129.0, 128.0, 127.7, 118.2, 67.9, 59.7, 58.1, 55.5, 48.2, 44.4, 42.7, 30.6, 21.5; IR (neat) 3421, 2960, 1681, 1649, 1457, 1124 cm$^{-1}$; MS (ES+) m/z 330.1 (M+H$^+$); HRMS calcd for $C_{19}H_{24}NO_4$ (M+H$^+$): 330.1705, found 330.1538.

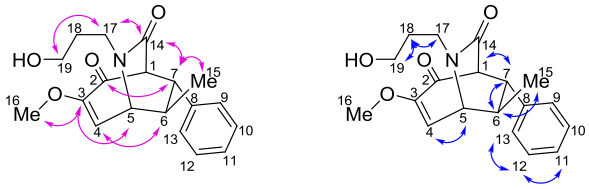

**(*E*)-6-(3-Hydroxypropyl)-3-methoxy-9-methyl-8-phenyl-6-azabicyclo[3.2.2]non-3-ene-2,7-dione (69b).** Compound **69b** was proposed based on the distinctive $^1$H and $^{13}$C chemical shift of C1, C5, C14, C17 and C19 in addition to connectivity data derived from HMBC and COSY. C1 appears at 67.9 ppm in the $^{13}$C and the $^1$H shows a doublet at 3.95 ppm, consistent with a bridgehead methylene between electron withdrawing groups such as an α-methoxy ketone and a lactam. C5

appears at 59.7 ppm in the $^{13}C$ and the $^{1}H$ shows a doublet at 3.89 ppm, consistent with the assignment of C5 as the bridgehead position between two electron withdrawing groups such as nitrogen and an olefin. C14 appears at 169.5 ppm in the $^{13}C$, typical of a lactam. C17 and C19 appear at 44.4 ppm and 58.1 ppm, respectively in the $^{13}C$ and the $^{1}H$ shows multiplets at 3.82 ppm, 3.59 ppm, and 3.41-3.51, suggesting C17 and C19 to be methylenes with diastereotopic hydrogens adjacent to heteroatoms such as nitrogen and oxygen. The HMBC supports the retention of the major bicyclic structure through the 3-bond correlations between C3 and C16, C3 and C5, C4 and C6, C2 and C7, and C7 and C15. In addition, the HMBC supports the assigned regioisomer of nitrogen insertion with the 3-bond correlations between C7 and C14, C14 and C17, and C17 and C19. The COSY reaffirms this conclusion by showing the retention of the carbon connectivity throughout the bicycle with correlations between C1, C4, C5, C6, C7, and C15, as well as between C11, C12, and C13. COSY data also shows the retention of the carbon connectivity between C15, C16, and C17.

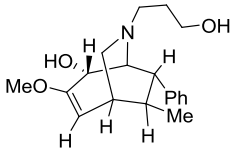


**(*E*)-6-(3-Hydroxypropyl)-3-methoxy-8-methyl-9-phenyl-6-azabicyclo[3.2.2]non-2-en-4-ol (83).** Sodium borohydride (23.6 mg, 0.607 mmol) was added to a solution of bicyclic iminium ether **67** (70.0 mg, 0.152 mmol) in ethanol (7.0 mL). The reaction was stirred at rt for 3 h. The reaction was quenched

with sat. aq. $NaHCO_3$ and was extracted with $CH_2Cl_2$ (3 × 10 mL). The organic extracts were combined, washed with brine, dried over anhydrous $Na_2SO_4$, and reduced to give a yellow oil. The crude material was purified by silica gel preparative thin layer chromatography to afford 21.4 mg (59% based on the major regioisomer in reactant) of **83** as a yellow oil. $R_f$ = 0.29 (10% MeOH/$CH_2Cl_2$); $^1$H NMR (400 MHz, $CDCl_3$) $\delta_H$ 7.26-7.33 (m, 4H), 7.17 (tt, *J* = 6.8, 2.0 Hz, 1H), 5.18 (d, *J* = 9.6 Hz, 1H), 4.42 (d, *J* = 6.0 Hz, 1H), 3.83 (m, 2H), 3.52 (s, 3H), 3.28 (dd, *J* = 6.0, 3.2 Hz, 1H), 3.02 (m, 3H), 2.83 (dd, *J* = 10.4, 2.8 Hz, 1H), 2.69 (m, 2H), 2.15 (dt, *J* = 9.6, 2.8 Hz, 1H), 1.75 (m, 2H), 0.99 (d, *J* = 6.8 Hz, 3H); $^{13}$C NMR (100 MHz, $CDCl_3$) $\delta_C$ 157.3, 141.8, 128.5, 128.3, 126.1, 102.2, 75.9, 65.4, 64.7, 57.2, 54.6, 49.9, 47.6, 37.6, 35.5, 28.4, 19.9; IR (neat) 3421, 1645 cm$^{-1}$; MS (ES+) m/z 318.2 (M+H$^+$); HRMS calcd for $C_{19}H_{28}NO_3$ (M+H$^+$): 318.2069, found 318.2067.

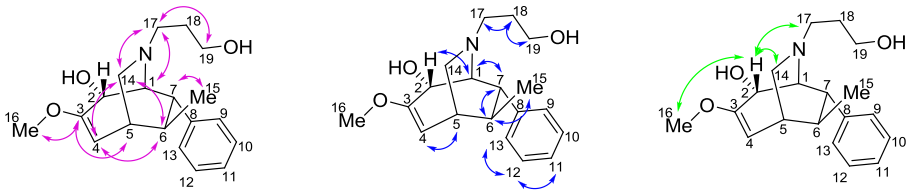

**(*E*)-6-(3-Hydroxypropyl)-3-methoxy-8-methyl-9-phenyl-6-azabicyclo[3.2.2]non-2-en-4-ol (83).** Compound **83** was proposed based on the distinctive $^1$H and $^{13}$C chemical shift of C2, C14, and C19 in addition to connectivity data derived from HMBC and COSY. C2 appears at 75.9 ppm in the $^{13}$C and the $^1$H shows a doublet at 4.42 ppm with an integration of 1.0, consistent with the assignment of C2 as a secondary alcohol. C14 appears at 57.2 ppm in the $^{13}$C and the

$^{1}$H shows a multiplet at 3.02 ppm with an integration of two, evidence for the direct reduction of the iminium ether. C19 appears at 64.7 ppm in the $^{13}$C and the $^{1}$H shows a multiplet at 3.83 ppm, suggesting C19 to be a methylene to a heteroatom such as oxygen. The HMBC supports the retention of the major bicyclic structure through the 3-bond correlations between C3 and C16, C3 and C5, C4 and C6, and C7 and C15. In addition, the HMBC supports the assigned regioisomer with the 3-bond correlations between C4 and C14, C6 and C14, C14 and C17, and C17 and C19. The COSY reaffirms this conclusion by showing the retention of the carbon connectivity throughout the bicycle with correlations between C1, C4, C5, C6, C7, and C15, as well as between C11, C12, and C13. COSY data also shows the retention of the carbon connectivity between C15, C16, and C17. NOSEY coupling of the proton on C2 with protons on C16, C17, and C14 support the assigned face of hydride addition.

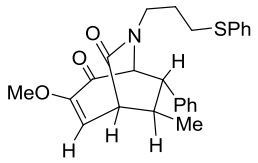


**(*E*)-3-Methoxy-8-methyl-9-phenyl-6-(3-(phenylthio)propyl)-6-azabicyclo[3.2.2]non-2-ene-4,7-dione (84).** To a solution of potassium hydride (13.0 mg, 0.325 mmol) in anhydrous DMF (0.5 mL) was added a solution of benzenethiol (33.0 μL, 0.325 mmol) in anhydrous DMF (0.5 mL). The mixture was stirred at rt for 5 min and bicyclic iminium ether **67** was added to the flask. The reaction mixture was stirred at 80 °C for 24 h. After cooling, the solution was diluted with water and

extracted with diethyl ether (3 × 10 mL). The organic extracts were combined, washed with brine, dried over anhydrous $Na_2SO_4$, and reduced to give a yellow oil. The crude material was purified by silica gel preparative thin layer chromatography (3:2 EtOAc-Hex) to afford 21.2 mg (62% based on the major regioisomer in reactant) of **84** as a yellow oil. $R_f$ = 0.46 (66% Hex/EtOAc); $^1$H NMR (400 MHz, $CDCl_3$) $\delta_H$ 7.17-7.35 (m, 8H), 7.02-7.05 (m, 2H), 6.32 (d, *J* = 10.4 Hz, 1H), 4.07 (d, *J* = 5.6 Hz, 1H), 3.67 (s, 3H), 3.53 (t, *J* = 6.8 Hz, 2H), 3.30 (dd, *J* = 10.0, 1.2 Hz, 1H), 3.04 (t, *J* = 6.2 Hz, 1H), 2.88 (t, *J* = 7.2 Hz, 2H), 2.57 (p, *J* = 6.8 Hz, 1H), 1.84 (p, *J* = 7.2 Hz, 2H), 1.20 (d, *J* = 6.8 Hz, 3H); $^{13}$C NMR (100 MHz, $CDCl_3$) $\delta_C$ 189.1, 171.4, 153.3, 137.6, 135.7, 129.8, 129.1, 129.0, 128.4, 127.8, 126.3, 116.9, 72.8, 55.4, 52.9, 49.3, 45.9, 41.1, 31.3, 27.8, 22.9; IR (neat) 2923, 1672, 1620, 1456, 1126, 700 cm$^{-1}$; MS (ES+) m/z 422.1 (M+H$^+$); HRMS calcd for $C_{25}H_{28}NO_3S$ (M+H$^+$): 422.1790, found 422.1785.

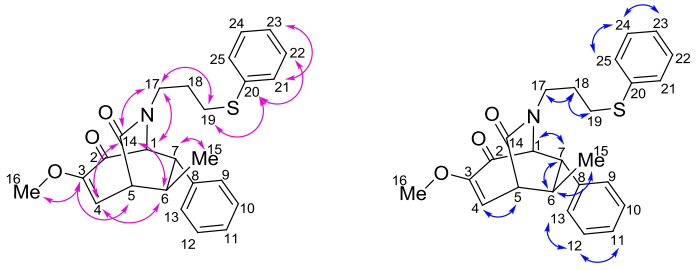

**(*E*)-3-Methoxy-8-methyl-9-phenyl-6-(3-(phenylthio)propyl)-6-azabicyclo[3.2.2]non-2-ene-4,7-dione (84).** Compound **84** was proposed based on the distinctive $^1$H and $^{13}$C chemical shift of C1, C5, C14, C17, and C19 in addition to connectivity data derived from HMBC and COSY. C1 appears at 72.8 ppm in the $^{13}$C

and the $^{1}H$ shows a doublet at 4.07 ppm with an integration of 1.0, consistent with the assignment of C1 as the bridgehead position between two electron withdrawing groups such as nitrogen and an α-methoxy ketone. C5 appears at 49.3 ppm in the $^{13}C$ and the $^{1}H$ shows a doublet of doublets at 3.30 ppm, consistent with a bridgehead methylene between slight electron withdrawing groups such as an olefin and an amide. C14 appears at 171.4 ppm in the $^{13}C$, typical of a lactam. C17 and C19 appear at 45.9 ppm and 31.3 ppm respectively in the $^{13}C$. C17 appears as a clean triplet in the $^{1}H$ at 3.53 ppm with an integration of 2.0. C19 appears as a clean triplet in the $^{1}H$ NMR at 2.88 ppm with an integration of 2.0. This data supports C17 and C19 as methylenes adjacent to heteroatoms such as nitrogen and sulfur, respectively. The HMBC supports the retention of the major bicyclic structure through the 3-bond correlations between C3 and C16, C3 and C5, C4 and C6, and C7 and C15. In addition, the HMBC supports the assigned regioisomer of nitrogen insertion with 3-bond correlations between C4 and C14, C6 and C14, C14 and C17, and C17 and C19. The connection of the aryl ring to the bicyclic core through the presence of a thioether bond is supported by the 3-bond HMBC correlation between C19 and C20. The COSY reaffirms this conclusion by showing the retention of the carbon connectivity throughout the bicycle with correlations between C1, C4, C5, C6, C7, and C15, as well as between C11, C12, and C13. COSY data also shows the retention of the carbon connectivity between C15, C16, and C17, as well as between C23, C24, and C25 of the thiophenol.

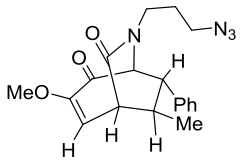


**(*E*)-6-(3-Azidopropyl)-3-methoxy-8-methyl-9-phenyl-6-azabicyclo[3.2.2]non-2-ene-4,7-dione (85)**. To a solution of sodium azide (21.1 mg, 0.325 mmol) in acetonitrile was added bicyclic iminium ether **67** (50.0 mg, 0.108 mmol). The reaction was heated to 80 °C for 24 h. After cooling, the reaction was diluted with water and extracted with diethyl ether (3 × 10 mL). The organic extracts were combined, washed with brine, dried over anhydrous $Na_2SO_4$, and reduced give a yellow oil. The crude material was purified by silica gel preparative thin layer chromatography (66% Hex/EtOAc) to afford 20.0 mg, (70% based on the major regioisomer in reactant) of **85** as a yellow oil. $R_f$ = 0.36 (66% Hex/EtOAc); $^1$H NMR (400 MHz, $CDCl_3$) $\delta_H$ 7.23-7.32 (m, 3H), 7.09-7.11 (m, 2H), 6.34 (d, *J* = 10.4 Hz, 1H), 4.10 (d, *J* = 5.6 Hz, 1H), 3.70 (s, 3H), 3.61 (m, 1H), 3.42 (m, 1H), 3.32 (d, *J* = 6.4 Hz, 1H), 3.30-3.31 (m, 2H), 3.11 (t, *J* = 6.0 Hz, 1H), 2.59 (p, *J* = 6.8 Hz, 1H), 1.76 (p, *J* = 6.8 Hz, 2H), 1.22 (d, *J* = 6.8 Hz, 3H); $^{13}$C NMR (100 MHz, $CDCl_3$) $\delta_C$ 189.2, 171.3, 153.3, 137.6, 129.1, 128.3, 127.8, 116.9, 72.9, 55.5, 52.8, 49.2, 48.9, 44.6, 41.2, 27.7, 22.9; IR (neat) 2925, 2096, 1670,1620, 1458, 1211 $cm^{-1}$; MS (ES+) m/z 355.1 ($M+H^+$); HRMS calcd for $C_{19}H_{23}N_4O_3$ ($M+H^+$): 355.1770, found 355.1824.

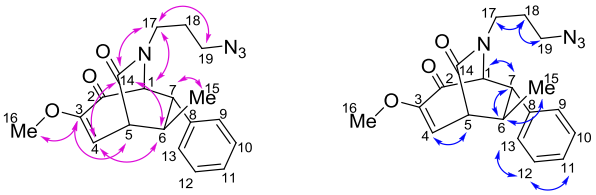

**(*E*)-6-(3-Azidopropyl)-3-methoxy-8-methyl-9-phenyl-6-azabicyclo[3.2.2]non-2-ene-4,7-dione (85)**. Compound **85** was proposed based on the distinctive $^{1}$H and $^{13}$C chemical shift of C1, C5, C14, C17, and C19 in addition to connectivity data derived from HMBC and COSY. C1 appears at 72.9 ppm in the $^{13}$C and the $^{1}$H shows a doublet at 4.10 ppm with an integration of 1.0, consistent with the assignment of C1 as the bridgehead position between two electron withdrawing groups such as nitrogen and an α-methoxy ketone. C5 appears at 48.9 ppm in the $^{13}$C and overlaps with C19 in the $^{1}$H showing a multiplet at 3.30 ppm. This data supports the assignment of C5 as a bridgehead methylene between slight electron withdrawing groups such as an olefin and an amide. C14 appears at 171.3 ppm in the $^{13}$C, typical of a lactam. C17 and C19 appear at 44.6 ppm and 49.2 ppm respectively in the $^{13}$C. C17 appears as a pair of multiplets in the $^{1}$H at 3.61 ppm and 3.42 ppm with an integration of 1.0 each, supporting the assignment of C17 as a methylene with diastereotopic hydrogens adjacent to a heteroatom such as nitrogen. C19 overlaps with C5 in the $^{1}$H, as previously mentioned, appearing at 3.30 ppm as a multiplet. This data plausibly supports C19 as a methylene adjacent to azide. The HMBC supports the retention of the major bicyclic structure through the 3-bond correlations between C3 and C16, C3 and C5, C4 and C6, and C7 and C15. In addition, the HMBC supports the assigned regioisomer of nitrogen insertion with 3-bond

correlations between C4 and C14, C6 and C14, C14 and C17, and C17 and C19. The COSY reaffirms this conclusion by showing the retention of the carbon connectivity throughout the bicycle with correlations between C1, C4, C5, C6, C7, and C15, as well as between C11, C12, and C13. COSY data also shows the retention of the carbon connectivity between C15, C16, and C17.

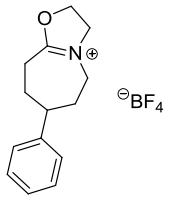


**7-Phenyl-3,5,6,7,8,9-hexahydro-2H-oxazolo[3,2-a]azepin-4-ium tetrafluoroborate salt (87)**. $BF_3 \cdot OEt_2$ (2.87 mL, 22.9 mmol) was added dropwise over 5 min to a solution of 4-phenyl cycohexanone (2.00 g, 11.4 mmol) and 2-azido-1-ethanol (1.50 g, 17.2 mmol) in $CH_2Cl_2$ (60 mL) at 0 °C. Gas evolution appeared upon acid addition. The reaction was warmed to rt, stirred for 12 h and, upon concentration in vacuo, yielded a colorless oil. The crude oil was purified by silica gel column chromatography (10% MeOH/$CH_2Cl_2$) to afford 3.38 g (97%) of **87** as a white solid. $R_f$ = 0.33 (10% MeOH/$CH_2Cl_2$); mp 127.0-128.5 °C; $^1$H NMR (400 MHz, DMSO-d6) $\delta_H$ 7.31-7.35 (m, 2H), 7.22-7.24 (m, 3H), 4.86-4.97 (m, 2H), 4.28 (app q, *J* = 10.0 Hz, 1H), 4.16 (app q, *J* = 10.0 Hz, 1H), 3.78-3.88 (m, 2H), 2.91-3.03 (m, 3H), 1.83-2.03 (m, 4H); $^{13}$C NMR (100 MHz, DMSO-d6) $\delta_c$ 179.1, 146.2, 128.5, 126.4 (2), 72.1, 52.4, 46.4, 45.5, 31.4, 27.6, 25.8; IR (neat) 2985, 1739, 1246, 1047

$cm^{-1}$; MS (ES+) m/z 216.1 ($M^+$); HRMS calcd for $C_{14}H_{18}NO$ ($M^+$): 216.1388, found 216.1377.

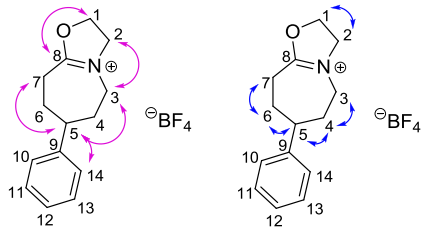

**7-Phenyl-3,5,6,7,8,9-hexahydro-2H-oxazolo[3,2-a]azepin-4-ium tetrafluoroborate salt (87)**. Compound **87** was proposed based on the presence on the presence of a 3-bond correlation between C1 and C8 in addition to the three bond correlation between C2 and C3 in the HMBC. This supports the incorporation of the hydroxyalkyl azide to form a fused bicycle. The COSY reaffirms this conclusion by showing the retention of the expected carbon connectivity between C1 and C2, as well as between C3, C4, C5, C6, and C7. This information is in accordance with similar iminium ethers that were previously synthesized.[105,106]

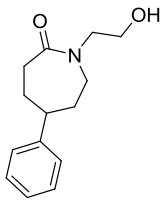

**1-(2-Hydroxyethyl)-5-phenylazepan-2-one (88)**. 1M NaOH solution (1.0 mL) was added to a solution of 7-phenyl-3,5,6,7,8,9-hexahydro-2H-oxazolo[3,2-a]azepin-4-ium tetrafluoroborate salt **20** (100 mg, 0.330 mmol) in $CH_2Cl_2$ (1 mL) and

the biphasic mixture was stirred at rt for 2 h. The reaction was diluted with water (5 mL) and extracted with $CH_2Cl_2$ (3 × 5 mL). The organic extracts were combined, washed with brine (10 mL), dried over anhydrous sodium sulfate, concentrated, and dried to afford 72.4 mg (94%) of **88** as a white solid. $R_f$ = 0.43 (10% MeOH/$CH_2Cl_2$); mp 109.5-110.0 °C; $^1$H NMR (400 MHz, $CDCl_3$) $\delta_H$ 7.26-7.29 (m, 2H), 7.14-7.20 (m, 3H), 3.63-3.76 (m, 5H), 3.51 (dt, *J* = 13.8, 5.2 Hz, 1H), 3.38 (dd, *J* = 15.2, 5.6 Hz, 1H), 2.59-2.78 (m, 3H), 1.97-2.00 (m, 2H), 1.74 (q, *J* = 12.0 Hz, 2H); $^{13}$C NMR (100 MHz, $CDCl_3$) $\delta_C$ 176.7, 145.9, 128.4, 126.5, 126.4, 61.3, 51.5, 50.1, 48.0, 36.3, 35.8, 30.5; IR (neat) 3428, 1616, 1056, 701 cm$^{-1}$; MS (ES+) m/z 234.1 ($M+H^+$); HRMS calcd for $C_{14}H_{20}NO_2$ ($M+H^+$): 234.1494, found 234.1452.

**General procedure for the addition of nucleophiles to tetrafluoroborate salt (87).** Diisopropylethylamine (86.0 μL, 0.495 mmol) was added to a solution of homophthalic anhydride (80.1 mg, 0.495 mmol) in anhydrous acetonitrile (1 mL) and the resulting solution was stirred at rt for 5 min. Iminium ether 7-phenyl-3,5,6,7,8,9-hexahydro-2-H-oxazolo[3,2-a]azepin-4-ium tetrafluoroborate salt (50.0 mg, 0.164 mmol) was added to the solution and the reaction was heated to 80 °C and stirred for 24 h. After cooling to rt, the crude solution was directly analyzed by LCMS and purified by mass-directed fractionation. Additional purification for characterization (if necessary) was completed by $SiO_2$ preparative thin layer chromatography (5:95 MeOH-$CH_2Cl_2$).

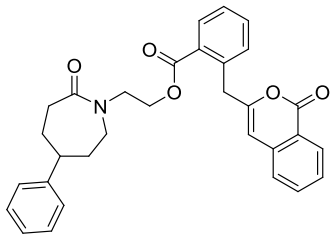

**2-(2-Oxo-5-phenylazepan-1-yl)ethyl-2-((1-oxo-1*H*-isochromen-3-yl)methyl)benzoate (113).** Yellow oil (35.0 mg, 43%); $R_f$ = 0.34, (5% MeOH/$CH_2Cl_2$); $^1$H NMR (400 MHz, $CDCl_3$) $\delta_H$ 8.23 (d, *J* = 8.0 Hz, 1H), 8.03 (dd, *J* = 8.0, 1.2 Hz, 1H), 7.64 (dt, *J* = 7.6, 1.6 Hz, 1H), 7.54 (dt, *J* = 7.6, 1.6 Hz, 1H), 7.37-7.46 (m, 3H), 7.26-7.29 (m, 3H), 7.21 (m, 1H), 7.08-7.10 (m, 2H), 6.16 (s, 1H), 4.47 (t, *J* = 5.8 Hz, 2H), 4.33 (s, 2H), 3.88 (m, 1H), 3.66-3.78 (m, 2H), 3.39 (dd, *J* = 6.2, 1.2 Hz, 1H), 2.72 (tt, *J* = 12.4, 3.4 Hz, 1H), 2.61-2.67 (m, 2H), 1.92-2.01 (m, 2H), 1.63-1.80 (m, 2H); $^{13}$C NMR (100 MHz, $CDCl_3$) $\delta_C$ 175.5, 166.7, 162.7, 156.6, 145.9, 137.5, 137.4, 134.7, 132.6, 132.1, 131.1, 129.4, 129.3, 128.5, 127.7, 127.5, 126.6, 126.5, 125.3, 120.1, 103.9, 62.9, 49.9, 48.1, 47.4, 37.6, 36.4, 36.1, 30.7; IR (neat) 1724, 1652, 1487, 1257, 1134 cm$^{-1}$; MS (ES+) m/z 496.2 (M+H$^+$); HRMS calcd for $C_{31}H_{30}NO_5$ (M+H$^+$): 496.2046, found 496.1951.

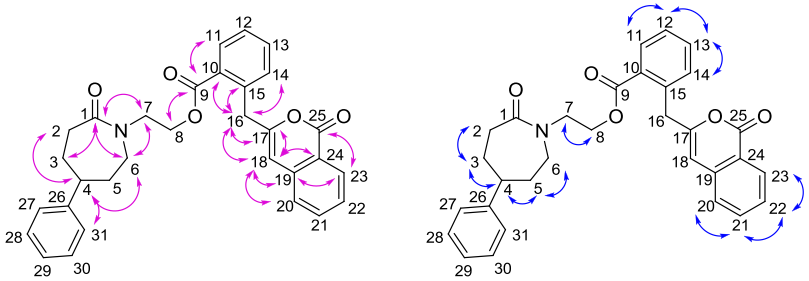

**2-(2-Oxo-5-phenylazepan-1-yl)ethyl-2-((1-oxo-1H-isochromen-3-yl)methyl)benzoate (113).** Compound **113** was proposed based on the distinctive $^{1}H$ and $^{13}C$ data for C8, C16, and C18 in addition to connectivity data derived from HMBC and COSY. C8 appears at 62.9 ppm in the $^{13}C$ and the $^{1}H$ shows a triplet at 4.47 ppm with an integration of 2.0. This evidence supports the assignments of C8 as a methylene adjacent to a heteroatom, such as oxygen. C16 appears at 37.6 ppm in the $^{13}C$ and the $^{1}H$ shows a sharp singlet at 4.33 ppm with an integration of 2.0, consistent with a benzylic methylene. Additionally, C18 appears at 103.9 ppm in the $^{13}C$ and the $^{1}H$ shows a sharp singlet at 6.16 ppm with an integration of 1.0, consistent with a conjugated tri-substituted olefin. Distinctive 3-bond correlations in the HMBC map through the extended structure of the side chain to give the proposed atom placement. Key connections include C8 to C9, C10 to C16, C16 to C18, C18 to C20, C18 to C24, C19 to C23, and C23 to C25. Important 2-bond HMBC correlations include C16 to C17, C17 to C18, and C18 to C19. The COSY reaffirms the proposed structure by showing the retention of the expected carbon connectivity between C7 and C8, as well as between C2, C3, C4, C5, and C6. In addition, the COSY data was vital in distinguishing the atoms of the aromatic rings of the side chain. Important connections exist between C11, C12, C13, and C14, as well as between C20, C21, C22, and C23. This information is in accordance with similar products derived from reactions of homophthalic anhydride.[105]

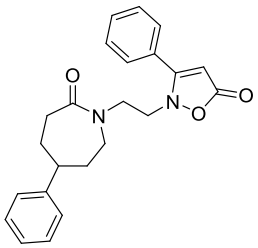

**2-(2-(2-Oxo-5-phenylcycloheptyl)ethyl)isoxazole-5(2*H*)-one (114)**.

Synthesized according to the general procedure where 3-phenyl-5-isoxazolone (79.7 mg, 0.495 mmol) was substituted for homophthalic anhydride. Clear oil (47.5 mg, 87%); $R_f$ = 0.41, (5% MeOH/$CH_2Cl_2$); $^1$H NMR (400 MHz, $CDCl_3$) $\delta_H$ 7.42-7.54 (m, 5H), 7.24-7.27 (m, 2H), 7.17 (m, 1H), 7.10-7.12 (m, 2H), 5.44 (s, 1H), 3.79-3.90 (m, 2H), 3.60-3.73 (m, 2H), 3.48 (m, 1H), 3.33 (dd, *J* = 15.1, 5.4 Hz, 1H), 2.71 (tt, *J* = 12.0, 3.6 Hz, 1H), 2.54 (m, 2H), 1.97 (m, 2H), 1.62-1.73 (m, 2H); $^{13}$C NMR (100 MHz, $CDCl_3$) $\delta_C$ 175.4, 170.5, 169.2, 145.7, 131.7, 129.3, 128.5, 127.5, 126.9, 126.5, 126.4, 90.9, 51.8, 50.8, 47.9, 47.1, 36.3, 35.9, 30.5; IR (neat) 2927, 1737, 1643, 1490, 1450, 761, 700 cm$^{-1}$; MS (ES+) m/z 377.1 ($M+H^+$); HRMS calcd for $C_{23}H_{25}N_2O_3$ ($M+H^+$): 377.1991, found 377.1700.

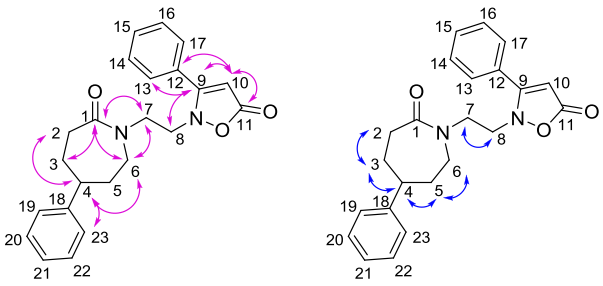

**2-(2-(2-Oxo-5-phenylcycloheptyl)ethyl)isoxazole-5(2H)-one (114)**.

Compound **114** was proposed based on the distinctive $^1$H and $^{13}$C chemical shifts of

C8 and C10 in addition to connectivity data derived from HMBC and COSY. C8 appears at 51.8 ppm in the $^{13}C$ and the $^{1}H$ shows a pair of multiplets at 3.79-3.90 ppm and 3.60-3.73 ppm suggesting C8 to be a methylene with diastereotopic hydrogens adjacent to a heteroatom, such as nitrogen. C10 appears at 90.9 ppm, in the $^{13}C$ and the $^{1}H$ shows as a sharp singlet at 5.44 ppm with an integration of 1.0, this data supports the assignment of C10 as a carbon of the tri-substituted olefin. Additionally, the presence of two characteristic 3-bond HMBC correlations to C9 further supports the proposed structure. First, the correlation between C9 and C13 suggests that C9 (169.2 ppm) is the isoxazolone carbon α to nitrogen and not the carbon of ester. Second, the correlation between C9 and C8 suggests that the isoxazolone ring is connected to the parent amide through a carbon-nitrogen bond to C8. The COSY reaffirms this conclusion by showing the retention of the expected carbon connectivity between C7 and C8, as well as between C2, C3, C4, C5, and C6.

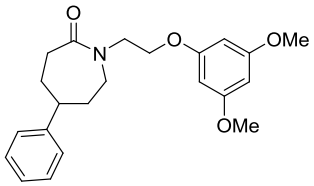


**1-(2-(3,5-Dimethoxyphenoxy)ethyl)-5-phenylazepan-2-one) (115).**

Synthesized according to the general procedure where 3,5-dimethoxyphenol (76.3 mg, 0.495 mmol) was substituted for homophthalic anhydride. Yellow oil (17.4 mg, 29%); $R_f$ 0.81, (10% MeOH/$CH_2Cl_2$); $^{1}H$ NMR (400MHz, $CDCl_3$) $\delta_H$ 7.26-7.29 (m, 2H), 7.19 (m, 1H), 7.11-7.13 (m, 2H), 6.10 (m, 1H), 6.07-6.08 (m, 2H), 4.08-4.17 (m,

2H), 3.85 (m, 1H), 3.78-3.71 (m, 2H), 3.75 (s, 6H), 3.53 (ddd, *J* = 15.6, 6.0, 1.2 Hz, 1H), 2.74 (tt, *J* = 12.4, 3.6 Hz, 1H), 2.62-2.69 (m, 2H), 1.96-2.04 (m, 2H), 1.66-1.85 (m, 2H); $^{13}$C NMR (100 MHz, $CDCl_3$) $\delta_C$ 175.4, 161.6, 160.4, 146.2, 128.6, 126.7, 126.5, 93.3, 93.2, 66.9, 55.3, 50.8, 48.6, 48.2, 36.6, 36.0, 30.8; IR (neat) 2935, 1645, 1600,1477, 1454, 1203, 1193, 1151, 1068 $cm^{-1}$; MS (ES+) m/z 370.1 ($M+H^+$); HRMS calcd for $C_{22}H_{28}NO_4$ ($M+H^+$): 370.1940, found 370.2029.

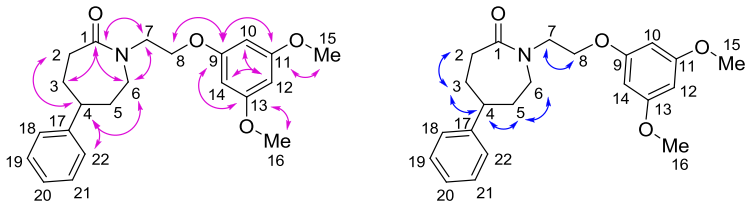

**1-(2-(3,5-Dimethoxyphenoxy)ethyl)-5-phenylazepan-2-one) (115).**

Compound **115** was proposed based on the distinctive $^1$H and $^{13}$C chemical shifts of C8, C9, C10, C11, and C12 in addition to connectivity data derived from HMBC and COSY. C8 appears at 66.9 ppm in the $^{13}$C and the $^1$H shows a multiplet at 4.08-4.17 ppm with an integration of 2.0. This evidence supports the assignment of C8 as a methylene adjacent to a heteroatom, such as oxygen. C9 and C11 appear at 160.4 ppm and 161.6 ppm in the $^{13}$C, respectively, typical of *O*-substituted methoxyphenols. C10 and C12 appear at 93.2 ppm and 93.3 ppm in the $^{13}$C and at 6.08 ppm and 6.10ppm in the $^1$H respectively, data typical of symmetrical *O*-substituted methoxyphenols. The 3-bond HMBC correlations of C8 and C11 with C9 support the presence of an ether linkage between C8 and C9 connecting the parent amide to the phenol. The COSY reaffirms this conclusion by showing retention of the expected

connectivity of the parent amide between C7 and C8, as well as between C2, C3, C4, C5, and C6.

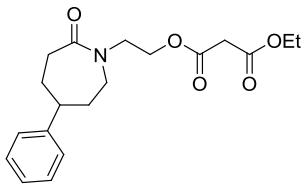


**Ethyl 2-(2-oxo-5-phenylazepan-1-yl)ethyl malonate (116).** Synthesized according to the general procedure except diethylmalonate (75.0 μL, 0.495 mmol) was substituted for homophthalic anhydride. Yellow oil (13.0 mg, 23% yield); $R_f$ = 0.24 (66% Hex/EtOAc); $^1$H NMR (400 MHz, $CDCl_3$) $\delta_H$ 7.16-7.32 (m, 5H), 4.27-4.37 (m, 2H), 4.17 (q, *J* = 7.2 Hz, 2H), 3.61-3.78 (m, 3H), 3.41 (m, 1H), 3.37 (s, 2H), 2.75 (tt, *J* = 12.4, 3.6 Hz, 1H), 2.64-2.68 (m, 2H), 1.98-2.03 (m, 2H), 1.62-1.80 (m, 2H), 1.25 (t, *J* = 7.2 Hz, 3H); $^{13}$C NMR (125 MHz, $CDCl_3$) $\delta_C$ 175.5, 166.4, 166.3, 146.0, 128.6, 126.8, 126.5, 63.8, 61.6, 50.1, 48.2, 47.4, 41.5, 36.5, 36.2, 30.6, 14.1; IR (neat) 2927, 1751, 1731, 1647, 1031 cm$^{-1}$; MS (ES+) m/z 348.2 (M+H$^+$); HRMS calcd for $C_{19}H_{26}NO_5$ (M+H$^+$): 348.1733, found 348.1578.

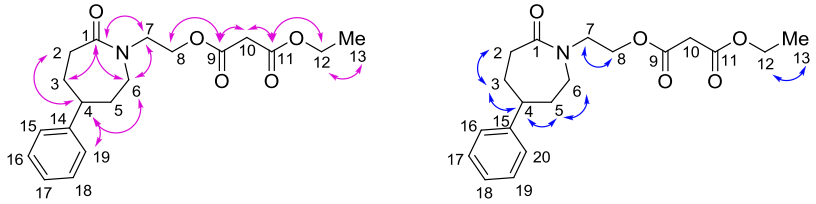


**Ethyl 2-(2-oxo-5-phenylazepan-1-yl)ethyl malonate (116).** Compound **116** was proposed based on the distinctive $^1$H and $^{13}$C data for C8 and C10 in addition to

connectivity data derived from HMBC and COSY. C8 appears at 63.8 ppm in the $^{13}C$ and the $^{1}H$ shows a multiplet at 4.27-4.37 ppm with an integration of 2.0. This evidence supports the assignment of C8 as a methylene adjacent to a heteroatom, such as oxygen. C10 appears at 41.5 ppm in the $^{13}C$ and in the $^{1}H$ shows a sharp singlet at 3.37 ppm with an integration of 2.0. This evidence supports the assignment of C10 as the α methylene of the malonate. The 3-bond HMBC correlations between C8 and C9 along with the 2-bond HMBC correlations of C9 and C11 with C10 support the connection of the parent amide to malonate through an ester bond with C8. The COSY reaffirms this conclusion by showing retention of the expected connectivity of the parent amide between C7 and C8, as well as between C2, C3, C4, C5, and C6. In addition, the COSY correlation between C12 and C13 shows the retention of one ethyl ester from the parent diethyl malonate.

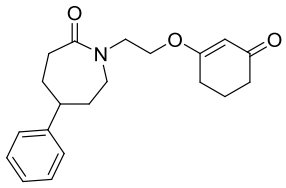


**1-(2-(3-Oxocyclohex-1-enyloxy)ethyl)-5-phenylazepan-2-one (117).**

Synthesized according to the general procedure where 1,3-cyclohexadione (55.4 mg, 0.495 mmol) was substituted for homophthalic anhydride. Yellow oil (30.2 mg, 58%); $R_f$ = 0.38, (5% MeOH/$CH_2Cl_2$); $^{1}H$ NMR (400 MHz, $CDCl_3$) $\delta_H$ 7.25-7.30 (m, 2H), 7.20 (m, 1H), 7.12-7.14 (m, 2H), 5.35 (s, 1H), 3.98 (t, *J* = 5.2 Hz, 2H), 3.68-3.81 (m, 3H), 3.43 (m, 1H), 2.74 (t, *J* = 3.6 Hz, 1H), 2.63-2.67 (m, 2H), 2.31-2.40 (dt, *J* =

20.8, 6.4 Hz, 4H), 1.92-2.03 (m, 4H), 1.63-1.77 (m, 2H); $^{13}$C NMR (100 MHz, $CDCl_3$) $\delta_C$ 199.4, 177.1, 175.4, 145.9, 128.6, 126.5 (2), 103.0, 66.9, 50.4, 48.0, 47.6, 36.6, 36.4, 36.1, 30.6, 28.9, 21.1; IR (neat) 1639,1180 $cm^{-1}$; MS (ES+) m/z 328.1 ($M+H^+$); HRMS calcd for $C_{20}H_{26}NO_3$ ($M+H^+$): 328.1834, found 328.1878.

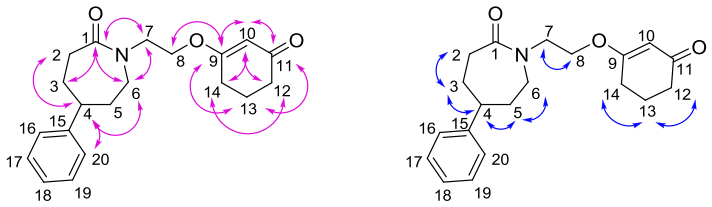

**1-(2-(3-Oxocyclohex-1-enyloxy)ethyl)-5-phenylazepan-2-one (117).**

Compound **117** was proposed based on the distinctive $^1$H and $^{13}$C chemical shifts of C8 and C10 in addition to connectivity data derived from HMBC and COSY. C8 appears at 66.9 ppm in the $^{13}$C and the $^1$H shows a triplet at 3.98 ppm with an integration of 2.0. This evidence supports the assignment of C8 as a methylene adjacent to a heteroatom, such as oxygen. C10 appears at 103 ppm, in the $^{13}$C and the $^1$H shows a sharp singlet at 5.35 ppm with an integration of 1.0, suggesting the identity of C10 as the α-carbon of an enol ether. The 3-bond HMBC correlations between C8 and C9, in addition to the 2-bond HMBC correlations of C9 and C11 with C10 support the connection of the diketone to the parent amide through an enol ether bond to C8. The COSY reaffirms this conclusion by showing retention of the expected carbon connectivity of the parent amide between C7 and C8, as well as between C2, C3, C4, C5, and C6. In addition the carbon connectivity of the diketone was retained between C12, C13, and C14.

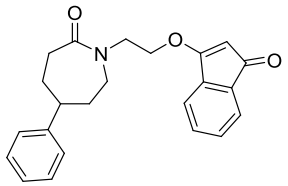

**1-(2-(1-Oxo-1*H*-inden-3-yloxy)ethyl)-5-phenylazepan-2-one (118).**

Synthesized according to the general procedure where 1,3-indanedione (72.3 mg, 0.495 mmol) was substituted for homophthalic anhydride. Yellow oil (14.8 mg, 25%); $R_f$ = 0.50, (5% MeOH/$CH_2Cl_2$); $^1$H NMR (400 MHz, $CDCl_3$) $\delta_H$ 7.48 (m, 1H), 7.33-7.38 (m, 2H), 7.26-7.29 (m, 2H), 7.21-7.23 (m, 2H), 7.10-7.12 (m, 2H), 5.11, (s, 1H), 4.32-4.42 (m, 2H), 3.91-3.94 (m, 2H), 3.83 (dd, *J* = 15.2, 10.4 Hz, 1H), 3.55 (ddd, *J* = 8.8, 6.4, 1.2 Hz, 1H), 2.79 (t, *J* = 3.6 Hz, 1H), 2.65-2.73 (m, 2H), 2.01-2.10 (m, 2H), 1.72-1.85 (m, 2H); $^{13}$C NMR (100 MHz, $CDCl_3$) $\delta_C$ 194.5, 178.4, 175.7, 145.8, 139.3, 133.1, 132.2, 130.4, 128.6, 126.6, 126.5, 121.3, 118.5, 96.9, 70.5, 50.8, 48.1 (2), 36.5, 36.1, 30.7; IR (neat) 1697, 1637, 1618, 1562, 754 cm$^{-1}$; MS (ES+) m/z 362.1 (M+H$^+$); HRMS calcd for $C_{23}H_{24}NO_3$ (M+H$^+$): 362.1678, found 362.1725.

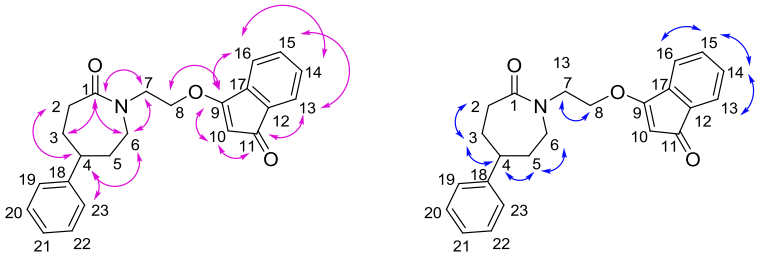

**1-(2-(1-Oxo-1*H*-inden-3-yloxy)ethyl)-5-phenylazepan-2-one (118).**

Compound **118** was proposed based on the distinctive $^1$H and $^{13}$C chemical shifts of

C8 and C10 in addition to connectivity data derived from HMBC and COSY. C8 appears at 70.5 ppm in the $^{13}C$ and the $^{1}H$ shows a multiplet at 4.32-4.42 ppm with an integration of 2.0. This evidence supports the assignment of C8 as a methylene adjacent to a heteroatom, such as oxygen. C10 appears at 96.9 ppm, in the $^{13}C$ and the $^{1}H$ shows as a sharp singlet at 5.11 ppm with an integration of 1.0. This data supports the identity of C10 as the α-carbon of an enol ether in conjugation with the aromatic ring. The 3-bond HMBC correlations of C8 and C17 with C9, as well as 2-bond HMBC correlations of C9 and C11 with C10 support the connection of the diketone to the parent amide through the presence of an enol ether bond to C8. The COSY reaffirms this conclusion by showing retention of the expected carbon connectivity of the parent amide between C7 and C8, as well as between C2, C3, C4, C5, and C6. In addition the carbon connectivity of the diketone was retained between C13, C14, C15 and C16.

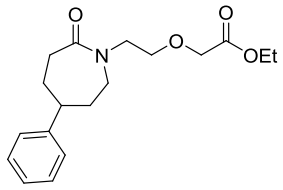


**Ethyl 2-(2-(2-oxo-5-phenylazepan-1-yl)ethoxy)acetate (119).** Synthesized according to the general procedure where ethyl bromoacetate (55.0 μL, 0.495 mmol) was substituted for homophthalic anhydride. Clear oil (3.8 mg, 7%); $R_f$ = 0.84, (66% Hex/EtOAc); $^{1}$NMR (500 MHz, $CDCl_3$) 7.75-7.30 (m, 2H), 7.17-7.21 (m, 3H), 4.62 (dt, *J* = 11.5, 3.0 Hz, 1H), 4.13 (q, *J* = 7.5 Hz, 2H), 3.92 (d, *J* = 11.0 Hz, 1H), 3.45 (d,

*J* = 17.5 Hz, 1H), 3.32 (dd, *J* = 17.5, 1.0 Hz, 1H), 3.06 (m, 1H), 2.86-2.95 (m, 3H), 2.76 (m, 1H), 2.49 (m, 1H), 2.37 (m, 1H), 2.11 (m, 1H), 1.82 (m, 1H), 1.72 (m, 1H), 1.61 (m, 1H), 1.24 (t, *J* = 7.0 Hz, 3H); $^{13}$C NMR (125 MHz, $CDCl_3$) $\delta_C$ 173.7, 171.6, 147.0, 128.4, 127.7, 126.0, 63.8, 60.3, 55.1, 53.4, 52.6, 39.7, 33.9 (2), 30.3, 14.3; IR (neat) 1731, 1633, 1454, 1195, 1029, 702 cm$^{-1}$; MS (ES+) m/z 320.2 ($M+H^+$); HRMS calcd for $C_{18}H_{26}NO_4$ ($M+H^+$): 320.1784, found 320.1788.

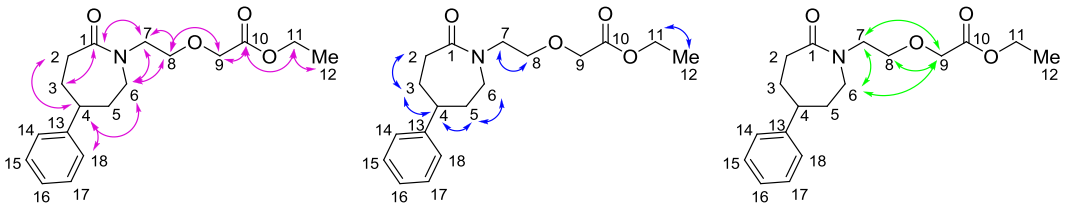

**Ethyl 2-(2-(2-oxo-5-phenylazepan-1-yl)ethoxy)acetate (119).** Compound **119** was proposed based on the distinctive $^1$H and $^{13}$C data for C8, C9, and C10 in addition to connectivity data derived from HMBC and COSY. C8 appears at 53.4 ppm in the $^{13}$C and the $^1$H shows a pair of triplets at 3.00 ppm and 2.95 ppm. C9 appears at 55.1 ppm in the $^{13}$C and the $^1$H shows a pair of doublets at 3.45 ppm and 3.52 ppm. C 10 appears at 173.7 ppm in the $^{13}$C, consistent with an α-alkoxy ester. The 3-bond HMBC correlations between C8 and C9, as well as the 2-bond HMBC correlations between C7 and C8, and C9 and C10 support the connection of the ethyl ester to the parent amide through the presence of an ether linkage of C8 and C9. The COSY reaffirms this conclusion by showing retention of the expected carbon connectivity of the parent amide between C7 and C8, as well as between C2, C3, C4,

C5, and C6. In addition the carbon connectivity of the ethyl ester was retained between C11 and C12.

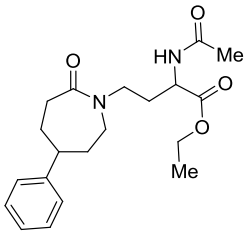


**Ethyl 2-acetamido-4-(2-oxo-5-phenylazepan-1-yl)butanoate (120).** Iminium ether 7-phenyl-3,5,6,7,8,9-hexahydro-2-H-oxazolo[3,2-a]azepin-4-ium tetrafluoroborate salt **87** (50.0 mg, 0.160 mmol) was added to a solution of ethyldiazoacetate (52.0 μL, 0.160 mmol) in anhydrous acetonitrile (1 mL). The resulting solution was sealed in a pressure tube and stirred at 135 °C for 24 h. After cooling to rt, the crude material was directly analyzed by LCMS and purified by mass-directed fractionation to afford 15.0 mg (13%) of **120** as a yellow oil. The product slowly decomposed upon purification under acidic conditions and the corresponding NMR appeared as a mixture of rotamers in an approximate 1:1 ratio, as estimated by $^{13}$C NMR. $R_f$ = 0.38, (5% MeOH/$CH_2Cl_2$); $^1$H NMR (500 MHz, $CDCl_3$) $\delta_H$ 7.28-7.32 (m, 2H), 7.19-7.24 (m, 1H), 7.15-7.16 (m, 2H), 4.04-4.25 (m, 4H), 3.62-3.78 (m, 2H), 3.55 (t, *J* = 7.0 Hz, 1H), 3.29-3.46 (m, 2H), 2.76 (m, 1H), 2.55-2.67 (m, 2H), 2.23 (s, 1H), 2.02 (s, 2H), 1.96-2.08 (m, 1H), 1.62-1.81 (m, 4H), 1.28 (dt, *J* = 12.5, 7.0 Hz, 3H); $^{13}$C NMR (125 MHz, $CDCl_3$) $\delta_C$ 175.7, 175.6*, 171.4, 171.3*, 169.4, 169.4*, 146.0, 145.7*, 128.7*, 128.6, 126.7, 126.6*, 126.6*, 126.5, 61.7, 61.3*, 50.7, 50.4* 49.4*, 48.2, 48.1*, 48.0, 47.9*, 47.7, 45.4*, 44.7, 36.5, 36.5*,

36.3*, 36.0, 30.8, 30.6*, 21.5, 21.0*, 14.2*, 14.1; IR (neat) 2931, 1743, 1645, 1205, 1029 $cm^{-1}$; MS (ES+) m/z 361.2 ($M+H^+$); HRMS calcd for $C_{20}H_{29}N_2O_4$ ($M+H^+$): 361.2049, found 361.2122.

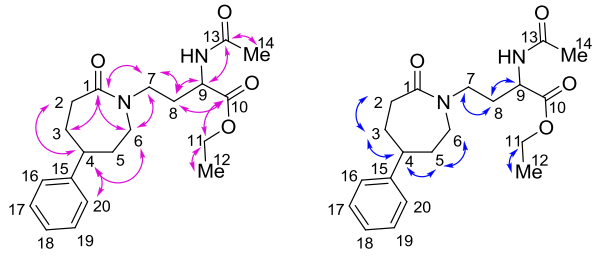

**Ethyl 2-acetamido-4-(2-oxo-5-phenylazepan-1-yl)butanoate (120).** Compound **120** was proposed based on the distinctive $^1H$ and $^{13}C$ chemical shift of C9 in addition to connectivity data derived from HMBC and COSY. C9 appears at 47.7 ppm in the $^{13}C$ and the $^1H$ shows a clear triplet at 3.55 ppm with an integration of 1.0, suggesting C9 to be adjacent to a methylene in addition to a proximity to electron withdrawing groups such as nitrogen and an ester. The HMBC gives critical information regarding the position of C9, showing a 3-bond correlation between C9 and C13, and a 2-bond correlation between C8 and C9. Further connectivity is established through the key 3-bond correlations between C1 and C7, C6 and C7, C8 and C10, and C10 and C11. Key 2-bond correlations occur between C7 and C8, C8 and C9, C11 and C12, and C13 and C14. The COSY reaffirms this conclusion by showing the retention of the expected carbon connectivity of between C2, C3, C4, C5 and C6. COSY correlations between C7, C8, and C9 are in accordance with the

proposed carbon-carbon bond formation at C8, and the correlation between C11 and C12 shows retention of the ethyl ester of the starting ethyl diazoacetate compound.

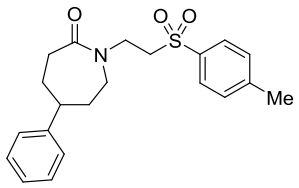


**5-Phenyl-1-(2-tosylethyl)azepan-2-one (121).** Method A: Synthesized according to the general procedure except *p*-toluenesulfonylmethyl isocyanate (96.5 mg, 0.495 mmol) was substituted for homophthalic anhydride, clear oil (24.3 mg, 40%). Method B: Thioether phenyl-1-(2-(*p*-tolythio)ethyl)azepan-2-one **122** (13.4 mg, 0.0395 mmol) was dissolved in $CCl_4$ (2 mL) and *m*-CPBA (20.4 mg, 0.118 mmol), was added to the solution at 0 °C. The mixture was warmed to rt and stirred for 5 h. The reaction was quenched by the addition of 10% sodium sulfite solution and was diluted with $CH_2Cl_2$, and extracted (3 × 10 mL). The organic extracts were collected, washed with brine, dried over anhydrous $Na_2SO_2$, and reduced to give a yellow oil. The crude material was purified by $SiO_2$ preparative thin layer chromatography (66% Hex/EtOAc) to afford 14.5 mg (99%) of **121** as a clear oil. $R_f$ = 0.32, (66% Hex/EtOAc); $^1$H NMR (500 MHz, $CDCl_3$) $\delta_H$ 7.79-7.81 (m, 2H), 7.37 (d, *J* = 8.0 Hz, 2H), 7.29 (t, *J* = 7.5 Hz, 2H), 7.21 (tt, *J* = 7.0, 1.5 Hz, 1H), 7.13-7.15 (m, 2H), 3.91 (ddd, *J* = 13.5, 7.5, 5.5 Hz, 1H), 3.61-3.69 (m, 2H), 3.40-3.49 (m, 2H), 3.33 (ddd, *J* = 13.5, 7.5, 5.5 Hz, 1H), 2.72 (tt, *J* = 12.0, 3.5 Hz, 1H), 2.56-2.58 (m, 2H), 2.45 (s, 3H), 1.94-2.04 (m, 2H), 1.65-1.73 (m, 2H); $^{13}$C NMR (125 MHz,

$CDCl_3$) $\delta_C$ 175.5, 145.8, 144.9, 136.2, 129.9, 128.6, 127.8, 126.6, 126.5, 54.0, 50.5, 48.1, 43.6, 36.4, 36.1, 30.5, 21.7; IR (neat) 2925, 1643, 1299, 1145 $cm^{-1}$; MS (ES+) m/z 372.1 ($M+H^+$); HRMS calcd for $C_{21}H_{26}NO_3S$ ($M+H^+$): 372.1555, found 372.1485.

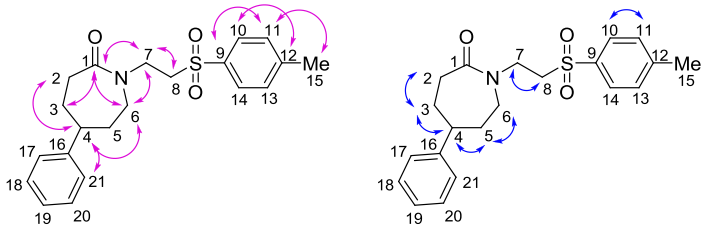

**5-Phenyl-1-(2-tosylethyl)azepan-2-one (121).** Compound **121** was proposed based on the distinctive $^1H$ and $^{13}C$ chemical shift of C8 in addition to connectivity data derived from HMBC and COSY. C8 appears at 54.0 ppm in the $^{13}C$ and the $^1H$ shows a pair of multiplets at 3.40-3.49 ppm and 3.33 ppm suggesting C8 to be a methylene with diastereotopic hydrogens adjacent to a heteroatom, like a sulfoxide group. Additionally, the HMBC spectrum shows two distinct regions of connectivity within the molecule. The 3-bond correlations between C11 and C15, C10 and C11, as well as C9 and C11 suggest the retention of *p*-toluenesulfonyl methyl moiety. The 2-bond correlation between C7 and C8, in addition to the 3-bond correlations between C1 and C7, and C6 and C7 suggest attachment of the *p*-toluenesulfonyl methyl group to C8. The COSY reaffirms this conclusion by showing the retention of the expected carbon connectivity between C7 and C8, as well as between C2, C3, C4, C5, and C6. COSY data was also present for the *p*-toluenesulfonyl methyl group between C10 and C11.

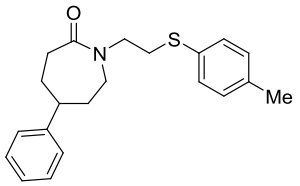


**5-Phenyl-1-(2-(*p*-tolythio)ethyl)azepan-2-one (122).** To a solution of potassium hydride (10.0 mg, 0.247 mmol) in anhydrous DMF (1.0 mL) was added a solution of 4-methylbenzenethiol (30.7 mg, 0.247 mmol) in anhydrous DMF (0.5 mL). The mixture was stirred at rt for 5 min and iminium ether 7-phenyl-3,5,6,7,8,9-hexahydro-2-H-oxazolo[3,2-a]azepin-4-ium tetrafluoroborate salt **87** (25.0 mg, 0.0824 mmol) was added to the flask. The reaction mixture was stirred at 80 °C for 24 h. After cooling, the solution was diluted with water and extracted with diethyl ether (3 × 10 mL). The organic extracts were combined, washed with brine, dried over anhydrous $Na_2SO_4$, and reduced to give a yellow oil. The crude material was purified by silica gel preparative thin layer chromatography (66% Hex/EtOAc) to afford 26.3 mg (94%) of **122** as a clear oil. $R_f$ = 0.61, (66% Hex/EtOAc); $^1$H NMR (400 MHz, $CDCl_3$) 7.28-7.32 (m, 4H), 7.20 (m, 1H), 7.11-7.15 (m, 4H), 3.60-3.74 (m, 2H), 3.52 (m, 1H), 3.29 (dd, *J* = 14.4, 6.4 Hz, 1H), 3.10 (t, *J* = 6.8 Hz, 2H), 2.72 (tt, *J* = 12.0, 3.6 Hz, 1H), 2.60-2.63, (m, 2H), 2.31 (s, 3H), 1.98-2.01 (m, 2H), 1.68-1.79 (m, 2H); $^{13}$C NMR (100 MHz, $CDCl_3$) $\delta_C$ 175.3, 146.0, 136.2, 131.8, 129.8, 129.6, 128.6, 126.6, 126.5, 50.1, 48.8, 48.2, 36.5, 36.4, 32.0, 30.6, 20.9; IR (neat) 2921, 1645, 1492, 1450,1419, 1176, 700 cm$^{-1}$; MS (ES+) m/z 340.2 (M+H$^+$); HRMS calcd for $C_{21}H_{26}NOS$ (M+H$^+$): 340.1735, found 340.1745.

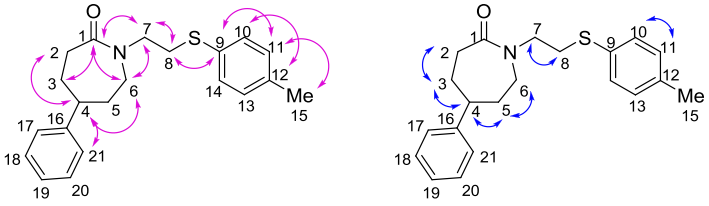


**5-Phenyl-1-(2-(*p*-tolythio)ethyl)azepan-2-one (122).** Compound **122** was proposed based on the distinctive $^{1}H$ and $^{13}C$ chemical shift of C8 in addition to connectivity data derived from HMBC and COSY. C8 appears at 32.0 ppm in the $^{13}C$ and the $^{1}H$ shows a triplet at 3.10 ppm suggesting C8 to be a methylene adjacent to a heteroatom, such as sulfur. Additionally, the HMBC spectrum shows two distinct regions of connectivity within the molecule. The 3-bond correlations between C11 and C15, C10 and C12, as well as C9 and C11 supports the retention of the 4-methylthiobenzene moiety. The 2-bond correlation between C7 and C8, in addition to the 3-bond correlations between C1 and C7, and C6 and C7 suggest attachment of the 4-methylthiobenzene group to C8. The COSY reaffirms this conclusion by showing the retention of the expected carbon connectivity between C7 and C8, as well as between C2, C3, C4, C5, and C6. COSY data was also present for the 4-methylthiobenzene group between C10 and C11.

**Control reaction: synthesis of 1-(benzylsulfonyl)-4-methylbenzene.**

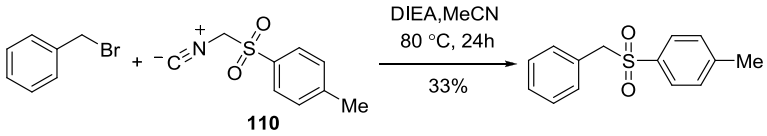


Diisopropylethylamine (0.113 mL, 0.650 mmol) was added to a solution of *p*-toluenesulfonylmethyl isocyanate (127 mg, 0.650 mmol) in anhydrous acetonitrile (1 mL) and the resulting solution was stirred at rt for 5 min. Benzylbromide (20.0 μL, 0.216 mmol) was added to the solution and the reaction was heated to 80 °C and stirred for 24 h. After cooling to rt, the crude solution was directly analyzed by LCMS and purified by mass-directed fractionation. Additional purification was completed with $SiO_2$ preparative thin layer chromatography (20% EtOAc/Hex) to afford 17.4 mg, (33%) as a white solid. The observed characterization data matched that previously reported.[106] $R_f$ = 0.34 (20% EtOAc/Hex); mp 141.0-142.0 °C ; $^1$H NMR (400 MHz, $CDCl_3$) $\delta_H$ 7.40-7.42 (d, *J* = 8.4 Hz, 2H), 7.13-7.24 (m, 5H), 6.98-7.01 (d, *J* = 8.4 Hz, 2H), 4.20 (s, 2H), 2.33 (s, 3H); $^{13}$C NMR (100 MHz, $CDCl_3$) $\delta_C$ 144.6, 134.9, 130.8, 129.4, 128.6, 128.5, 128.3, 128.1, 62.9, 21.6; IR (neat) 2923, 1301, 1128, 783 $cm^{-1}$; MS (ES+) m/z 247.1 ($M+H^+$); HRMS calcd for $C_{14}H_{15}O_2S$ ($M+H^+$): 247.0793, found 247.0803.

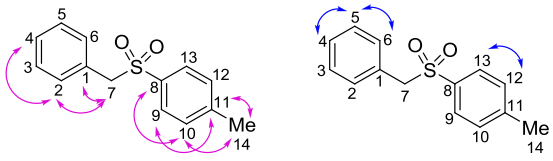

**1-(Benzylsulfonyl)-4-methylbenzene.** This compound was proposed based on the distinctive $^{1}H$ and $^{13}C$ chemical shift of C7 in addition to connectivity data derived from HMBC and COSY. C7 appears at 62.9 ppm in the $^{13}C$ and the $^{1}H$ shows a sharp singlet at 4.20 ppm suggesting C7 to be a benzylic methylene adjacent to a heteroatom, such as sulfoxide. Additionally, the HMBC spectrum shows two distinct regions of connectivity within the molecule. The 3-bond correlations between C8 and C10, C9 and C11, and C10 and C14, in addition to the 2-bond correlation between C11 and C14 suggest the presence of *p*-toluenesulfonyl methyl moiety. The 2-bond correlation between C1 and C7, and the 3-bond correlations between C2 and C4, and C2 and C7 suggest attachment of the 4-methylthiobenzene group to C7. The COSY reaffirms this conclusion by showing the retention of the expected carbon connectivity between the benzylic and *p*-toluenesulfonyl methyl regions of the molecule with correlations between C4, C5, and C6, as well as between C12 and C13.

**General procedure for the addition of nucleophiles to bicyclic iminium ether triflate salt.** Diisopropylethylamine (112.0 μL, 0.650 mmol) was added to a solution of homophthalic anhydride (105 mg, 0.650 mmol) in anhydrous acetonitrile (2 mL) and the resulting solution was stirred at rt for 5 min. Bicyclic iminium ether **67** (100.0 mg, 0.216 mmol) was added to the solution and the reaction was heated to 80 °C and stirred for 24 h. After cooling to rt, the crude solution was directly analyzed by LCMS and purified by mass-directed fractionation. Additional purification for characterization (if necessary) was completed by silica gel preparative

thin layer chromatography (5% MeOH/$CH_2Cl_2$). Alternatively, some reactions were similarly completed on a 0.216 mmol scale using proportional amounts of the necessary reagents.

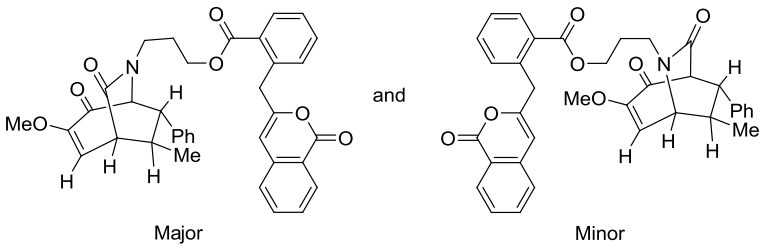


**(*E*)-3-(3-Methoxy-8-methyl-4,7-dioxo-9-phenyl-6-azabicyclo[3.2.2]non2-en-6-yl)propyl 2-((1-oxo-1*H*-isochromen-3-yl)methyl)benzoate (123a) and (*E*)-3-(3-methoxy-9-methyl-2,7-dioxo-8-phenyl-6-azabicyclo[3.2.2]non-3-en-6-yl)propyl-2-((1-oxo-1*H*-isochromen-3-yl)mehtyl)benzoate (123b).** Clear oil (32.6 mg, 25% as an inseparable mixture of regioisomers); $R_f$ = 0.25 (66% Hex/EtOAc); $^1$NMR (400 MHz, $CDCl_3$) $\delta_H$ 8.21 (dd, *J* = 8.0, 0.4 Hz, 1H), 8.02 (dd, *J* = 8.0, 1.2 Hz, 1H), 7.61 (dt, *J* = 7.6, 1.2 Hz, 1H), 7.51 (dt *J* = 7.6, 1.2 Hz, 1H), 7.36-7.43 (m, 3H), 7.21-7.29 (m, 4H), 7.10 (m, 2H), 7.02* (m, 0.46), 6.42* (d, *J* = 9.2 Hz, 0.23H) 6.33 (d, *J* = 10.4 Hz, 1H), 6.11 (s, 1H), 6.09* (s, 0.23H), 4.29 (s, 2H), 4.21-4.32 (m, 2H), 4.11 (d, *J* = 5.6 Hz, 1H), 3.91* (d, *J* = 4.8 Hz, 0.23H), 3.88* (m, 0.23H), 3.77* (m, 0.23H), 3.68 (s, 3H), 3.65* (s, 0.69H), 3.63 (m, 1H), 3.51 (m, 1H), 3.38* (m, 0.23H), 3.29 (dd, *J* = 10.0, 1.2 Hz, 1H), 3.15 (t, *J* = 6.4 Hz, 1H), 2.94* (t, *J* = 5.4 Hz, 0.23H), 2.58 (p, *J* = 6.8 Hz, 1H), 1.89-2.03 (m, 2H), 1.20 (d, *J* = 7.2 Hz, 3H), 1.18* (d, *J* = 6.8 Hz, 0.69H); $^{13}$C NMR (100 MHz, $CDCl_3$) $\delta_C$ 189.2, 186.6*, 171.3, 169.4*, 166.9*,

166.8, 162.7, 160.5*, 156.8, 153.3, 152.2*, 138.6*, 138.9*, 137.3, 137.4, 137.2, 136.9*, 134.8*, 134.6, 132.3*, 132.5, 132.0*, 131.9, 131.2, 129.6, 129.4, 129.3*, 129.0, 128.9*, 128.4, 128.0*, 127.8*, 127.7, 127.6, 127.5*, 127.4, 125.3*, 125.3, 120.0, 118.6*, 117.5*, 117.0, 103.8, 103.8*, 72.7, 68.2*, 62.6*, 62.0, 59.4*, 55.4, 55.4*, 52.7, 49.2, 48.1*, 44.9*, 43.7, 42.7*, 41.2, 37.8*, 37.6, 27.7*, 27.4, 22.9, 21.4*; IR (neat) 1720, 1670, 1622, 1456, 1259, 1130, 730 $cm^{-1}$; MS (ES+) m/z 592.2 ($M+H^+$); HRMS calcd for $C_{36}H_{34}NO_7$ ($M+H^+$): 592.2257, found 592.2310.

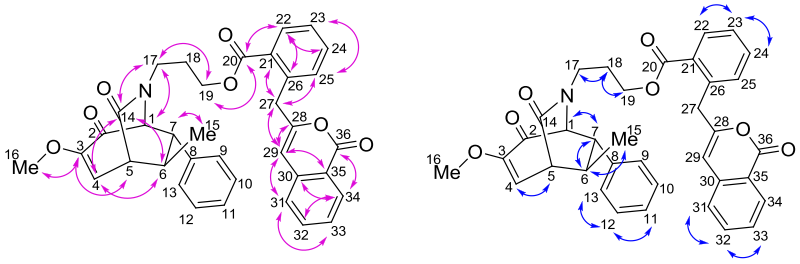

**(*E*)-3-(3-Methoxy-8-methyl-4,7-dioxo-9-phenyl-6-azabicyclo[3.2.2]non2-en-6-yl)propyl 2-((1-oxo-1*H*-isochromen-3-yl)methyl)benzoate (123).** Compound **123** was proposed based on the distinctive $^1H$ and $^{13}C$ chemical shift of C1, C5, C14, C17, C19, C20, C27, C29 and C36 in addition to connectivity data derived from HMBC and COSY. C1 appears at 72.7 ppm in the $^{13}C$ and the $^1H$ shows a doublet at 4.11 ppm with an integration of 1.0, consistent with the assignment of C1 as the bridgehead position between two electron withdrawing groups such as nitrogen and an α-methoxy ketone. C5 appears at 49.2 ppm in the $^{13}C$ and the $^1H$ shows a doublet of doublets at 3.29 ppm, consistent with a bridgehead methylene between slight electron withdrawing groups such as an olefin and an amide. C14 appears at 171.3

ppm in the $^{13}C$, typical of a lactam. C17 and C19 appear at 43.7 ppm and 62.0 ppm respectively in the $^{13}C$. C17 appears as a pair of multiplets in the $^{1}H$ at 3.63 ppm and 3.51 ppm, supporting the assignment of C17 as a methylene with diastereotopic hydrogens adjacent to a heteroatom such as nitrogen. C19 appears as a multiplet in the $^{1}H$ at 4.21-4.32 ppm. This data supports the assignment of C19 as a methylene adjacent to a heteroatom such as oxygen. C20 and C36 appear at 166.7 ppm and 162.7 ppm respectively in the $^{13}C$, common shifts for benzylic esters and lactones. C27 appears at 37.6 ppm in the $^{13}C$ and the $^{1}H$ shows a sharp singlet at 4.29 ppm with an integration of 2.0, consistent with a benzylic methylene. Additionally, C29 appears at 103.8 ppm in the $^{13}C$ and the $^{1}H$ shows a sharp singlet at 6.11 ppm with an integration of 1.0, consistent with a conjugated tri-substituted olefin. Distinctive 3-bond correlations in the HMBC map through the extended structure of the side chain to give the proposed atom placement. Key connections include C19 to C20, C21 to C27, C27 to C29, C29 to C31, C29 to C35, C30 to C34, and C34 to C36. In addition, the observed connection between C28 to C29 is an important 2-bond HMBC correlation. HMBC data also supports the assigned regioisomer of nitrogen insertion with the 3-bond correlations between C4 and C14, C6 and C14, C14 and C17, C1 and C17, and C17 and C19. The COSY reaffirms this conclusion by showing the retention of the carbon connectivity throughout the bicycle with correlations between C1, C4, C5, C6, C7, and C15, as well as between C11, C12, and C13. Retention of the carbon connectivity between C15, C16, and C17 is also observed. In addition, COSY was vital in distinguishing the atoms of the aromatic rings of the side chain. Important

connections exist between C22, C23, and C24, as well as between C31, C32, and C33. This information is in accordance with similar products derived from reactions of homophthalic anhydride.[124,126,166]

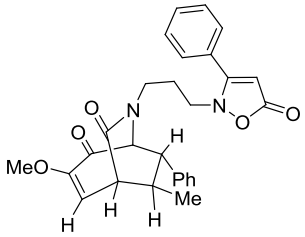


**(*E*)-3-Methoxy-8-methyl-6-(3-5-oxo-3-phenylisoxazol-2(5H)-yl)propyl)-9-phenyl-6-azabicyclo[3.2.2]non-2-ene-4,7-dione (124).** Synthesized according to the general procedure where 3-phenyl-5-isoxazolone (52.4 mg, 0.325 mmol) was substituted for homophthalic anhydride. Yellow oil (10.0 mg, 26% based on the major regioisomer in reactant); $R_f$ = 0.75 (5% MeOH/$CH_2Cl_2$); $^1$NMR (500 MHz, $CDCl_3$) $\delta_H$ 7.43-7.56 (m, 5H), 7.23-7.32 (m, 3H), 7.08-7.09 (m, 2H), 7.01-7.02* (m, 0.34H), 6.45* (d, *J* = 9.0 Hz, 0.17H), 6.29 (d, *J* = 10.0 Hz, 1H), 5.48 (s, 1H), 5.30* (s, 0.17H), 4.08 (d, *J* = 5.5 Hz, 1H), 3.90* (d, *J* = 5.0 Hz, 0.17 H), 3.81* (m, 0.17H), 3.71* (s, 0.51H), 3.65 (s, 3H), 3.60 (m, 1H), 3.41-3.54 (m, 3H), 3.28 (dd, *J* = 10.0, 1.5 Hz, 1H), 3.05 (t, *J* = 6.0 Hz, 1H), 2.92* (t, *J* = 6.0 Hz, 0.17H), 2.63* (p, *J* = 6.5 Hz, 0.17H), 2.57 (p, *J* = 6.5 Hz, 1H), 1.85-2.03 (m, 2H), 1.21* (d, *J* = 7.0 Hz, 0.51H), 1.16 (d, *J* = 7.0 Hz, 3H); $^{13}$C NMR (125 MHz, $CDCl_3$) $\delta_C$ 188.9, 186.5*, 171.5, 170.7*, 170.5, 170.0*, 169.8, 168.2*, 155.0*, 153.2, 138.5*, 137.5, 131.9*, 131.6, 129.5*, 129.4, 129.0, 128.9*, 128.4, 128.0*, 127.9, 127.9*, 127.8, 127.7*, 127.6,

127.3*, 118.4*, 116.8, 92.6, 92.2*, 72.3, 68.2*, 59.1*, 55.6*, 55.4, 52.7, 51.7, 51.5*, 49.2, 49.1*, 44.7*, 43.9, 42.6*, 41.2, 29.7*, 25.4, 22.9, 21.5*; IR (neat) 1739, 1670, 1618, 1452, 1126, 912, 730 $cm^{-1}$; MS (ES+) m/z 473.2 ($M+H^+$); HRMS calcd for $C_{28}H_{29}N_2O_5$ ($M+H^+$): 473.1998, found 473.2299.

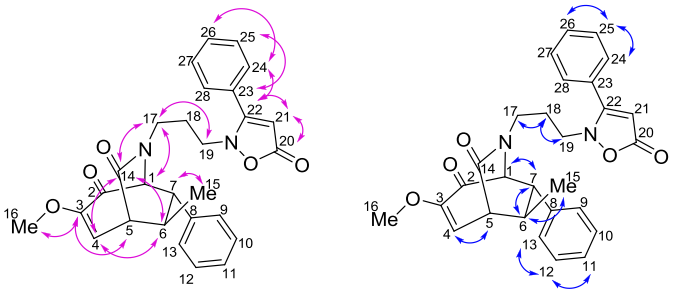

**(*E*)-3-Methoxy-8-methyl-6-(3-5-oxo-3-phenylisoxazol-2(5H)-yl)propyl)-9-phenyl-6-azabicyclo[3.2.2]non-2-ene-4,7-dione (124).** Compound **124** was proposed based on the distinctive $^1H$ and $^{13}C$ chemical shifts of C1, C5, C14, C17, C19, and C21 in addition to connectivity data derived from HMBC and COSY. C1 appears at 72.3 ppm in the $^{13}C$ and the $^1H$ shows a doublet at 4.08 ppm with an integration of 1.0, consistent with the assignment of C1 as the bridgehead position between two electron withdrawing groups such as nitrogen and an α-methoxy ketone. C5 appears at 49.2 ppm in the $^{13}C$ and $^1H$ shows a doublet at 3.28 ppm. This data supports the assignment of C5 as a bridgehead methylene between slight electron withdrawing groups such as an olefin and an amide. C14 appears at 171.5 ppm in the $^{13}C$, typical of a lactam. C17 and C19 appear at 43.9 ppm and 51.7 ppm respectively in the $^{13}C$. C17 appears as a pair of multiplets in the $^1H$ at 3.60 and 3.41-3.54 ppm, supporting the assignment of C17 as a methylene with diastereotopic hydrogens adjacent to a

heteroatom such as nitrogen. C19 overlaps with C17 in the $^{1}H$ appearing at 3.41-3.54 ppm as a multiplet. This data plausibly supports C19 as a methylene adjacent to a heteroatom such as nitrogen. C21 appears at 92.6 ppm, in the $^{13}C$ and the $^{1}H$ shows as a sharp singlet at 5.48 ppm with an integration of 1.0, this data supports the assignment of C21 as the carbon of the tri-substituted olefin. The presence of a key 3-bond HMBC correlation between C22 and C24, in addition to two key 2-bond HMBC correlations between C20 and C21, and C21 and C22 suggests that C22 (169.8 ppm) is the isoxazolone carbon α to nitrogen, and not the carbon of ester, as the proposed point of attachment to the bicyclic structure. The HMBC also shows the retention of the major bicyclic structure through the 3-bond correlations between C3 and C16, C3 and C5, C4 and C6, and C7 and C15. In addition, the HMBC supports the assigned regioisomer of nitrogen insertion with 3-bond correlations between C4 and C14, C6 and C14, C14 and C17, and C17 and C19. The COSY reaffirms this conclusion by showing the retention of the carbon connectivity throughout the bicycle with correlations between C1, C4, C5, C6, C7, and C15, as well as between C11, C12, and C13. COSY data also shows the retention of the carbon connectivity between C15, C16, and C17, as well as between C24, C25, and C26 of the aryl group on the isoxazolone ring.

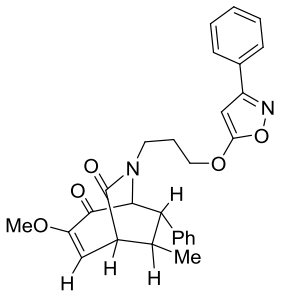


**(*E*)-3-Methoxy-8-methyl-9-phenyl-6-(3-(3-phenylisoxazol-5-yloxy)propyl)-6-azabicyclo[3.2.2]non-2-ene-4,7-dione (125).** Synthesized according to the general procedure where 3-phenyl-5-isoxazolone (52.4 mg, 0.325 mmol) was substituted for homophthalic anhydride. Yellow oil (10.6 mg, 28% based on the major regioisomer in reactant); $R_f$ = 0.58 (5% MeOH/$CH_2Cl_2$); $^1$NMR (400 MHz, $CDCl_3$) $\delta_H$ 7.73-7.75 (m, 2H), 7.43-7.45 (m, 3H), 7.22-7.31 (m, 3H), 7.09-7.10 (m, 2H), 6.34 (d, *J* = 10.4 Hz, 1H), 5.53 (s, 1H), 4.27 (t, *J* = 6.4 Hz, 2H), 4.14 (d, *J* = 5.6 Hz, 1H), 3.75 (m, 1H), 3.70 (s, 3H), 3.55 (m, 1H), 3.32 (dd, *J* = 10.4, 1.2 Hz, 1H), 3.16 (t, *J* = 6.0 Hz, 1H), 2.61 (t, *J* = 6.8 Hz, 1H), 2.06 (p, *J* = 6.4 Hz, 2H), 1.22 (d, *J* = 6.8 Hz, 3H); $^{13}$C NMR (100 MHz, $CDCl_3$) $\delta_C$ 189.2, 173.3, 171.5, 164.2, 153.3, 137.6, 130.0 (2), 129.0, 128.8, 128.4, 127.8, 126.5, 116.9, 76.2, 73.0, 69.9, 55.5, 52.7, 49.2, 44.1, 41.2, 27.8, 22.9; IR (neat) 1666, 1608, 1579, 1458, 1209, 732 $cm^{-1}$; MS (ES+) m/z 473.2 ($M+H^+$); HRMS calcd for $C_{28}H_{29}N_2O_5$ ($M+H^+$): 473.1998, found 473.1838.

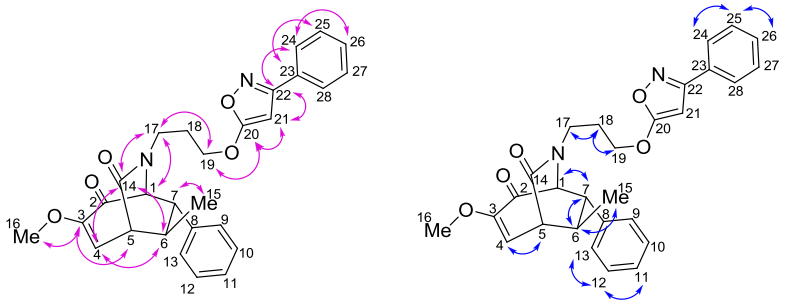

**(*E*)-3-Methoxy-8-methyl-9-phenyl-6-(3-(3-phenylisoxazol-5-yloxy)propyl)-6-azabicyclo[3.2.2]non-2-ene-4,7-dione (125a).** Compound **125a** was proposed based on the distinctive $^{1}H$ and $^{13}C$ chemical shifts of C1, C5, C14, C17, C19, and C21 in addition to connectivity data derived from HMBC and COSY. C1 appears at 73.0 ppm in the $^{13}C$ and the $^{1}H$ shows a doublet at 4.14 ppm with an integration of 1.0, consistent with the assignment of C1 as the bridgehead position between two electron withdrawing groups such as nitrogen and an α-methoxy ketone. C5 appears at 49.2 ppm in the $^{13}C$ and $^{1}H$ shows a doublet at 3.32 ppm. This data supports the assignment of C5 as a bridgehead methylene between slight electron withdrawing groups such as an olefin and an amide. C14 appears at 171.5 ppm in the $^{13}C$, typical of a lactam. C17 and C19 appear at 44.1 ppm and 69.9 ppm respectively in the $^{13}C$. C17 appears as a pair of multiplets in the $^{1}H$ at 3.75 and 3.55 ppm, supporting the assignment of C17 as a methylene with diastereotopic hydrogens adjacent to a heteroatom such as nitrogen. C19 appears as a triplet in the $^{1}H$ at 4.27 ppm. This data supports the assignment of C19 as a methylene adjacent to a heteroatom such as oxygen. C21 appears at 76.2 ppm, in the $^{13}C$ and the $^{1}H$ shows as a sharp singlet at 5.53 ppm with an integration of 1.0, this data supports the assignment of C21 as the carbon of the tri-substituted olefin. Critical 3- and 2-bond HMBC correlations

between C20, C21, C22, and C14 identify C20 as the enol ether at 173.3 ppm and C22 as the carbon α to nitrogen in the isoxazolone ring at 164.2 ppm. The presence of a 3-bond HMBC correlation between C19 and C20 is consistent with the proposed point of attachment to the bicycle through the enol ether oxygen and not through the nitrogen of the isoxazolone ring. Also, the HMBC supports the retention of the major bicyclic structure through the 3-bond correlations between C3 and C16, C3 and C5, C4 and C6, and C7 and C15. It also supports the assigned regioisomer of nitrogen insertion with 3-bond correlations between C4 and C14, C6 and C14, C14 and C17, and C17 and C19. The COSY reaffirms this conclusion by showing the retention of the carbon connectivity throughout the bicycle with correlations between C1, C4, C5, C6, C7, and C15, as well as between C11, C12, and C13. COSY data also shows the retention of the carbon connectivity between C15, C16, and C17 of the side chain, as well as between C24, C25, and C26 of the aryl group on the isoxazolone ring.

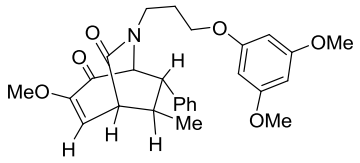


**(*E*)-6-(3-(3,5-Dimethoxyphenoxy)propyl)-3-methoxy-8-methyl-9-phenyl-6-azabicyclo[3.2.2]non-2-ene-4,7-dione (126).** Synthesized according to the general procedure where 3,5-dimethoxyphenol (50.0 mg, 0.325 mmol) was substituted for homophthalic anhydride. Clear oil (32.3 mg, 57% based on the major regioisomer in reactant); $R_f$ = 0.26 (66% Hex/EtOAc); $^1$NMR (400 MHz, $CDCl_3$) $\delta_H$ 7.23-7.28 (m, 3H), 7.00-7.02 (m, 2H), 6.34 (d, *J* = 10.4 Hz, 1H), 6.09-6.12 (m, 3H), 4.18 (d, *J* = 5.6

Hz, 1H), 3.92-3.98 (m, 2H), 3.76 (s, 6H), 3.70 (s, 3H), 3.62 (m, 2H), 3.32 (dd, *J* = 10.4, 1.2 Hz, 1H), 3.13 (t, *J* = 6.4 Hz, 1H), 2.60 (p, *J* = 6.4 Hz, 1H), 1.99-2.07 (m, 2H), 1.23 (d, *J* = 7.2 Hz, 3H); $^{13}$C NMR (100 MHz, $CDCl_3$) $\delta_C$ 189.2, 171.4, 161.5, 160.5, 153.3, 137.7, 128.9, 128.3, 127.7, 116.8, 93.3, 93.4, 73.1, 65.1, 55.4, 55.3, 52.6, 49.2, 44.6, 40.9, 27.9, 22.9; IR (neat) 2956, 1672, 1600, 1456, 1151, 1064 $cm^{-1}$; MS (ES+) m/z 466.2 ($M+H^+$); HRMS calcd for $C_{27}H_{32}NO_6$ ($M+H^+$):466.2151, found 466.2200.

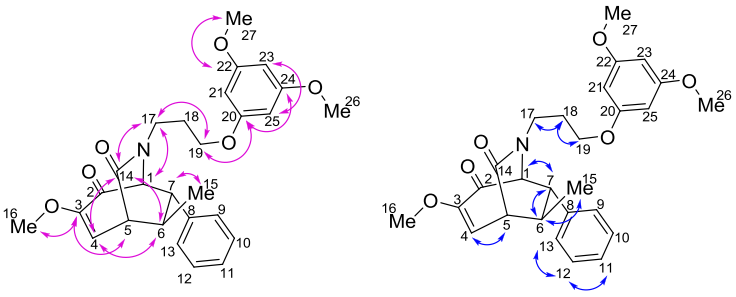

**(*E*)-6-(3-(3,5-Dimethoxyphenoxy)propyl)-3-methoxy-8-methyl-9-phenyl-6-azabicyclo[3.2.2]non-2-ene-4,7-dione (126).** Compound **126** was proposed based on the distinctive $^1$H and $^{13}$C chemical shift of C1, C5, C14, C17, C19, C20, C21, and C22 in addition to connectivity data derived from HMBC and COSY. C1 appears at 73.1 ppm in the $^{13}$C and the $^1$H shows a doublet at 4.18 ppm with an integration of 1.0, consistent with the assignment of C1 as the bridgehead position between two electron withdrawing groups such as nitrogen and an α-methoxy ketone. C5 appears at 49.2 ppm in the $^{13}$C and the $^1$H shows a doublet at 3.32 ppm, consistent with a bridgehead methylene between slight electron withdrawing groups such as an olefin and an amide. C14 appears at 171.4 ppm in the $^{13}$C, typical of a lactam. C17 and C19

appear at 44.6 ppm and 65.1 ppm respectively in the $^{13}C$. C17 appears as a multiplet in the $^{1}H$ at 3.62 ppm, supporting the assignment of C17 as a methylene adjacent to a heteroatom such as nitrogen. C19 appears as a multiplet in the $^{1}H$ at 3.92-3.98 ppm. This data supports the assignment of C19 as a methylene adjacent to a phenol. C20 and C22 appear at 160.5 ppm and 161.5 ppm in the $^{13}C$, typical of *O*-substituted methoxyphenols. C21 and C23 appear at 93.3 ppm and 93.4 ppm, respectively in the $^{13}C$ and at 6.09-6.12 ppm in the $^{1}H$, data typical of symmetrical *O*-substituted methoxyphenols. The 3-bond HMBC correlations of C19 and C24 with C20 support the presence of an ether linkage between C19 and C20 connecting the parent amide to the phenol. The HMBC supports the retention of the major bicyclic structure through the 3-bond correlations between C3 and C16, C3 and C5, C4 and C6, and C7 and C15. In addition, the HMBC supports the assigned regioisomer of nitrogen insertion with the 3-bond correlations between C4 and C14, C6 and C14, C14 and C17, and C17 and C19. The COSY reaffirms this conclusion by showing the retention of the carbon connectivity throughout the bicycle with correlations between C1, C4, C5, C6, C7, and C15, as well as between C11, C12, and C13. COSY data also shows the retention of the carbon connectivity between C15, C16, and C17.

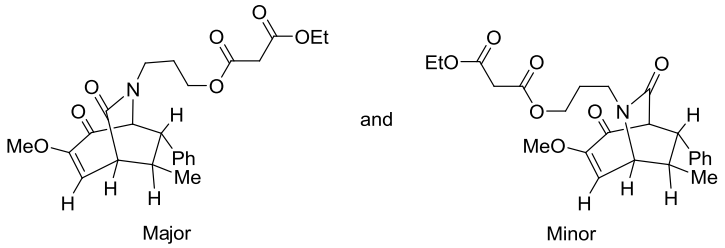

**(*E*)-Ethyl-3-(3-methoxy-8-methyl-4,7-dioxo-9-phenyl-6-azabicyclo[3.2.2]non-2-en-6-yl)propyl malonate (127a) and (*E*)-ethyl-3-(3-methoxy-9-methyl-2,7-dioxo-8-phenyl-6-azabicyclo[3.2.2]non-3-en-6-yl)propyl malonate (127b).** Synthesized according to the general procedure where diethyl malonate (49.0 μL, 0.325 mmol) was substituted for homophthalic anhydride. Yellow oil (10.1 mg, 21% as an inseparable mixture of regioisomers); $R_f$ = 0.24 (66% Hex/EtOAc); $^1$H NMR (500 MHz, $CDCl_3$) $\delta_H$ 7.23-7.31 (m, 4.8H), 7.09-7.11 (m, 2H), 7.02-7.04* (m, 1.2H), 6.43* (d, *J* = 9.0 Hz, 0.6H), 6.33 (d, *J* = 10.0 Hz, 1H), 4.22* (q, *J* = 7.0 Hz, 1.2H), 4.18 (q, *J* = 7.0 Hz, 2H), 4.13-4.27* (m, 1.2H), 4.10 (d, *J* = 5.5 Hz, 1H), 4.06-4.11 (m, 1H), 3.94* (d, *J* = 9.0 Hz, 0.6H), 3.92* (d, *J* = 5.0 Hz, 0.6H), 3.80* (m, 0.6H), 3.69 (s, 3H), 3.68* (s, 1.8H), 3.57 (m, 1H), 3.47 (m, 1H), 3.41* (d, *J* = 2.0 Hz, 1.2H), 3.38 (s, 2H), 3.35* (m, 0.6H), 3.30 (dd, *J* = 10.0, 1.0 Hz, 1H), 3.14 (t, *J* = 6.0 Hz, 1H), 2.96* (t, *J* = 6.0 Hz, 0.6H), 2.56-2.63 (m, 1.6H), 1.91-1.99* (m, 1.2H), 1.83-1.89 (m, 2H), 1.21-1.31 (m, 9.6H); $^{13}$C NMR (125 MHz, $CDCl_3$) $\delta_C$ 189.2, 186.7*, 171.4, 168.1*, 166.8*, 166.5*, 166.5, 166.4, 154.9*, 153.3, 138.7*, 137.7, 129.0, 128.9*, 128.4, 128.0*, 127.8, 127.5*, 118.6*, 116.9, 72.8, 68.3*, 62.8*, 62.4, 61.7*, 61.6, 59.6*, 55.5, 55.5*, 52.7, 49.2, 48.1*, 44.9*, 43.8, 42.7*, 41.5*, 41.4, 41.2, 27.4*, 27.2, 22.9, 21.4*, 14.1*, 14.0; IR (neat) 2960, 1747, 1731, 1681, 1674, 1622, 1151, 1031 $cm^{-1}$; MS (ES+) m/z 444.2 ($M+H^+$); HRMS calcd for $C_{24}H_{30}NO_7$ ($M+H^+$): 444.1944, found 444.1896.

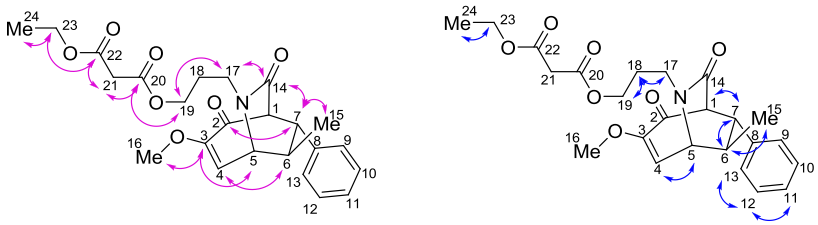

**(*E*)-Ethyl-3-(3-methoxy-9-methyl-2,7-dioxo-8-phenyl-6-azabicyclo[3.2.2]non-3-en-6-yl)propyl malonate (127b).** Compound **127b** was proposed based on the distinctive $^{1}H$ and $^{13}C$ chemical shift of C1, C5, C14, C17, C19, C20, C21, and C22, in addition to connectivity data derived from HMBC and COSY. C1 appears at 68.3 ppm in the $^{13}C$ and the $^{1}H$ shows a doublet at 3.92 ppm with an integration of 1.0, consistent with the assignment of C1 as a bridgehead methylene between electron withdrawing groups such as an α-methoxy ketone and a lactam. C5 appears at 59.6 ppm in the $^{13}C$ and the $^{1}H$ shows a doublet at 3.94 ppm, consistent with the assignment of C5 as the bridgehead position between two electron withdrawing groups such as nitrogen and an olefin. C14 appears at 168.1 ppm in the $^{13}C$, typical of a lactam. C17 and C19 appear at 45.0 ppm and 62.8 ppm respectively in the $^{13}C$. C17 appears as a pair of multiplets at 3.80 ppm and 3.35 ppm in the $^{1}H$, common for a methylene with diastereotopic hydrogens adjacent to a heteroatom such as nitrogen. C19 appears as a multiplet at 4.13-4.27 ppm in the $^{1}H$, common for a methylene adjacent to a heteroatom such as oxygen. C20 and C22 appear at 166.5 ppm and 166.8 ppm in the $^{13}C$ NMR, consistent with a 1,3-diester. C21 appears at 41.2 ppm in the $^{13}C$ and the $^{1}H$ shows a sharp singlet at 3.38 ppm, corresponding to the methylene α to the malonate. The 3-bond HMBC correlation between C19 and C20 along with the 2-bond HMBC correlations of 20 and C22 with C21 support the

connection of the parent amide to malonate through an ester bond with C19. The HMBC supports the retention of the major bicyclic structure through the 3-bond correlations between C3 and C16, C3 and C5, C4 and C6, C2 and C7, and C7 and C15. In addition, the HMBC supports the assigned regioisomer of nitrogen insertion with the 3-bond correlations between C7 and C14, C14 and C17, and C17 and C19. The COSY reaffirms this conclusion by showing the retention of the carbon connectivity throughout the bicycle with correlations between C1, C4, C5, C6, C7, and C15, as well as between C11, C12, and C13. COSY data also shows the retention of the carbon connectivity between C15, C16, and C17. In addition a COSY correlation between C23 and C24 show the retention of one ethyl ester from the parent diethyl malonate.

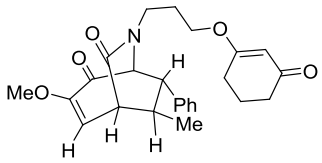


**(*E*)-3-Methoxy-8-methyl-6-(3-(3-oxocyclohex-1-enyloxy)propyl)-9-phenyl-6-azabicyclo[3.2.2]non-2-ene-4,7-dione (128).** Synthesized according to the general procedure where 1,3-cyclohexadione (36.4 mg, 0.325 mmol) was substituted for homophthalic anhydride. Clear oil (21.6 mg, 63% based on the major regioisomer in reactant); $R_f$ = 0.42 (5% MeOH/$CH_2Cl_2$); $^1$H NMR (400 MHz, $CDCl_3$) $\delta_H$ 7.24-7.31 (m, 3H), 7.06-7.09 (m, 2H), 6.33 (d, *J* = 10.0 Hz, 1H), 5.29, (s, 1H), 4.08 (d, *J* = 5.2 Hz, 1H), 3.77 (t, *J* = 6.0 Hz, 2H), 3.68 (s, 3H), 3.74 (m, 1H), 3.44 (m, 1H), 3.30 (dd, *J* = 10.0, 1.2 Hz, 1H), 3.08 (t, *J* = 6.0 Hz, 1H), 2.58 (t, *J* = 6.8 Hz, 1H), 2.39 (t, *J* = 6.4

Hz, 2H), 2.33 (t, *J* = 6.4 Hz, 2H), 1.94 (m, 4H), 1.20 (d, *J* = 7.2 Hz, 3H); $^{13}$C NMR (100 MHz, $CDCl_3$) $\delta_C$ 199.7, 189.2, 177.6, 171.3, 153.2, 137.6, 129.0, 128.3, 127.8, 117.0, 102.9, 73.0, 65.3, 55.5, 52.9, 49.2, 43.9. 41.2, 36.7, 28.8, 27.3, 22.8, 21.1; IR (neat) 1643, 1600, 1218, 1184 cm$^{-1}$; MS (ES+) m/z 424.2 (M+H$^+$); HRMS calcd for $C_{25}H_{30}NO_5$ (M+H$^+$): 424.2046, found 424.2112.

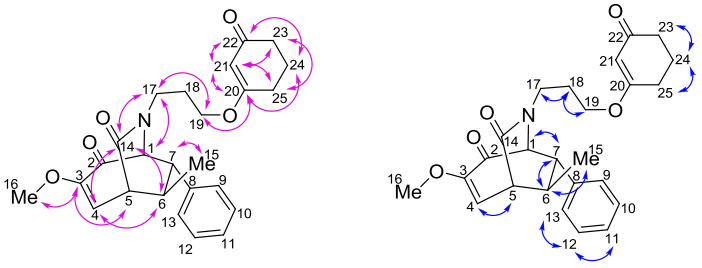

**(*E*)-3-Methoxy-8-methyl-6-(3-(3-oxocyclohex-1-enyloxy)propyl)-9-phenyl-6-azabicyclo[3.2.2]non-2-ene-4,7-dione (128).** Compound **128** was proposed based on the distinctive $^1$H and $^{13}$C chemical shift of C1, C5, C14, C17, C19, C20, C21, and C22, in addition to connectivity data derived from HMBC and COSY. C1 appears at 73.0 ppm in the $^{13}$C and the $^1$H shows a doublet at 4.08 ppm with an integration of 1.0, consistent with the assignment of C1 as the bridgehead position between two electron withdrawing groups such as nitrogen and an α-methoxy ketone. C5 appears at 49.2 ppm in the $^{13}$C and the $^1$H shows a doublet of doublets at 3.30 ppm, consistent with a bridgehead methylene between slight electron withdrawing groups such as an olefin and an amide. C14 appears at 171.3 ppm in the $^{13}$C, typical of a lactam. C17 and C19 appear at 65.3 ppm and 73.0 ppm respectively in the $^{13}$C. C17 appears as a pair of multiplets at 3.44 ppm and 3.74 ppm in the $^1$H, common for a methylene with

diastereotopic hydrogens adjacent to a heteroatom such as nitrogen. C19 appears as a triplet at 3.77 ppm in the $^{1}H$, common for a methylene adjacent to a heteroatom such as oxygen. C20 and C22 appear at 177.6 ppm and 199.2 ppm respectively in the $^{13}C$ NMR, consistent with an enol ether and a conjugated ketone. C21 appears at 102.9 ppm in the $^{13}C$ and the $^{1}H$ shows a sharp singlet at 5.32 ppm, corresponding to the methylene α to the malonate. The 3-bond HMBC correlations between C19 and C20 along with the 2-bond HMBC correlations of C20 and C22 with C21 support the connection of the diketone to the parent amide through the presence of an enol ether bond to C19. The HMBC shows the retention of the major bicyclic structure through the 3-bond correlations between C3 and C16, C3 and C5, C4 and C6, and C7 and C15. In addition, the HMBC supports the assigned regioisomer of nitrogen insertion with the 3-bond correlations between C4 and C14, C6 and C14, C14 and C17, C1 and C17, and C17 and C19. The COSY reaffirms the above conclusions by showing the preservation of the carbon connectivity throughout the bicycle with correlations between C1, C4, C5, C6, C7, and C15, as well as between C11, C12, and C13. COSY data also shows the retention of the carbon connectivity between C15, C16, and C17. In addition the carbon connectivity of the diketone was retained between C23, C24, and C25.

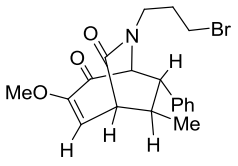

**(*E*)-6-(3-Bromopropyl)-3-methoxy-8-methyl-9-phenyl-6-azabicyclo[3.2.2]non-2-ene-4,7-dione (129).** Synthesized according to the general procedure where ethyl bromoacetate (36.0 μL, 0.325 mmol) was substituted for homophthalic anhydride. Yellow oil (17.1 mg, 64% based on the major regioisomer in reactant); $R_f$ = 0.74, (5% MeOH/$CH_2Cl_2$); $^1$H NMR (400 MHz, $CDCl_3$) $\delta_H$ 7.22-7.35 (m, 3H), 7.09-7.11 (m, 2H), 6.33 (d, *J* = 10.4 Hz, 1H), 4.14 (d, *J* = 5.6 Hz, 1H), 3.69 (s, 3H), 3.64 (m, 1H), 3.49 (m, 1H), 3.29-3.37 (m, 3H), 3.12 (t, *J* = 6.4 Hz, 1H), 2.59 (p, *J* = 6.8 Hz, 1H), 2.00-2.14 (m, 2H), 1.21 (d, *J* = 6.8 Hz, 3H); $^{13}$C NMR (100 MHz, $CDCl_3$) $\delta_C$ 189.1, 171.5, 153.3, 137.6, 129.0, 128.3, 127.8, 116.9, 73.2, 55.5, 52.8, 49.2, 46.1, 41.0, 31.1, 29.9, 22.9; IR (neat) 1664, 1649, 1209,702 cm$^{-1}$; MS (ES+) m/z 392.0 (M+H$^+$); HRMS calcd for $C_{19}H_{23}BrNO_3$ (M+H$^+$): 392.0783, found 392.0631 and 394.0617.

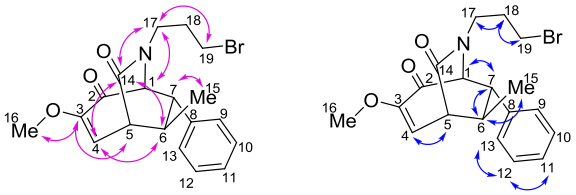


**(*E*)-6-(3-Bromopropyl)-3-methoxy-8-methyl-9-phenyl-6-azabicyclo[3.2.2]non-2-ene-4,7-dione (129).** Compound **129** was proposed based on the distinctive $^1$H and $^{13}$C chemical shift of C1, C5, C14, C17, and C19 in addition to connectivity data derived from HMBC and COSY. C1 appears at 73.2 ppm in the $^{13}$C and the $^1$H shows a doublet at 4.14 ppm with an integration of 1.0, consistent with the assignment of C1 as the bridgehead position between two electron withdrawing

groups such as nitrogen and an α-methoxy ketone. C5 appears at 49.2 ppm in the $^{13}C$ and overlaps with C19 in the $^{1}H$ showing a multiplet at 3.29-3.37 ppm. This data supports the assignment of C5 as a bridgehead methylene between slight electron withdrawing groups such as an olefin and an amide. C14 appears at 171.5 ppm in the $^{13}C$, typical of a lactam. C17 and C19 appear at 46.1 ppm and 29.9 ppm respectively in the $^{13}C$. C17 appears as a pair of multiplets in the $^{1}H$ at 3.64 ppm and 3.49 ppm with an integration of 1.0 each, supporting the assignment of C17 as a methylene with diastereotopic hydrogens adjacent to a heteroatom such as nitrogen. C19 overlaps with C5 in the $^{1}H$, as previously mentioned, appearing at 3.29-3.37 ppm as a multiplet. This data plausibly supports C19 as a methylene adjacent to bromide. The HMBC supports the retention of the major bicyclic structure through the 3-bond correlations between C3 and C16, C3 and C5, C4 and C6, and C7 and C15. In addition, the HMBC supports the assigned regioisomer of nitrogen insertion with 3-bond correlations between C4 and C14, C6 and C14, C14 and C17, and C17 and C19. The COSY reaffirms this conclusion by showing the retention of the carbon connectivity throughout the bicycle with correlations between C1, C4, C5, C6, C7, and C15, as well as between C11, C12, and C13. COSY data also shows the retention of the carbon connectivity between C15, C16, and C17.

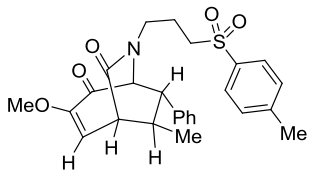

**(*E*)-3-Methoxy-8-methyl-9-phenyl-6-(3-tosylpropyl)-6-azabicyclo[3.2.2]non-2-ene-4,7-dione (130).** Synthesized according to the general procedure where *p*-toluenesulfonylmethyl isocyanide (127 mg, 0.651 mmol) was substituted for homophthalic anhydride and the reaction was completed on a 0.216 mmol scale. The corresponding NMR appeared as a mixture of rotamers in an approximate 1:1 ratio, as estimated by $^{13}$C NMR. Clear oil (48.6 mg, 64% based on the major regioisomer in reactant); $R_f$ = 0.30, (66% Hex/EtOAc); $^{1}$NMR (400 MHz, $CDCl_3$) $\delta_H$ 7.60-7.59 (ovrlp dd, *J* = 8.5, 8.0 Hz, 2H), 7.24-7.33 (m, 5H), 7.09-7.12 (m, 2H), 6.31-6.30 (ovrlp dd, *J* = 10.4, 10.4 Hz, 1H), 4.10 (d, *J* = 5.6 Hz, 0.6H), 4.06* (d, *J* = 5.6 Hz, 0.4H), 4.01 (m, 1H), 3.68 (s, 1.8H), 3.67* (s, 1.2H), 3.62 (m, 1H), 3.40-3.55 (m, 2H), 3.29-3.28 (ovrlp dd, *J* = 10.0, 1.2 Hz, 1H), 3.14 (t, *J* = 6.0 Hz, 0.6H), 3.09* (t, *J* = 6.0 Hz, 0.4H), 2.57 (p, *J* = 6.8 Hz, 0.6H), 2.43* (m, 0.4H), 2.41 (s, 3H), 1.77-1.88 (m, 2H), 1.19-1.18 (ovrlp dd, *J* = 7.2, 7.2 Hz, 3H); $^{13}$C NMR (100 MHz, $CDCl_3$) $\delta_C$ 189.2, 171.4, 171.3*, 153.3, 153.3*, 142.9, 142.8*, 141.4*, 141.2, 137.7, 137.7*, 129.8, 129.0, 128.4, 128.4*, 127.7, 125.3, 125.2*, 116.8*, 116.8, 72.9, 72.7*, 61.7*, 60.7, 55.4, 55.4*, 52.6*, 52.5, 49.2, 44.1, 44.0*, 41.1*, 41.0, 28.5*, 28.4, 22.9, 21.5; IR (neat) 1672, 1620, 1456, 1128 cm$^{-1}$; MS (ES+) m/z 468.2 ($M+H^+$); HRMS calcd for $C_{26}H_{30}NO_5S$ ($M+H^+$): 468.1766, found 468.1831.

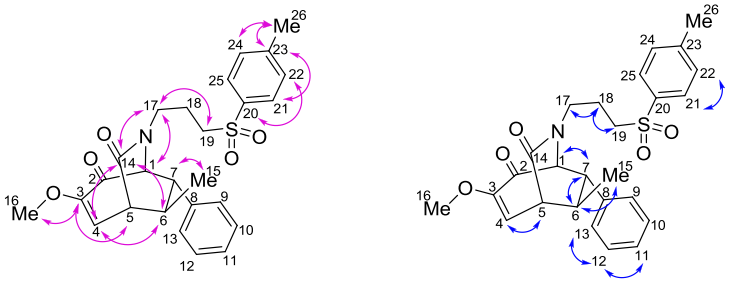

**(*E*)-3-Methoxy-8-methyl-9-phenyl-6-(3-tosylpropyl)-6-azabicyclo[3.2.2]non-2-ene-4,7-dione (130).** Compound **130** was proposed based on the distinctive $^{1}H$ and $^{13}C$ chemical shift of C1, C5, C14, C17, and C19 in addition to connectivity data derived from HMBC and COSY. C1 appears at 72.9 ppm in the $^{13}C$ and the $^{1}H$ shows a doublet at 4.10 ppm with an integration of 1.0, consistent with the assignment of C1 as the bridgehead position between two electron withdrawing groups such as nitrogen and an α-methoxy ketone. C5 appears at 49.2 ppm in the $^{13}C$ and the $^{1}H$ shows a doublet of doublets at 3.28 ppm, consistent with a bridgehead methylene between slight electron withdrawing groups such as an olefin and an amide. C14 appears at 171.4 ppm in the $^{13}C$, typical of a lactam. C17 and C19 appear at 44.1 ppm and 60.7 ppm respectively in the $^{13}C$. C17 appears as a multiplet in the $^{1}H$ at 3.40-3.55 ppm. C19 appears as a pair of multiplets in the $^{1}H$ at 4.01 ppm and 3.62 ppm. This data supports C17 and C19 as methylenes adjacent to heteroatoms such as nitrogen and a sulfoxide group, respectively. The HMBC spectrum shows two distinct regions of connectivity within the molecule. The 3-bond correlations between C20 and C22, C21 and C23, as well as C24 and C26 suggest the retention of *p*-toluenesulfonyl methyl moiety with the point of attachment to the bicycle at C19. The HMBC supports the retention of the major bicyclic structure through the 3-bond

correlations between C3 and C16, C3 and C5, C4 and C6, and C7 and C15. In addition, the HMBC supports the assigned regioisomer of nitrogen insertion with 3-bond correlations between C4 and C14, C6 and C14, C14 and C17, and C17 and C19. The COSY reaffirms the aforementioned conclusion by showing the retention of the carbon connectivity throughout the bicycle with correlations between C1, C4, C5, C6, C7, and C15, as well as between C11, C12, and C13. COSY data also shows the retention of the carbon connectivity between C15, C16, and C17, as well as between C21, and C22 *p*-methylthiophenol.

**General Procedure for the Synthesis of Polycyclic Cyclopropanes.** (Synthesis of cyclopropanes **135** and **140**-**144**). To a dry pyrex-rayonet tube containing a small magnetic cross stir bar was added bicyclo[3.2.1]octanoid (1.51 mmol) followed by the addition of acetone (10 mL). The reaction vessel was capped with rubber septa and degassed by bubbling argon *via* balloon (15 min). The vessel was sealed by wrapping several layers of parafilm around the septa. Next the reaction vessel was placed in a Hanovia lamp photoreactor with no filter (quartz) and was stirred at approximately 20 $^{o}$C (rt) for 4 h. A small aliquot was analyzed by UPLC/MS/ELS which indicated 100 % conversion to product. The reaction was concentrated to afford cyclopropane without the need for purification. Note: the cyclopropane products are generally not stable to purification *via* silica gel chromatography.

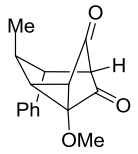


**Cyclopropane (135).** Bicyclo[3.2.1]octanoid **63** (32 mg, 0.125 mmol) in 5 mL acetone afforded cyclopropane **135** (32 mg, 0.125 mmol, 99%) as a white solid. mp = 95.0-98.0 $^{o}$C; $^{1}$H NMR (400 MHz, $CDCl_3$) $\delta_H$ 7.35-7.27 (m, 3H), 7.14 (d, *J* = 7.0 Hz, 2H), 3.61 (s, 3H), 3.11 (dd, *J* = 8.9, 1.8 Hz, 1H), 3.01 (dd, *J* = 6.4, 2.1 Hz, 1H), 2.81 (dd, *J* = 8.9, 1.5 Hz, 1H), 2.68 (dd, *J* = 2.1, 1.8 Hz, 1H), 2.67-2.59 (dquin, *J*

= 6.8, 1.5 Hz, 1H), 1.25 (d, *J* = 7.0 Hz, 3H); $^{13}$C NMR (100 MHz, $CDCl_3$) $\delta_c$ 200.4, 199.7, 140.7, 128.9, 127.7, 127.4, 83.5, 61.2, 59.1, 58.2, 49.5, 47.9, 34.3, 20.5; IR (thin film) 2963, 2935, 1762, 1716, 1456, 1298, 1206, 1162, 1080, 1063, 887, 758, 735, 701 $cm^{-1}$; MS (ES+) m/z 535.2 ($2M+Na^+$); HRMS calcd for $C_{32}H_{32}O_6Na$ ($2M+Na^+$): 535.2097, found 535.2091.

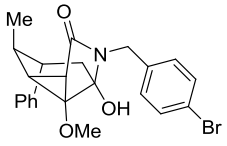


***N*-Acylhemiaminal (136).** To a dry vial containing a small magnetic stir bar was added cyclopropane **135** (50 mg, 0.195 mmol) and 1.2 mL DMSO followed by the addition of 4-bromobenzylamine (49.3 μL, 0.390 mmol). Next DBU (35.0 μL, d=1.018, 0.195 mmol) was added quickly and the reaction was stirred for 45 min at room temp. The reaction was stopped with the addition of acetic anhydride (390 μL of 10% by volume in DMSO, approx. 0.390 mmol) followed by continued stirring for 10 min. DMSO was removed by portioning the reaction into water and extracting the product with $CH_2Cl_2$ (x 3). The organic fractions were combined, dried over sodium sulfate, filtered, and concentrated *in vacuo*. The crude extract was purified by flash silica gel chromatography (50% EtOAc/Hex) to afford *N*-acylhemiaminal **136** as a white solid. mp 197-198 ºC; $^1$H NMR (400 MHz, $CDCl_3$) δ 7.43-7.39 (m, 2H), 7.34-7.30 (m, 2H), 7.28 (s, 2H), 7.24-7.18 (m, 1H), 6.91 (d, *J* = 6.6 Hz, 2H), 4.43 (d, *J* = 14.8 Hz, 1H), 4.04 (d, *J* = 14.8 Hz, 1H), 3.59 (s, 3H), 3.49 (s, 1H), 2.33 (ddq, *J* = 10.6, 6.6, 5.5 Hz, 1H), 2.24 (d, *J* = 9.8 Hz, 1H), 2.16 (dd, *J* = 9.8, 5.5 Hz, 1H), 2.08

(ovrlp d, *J* = 5.1 Hz, 1H), 2.07 (ovrlp d, *J* = 11.3 Hz, 1H), 1.70 (ddd, *J* = 11.3, 10.6, 5.1 Hz, 1H), 0.92 (d, *J* = 6.6 Hz, 3H); $^{13}$C NMR (100 MHz, $CDCl_3$) $\delta_C$ 170.1, 142.8, 136.9, 131.6, 130.8, 128.6, 127.6, 126.9, 121.4, 87.7, 73.7, 58.4, 44.9, 42.1, 40.6, 36.5, 35.3, 31.4, 18.4; IR (thin film) 3345, 2957, 2929, 1668, 1488, 1453, 1401, 1134, 1070, 1013, 736, 703 cm$^{-1}$; MS (ES+) m/z 442.1 (M+H$^+$); HRMS calcd for $C_{23}H_{25}BrNO_3$ (M+H$^+$): 442.1018, found 442.1024.

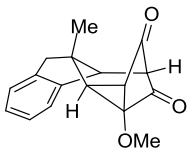


**Cyclopropane (140).** Bicyclo[3.2.1]octanoid **75** (405 mg, 1.51 mmol) and 10 mL acetone afford cyclopropane **140** (391 mg, 1.46 mmol, 96%) as a white solid. $^1$H NMR (400 MHz, $CDCl_3$-d) $\delta_H$ 7.26-7.21 (m, 2H), 7.18-7.10 (m, 2H), 3.62 (d, *J* = 3.5 Hz, 1H), 3.50 (s, 3H), 3.31 (d, *J* = 17.2 Hz, 1H), 3.10 (dd, *J* = 9.0, 2.0 Hz, 1H), 3.05 (d, *J* = 17.2 Hz, 1H), 2.91 (ovrlp d, *J* = 9.0 Hz, 1H), 2.91(ovrlp dd, J = 3.5, 2.0 Hz, 1H), 1.42 (s, 3H); $^{13}$C NMR (100 MHz, $CDCl_3$) $\delta_C$ 200.3, 199.0, 140.8, 139.4, 128.6, 127.5, 125.1, 124.1, 82.6, 64.3, 60.8, 58.0, 55.0, 48.4, 46.7, 40.9, 28.7; IR (thin film) 2956, 1764, 1719, 1457, 1302, 1210, 1060, 758, 737 cm$^{-1}$; MS (ES+) m/z 559.2 (M+Na$^+$); HRMS calcd for $C_{34}H_{32}O_6Na$ (M+Na$^+$): 559.2097, found 559.2117.

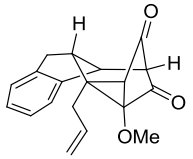

**Cyclopropane (141).** Bicyclo[3.2.1]octanoid **137** (444 mg, 1.51 mmol) and 10 mL acetone afford cyclopropane **141** (438 mg, 1.49 mmol, 99%) as a white solid. $^{1}$H NMR (400 MHz, $CDCl_3$) $\delta_H$ 7.25-7.07 (m, 4H), 5.91 (ddd, *J* = 14.1, 8.3, 5.9 Hz, 1H), 5.30-5.21 (m, 2H), 4.01 (dd, *J* = 9.2, 3.0 Hz, 1H), 3.53 (s, 3H), 3.40-3.26 (m, 2H), 3.00-2.92 (ovrlp m, 1H), 2.94 (ovrlp dd, *J* = 3.0, 2.0 Hz, 1H), 2.88 (d, *J* = 2.0 Hz, 1H), 2.60 (dd, *J* = 15.1, 8.3 Hz, 1H), 2.37 (dd, *J* = 15.1, 5.9 Hz, 1H); $^{13}$C NMR (100 MHz, $CDCl_3$) $\delta_C$ 201.2, 199.3, 141.2, 139.7, 133.2, 128.4, 127.4, 124.9, 124.1, 119.1, 85.8, 61.9, 58.2, 57.8, 55.8, 52.1, 37.6, 37.0, 35.1; IR (thin film) 2939, 1761, 1710, 1450, 1284, 1220, 1093, 1010, 879, 762 $cm^{-1}$; MS (ES+) m/z 317.1 ($M+Na^+$); HRMS calcd for $C_{19}H_{18}O_3Na$ ($M+Na^+$): 317.1154, found 317.1142.

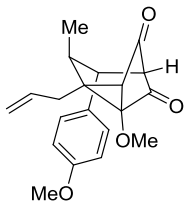


**Cyclopropane (142).** Bicyclo[3.2.1]octanoid **77** (489 mg, 1.50 mmol) and 10 mL acetone afford cyclopropane **142** (474 mg, 1.45 mmol, 97%) as a viscous oil. $^{1}$H NMR (400 MHz, $CDCl_3$) $\delta_H$ 7.03 (d, *J* = 8.6 Hz, 2H), 6.84 (d, *J* = 8.6 Hz, 2H), 5.85 (dddd, *J* = 17.2, 9.9, 9.6, 4.5 Hz, 1H), 5.23-5.13 (m, 2H), 3.78 (s, 3H), 3.60 (s, 3H), 2.97 (dd, *J* = 6.3, 2.5 Hz, 1H), 2.80 (d, *J* = 2.0 Hz, 1H), 2.76 (dd, *J* = 14.7, 9.6 Hz, 1H), 2.66 (dd, *J* = 2.5, 2.0 Hz, 1H), 2.52 (dd, *J* = 6.6, 6.3 Hz, 1H), 2.32-2.24 (m, 1H), 1.18 (d, *J* = 6.6 Hz, 3H); $^{13}$C NMR (100 MHz, $CDCl_3$) $\delta_C$ 200.6, 199.8, 159.0, 133.3, 132.7, 128.6, 118.7, 114.2, 86.9, 61.9, 58.2, 57.8, 56.5, 55.2, 51.9, 36.0, 35.0, 18.0;

IR (thin film) 2936, 1761, 1713, 1611, 1514, 1250, 1216, 1182, 1034, 838 $cm^{-1}$; MS (ES+) m/z 327.1 ($M+H^+$); HRMS calcd for $C_{30}H_{23}O_4$ ($M+H^+$): 327.1596, found 327.1597.

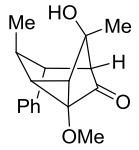


**Tertiary alcohol (145).** To an oven-dried vial was added cyclopropane **135** (40 mg, 0.156 mmol) and anhydrous THF (4.0 mL). The reaction mixture was cooled to 0 $^oC$ while under argon. To this mixture was added 3.0 M methylmagnesium bromide in THF (167 μL, 0.468 mmol) dropwise *via* syringe over 1 min while at 0 $^oC$. The reaction was held at 0 $^oC$ for 1 h with continual stirring. The reaction was quenched while at 0 $^oC$ with the addition of water (40 μL). This mixture was warmed to rt, diluted with water (20 mL), and extracted into $CH_2Cl_2$ (20 mL x 3). The organic fractions were combined, washed with brine (20 mL), dried over sodium sulfate, filtered and evaporated *in vacuo*. The crude product was purified by silica gel flash chromatography (0.03% EtOAc/$CH_2Cl_2$) to afford the tertiary alcohol **145** as a single diastereomer (31.9 mg, 0.117 mmol, 75%) as an amorphous white solid. $^1H$ NMR (400 MHz, CDCl3) $\delta_H$ 7.32-7.25 (m, 2H), 7.24-7.18 (m, 1H), 7.15 (d, *J* = 7.0 Hz, 2H), 3.53 (s, 3H), 3.24 (dd, *J* = 6.6, 2.3 Hz, 1H), 2.54-2.45 (m, 2H), 2.19 (dd, *J* = 8.2, 2.0 Hz, 1H), 2.01 (dd, *J* = 2.3, 2.0 Hz, 1H), 1.99 (s, 1H), 1.46 (s, 3H), 1.28 (d, *J* = 6.6 Hz, 3H); $^{13}C$ NMR (100 MHz, CDCl3) $\delta_C$ 207.7, 143.6, 128.5, 128.1, 126.8, 75.8, 71.2, 58.7, 57.4, 49.4, 41.8, 41.1, 33.4, 28.4, 20.4; IR (thin film) 3446, 2962, 2930,

1717, 1456, 1375, 1148, 1110, 1053, 701 $cm^{-1}$; MS (ES+) m/z 273.1 ($M+H^+$); HRMS calcd for $C_{17}H_{21}O_3$ ($M+H^+$): 273.1491, found 273.1503.

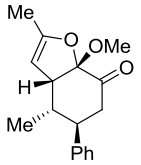


**(3aS,4R,5S,7aR)-7a-Methoxy-2,4-dimethyl-5-phenyl-3a,4,5,6-tetrahydro benzofuran-7(7aH)-one (147).** To an oven-dried vial was added cyclopropane **135** (40 mg, 0.156 mmol) and anhydrous THF (4.0 mL). The reaction mixture was cooled to 0 $^oC$ while under argon. To this mixture was added 3.0 M methylmagnesium bromide in THF (167 μL, 0.468 mmol) dropwise *via* syringe over 1 min while at 0 $^oC$. The reaction was held at 0 $^oC$ with continued stirring for 15 min then warmed to rt for additional 1 h. The reaction was cooled back down to 0 $^oC$ then quenched with the addition of water (40 μL). This mixture was warmed to rt, diluted with water (20 mL) and extracted into $CH_2Cl_2$ (20 mL x 3). The organic fractions were combined, washed with brine (20 mL), dried over sodium sulfate, filtered, and evaporated *in vacuo*. The crude product was purified by silica gel flash chromatography (0.03% EtOAc/$CH_2Cl_2$) to afford acetal **147** (34.8 mg, 0.128 mmol, 82%) as an amorphous white solid. $^1H$ NMR (400 MHz, $CDCl_3$) $\delta_H$ 7.33-7.28 (m, 2H), 7.25-7.19 (m, 1H), 7.13 (d, *J* = 7.0 Hz, 2H), 4.78-4.72 (m, 1H), 3.49 (s, 3H), 3.26-3.18 (m, 1H), 3.03 (dd, *J* = 16.4, 8.2 Hz, 1H), 2.91 (ddd, *J* = 11.6, 9.0, 8.2 Hz, 1H), 2.51 (dd, *J* = 16.4, 9.0 Hz, 1H), 2.06-1.94 (m, 4H), 0.62 (d, *J* = 6.6 Hz, 3H); $^{13}C$ NMR (100 MHz, $CDCl_3$) $\delta_C$

204.8, 155.1, 143.6, 128.6, 127.7, 126.6, 107.6, 95.5, 56.2, 51.5, 45.8, 43.1, 37.2, 16.2, 13.5; IR (thin film) 3420, 2958, 2926, 1722, 1453, 1373, 1220, 1204, 1131, 1095, 1056, 1037, 1007, 761, 702 $cm^{-1}$; MS (ES+) m/z 295.1 ($M+Na^+$); HRMS calcd for $C_{17}H_{20}O_3Na$ ($M+Na^+$): 295.1310, found 295.1314.

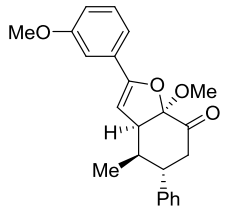


**(3aS,4R,5S,7aR)-7a-Methoxy-2-(3-methoxyphenyl)-4-methyl-5-phenyl-3a,4,5,6-tetrahydrobenzofuran-7(7aH)-one (148).** To an oven-dried vial was added cyclopropane **135** (40 mg, 0.156 mmol) and anhydrous THF (4.0 mL). The reaction mixture was cooled to 0 $^oC$ while under argon. To this mixture was added 1.0 M 3-methoxyphenylmagnesium bromide in THF (468 μL, 0.468 mmol) dropwise *via* syringe over 1 min while at 0 $^oC$. The reaction was held at 0 $^oC$ for 1 h with continual stirring. The reaction was quenched while at 0 $^oC$ with the addition of water (40 μL). This mixture was warmed to rt, diluted with water (20 mL) and extracted into $CH_2Cl_2$ (20 mL x 3). The organic fractions were combined, washed with brine (20 mL), dried over sodium sulfate, filtered, and evaporated *in vacuo*. The crude product was purified by silica gel flash chromatography (0.03% EtOAc/$CH_2Cl_2$) to afford the acetal **148** (43.9 mg, 0.120 mmol, 77 %) as an amorphous white solid. $R_f$ = 0.27 (50%, $CH_2Cl_2$/Hex); $R_f$ = 0.67 (100% $CH_2Cl_2$); $^1H$ NMR (400 MHz, $CDCl_3$) $\delta_H$ 7.36-7.25 (m, 4H), 7.24-7.19 (m, 2H), 7.11 (d, *J* = 7.0 Hz, 2H), 6.96-6.91 (m, 1H), 5.56-

5.47 (m, 1H), 3.87 (s, 3H), 3.56 (s, 3H), 3.46-3.37 (m, 1H), 3.12 (dd, *J* = 16.9, 8.5 Hz, 1H), 2.98 (ddd, *J* = 11.9, 8.9, 8.5 Hz, 1H), 2.54 (dd, *J* = 16.9, 8.9 Hz, 1H), 2.14-2.00 (m, 1H), 0.71 (d, *J* = 6.8 Hz, 3H); $^{13}$C NMR (100 MHz, $CDCl_3$) $\delta_C$ 204.4, 159.7, 155.8, 143.5, 130.9, 129.6, 128.7, 127.7, 126.7, 118.0, 114.8, 110.8, 107.3, 95.8, 56.6, 55.4, 51.7, 45.9, 43.0, 37.6, 16.3; IR (thin film) 2959, 1732, 1601, 1582, 1490, 1454, 1288, 1264, 1208, 1132, 1032, 771, 702 cm$^{-1}$; MS (ES+) m/z 365.1 (M+H$^+$); HRMS calcd for $C_{23}H_{25}O_4$ (M+H$^+$): 365.1753, found 365.1842.

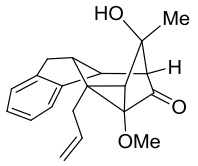


**Tertiary alcohol (149).** To an oven-dried vial was added cyclopropane **141** (60 mg, 0.170 mmol) and anhydrous THF (6.0 mL). The reaction mixture was cooled to 0 $^o$C while under argon. To this mixture was added 3.0 M methylmagnesium bromide in THF (219 μL, 0.612 mmol) dropwise *via* syringe over 1 min while at 0 $^o$C. The reaction was held at 0 $^o$C for 1 h with continual stirring. The reaction was quenched while at 0 $^o$C with the addition of water (40 μL). This mixture was warmed to rt, diluted with water (20 mL), and extracted into $CH_2Cl_2$ (20 mL x 3). The organic fractions were combined, washed with brine (20 mL), dried over sodium sulfate, filtered, and evaporated *in vacuo*. The crude product was purified by silica gel flash chromatography (0.03% EtOAc/$CH_2Cl_2$) to afford the tertiary alcohol **149** as single diastereomer (51.7 mg, 0.167 mmol, 83%) as an amorphous white solid. $^1$H NMR

(400 MHz, $CDCl_3$) $\delta_H$ 7.19-7.07 (m, 4H), 5.92 (dddd, *J* = 17.0, 10.1, 8.1, 5.7 Hz, 1H), 5.29-5.14 (m, 2H), 3.97 (dd, *J* = 9.4, 3.5 Hz, 1H), 3.44-3.40 (m, 3H), 3.36 (dd, *J* = 16.5, 9.8 Hz, 1H), 3.25-3.17 (m, 1H), 2.90 (dd, *J* = 16.5, 6.0 Hz, 1H), 2.56 (dd, *J* = 14.9, 8.1 Hz, 1H), 2.38 (dd, *J* = 3.5, 1.6 Hz, 1H), 2.27 (d, *J* = 1.6 Hz, 1H), 2.16 (dd, *J* = 14.9, 5.7 Hz, 1H), 1.95 (s, 1H), 1.46 (s, 3H); $^{13}C$ NMR (100 MHz, $CDCl_3$) $\delta_C$ 205.9, 142.2, 141.6, 134.7, 127.3, 126.9, 124.6, 123.9, 117.8, 78.7, 71.7, 59.1, 57.6, 48.3, 47.2, 46.5, 38.5, 34.9, 34.8, 27.8; IR (thin film) 3443, 2962, 2929, 1718, 1447, 1377, 1178, 1149, 1102, 1024, 932, 752, 735 $cm^{-1}$; MS (ES+) m/z 333.1 ($M+Na^+$); HRMS calcd for $C_{20}H_{22}O_3Na$ ($M+Na^+$): 333.1467, found 333.1462.

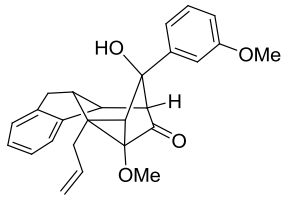


**Tertiary alcohol (150).** To an oven-dried vial was added cyclopropane **141** (50.0 mg, 0.170 mmol) and anhydrous THF (4.0 mL). The reaction mixture was cooled to 0 $^oC$ while under argon. To this mixture was added 1.0 M 3-methoxyphenylmagnesium bromide in THF (510 μL, 0.510 mmol) dropwise *via* syringe over 1 min while at 0 $^oC$. The reaction was held at 0 $^oC$ for 1 h with continual stirring. The reaction was quenched while at 0 $^oC$ with the addition of water (40 μL). This mixture was warmed to rt, diluted with water (20 mL) and extracted into $CH_2Cl_2$ (20 mL x 3). The organic fractions were combined, washed with brine (20 mL), dried over sodium sulfate, filtered, and evaporated *in vacuo*. The crude product was

purified by silica gel flash chromatography (0.03% EtOAc/$CH_2Cl_2$) to afford tertiary alcohol **150** (56.3 mg, 0.140 mmol, 82%) as an amorphous white solid. $R_f$ = 0.37 (0.03%, EtOAc/$CH_2Cl_2$); $R_f$ = 0.58 (0.05% EtOAc/$CH_2Cl_2$); $^1$H NMR (400 MHz, $CDCl_3$) $\delta_H$ 7.30-7.22 (m, 1H), 7.16-7.13 (m, 4H), 7.13-7.10 (m, 1H), 7.09-7.05 (m, 1H), 6.83 (dd, *J* = 8.2, 2.3 Hz, 1H), 5.98 (dddd, *J* = 17.1, 10.2, 8.0, 5.7 Hz, 1H), 5.32-5.18 (m, 2H), 4.20 (dd, *J* = 9.1, 3.7 Hz, 1H), 3.79 (s, 3H), 3.40 (dd, *J* = 15.8, 9.8 Hz, 1H), 3.36-3.31 (m, 1H), 3.31 (s, 3H), 2.94 (dd, *J* = 15.8, 5.3 Hz, 1H), 2.86-2.79 (m, 1H), 2.63 (dd, *J* = 15.1, 8.0 Hz, 1H), 2.55-2.47 (m, 1H), 2.23 (ovrlp dd, *J* = 15.1, 5.7 Hz, 1H), 2.22 (ovrlp s, 1H); $^{13}$C NMR (100 MHz, $CDCl_3$) $\delta_C$ 205.8, 160.0, 146.5, 142.0, 141.7, 134.6, 129.9, 127.4, 126.9, 124.6, 124.0, 117.8, 117.2, 113.6, 111.0, 78.8, 75.4, 59.0, 58.0, 55.3, 48.6, 48.2, 46.8, 38.6, 34.9, 34.8; IR (thin film) 3441, 2935, 1730, 1601, 1486, 1292, 1261, 1047, 752, 735, 701 $cm^{-1}$; MS (ES+) m/z 425.1 ($M+Na^+$); HRMS calcd for $C_{26}H_{26}O_4Na$ ($M+Na^+$): 425.1729, found 425.1739.

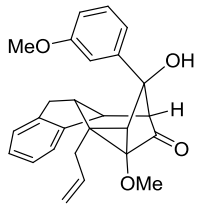


**Tertiary alcohol (151).** To an oven-dried vial was added cyclopropane **141** (60 mg, 0.204 mmol) and anhydrous THF (6.0 mL). The reaction mixture was cooled to 0 $^o$C while under argon. To this mixture was added 1.0 M 3-methoxyphenylmagnesium bromide in THF (612 μL, 0.612 mmol) dropwise *via* syringe over 1 min while at 0 $^o$C. The reaction was stirred for 15 min then warmed to

rt with continued stirring for 1 h. The reaction was cooled back down to 0 $^{o}$C and quenched while at 0 $^{o}$C with the addition of water (40 μL). This mixture was warmed to rt, diluted with water (20 mL) and extracted into $CH_2Cl_2$ (20 mL x 3). The organic fractions were combined, washed with brine (20 mL), dried over sodium sulfate, filtered, and evaporated *in vacuo*. The crude product was purified by silica gel flash chromatography (0.03% EtOAc/$CH_2Cl_2$) to afford the tertiary alcohol **150** (9.3 mg, 0.023 mmol, 11%) and tertiary alcohol **151** (45.5 mg, 0.113 mmol, 55 %) as amorphic white solids. Tertiary alchohol **150**: $R_f$ = 0.37 (0.03% EtOAc/$CH_2Cl_2$); $R_f$ = 0.58 (0.05% EtOAc/$CH_2Cl_2$) ; Tertiary alcohol **151**: $R_f$ = 0.08 (0.03%, EtOAc/$CH_2Cl_2$); $R_f$ = 0.19 (0.05% EtOAc/$CH_2Cl_2$); Characterization data for **151**: $^{1}$H NMR (400 MHz, $CDCl_3$) $\delta_H$ 7.37 (t, *J* = 8.0 Hz, 1H), 7.16 (d, *J* = 7.8 Hz, 1H), 7.13-7.06 (m, 4H), 7.02-6.98 (m, 1H), 6.91 (dd, *J* = 8.2, 2.3 Hz, 1H), 6.23-6.09 (m, 1H), 5.35-5.27 (m, 2H), 3.86 (s, 3H), 3.54 (s, 3H), 3.28 (ddd, *J* = 16.4, 9.4, 4.7 Hz, 1H), 3.02-2.96 (m, 2H), 2.96-2.85 (m, 1H), 2.64 (dd, *J* = 14.8, 8.2 Hz, 1H), 2.62 (s, 1H), 2.55 (d, *J* = 2.0 Hz, 1H), 2.49 (s, 1H), 2.37 (dd, *J* = 14.5, 7.0 Hz, 1H); $^{13}$C NMR (100 MHz, $CDCl_3$) $\delta_C$ 207.6, 160.0, 143.5, 141.5, 141.4, 134.3, 130.0, 127.5, 126.9, 124.5, 123.9, 118.7, 118.5, 114.0, 111.9, 79.1, 75.5, 60.4, 57.9, 55.4, 49.3, 49.1, 44.1, 38.3, 35.4, 35.0; IR (thin film) 3365, 2934, 1734, 1487, 1457, 1436, 1262, 1036, 752 cm$^{-1}$; MS (ES+) m/z 425.1 (M+Na$^{+}$); HRMS calcd for $C_{26}H_{26}O_4Na$ (M+Na$^{+}$): 425.1729, found 425.1742.

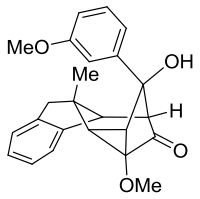


***Epi*-Product derived from cyclopropane 140**: Followed procedure for tertiary alcohol **151**. Reaction using cyclopropane **140** (70 mg, 0.224 mmol) and 1 M 3-methoxyphenylmagnesium bromide in THF (671 μL, 0.671 mmol) afforded the tertiary alcohol (49.0 mg, 0.129 mmol, 50%) as an amorphic white solid. $R_f$ = 0.31 (11% EtOAc/$CH_2Cl_2$); $R_f$ = 0.52 (20% EtOAc/$CH_2Cl_2$); $^1$H NMR (400 MHz, $CDCl_3$) $\delta_H$ 7.40 (t, *J* = 8.0 Hz, 1H), 7.20 (d, *J* = 7.8 Hz, 1H), 7.17-7.10 (m, 3H), 7.08-7.01 (m, 2H), 6.92 (dd, *J* = 8.2, 2.7 Hz, 1H), 3.86 (s, 3H), 3.51 (s, 3H), 3.15 (d, *J* = 16.8 Hz, 1H), 2.92 (dd, *J* = 8.6, 2.0 Hz, 1H), 2.85 (ovrlp s, 1H), 2.83 (ovrlp d, *J* = 16.8 Hz, 1H), 2.73-2.66 (m, 2H), 2.48 (d, *J* = 8.6 Hz, 1H), 1.06 (s, 3H); $^{13}$C NMR (100 MHz, $CDCl_3$) $\delta_C$ 208.1, 159.9, 143.0, 141.3, 141.2, 130.0, 127.5, 126.9, 124.7, 124.1, 118.7, 113.6, 112.7, 78.2, 72.3, 59.6, 57.5, 56.7, 55.3, 49.0, 47.5, 40.7, 40.0, 28.3; IR (thin film) 3420, 2957, 1742, 1452, 1265, 1072, 1030, 736 cm$^{-1}$; MS (ES+) m/z 399.1 (M+Na$^+$); HRMS calcd for $C_{24}H_{24}O_4Na$ (M+Na$^+$): 399.1572, found 399.1569.

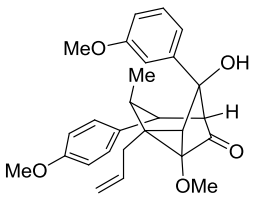


***Epi*-Product derived from cyclopropane 142**: Followed procedure for tertiary alcohol **151**. Reaction using cyclopropane **142** (70 mg, 0.214 mmol) and 1.0

M 3-methoxyphenylmagnesium bromide in THF (643 μL, 0.643 mmol) afforded the tertiary alcohol (53.4 mg, 0.123 mmol, 67%) as an amorphic white solid. $R_f$ = 0.42 (10% EtOAc/$CH_2Cl_2$); $R_f$ = 0.75 (20% EtOAc/$CH_2Cl_2$); $^1$H NMR (400 MHz, $CDCl_3$) $\delta_H$ 7.38 (t, *J* = 8.0 Hz, 1H), 7.07 (d, *J* = 7.4 Hz, 1H), 7.03 (s, 1H), 6.93 (dd, *J* = 8.2, 2.3 Hz, 1H), 6.87 (d, *J* = 8.6 Hz, 2H), 6.74 (d, *J* = 8.6 Hz, 2H), 5.93 (dddd, *J* = 17.1, 10.2, 9.8, 4.7 Hz, 1H), 5.15 (d, *J* = 17.2 Hz, 1H), 5.10 (d, *J* = 10.2 Hz, 1H), 3.85 (s, 3H), 3.74 (s, 3H), 3.57 (s, 3H), 2.77 (dd, *J* = 14.7, 9.6 Hz, 1H), 2.56-2.53 (m, 2H), 2.44-2.40 (m, 1H), 2.34-2.27 (m, 1H), 2.24-2.15 (m, 2H), 0.87 (d, *J* = 6.3 Hz, 3H); $^{13}$C NMR (100 MHz, $CDCl_3$) $\delta_H$ 209.4, 160.0, 158.4, 143.5, 135.0, 134.8, 130.1, 128.9, 118.7, 117.6, 113.8, 113.8, 112.5, 79.4, 76.8 59.3, 57.7, 55.3, 55.2, 51.0, 47.1, 44.1, 36.0, 35.3, 17.0; IR (thin film) 3421, 2936, 1734, 1514, 1457, 1251, 1180, 1046, 788 cm$^{-1}$; MS (ES+) m/z 417.2 (M-$H_2O$); HRMS calcd for $C_{27}H_{28}O_4$ (M-$H_2O$): 417.2066, found 417.2078.

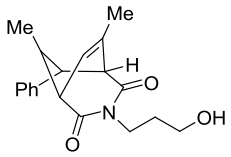


**3-(3-Hydroxypropyl)-6,8-dimethyl-7-phenyl-3-azabicyclo [3.2. 2]non-8-ene-2,4-dione (152).** 3-Azido-1-propanol (39.3 mg, 0.390 mmol) was added to a solution of **145** (106 mg, 0.390 mmol) in $CH_2Cl_2$ (1.0 mL) at 0 ºC and the solution was stirred for 5 min. Triflic acid stock solution (1.03 mL, 1.17 mmol) was slowly added dropwise and the solution gradually turned black. The acid stock solution was prepared fresh by the addition of triflic acid (0.20 mL) to a mixture of $CH_2Cl_2$ (1.45

mL) and MeCN (0.35 mL). The solution was gradually warmed to rt and stirred for 12 h. The reaction was diluted with $CH_2Cl_2$ (5.0 mL) and quenched by the addition of sat. aq $NaHCO_3$ (5.0 mL) and the biphasic solution was stirred at rt for 2 h. The layers were then separated and the aqueous layer was extracted with $CH_2Cl_2$ (10 mL x 3). The organic extracts were combined, washed with brine (10 mL), dried (anhydrous $Na_2SO_4$), filtered, and evaporated *in vacuo*. The crude material was purified by $SiO_2$ preparative TLC (10% MeOH/$CH_2Cl_2$) to afford **152** (21.5 mg, 0.0684 mmol, 18%) as a yellow oil. $R_f$ = 0.20 (10% MeOH:$CH_2Cl_2$); $^1$H NMR (500 MHz, $CDCl_3$) $\delta_H$ 7.33-7.29 (m, 2H), 7.27-7.24 (m, 1H), 7.19-7.10 (m, 2H), 5.93 (d, *J* = 7.0 Hz, 1H), 3.87 (td, *J* = 6.5, 2.0 Hz, 2H), 3.53 (dd, *J* = 7.5, 1.0 Hz, 1H), 3.51 (dd, *J* = 4.0, 1.5 Hz, 1H), 3.48-3.40 (m, 2H), 2.67-2.62 (m, 1H), 2.59 (dd, *J* = 7.5, 4.0 Hz, 1H), 1.94 (d, *J* = 1.5 Hz, 3H); $^{13}$C NMR (125 MHz, $CDCl_3$) $\delta_C$ 175.2, 172.2, 141.4, 140.2, 128.8 (2), 127.6 (2), 127.5, 120.0, 60.6, 59.0, 53.9, 51.8, 37.8, 37.0, 30.7, 22.5, 21.1; IR (neat) 2962, 1729, 1710, 1656, 726 cm$^{-1}$; MS (ES+) m/z 314.1 (M+H$^+$); HRMS calcd for $C_{19}H_{24}NO_3$ (M+H$^+$): 314.1756, found 314.1771.

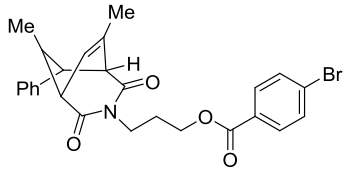


**(6,8-Dimethyl-2,4-dioxo-7-phenyl-3-azabicyclo [3.2.2]non-8-en-3-yl)propyl-4-bromobenzoate (153).** A solution of **145** (120 mg, 0.383 mmol) in $CH_2Cl_2$ (4.0 mL) was treated with pyridine (60.6 mg, 0.766 mmol), followed by 4-

bromobenzoyl chloride (168 mg, 0.766 mmol). The reaction was stirred overnight at rt. The solution was quenched with brine (5.0 mL) and diluted with $CH_2Cl_2$ (5.0 mL). The layers were separated and the aqueous layer was extracted with $CH_2Cl_2$ (10 mL x 3). The organic extracts were combined, washed with brine (10 mL), dried (anhydrous $Na_2SO_4$), filtered, and evaporated *in vacuo*. The crude material was purified by $SiO_2$ preparative TLC (1:5 EtOAc:Hex) to afford **153** (139.7 mg, 0.281 mmol, 73%) as a white solid. The pure material was recrystallized with EtOAc-Hex to give single crystals for X-ray analysis. $R_f$ = 0.39 (20% EtOAc:Hex); mp 99.5-100.0 ºC; $^1$H NMR (400 MHz, $CDCl_3$) $\delta_H$ 7.92 (dt, *J* = 7.2, 1.6 Hz, 2H), 7.56 (dt, *J* = 7.2, 1.6 Hz, 2H), 7.32-7.29 (m, 2H), 7.27-7.23 (m, 1H), 7.12-7.10 (m, 2H), 5.91 (d, *J* = 5.6 Hz, 1H), 4.28 (t, *J* = 4.8 Hz, 2H), 3.91 (t, *J* = 6.0 Hz, 2H), 3.52 (dd, *J* = 6.0, 0.8 Hz, 1H), 3.49 (dd, *J* = 3.2, 1.2 Hz, 1H), 2.64 (m, 1H), 2.58 (dd, *J* = 6.0, 3.2 Hz, 1H), 2.00-1.94 (m, 2H), 1.93 (d, *J* = 1.2 Hz, 3H) 1.09 (d, *J* = 6.4 Hz, 3H); $^{13}$C NMR (100 MHz, $CDCl_3$) $\delta_C$ 174.3, 171.3, 165.7, 141.3, 140.3, 131.6 (2), 131.1 (2), 129.1, 128.8 (2), 127.9, 127.7 (2), 127.4, 120.0, 62.9, 60.7, 53.9, 52.0, 38.5, 37.1, 27.1, 22.6, 21.2; IR (neat) 2962, 1717, 1662, 1271 cm$^{-1}$; MS (ES+) m/z 496.1 (M+H$^+$); HRMS calcd for $C_{26}H_{27}BrNO_4$ (M+H$^+$): 496.1123, found 496.1129.

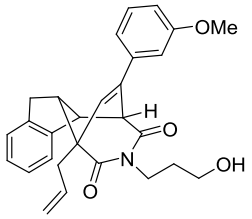

**Indene-derived bicyclic imide (155).** 3-Azido-1-propanol (17.5 mg, 0.173 mmol) was added to a solution of **150** (69.0 mg, 0.171 mmol) in $CH_2Cl_2$ (2.0 mL) at 0 ºC and the solution was stirred for 5 min. Triflic acid stock solution (0.455 mL, 0.514 mmol) was slowly added dropwise and the solution gradually turned black. The acid stock solution was prepared fresh by the addition of triflic acid (0.20 mL) to a mixture of $CH_2Cl_2$ (1.45 mL) and MeCN (0.35 mL). The solution was gradually warmed to rt and stirred for 12 h. The reaction was diluted with $CH_2Cl_2$ (10 mL) and quenched by the addition of sat. aq $NaHCO_3$ (5.0 mL) and the biphasic solution was stirred at rt for 2 h. The layers were then separated and the aqueous layer was extracted with $CH_2Cl_2$ (10 mL x 3). The organic extracts were combined, washed with brine (10 mL), dried (anhydrous $Na_2SO_4$), filtered, and evaporated *in vacuo*. The crude material was purified by $SiO_2$ preparative TLC (5% MeOH/$CH_2Cl_2$) to afford **155** (15.0 mg, 0.0337 mmol, 20%) as a yellow oil. $R_f$ = 0.41 (5% MeOH/$CH_2Cl_2$); $^1$H NMR (500 MHz, $CDCl_3$) δ 7.35-7.31 (m, 2H), 7.24-7.16 (m, 3H), 7.12 (ddd, *J* = 7.5, 1.5, 1.0 Hz, 1H), 7.05 (t, *J* = 2.5 Hz, 1H), 6.90 (ddd, *J* = 8.0, 2.5, 0.5 Hz, 1H), 6.40, (d, *J* = 1.5 Hz, 1H), 6.00-5.91 (m, 1H), 5.32-5.26 (m, 2H), 4.75 (dd, *J* = 6.5, 2.0 Hz, 1H), 4.03 (dd, *J* = 10.0, 6.5 Hz, 1H), 3.87 (s, 3H), 3.62-3.57 (m, 1H), 3.55-3.49 (m, 1H), 3.26 (dd, *J* = 17.5, 10.0 Hz, 1H), 3.01-2.95 (m, 2H), 2.92-2.87 (m, 1H), 2.84 (dd, *J* = 17.5, 4.0 Hz, 1H), 2.65-2.60 (m, 1H), 2.54 (dd, *J* = 14.0, 8.5 Hz, 1H), 1.62-1.21 (m, 2H); $^{13}$C NMR (125 MHz, $CDCl_3$) $\delta_C$ 173.4, 172.7, 159.9, 142.5,140.5, 140.5, 139.1, 133.8, 129.8, 129.3, 128.1, 127.1, 125.0, 124.9, 119.7, 117.9, 113.7, 111.3, 58.3, 55.4, 55.3, 54.5,

48.0, 43.4, 40.5, 38.0, 33.2, 30.4; IR (neat) 3487, 1702, 1653 $cm^{-1}$; MS (ES+H) m/z 444.2 ($M+H^+$); HRMS calcd for $C_{28}H_{30}NO_4$ ($M+H^+$): 444.2175, found 444.2151.

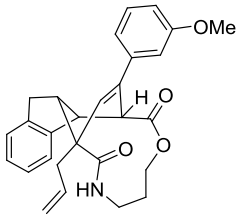


**Indene-derived macrocyclic ester (156).** 3-Azido-1-propanol (17.5 mg, 0.173 mmol) was added to a solution of **151** (69.0 mg, 0.171 mmol) in $CH_2Cl_2$ (2.0 mL) at 0 ºC and the solution was stirred for 5 min. Triflic acid stock solution (0.455 mL, 0.514 mmol) was slowly added dropwise and the solution gradually turned black. The acid stock solution was prepared fresh by the addition of triflic acid (0.20 mL) to a mixture of $CH_2Cl_2$ (1.45 mL) and MeCN (0.35 mL). The solution was gradually warmed to rt and stirred for 12 h. The reaction was diluted with $CH_2Cl_2$ (10 mL) and quenched by the addition of sat. aq $NaHCO_3$ (5.0 mL) and the biphasic solution was stirred at rt for 2 h. The layers were then separated and the aqueous layer was extracted with $CH_2Cl_2$ (10 mL x 3). The organic extracts were combined, washed with brine (10 mL), dried (anhydrous $Na_2SO_4$), filtered, and evaporated *in vacuo*. The crude material was purified by $SiO_2$ preparative TLC (5% MeOH/$CH_2Cl_2$) to afford **156** (13.2 mg, 0.0297 mmol, 17%) as a yellow oil. $R_f$ = 0.50 (5% MeOH/$CH_2Cl_2$); $^1H$ NMR (500 MHz, $CDCl_3$) $\delta_H$ 7.35 (t, *J* = 8.0 Hz, 1H), 7.24-7.14 (m, 6H), 6.92 (dd, *J* = 8.0, 2.0 Hz, 1H), 6.45 (s, 1H), 6.33, (d, *J* = 8.0 Hz, NH), 5.86-5.78 (m, 1H), 5.26-5.19 (m, 2H), 4.25 (ddd, *J* = 11.0, 8.0, 2.5 Hz, 1H), 4.07 (ddd, *J* = 11.0, 7.5, 3.0 Hz, 1H),

4.00 (d, $J$ = 6.0 Hz, 1H), 3.90-3.83 (m, 1H), 3.86 (s, 3H), 3.51 (dd, $J$ = 10.0, 5.5 Hz, 1H), 3.25 (dd, $J$ = 16.5, 9.0 Hz, 1H), 3.05-2.83 (m, 4H), 2.52 (dd, $J$ = 13.5, 9.0 Hz, 1H), 1.89-1.84 (m, 1H), 1.63-1.59 (m, 1H); $^{13}$C NMR (125 MHz, $CDCl_3$) $\delta_C$ 173.3, 169.7, 159.8, 144.4, 142.0, 141.8, 141.4, 133.7, 131.4, 129.7, 127.2, 126.3, 124.4, 123.6, 119.5, 118.4, 113.1, 112.1, 65.5, 55.3, 52.1, 48.8, 48.4, 45.8, 45.3, 40.1, 36.8, 26.4; IR (neat) 3413, 2929, 1726, 1665 cm$^{-1}$; MS (ES+) m/z 444.2 (M+H$^+$); HRMS calcd for $C_{28}H_{30}NO_4$ (M+H$^+$): 444.2175, found 444.2149.

**General procedure for the synthesis of polycyclic imines 157-160.** To an oven-dried vial was added cyclopropane **135** (30 mg, 0.117 mmol) and anhydrous nitromethane (450 μL) followed by the addition of benzonitrile (60 μL, 0.585 mmol). To this mixture was added TMSOTf (21.0 μL, 0.039 mmol) in anhydrous nitromethane (300 μL) while at 0 $^o$C. The reaction was warmed to rt and stirred for 4 h. Next, the reaction was cooled to 0 $^o$C and slowly quenched with the addition of saturated $NaHCO_3$ (400 μL), diluted with water (5 mL), and extracted into $CH_2Cl_2$ (5 mL x 3). The organic fractions were combined, washed with brine (10 mL), dried over sodium sulfate, filtered, and evaporated *in vacuo*. The crude product was purified by flash chromatography ($SiO_2$, 100 % $CH_2Cl_2$ to 30:1 $CH_2Cl_2$:EtOAc).

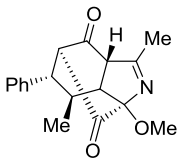

**Polycyclic imine (157).** Reaction of cyclopropane **135** (40 mg, 0.156 mmol) with anhydrous acetonitrile (neat) afford polycyclic imine **157** (23.7 mg, 0.080 mmol, 51%) as an amorphous white solid. The product was purified by silica gel flash chromatography (0.03% EtOAc/$CH_2Cl_2$ to 0.06% EtOAc/$CH_2Cl_2$). $R_f$ = 0.22 (0.03 EtOAc/$CH_2Cl_2$); $^1$H NMR (400 MHz, $CDCl_3$) $\delta_H$ 7.36-7.25 (m, 3H), 7.15 (d, *J* = 6.6 Hz, 2H), 3.90 (d, *J* = 5.1 Hz, 1H), 3.79 (s, 3H), 3.21-3.17 (m, 1H), 3.12-3.07 (m, 2H), 2.67-2.57 (m, 1H), 2.18 (s, 3H), 1.17 (d, *J* = 7.0 Hz, 3H); $^{13}$C NMR (100 MHz, $CDCl_3$) $\delta_C$ 198.9, 197.8, 173.9, 139.4, 128.9, 128.1, 127.9, 105.2, 71.1, 64.1, 57.4, 56.1, 53.0, 29.9, 21.0, 20.4; IR (thin film) 2959, 1749, 1718, 1624, 1272, 1142, 1032, 731, 701 cm$^{-1}$; MS (ES+) m/z 298.1 (M+H$^+$); HRMS calcd for $C_{18}H_{20}NO_3$ (M+H$^+$): 298.1443, found 298.1445.

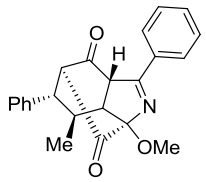


**Polycyclic imine (158).** Reaction of cyclopropane **135** (30 mg, 0.117 mmol) and benzonitrile (60 μL, 0.585 mmol) afford polycyclic imine **158** (39.7 mg, 0.110 mmol, 94%) as an amorphous off-white solid. The product was purified by silica gel flash chromatography (100% $CH_2Cl_2$ to 0.03% EtOAc/$CH_2Cl_2$). $R_f$ = 0.49 (0.03% EtOAc/$CH_2Cl_2$); $^1$H NMR (400 MHz, $CDCl_3$) $\delta_H$ 8.06 (d, *J* = 7.0 Hz, 2H), 7.57-7.51 (m, 1H), 7.51-7.45 (m, 2H), 7.38-7.32 (m, 2H), 7.31-7.25 (m, 1H), 7.20 (d, *J* = 7.4 Hz, 2H), 4.59 (d, *J* = 5.5 Hz, 1H), 3.87 (s, 3H), 3.25-3.18 (m, 3H), 2.76-2.65 (m, 1H),

1.25 (d, $J$ = 7.0 Hz, 3H); $^{13}$C NMR (100 MHz, $CDCl_3$) $\delta_C$ 199.7, 197.4, 169.8, 139.5, 132.5, 131.5, 128.9, 128.8, 128.6, 128.2, 127.9, 105.0, 71.5, 59.9, 57.7, 56.7, 53.0, 30.0, 21.1; IR (thin film) 2959, 1749, 1723, 1568, 1456, 1210, 1147, 1070, 1032, 735, 700 cm$^{-1}$; MS (ES+) m/z 360.1 (M+H$^+$); HRMS calcd for $C_{23}H_{22}NO_3$ (M+H$^+$): 360.1600, found 360.1593.

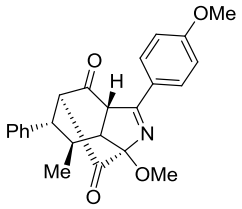


**Polycyclic imine (159).** Reaction of cyclopropane **135** (30 mg, 0.117 mmol) and 4-methoxybenzonitrile (78 μL, 0.585 mmol) afford polycyclic imine **159** (36.4 mg, 0.093 mmol, 80%) as an amorphic solid. The product was purified by silica gel flash chromatography (100% $CH_2Cl_2$ to 0.03% EtOAc/$CH_2Cl_2$). $R_f$ = 0.39 (0.03% EtOAc/$CH_2Cl_2$); $^1$H NMR (400 MHz, $CDCl_3$) $\delta_H$ 8.00 (d, $J$ = 9.0 Hz, 2H), 7.37-7.32 (m, 2H), 7.30-7.25 (m, 1H), 7.20 (d, $J$ = 7.4 Hz, 2H), 6.97 (d, $J$ = 9.0 Hz, 2H), 4.54 (d, $J$ = 5.1 Hz, 1H), 3.86 (s, 3H), 3.85 (s, 3H), 3.23-3.21 (m, 1H), 3.21-3.16 (m, 2H), 2.76-2.65 (m, 1H), 1.24 (d, $J$ = 7.0 Hz, 3H); $^{13}$C NMR (100 MHz, $CDCl_3$) $\delta_C$ 199.9, 197.5, 168.9, 163.1, 139.6, 130.6, 128.9, 128.2, 127.8, 124.2, 114.1, 105.0, 71.3, 59.7, 57.3, 56.7, 55.4, 52.8, 30.0, 21.1; IR (thin film)x2959, 1750, 1723, 1607, 1513, 1256, 1174, 1031, 735, 701 cm$^{-1}$; MS (ES+) m/z 390.1 (M+H$^+$); HRMS calcd for $C_{24}H_{24}NO_4$ (M+H$^+$): 390.1705, found 390.1717.

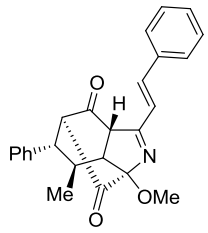


**Polycyclic imine (160).** Reaction with cyclopropane **135** (40 mg, 0.156 mmol) and cinnamonitrile (98 μL, 0.78 mmol) afford polycyclic imine **160** (28.6 mg, 0.074 mmol, 47%) as an amorphous solid. The product was purified by silica gel flash chromatography (100% $CH_2Cl_2$ to 0.03% EtOAc/$CH_2Cl_2$). $R_f$ = 0.14 (0.03% EtOAc/$CH_2Cl_2$). $^1$H NMR (400 MHz, $CDCl_3$) $\delta_H$ 7.59-7.55 (m, 2H), 7.45 (d, *J* = 16.4 Hz, 1H), 7.42-7.38 (m, 3H), 7.38-7.32 (m, 2H), 7.31-7.26 (m, 1H), 7.20 (d, *J* = 7.4 Hz, 2H), 7.01 (d, *J* = 16.4 Hz, 1H), 4.41 (d, *J* = 5.1 Hz, 1H), 3.85 (s, 3H), 3.23 (d, *J* = 2.0 Hz, 1H), 3.19-3.12 (m, 2H), 2.74-2.65 (m, 1H), 1.24 (d, *J* = 7.0 Hz, 3H); $^{13}$C NMR (100 MHz, $CDCl_3$) $\delta_C$ 199.5, 197.4, 169.9, 144.2, 139.5, 134.9, 130.3, 129.0, 128.9, 128.2, 128.0, 127.9, 121.9, 105.0, 71.4, 59.1, 57.4, 56.7, 53.1, 30.0, 21.1; IR (thin film) 2958, 1750, 1724, 1628, 1559, 1578, 1456, 1201, 1143, 754, 735, 700 cm$^{-1}$; MS (ES+) m/z 386.1 (M+H$^+$); HRMS calcd for $C_{25}H_{24}NO_3$ (M+H$^+$): 386.1756, found 386.1765.

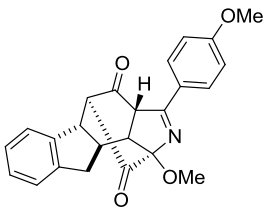

**Polycyclic imine (161).** Reaction with cyclopropane **141** (45.9 mg, 0.156 mmol) and 4-methoxybenzonitrile (104 mg, 0.780 mmol) afford imine **161** (36.2 mg, 0.085 mmol, 54%) as an amorphous solid. The product was purified by prep $SiO_2$ TLC (0.03% EtOAc/$CH_2Cl_2$). $R_f$ = 0.76 (0.03% EtOAc/$CH_2Cl_2$); $^1$H NMR (400 MHz, $CDCl_3$) $\delta_H$ 7.96 (d, *J* = 9.0 Hz, 2H), 7.26-7.21 (m, 3H), 7.21-7.17 (m, 1H), 6.97 (d, *J* = 8.6 Hz, 2H), 5.78 (dddd, *J* = 16.8, 10.2, 7.4, 7.4 Hz, 1H), 5.13 (dd, *J* = 10.6, 1.6 Hz, 1H), 5.04 (dd, *J* = 16.8, 1.2 Hz, 1H), 4.32 (s, 1H), 4.08 (dd, *J* = 9.0, 3.5 Hz, 1H), 3.90 (s, 3H), 3.87 (s, 3H), 3.70-3.60 (m, 1H), 3.58 (d, *J* = 3.5 Hz, 1H), 3.18-3.14 (m, 2H), 2.59 (dd, *J* = 14.5, 7.4 Hz, 1H), 2.18 (dd, *J* = 14.5, 7.4 Hz, 1H); $^{13}$C NMR (100 MHz, $CDCl_3$) $\delta_H$ 200.2, 198.9, 168.0, 163.0, 142.3, 139.6, 133.1, 130.5, 128.4, 127.1, 125.2, 124.5, 124.5, 119.4, 114.2, 105.2, 69.2, 67.5, 65.0, 56.4, 55.5, 51.5, 35.3, 33.7, 33.7; IR (thin film) 2943, 1719, 1606, 1513, 1251, 1174, 1027, 739 $cm^{-1}$; MS (ES+) m/z 428.1 ($M+H^+$); HRMS calcd for $C_{27}H_{26}NO_4$ ($M+H^+$): 428.1862, found 428.1864.

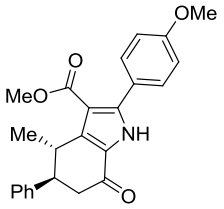


**Methyl-3-(4-methoxyphenyl)-7-methyl-4-oxo-6-phenyl-4,5,6,7-tetrahydro-2*H*-isoindole-1-carboxylate (162).** A solution of **159** (100 mg, 0.256 mmol) dissolved in dry MeOH (5.0 mL) was heated in a sealed tube at 100 ºC for 12 h. After cooling, the solvent was removed *in vacuo* and the crude material was directly purified by $SiO_2$ preparative TLC (66% $Et_2O$/Hex) to afford **162** (83.5 mg, 0.214

mmol, 84%) as a white solid. $R_f$ = 0.28 (66% $Et_2O$/Hex); mp 86.6-90.0 ºC; $^1$H NMR (400 MHz, $CDCl_3$) $\delta_H$ 10.04 (s, 1H), 7.53-7.50 (m, 2H), 7.28-7.24 (m, 2H), 7.20-7.17 (m, 3H), 6.93-6.91 (m, 2H), 3.85 (s, 3H), 3.85-3.79 (m, 1H), 3.75 (s, 3H), 3.42 (q, *J* = 4.0 Hz, 1H), 3.12 (dd, *J* = 17.2, 2.8 Hz, 1H), 2.78 (dd, *J* = 17.2, 4.0 Hz, 1H), 1.54 (d, *J* = 7.2 Hz, 3H); $^{13}$C NMR (100 MHz, $CDCl_3$) $\delta_C$ 187.1, 164.8, 160.2, 144.1, 143.9, 142.4, 130.6 (2), 128.3 (2), 127.4 (2), 126.5, 126.2, 123.0, 113.3 (2), 110.9, 55.2, 50.9, 47.8, 39.4, 34.5, 20.9; IR (neat) 3209, 2953, 1702, 1634 cm$^{-1}$; MS (ES+) m/z 390.1 (M+H$^+$); HRMS calcd for $C_{24}H_{24}NO_4$ (M+H$^+$): 390.1705, found 390.1678.

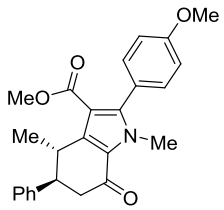


**Methyl-3-(4-methoxyphenyl)2,7-dimethyl-4-oxo-6-phenyl-4,5,6,7-tetrahydro-2*H*-isoindole-1-carboxylate (163).** A solution of **162** (100 mg, 0.256 mmol), iodomethane (109 mg, 0.770 mmol), and $K_2CO_3$ (107 mg, 0.770 mmol) in dry MeCN (5.0 mL) was heated in a sealed tube at 82 ºC for 24 h. After cooling, the solvent was removed and the residue was taken up in $CH_2Cl_2$ (5.0 mL). The solution was washed with water (10 mL) and the aqueous layer was extracted with $CH_2Cl_2$ (5.0 mL x 3). The organic extracts were collected, dried (anhydrous $Na_2SO_4$), filtered, and evaporated *in vacuo* to give a pale yellow oil. The crude material was purified by $SiO_2$ column chromatography (66% $Et_2O$/Hex) to afford **163** (55.5 mg, 0.137 mmol, 54%) as a white solid. $R_f$ = 0.43 (66% $Et_2O$/Hex); mp 146.6-152.7 ºC; $^1$H NMR (500

MHz, $CDCl_3$) $\delta_H$ 7.31-7.20 (m, 7H), 7.02 (d, *J* = 9.0 Hz, 2H), 3.95-3.89 (m, 1H), 3.90 (s, 3H), 3.74 (s, 3H), 3.65 (s, 3H), 3.43-3.40 (m, 1H), 3.20 (dd, *J* = 17.0, 5.5 Hz, 1H), 2.86 (dd, *J* = 17.0, 4.0 Hz, 1H), 1.57 (d, *J* = 7.0 Hz, 3H); $^{13}$C NMR (125 MHz, $CDCl_3$) $\delta_C$ 187.6, 164.5, 159.9, 145.7, 144.2, 141.4, 131.3 (2), 128.2 (2), 127.4 (2), 126.1, 126.0, 122.4, 113.4 (2), 111.2, 55.1, 50.7, 46.9, 40.7, 34.3, 34.1 21.3; IR (neat) 1702, 1649, 1456, 1247 $cm^{-1}$; MS (ES+) m/z 404.1 ($M+H^+$); HRMS calcd for $C_{25}H_{26}NO_4$ ($M+H^+$): 404.1862, found 404.1859.

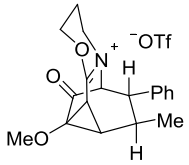


**Cyclopropyl iminium ether (165).** A solution of polycyclic iminium ethers **67a/67b** (5.00 mg, 0.011 mmol) dissolved in acetone-d6 (1.0 mL) in an NMR tube was irradiated in a photoreactor at 300 nm for 30 min. The solvent was then removed *in vacuo*. The isolated product required no additional purification and was unstable to $SiO_2$. The reaction afforded **165** (4.31 mg, 0.0138 mmol, 86%) as a yellow oil. $^1$H NMR (500 MHz, Acetone-d6) $\delta_H$ 7.35-7.38 (m, 2H), 7.27-7.32 (m, 3H), 5.07 (ddt, *J* = 11.0, 4.5, 2.0 Hz, 1H), 4.83 (ddd, *J* = 11.5, 10.5, 4.0 Hz, 1H), 4.23-4.28 (m, 1H), 4.04 (d, *J* = 3.0 Hz, 1H), 3.98 (ddd, *J* = 14.5, 10.0, 5.5 Hz, 1H), 3.90 (s, 1H), 3.57 (s, 3H), 3.30-3.34 (m, 3H), 2.54-2.66 (m, 2H), 1.47 (d, *J* = 7.0 Hz, 3H); $^{13}$C NMR (125 MHz, Acetone-d6) $\delta_C$ 195.2, 172.6, 141.6, 130.6 (2), 129.7, 129.6 (2), 72.7, 72.4, 72.2, 58.9

53.9, 48.6, 45.2, 35.7, 34.3, 23.8, 21.4; IR (neat) 1739, 1652, 1274 $cm^{-1}$; MS (ES+) m/z 312.1 ($M^+$); HRMS calcd for $C_{19}H_{22}NO_3$ ($M^+$): 312.1600, found 312.1595.

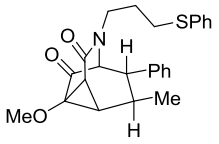


**Cyclopropyl-γ-thiophenyl lactam (166**). A solution of polycyclic iminium ether **67a/67b** (10.0 mg, 0.022 mmol) dissolved in acetone-d6 (1.0 mL) in an NMR tube was irradiated in a photoreactor at 300 nm for 30 min. The solution was transferred to a round-bottom flask and solvent was removed *in vacuo*. In a separate flask benzenethiol (9.55 mg, 0.086 mmol) was added to a mixture of potassium hydride (3.50 mg, 0.086 mmol) in DMF (1.0 mL). The cyclopropane iminium ether residue was taken up in DMF (0.50 mL) and added to the potassium hydride solution. The reaction was heated at 80 ºC for 24 h. After cooling, the reaction was quenched with water (5.0 mL) and extracted with $Et_2O$ (5.0 mL x 3). The organic extracts were combined, washed with brine (5.0 mL), dried (anhydrous $Na_2SO_4$), filtered and concentrated. The crude material was purified by $SiO_2$ preparative TLC (7% MeOH/$CH_2Cl_2$) to afford γ-thiophenyl lactam **166** (6.80 mg, 0.0161 mmol, 99% derived according to reaction of the major regioisomer of substrate) as a yellow oil. $R_f$ = 0.55 (7% MeOH/$CH_2Cl_2$); $^1$H NMR (400 MHz, $CDCl_3$) $\delta_H$ 7.25-7.34 (m, 7H), 7.16-7.20 (m, 1H), 7.05-7.07 (m, 2H), 3.85 (ddd, *J* = 14.4, 13.6, 7.2 Hz, 1H), 3.55 (s, 3H), 3.36 (d, *J* = 2.4 Hz, 1H), 3.14 (dt, *J* = 14.0, 6.8 Hz, 1H), 3.08 (t, *J* = 2.4 Hz, 1H), 2.90-3.02 (m, 1H), 2.90 (t, *J* = 7.2 Hz, 2H), 2.65 (d, *J* = 10.4 Hz, 1H), 2.55 (ddd, *J* =

10.4, 5.2, 0.8 Hz, 1H), 1.86 (p, *J* = 7.2 Hz, 2H), 2.32 (d, *J* = 7.2 Hz, 3H); $^{13}$C NMR (125 MHz, $CDCl_3$) $\delta_C$ 198.0, 166.5, 140.9, 136.9, 135.3, 130.6, 129.7, 129.1, 129.0 (2), 127.6, 127.3, 127.0, 126.3, 70.0, 67.9, 57.4, 55.4, 45.6, 41.7, 36.9, 33.2, 31.0, 27.3, 22.2; IR (neat) 1726, 1662, 1477 $cm^{-1}$; MS (ES+) m/z 422.1 ($M+H^+$); HRMS calcd for $C_{25}H_{28}NO_3S$ ($M+H^+$): 422.1790, found 422.1777.

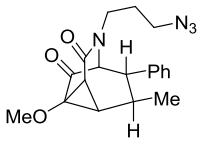


**Cyclopropyl-γ-azido lactam (167).** A solution of polycyclic iminium ether **67a/67b** (10.0 mg, 0.022 mmol) dissolved in acetone-d6 (1.0 mL) in an NMR tube was irradiated in a photoreactor at 300 nm for 30 min. The solution was transferred to a round-bottom flask and solvent was removed in vacuo. In a separate flask sodium azide (5.63 mg, 0.86 mmol) was dissolved in DMF (1.0 mL). The cyclopropane iminium ether residue was taken up in DMF (0.50 mL) and added to the sodium azide solution. The reaction was heated at 80 ºC for 24 h. After cooling, the reaction was quenched with water (5.0 mL) and extracted with $Et_2O$ (5.0 mL x 3). The organic extracts were combined, washed with brine (5.0 mL), dried (anhydrous $Na_2SO_4$), filtered and concentrated. The crude material was purified by $SiO_2$ preparative TLC (7% MeOH/$CH_2Cl_2$) to afford γ-azido lactam **167** (5.20 mg, 0.0137 mmol, 91% derived according to reaction of the major regioisomer of substrate) as a yellow oil. $R_f$ = 0.45 (7% MeOH/$CH_2Cl_2$); $^1$H NMR (500 MHz, $CDCl_3$) $\delta_H$ 7.22-7.35 (m, 3H), 7.10-7.12 (m, 2H), 3.90 (dt, *J* = 14.0, 7.0 Hz, 1H), 3.57 (s, 3H), 3.39 (d, *J* = 2.5 Hz,

1H), 3.32-3.36 (m, 2H), 3.13 (t, *J* = 2.5 Hz, 1H), 2.95-3.03 (m, 2H), 2.67 (d, *J* = 10.5 Hz, 1H), 2.57 (ddd, *J* = 10.5, 5.5, 1.0 Hz, 1H), 1.77-1.84 (m, 2H), 1.34 (d, *J* = 7.0 Hz, 3H); $^{13}$C NMR (125 MHz, $CDCl_3$) $\delta_C$ 198.0, 166.6, 140.9, 129.1 (2), 127.7, 127.0 (2), 70.0, 68.0, 57.4, 55.3, 48.7, 44.2, 41.7, 36.9, 33.3, 27.4, 22.2; IR (neat) 2098, 1726, 1650 1456 $cm^{-1}$; MS (ES+) m/z 377.1 ($M+Na^+$); HRMS calcd for $C_{19}H_{22}N_4O_3Na$ ($M+Na^+$): 377.1590, found 377.1653.

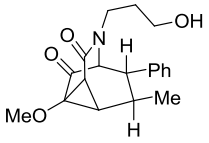


**Cyclopropyl-γ-hydroxy lactam (168).** A solution of polycyclic iminium ether **67a/67b** (400 mg, 0.867 mmol) dissolved in acetone-d6 (8.0 mL) divided amongst eight NMR tubes was irradiated in a photoreactor at 300 nm for 1 h. The solutions were combined and the solvent was removed in vacuo. The residue was taken up in $CH_2Cl_2$ (10 mL) and sat. aq $NaHCO_3$ (10 mL) was added. The biphasic mixture was vigorously stirred for 3 h. The layers were separated and the aqueous layer was extracted with $CH_2Cl_2$ (10 mL x 3). The organic extracts were combined, washed with brine, dried (anhydrous $Na_2SO_4$), filtered and concentrated to give pure product. The reaction afforded **168** (268 mg, 0.811 mmol, 94% derived according to reaction of the major regioisomer of substrate) as a fluffy yellow solid. $R_f$ = 0.49 (7% MeOH/$CH_2Cl_2$); mp 98.0-100.0 ºC; $^1$H NMR (500 MHz, $CDCl_3$) $\delta_H$ 7.33 (t, *J* = 7.5 Hz, 2H), 7.25-7.28 (m, 1H), 7.11 (d, *J* = 7.0 Hz, 2H), 4.02 (ddd, *J* = 14.0, 10.0, 4.5 Hz, 1H), 3.57-3.62 (m, 1H), 3.57 (s, 3H), 3.45 (ddd, *J* = 12.5, 9.5, 3.5 Hz, 1H), 3.36

(d, *J* = 2.5 Hz, 1H), 3.15 (t, *J* = 2.5 Hz, 1H), 2.99-3.04 (m, 2H), 2.68 (d, *J* = 10.5 Hz, 1H), 2.59 (ddd, *J* = 10.5, 5.5, 0.5 Hz, 1H), 1.74-1.80 (m, 1H), 1.57-1.65 (m, 1H), 1.36 (d, *J* = 7.0 Hz, 3H); $^{13}$C NMR (125 MHz, $CDCl_3$) $\delta_C$ 198.0, 167.8, 140.9, 129.1 (2), 127.7, 127.1 (2), 70.2, 67.7, 58.0, 57.4, 55.2, 42.9, 41.9, 36.8, 33.4, 30.1, 22.3; IR (neat) 3421, 1726, 1648, 1265 cm$^{-1}$; MS (ES+) m/z 330.2 ($M+H^+$); HRMS calcd for $C_{19}H_{24}NO_4$ ($M+H^+$): 330.1705, found 330.1709.

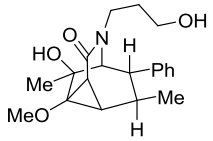


**Cyclopropyl-γ-hydroxy lactam tertiary alcohol (Lithiate addition product) (169).** Methylmagnesium bromide (0.097 mL of 3.0 M in $Et_2O$, 0.291 mmol) was added dropwise to a solution of **37** (32.0 mg, 0.97 mmol) in THF (0.75 mL) at 0 ºC. The solution was warmed to rt and stirred for 1 h. The reaction was quenched with water (2.0 mL), dropwise, and the mixture was extracted with $CH_2Cl_2$ (5.0 mL x 3). The organic extracts were collected, washed with brine, dried (anhydrous $Na_2SO_4$), filtered and concentrated to afford tertiary alcohol (18.5 mg, 0.534 mmol, 55%) as a yellow oil. $R_f$ = 0.30 (5% MeOH/$CH_2Cl_2$); $^1$H NMR (400 MHz, $CDCl_3$) $\delta_H$ 7.39-7.41 (m, 2H), 7.29-7.33 (m, 2H), 7.20-7.25 (m, 1H), 3.82-3.89 (m, 1H), 3.59-3.66 (m, 1H), 3.50-5.58 (m, 1H), 3.49 (s, 3H), 3.23 (m, 1H), 3.04-3.10 (m, 2H), 2.59 (d, *J* = 7.6 Hz, 1H), 2.17 (d, *J* = 10.4 Hz, 1H), 1.97 (dd, *J* = 10.4, 2.8 Hz, 1H), 1.85 (brs, 1H), 1.71-1.80 (m, 1H), 1.53-1.64 (m, 1H), 1.48 (s, 3H), 1.15 (d, *J* = 7.2 Hz, 3H); $^{13}$C NMR (125 MHz, CDCl3) $\delta_C$ 170.1, 143.1, 128.7 (2), 128.5 (2),

126.8, 72.5, 69.2, 68.8, 58.3, 57.0, 52.4, 43.1, 33.1, 32.5, 30.0, 29.8, 24.3, 22.7; IR (neat) 3364, 2921, 1627 $cm^{-1}$; MS (ES+) m/z 346.2 ($M+H^+$); HRMS calcd for $C_{20}H_{28}NO_4$ ($M+H^+$): 346.2018, found 346.2014.

## References


1. a) Schreiber, S. L. *Science* **2000**, *287*, 1964-1969. b) Hulme, C.; Gore, V. *Curr. Med. Chem.* **2003**, *10*, 51-80. c) Schreiber, S. L. *Chem. Eng. News* **2003**, *81*, 51-61. d) Bender, A.; Fergus, S.; Galloway, W. R. J. D.; Glansdrop, F. G.; Marsden, D. M.; Nicholson, R. L.; Spandl, R. J.; Thomas, G. L.; Wyatt, E. E.; Glen, R. G.; Spring, D. R. *Chemical Genomics*; Jaroch, S., Weinmann, H., Eds.; Springer: New York, 2006, pp 47-60.
2. a) Wender, P. A.; Handy, S. T.; Wright, D. L. *Chem. Ind.* **1997**, 765, 767-769. b) Andraos, J. *Org. Process Res. Dev.* **2005**, *9*, 404-431.
3. Weber, L.; Illgen, K.; Almstetter, M. *Synlett* **1999**, 366-374.
4. Kelly, T. R.; Liu, H.-T. *J. Am. Chem. Soc.* **1985**, *107*, 4998-4999.
5. Grieco, P. A.; Bahsas, A. *Tetrahedron Lett.* **1988**, *29*, 5855-5858.
6. a) Kurti, L.; Czako, B. *Strategic Applications of Named Reactions in Organic Synthesis*; Elsevier Academic Press: Burlington, 2005, pp 384-385. b) Lazarski, K. E.; Rich, A. A.; Mascarenhas, C. M. *J. Chem. Educ.* **2008**, *85*, 1531-1533.
7. a) Eder, U.; Sauer, G.; Wiechert, R. *Angew. Chem. Int. Ed.* **1971**, *10*, 496-497. b) Hajos, Z. G.; Parrish, D. R. *J. Org. Chem.* **1974**, *39*, 1615-1621. c) Fuentes de Arriba, A. L.; Simón, L.; Raposo, C.; Alcázar, V.; Morán, J. R. *Tetrahedron* **2009**, *65*, 4841-4845.
8. Hajos, Z. G.; Parrish, D. R. *Organic Syntheses;* Wiley: New York, 1990; Collect. Vol. VII, p 393.

9. Weber, L. In *Multicomponent Reactions*; Zhu, J., Bienayme, H., Eds.; Wiley-VCH: Morlenbach, 2005, pp 300-310.

10. James, C. A.; Weininger, D.; Delaney, J. *Daylight Theory Manual, Daylight Chemical Information Systems* Irvine, 11, Feb. 1997.

11. a) Badorrey, R.; Cativiela, C.; Diaz-De-Villegas, M. D.; Galvez, J. A. *Tetrahedron Lett.* **1997**, *38*, 2547-2550. b) Danishefsky, S.; Langer, M. E.; Vogel, C. *Tetrahedron Lett.* **1985**, *26*, 5983-5986.

12. Lack, O.; Weber, L. *Chimia* **1996**, *50*, 445-447.

13. a) Dömling, A. *Curr. Opin. Chem. Biol.* **2000**, *4*, 318-323. b) Dömling, A. In *Multicomponent Reactions*; Zhu, J., Bienayme, H., Eds.; Wiley: Morlenbach, 2005, pp 76-94.

14. a) Balkenhohl, F.; von dem Bussche-Hünnefeld, C.; Lansky, A.; Zechel, C. *Angew. Chem. Int. Ed.* **1996**, *35*, 2288-2337. b) Ley, S. V.; Baxendale, I. R.; Myers, R. M. *The Chemical Theatre of Biological Systems*; Hicks, M. G., Kettner, C., Eds.; Beilstein-Institut: Bozen, May 24-28, 2004.

15. a) Felder, E. R.; Berta, D. G. *Combinatorial Chemistry and Technologies Methods and Applications*; Second ed.; Fassina, G., Miertus, S., Eds.; CRC Press: Boca Raton, 2005, pp 75-106. b) Kurth, M. J. *Combinatorial Chemistry*; Wilson, S. R., Czarnik, A. W., Eds.; John Wiley & Sons, Inc.: New York, NY, 1997, pp 39-64.

16. Ferritto, R.; de Magistris, E.; Missio, A.; Paio, A.; Seneci, P. *Combinatorial Chemistry and Technologies Methods and Applications*; 2nd ed.; Fassina, G., Miertus, S., Eds.; CRC Press: Boca Raton, 2005, pp 107-152.

17. a) Harre, M.; Neh, H.; Schulz, C.; Tilstam, U.; Wessa, T.; Weinmann, H. *Org. Process Res. Dev.* **2001**, *5*, 335-339. b) Dinter, C.; Weinmann, H.; Merten, C.; Schuetz, A.; Blume, T.; Sander, M.; Harre, M.; Neh, H. *Org. Process Res. Dev.* **2004**, *8*, 482-487.

18. a) Jandeleit, B.; Schaefer, D. J.; Powers, T. S.; Turner, H. W.; Weinberg, W. H. *Angew. Chem. Int. Ed.* **1999**, *38*, 2494-2532. b) Geyer, K.; Codee, J. D. C.; Seeberger, P. H. *Chem.-Eur. J.* **2006**, *12*, 8434-8442. c) Dittrich, P. S.; Manz, A. *Nat. Rev. Drug Discovery* **2006**, *5*, 210-218. d) Luisi, R.; Musio, B.; Degennaro, L. *Chimica e l'industria* **2011**, *93*, 114-123.

19. a) Chen, Y.; Kamlet, A. S.; Steinman, J. B.; Liu, D. R. *Nat. Chem.* **2011**, *3*, 146-153. b) Kanan, M. W.; Rozenman, M. M.; Sakurai, K.; Snyder, T. M.; Liu, D. R. *Nature* **2004**, *431*, 545-549. c) Rozenman, M. M.; Kanan, M. W.; Liu, D. R. *J. Am. Chem. Soc.* **2007**, *129*, 14933-14938.

20. Beck-Sickinger, A.; Weber, P. *Combinatorial Strategies in Biology and Chemistry*; John Wiley & Sons, Inc.: New York, 2002, pp 105-142.

21. Potyrailo, R. A.; Wroczynski, R. J.; Lemmon, J. P.; Flanagan, W. P.; Siclovan, O. P. *Analysis and Purification Methods in Combinatorial Chemistry*; Yan, B., Ed.; John Wiley & Sons, Inc.: Hoboken, 2004, pp 87-124.

22. a) Dreher, S. D.; Dormer, P. G.; Sandrock, D. L.; Molander, G. A. *J. Am. Chem. Soc.* **2008**, *130*, 9257-9259. b) Spivack, J. L.; Cawse, J. N.; Whisenhunt, D. W.; Johnson, B. F.; Shalyaev, K. V.; Male, J.; Pressman, E. J.; Ofori, J. Y.; Soloveichik, G. L.; Patel, B. P.; Chuck, T. L.; Smith, D. J.; Jordan, T. M.; Brennan, M. R.; Kilmer, R. J.; Williams, E. D. *Appl. Catal., A* **2003**, *254*, 5-25. c) Smalley, J.; Xin, B.; Olah, T. V. *Rapid Commun. Mass Spectrom.* **2009**, *23*, 3457-3464.

23. Stambuli, J. P.; Hartwig, J. F. *Curr. Opin. Chem. Biol.* **2003**, *7*, 420-426.

24. a) Lingard, I.; Bhalay, G.; Bradley, M. *Chem. Commun. (Cambridge, U. K.)* **2003**, 2310-2311. b) Taylor, S. J.; Morken, J. P. *Science* **1998**, *280*, 267-270. c) Holzwarth, A.; Schmidt, H.-W.; Maier, W. F. *Angew. Chem. Int. Ed.* **1998**, *37*, 2644-2647.

25. a) Kawatsura, M.; Hartwig, J. F. *Organometallics* **2001**, *20*, 1960-1964. b) Loeber, O.; Kawatsura, M.; Hartwig, J. F. *J. Am. Chem. Soc.* **2001**, *123*, 4366-4367. c) Cooper, A. C.; McAlexander, L. H.; Lee, D.-H.; Torres, M. T.; Crabtree, R. H. *J. Am. Chem. Soc.* **1998**, *120*, 9971-9972.

26. Reddington, E.; Sapienza, A.; Gurau, B.; Viswanathan, R.; Sarangapani, S.; Smotkin, E. S.; Mallouk, T. E. *Science* **1998**, *280*, 1735-1737.

27. a) Shaughnessy, K. H.; Kim, P.; Hartwig, J. F. *J. Am. Chem. Soc.* **1999**, *121*, 2123-2132. b) Evans, C. A.; Miller, S. J. *Curr. Opin. Chem. Biol.* **2002**, *6*, 333-338.

28. a) Stauffer, S. R.; Hartwig, J. F. *J. Am. Chem. Soc.* **2003**, *125*, 6977-6985. b) Stauffer, S. R.; Beare, N. A.; Stambuli, J. P.; Hartwig, J. F. *J. Am. Chem. Soc.* **2001**, *123*, 4641-4642.

29. a) Ding, K.; Du, H.; Yuan, Y.; Long, J. *Chem.--Eur. J.* **2004**, *10*, 2872-2884. b) Traverse, J. F.; Snapper, M. L. *Drug Discovery Today* **2002**, *7*, 1002-1012.

30. Francis, M. B.; Jacobsen, E. N. *Angew. Chem., Int. Ed.* **1999**, *38*, 937-941.

31. Seneci, P. *Combinatorial Chemistry and Technologies Methods and Applications*; 2nd ed.; Fassina, G., Miertus, S., Eds.; CRC Press: Boca Raton, 2005, pp 153-192.

32. Colombo, M.; Peretto, I. *Drug Discov. Today* **2008**, *13*, 677-684.

33. Baumann, M.; Baxendale, I. R.; Ley, S. V.; Nikbin, N.; Smith, C. D.; Tierney, J. P. *Org. Biomol. Chem.* **2008**, *6*, 1577-1586.

34. Wild, G. P.; Wiles, C.; Watts, P. *Lett. Org. Chem.* **2006**, *3*, 419-425.

35. Davis, G. *Innovations Pharm. Technol.* **2008**, *25*, 24-27.

36. Balagadde, F. K.; You, L.; Hansen, C. L.; Arnold, F. H.; Quake, S. R. *Science* **2005**, *309*, 137-140.

37. a) Kang, L.; Chung, B. G.; Langer, R.; Khademhosseini, A. *Drug Discov. Today* **2008**, *13*, 1-13. b) Song, H.; Chen, D. L.; Ismagilov, R. F. *Angew. Chem. Int. Ed.* **2006**, *45*, 7336-7356. c) Zheng, B.; Gerdts, C. J.; Ismagilov, R. F. *Curr. Opin. Struct. Biol.* **2005**, *15*, 548-555.

38. Watts, P.; Haswell, S. J. *Drug Discov. Today* **2003**, *8*, 586-593.

39. Wiles, C.; Watts, P. *Expert Opin. Drug Discov.* **2007**, *2*, 1487-1503.

40. Lu, H.; Schmidt, M. A.; Jensen, K. F. *Lab Chip* **2001**, *1*, 22-28.

41. ThalesNano Homepage. http://thalesnano.com/products/h-cube (accessed June 23, 2011).

42. Uniqsis Homepage. http://uniqsis.com (accessed June 23, 2011).

43. Vapourtec Homepage. http://vapourtec.co.uk (accessed June 23, 2011).

44. Syrris Homepage. http://syrris.com (accessed June 23, 2011).

45. YMC Europe Homepage. http://ymc.de/ymceurope (accessed June 23, 2011).

46. Jas, G.; Kirschning, A. *Chem.-Eur. J.* **2003**, *9*, 5708-5723.

47. Zhang, X.; Stefanick, S.; Villani, F. J. *Org. Process Res. Dev.* **2004**, *8*, 455-460.

48. Baxendale, I. R.; Deeley, J.; Griffiths-Jones, C. M.; Ley, S. V.; Saaby, S.; Tranmer, G. K. *Chem. Commun.* **2006**, 2566-2568.

49. Valera, F. E.; Quaranta, M.; Moran, A.; Blacker, J.; Armstrong, A.; Cabral, J. T.; Blackmond, D. G. *Angew. Chem. Int. Ed.* **2010**, *49*, 2478-2485.

50. Wheeler, R. C.; Benali, O.; Deal, M.; Farrant, E.; MacDonald, S. J. F.; Warrington, B. H. *Org. Process Res. Dev.* **2007**, *11*, 704-710.

51. Eguchi, S.; Kita, M.; Kiyota, H.; Nishino, H.; Ohno, M.; Somei, M.; Uemura, D. *Bioactive Heterocycles I*; Eguchi, S., Ed.; Springer: Berlin, 2006, pp 1-214.

52. Pozharskii, A. F.; Soldatenkov, A. T.; Katritzky, A. R. *Heterocycles in Life and Society*; John Wiley & Sons Inc.: New York, 1997, pp 1-35.

53. *The PDR Pocket Guide to Prescription Drugs*; 9th ed.; Kennedy, B., Ed.; Pocket Books, A Division of Simon & Schuster, Inc.: New York, 2010.

54. Broughton, H. B.; Watson, I. A. *J. Mol. Graphics Modell.* **2004**, *23*, 51-58.

55. Kabalka, G. W.; Mereddy, A. R. *Tetrahedron Lett.* **2006**, *47*, 5171-5172.

56. a) Sisko, J.; Mellinger, M. *Pure Appl. Chem.* **2002**, *74*, 1349-1357. b) Gelens, E.; De Kanter, F. J. J.; Schmitz, R. F.; Sliedregt, L. A. J. M.; Van Steen. B. J.; Kruse, C. G.; Leurs, R.; Groen, M. B.; Orru, R. V. A. *Mol. Diversity* **2006**, *10*, 17-22.

57. Ballini, R.; Barboni, L.; Giarlo, G. *J. Org. Chem.* **2003**, *68*, 9173-9176.

58. *Microwave-Assisted Synthesis of Heterocycles*; Van der Eycken, E.; Kappe, C. O., Eds.; Springer: Berlin, 2006, pp 1-78.

59. Photographs courtesy of Christina Thompson, Abbott Laboratories.

60. Lieke, W. *Justus Liebigs Ann. Chem.* **1859**, *112*, 316-321.

61. Gautier, A. *Justus Liebigs Ann. Chem.* **1867**, *142*, 289-294.

62. Hofmann, A. W. *Ber. Drsch. Chem. Ges.* **1870**, *3*, 761-772.

63. Ugi, I.; Fetzer, U.; Eholzer, U.; Knupfer, H.; Offermann, K. *Angew. Chemie Int. Ed.* **1965**, *4*, 472-484.

64. a) Ugi, L.; Werner, B.; Dömling, A. *Molecules* **2003**, *8*, 53-66. b) Hagedorn, I.; Tonjes, H. *Pharmazie* **1956**, *11*, 409-410. c) Hagedorn, I.; Eholzer, U.; Luttringhaus, A. *Chem. Ber.* **1960**, *93*, 1584-1590.

65. Pirrung, M. C.; Ghorai, S.; Ibarra-Rivera, T. R. *J. Org. Chem.* **2009**, *74*, 4110-4117.

66. Dömling, A. *Chem. Rev.* **2006**, *106*, 17-89.

67. Akritopoulou-Zanze, I. *Curr. Opin. Chem. Biol.* **2008**, *12*, 324-331.

68. Norris, J. F. *Experimental Organic Chemistry*; McGraw-Hill: New York, 1915, pp 95-98.

69. Burr, C. *The Emperor of Scent: A Story of Perfume, Obsession, and the Last Mystery of the Senses*; Random House: New York, 2002.

70. Pinney, V. R. March 5, 2002; Vol. US Pat. 6 352 032.

71. Creedon, S. M.; Crowley, H. K.; McCarthy, D. G. *J. Chem. Soc., Perkin Trans. 1* **1998**, 1015-1018.

72. Berlozecki, S.; Szymanski, W.; Ostaszewski, R. *Synth. Commun.* **2008**, *38*, 2714-2721.

73. Appel, R.; Kleinstueck, R.; Ziehn, K. D. *Angew. Chem. Int. Ed.* **1971**, *10*, 132.

74. Azuaje, J.; Coelho, A.; El, M. A.; Blanco, J. M.; Sotelo, E. *ACS Comb. Sci.*, *13*, 89-95.

75. a) Hünig, S. *Angew. Chem. Int. Ed.*. **1964**, *3*, 548-560. b) Hünig, S.; Geldern, L. *J. Prakt. Chem.* **1964**, *24*, 246-268.

76. Pittman, C. U., Jr.; McManus, S. P.; Larsen, J. W. *Chem. Rev.* **1972**, *72*, 357-438.

77. Frump, J. A. *Chem. Rev.* **1971**, *71*, 483-506.

78. a) Gracias, V.; Milligan, G. L.; Aubé, J. *J. Org. Chem.* **1996**, *61*, 10-11. b) Fenster, E.; Smith, B. T.; Gracias, V.; Milligan, G. L.; Aubé´, J. *J. Org. Chem.* **2008**, *73*, 201-205. c) Gracias, V.; Milligan, G. L.; Aubé´, J. *J. Am. Chem. Soc.* **1995**, *117*, 8047-8048. d) Gracias, V.; Milligan, G. L.; Aubé´, J. *J. Org. Chem.* **1996**, *61*, 10-11.

79. a) Fazio, M. J. *J. Org. Chem.* **1984**, *49*, 4889-4893. b) Meyers, A. I.; Temple, D. L., Jr. *J. Amer. Chem. Soc.* **1970**, *92*, 6644-6646. c) Meyers, A. I.; Temple, D. L., Jr. *J. Amer. Chem. Soc.* **1970**, *92*, 6646-6647. d) Meyers, A. I.; Collington, E. W. *J. Amer. Chem. Soc.* **1970**, *92*, 6676-6678.

80. Goodell, J. R.; McMullen, J. P.; Zaborenko, N.; Maloney, J. R.; Ho, C.-X.; Jensen, K. F.; Porco, J. J. A.; Beeler, A. B. *J. Org. Chem.* **2009**, *74*, 6169-6180.

81. Photograph courtesy of the Center for Chemical Methodology and Library Development at Boston University.

82. Beeler, A. B.; Su, S.; Singleton, C. A.; Porco, J. A., Jr. *J. Am. Chem. Soc.* **2007**, *129*, 1413-1419.

83. a) Goldfarb, D. S.; Method Using Lifespan-Altering Compounds for Altering the Lifespan of Eukaryotic Organisms, and Screening for Such Compounds. U.S. Patent Applications 2008-341615 and 2009-163545, Dec. 22, 2008. b) McDougal, N. T.; Schaus, S. E. *J. Am. Chem. Soc.* **2003**, *125*, 12094-12095. c) Smissman, E. E.; Diebold, J. L. *J. Org. Chem.* **1965**, *30*, 4002-4005. d) Grecian, S.; Wrobleski, A. D.; Aubé, J. *Org. Lett.* **2005**, *7*, 3167-3170.

84. a) Büchi, G.; Mak, C.-P. *J. Am. Chem. Soc.* **1977**, *99*, 8073-8075. b) Collins, J. L.; Grieco, P. A.; Walker, J. K. *Tetrahedron Lett.* **1997**, *38*, 1321-1324. c) Engler, T. A.; Letavic, M. A.; Combrink, K. D.; Takusagawa, F. *J. Org. Chem.* **1990**, *55*, 5810-5812. d) Harmata, M.; Rashatasakhon, P. *Tetrahedron* **2003**, *59*, 2371-2395.

85. Smith, B. T.; Gracias, V.; Aubé´, J. *J. Org. Chem.* **2000**, *65*, 3771-3774.

86. Mazzeo, J. R.; Neue, U. D.; Kele, M.; Plumb, R. S. *Anal. Chem.* **2005**, *77*, 460 A - 470 A.

87. a) Ayyangar, N. R.; Srinivasan, K. V. *Indian J. Chem., Sect. B* **1983**, *22B*, 1108-1115. b) Ozcan, S.; Sahin, E.; Balci, M. *Tetrahedron Lett.* **2007**, *48*, 2151-2154. c) Duddeck, H.; Kaiser, M. *Spectrochim. Acta, Part A* **1985**, *41A*, 913-924.

88. Van Leusen, D.; van Leusen, A. M. *Org. React.* **2001**, *57*, 417-666.

89. a) Van Leusen, A. M.; Wildeman, J.; Oldenziel, O. H. *J. Org. Chem.* **1977**, *42*, 1153-1159. b) Larionov, O. V.; de Meijere, A. *Angew. Chem. Int. Ed.* **2005**, *44*, 5664-5667. c) Grigg, R.; Lansdell, M. I.; Thorton-Pett, M. *Tetrahedron* **1999**, *55*, 2025-2044.

90. Bull, J. R.; Tuinman, A. *Tetrahedron* **1975**, *31*, 2151-2155.

91. a) Ibata, T.; Sato, R. *Chem. Lett.* **1978**, 1129-1130. b) Doyle, M. P.; Buhro, W. E.; Davidson, J. G.; Elliott, R. C.; Hoekstra, J. W.; Oppenhuizen, M. *J. Org. Chem.* **1980**, *45*, 3657-36564. c) Saegusa, T.; Ito, Y.; Shimizu, T.; Kobayashi, S. *Bull. Chem. Soc. Jap.* **1969**, *42*, 3535-3538.

92. a) Treece, J. L.; Goodell, J. R.; Vander Velde, D.; Porco, J. A., Jr.; Aubé, J. *J. Org. Chem.* **2010**, *75*, 2028-2038. b) Goodell, J. R.; Leng, B.; Snyder, T. K.; Beeler, A. B.; Porco, J. A., Jr. *Synthesis* **2010**, 2254-2270. c) Liang, B.; Kalidindi, S.; Porco, J. A., Jr.; Stephenson, C. R. J. *Org. Lett.* **2010**, *12*, 572-575. d) Kinoshita, H.; Ong, W. W.; Ingham, O. J.; Beeler, A. B.; Porco, J. A.,

Jr. *J. Am. Chem. Soc.* **2010**, *132*, 6412-6418. e) Han, C.; Rangarajan, S.; Voukides, A. C.; Beeler, A. B.; Porco, J. A., Jr. *Org. Lett.* **2009**, *11*, 413-416.

93. Reissig, H.-U.; Zimmer, R. *Chem. Rev.* **2003**, *103*, 1151-1196.

94. Supporting X-ray crystal structures available in the appendix of this dissertation.

95. Zimmerman, H. E.; Armesto, D. *Chem. Rev.* **1996**, *96*, 3065-3112.

96. a) Boyer, J. H.; Canter, F. C.; Hamer, J.; Putney, R. L. *J. Am. Chem. Soc.* **1956**, *78*, 325-327. b) Boyer, J. H.; Hamer, J. *J. Am. Chem. Soc.* **1955**, *77*, 951-954.

97. a) Gutke, H.-J.; Braun, N. A.; Spitzner, D. *Tetrahedron* **2004**, *60*, 8137-8141. b) Penkett, C. S.; Byrne, P. W.; Teobald, B. J.; Rola, B.; Ozanne, A.; Hitchcock, P. B. *Tetrahedron* **2004**, *60*, 2771-2784. c) Sagawa, S.; Nagaoka, H.; Yamada, Y. *Tetrahedron Lett.* **1994**, *35*, 603-604.

98. Forsee, J. E.; Aubé, J. *J. Org. Chem.* **1999**, *64*, 4381-4385.

99. a) Yu, M.; Pagenkopf, B. L. *J. Am. Chem. Soc.* **2003**, *125*, 8122-8123. b) Morra, N. A.; Morales, C. L.; Bajtos, B.; Wang, X.; Jang, H.; Wang, J.; Yu, M.; Pagenkopf, B. L. *Adv. Synth. Catal.* **2006**, *348*, 2385-2390. c) Bajtos, B.; Yu, M.; Zhao, H.; Pagenkopf, B. L. *J. Am. Chem. Soc.* **2007**, *129*, 9631-9634. d) Morales, C. L.; Pagenkopf, B. L. *Org. Lett.* **2008**, *10*, 157-159. e) Sugita, Y.; Kimura, C.; Hosoya, H.; Yamadoi, S.; Yokoe, I. *Tetrahedron Lett.* **2001**, *42*, 1095-1098. f) Fang, J.; Ren, J.; Wang, Z. *Tetrahedron Lett.* **2008**, *49*,

6659-6662. g) Pohlhaus, P. D.; Sanders, S. D.; Parsons, A. T.; Li, W.; Johnson, J. S. *J. Am. Chem. Soc.* **2008**, *130*, 8642-8650.

100. a) Ortiz, M. J.; Agarrabeitia, A. R.; Aparicio-Lara, S.; Armesto, D. *Tetrahedron Lett.* **1999**, *40*, 1759-1762. b) Armesto, D.; Ortiz, M. J.; Agarrabeitia, A. R.; Aparicio-Lara, S.; Martin-Fontecha, M.; Liras, M.; Paz, M.-A. M. *J. Org. Chem.* **2002**, *67*, 9397-9405. c) Armesto, D.; Caballero, O.; Ortiz, M. J.; Agarrabeitia, A. R.; Martin-Fontecha, M.; Torres, M. R. *J. Org. Chem.* **2003**, *68*, 6661-6671.

101. a) Mariano, P. S.; Stavinoha, J.; Bay, E. *Tetrahedron* **1981**, *37*, 3385-3395. b) Mariano, P. S. *Tetrahedron* **1983**, *39*, 3845-3879.

102. a) Stavinoha, J.; Bay, E.; Leone, A.; Mariano, P. S. *Tetrahedron Lett.* **1980**, *21*, 3455-3458. b) Stavinoha, J. L.; Mariano, P. S. *J. Am. Chem. Soc.* **1981**, *103*, 3136-3148. c) Mariano, P. S. *Acc. Chem. Res.* **1983**, *16*, 130-137. d) Cho, I. S.; Tu, C. L.; Mariano, P. S. *J. Am. Chem. Soc.* **1990**, *112*, 3594-3607.

103. Mariano, P. S.; Stavinoha, J. L.; Swanson, R. *J. Am. Chem. Soc.* **1977**, *99*, 6781-6782.

104. Pangborn, A. B.; Giardello, M. A.; Grubbs, R. H.; Rosen, R. K.; Timmers, F. J. *Organometallics* **1996**, *15*, 1518-1520.

105. Oezcan, S.; Sahin, E.; Balci, M. *Tetrahedron Lett.* **2007**, *48*, 2151-2154.

106. a) Crandall, J. K.; Pradat, C. *J. Org. Chem.* **1984**, *50*, 1327-1329. b) Wildeman, J; van Lusen, A. M. *Synthesis* **1979**, 733.

# Appendix

## Single Crystal X-Ray Analysis

**General methods.** All x-ray crystal structure determinations were performed by either Dr. Victor Day, Ph.D. (University of Kansas), Dr. Jeff Bacon Ph.D. (Boston University), or Dr. Emil Lobkovsky, Ph.D. (Cornell University). Intensity data collected at the University of Kansas were collected using a Bruker APEX ccd area detector[1] mounted on a Bruker D8 goniometer with graphite-monochromated Mo Kα radiation (λ = 0.71071 Å). All samples were cooled to 100 K.[2] The intenisty data were measured as a series of ω oscillation frames, each at the indicated angle and time per frame specified for each sample. The detector operated in 512 x 512 mode and was positioned 5.054 cm from each sample.

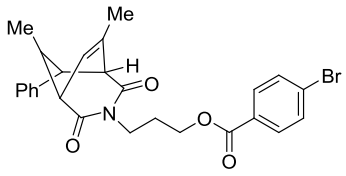


**X-Ray crystallographic data for bicyclic imide (153).** Crystals of compound **153** suitable for X-ray analysis were obtained by dissolving the material in a minimal amount of ethyl acetate, placing the vial of solution in a larger vial containing hexanes, and sealing the lid to allow slow solvent mixing. Crystallographic data have been deposited with the Cambridge Crystallographic Data Centre (CCDC # 818811). Copies of the data can be obtained free of charge on application to the CCDC, 12 Union Road, Cambridge CB21EZ, UK (fax: (+44)-1223-336-033; e-mail: deposit@ccdc.cam.ac.uk.

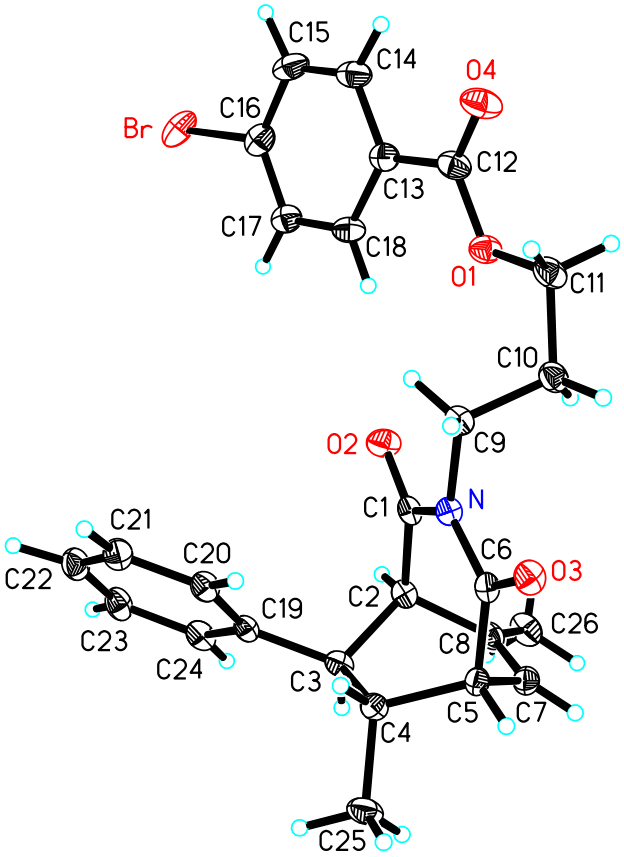


**Crystal data and structure refinement for compound 153**.

| | | |
|---|---|---|
| Identification Code | Compound **153** | |
| Empirical formula | $C_{26}H_{26}BrNO_4$ | |
| Formula weight | 496.39 | |
| Temperature | 100(2) K | |
| Wavelength | 0.71073 Å | |
| Crystal system | Triclinic | |
| Space group | $P\bar{1} - C_i^1$ (No. 2) | |
| Unit cell dimensions | a = 7.867(4) Å | α = 72.210(7)°. |
| | b = 11.447(6) Å | β = 86.597(8)°. |
| | c = 13.759(7) Å | γ = 76.128(8)°. |
| Volume | 1145(1)Å$^3$ | |
| Z | 2 | |
| Density (calculated) | 1.440 Mg/m$^3$ | |
| Absorption coefficient | 1.828 mm$^{-1}$ | |

| | |
|---|---|
| F(000) | 512 |
| Crystal size | 0.44 x 0.40 x 0.26 $mm^3$ |
| Theta range for data collection | 2.67 to 29.06°. |
| Index ranges | $-10 \leq h \leq 10$, $-15 \leq k \leq 15$, $-18 \leq l \leq 18$ |
| Reflections collected | 10050 |
| Independent reflections | 5356 [$R_{int}$ = 0.086] |
| Completeness to theta = 29.06° | 87.4 % |
| Absorption correction | Multi-scan |
| Max. and min. transmission | 1.000 and 0.784 |
| Refinement method | Full-matrix least-squares on $F^2$ |
| Data / restraints / parameters | 5356 / 0 / 393 |
| Goodness-of-fit on $F^2$ | 1.036 |
| Final R indices [I>2sigma(I)] | $R_1$ = 0.049, $wR_2$ = 0.133 |
| R indices (all data) | $R_1$ = 0.056, $wR_2$ = 0.151 |
| Largest diff. peak and hole | 1.11 and -0.89 $e^-/Å^3$ |

**Atomic coordinates ( x $10^4$) and equivalent isotropic displacement parameters ($Å^2$x$10^3$) for compound 153. U(eq) is defined as one third of the trace of the orthogonalized $U_{ij}$ tensor.**

| | x | y | z | U(eq) |
|---|---|---|---|---|
| Br | 1232(1) | 5683(1) | -2597(1) | 31(1) |
| O(1) | 3716(2) | 3314(2) | 2384(1) | 21(1) |
| O(2) | 2356(3) | 872(2) | 1913(1) | 23(1) |
| O(3) | 2019(2) | -529(2) | 5353(1) | 20(1) |
| O(4) | 3334(3) | 5358(2) | 2283(2) | 31(1) |
| N | 2105(3) | 132(2) | 3628(1) | 15(1) |
| C(1) | 2324(3) | -26(2) | 2650(2) | 16(1) |
| C(2) | 2561(3) | -1333(2) | 2531(2) | 16(1) |
| C(3) | 871(3) | -1862(2) | 2803(2) | 16(1) |
| C(4) | 508(3) | -2164(2) | 3957(2) | 17(1) |
| C(5) | 2107(3) | -2132(2) | 4566(2) | 16(1) |
| C(6) | 2078(3) | -800(2) | 4558(2) | 16(1) |
| C(7) | 3820(3) | -2688(2) | 4152(2) | 19(1) |
| C(8) | 4076(3) | -2272(2) | 3153(2) | 18(1) |
| C(9) | 2038(3) | 1409(2) | 3676(2) | 17(1) |
| C(10) | 3851(3) | 1579(2) | 3884(2) | 21(1) |
| C(11) | 3964(4) | 2949(3) | 3477(2) | 23(1) |
| C(12) | 3330(3) | 4550(2) | 1887(2) | 22(1) |
| C(13) | 2884(3) | 4793(2) | 798(2) | 20(1) |
| C(14) | 2675(4) | 6017(2) | 132(2) | 25(1) |
| C(15) | 2189(4) | 6291(3) | -878(2) | 27(1) |
| C(16) | 1922(4) | 5318(3) | -1217(2) | 24(1) |
| C(17) | 2109(3) | 4109(2) | -574(2) | 22(1) |
| C(18) | 2596(4) | 3837(2) | 435(2) | 22(1) |

| | | | | |
|---|---|---|---|---|
| C(19) | -639(3) | -1050(2) | 2096(2) | 16(1) |
| C(20) | -1871(3) | -67(2) | 2309(2) | 19(1) |
| C(21) | -3217(4) | 655(3) | 1616(2) | 22(1) |
| C(22) | -3346(4) | 417(3) | 689(2) | 24(1) |
| C(23) | -2111(3) | -546(3) | 465(2) | 23(1) |
| C(24) | -780(3) | -1274(3) | 1165(2) | 20(1) |
| C(25) | 83(4) | -3461(3) | 4378(2) | 26(1) |
| C(26) | 5668(4) | -2714(3) | 2595(2) | 25(1) |

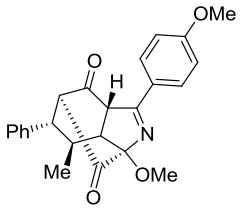


**X-Ray crystallographic data for caged imine (159).** Crystals of compound **27** suitable for X-ray analysis were obtained by slow evaporation from a minimal amount of ethyl acetate. Crystallographic data have been deposited with the Cambridge Crystallographic Data Centre (CCDC # 819148). Copies of the data can be obtained free of charge on application to the CCDC, 12 Union Road, Cambridge CB21EZ, UK (fax: (+44)-1223-336-033; e-mail: deposit@ccdc.cam.ac.uk.

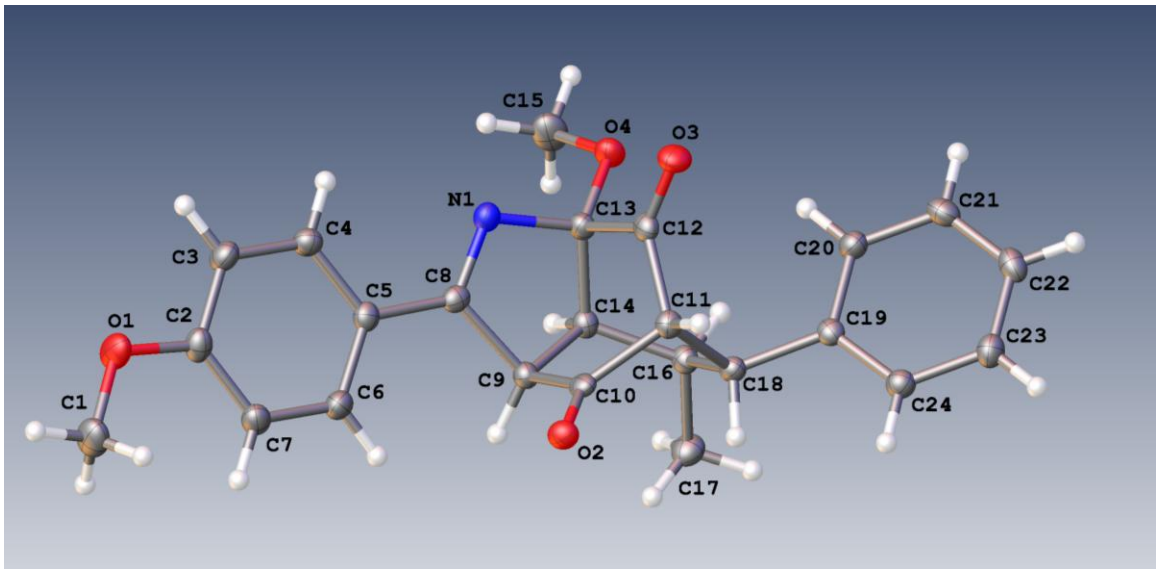


**Crystal data and structure refinement for compound 159.**

| | |
|---|---|
| Identification code | compound **159** |
| Empirical formula | C24 H23 N O4 |
| Formula weight | 389.43 |
| Temperature | 102(2) K |
| Wavelength | 1.54178 Å |
| Crystal system | Monoclinic |
| Space group | P2(1) |
| Unit cell dimensions | a = 13.337(4) Å |

| | |
|---|---|
| | b =17.093 (5) Å □= 105.324 (18)°<br>c = 17.547 (5) Å |
| Volume | 3857.9 (19) $Å^3$ |
| Z, Z' | 8, 4 |
| Density (calculated) | 1.341 $Mg/m^3$ |
| Absorption coefficient | 0.74 $mm^{-1}$ |
| F(000) | 1648 |
| Crystal size | 0.27 x 0.20 x 0.11 $mm^3$ |
| Theta range for data collection | 2.6 to 66.5°. |
| Index ranges | -14<=h<=15, -20<=k<=20, -19<=l<=20 |
| Reflections collected | 142546 |
| Independent reflections | 13252 [R(int) = 0.0341] |
| Completeness to theta = 66.5° | 97 % |
| Absorption correction | Semi-empirical from equivalents |
| Max. and min. transmission | 0.753 and 0.698 |
| Refinement method | Full-matrix least-squares on $F^2$ |
| Data / restraints / parameters | 13252 / 1 / 1058 |
| Goodness-of-fit on $F^2$ | 1.002 |
| Final R indices [I>2sigma(I)] | R1 = 0.0233, wR2 = 0.0667 |
| R indices (all data) | R1 = 0.0233, wR2 = 0.0668 |
| Largest diff. peak and hole | 0.21 and -0.13 $e.Å^{-3}$ |

**Atomic coordinates ( x $10^4$) and equivalent isotropic displacement parameters ($Å^2$x $10^3$) for compound 159. U(eq) is defined as one third of the trace of the orthogonalized $U^{ij}$ tensor.**

| | *x* | *y* | *z* | $U_{iso}$*/$U_{eq}$ |
|---|---|---|---|---|
| O1C | 1.02764 (7) | 0.64277 (6) | 1.10490 (5) | 0.0280 (2) |
| O4C | 0.93883 (6) | 0.53264 (5) | 1.57238 (5) | 0.02034 (17) |
| O3C | 0.87140 (6) | 0.68541 (5) | 1.55193 (5) | 0.02434 (18) |
| O2C | 1.13723 (6) | 0.77126 (5) | 1.47301 (5) | 0.02146 (17) |
| O1A | 1.19613 (7) | 0.43665 (6) | 1.37720 (5) | 0.0298 (2) |
| O4A | 1.30047 (6) | 0.54731 (5) | 0.91550 (5) | 0.02198 (18) |
| O3A | 1.34847 (6) | 0.39026 (5) | 0.92625 (5) | 0.02353 (18) |
| O2A | 1.07358 (6) | 0.32005 (5) | 1.00339 (5) | 0.02098 (17) |
| O1D | 0.47669 (8) | 0.17306 (6) | 0.89461 (5) | 0.0364 (2) |
| O3D | 0.63009 (6) | 0.22851 (5) | 0.43617 (5) | 0.02508 (18) |
| O4D | 0.60648 (6) | 0.06812 (5) | 0.44397 (5) | 0.02259 (18) |

| | | | | |
|---|---|---|---|---|
| O2D | 0.34823 (7) | 0.28404 (5) | 0.51066 (5) | 0.02538 (19) |
| O1B | 0.61044 (7) | 0.44321 (6) | 1.37784 (5) | 0.0308 (2) |
| O2B | 0.57158 (7) | 0.31910 (5) | 1.01625 (5) | 0.02501 (18) |
| O3B | 0.85633 (6) | 0.38471 (5) | 0.96390 (5) | 0.02484 (18) |
| O4B | 0.81473 (6) | 0.54215 (5) | 0.94873 (5) | 0.02230 (18) |
| N1C | 0.96961 (7) | 0.57747 (6) | 1.44959 (6) | 0.0183 (2) |
| N1A | 1.26482 (7) | 0.50091 (6) | 1.03581 (5) | 0.0190 (2) |
| N1D | 0.56209 (7) | 0.12139 (6) | 0.55750 (6) | 0.0202 (2) |
| N1B | 0.75644 (7) | 0.49731 (6) | 1.06039 (6) | 0.0193 (2) |
| C1C | 1.10790 (11) | 0.68199 (8) | 1.07976 (7) | 0.0273 (3) |
| H1CB | 1.1726 | 0.6520 | 1.0966 | 0.041* |
| H1CC | 1.1185 | 0.7343 | 1.1034 | 0.041* |
| H1CA | 1.0877 | 0.6866 | 1.0220 | 0.041* |
| C2C | 1.04008 (10) | 0.63447 (7) | 1.18435 (7) | 0.0216 (2) |
| C7C | 1.12894 (9) | 0.65521 (7) | 1.24267 (7) | 0.0217 (2) |
| H7C | 1.1869 | 0.6771 | 1.2284 | 0.026* |
| C6C | 1.13274 (9) | 0.64375 (7) | 1.32225 (7) | 0.0202 (2) |
| H6C | 1.1941 | 0.6571 | 1.3618 | 0.024* |
| C5C | 1.04806 (9) | 0.61302 (7) | 1.34446 (7) | 0.0185 (2) |
| C8C | 1.04842 (9) | 0.60336 (6) | 1.42792 (7) | 0.0165 (2) |
| C9C | 1.13764 (8) | 0.63077 (7) | 1.49740 (6) | 0.0162 (2) |
| H9C | 1.2086 | 0.6219 | 1.4901 | 0.019* |
| C14C | 1.11350 (8) | 0.58270 (6) | 1.56546 (6) | 0.0158 (2) |
| H14B | 1.1389 | 0.5278 | 1.5643 | 0.019* |
| C16C | 1.15210 (8) | 0.61633 (7) | 1.64932 (6) | 0.0162 (2) |
| H16B | 1.1114 | 0.5906 | 1.6827 | 0.019* |
| C18C | 1.12909 (9) | 0.70557 (7) | 1.64864 (6) | 0.0169 (2) |
| H18B | 1.1953 | 0.7329 | 1.6485 | 0.020* |
| C19C | 1.10034 (9) | 0.73236 (7) | 1.72309 (7) | 0.0185 (2) |
| C20C | 1.01470 (9) | 0.70242 (7) | 1.74434 (7) | 0.0232 (2) |
| H20B | 0.9695 | 0.6667 | 1.7103 | 0.028* |
| C21C | 0.99487 (10) | 0.72475 (8) | 1.81570 (7) | 0.0251 (3) |
| H21B | 0.9359 | 0.7043 | 1.8296 | 0.030* |
| C22C | 1.06055 (10) | 0.77661 (8) | 1.86651 (7) | 0.0251 (3) |

| | | | | |
|---|---|---|---|---|
| H22B | 1.0474 | 0.7910 | 1.9152 | 0.030* |
| C13C | 0.99385 (9) | 0.58460 (7) | 1.53685 (6) | 0.0169 (2) |
| C15C | 0.95852 (10) | 0.45123 (7) | 1.56228 (7) | 0.0255 (3) |
| H15I | 1.0292 | 0.4382 | 1.5930 | 0.038* |
| H15G | 0.9514 | 0.4405 | 1.5062 | 0.038* |
| H15H | 0.9084 | 0.4195 | 1.5807 | 0.038* |
| C12C | 0.95941 (8) | 0.66833 (7) | 1.55278 (6) | 0.0174 (2) |
| C11C | 1.04818 (9) | 0.72712 (7) | 1.56826 (6) | 0.0176 (2) |
| H11B | 1.0223 | 0.7820 | 1.5688 | 0.021* |
| C17C | 1.26643 (9) | 0.60131 (7) | 1.68794 (7) | 0.0201 (2) |
| H17H | 1.3086 | 0.6270 | 1.6572 | 0.030* |
| H17G | 1.2798 | 0.5449 | 1.6898 | 0.030* |
| H17I | 1.2847 | 0.6224 | 1.7418 | 0.030* |
| C23C | 1.14495 (11) | 0.80672 (8) | 1.84513 (7) | 0.0282 (3) |
| H23B | 1.1898 | 0.8427 | 1.8790 | 0.034* |
| C24C | 1.16512 (10) | 0.78473 (7) | 1.77403 (7) | 0.0228 (2) |
| H24B | 1.2239 | 0.8058 | 1.7602 | 0.027* |
| C10C | 1.11155 (8) | 0.71695 (7) | 1.50788 (6) | 0.0165 (2) |
| C4C | 0.95831 (9) | 0.59367 (7) | 1.28486 (7) | 0.0215 (2) |
| H4C | 0.8994 | 0.5734 | 1.2990 | 0.026* |
| C3C | 0.95448 (10) | 0.60371 (7) | 1.20587 (7) | 0.0242 (3) |
| H3C | 0.8936 | 0.5897 | 1.1663 | 0.029* |
| C1A | 1.11716 (11) | 0.39364 (9) | 1.39980 (8) | 0.0327 (3) |
| H1AA | 1.1084 | 0.3426 | 1.3735 | 0.049* |
| H1AB | 1.0515 | 0.4227 | 1.3843 | 0.049* |
| H1AC | 1.1372 | 0.3861 | 1.4572 | 0.049* |
| C2A | 1.18559 (10) | 0.44670 (7) | 1.29793 (7) | 0.0221 (2) |
| C7A | 1.09709 (10) | 0.42783 (7) | 1.23880 (7) | 0.0223 (2) |
| H7A | 1.0383 | 0.4061 | 1.2520 | 0.027* |
| C6A | 1.09474 (9) | 0.44094 (7) | 1.15991 (7) | 0.0210 (2) |
| H6A | 1.0335 | 0.4290 | 1.1197 | 0.025* |
| C5A | 1.18089 (9) | 0.47123 (7) | 1.13930 (7) | 0.0179 (2) |
| C8A | 1.18272 (8) | 0.48077 (7) | 1.05640 (7) | 0.0175 (2) |
| C9A | 1.09033 (9) | 0.46075 (7) | 0.98597 (6) | 0.0170 (2) |

| | | | | |
|---|---|---|---|---|
| H9A | 1.0208 | 0.4742 | 0.9938 | 0.020* |
| C14A | 1.12058 (9) | 0.50841 (7) | 0.92012 (6) | 0.0176 (2) |
| H14A | 1.1023 | 0.5648 | 0.9239 | 0.021* |
| C16A | 1.07485 (9) | 0.47885 (7) | 0.83529 (6) | 0.0177 (2) |
| H16A | 1.1127 | 0.5056 | 0.8005 | 0.021* |
| C18A | 1.09325 (9) | 0.38891 (7) | 0.83038 (6) | 0.0172 (2) |
| H18A | 1.0247 | 0.3627 | 0.8252 | 0.021* |
| C19A | 1.13134 (8) | 0.36338 (7) | 0.76000 (6) | 0.0173 (2) |
| C24A | 1.08590 (9) | 0.29930 (7) | 0.71433 (7) | 0.0202 (2) |
| H24A | 1.0308 | 0.2720 | 0.7275 | 0.024* |
| C23A | 1.12008 (9) | 0.27487 (7) | 0.64988 (7) | 0.0228 (2) |
| H23A | 1.0883 | 0.2311 | 0.6197 | 0.027* |
| C22A | 1.20022 (9) | 0.31400 (7) | 0.62938 (7) | 0.0232 (3) |
| H22A | 1.2229 | 0.2979 | 0.5849 | 0.028* |
| C4A | 1.26968 (9) | 0.48980 (7) | 1.19989 (7) | 0.0208 (2) |
| H4A | 1.3292 | 0.5105 | 1.1868 | 0.025* |
| C3A | 1.27186 (9) | 0.47845 (7) | 1.27839 (7) | 0.0230 (2) |
| H3A | 1.3320 | 0.4923 | 1.3189 | 0.028* |
| C13A | 1.23956 (9) | 0.49785 (7) | 0.94827 (6) | 0.0177 (2) |
| C15A | 1.30043 (11) | 0.62790 (8) | 0.93807 (8) | 0.0313 (3) |
| H15F | 1.3196 | 0.6319 | 0.9958 | 0.047* |
| H15D | 1.2309 | 0.6500 | 0.9166 | 0.047* |
| H15E | 1.3508 | 0.6569 | 0.9172 | 0.047* |
| C10A | 1.10555 (8) | 0.37351 (7) | 0.97137 (6) | 0.0170 (2) |
| C11A | 1.16827 (9) | 0.36055 (7) | 0.91099 (6) | 0.0174 (2) |
| H11A | 1.1874 | 0.3042 | 0.9084 | 0.021* |
| C21A | 1.24683 (9) | 0.37725 (8) | 0.67502 (7) | 0.0230 (2) |
| H21A | 1.3025 | 0.4040 | 0.6620 | 0.028* |
| C20A | 1.21291 (9) | 0.40188 (7) | 0.73967 (7) | 0.0208 (2) |
| H20A | 1.2456 | 0.4452 | 0.7702 | 0.025* |
| C17A | 0.96018 (9) | 0.49881 (8) | 0.80467 (7) | 0.0249 (3) |
| H17F | 0.9513 | 0.5557 | 0.8047 | 0.037* |
| H17E | 0.9214 | 0.4747 | 0.8389 | 0.037* |
| H17D | 0.9339 | 0.4788 | 0.7507 | 0.037* |

| | | | | |
|---|---|---|---|---|
| C12A | 1.26351 (9) | 0.41252 (7) | 0.92809 (6) | 0.0180 (2) |
| C1D | 0.38501 (13) | 0.19095 (9) | 0.91767 (8) | 0.0359 (3) |
| H1DA | 0.3332 | 0.1498 | 0.8988 | 0.054* |
| H1DB | 0.3572 | 0.2413 | 0.8947 | 0.054* |
| H1DC | 0.4014 | 0.1941 | 0.9754 | 0.054* |
| C2D | 0.46908 (11) | 0.16651 (8) | 0.81593 (7) | 0.0274 (3) |
| C7D | 0.37721 (10) | 0.17078 (8) | 0.75621 (8) | 0.0262 (3) |
| H7D | 0.3132 | 0.1805 | 0.7686 | 0.031* |
| C6D | 0.37950 (10) | 0.16072 (7) | 0.67768 (7) | 0.0238 (3) |
| H6D | 0.3164 | 0.1630 | 0.6370 | 0.029* |
| C5D | 0.47250 (9) | 0.14741 (7) | 0.65802 (7) | 0.0209 (2) |
| C8D | 0.47677 (9) | 0.13557 (7) | 0.57620 (7) | 0.0199 (2) |
| C9D | 0.38349 (9) | 0.14465 (7) | 0.50350 (7) | 0.0203 (2) |
| H9D | 0.3157 | 0.1272 | 0.5119 | 0.024* |
| C10D | 0.38710 (8) | 0.23149 (7) | 0.48216 (6) | 0.0200 (2) |
| C11D | 0.44616 (9) | 0.24484 (7) | 0.41937 (7) | 0.0199 (2) |
| H11 | 0.4565 | 0.3018 | 0.4108 | 0.024* |
| C18D | 0.37016 (9) | 0.20589 (7) | 0.34477 (7) | 0.0200 (2) |
| H18 | 0.2982 | 0.2217 | 0.3454 | 0.024* |
| C19D | 0.38602 (9) | 0.23433 (7) | 0.26664 (7) | 0.0190 (2) |
| C24D | 0.30562 (9) | 0.27277 (7) | 0.21283 (7) | 0.0224 (2) |
| H24 | 0.2419 | 0.2819 | 0.2259 | 0.027* |
| C23D | 0.31706 (10) | 0.29807 (7) | 0.14011 (7) | 0.0260 (3) |
| H23 | 0.2608 | 0.3233 | 0.1038 | 0.031* |
| C22D | 0.40941 (10) | 0.28676 (7) | 0.12042 (7) | 0.0253 (3) |
| H22 | 0.4175 | 0.3047 | 0.0711 | 0.030* |
| C4D | 0.56480 (10) | 0.14503 (8) | 0.71918 (7) | 0.0250 (3) |
| H4D | 0.6293 | 0.1369 | 0.7070 | 0.030* |
| C3D | 0.56275 (10) | 0.15433 (8) | 0.79679 (7) | 0.0282 (3) |
| H3D | 0.6258 | 0.1524 | 0.8376 | 0.034* |
| C16D | 0.37599 (9) | 0.11523 (7) | 0.35504 (7) | 0.0205 (2) |
| H16 | 0.4252 | 0.0950 | 0.3255 | 0.025* |
| C17D | 0.27068 (10) | 0.07693 (8) | 0.31992 (8) | 0.0274 (3) |
| H17C | 0.2218 | 0.0932 | 0.3499 | 0.041* |

| | | | | |
|---|---|---|---|---|
| H17B | 0.2784 | 0.0199 | 0.3226 | 0.041* |
| H17A | 0.2441 | 0.0930 | 0.2647 | 0.041* |
| C14D | 0.42141 (9) | 0.09528 (7) | 0.44270 (7) | 0.0190 (2) |
| H14 | 0.4115 | 0.0384 | 0.4517 | 0.023* |
| C13D | 0.53764 (9) | 0.11629 (7) | 0.47022 (7) | 0.0188 (2) |
| C12D | 0.54884 (9) | 0.20054 (7) | 0.44087 (6) | 0.0193 (2) |
| C15D | 0.60883 (10) | -0.01167 (8) | 0.46977 (7) | 0.0270 (3) |
| H15A | 0.5488 | -0.0398 | 0.4368 | 0.040* |
| H15C | 0.6062 | -0.0132 | 0.5250 | 0.040* |
| H15B | 0.6731 | -0.0366 | 0.4651 | 0.040* |
| C21D | 0.49053 (10) | 0.24881 (8) | 0.17362 (8) | 0.0278 (3) |
| H21 | 0.5546 | 0.2407 | 0.1607 | 0.033* |
| C20D | 0.47854 (10) | 0.22256 (8) | 0.24584 (7) | 0.0258 (3) |
| H20 | 0.5344 | 0.1962 | 0.2814 | 0.031* |
| C1B | 0.69766 (12) | 0.43694 (9) | 1.44557 (7) | 0.0336 (3) |
| H1BB | 0.7391 | 0.4850 | 1.4511 | 0.050* |
| H1BA | 0.7406 | 0.3922 | 1.4390 | 0.050* |
| H1BC | 0.6730 | 0.4293 | 1.4929 | 0.050* |
| C2B | 0.63042 (10) | 0.45213 (7) | 1.30589 (7) | 0.0240 (3) |
| C7B | 0.54449 (10) | 0.44787 (8) | 1.24051 (7) | 0.0258 (3) |
| H7B | 0.4776 | 0.4386 | 1.2481 | 0.031* |
| C6B | 0.55525 (9) | 0.45700 (7) | 1.16454 (7) | 0.0223 (2) |
| H6B | 0.4957 | 0.4545 | 1.1207 | 0.027* |
| C5B | 0.65347 (9) | 0.46982 (7) | 1.15207 (7) | 0.0187 (2) |
| C8B | 0.66852 (9) | 0.47861 (7) | 1.07240 (7) | 0.0177 (2) |
| C9B | 0.58531 (9) | 0.45944 (7) | 0.99562 (6) | 0.0180 (2) |
| H9B | 0.5126 | 0.4729 | 0.9964 | 0.022* |
| C14B | 0.62788 (9) | 0.50736 (7) | 0.93601 (6) | 0.0177 (2) |
| H14C | 0.6104 | 0.5639 | 0.9394 | 0.021* |
| C16B | 0.59501 (9) | 0.48031 (7) | 0.84925 (6) | 0.0176 (2) |
| H16C | 0.6453 | 0.5033 | 0.8221 | 0.021* |
| C18B | 0.60394 (9) | 0.38924 (7) | 0.84535 (6) | 0.0181 (2) |
| H18C | 0.5324 | 0.3679 | 0.8392 | 0.022* |
| C19B | 0.63735 (9) | 0.36327 (7) | 0.77291 (7) | 0.0186 (2) |

| | | | | |
|---|---|---|---|---|
| C24B | 0.56202 (10) | 0.34823 (8) | 0.70256 (7) | 0.0244 (3) |
| H24C | 0.4906 | 0.3506 | 0.7017 | 0.029* |
| C23B | 0.58960 (11) | 0.32967 (8) | 0.63322 (7) | 0.0283 (3) |
| H23C | 0.5368 | 0.3208 | 0.5857 | 0.034* |
| C22B | 0.69273 (10) | 0.32407 (7) | 0.63309 (7) | 0.0254 (3) |
| H22C | 0.7116 | 0.3110 | 0.5861 | 0.030* |
| C4B | 0.73868 (9) | 0.47273 (7) | 1.21825 (7) | 0.0217 (2) |
| H4B | 0.8060 | 0.4805 | 1.2109 | 0.026* |
| C3B | 0.72820 (10) | 0.46460 (7) | 1.29452 (7) | 0.0237 (3) |
| H3B | 0.7875 | 0.4676 | 1.3385 | 0.028* |
| C13B | 0.74456 (9) | 0.49453 (7) | 0.97354 (6) | 0.0184 (2) |
| C17B | 0.48704 (9) | 0.50909 (8) | 0.80594 (7) | 0.0231 (2) |
| H17L | 0.4860 | 0.5664 | 0.8064 | 0.035* |
| H17K | 0.4361 | 0.4890 | 0.8323 | 0.035* |
| H17J | 0.4695 | 0.4904 | 0.7512 | 0.035* |
| C11B | 0.67254 (9) | 0.35864 (7) | 0.92695 (7) | 0.0184 (2) |
| H11C | 0.6908 | 0.3022 | 0.9242 | 0.022* |
| C10B | 0.60400 (8) | 0.37182 (7) | 0.98342 (6) | 0.0184 (2) |
| C12B | 0.76909 (9) | 0.40907 (7) | 0.95505 (6) | 0.0189 (2) |
| C21B | 0.76817 (10) | 0.33788 (7) | 0.70295 (7) | 0.0253 (3) |
| H21C | 0.8395 | 0.3338 | 0.7038 | 0.030* |
| C20B | 0.74130 (9) | 0.35760 (7) | 0.77206 (7) | 0.0230 (2) |
| H20C | 0.7944 | 0.3673 | 0.8191 | 0.028* |
| C15B | 0.80547 (11) | 0.62427 (8) | 0.96217 (8) | 0.0292 (3) |
| H15L | 0.8047 | 0.6329 | 1.0172 | 0.044* |
| H15J | 0.7407 | 0.6440 | 0.9269 | 0.044* |
| H15K | 0.8647 | 0.6520 | 0.9516 | 0.044* |

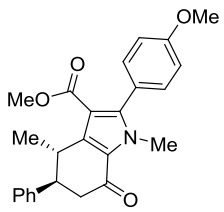


**X-Ray crystallographic data of *N*-acylhemiaminal (163).** Crystals of compound **3** suitable for X-ray analysis were obtained by dissolving the residue in a minimal amount of ethyl acetate and adding hexane very carefully as to produce two layers; the product crystallized as the layers diffused. Crystallographic data have been deposited with the Cambridge Crystallographic Data Centre (CCDC # 818952). Copies of the data can be obtained free of charge on application to the CCDC, 12 Union Road, Cambridge CB21EZ, UK (fax: (+44)-1223-336-033; e-mail: deposit@ccdc.cam.ac.uk.

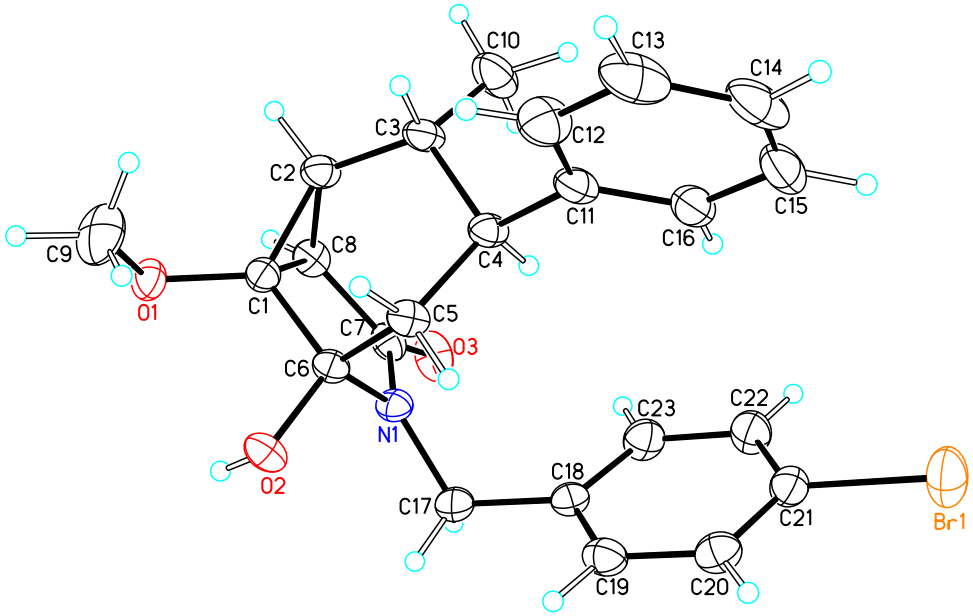


**Crystal data and structure refinement for compound 163.**

| | |
|---|---|
| Identification code | Compound **163** |
| Empirical formula | C23 H24 Br N O3 |

| | | |
|---|---|---|
| Formula weight | 442.34 | |
| Temperature | 173(2) K | |
| Wavelength | 0.71073 Å | |
| Crystal system | Monoclinic | |
| Space group | P2(1)/c | |
| Unit cell dimensions | a = 11.4651(3) Å | α= 90°. |
| | b = 10.4634(2) Å | β= 102.0840(10)°. |
| | c = 17.3065(5) Å | γ = 90°. |
| Volume | 2030.15(9) $Å^3$ | |
| Z | 4 | |
| Density (calculated) | 1.447 $Mg/m^3$ | |
| Absorption coefficient | 2.048 $mm^{-1}$ | |
| F(000) | 912 | |
| Crystal size | 0.40 x 0.35 x 0.30 $mm^3$ | |
| Theta range for data collection | 2.29 to 30.51°. | |
| Index ranges | -16<=h<=15, -14<=k<=14, -24<=l<=24 | |
| Reflections collected | 35229 | |
| Independent reflections | 6191 [R(int) = 0.0399] | |
| Completeness to theta = 30.51° | 100.0 % | |
| Absorption correction | Semi-empirical from equivalents | |
| Max. and min. transmission | 0.5785 and 0.4946 | |
| Refinement method | Full-matrix least-squares on $F^2$ | |
| Data / restraints / parameters | 6191 / 0 / 349 | |
| Goodness-of-fit on $F^2$ | 1.003 | |
| Final R indices [I>2sigma(I)] | R1 = 0.0341, wR2 = 0.0746 | |
| R indices (all data) | R1 = 0.0627, wR2 = 0.0851 | |
| Largest diff. peak and hole | 0.383 and -0.358 $e.Å^{-3}$ | |

**Atomic coordinates ( x $10^4$) and equivalent isotropic displacement parameters ($Å^2$x $10^3$) for compound 163. U(eq) is defined as one third of the trace of the orthogonalized $U^{ij}$ tensor.**

| | x | y | z | U(eq) |
|---|---|---|---|---|
| Br(1) | 338(1) | 2627(1) | 1162(1) | 40(1) |
| O(1) | 4385(1) | 10803(1) | 574(1) | 24(1) |
| O(2) | 3348(1) | 8799(1) | -347(1) | 24(1) |
| O(3) | 5705(1) | 6982(1) | 1808(1) | 31(1) |
| N(1) | 4209(1) | 7528(1) | 761(1) | 20(1) |
| C(1) | 4073(1) | 9736(1) | 969(1) | 19(1) |
| C(2) | 3839(1) | 9830(1) | 1776(1) | 22(1) |
| C(3) | 2779(1) | 9216(1) | 2025(1) | 24(1) |
| C(4) | 2182(1) | 8143(1) | 1468(1) | 20(1) |
| C(5) | 2182(1) | 8438(1) | 603(1) | 21(1) |
| C(6) | 3434(1) | 8624(1) | 462(1) | 18(1) |

| | | | | |
|---|---|---|---|---|
| C(7) | 5016(1) | 7770(1) | 1439(1) | 21(1) |
| C(8) | 4966(1) | 9153(1) | 1622(1) | 22(1) |
| C(9) | 3422(2) | 11673(2) | 314(1) | 42(1) |
| C(10) | 3108(2) | 8766(2) | 2879(1) | 37(1) |
| C(11) | 926(1) | 7865(1) | 1576(1) | 24(1) |
| C(12) | 31(1) | 8782(2) | 1415(1) | 34(1) |
| C(13) | -1118(1) | 8492(2) | 1495(1) | 42(1) |
| C(14) | -1396(1) | 7295(2) | 1725(1) | 42(1) |
| C(15) | -520(1) | 6384(2) | 1893(1) | 37(1) |
| C(16) | 634(1) | 6668(2) | 1825(1) | 29(1) |
| C(17) | 4128(1) | 6294(1) | 364(1) | 26(1) |
| C(18) | 3211(1) | 5382(1) | 561(1) | 23(1) |
| C(19) | 2217(1) | 5051(1) | -5(1) | 26(1) |
| C(20) | 1359(1) | 4225(1) | 167(1) | 26(1) |
| C(21) | 1516(1) | 3738(1) | 920(1) | 24(1) |
| C(22) | 2509(1) | 4025(1) | 1496(1) | 28(1) |
| C(23) | 3357(1) | 4844(1) | 1312(1) | 27(1) |

**References for X-Ray Structure Determinations**

(1) (a) Data Collection: SMART Software Reference Manual (1994). Bruker-AXS, 6300 Enterprise Dr. Madison, WI 53719-1173, USA. (b) Data Reduction: SAINT Software Reference Manual (1995). Bruker-AXS, 6300 Enterprise Dr. Madison, WI 53719-1173, USA.

(2) G.M. Sheldrick (2000). SADABS. Program for Empirical Adsorption Correction of Area Detector Data. University of Göttingen, Germany.

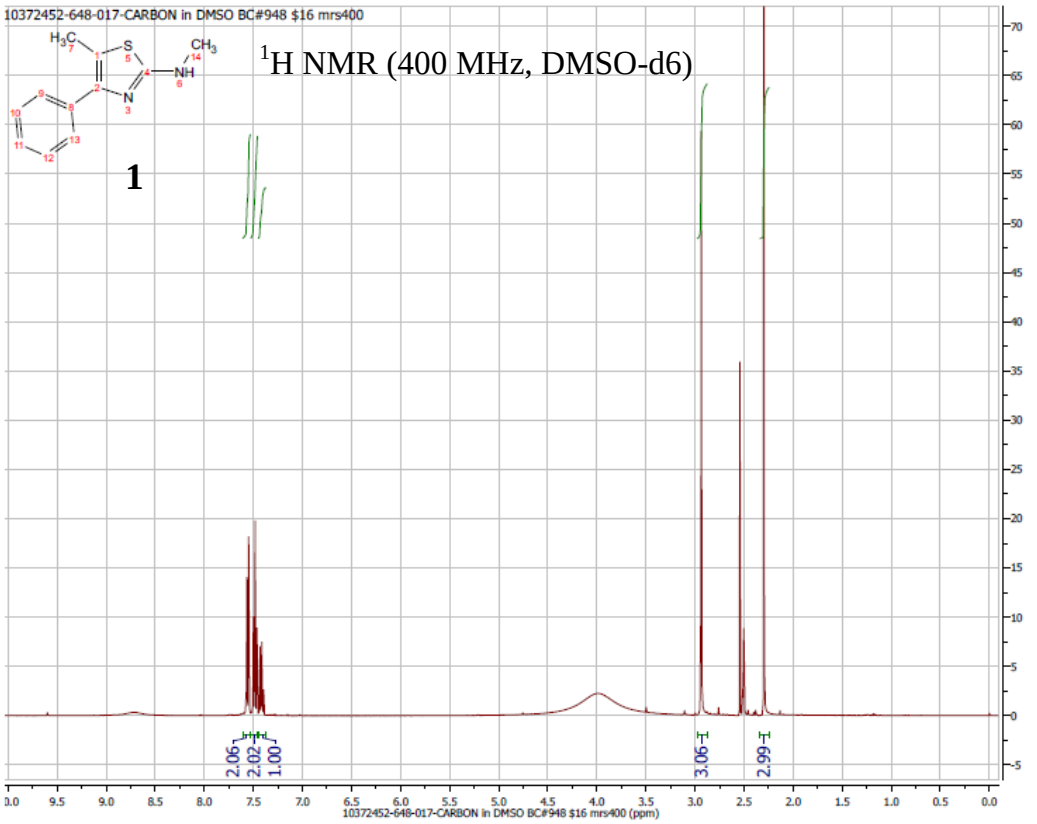


$^{1}$H NMR (400 MHz, DMSO-d6)

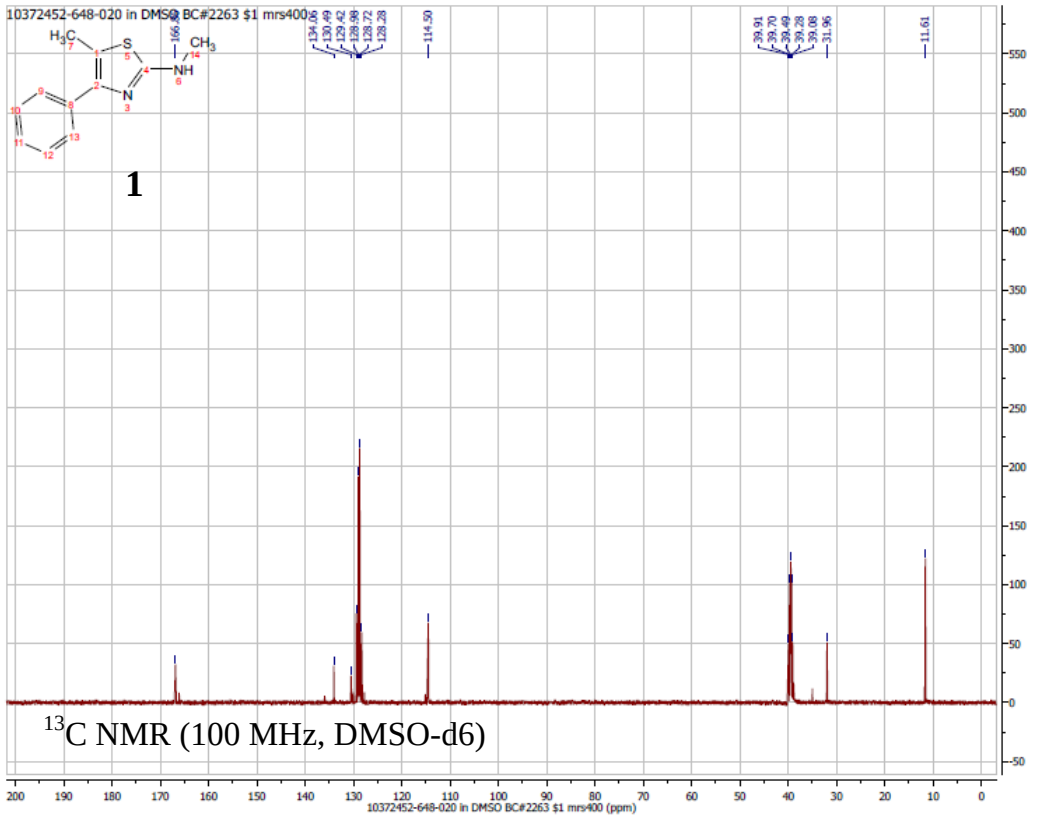


$^{13}$C NMR (100 MHz, DMSO-d6)

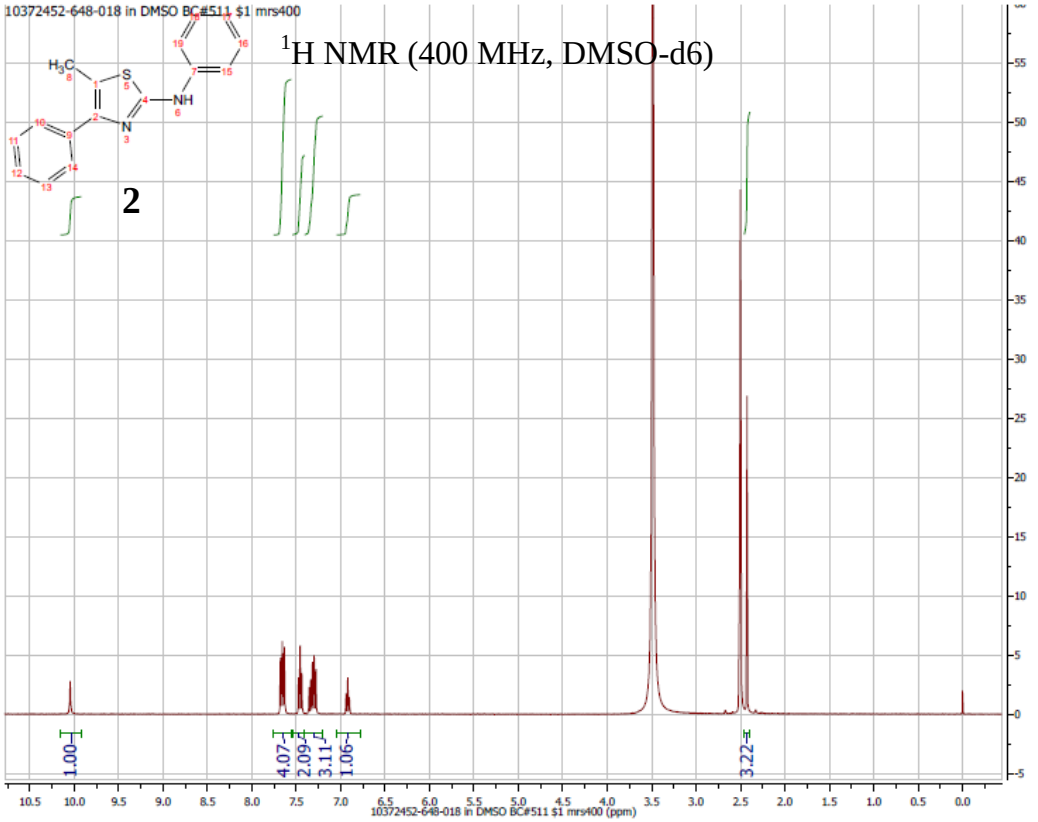


$^{1}$H NMR (400 MHz, DMSO-d6)

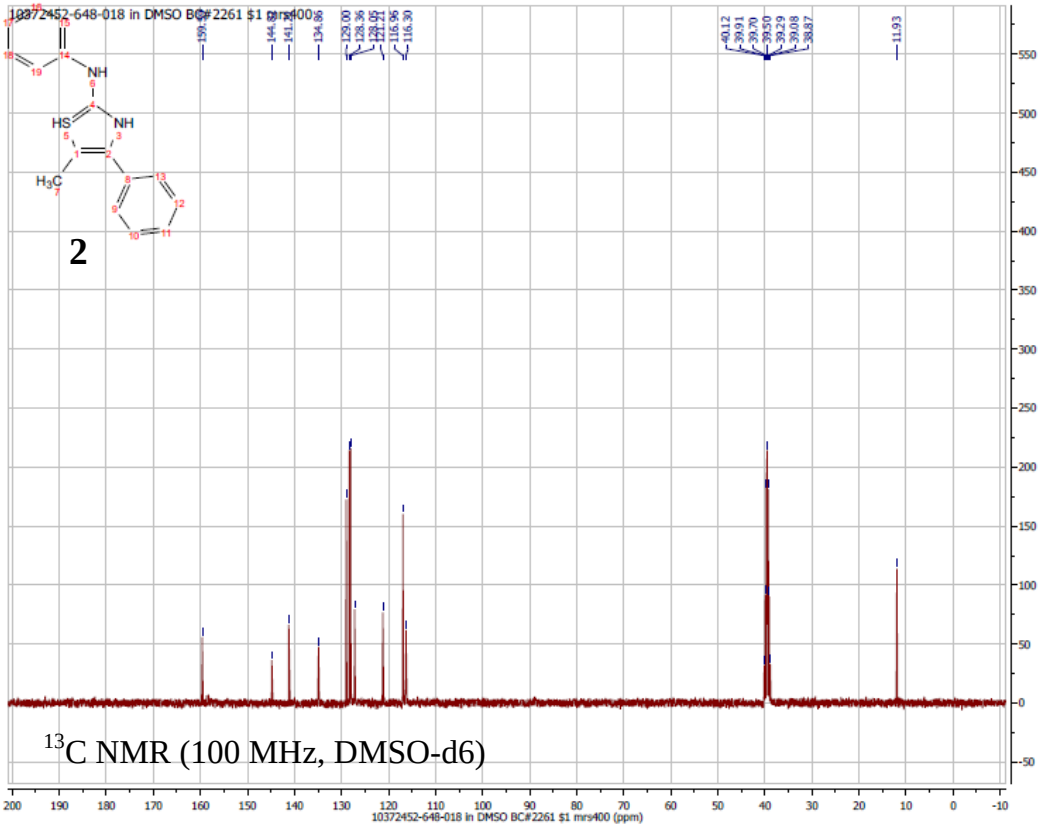


$^{13}$C NMR (100 MHz, DMSO-d6)

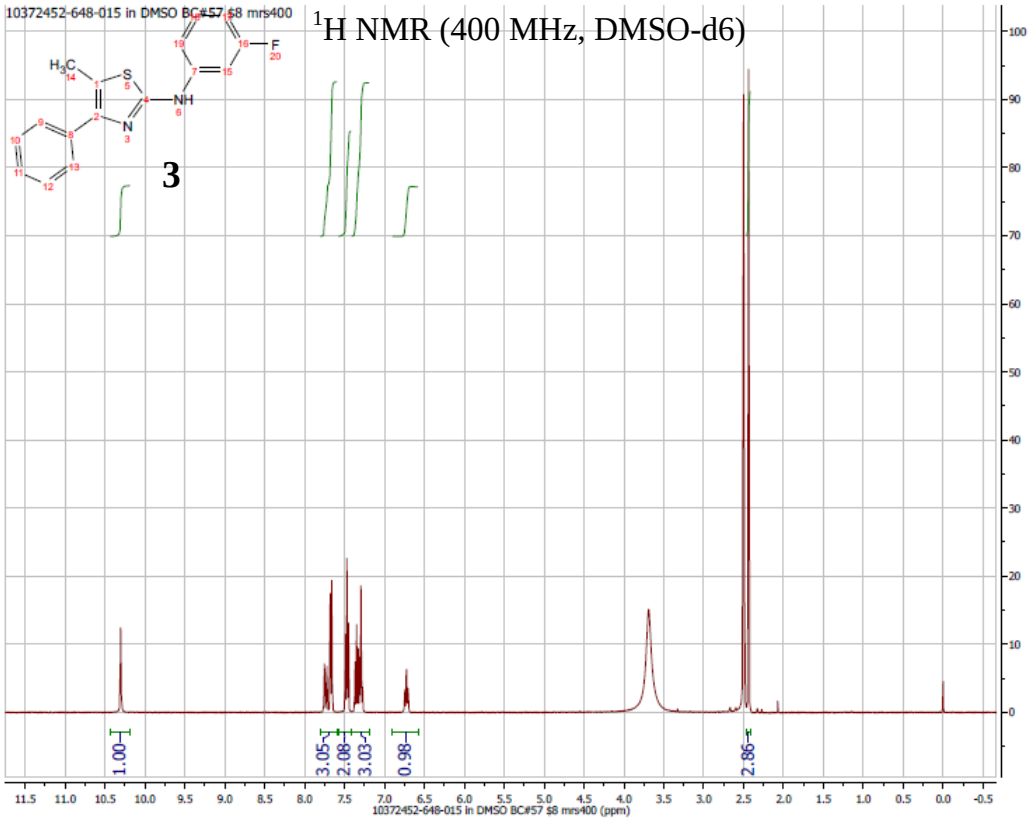


$^{1}$H NMR (400 MHz, DMSO-d6)

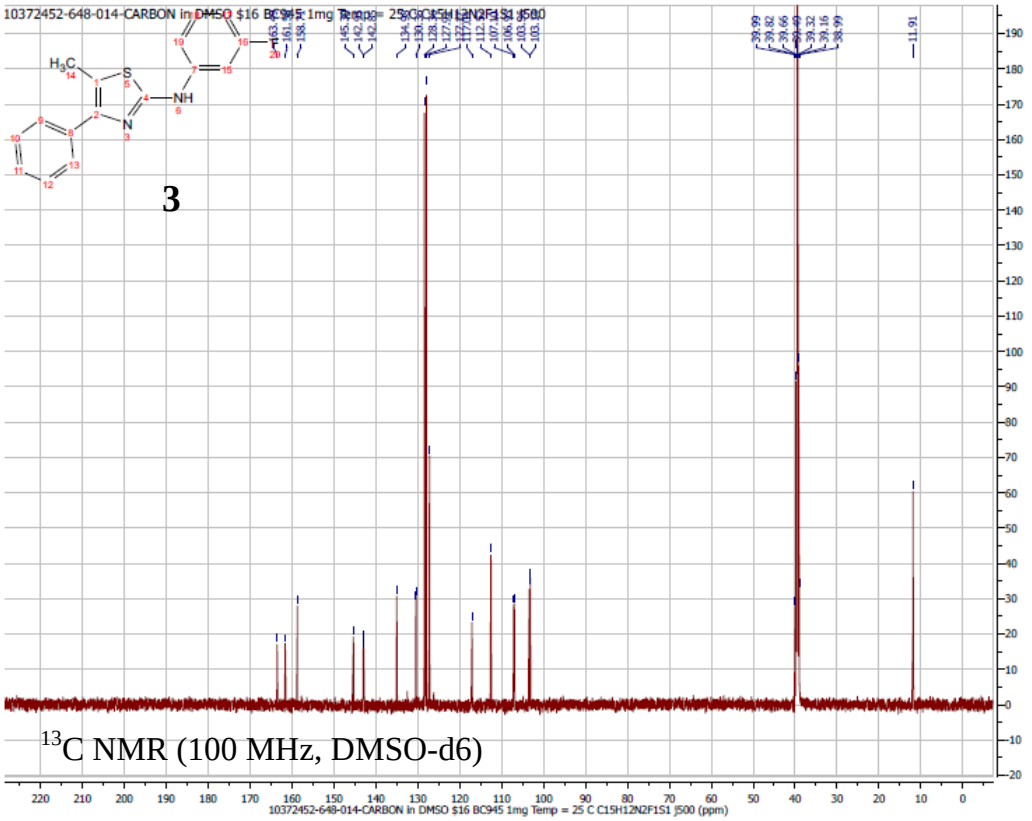


$^{13}$C NMR (100 MHz, DMSO-d6)

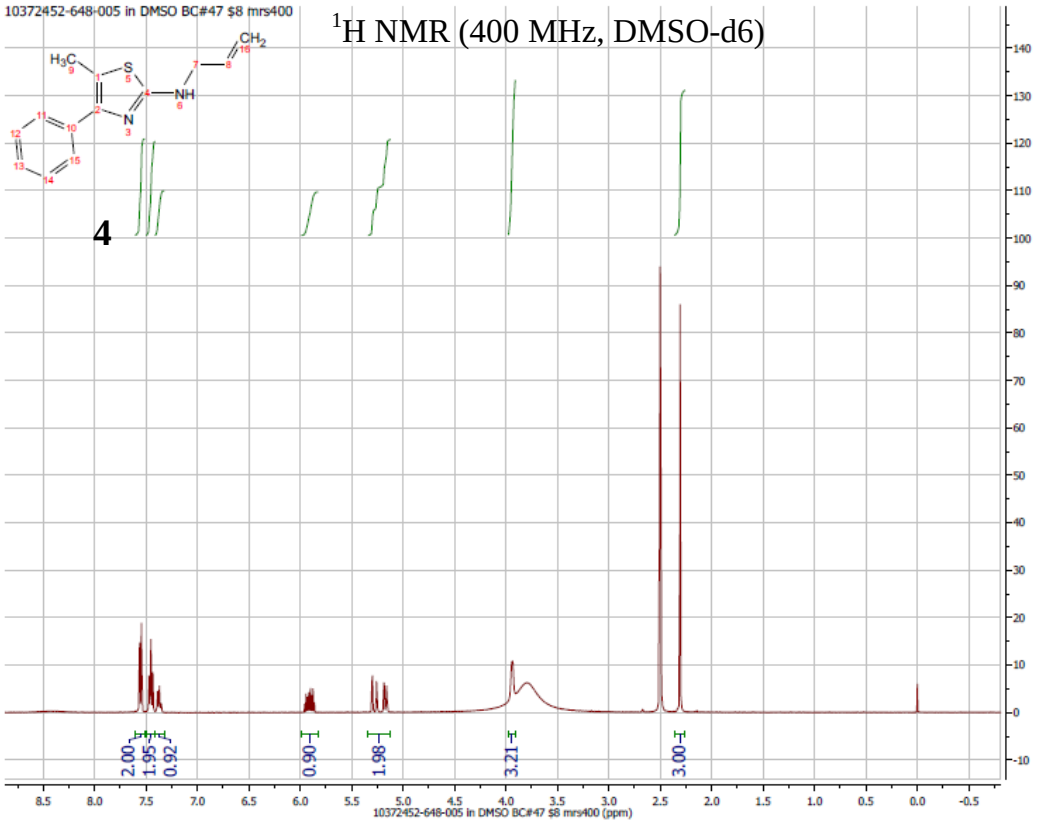


$^{1}$H NMR (400 MHz, DMSO-d6)

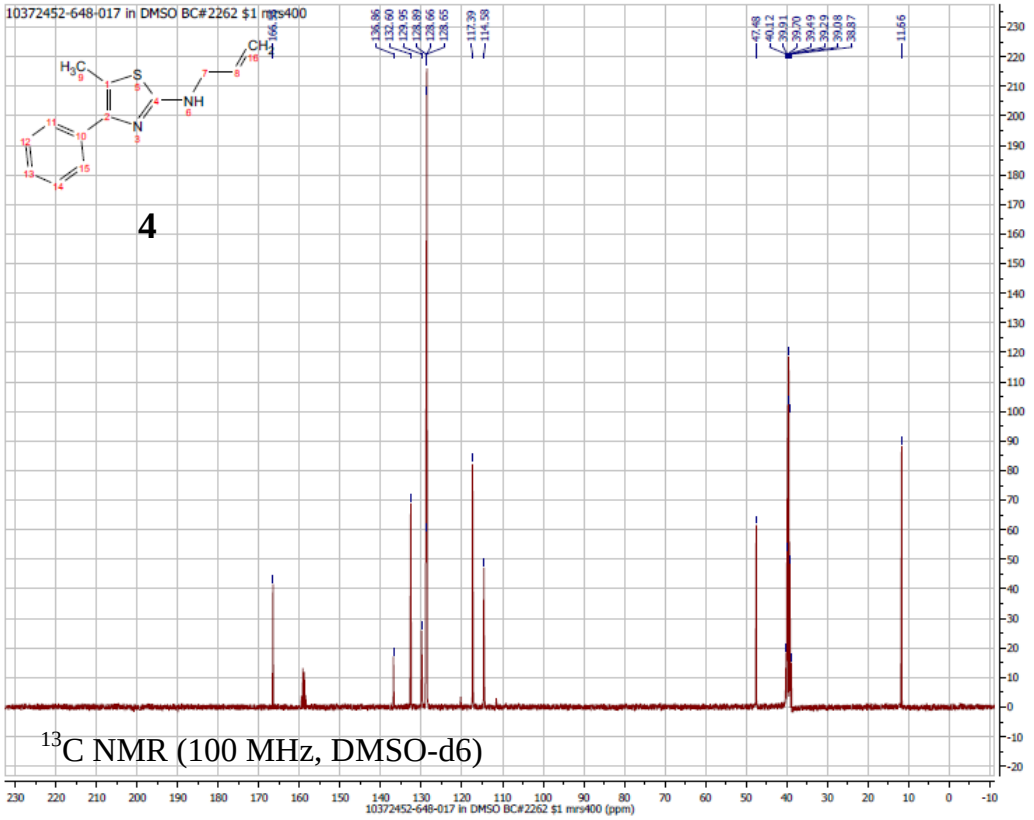


$^{13}$C NMR (100 MHz, DMSO-d6)

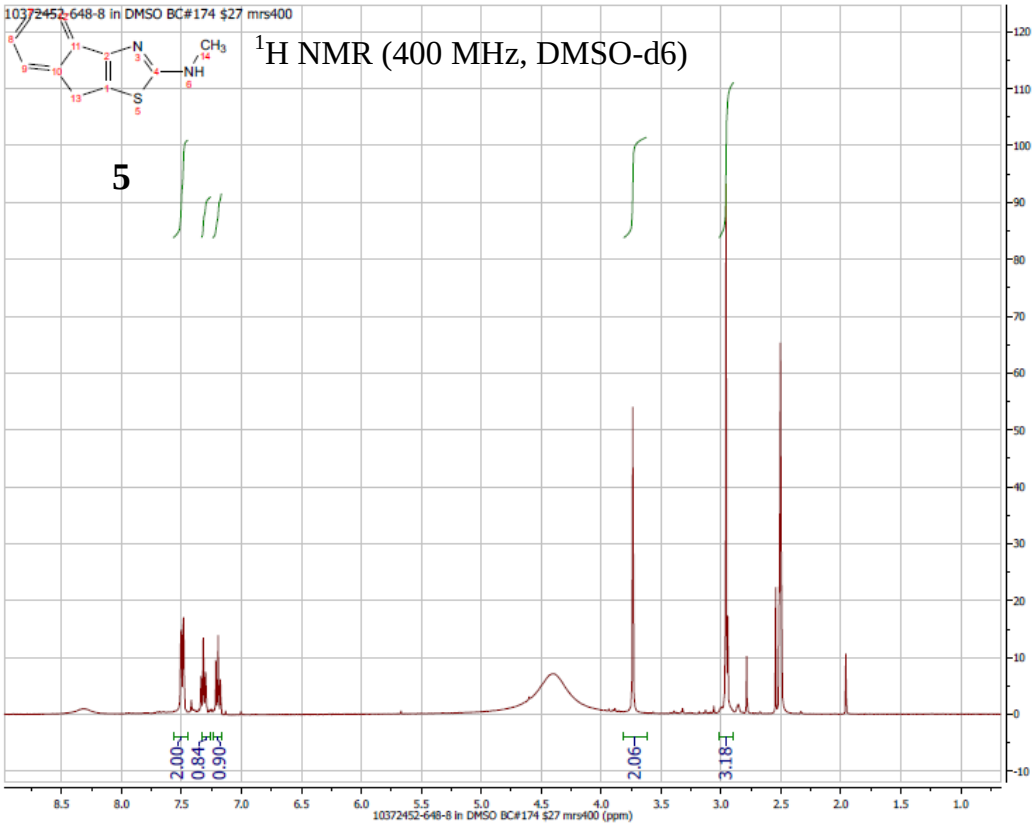
10372452-648-8 in DMSO BC#174 $27 mrs400
$^{1}$H NMR (400 MHz, DMSO-d6)
5
2.00
0.84
0.90
2.06
3.18
10372452-648-8 in DMSO BC#174 $27 mrs400 (ppm)

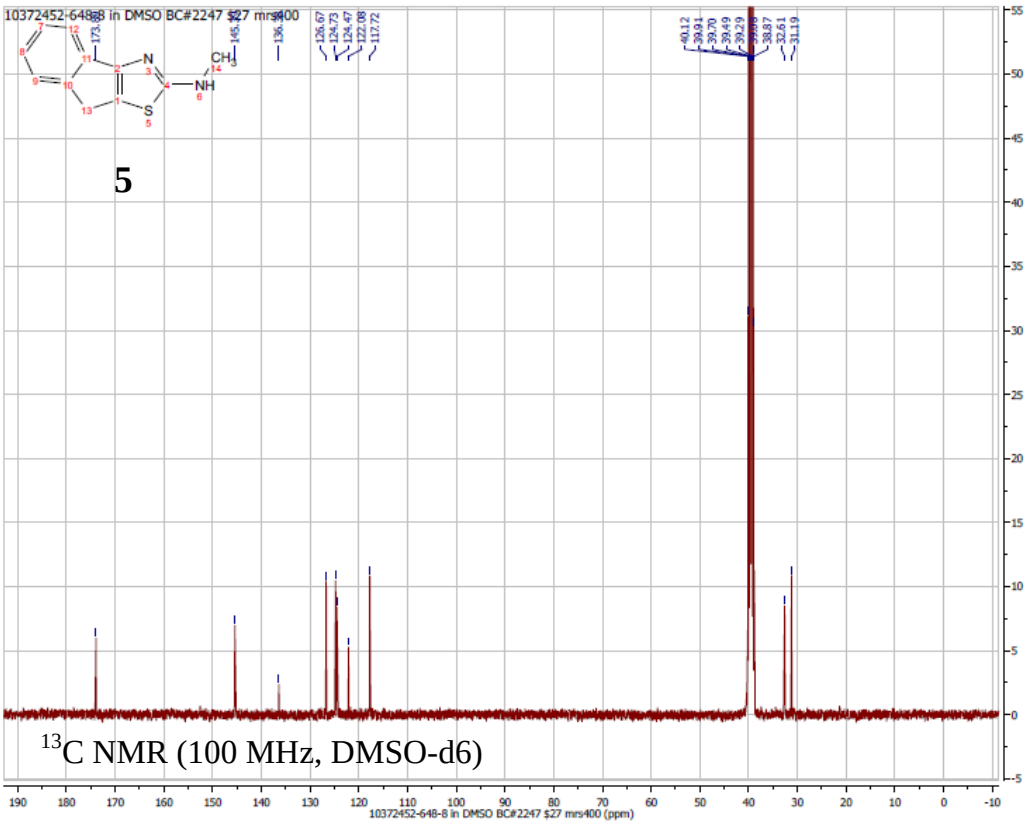
10372452-648-8 in DMSO BC#2247 $27 mrs400
5
$^{13}$C NMR (100 MHz, DMSO-d6)
10372452-648-8 in DMSO BC#2247 $27 mrs400 (ppm)

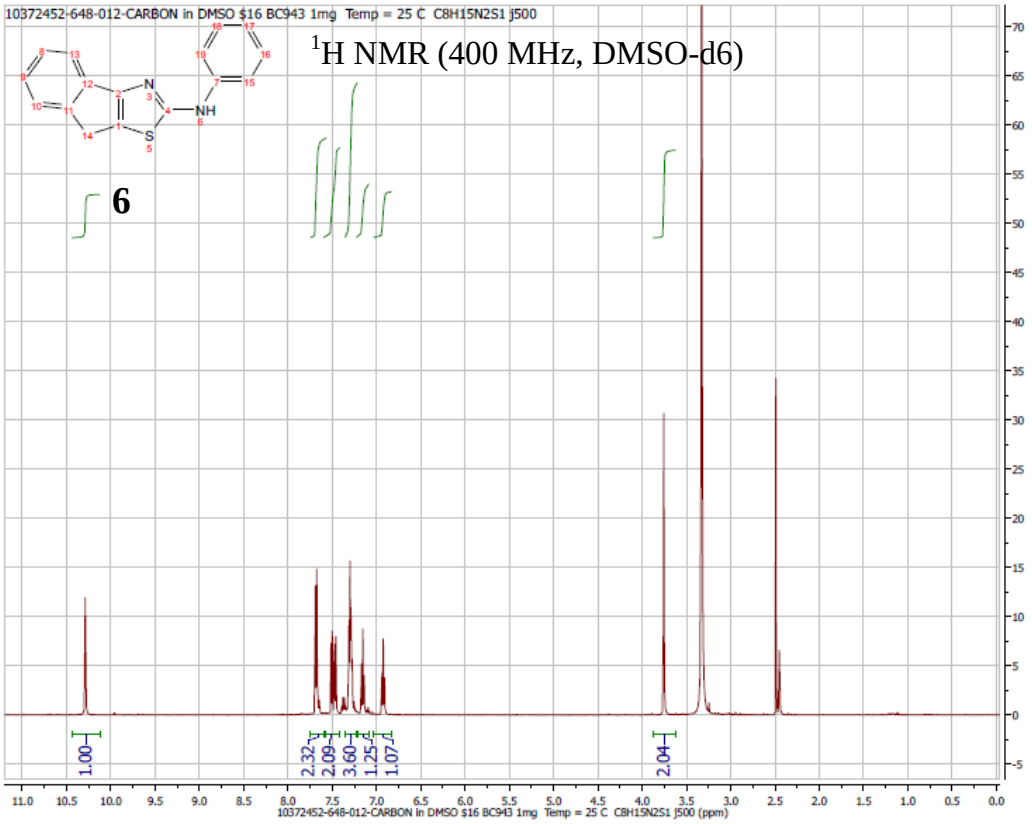


$^{1}$H NMR (400 MHz, DMSO-d6)

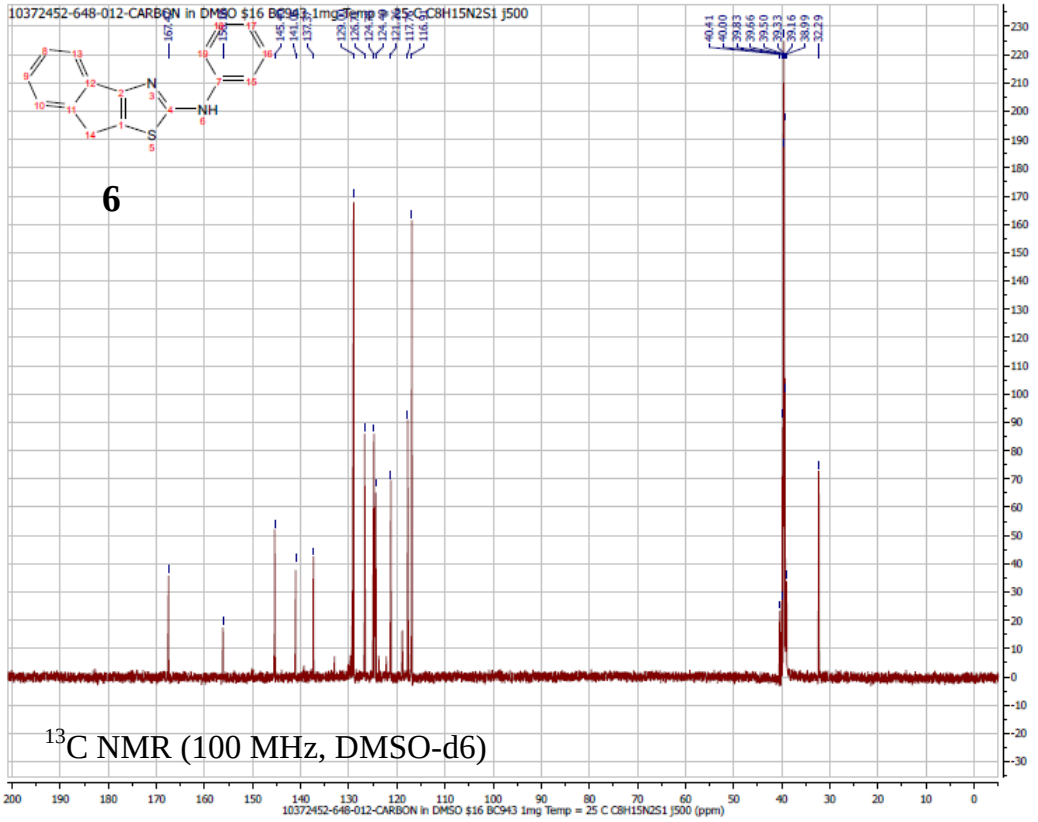


$^{13}$C NMR (100 MHz, DMSO-d6)

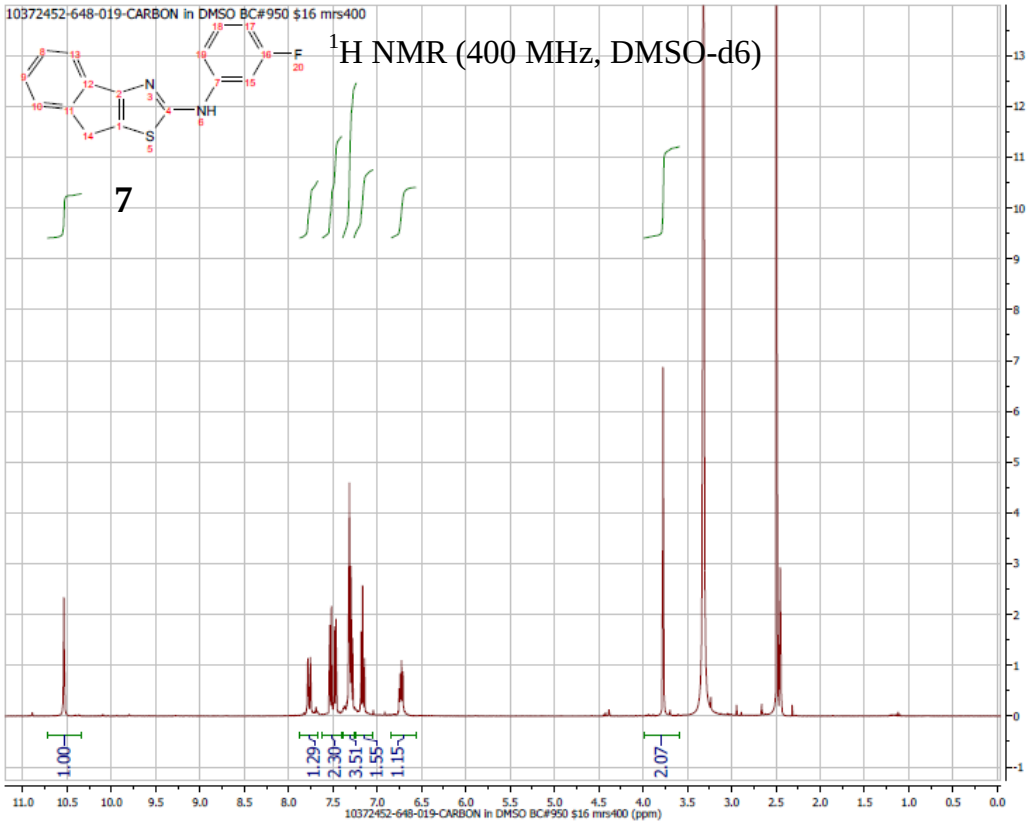


$^{1}$H NMR (400 MHz, DMSO-d6)

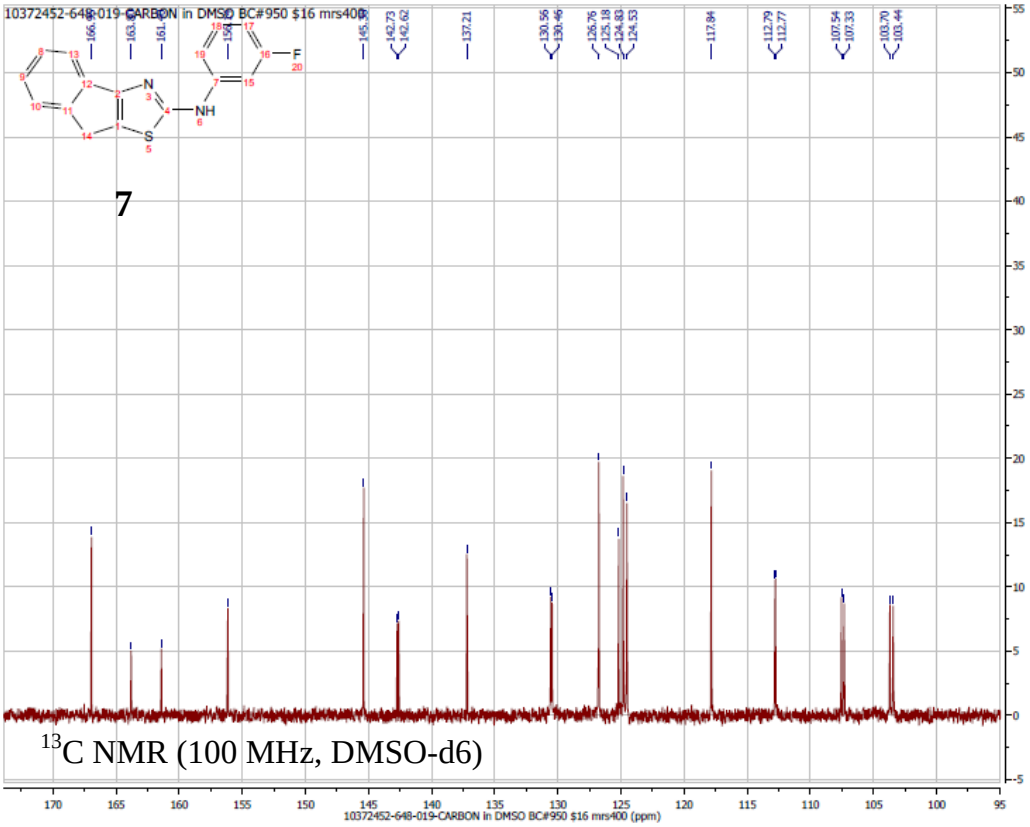


$^{13}$C NMR (100 MHz, DMSO-d6)

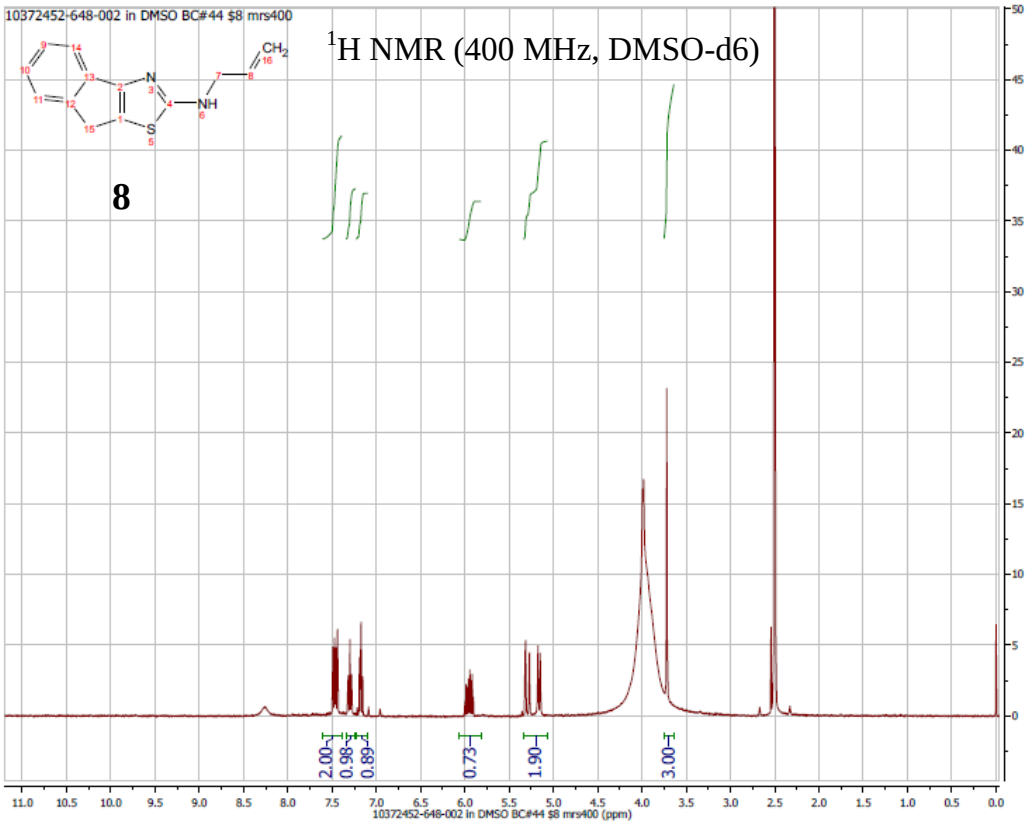
10372452-648-002 in DMSO BC#44 $8 mrs400
$^{1}$H NMR (400 MHz, DMSO-d6)
8
2.00
0.98
0.89
0.73
1.90
3.00
10372452-648-002 in DMSO BC#44 $8 mrs400 (ppm)

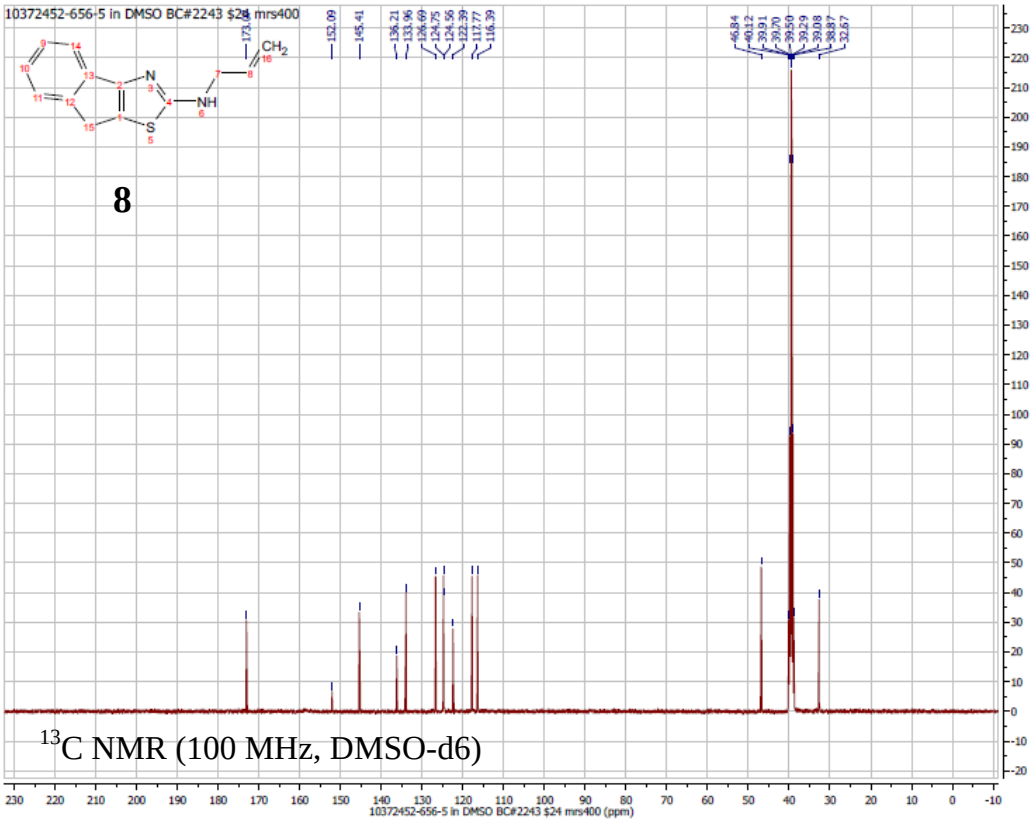
10372452-656-5 in DMSO BC#2243 $24 mrs400
8
$^{13}$C NMR (100 MHz, DMSO-d6)
10372452-656-5 in DMSO BC#2243 $24 mrs400 (ppm)

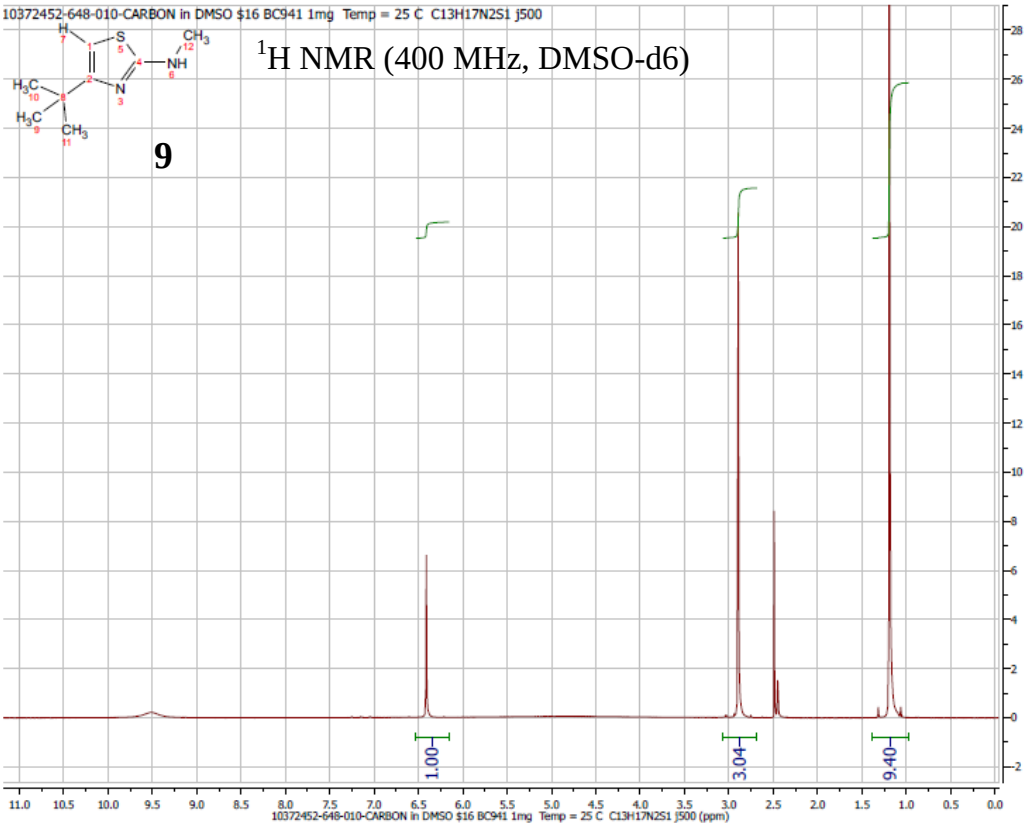


$^{1}$H NMR (400 MHz, DMSO-d6)

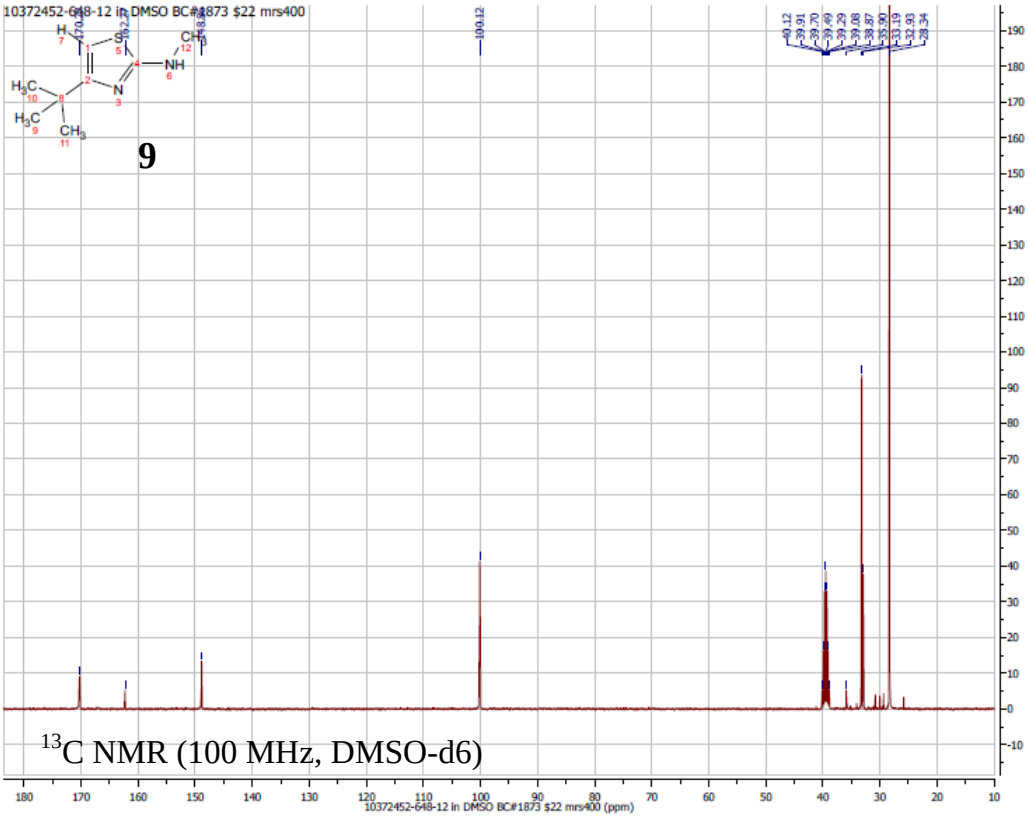


$^{13}$C NMR (100 MHz, DMSO-d6)

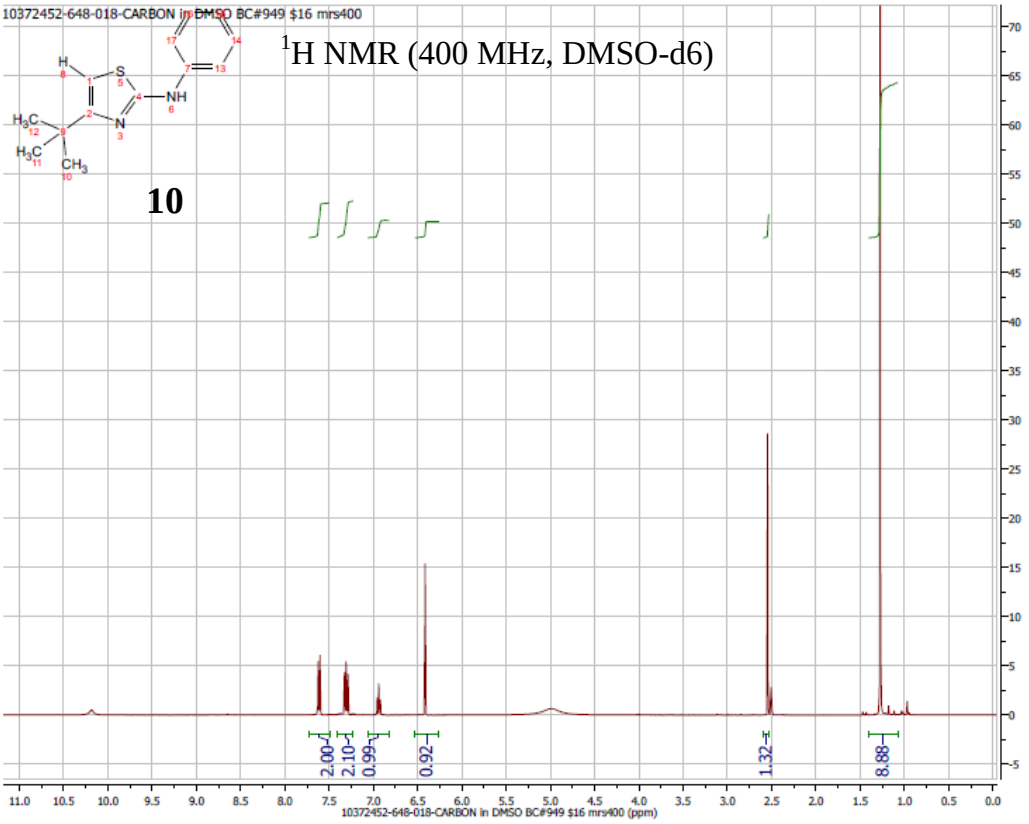


$^{1}$H NMR (400 MHz, DMSO-d6)

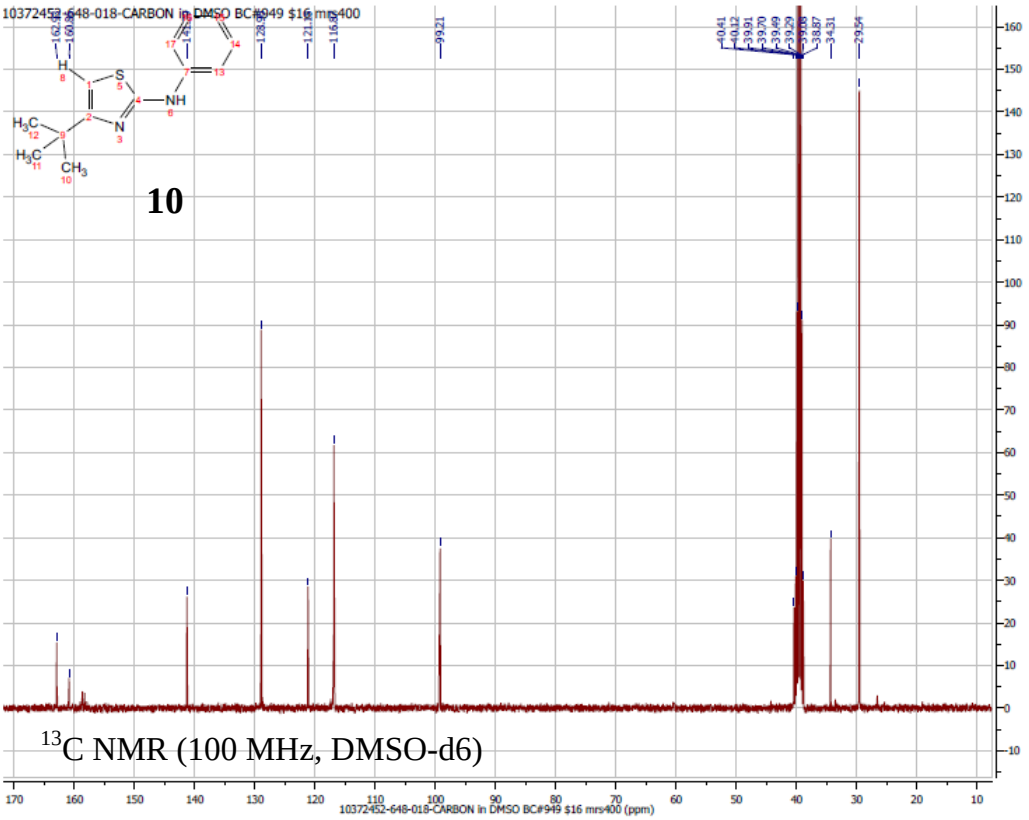


$^{13}$C NMR (100 MHz, DMSO-d6)

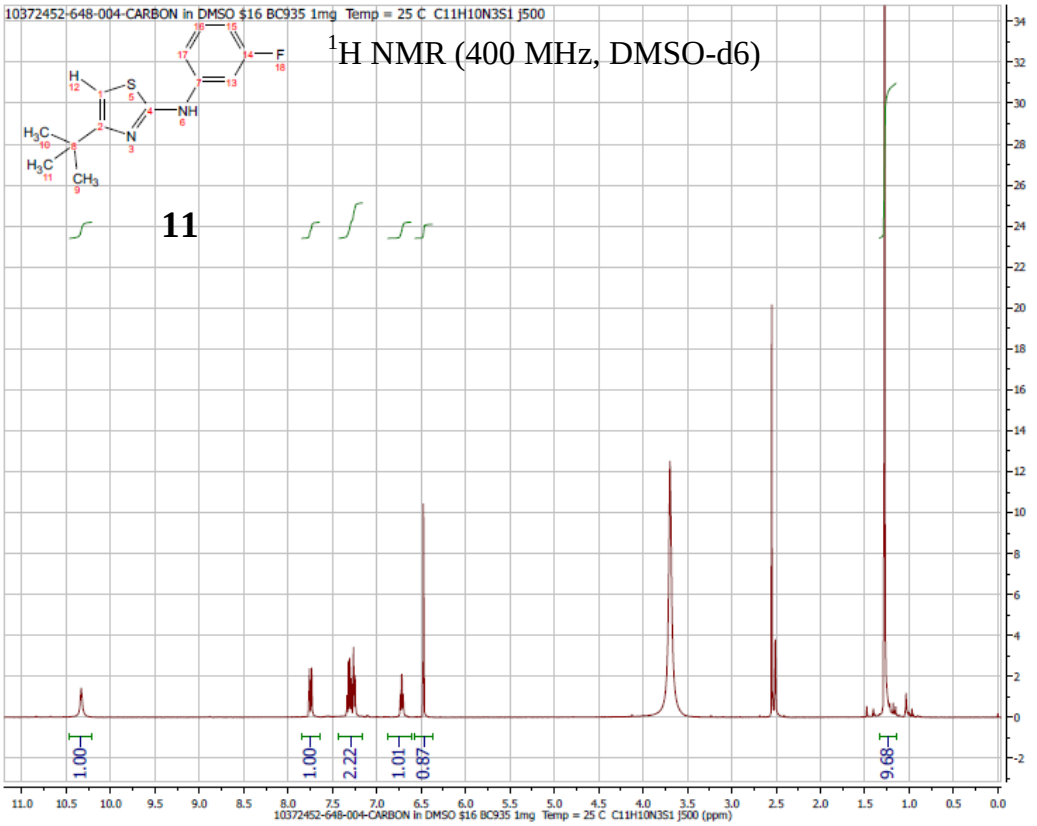


$^{1}$H NMR (400 MHz, DMSO-d6)

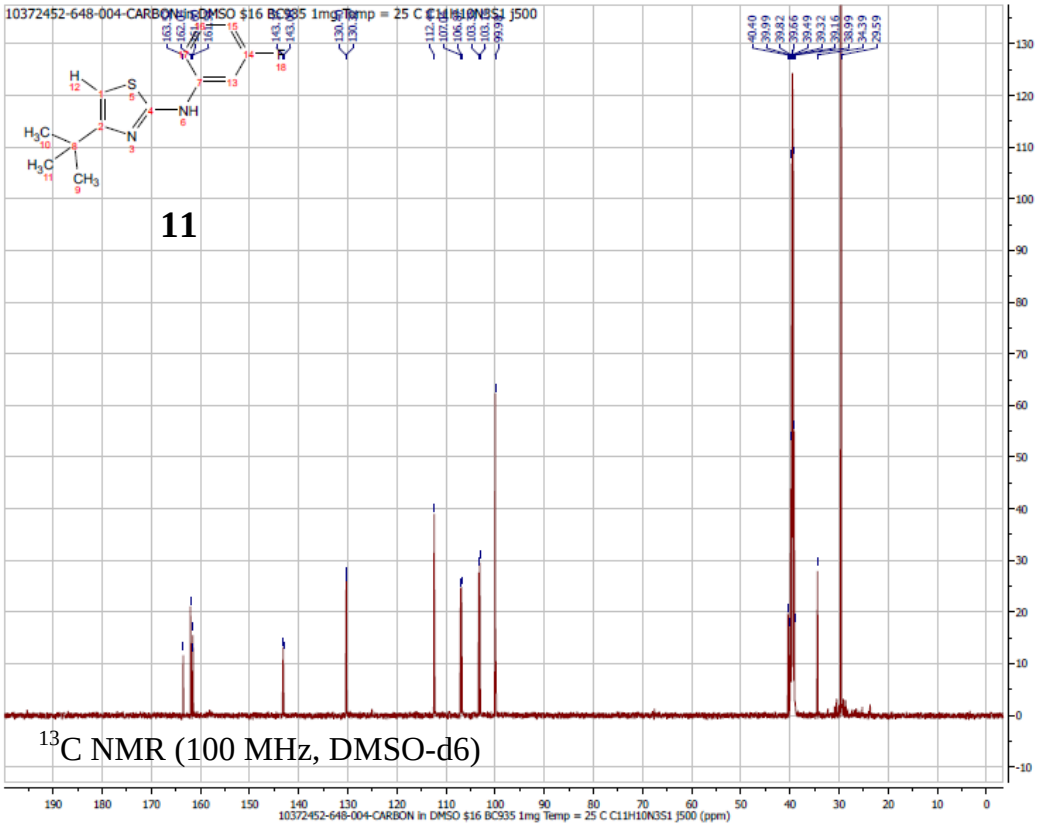


$^{13}$C NMR (100 MHz, DMSO-d6)

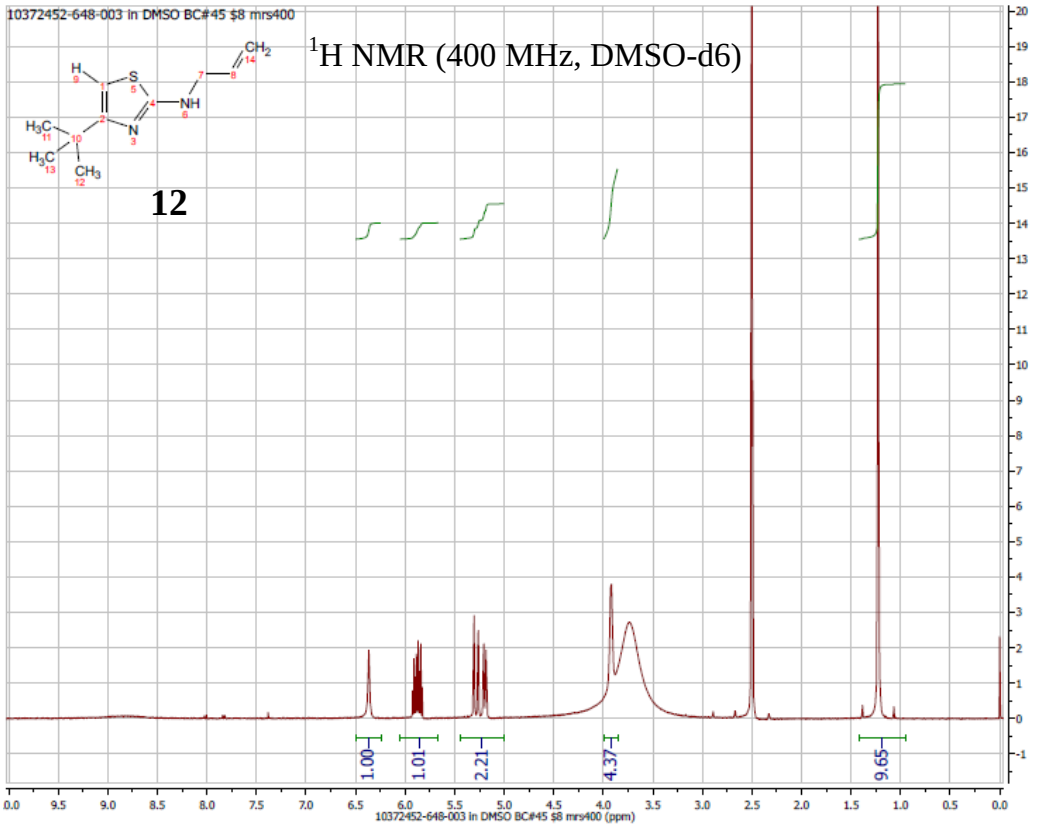


$^{1}$H NMR (400 MHz, DMSO-d6)

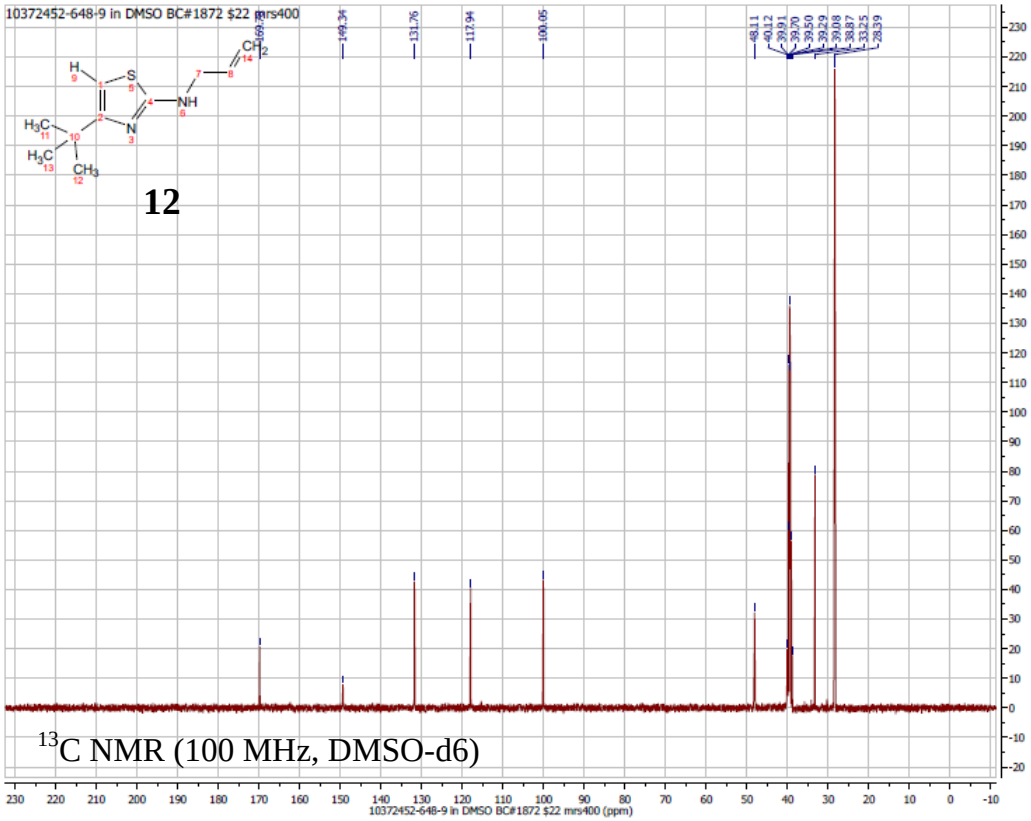


$^{13}$C NMR (100 MHz, DMSO-d6)

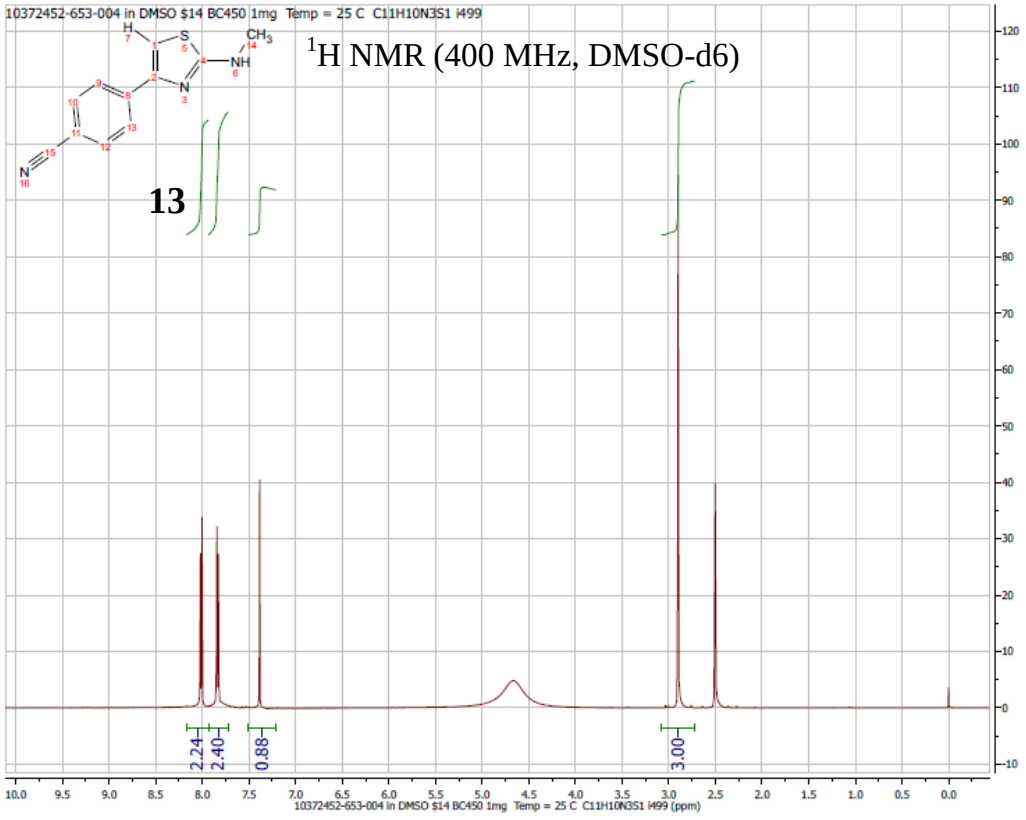


$^{1}$H NMR (400 MHz, DMSO-d6)

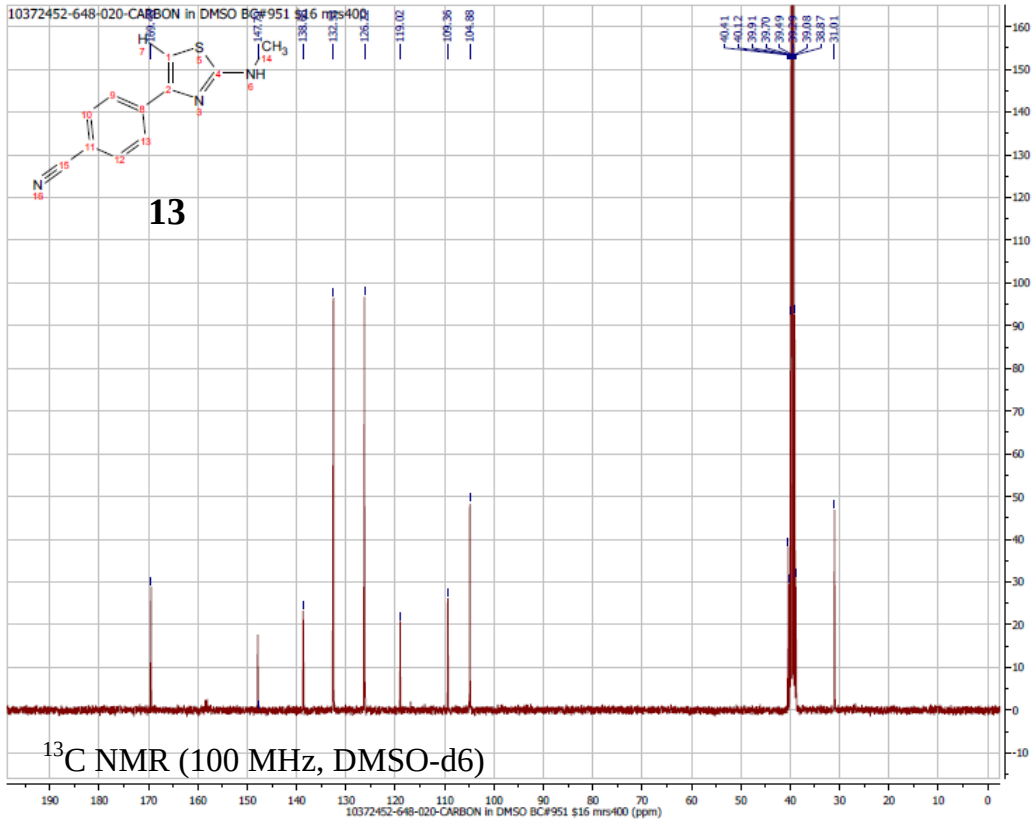


$^{13}$C NMR (100 MHz, DMSO-d6)

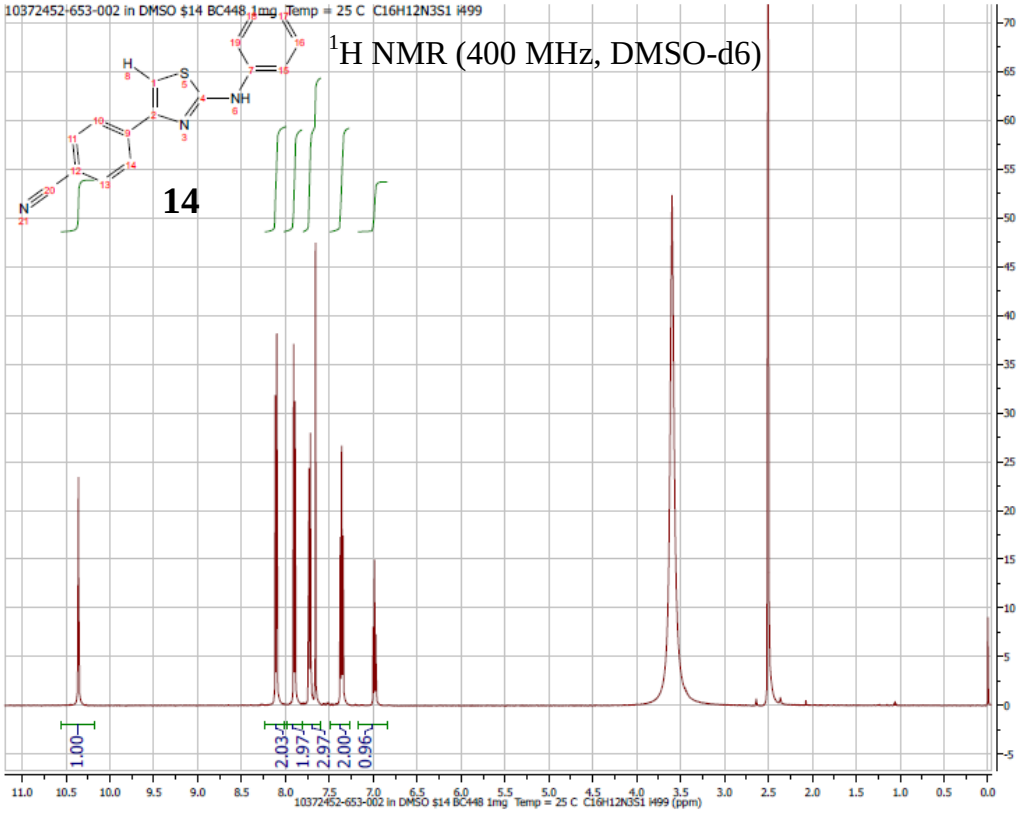


$^{1}$H NMR (400 MHz, DMSO-d6)

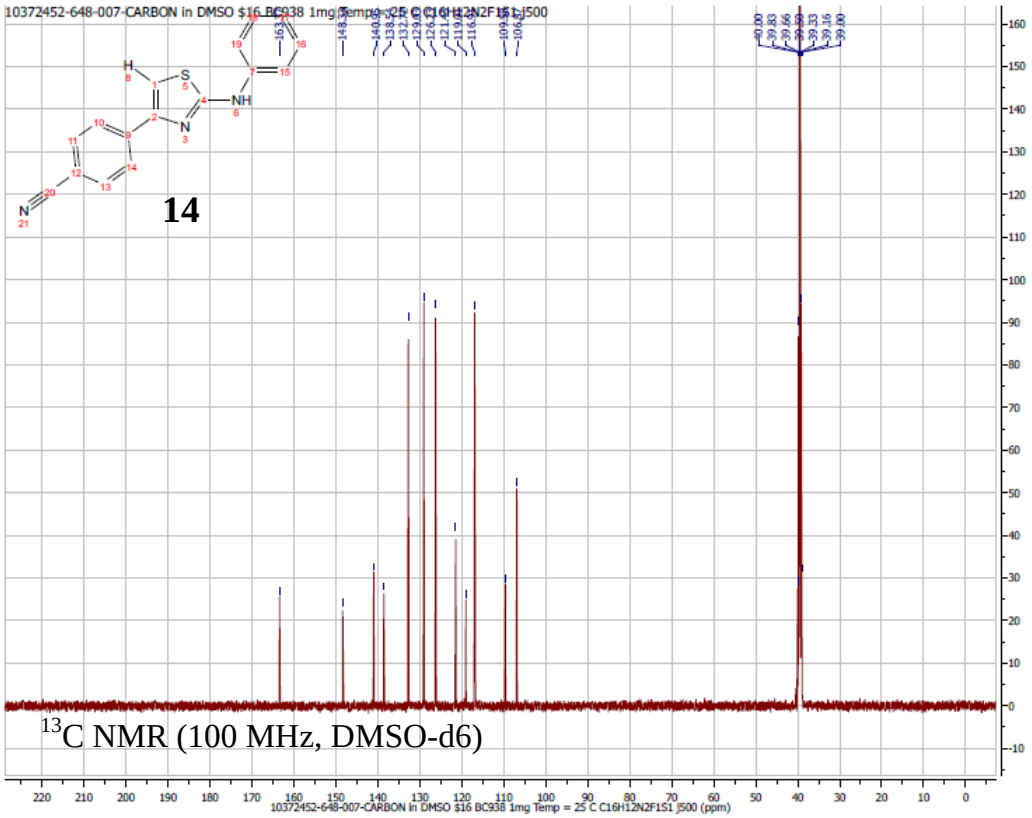


$^{13}$C NMR (100 MHz, DMSO-d6)

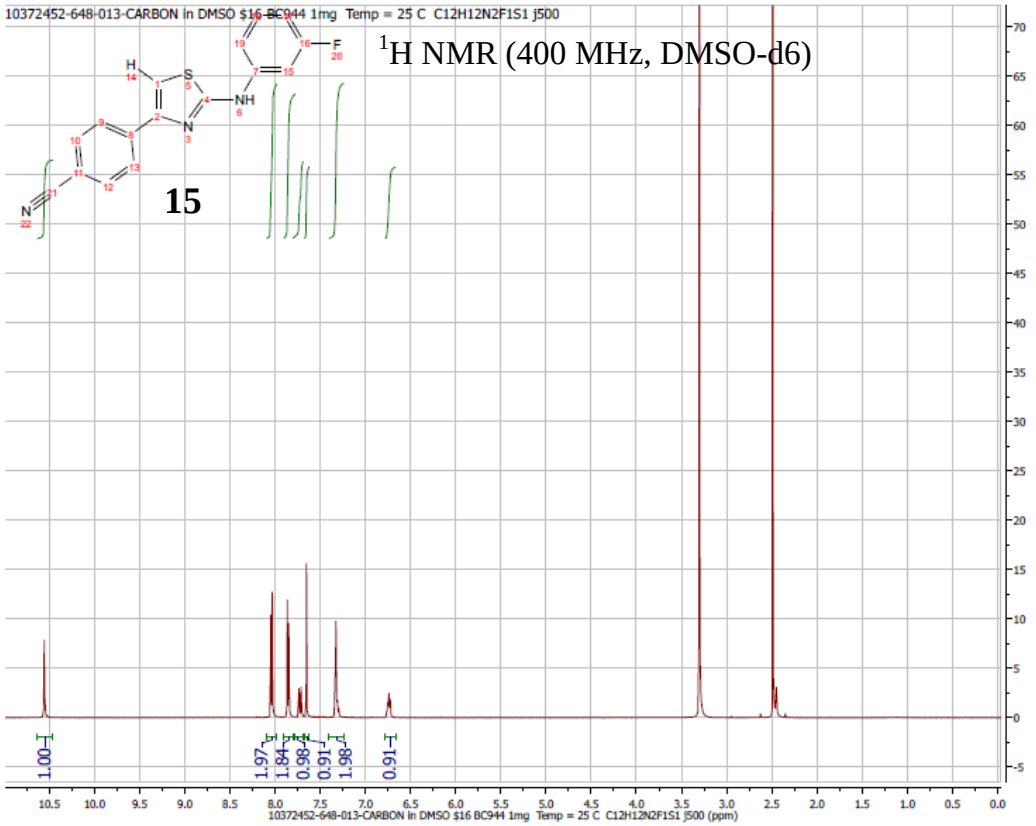


$^{1}$H NMR (400 MHz, DMSO-d6)

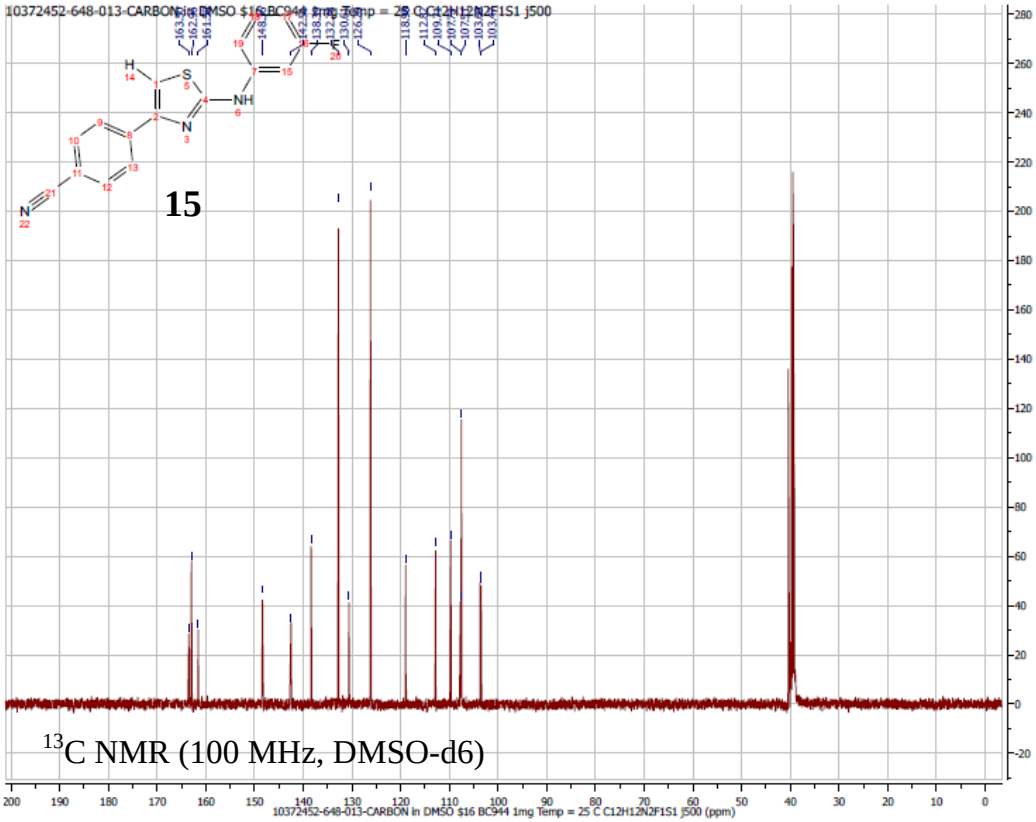


$^{13}$C NMR (100 MHz, DMSO-d6)

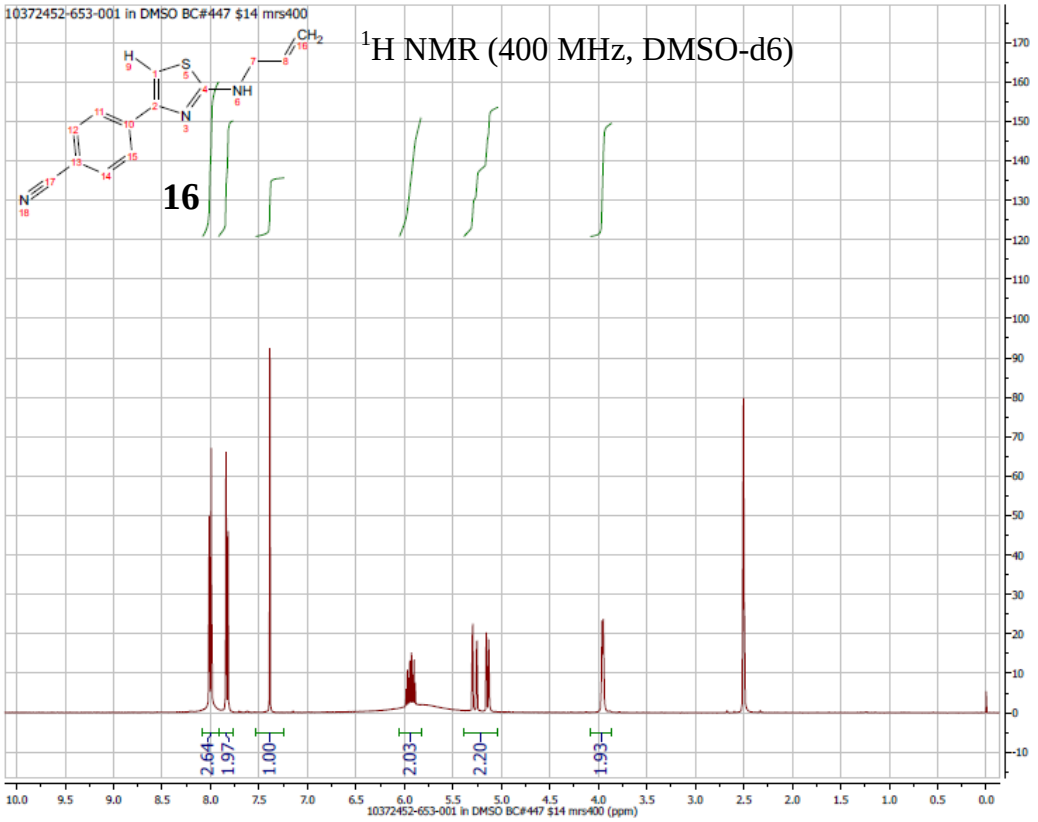


$^{1}$H NMR (400 MHz, DMSO-d6)

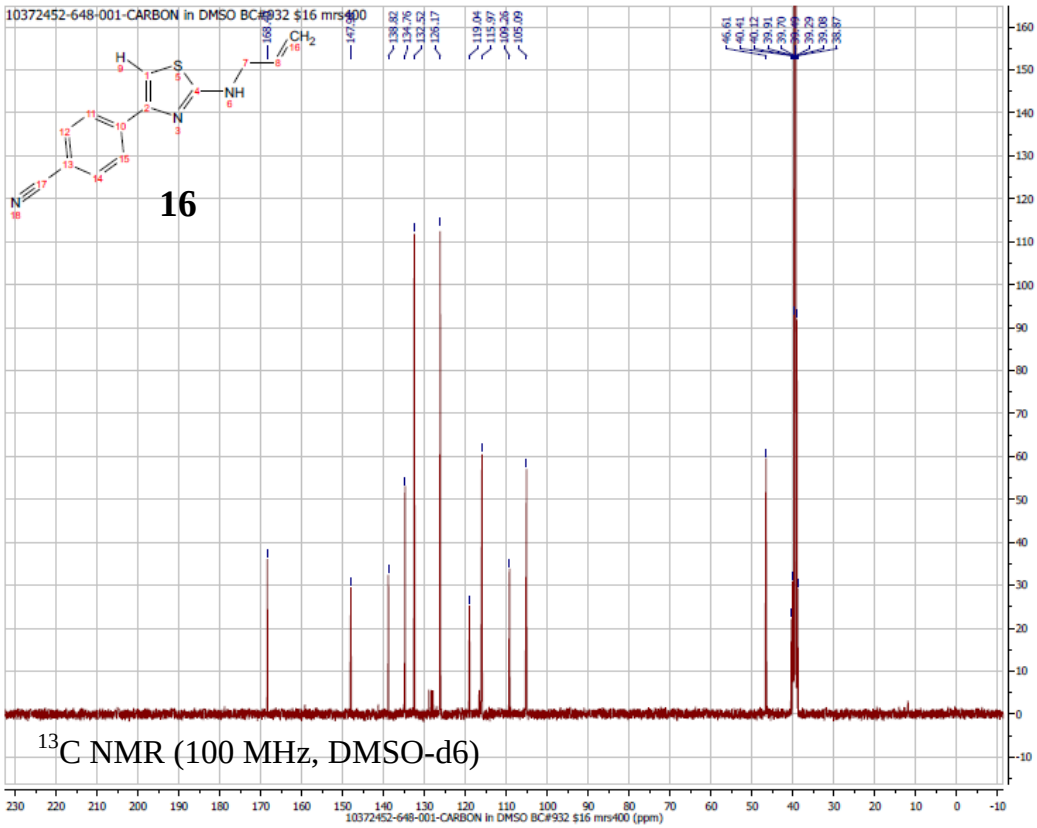


$^{13}$C NMR (100 MHz, DMSO-d6)

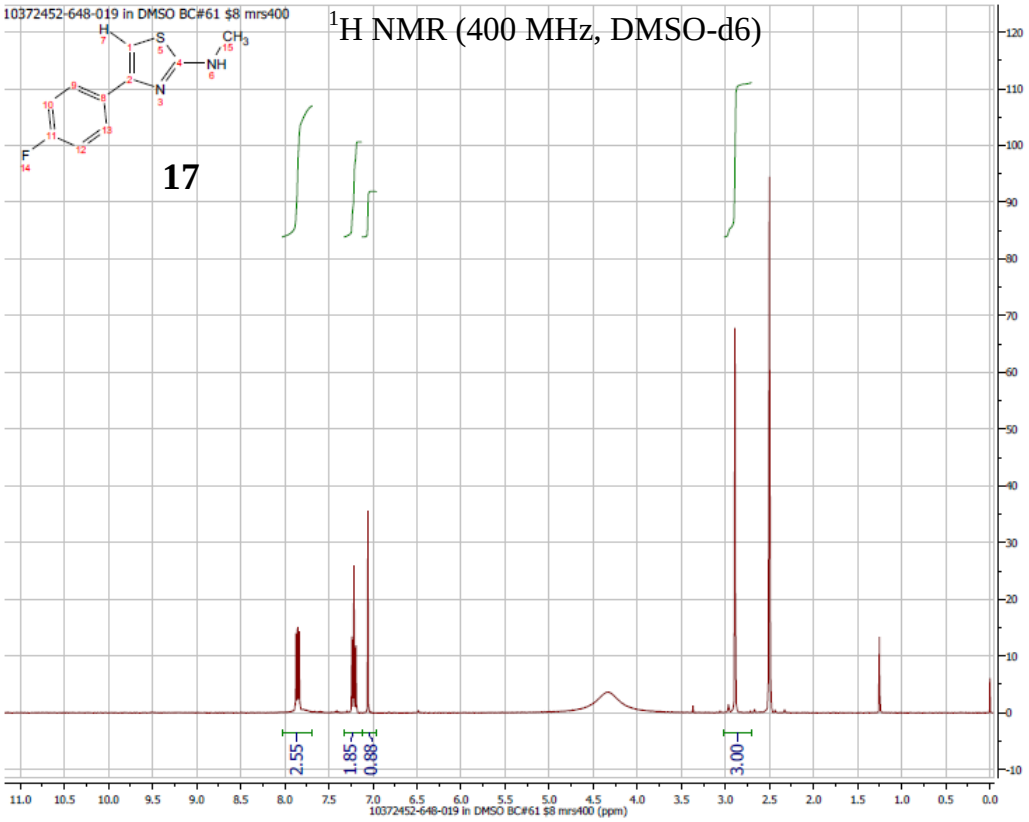


$^{1}$H NMR (400 MHz, DMSO-d6)

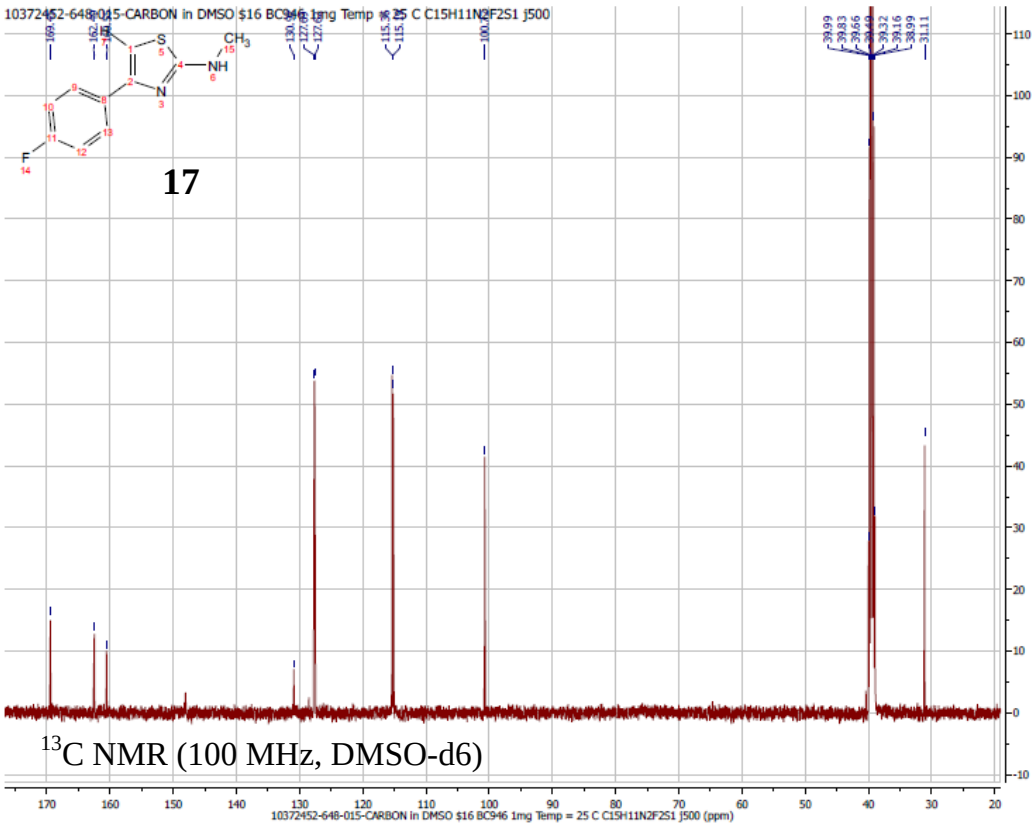


$^{13}$C NMR (100 MHz, DMSO-d6)

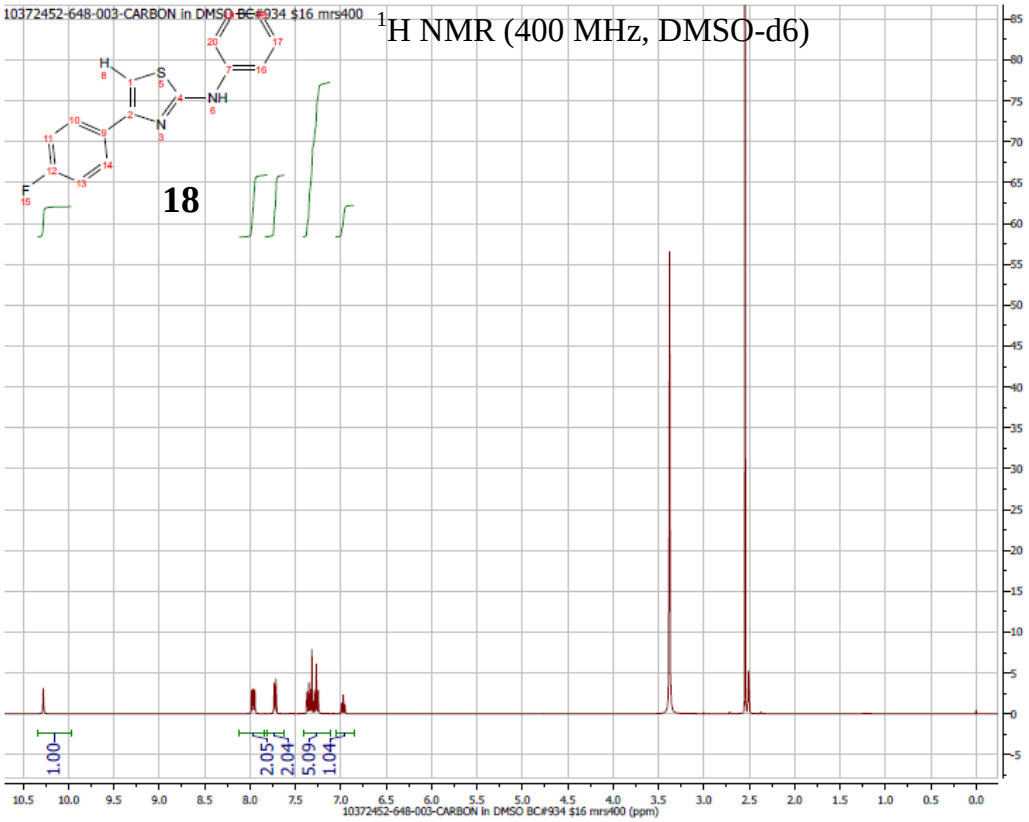


$^{1}$H NMR (400 MHz, DMSO-d6)

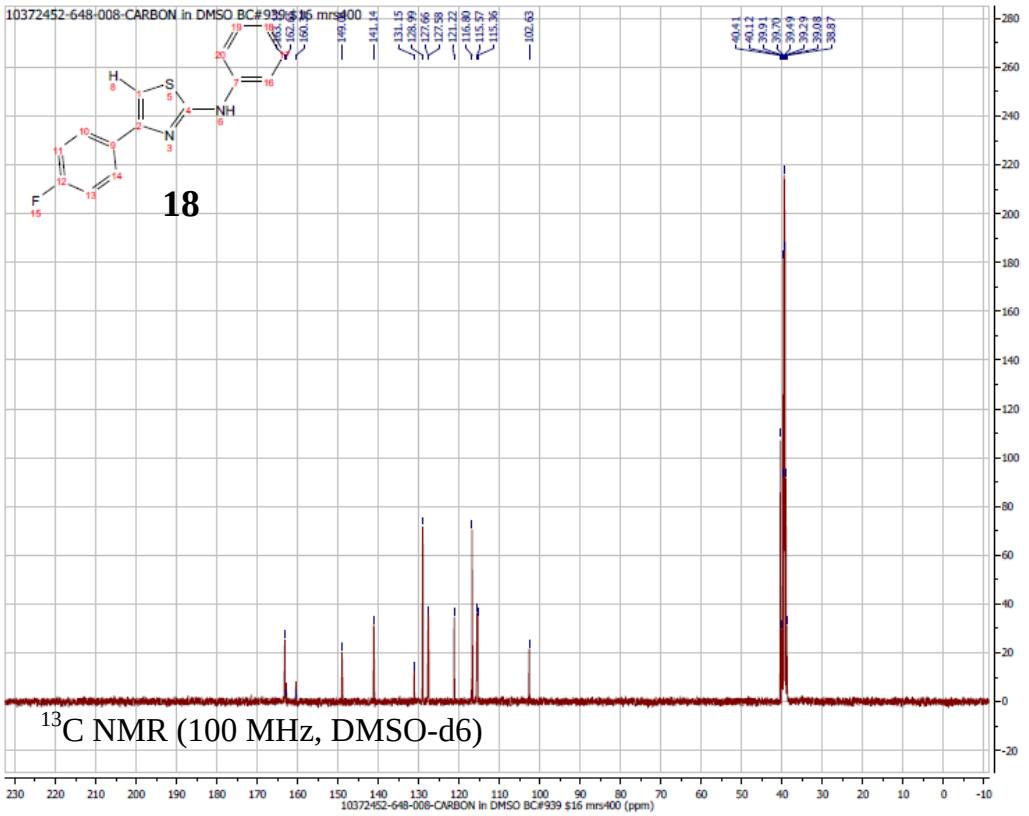


$^{13}$C NMR (100 MHz, DMSO-d6)

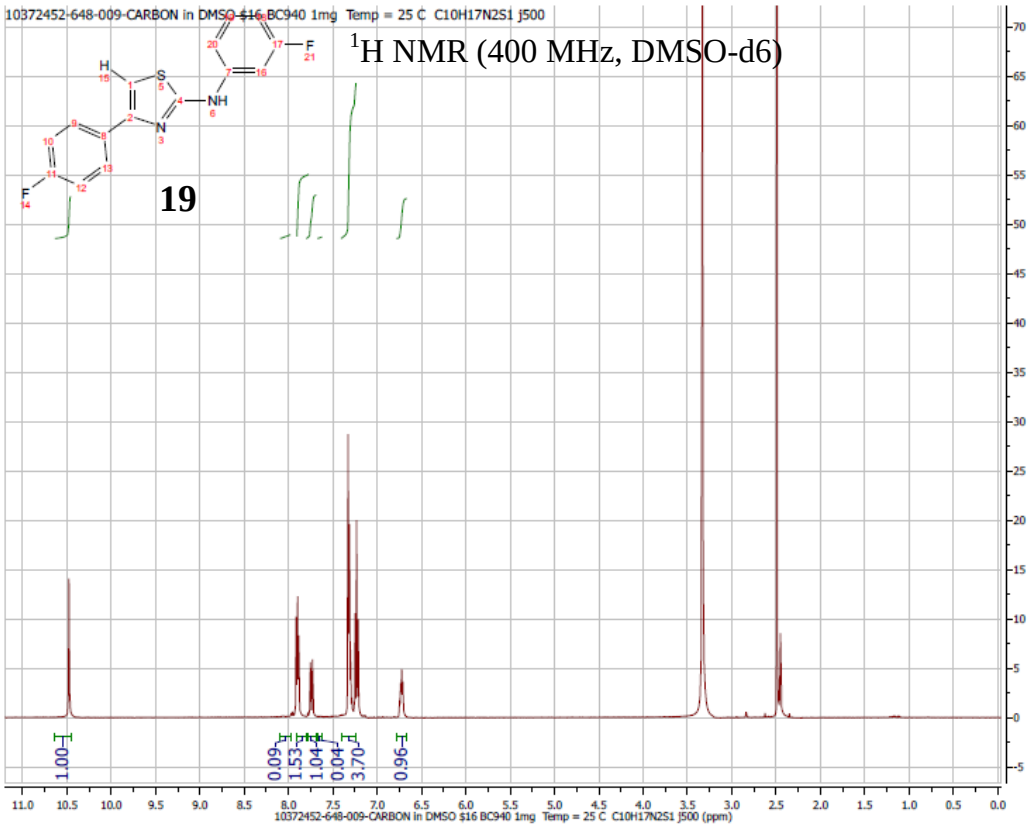


$^{1}$H NMR (400 MHz, DMSO-d6)

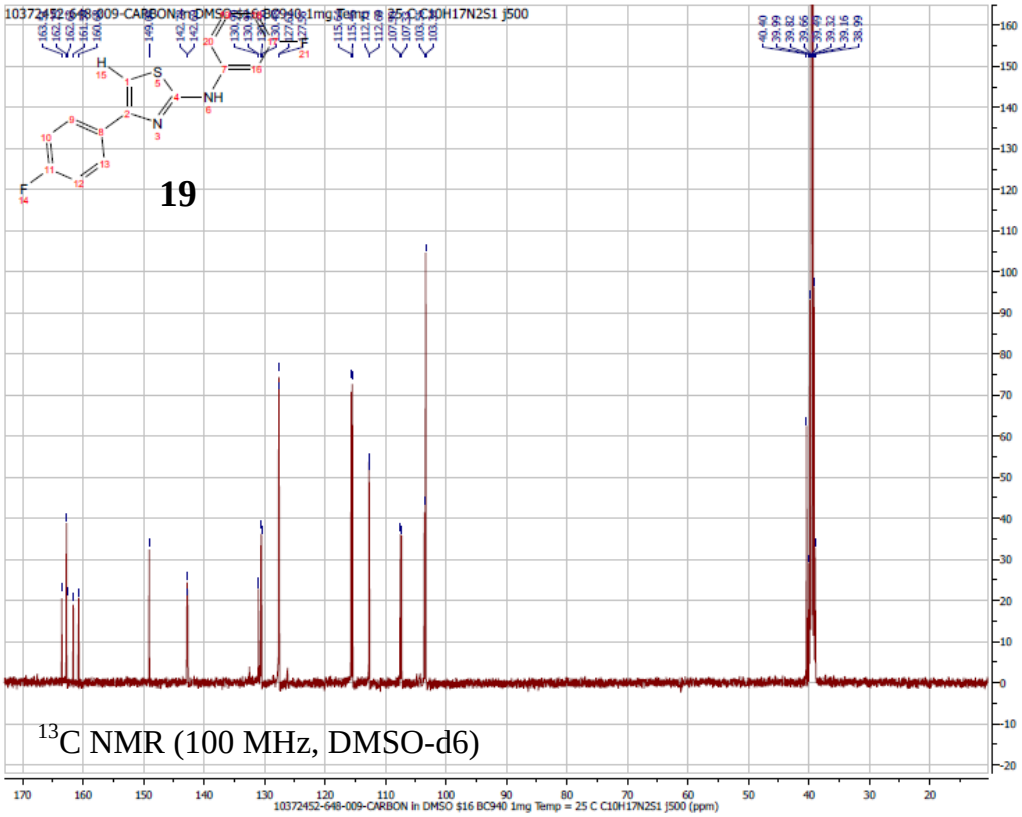


$^{13}$C NMR (100 MHz, DMSO-d6)

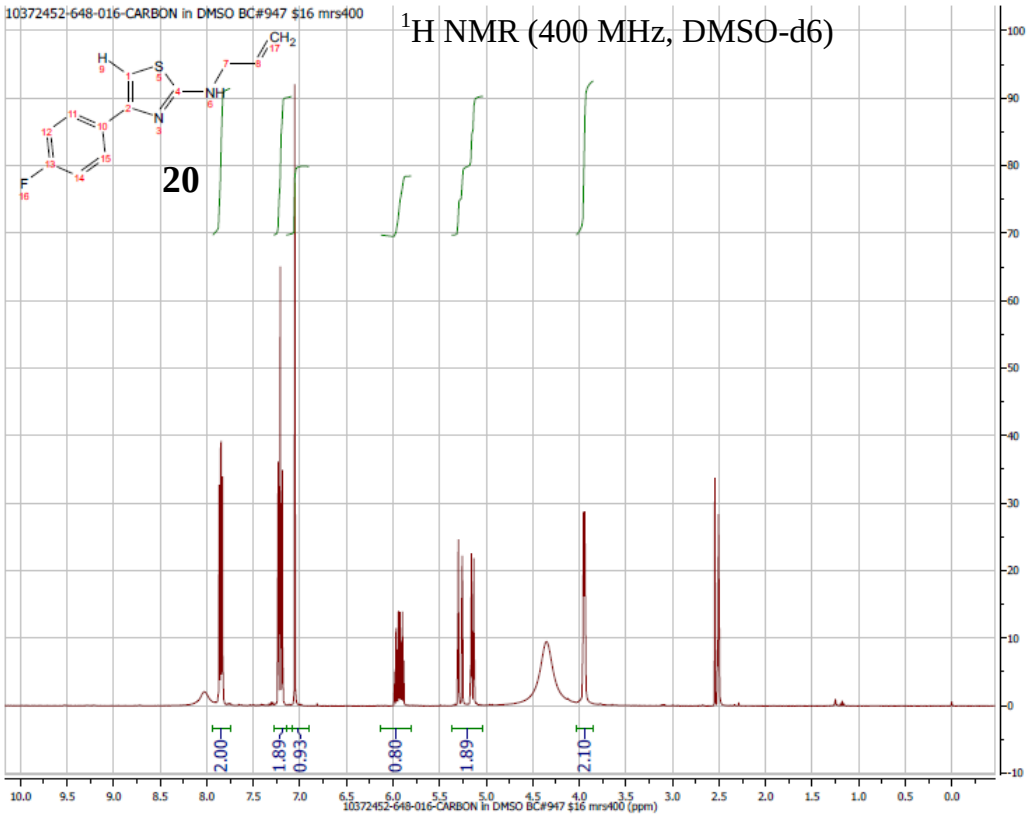


$^{1}$H NMR (400 MHz, DMSO-d6)

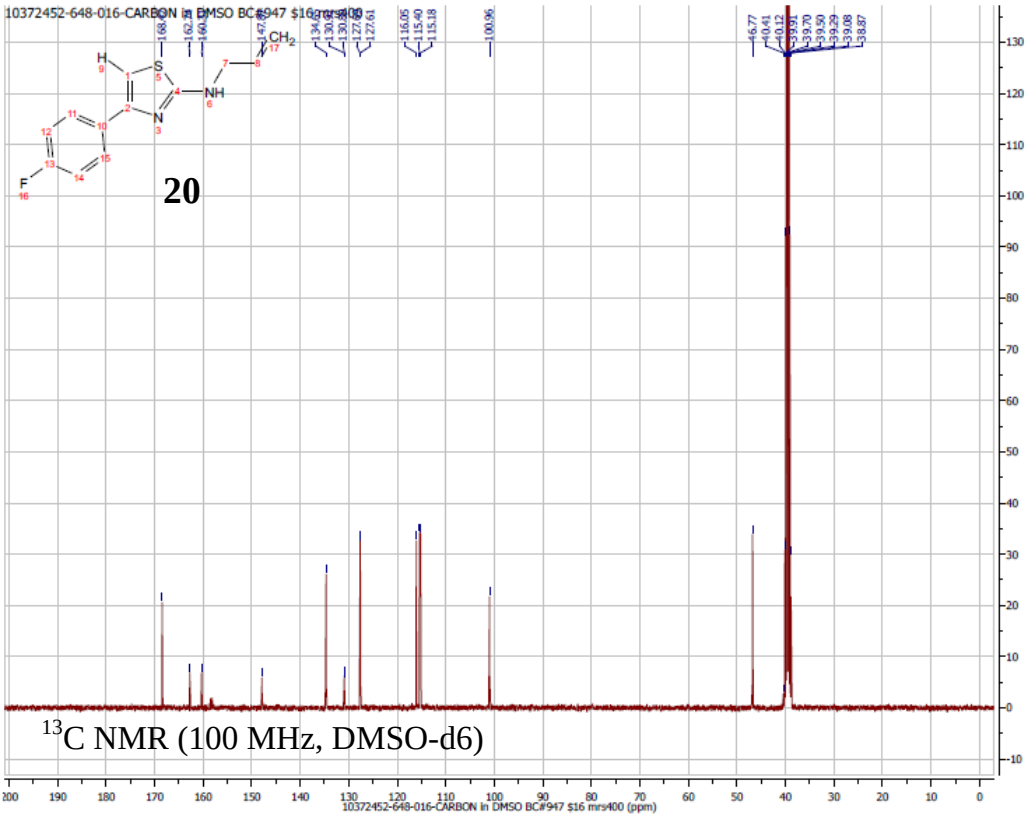


$^{13}$C NMR (100 MHz, DMSO-d6)

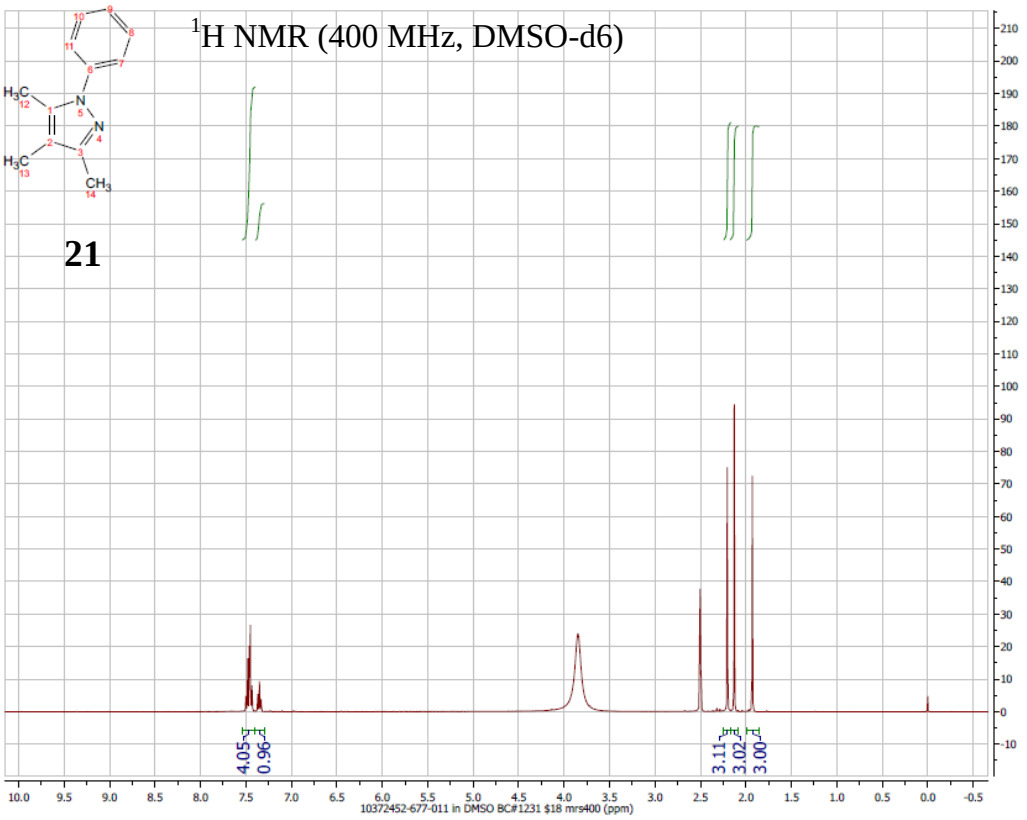
21
$^{1}$H NMR (400 MHz, DMSO-d6)
4.05
0.96
3.11
3.02
3.00
10372452-677-011 in DMSO BC#1231 $18 mrs400 (ppm)

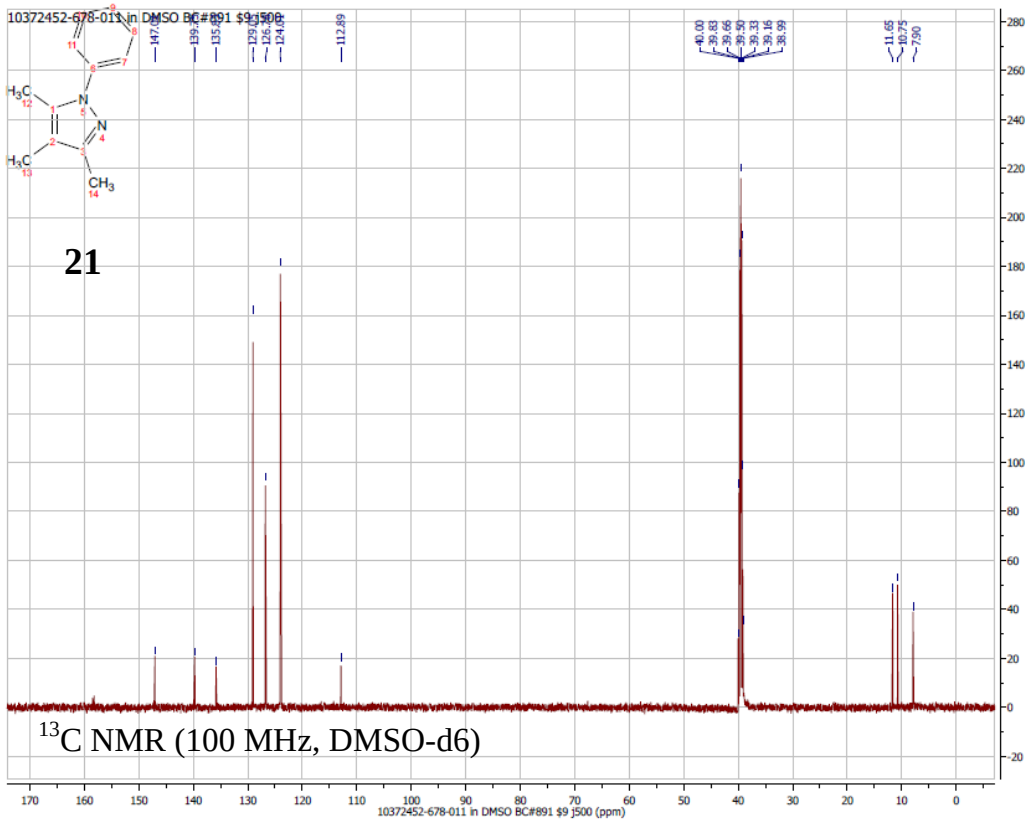
21
$^{13}$C NMR (100 MHz, DMSO-d6)
10372452-678-011 in DMSO BC#891 $9 j500 (ppm)

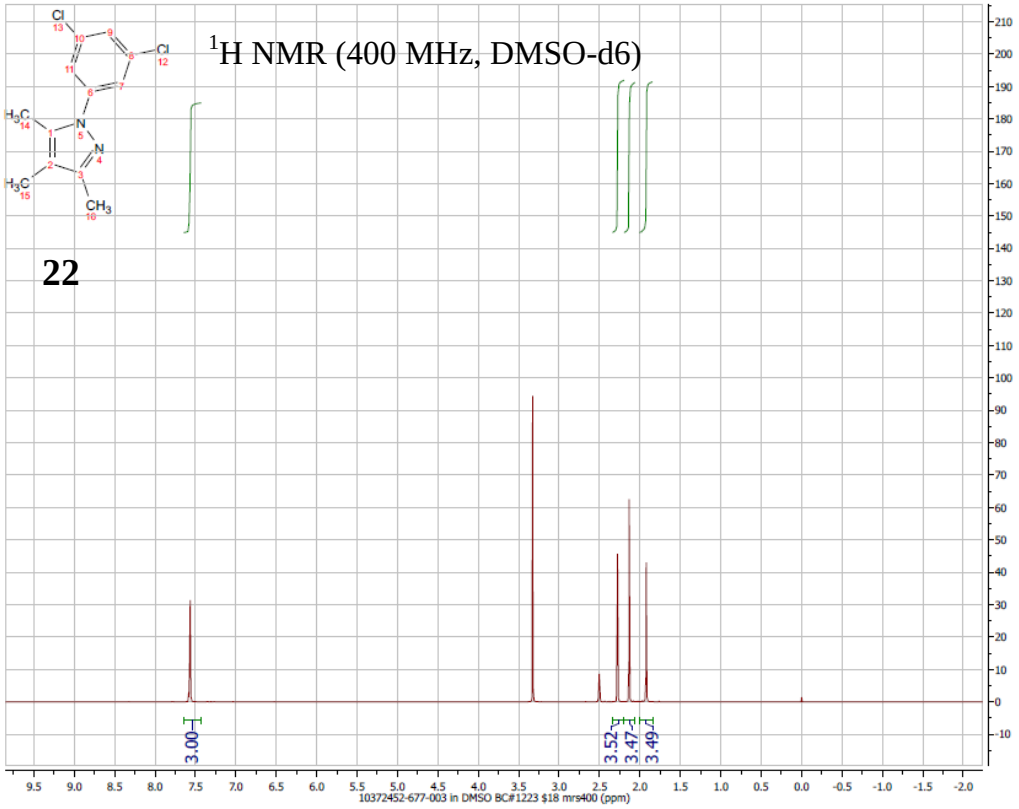
$^1$H NMR (400 MHz, DMSO-d6)
22
3.00
3.52
3.47
3.49
10372452-677-003 in DMSO BC#1223 $18 mrs400 (ppm)

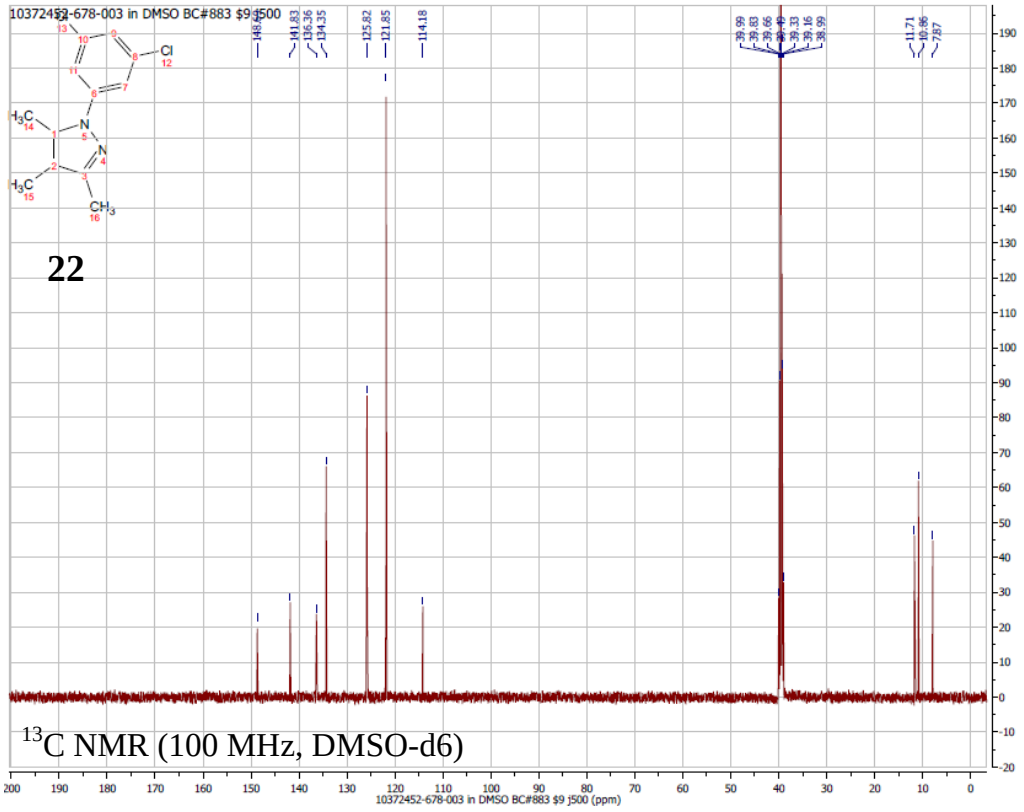
22
$^{13}$C NMR (100 MHz, DMSO-d6)
10372452-678-003 in DMSO BC#883 $9 j500 (ppm)

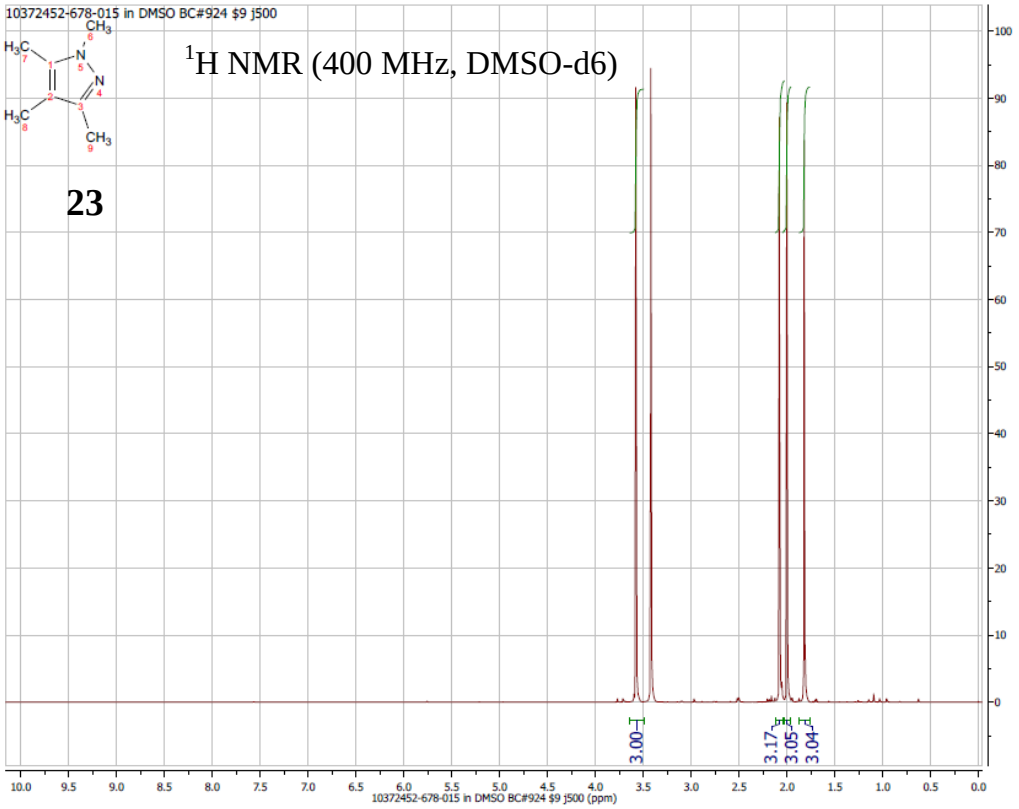
10372452-678-015 in DMSO BC#924 $9 j500
$^{1}$H NMR (400 MHz, DMSO-d6)
23
3.00
3.17
3.05
3.04
10372452-678-015 in DMSO BC#924 $9 j500 (ppm)

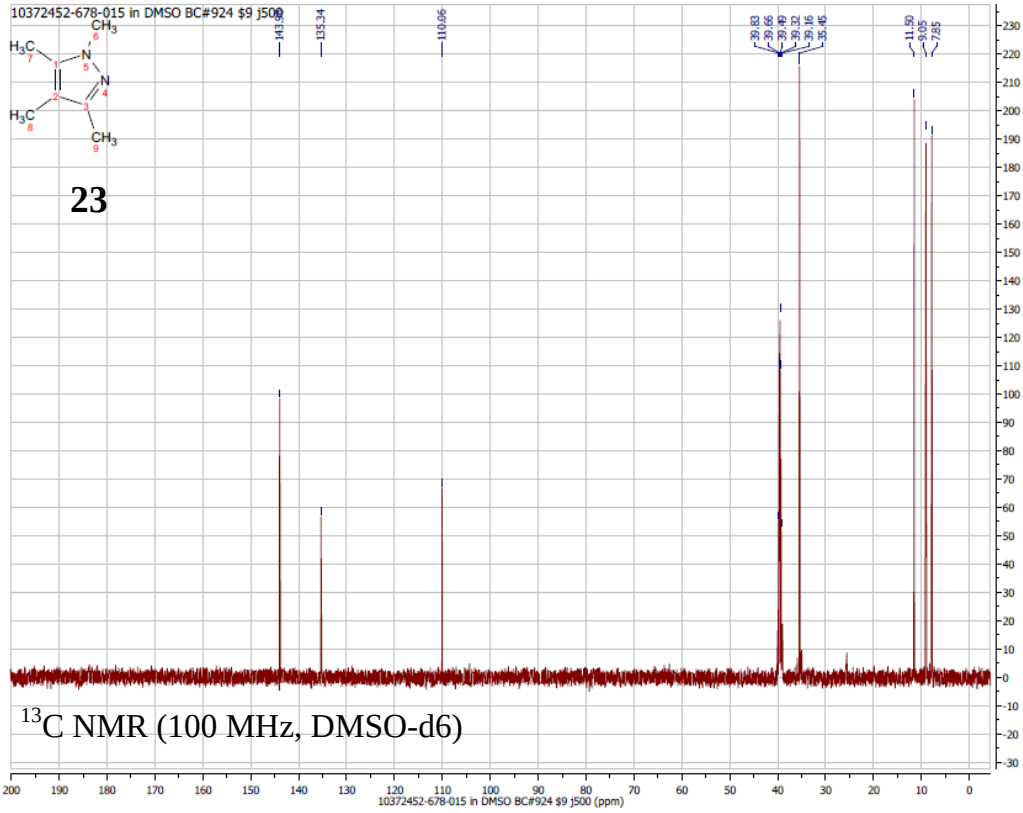
10372452-678-015 in DMSO BC#924 $9 j500
23
$^{13}$C NMR (100 MHz, DMSO-d6)
10372452-678-015 in DMSO BC#924 $9 j500 (ppm)

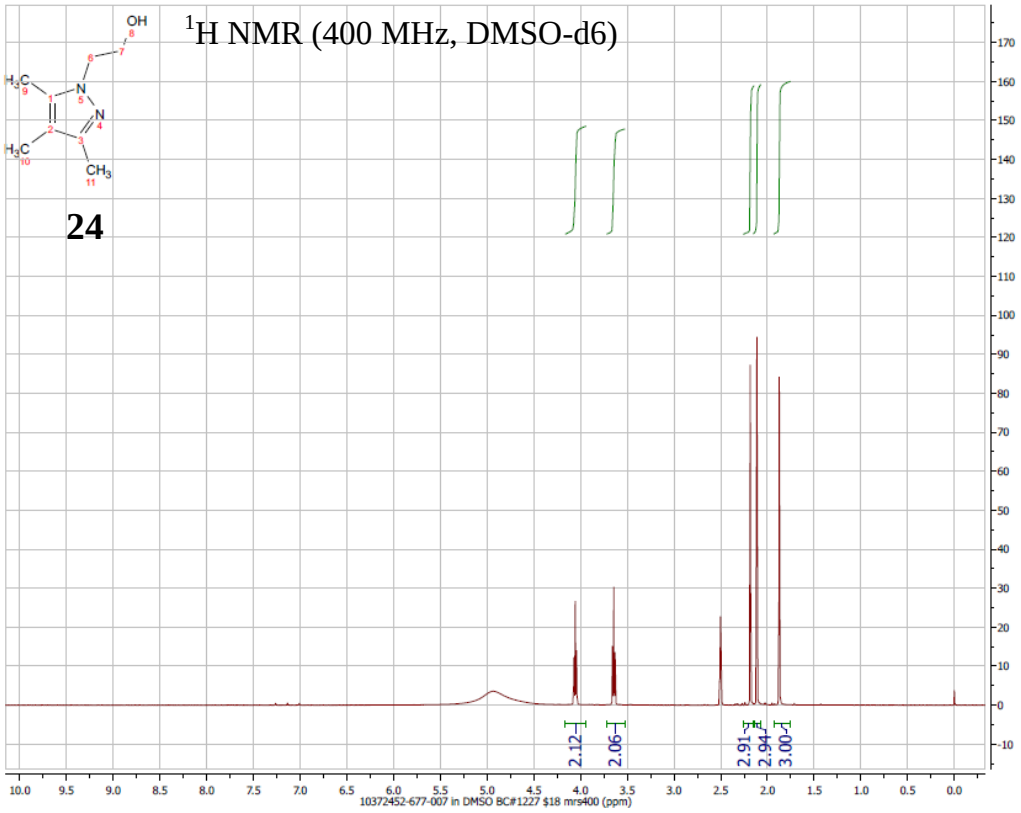
OH
H3C
N
N
H3C
CH3
24
1H NMR (400 MHz, DMSO-d6)
2.12
2.06
2.91
2.94
3.00
10372452-677-007 in DMSO BC#1227 $18 mrs400 (ppm)

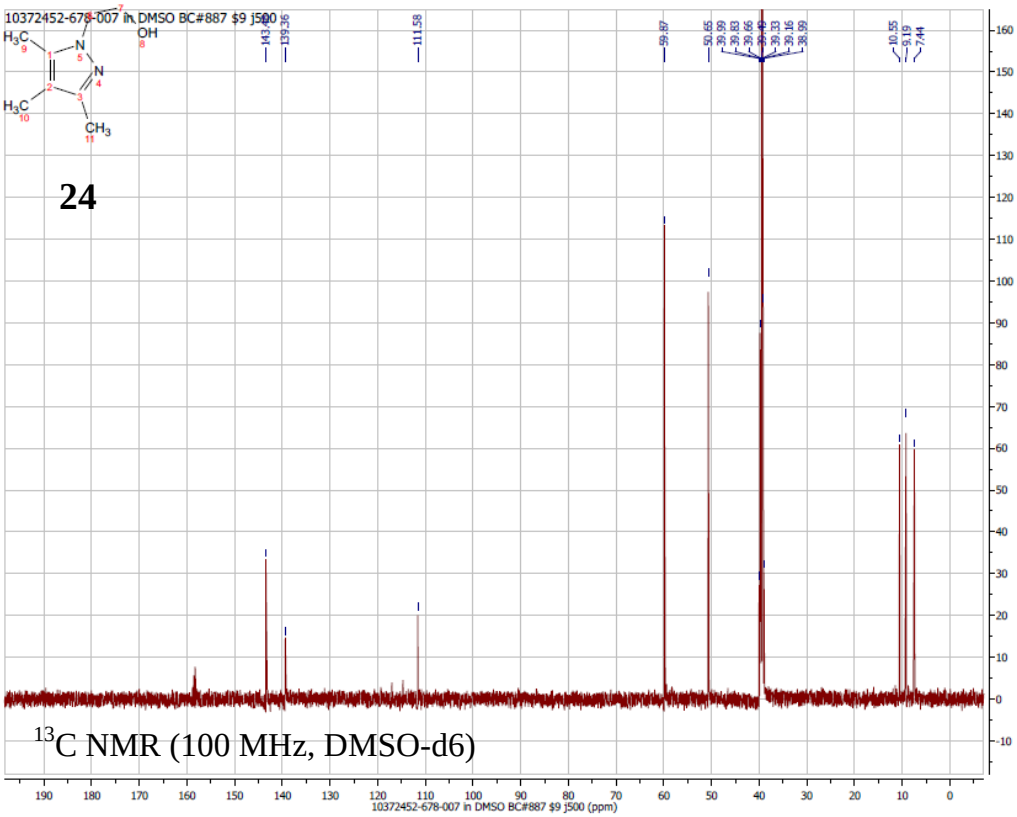
10372452-678-007 in DMSO BC#887 $9 j500
OH
H3C
N
N
H3C
CH3
24
13C NMR (100 MHz, DMSO-d6)
10372452-678-007 in DMSO BC#887 $9 j500 (ppm)

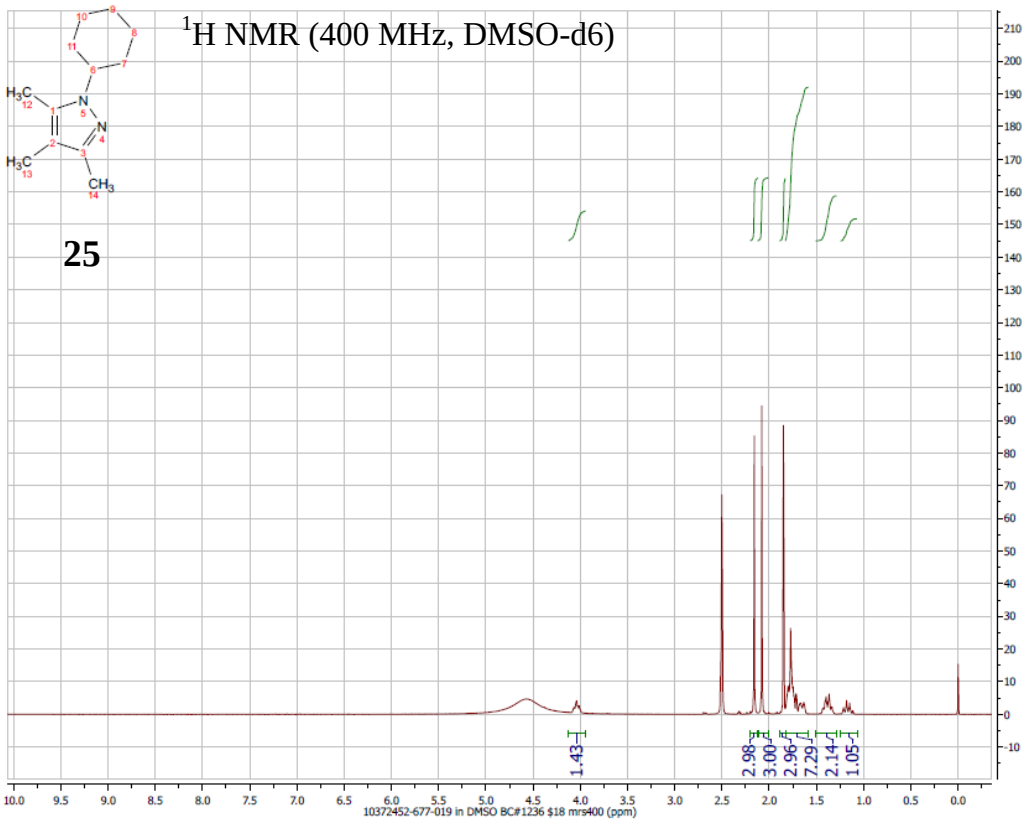
$^{1}$H NMR (400 MHz, DMSO-d6)
25
1.43
2.98
3.00
2.96
7.29
2.14
1.05
10372452-677-019 in DMSO BC#1236 $18 mrs400 (ppm)

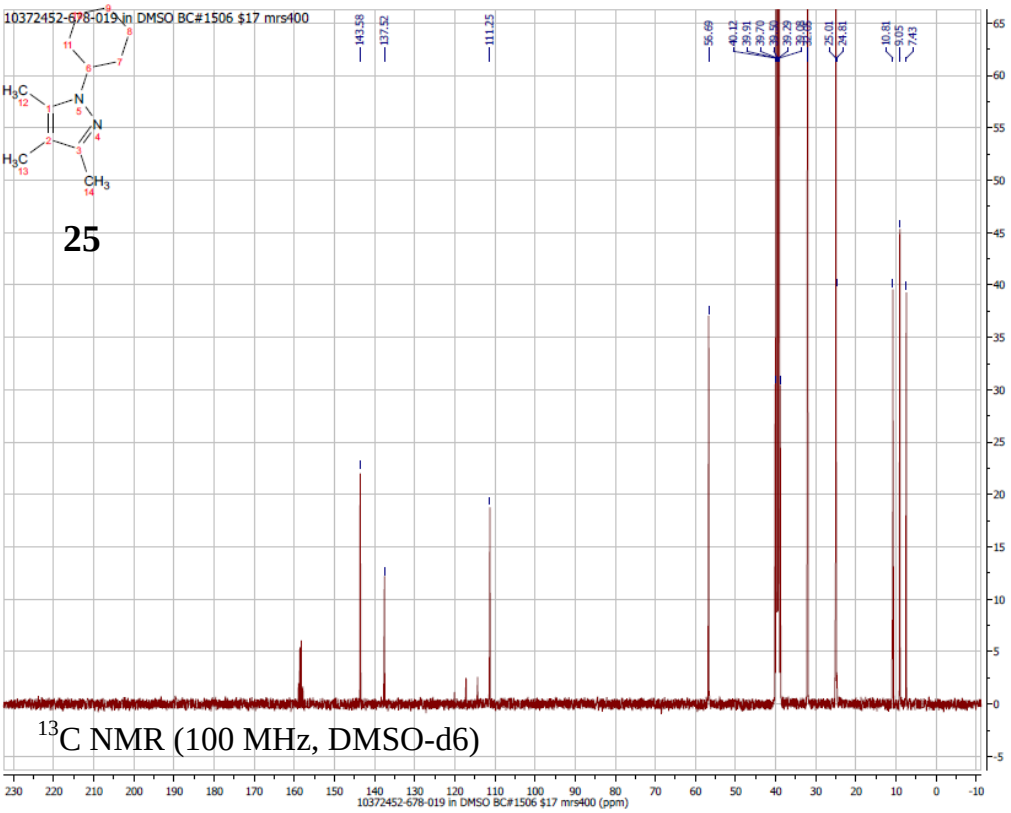
10372452-678-019 in DMSO BC#1506 $17 mrs400
25
$^{13}$C NMR (100 MHz, DMSO-d6)
10372452-678-019 in DMSO BC#1506 $17 mrs400 (ppm)

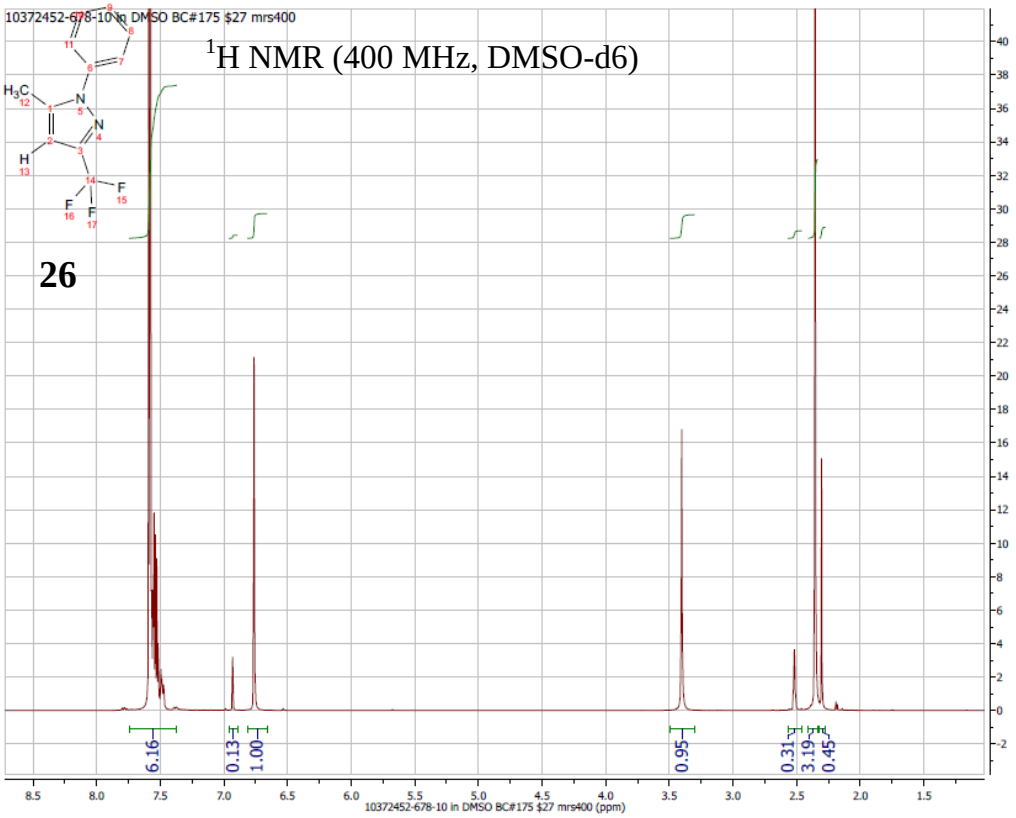
10372452-678-10 in DMSO BC#175 $27 mrs400
$^{1}$H NMR (400 MHz, DMSO-d6)
26
6.16
0.13
1.00
0.95
0.31
3.19
0.45
10372452-678-10 in DMSO BC#175 $27 mrs400 (ppm)

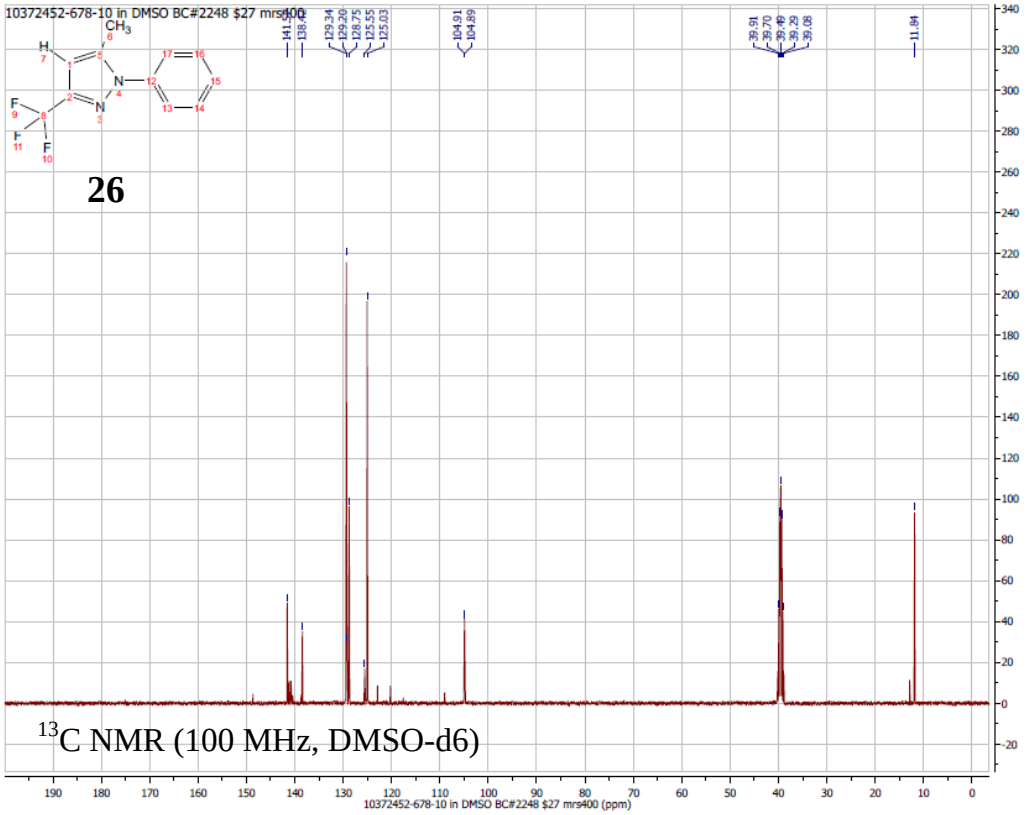
10372452-678-10 in DMSO BC#2248 $27 mrs400
26
$^{13}$C NMR (100 MHz, DMSO-d6)
10372452-678-10 in DMSO BC#2248 $27 mrs400 (ppm)

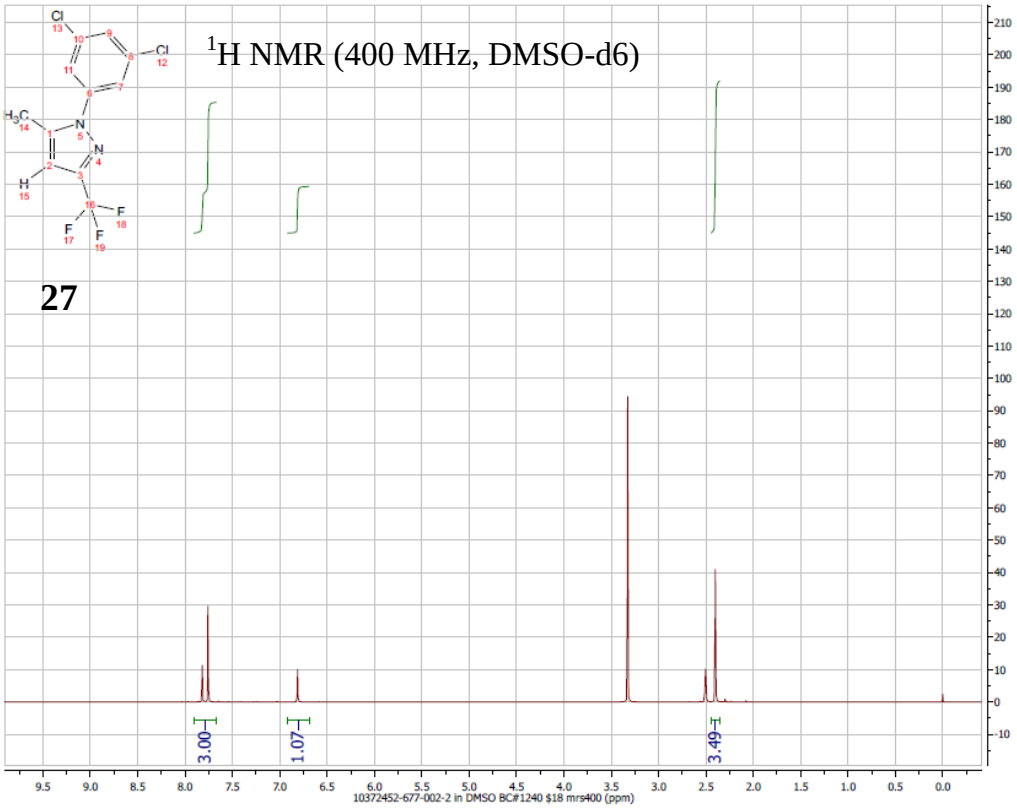
$^1$H NMR (400 MHz, DMSO-d6)
27
3.00
1.07
3.49
10372452-677-002-2 in DMSO BC#1240 $18 mrs400 (ppm)

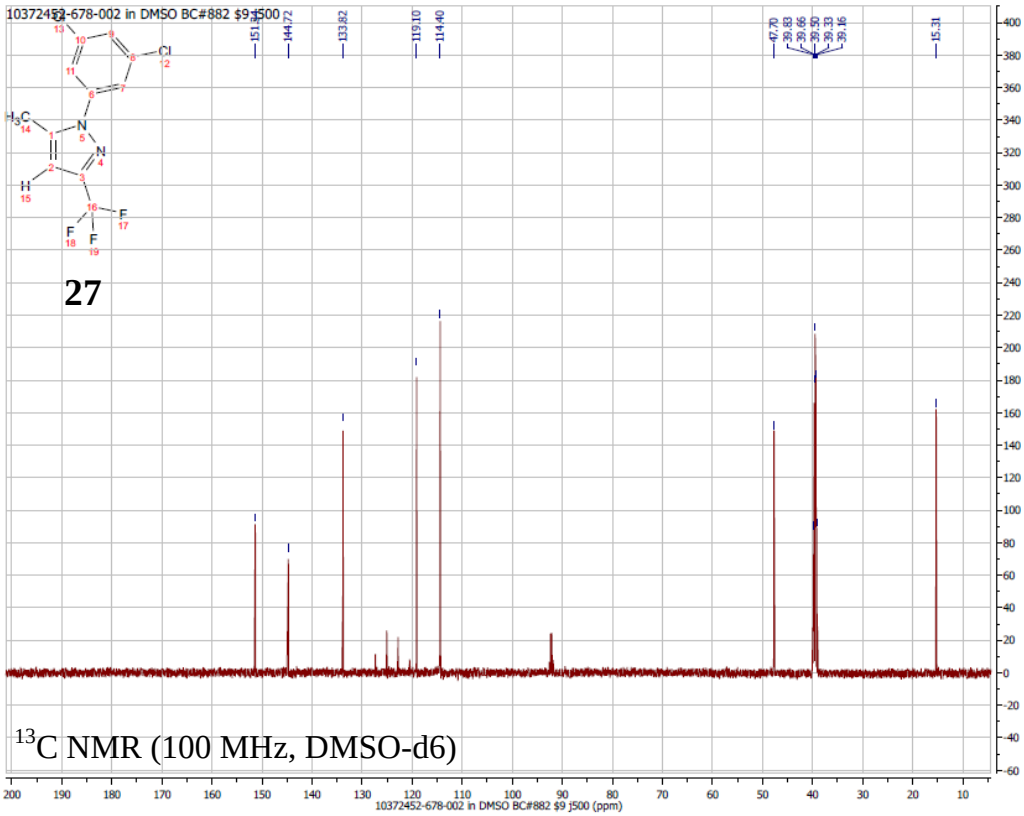
10372452-678-002 in DMSO BC#882 $9 j500
151.84
144.72
133.82
119.10
114.40
47.70
39.83
39.66
39.50
39.33
39.16
15.31
27
$^{13}$C NMR (100 MHz, DMSO-d6)
10372452-678-002 in DMSO BC#882 $9 j500 (ppm)

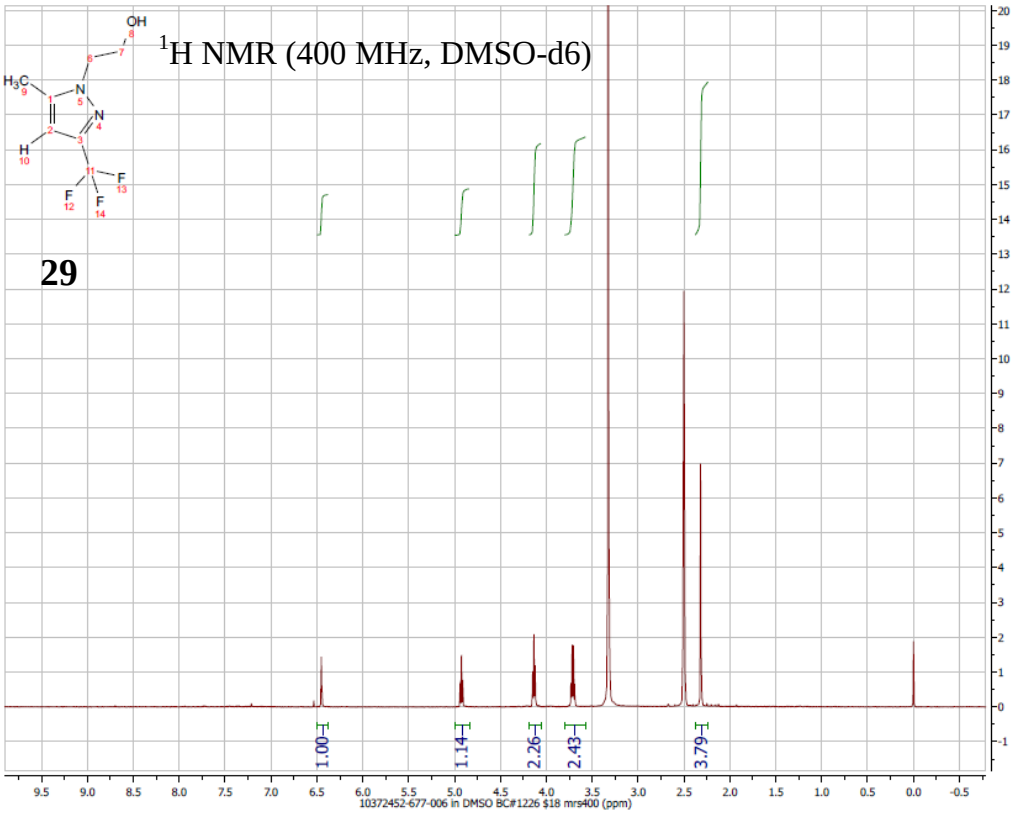
$^1$H NMR (400 MHz, DMSO-d6)
29
1.00
1.14
2.26
2.43
3.79
10372452-677-006 in DMSO BC#1226 $18 mrs400 (ppm)

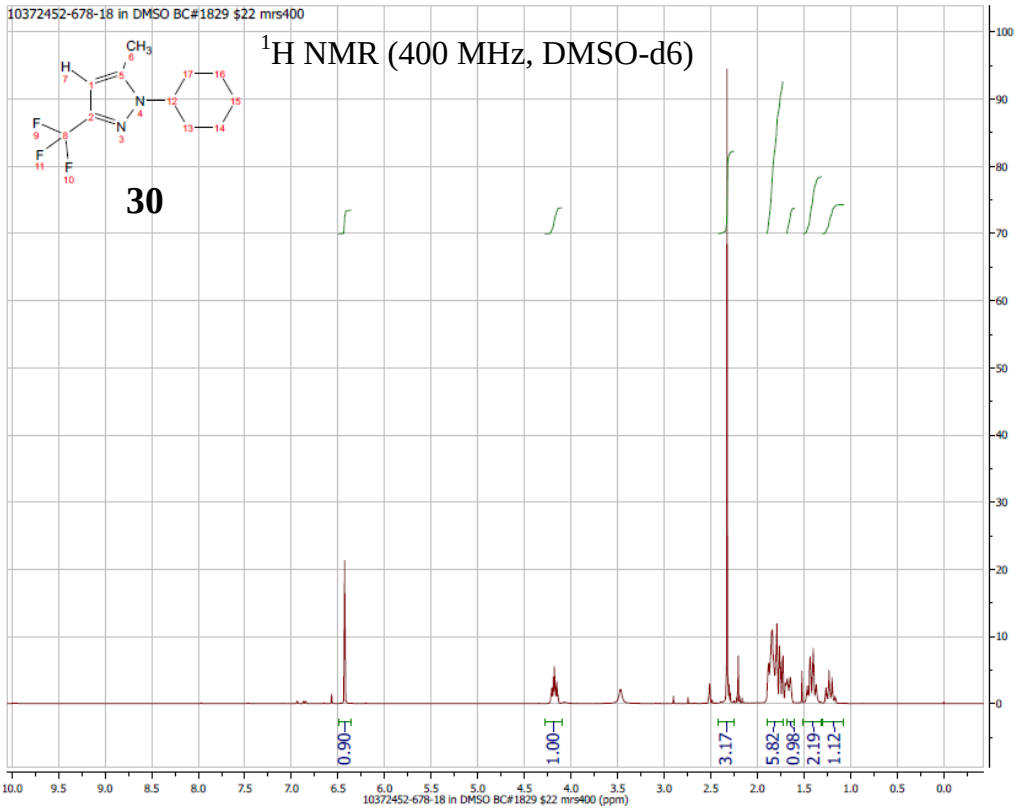
10372452-678-18 in DMSO BC#1829 $22 mrs400
$^{1}$H NMR (400 MHz, DMSO-d6)
30
0.90
1.00
3.17
5.82
0.98
2.19
1.12
10372452-678-18 in DMSO BC#1829 $22 mrs400 (ppm)

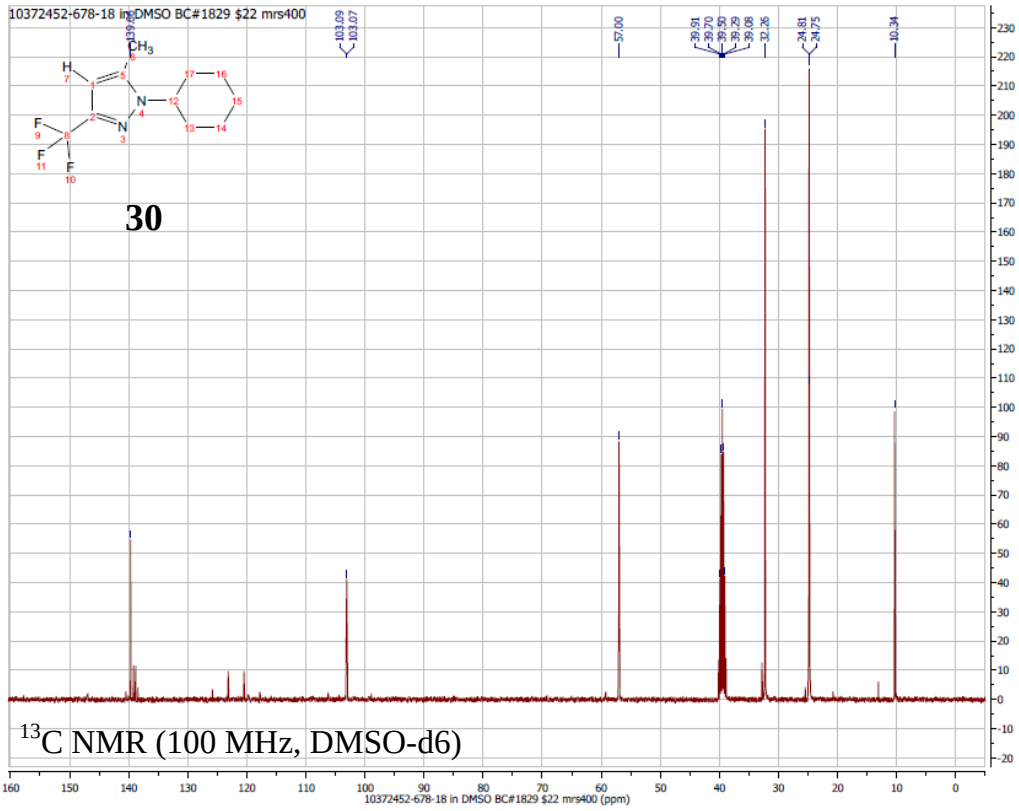
10372452-678-18 in DMSO BC#1829 $22 mrs400
103.09
103.07
57.00
39.91
39.70
39.50
39.29
39.08
32.26
24.81
24.75
10.34
30
$^{13}$C NMR (100 MHz, DMSO-d6)
10372452-678-18 in DMSO BC#1829 $22 mrs400 (ppm)

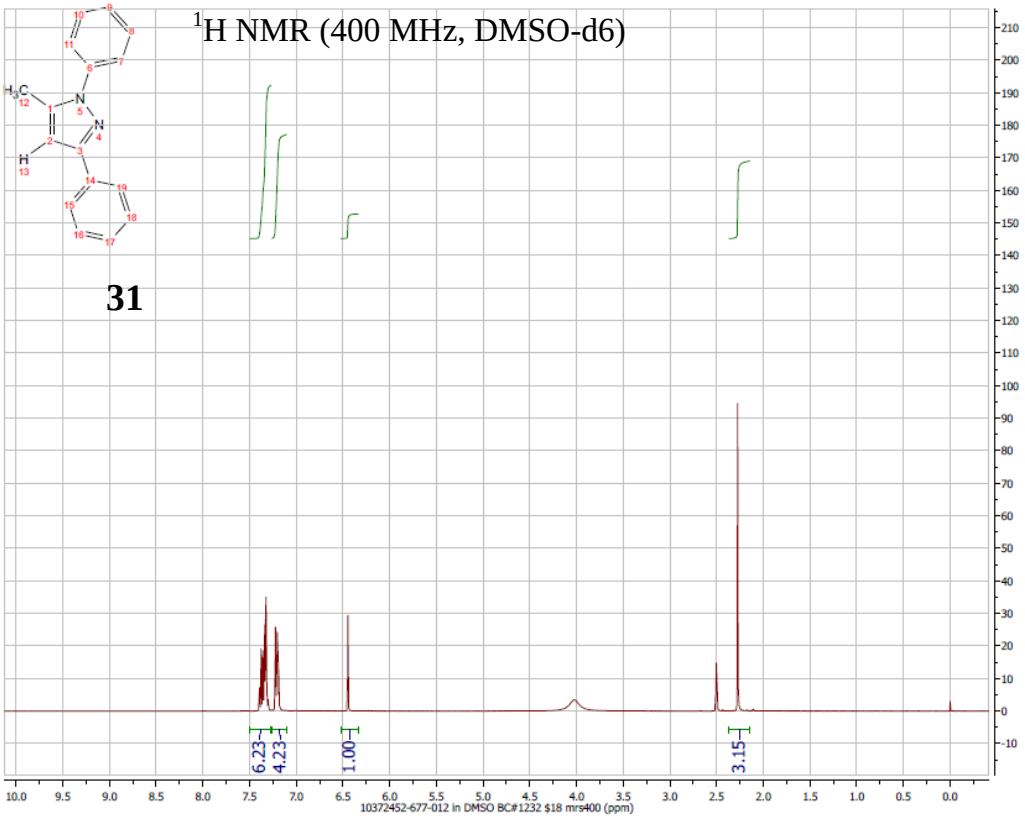
$^1$H NMR (400 MHz, DMSO-d6)
31
6.23
4.23
1.00
3.15
10372452-677-012 in DMSO BC#1232 $18 mrs400 (ppm)

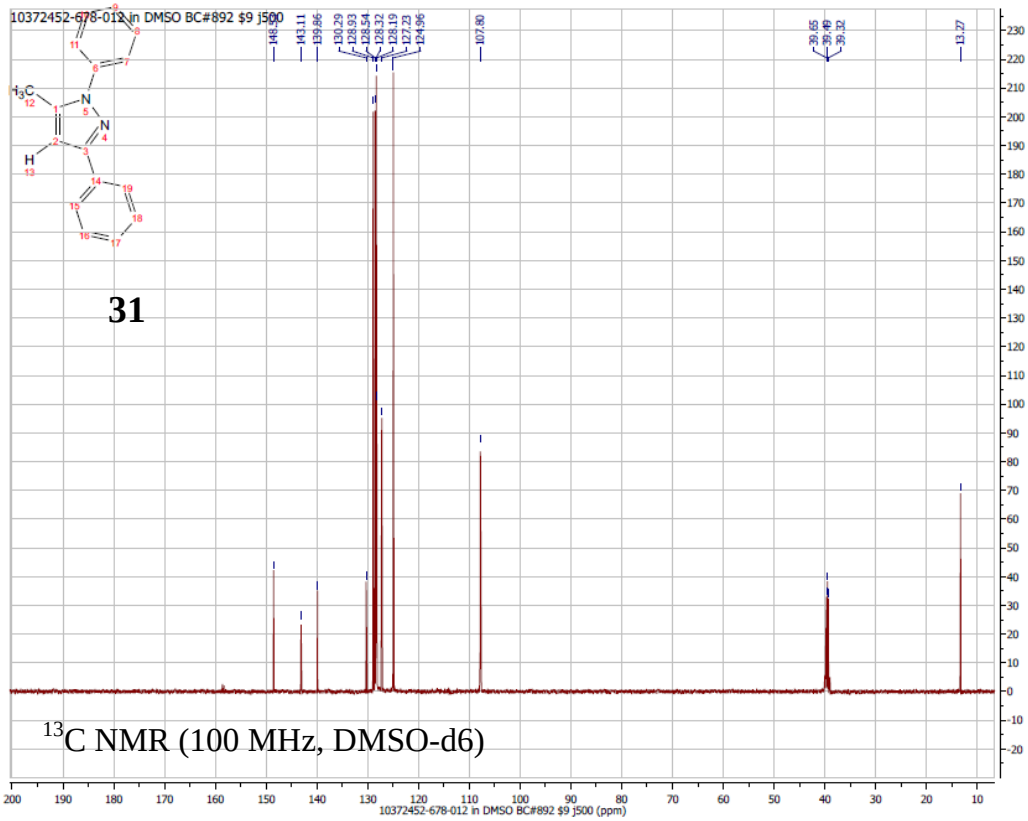
10372452-678-012 in DMSO BC#892 $9 j500
31
$^{13}$C NMR (100 MHz, DMSO-d6)
10372452-678-012 in DMSO BC#892 $9 j500 (ppm)

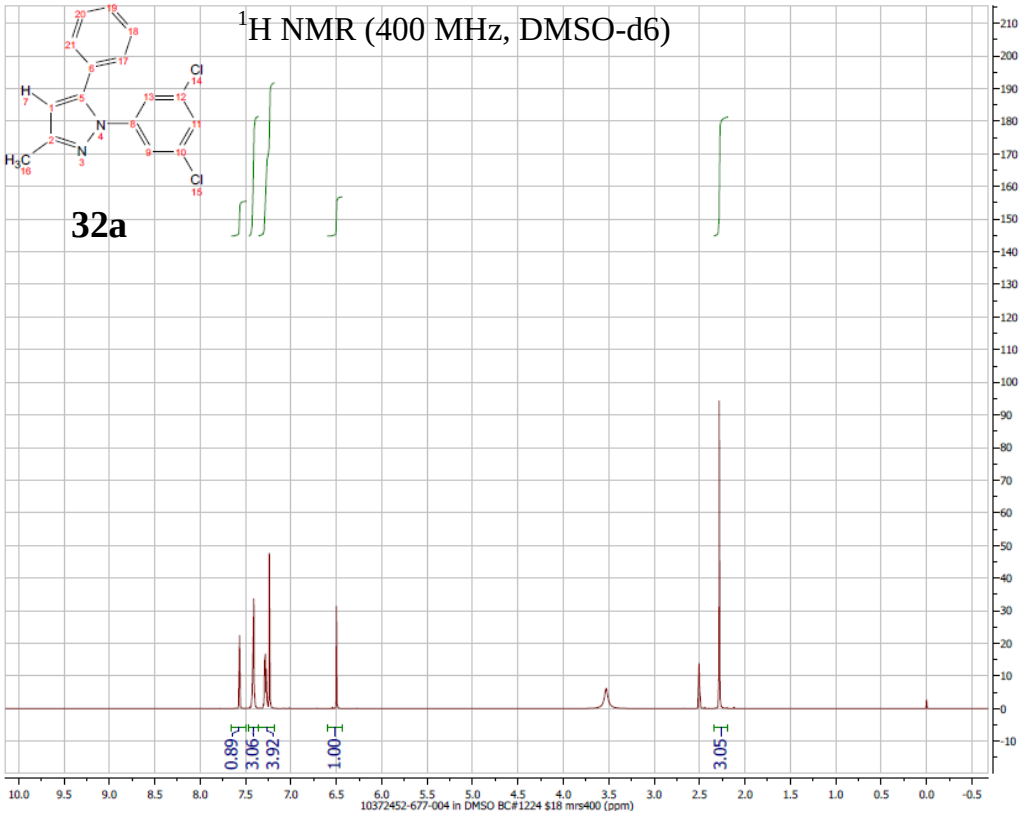
1H NMR (400 MHz, DMSO-d6)
32a
0.89
3.06
3.92
1.00
3.05
10372452-677-004 in DMSO BC#1224 $18 mrs400 (ppm)

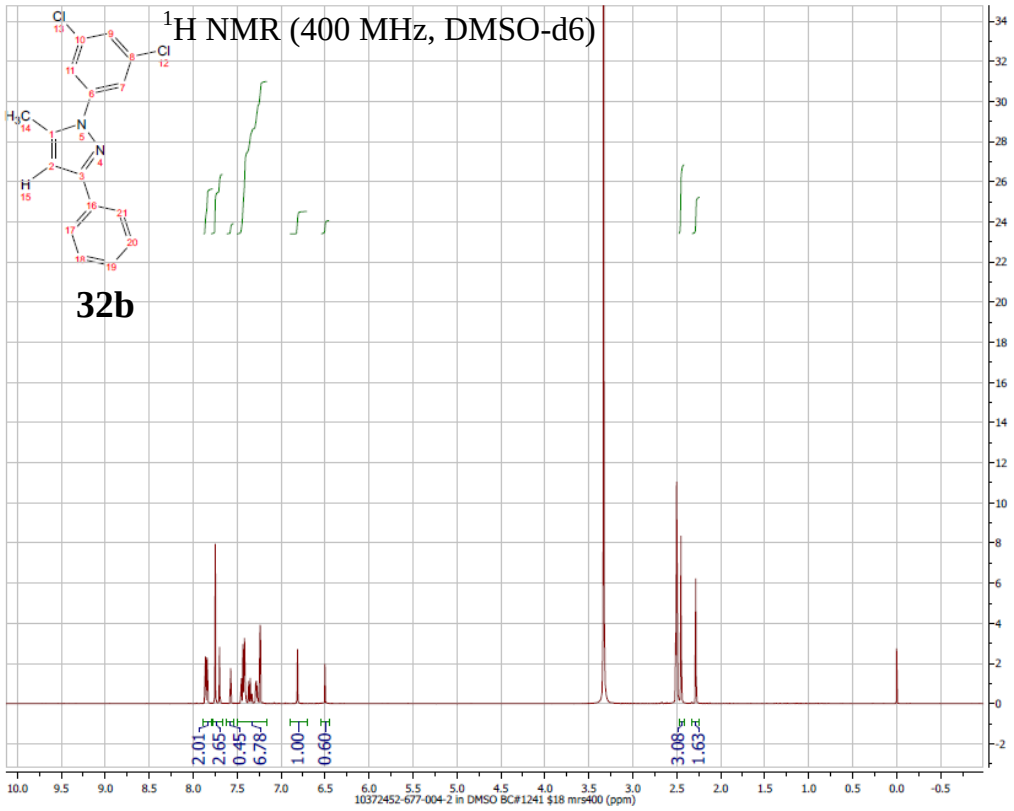
$^1$H NMR (400 MHz, DMSO-d6)
32b
2.01
2.65
0.45
6.78
1.00
0.60
3.08
1.63
10372452-677-004-2 in DMSO BC#1241 $18 mrs400 (ppm)

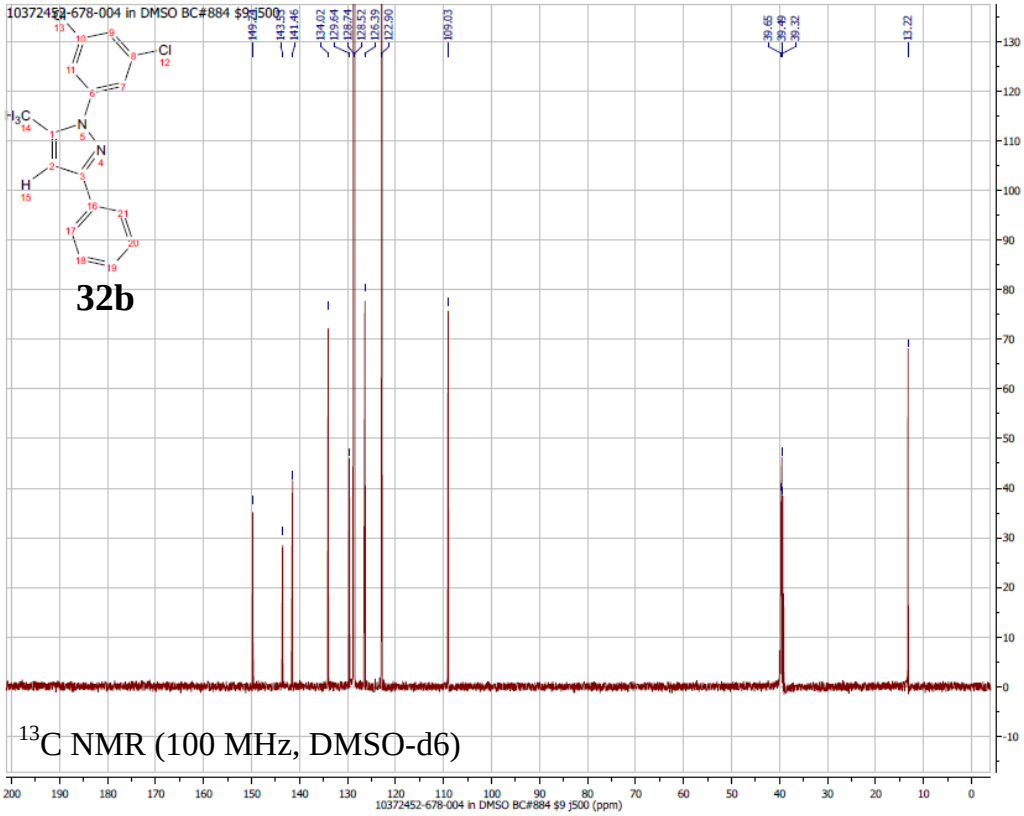
32b
$^{13}$C NMR (100 MHz, DMSO-d6)
10372452-678-004 in DMSO BC#884 $9 j500 (ppm)

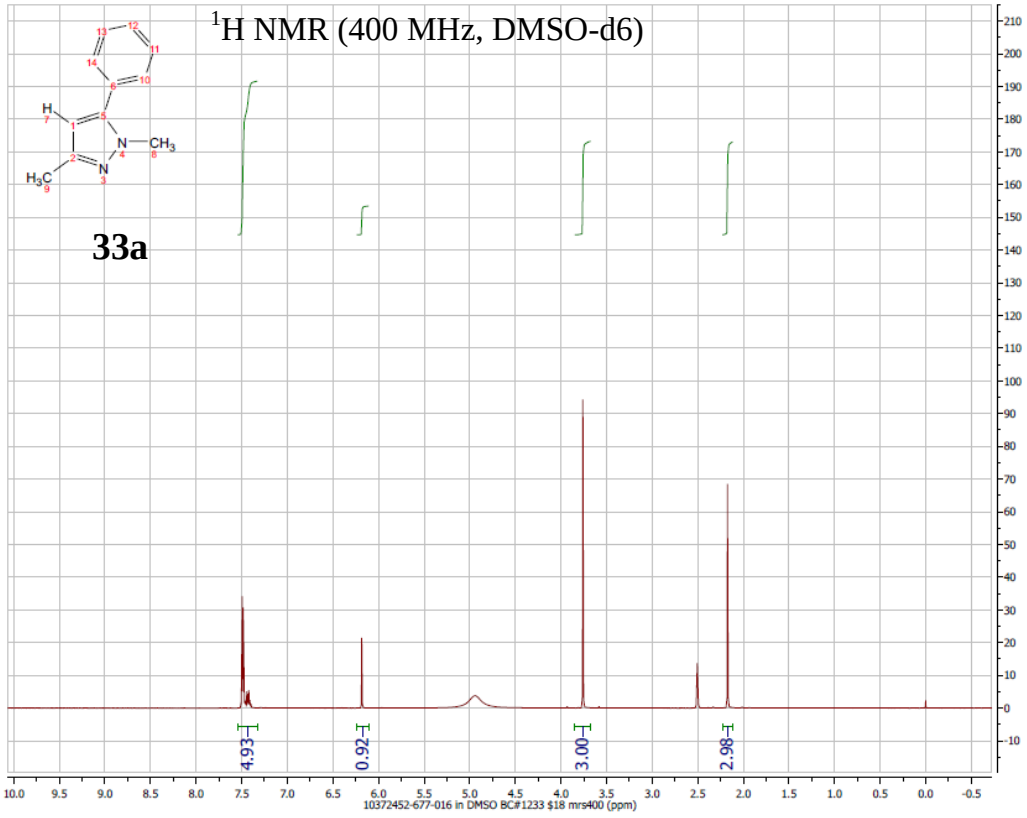
$^1$H NMR (400 MHz, DMSO-d6)
33a
4.93
0.92
3.00
2.98
10372452-677-016 in DMSO BC#1233 $18 mrs400 (ppm)

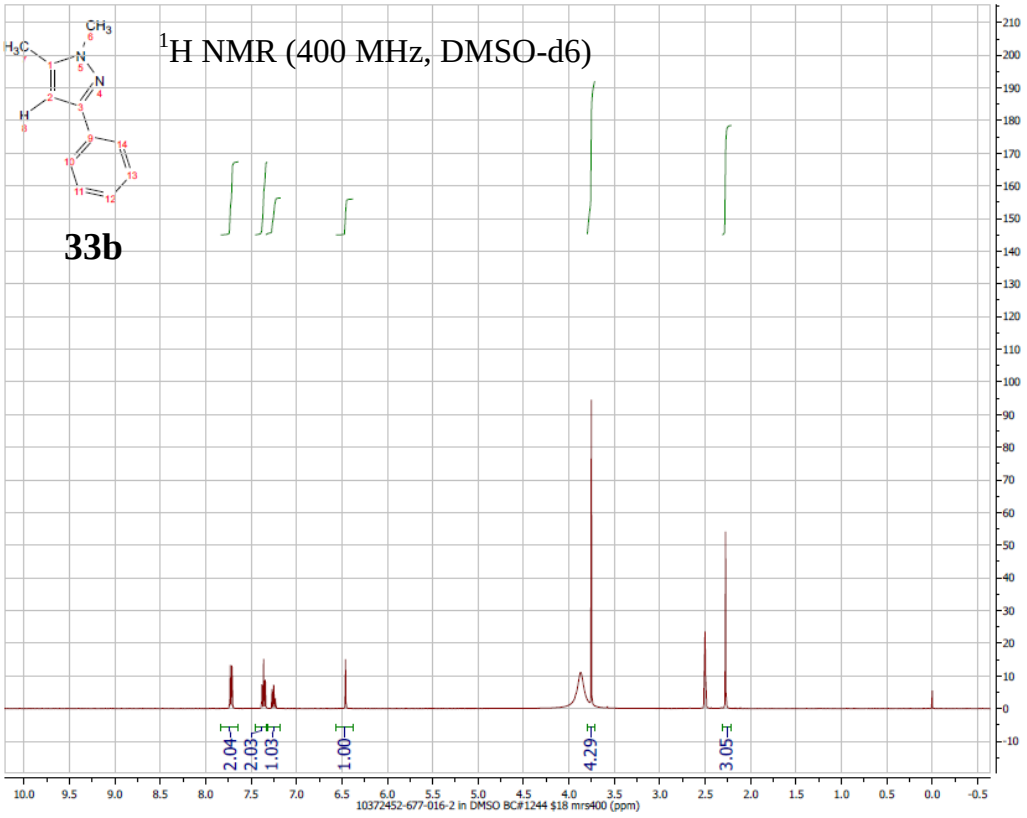
$^1$H NMR (400 MHz, DMSO-d6)
33b
2.04
2.03
1.03
1.00
4.29
3.05
10372452-677-016-2 in DMSO BC#1244 $18 mrs400 (ppm)

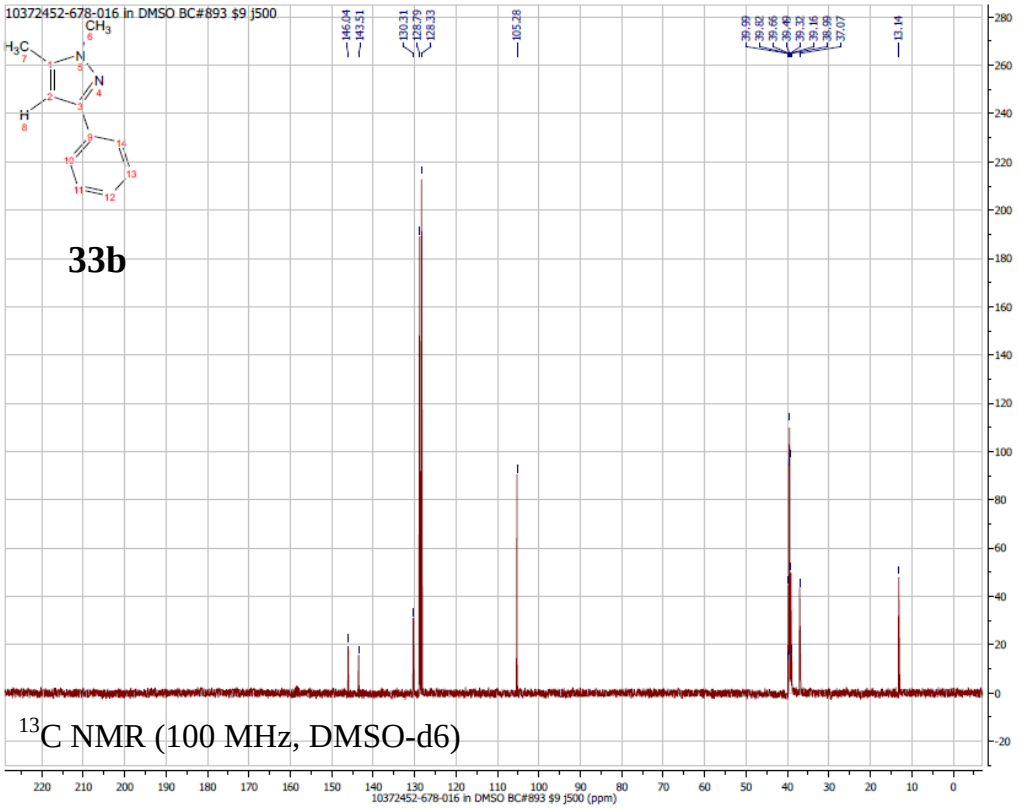
10372452-678-016 in DMSO BC#893 $9 j500
33b
$^{13}$C NMR (100 MHz, DMSO-d6)
10372452-678-016 in DMSO BC#893 $9 j500 (ppm)

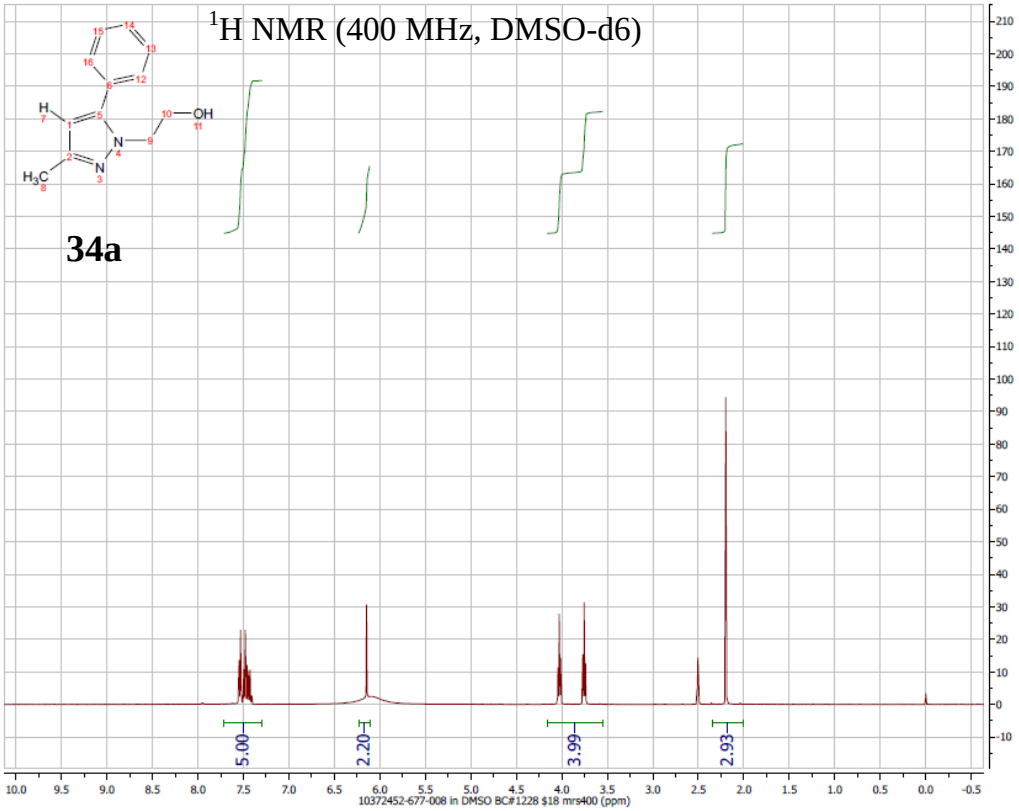
1H NMR (400 MHz, DMSO-d6)
34a
5.00
2.20
3.99
2.93
10372452-677-008 in DMSO BC#1228 $18 mrs400 (ppm)

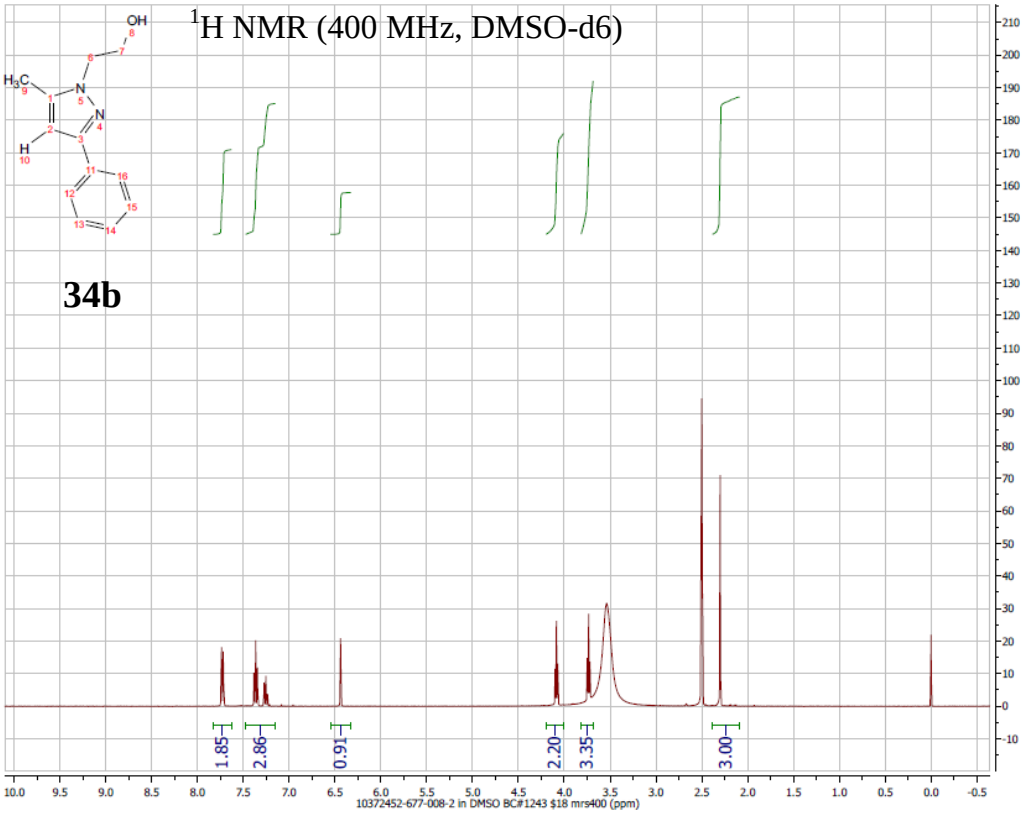


$^{1}$H NMR (400 MHz, DMSO-d6)

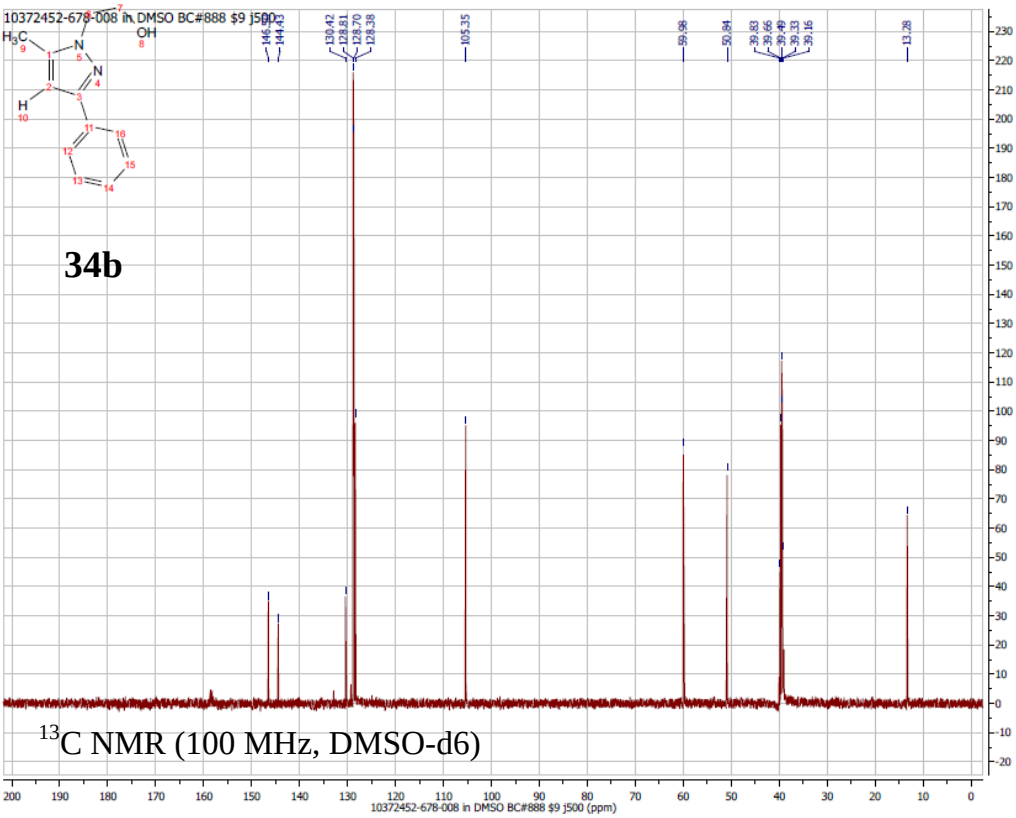


$^{13}$C NMR (100 MHz, DMSO-d6)

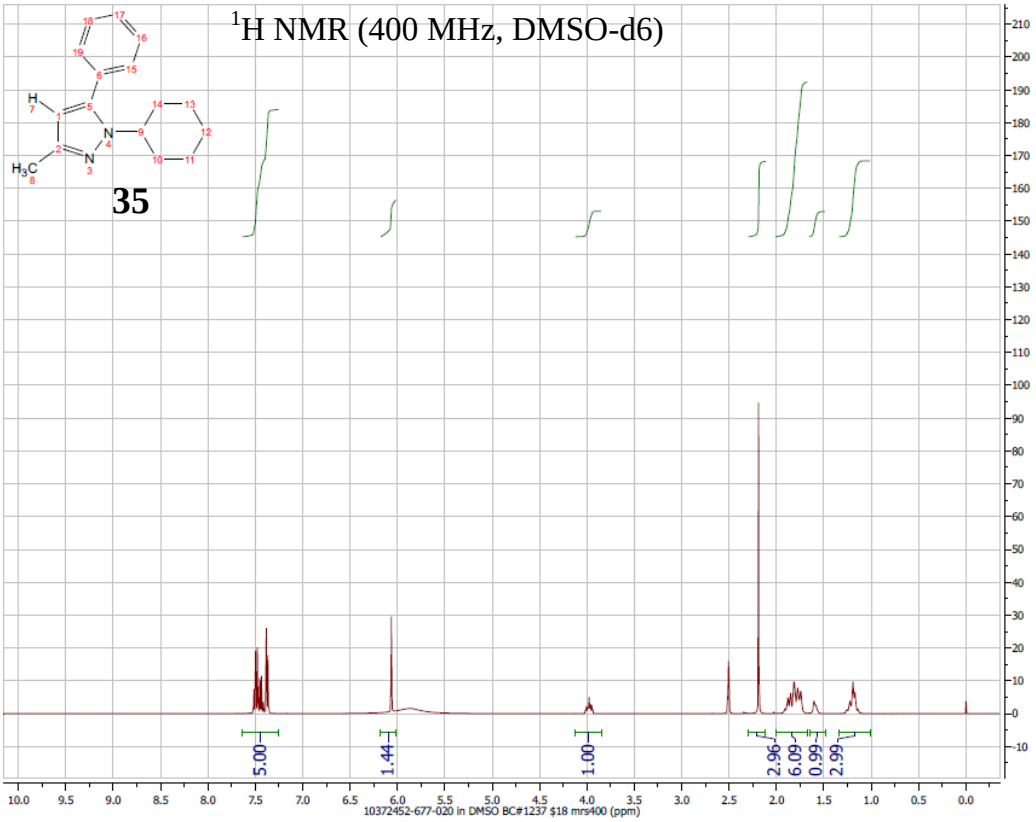


$^{1}$H NMR (400 MHz, DMSO-d6)

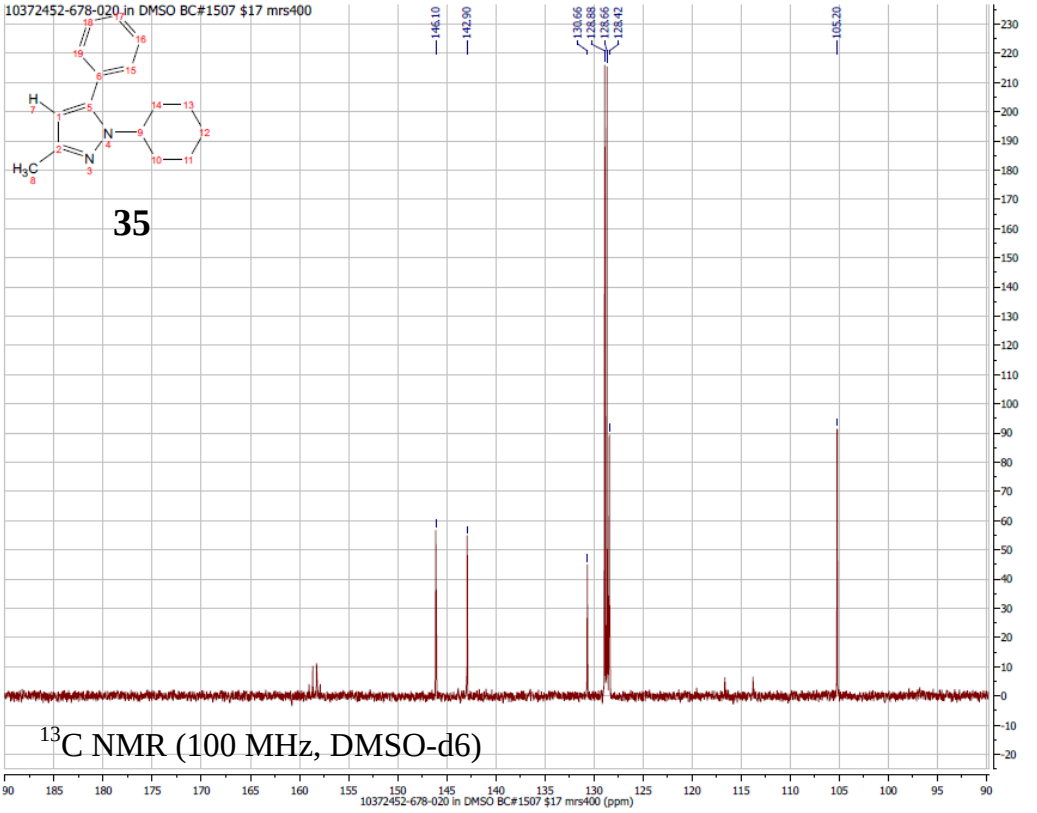


$^{13}$C NMR (100 MHz, DMSO-d6)

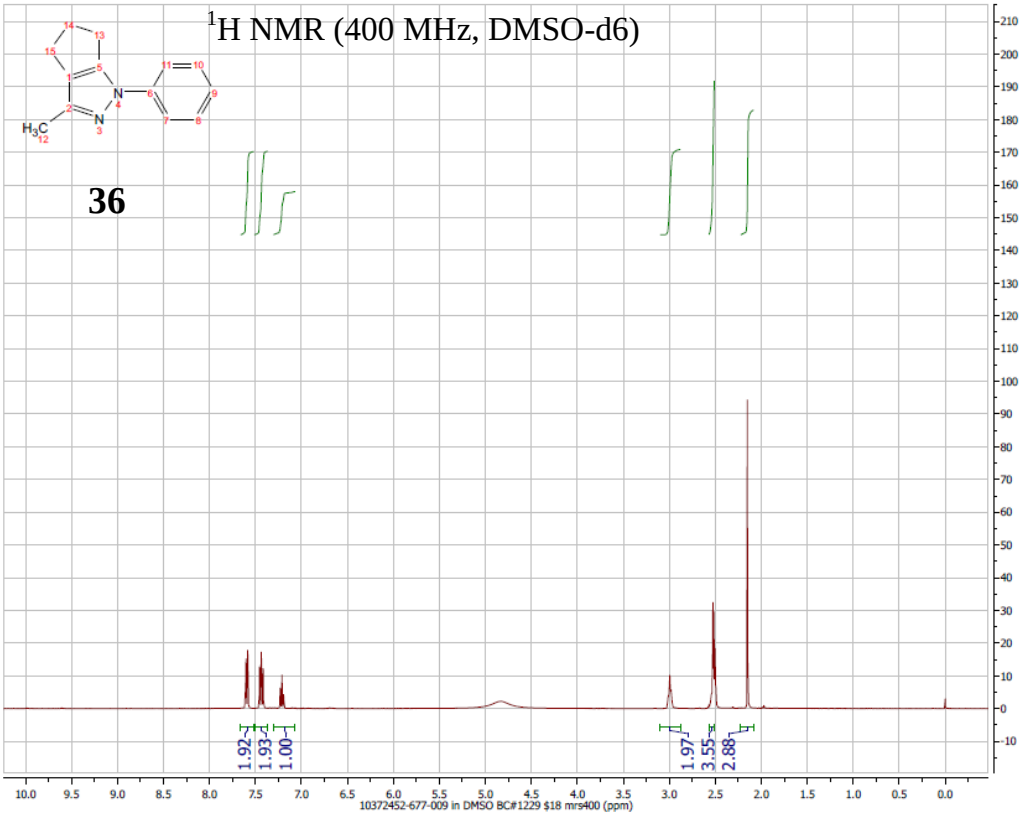
$^{1}$H NMR (400 MHz, DMSO-d6)
36
1.92
1.93
1.00
1.97
3.55
2.88
10372452-677-009 in DMSO BC#1229 $18 mrs400 (ppm)

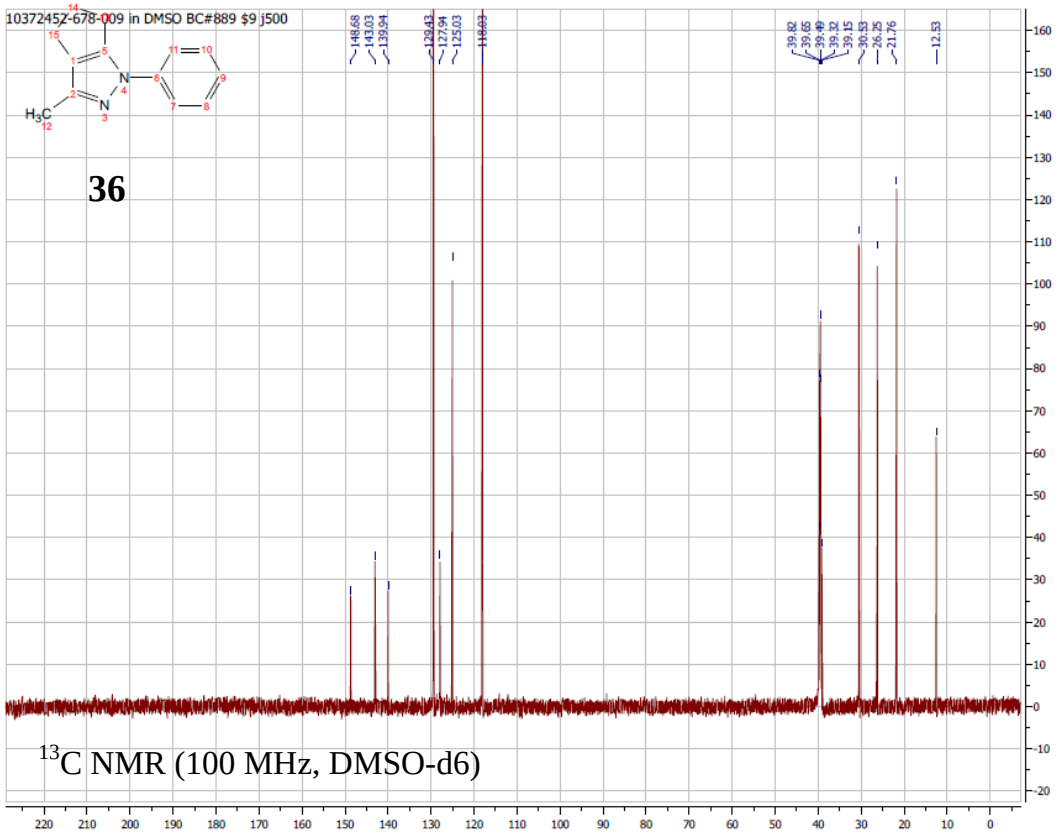
10372452-678-009 in DMSO BC#889 $9 j500
36
148.68
143.03
139.94
128.43
127.94
125.03
118.03
39.82
39.65
39.49
39.32
39.15
30.53
26.25
21.76
12.53
$^{13}$C NMR (100 MHz, DMSO-d6)

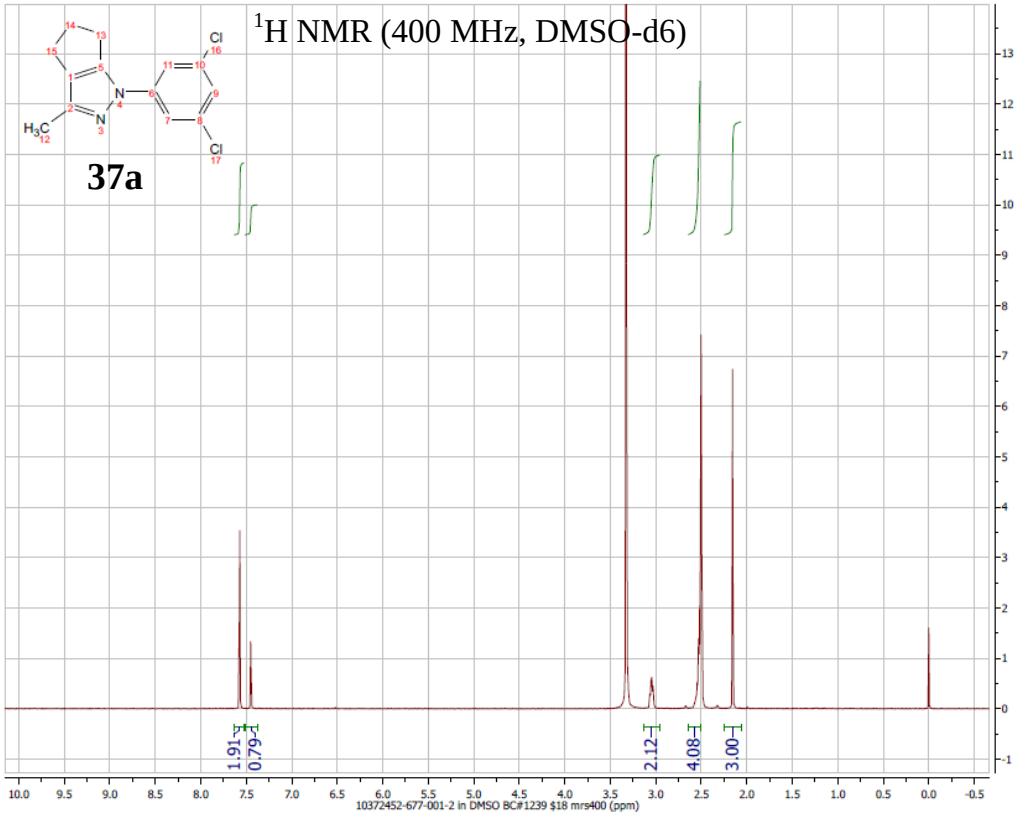
$^1$H NMR (400 MHz, DMSO-d6)
37a
1.91
0.79
2.12
4.08
3.00
10372452-677-001-2 in DMSO BC#1239 $18 mrs400 (ppm)

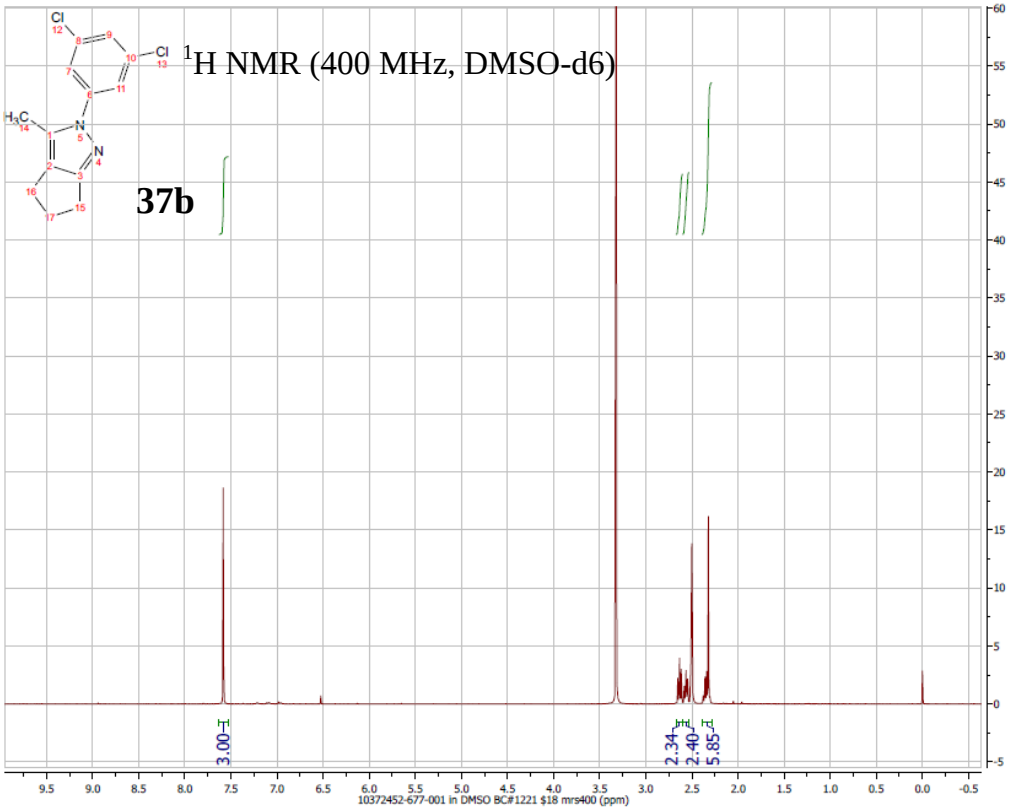
$^1$H NMR (400 MHz, DMSO-d6)
37b
3.00
2.34
2.40
5.85
10372452-677-001 in DMSO BC#1221 $18 mrs400 (ppm)

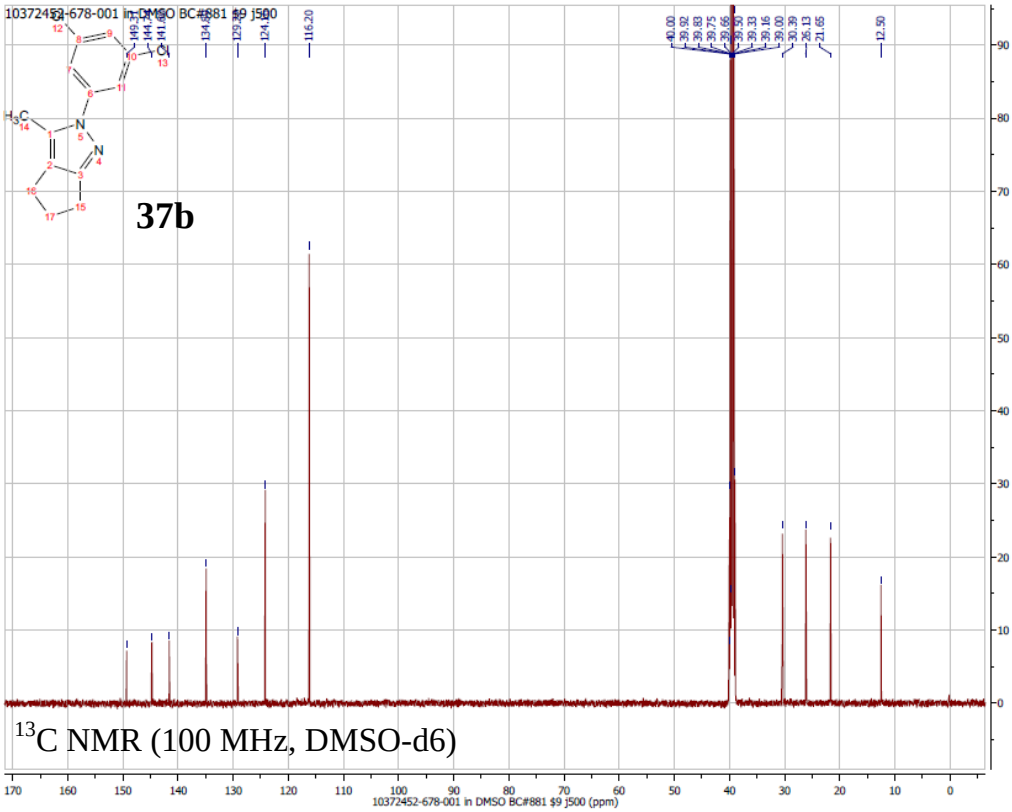
37b
$^{13}$C NMR (100 MHz, DMSO-d6)
10372452-678-001 in DMSO BC#881 $9 j500 (ppm)

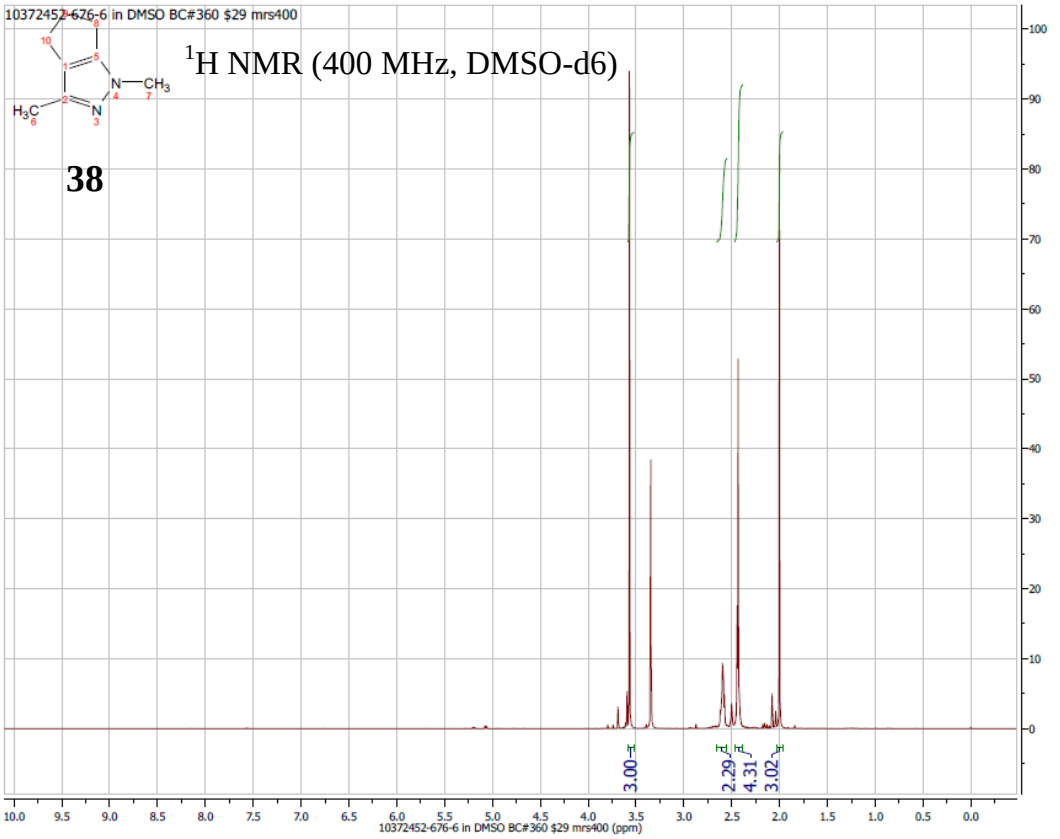
10372452-676-6 in DMSO BC#360 $29 mrs400
38
$^{1}$H NMR (400 MHz, DMSO-d6)
3.00
2.29
4.31
3.02
10372452-676-6 in DMSO BC#360 $29 mrs400 (ppm)

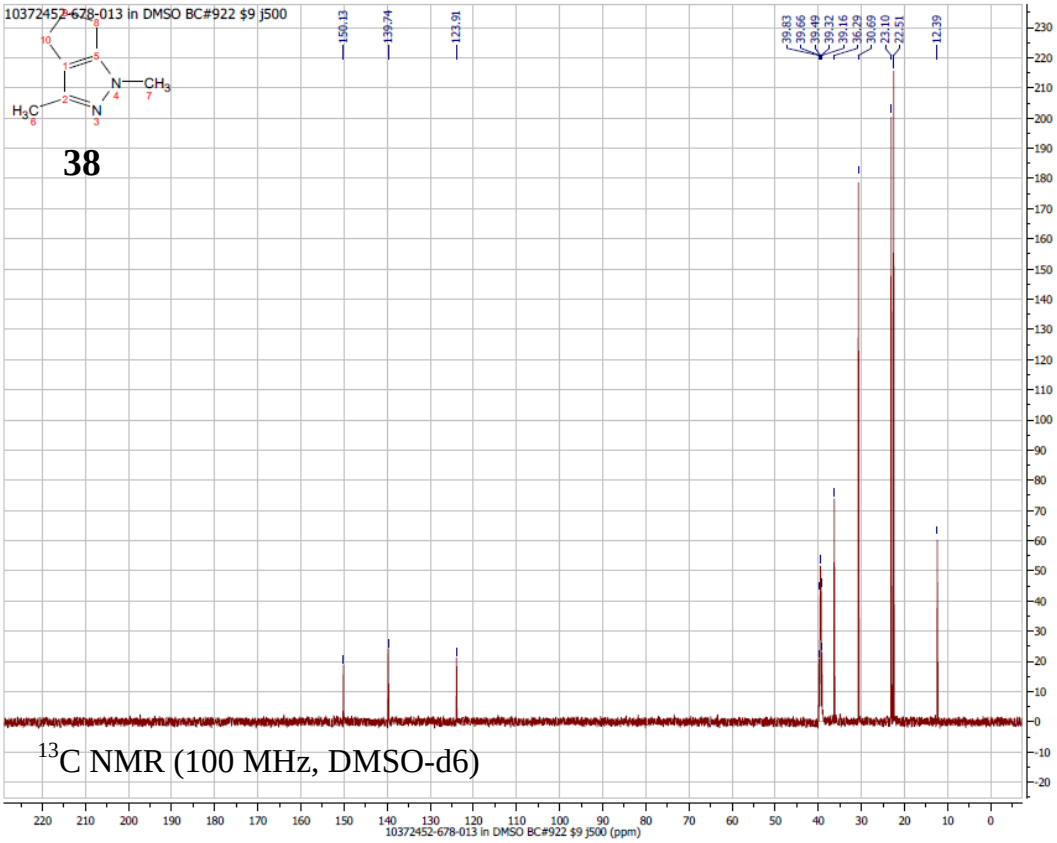
10372452-678-013 in DMSO BC#922 $9 j500
38
150.13
139.74
123.91
39.83
39.66
39.49
39.32
39.16
36.29
30.69
23.10
22.51
12.39
$^{13}$C NMR (100 MHz, DMSO-d6)
10372452-678-013 in DMSO BC#922 $9 j500 (ppm)

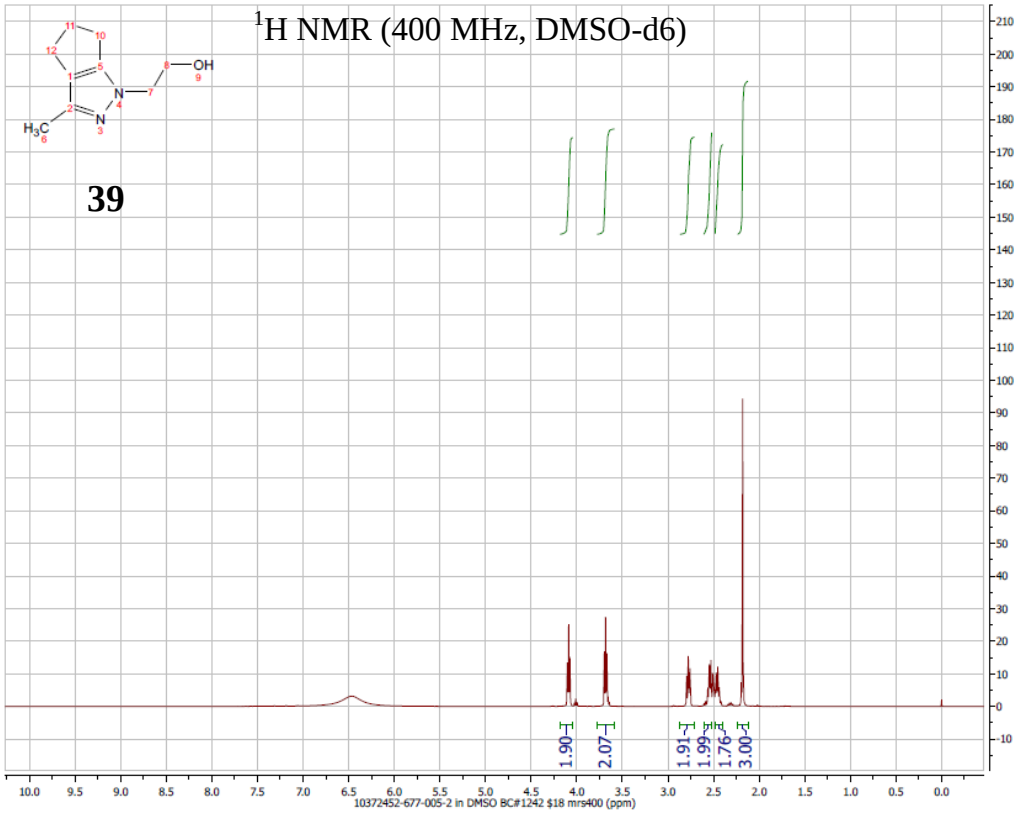
39
1H NMR (400 MHz, DMSO-d6)
1.90
2.07
1.91
1.99
1.76
3.00
10372452-677-005-2 in DMSO BC#1242 $18 mrs400 (ppm)

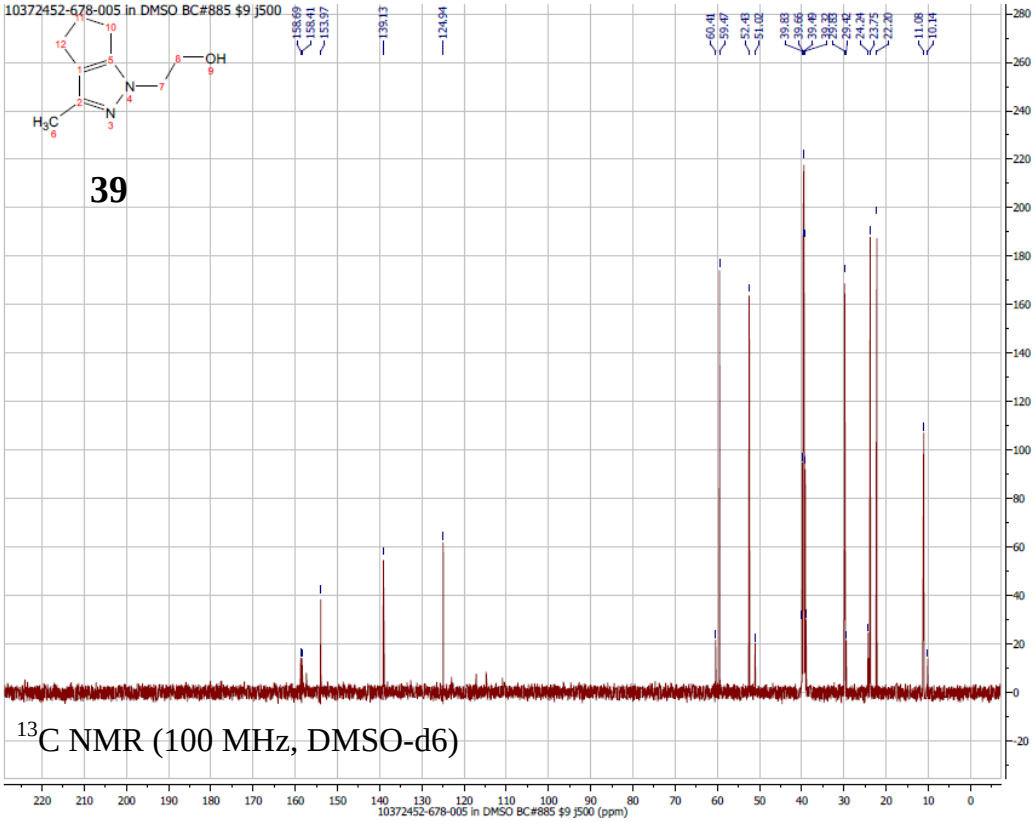
10372452-678-005 in DMSO BC#885 $9 j500
39
13C NMR (100 MHz, DMSO-d6)
158.69
158.41
153.97
139.13
124.94
60.41
59.47
52.43
51.02
39.83
39.66
39.49
39.33
29.42
24.24
23.75
22.20
11.08
10.14
10372452-678-005 in DMSO BC#885 $9 j500 (ppm)

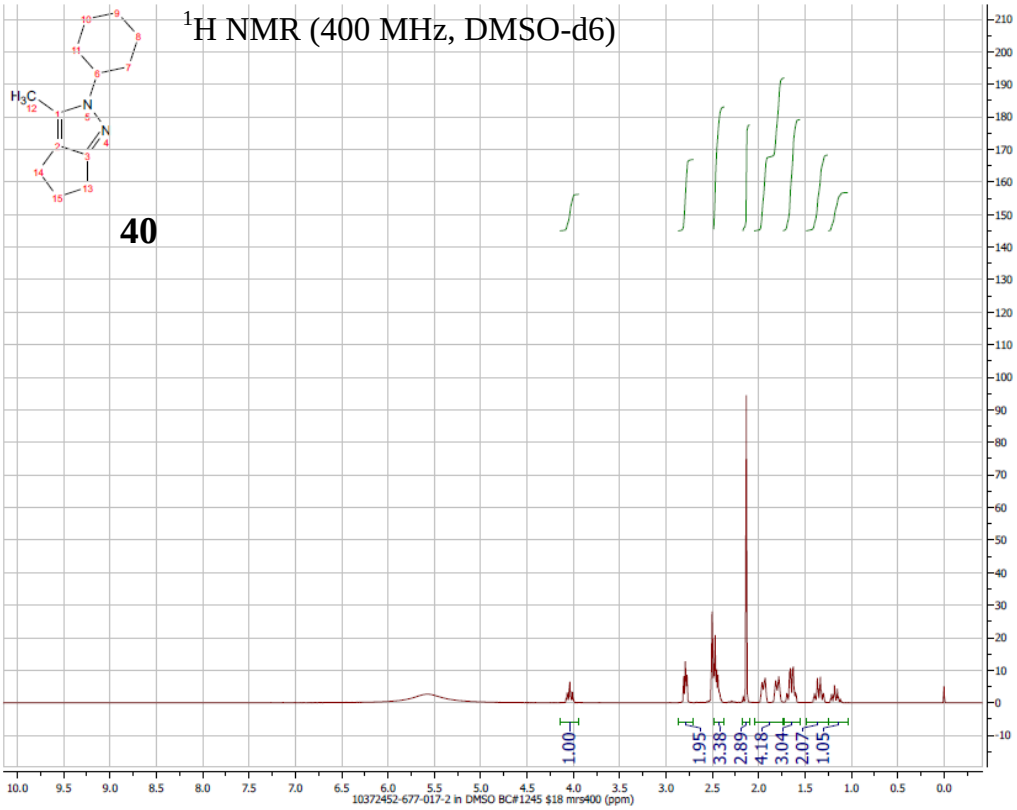
$^1$H NMR (400 MHz, DMSO-d6)
40
1.00
1.95
3.38
2.89
4.18
3.04
2.07
1.05
10372452-677-017-2 in DMSO BC#1245 $18 mrs400 (ppm)

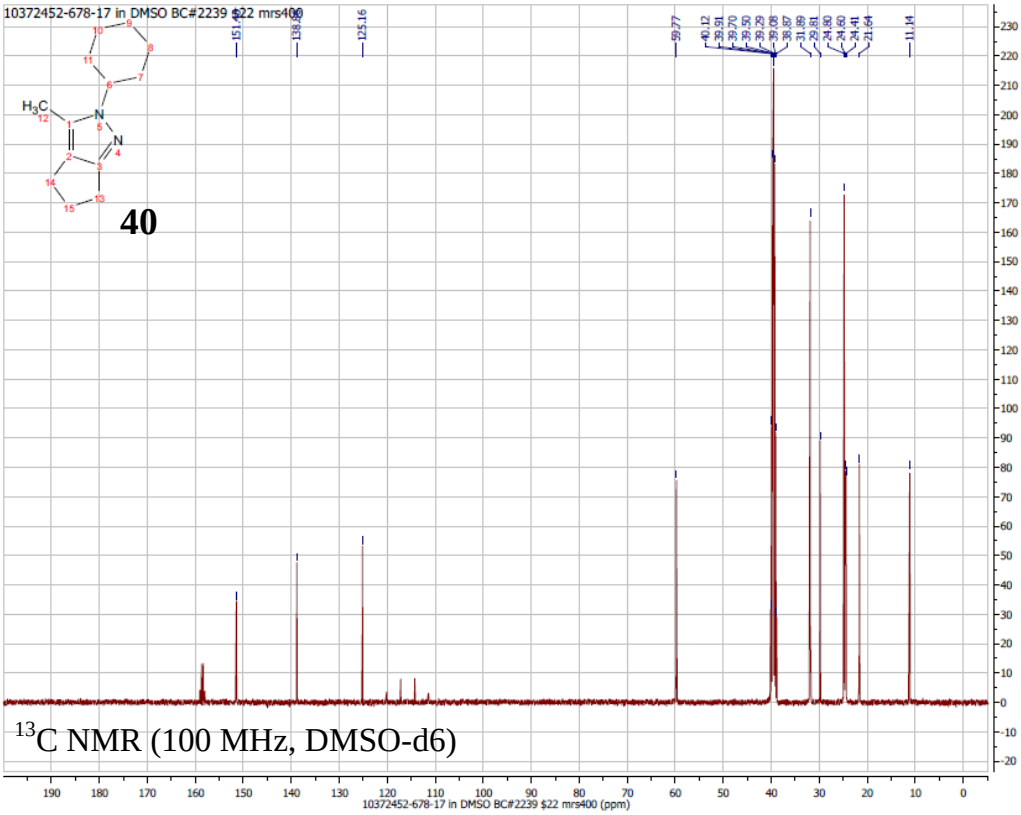
10372452-678-17 in DMSO BC#2239 $22 mrs400
40
$^{13}$C NMR (100 MHz, DMSO-d6)
10372452-678-17 in DMSO BC#2239 $22 mrs400 (ppm)

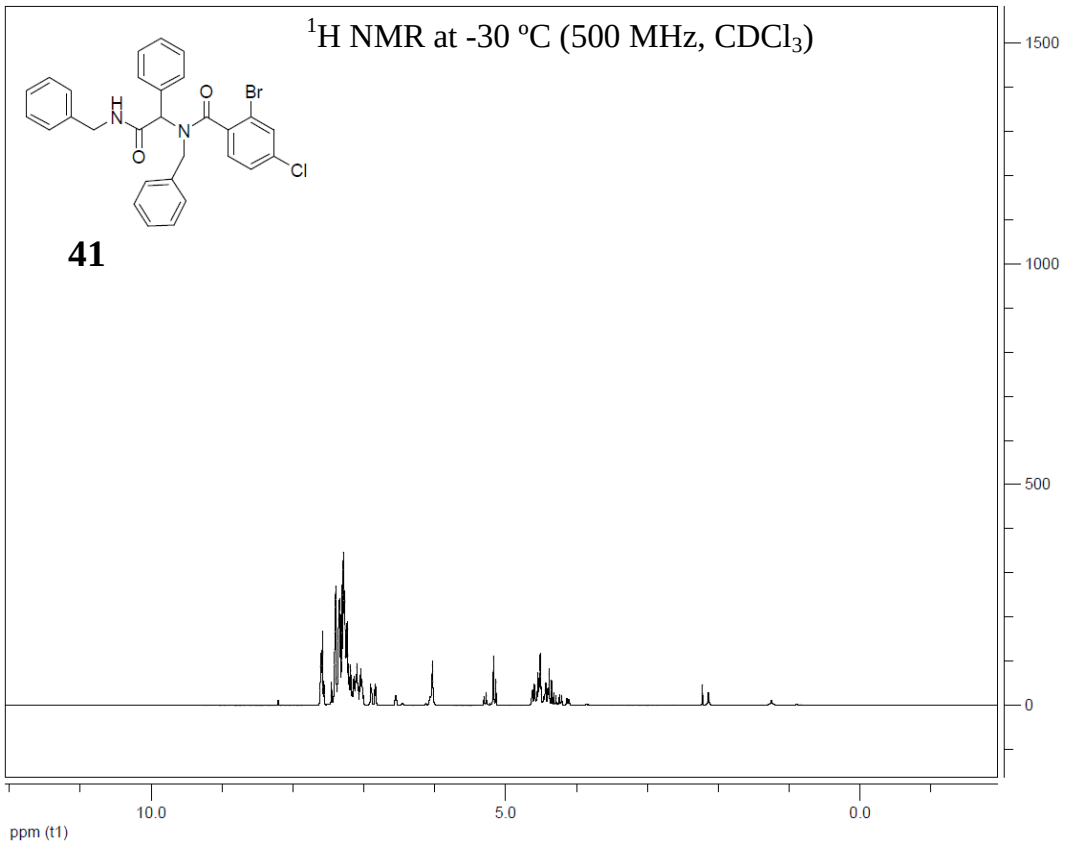
$^{1}$H NMR at -30 ºC (500 MHz, $CDCl_3$)
41
1500
1000
500
0
10.0
5.0
0.0
ppm (t1)

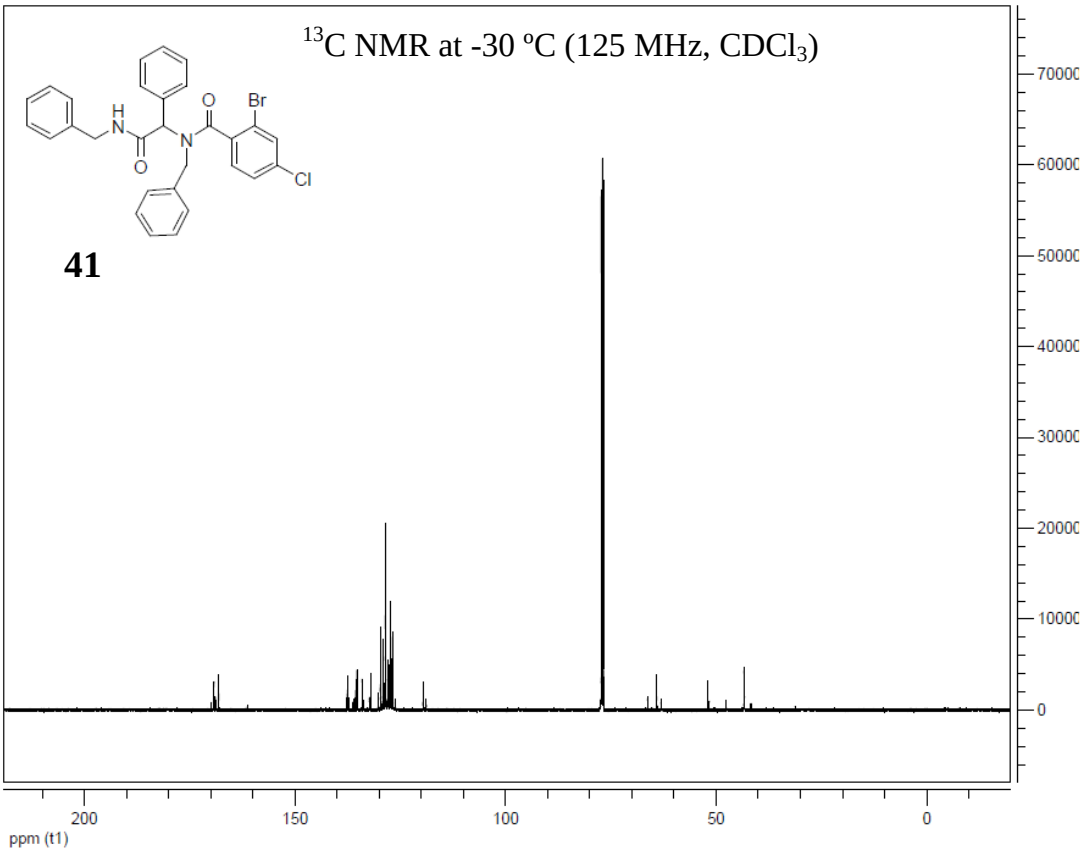
$^{13}$C NMR at -30 ºC (125 MHz, $CDCl_3$)
41
70000
60000
50000
40000
30000
20000
10000
0
200
150
100
50
0
ppm (t1)

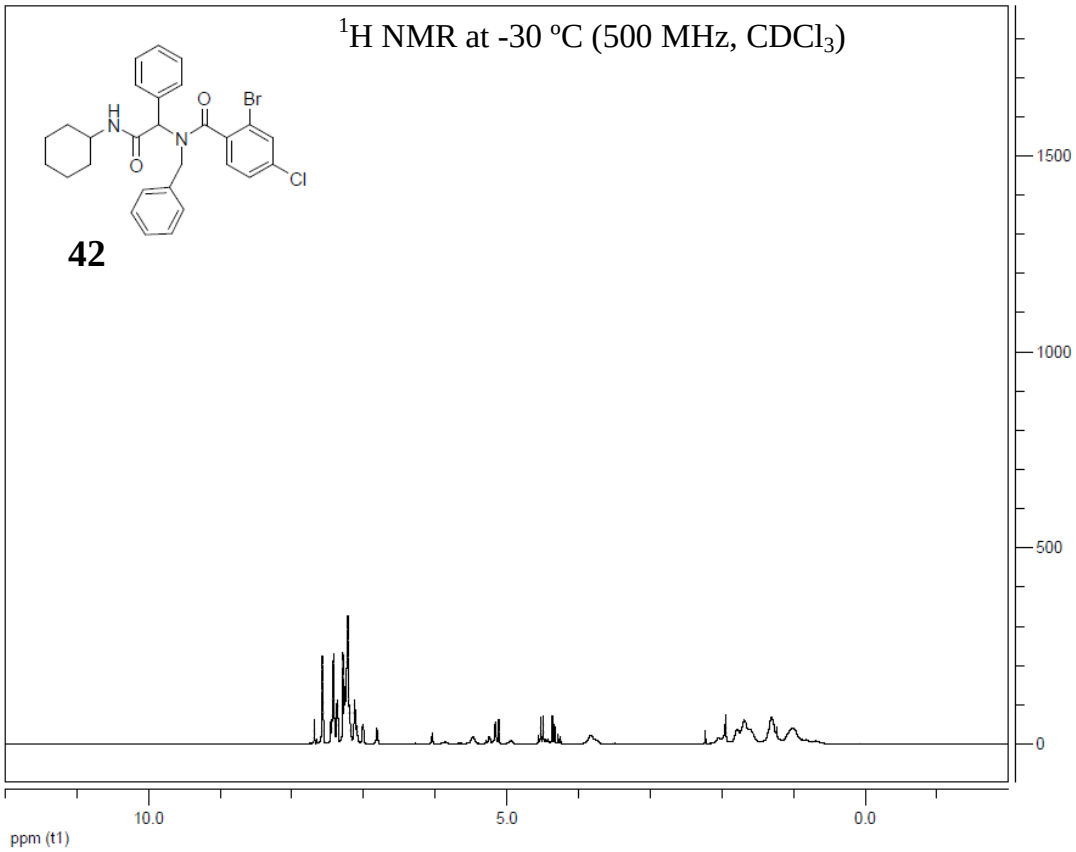
$^{1}$H NMR at -30 ºC (500 MHz, $CDCl_3$)
42
1500
1000
500
0
10.0
5.0
0.0
ppm (t1)

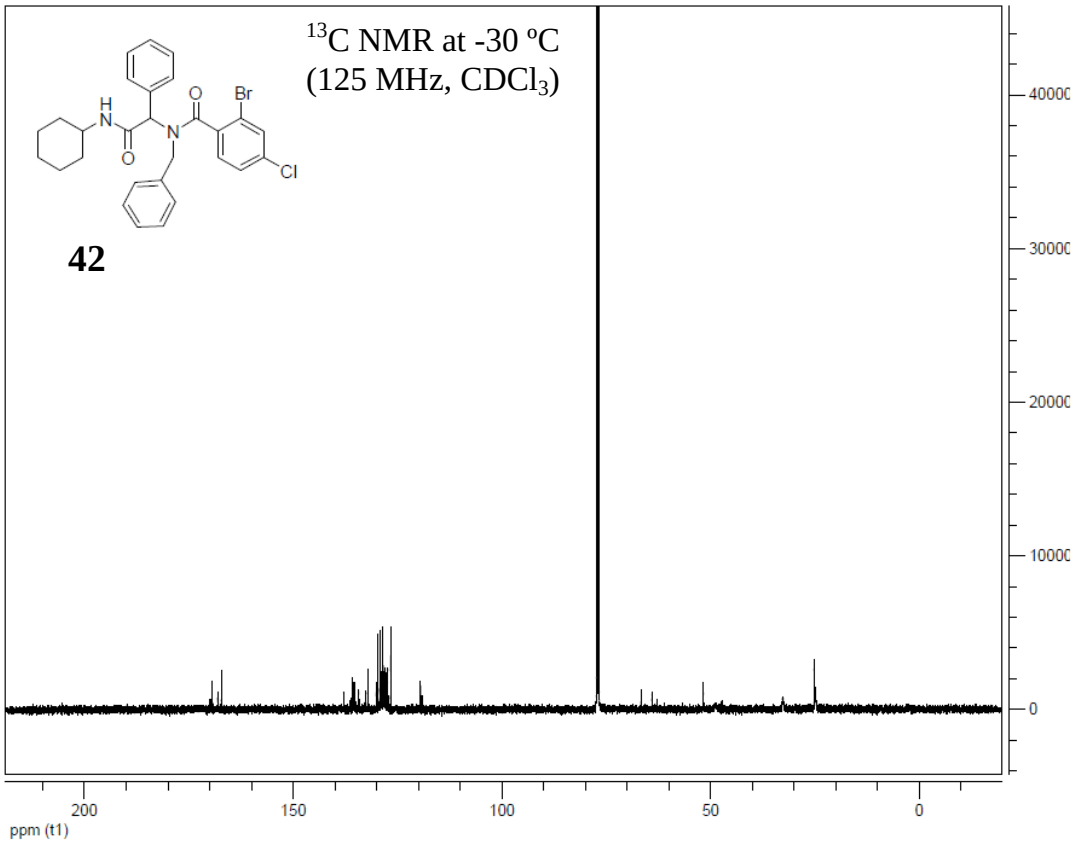
$^{13}$C NMR at -30 ºC
(125 MHz, $CDCl_3$)
42
40000
30000
20000
10000
0
200
150
100
50
0
ppm (t1)

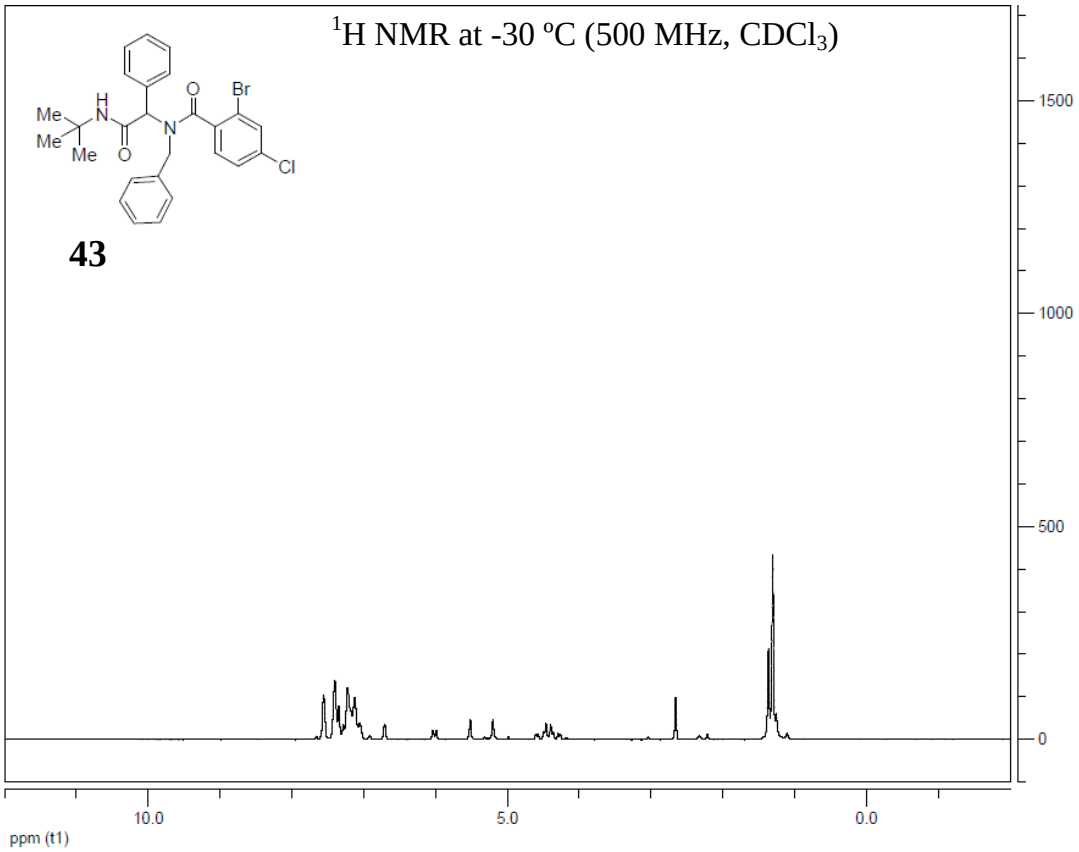
$^{1}$H NMR at -30 ºC (500 MHz, $CDCl_3$)
Me
Me
Me
H
N
O
O
N
O
Br
Cl
43
1500
1000
500
0
10.0
5.0
0.0
ppm (t1)

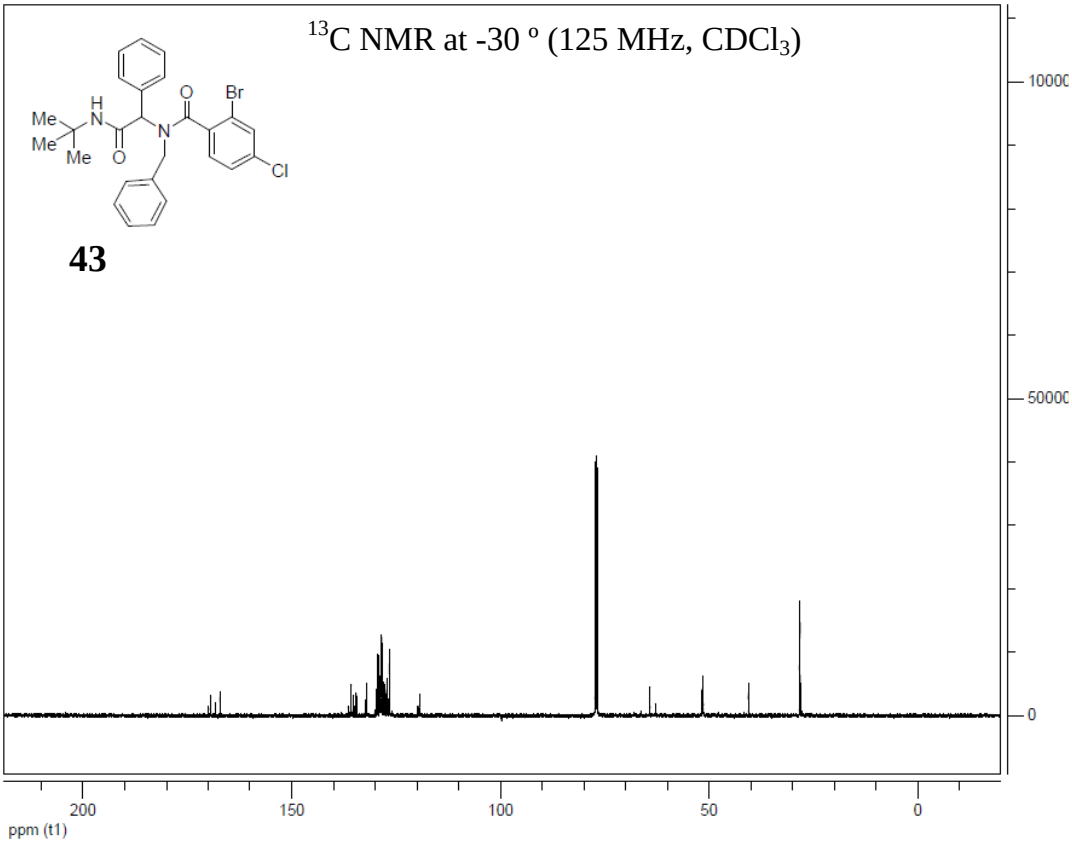
$^{13}$C NMR at -30 º (125 MHz, $CDCl_3$)
Me
Me
Me
H
N
O
O
N
O
Br
Cl
43
10000
50000
0
200
150
100
50
0
ppm (t1)

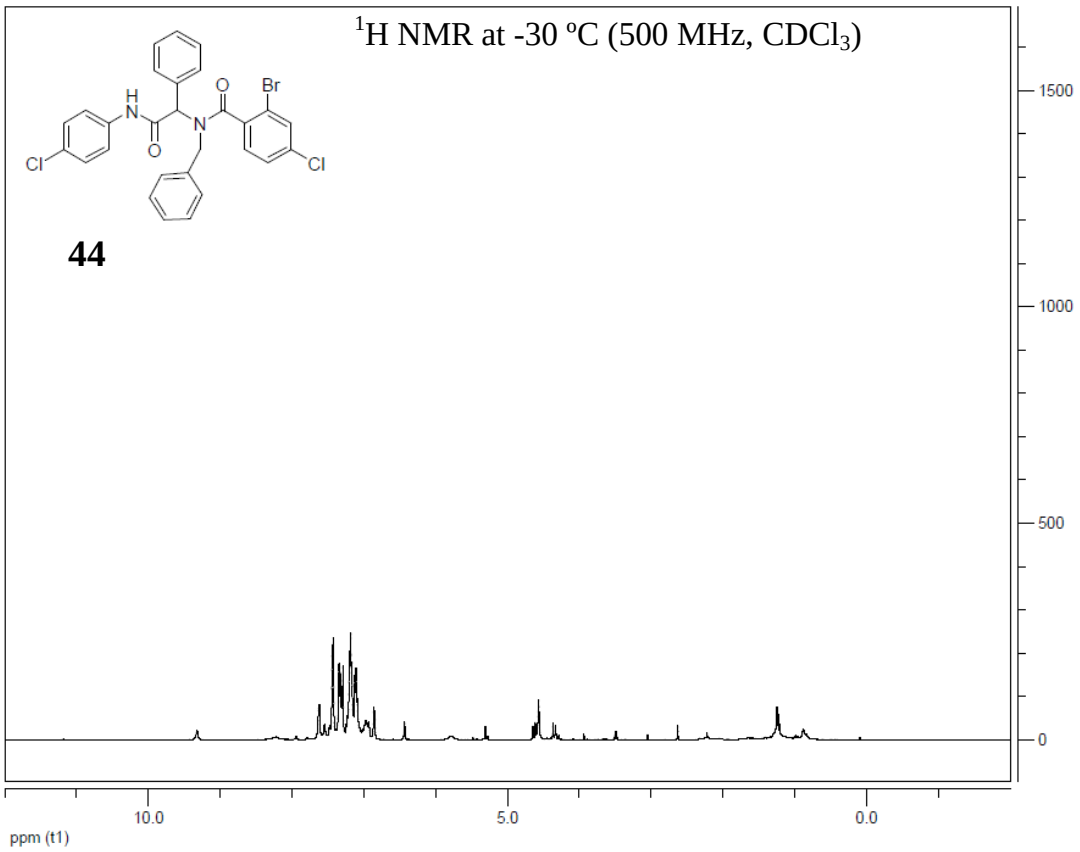
$^{1}$H NMR at -30 ºC (500 MHz, $CDCl_3$)
44
1500
1000
500
0
10.0
5.0
0.0
ppm (t1)

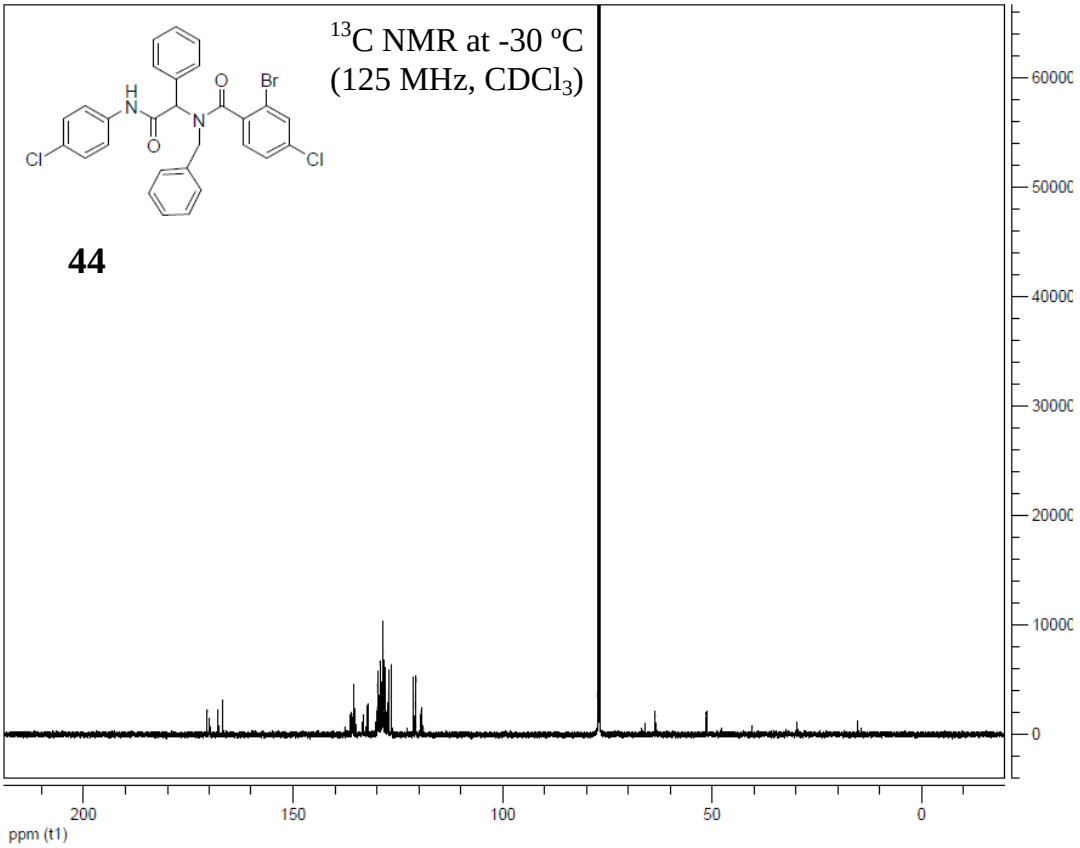
$^{13}$C NMR at -30 ºC
(125 MHz, $CDCl_3$)
44
60000
50000
40000
30000
20000
10000
0
200
150
100
50
0
ppm (t1)

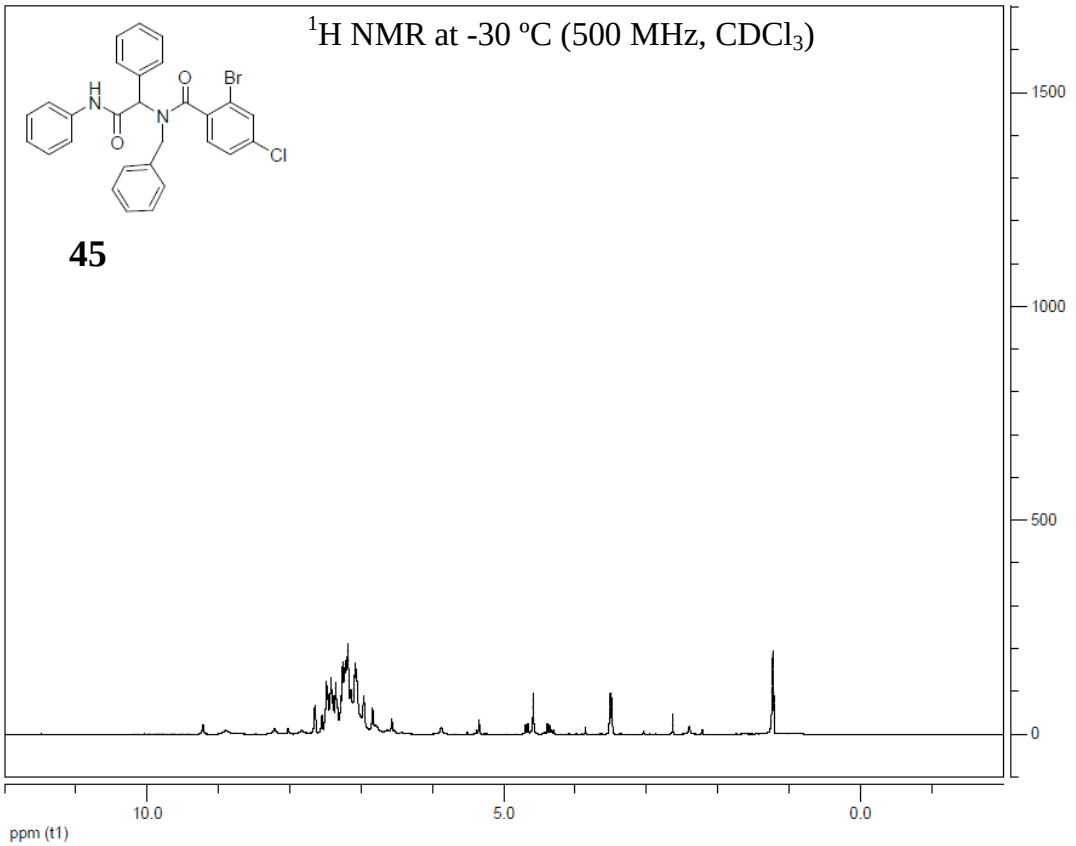
$^{1}$H NMR at -30 ºC (500 MHz, $CDCl_3$)
45
1500
1000
500
0
10.0
5.0
0.0
ppm (t1)

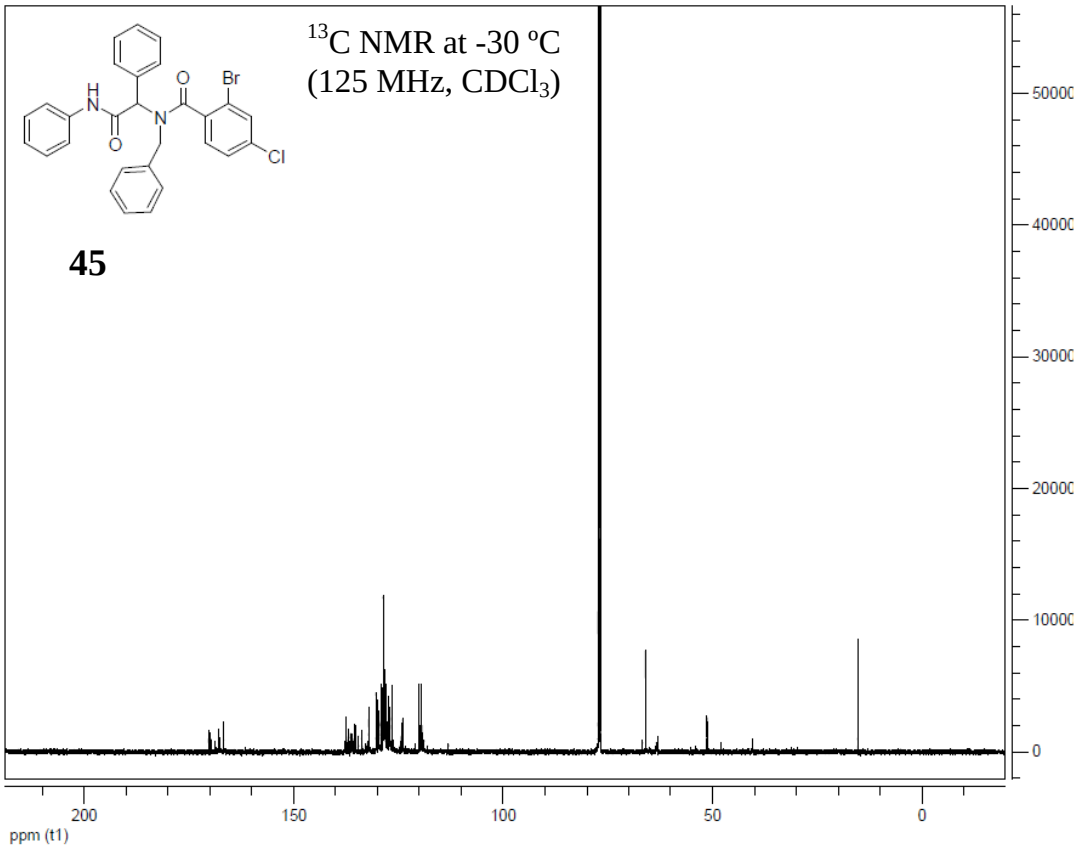
$^{13}$C NMR at -30 ºC
(125 MHz, $CDCl_3$)
45
50000
40000
30000
20000
10000
0
200
150
100
50
0
ppm (t1)

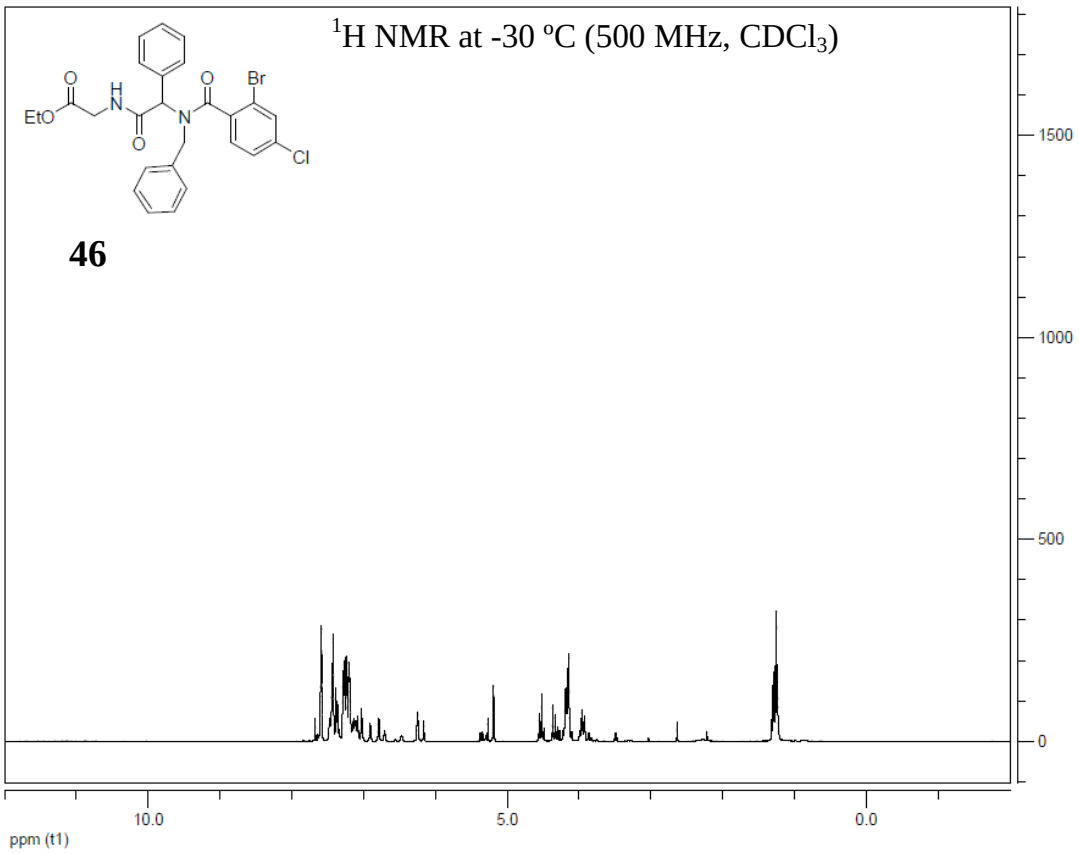
$^{1}$H NMR at -30 ºC (500 MHz, $CDCl_3$)
EtO
O
H
N
O
O
N
O
Br
Cl
46
1500
1000
500
0
10.0
5.0
0.0
ppm (t1)

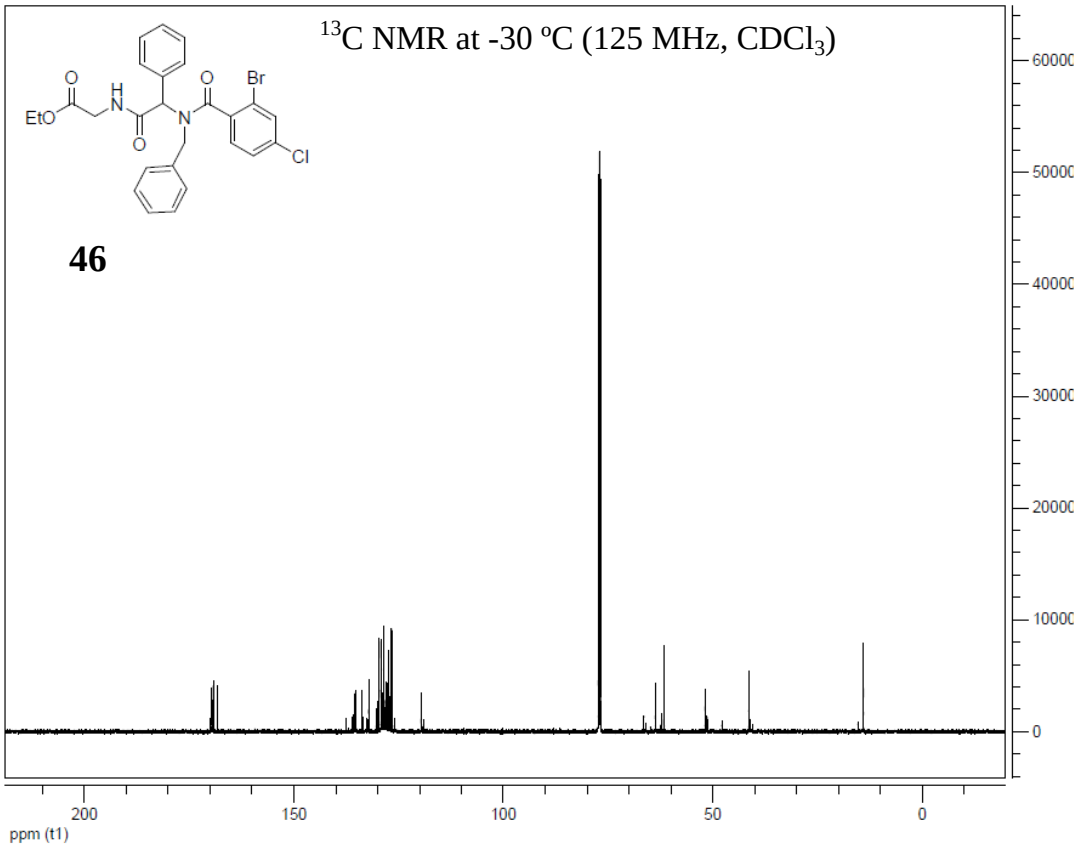
$^{13}$C NMR at -30 ºC (125 MHz, $CDCl_3$)
EtO
O
H
N
O
O
N
O
Br
Cl
46
60000
50000
40000
30000
20000
10000
0
200
150
100
50
0
ppm (t1)

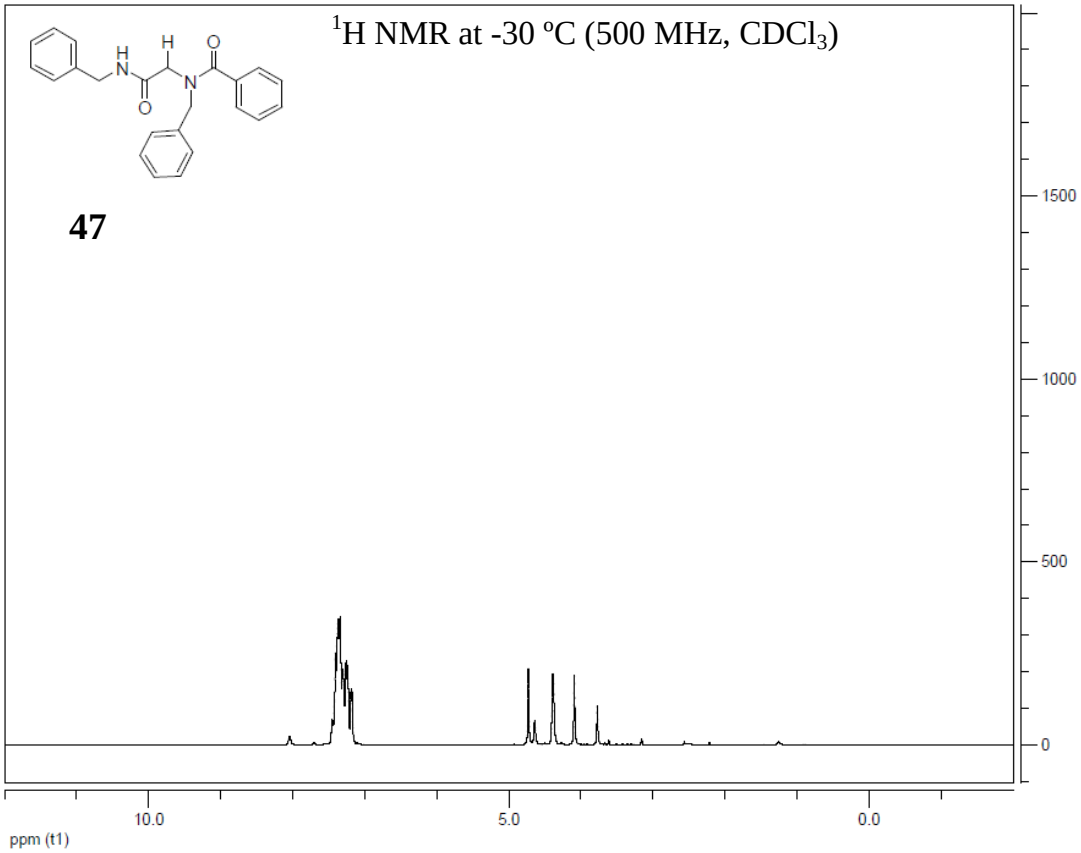


$^{1}$H NMR at -30 ºC (500 MHz, $CDCl_3$)

**47**

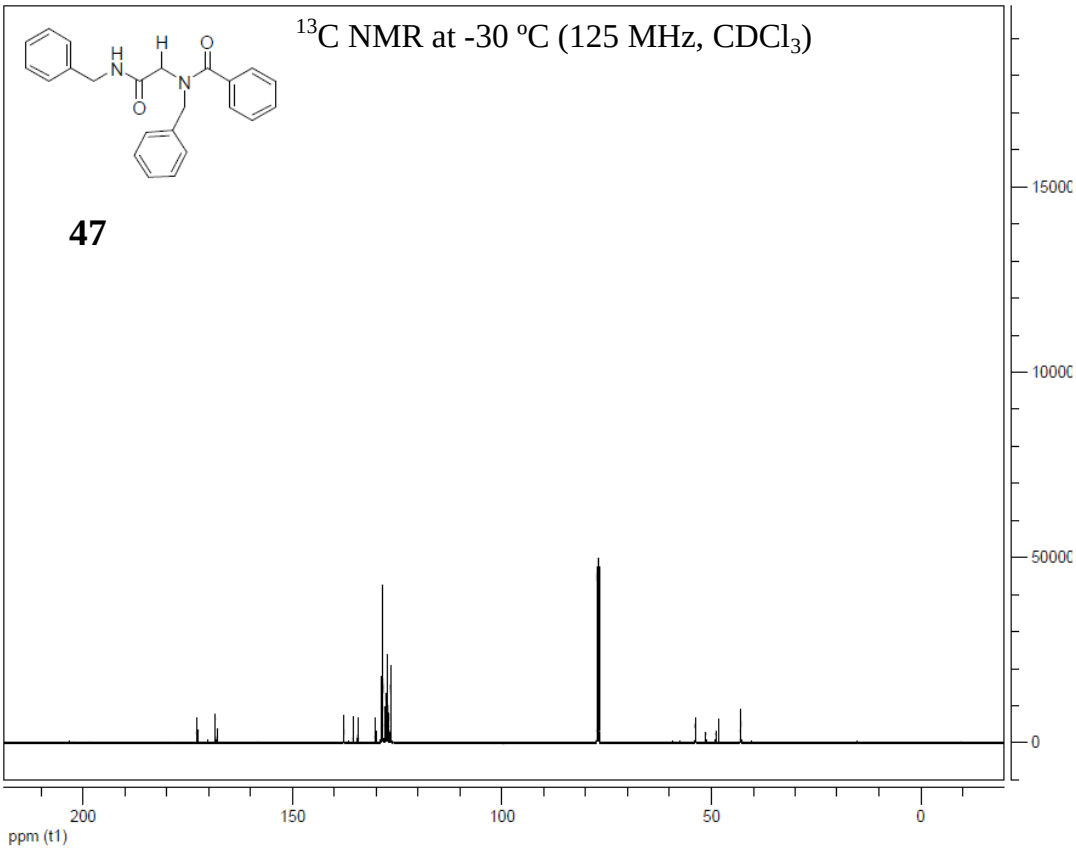


$^{13}$C NMR at -30 ºC (125 MHz, $CDCl_3$)

**47**

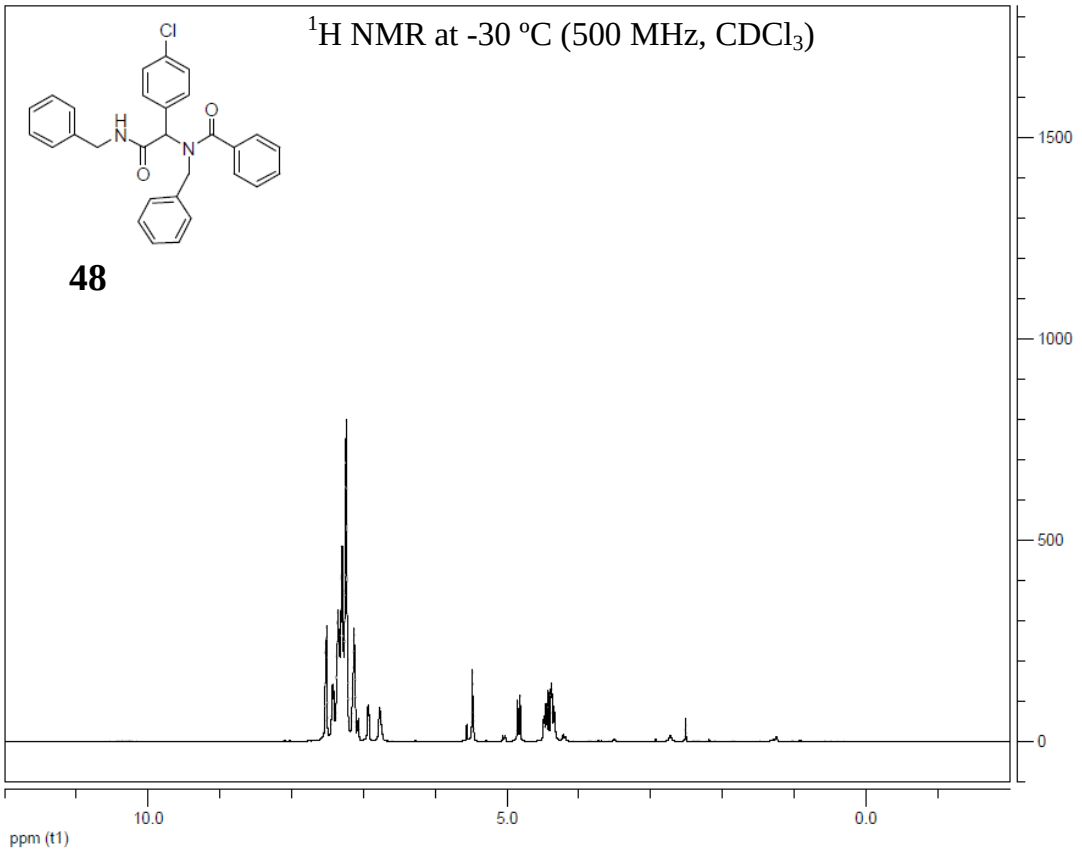


$^{1}$H NMR at -30 ºC (500 MHz, $CDCl_3$)

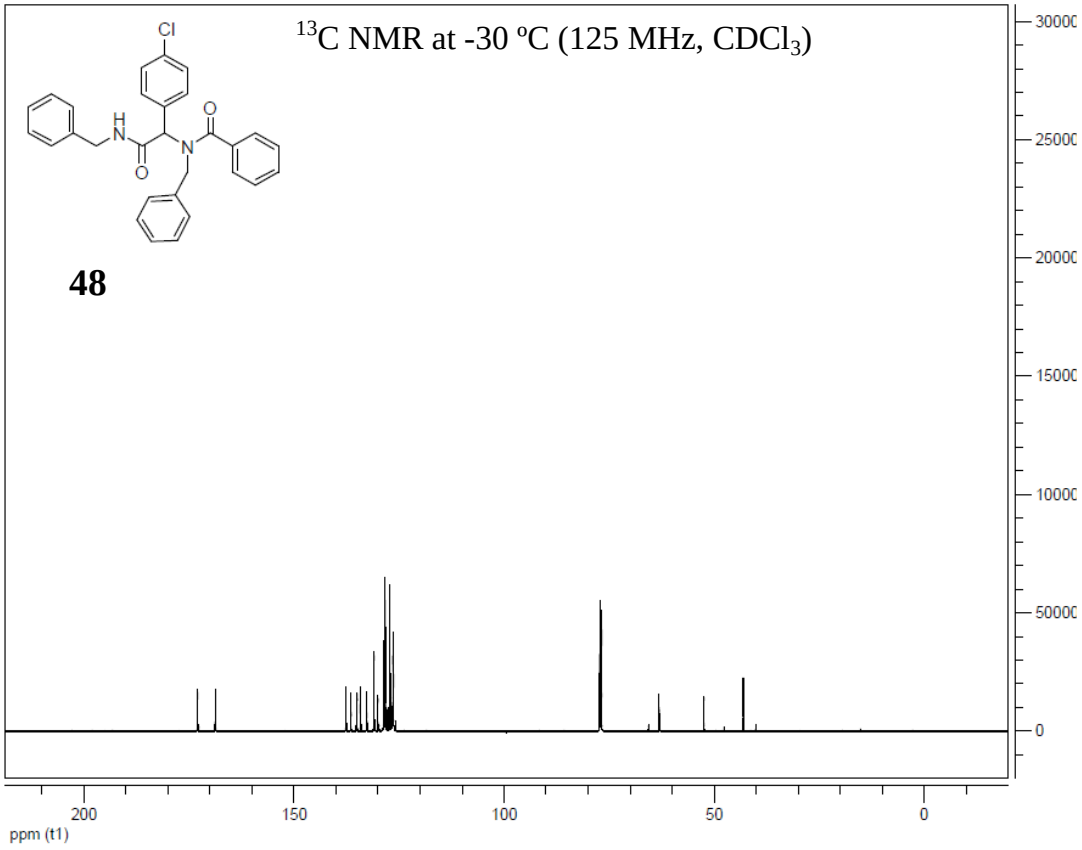


$^{13}$C NMR at -30 ºC (125 MHz, $CDCl_3$)

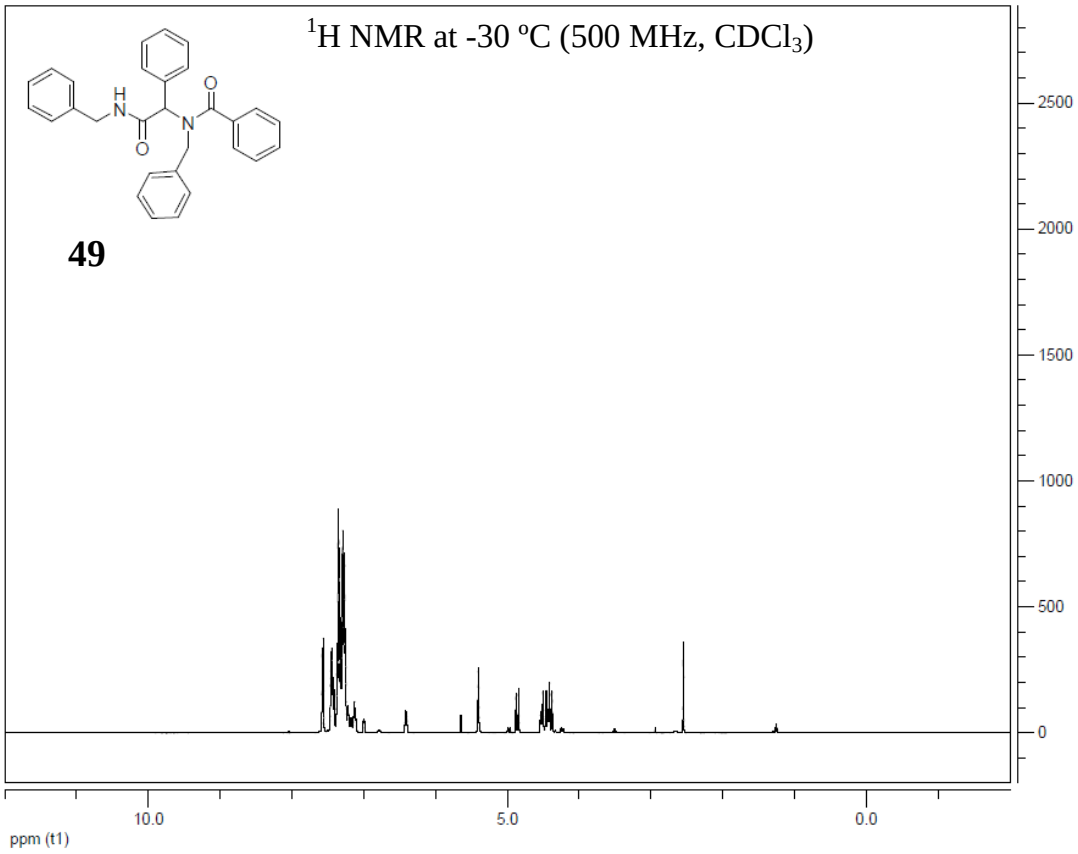
$^{1}$H NMR at -30 ºC (500 MHz, $CDCl_3$)
49
2500
2000
1500
1000
500
0
10.0
5.0
0.0
ppm (t1)

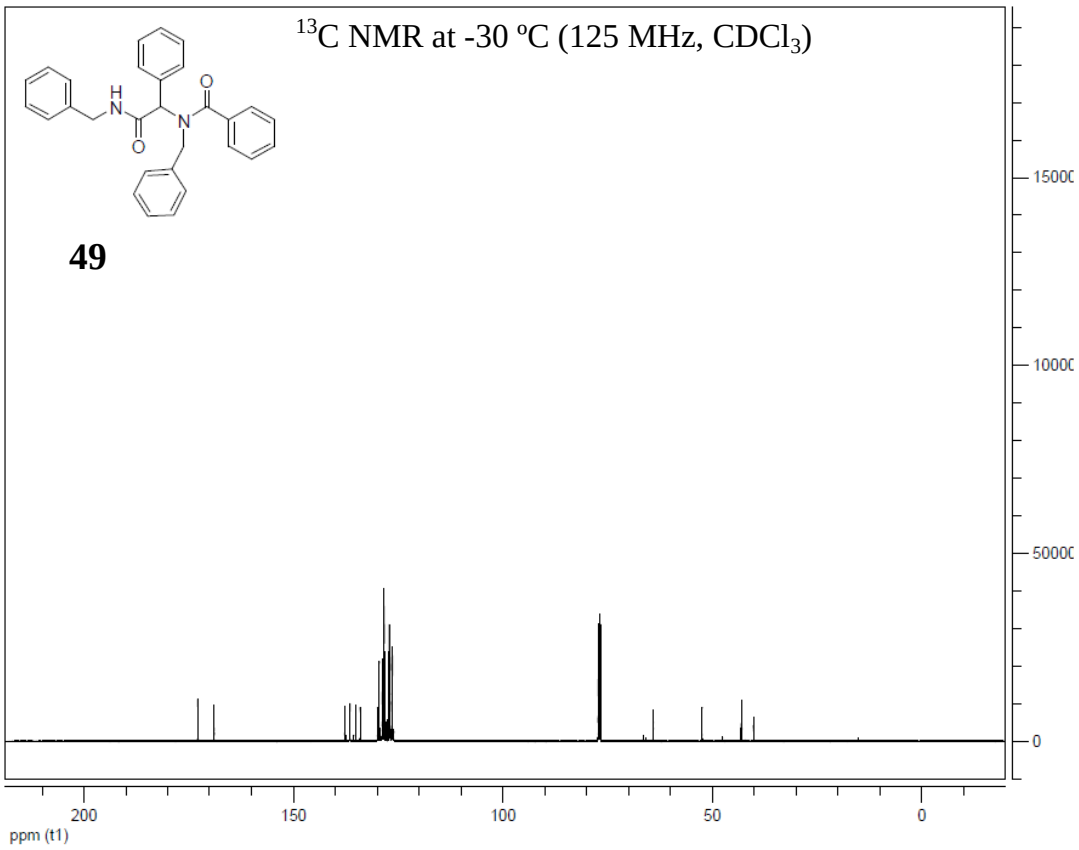
$^{13}$C NMR at -30 ºC (125 MHz, $CDCl_3$)
49
15000
10000
50000
0
200
150
100
50
0
ppm (t1)

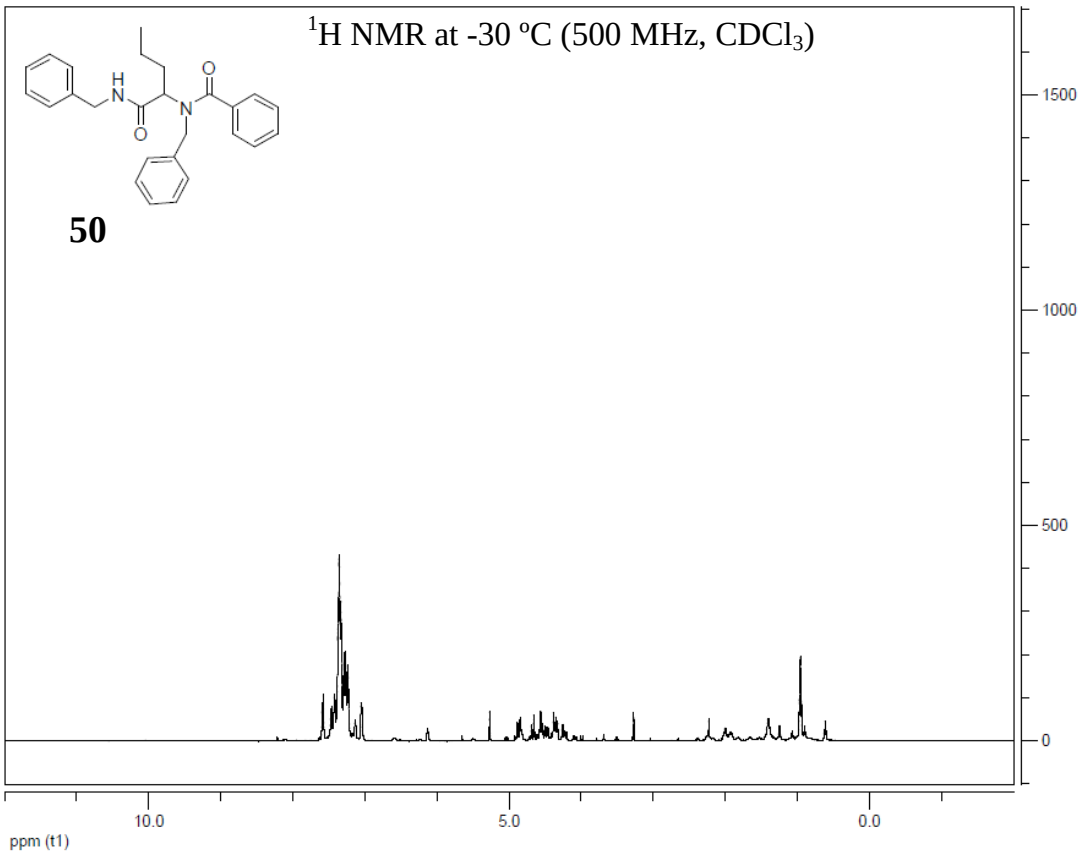
$^{1}$H NMR at -30 ºC (500 MHz, $CDCl_3$)
50
1500
1000
500
0
10.0
5.0
0.0
ppm (t1)

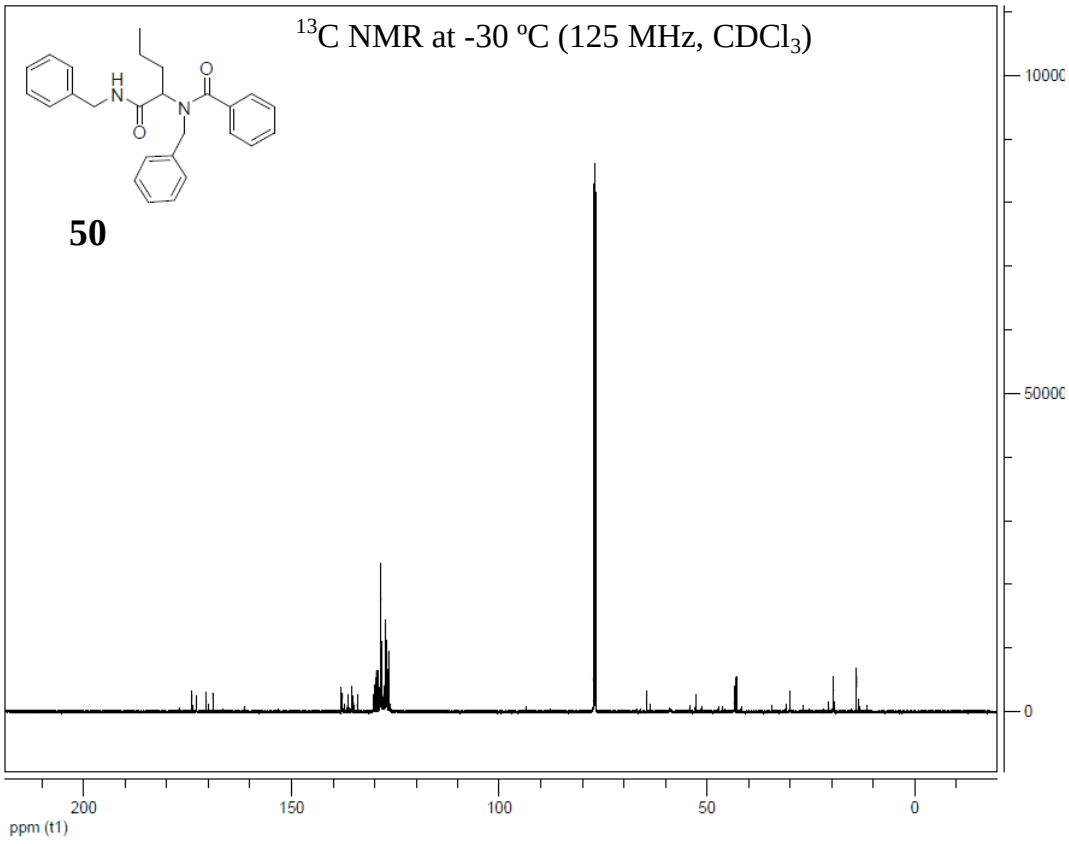
$^{13}$C NMR at -30 ºC (125 MHz, $CDCl_3$)
50
10000
50000
0
200
150
100
50
0
ppm (t1)

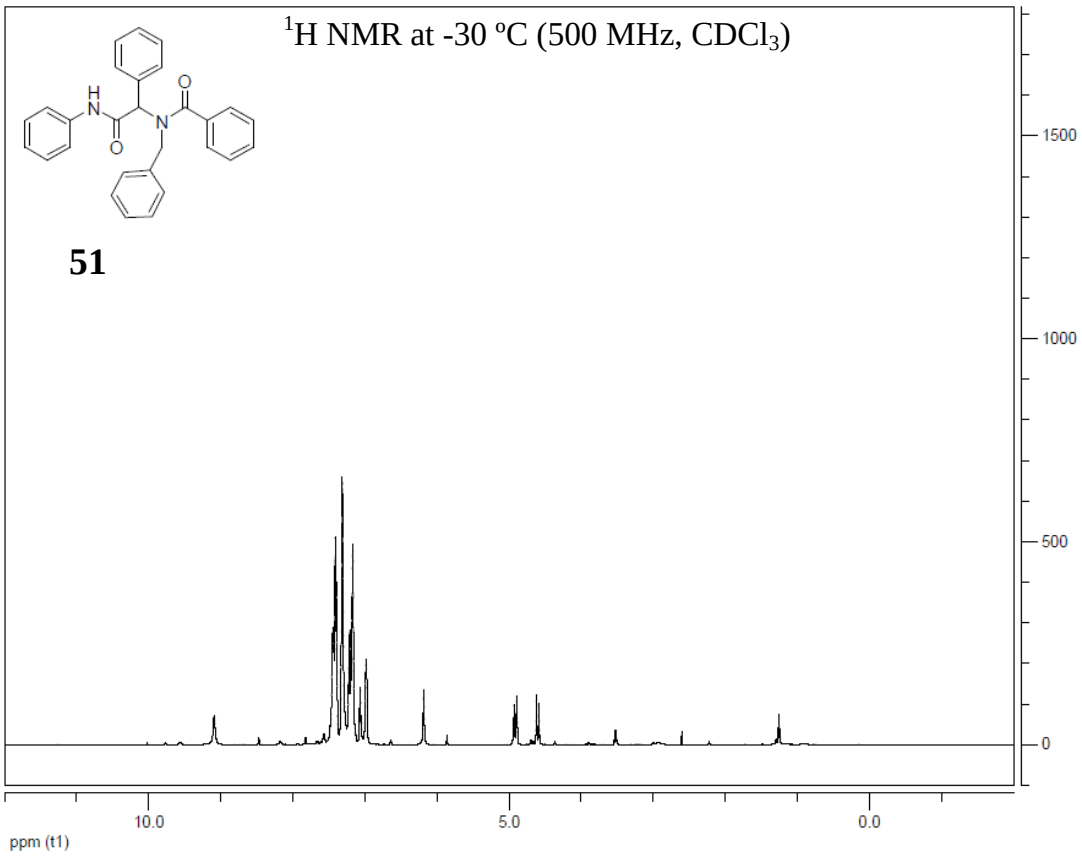
$^{1}$H NMR at -30 ºC (500 MHz, $CDCl_3$)
51
1500
1000
500
0
10.0
5.0
0.0
ppm (t1)

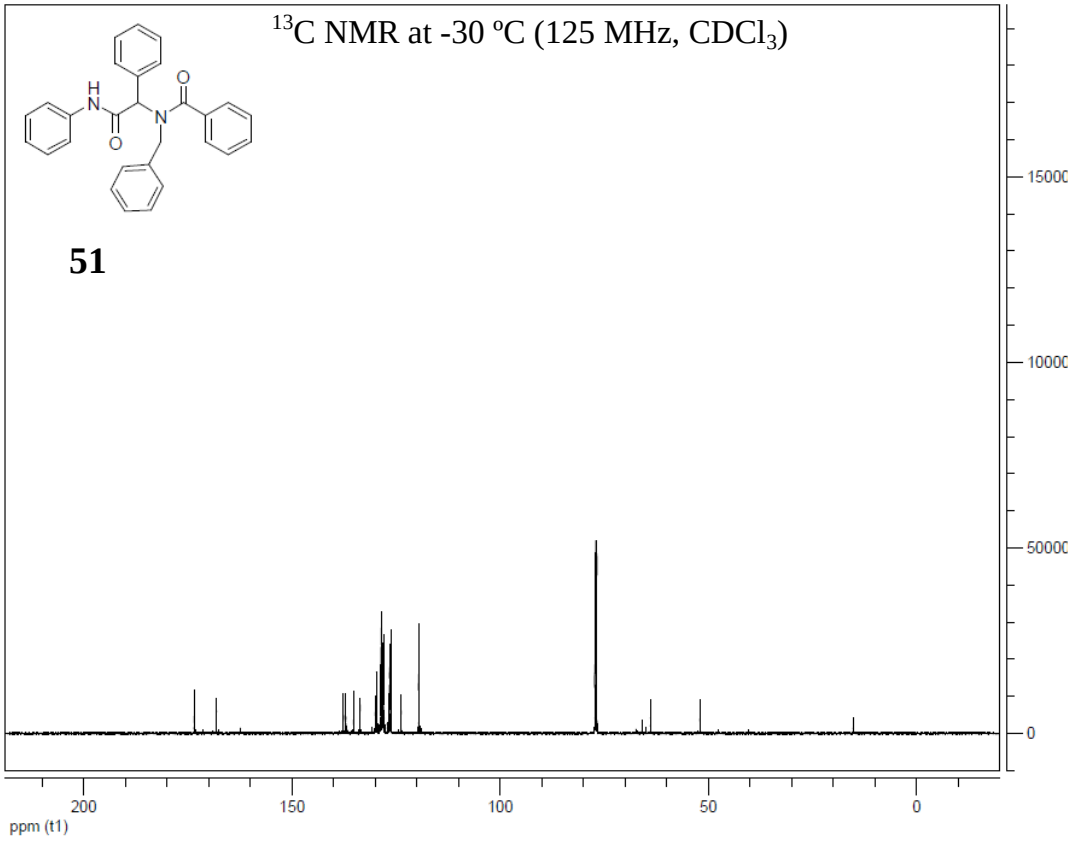
$^{13}$C NMR at -30 ºC (125 MHz, $CDCl_3$)
51
15000
10000
50000
0
200
150
100
50
0
ppm (t1)

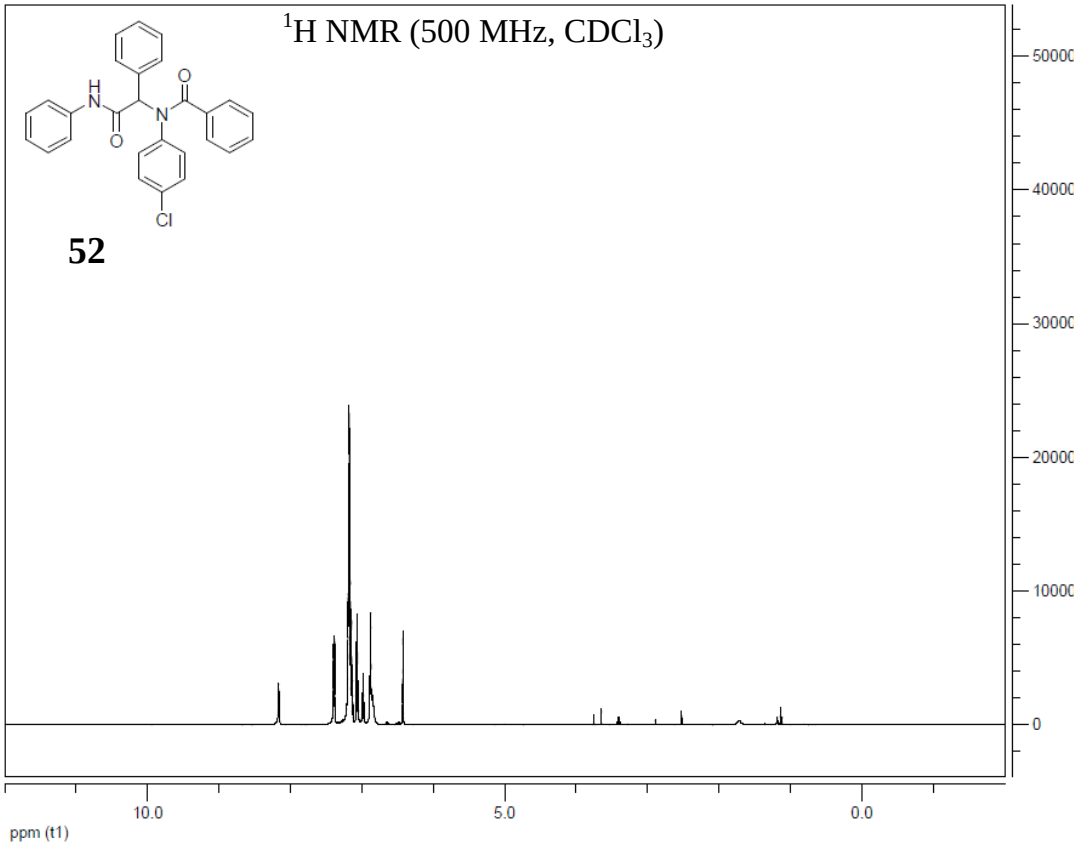
$^{1}$H NMR (500 MHz, $CDCl_3$)
52
10.0
5.0
0.0
ppm (t1)

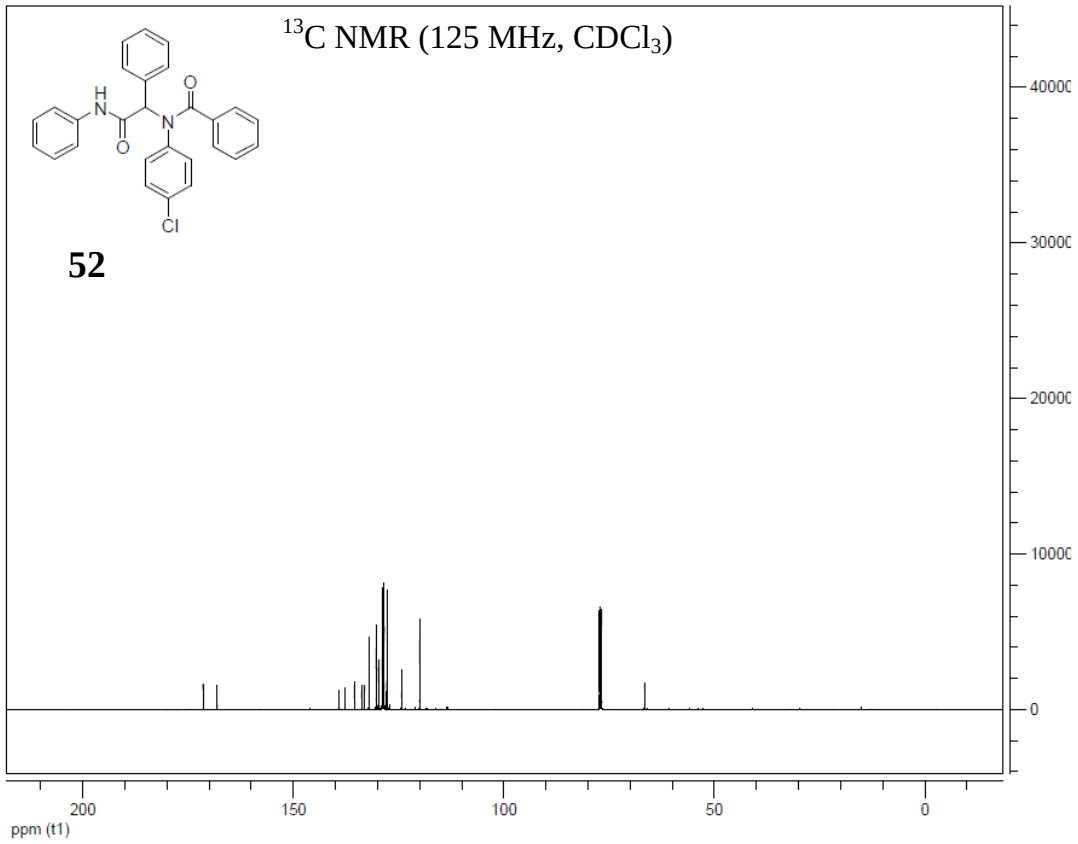
$^{13}$C NMR (125 MHz, $CDCl_3$)
52
200
150
100
50
0
ppm (t1)

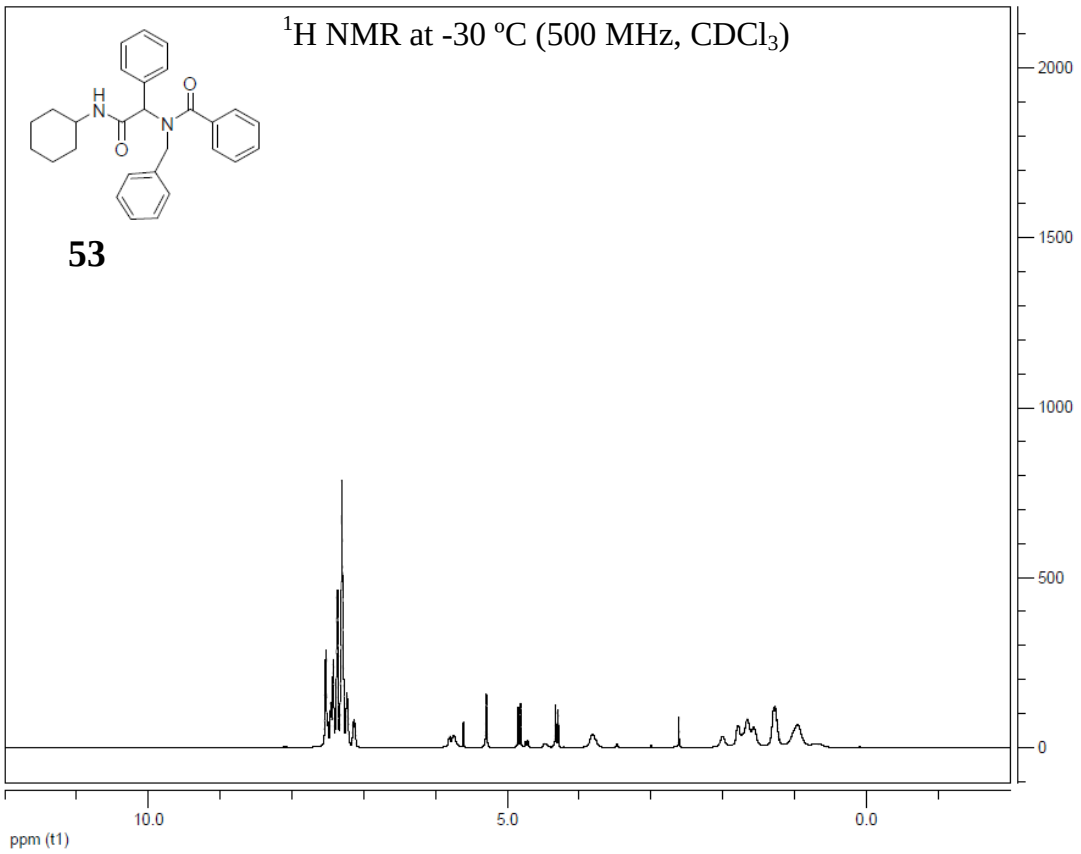
$^1$H NMR at -30 ºC (500 MHz, $CDCl_3$)
53
2000
1500
1000
500
0
10.0
5.0
0.0
ppm (t1)

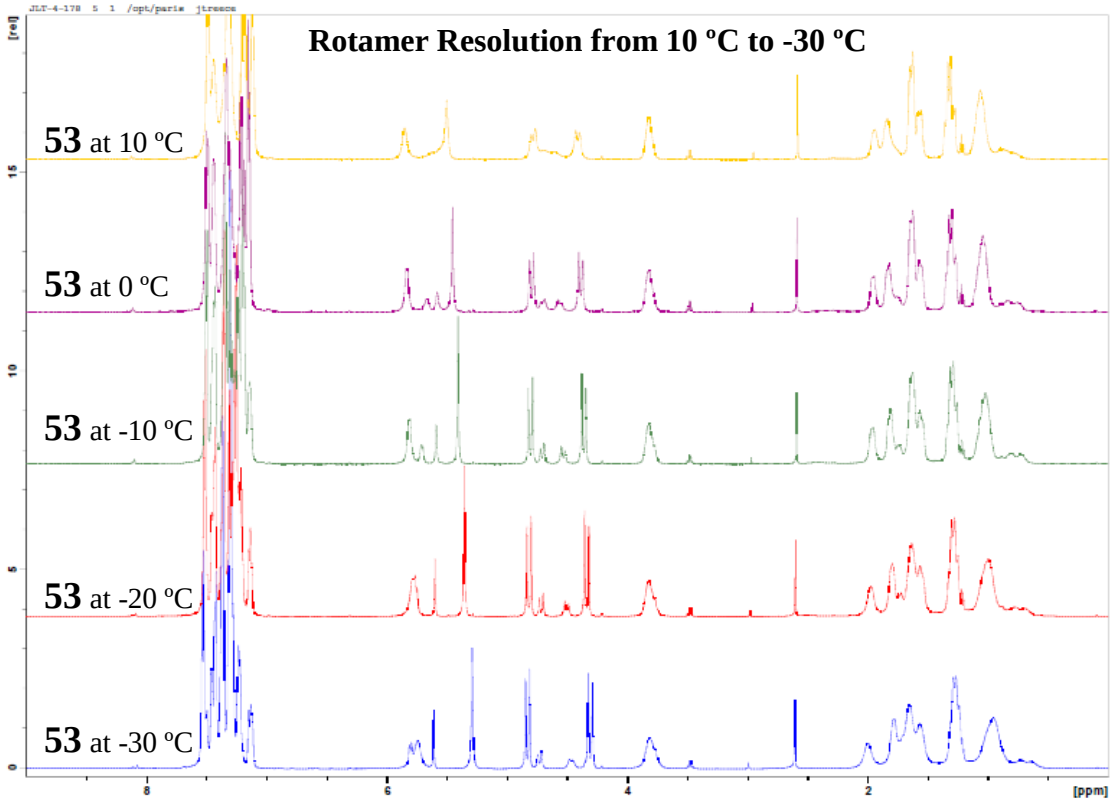
Rotamer Resolution from 10 ºC to -30 ºC
53 at 10 ºC
53 at 0 ºC
53 at -10 ºC
53 at -20 ºC
53 at -30 ºC
[ppm]

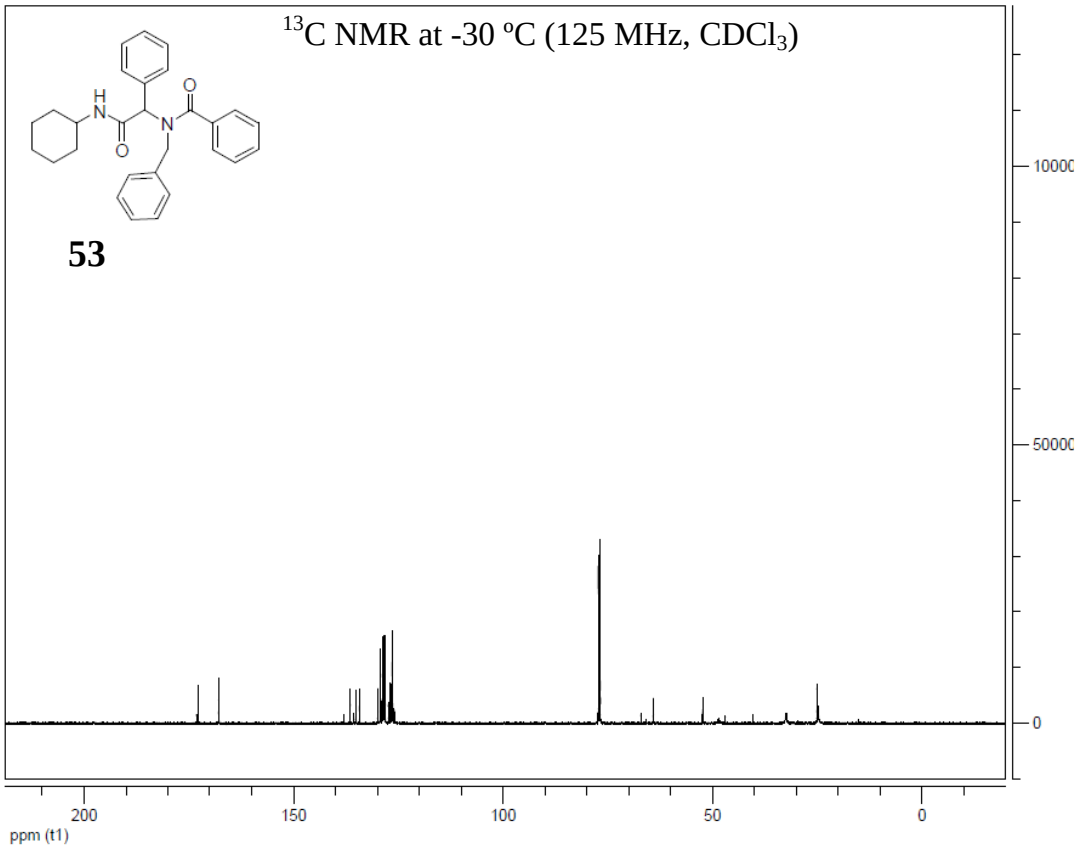
$^{13}$C NMR at -30 ºC (125 MHz, $CDCl_3$)
53
10000
50000
0
200
150
100
50
0
ppm (t1)

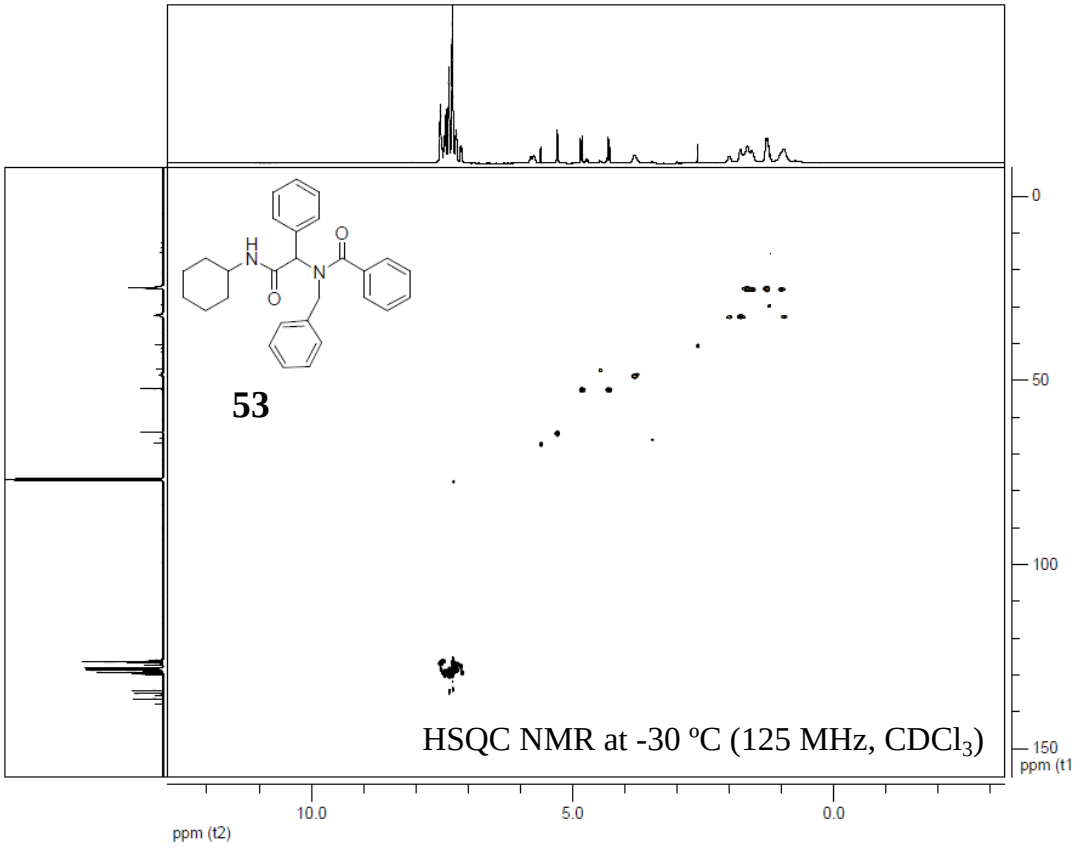
53
HSQC NMR at -30 ºC (125 MHz, $CDCl_3$)
0
50
100
150
ppm (t1
10.0
5.0
0.0
ppm (t2)

$^{1}$H NMR (500 MHz, $CDCl_3$)

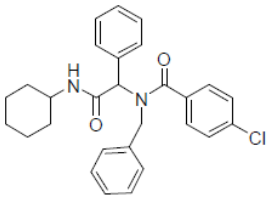

**54**




$^{13}$C NMR (125 MHz, $CDCl_3$)

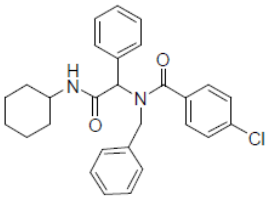

**54**

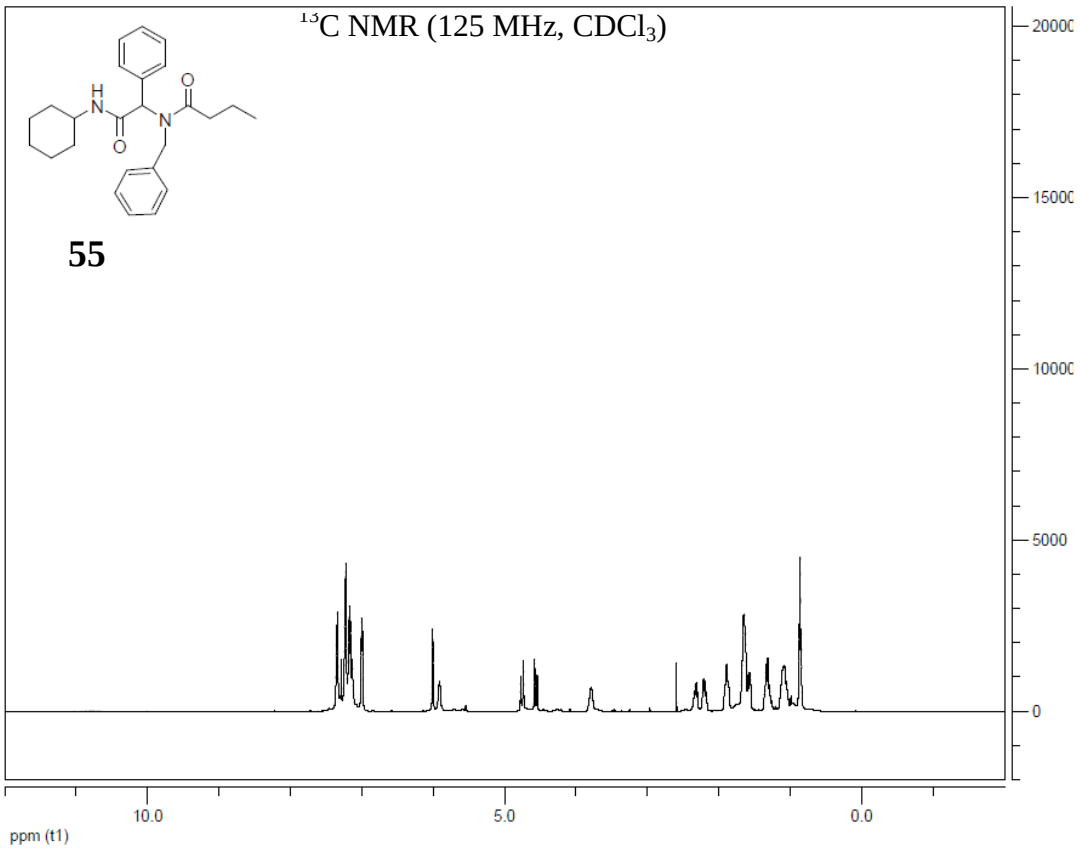
$^{13}$C NMR (125 MHz, CDCl$_3$)
55
20000
15000
10000
5000
0
10.0
5.0
0.0
ppm (t1)

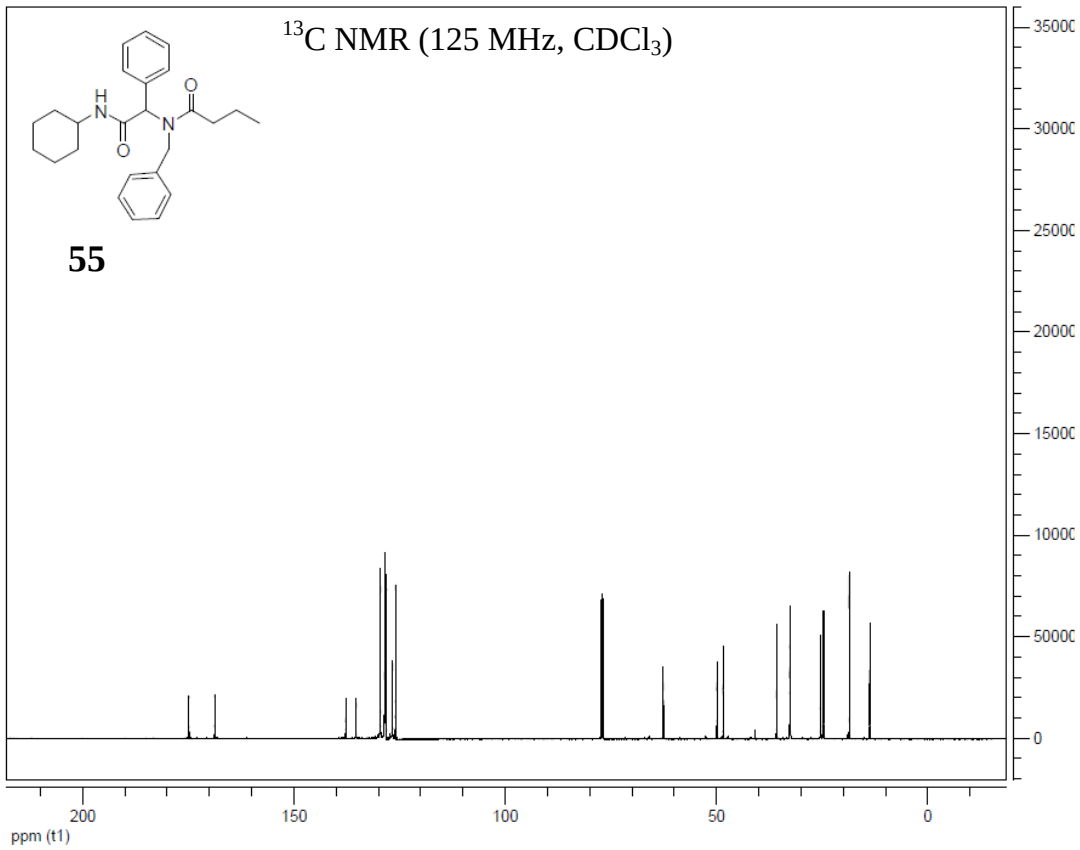
$^{13}$C NMR (125 MHz, CDCl$_3$)
55
35000
30000
25000
20000
15000
10000
5000
0
200
150
100
50
0
ppm (t1)

$^{1}$H NMR (500 MHz, $CDCl_3$)

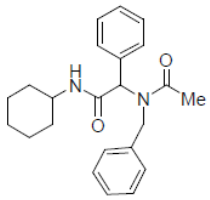


**56**




$^{13}$C NMR (125 MHz, $CDCl_3$)

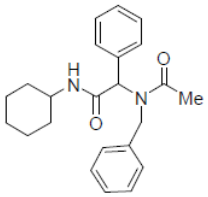


**56**

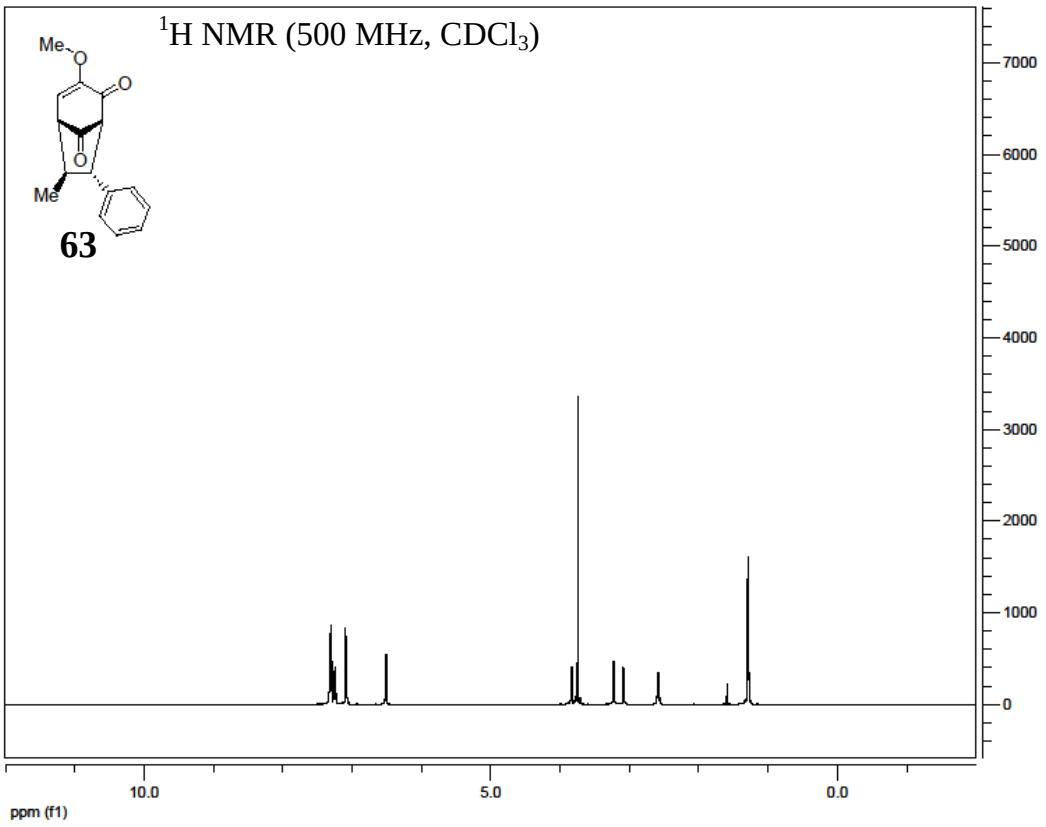
$^{1}$H NMR (500 MHz, $CDCl_3$)
Me
O
O
O
Me
63
7000
6000
5000
4000
3000
2000
1000
0
10.0
5.0
0.0
ppm (f1)

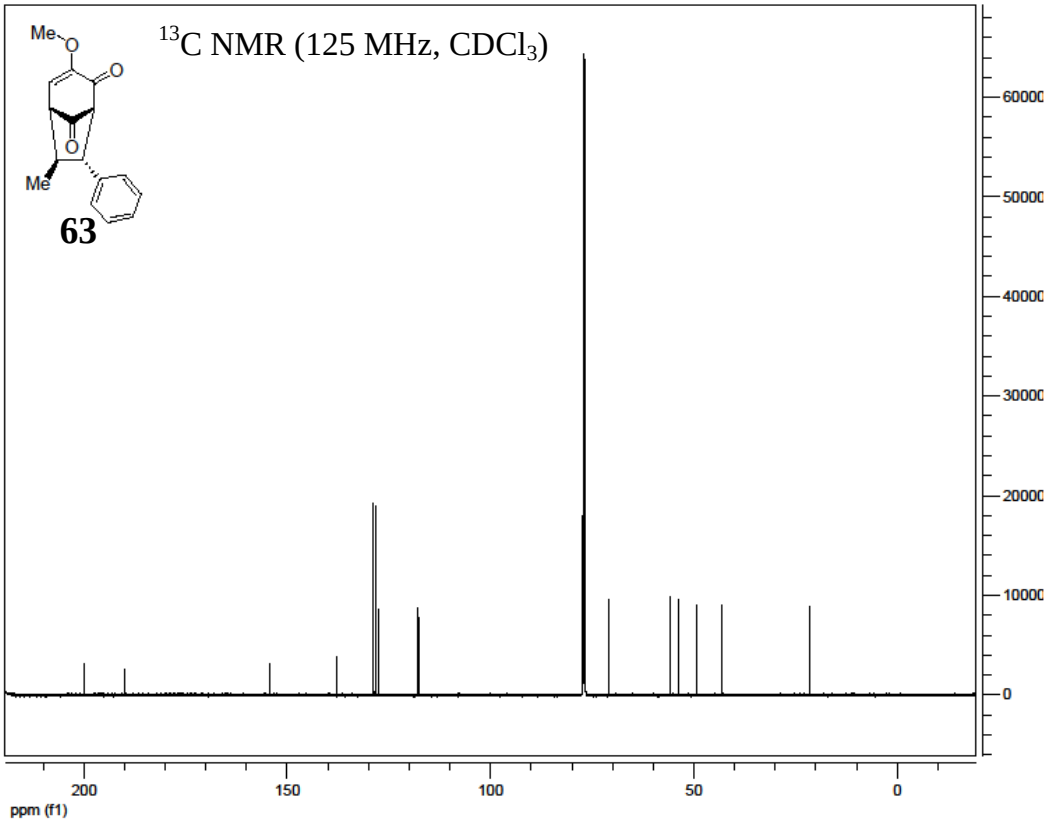
$^{13}$C NMR (125 MHz, $CDCl_3$)
Me
O
O
O
Me
63
60000
50000
40000
30000
20000
10000
0
200
150
100
50
0
ppm (f1)

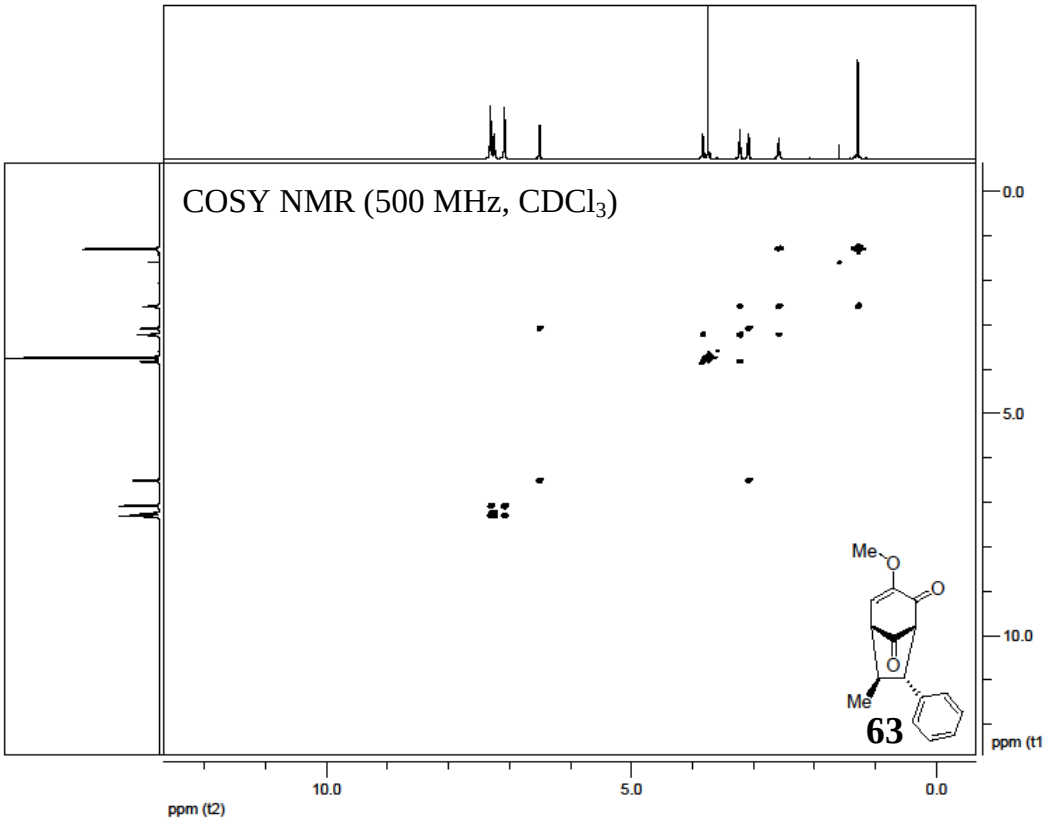
COSY NMR (500 MHz, CDCl3)
Me
O
O
O
Me
63
0.0
5.0
10.0
ppm (t1
10.0
5.0
0.0
ppm (t2)

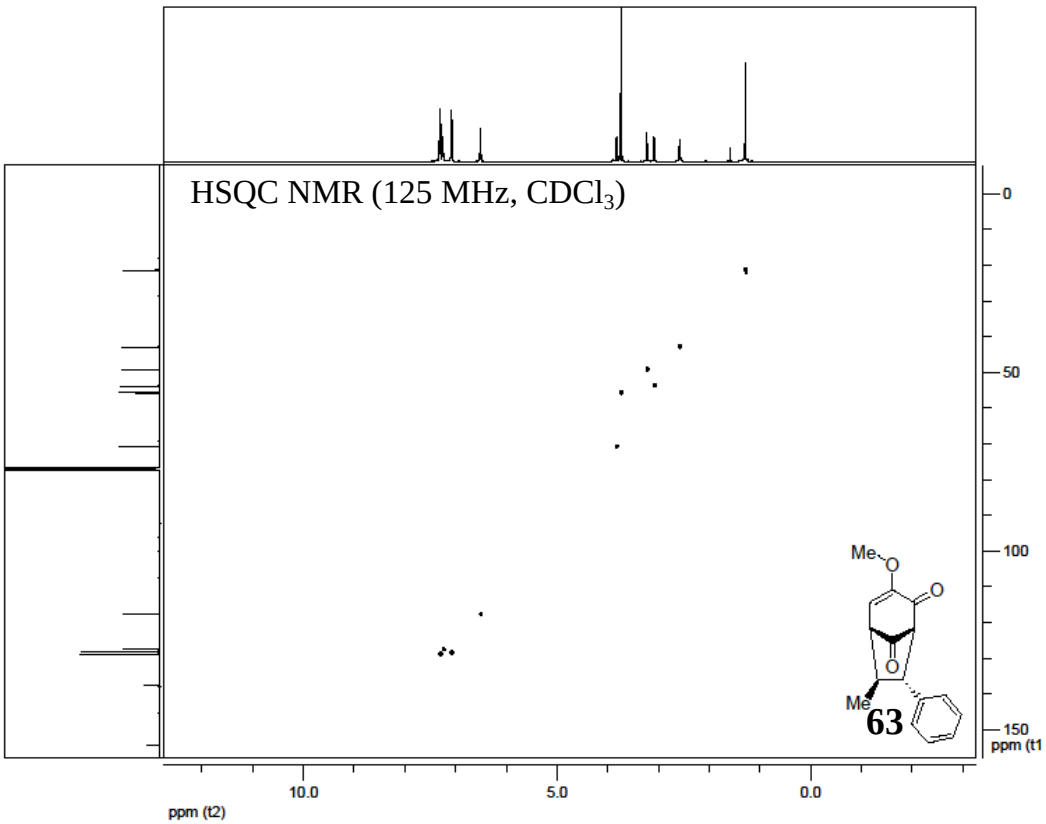
HSQC NMR (125 MHz, CDCl3)
Me
O
O
O
Me
63
0
50
100
150
ppm (t1
10.0
5.0
0.0
ppm (t2)

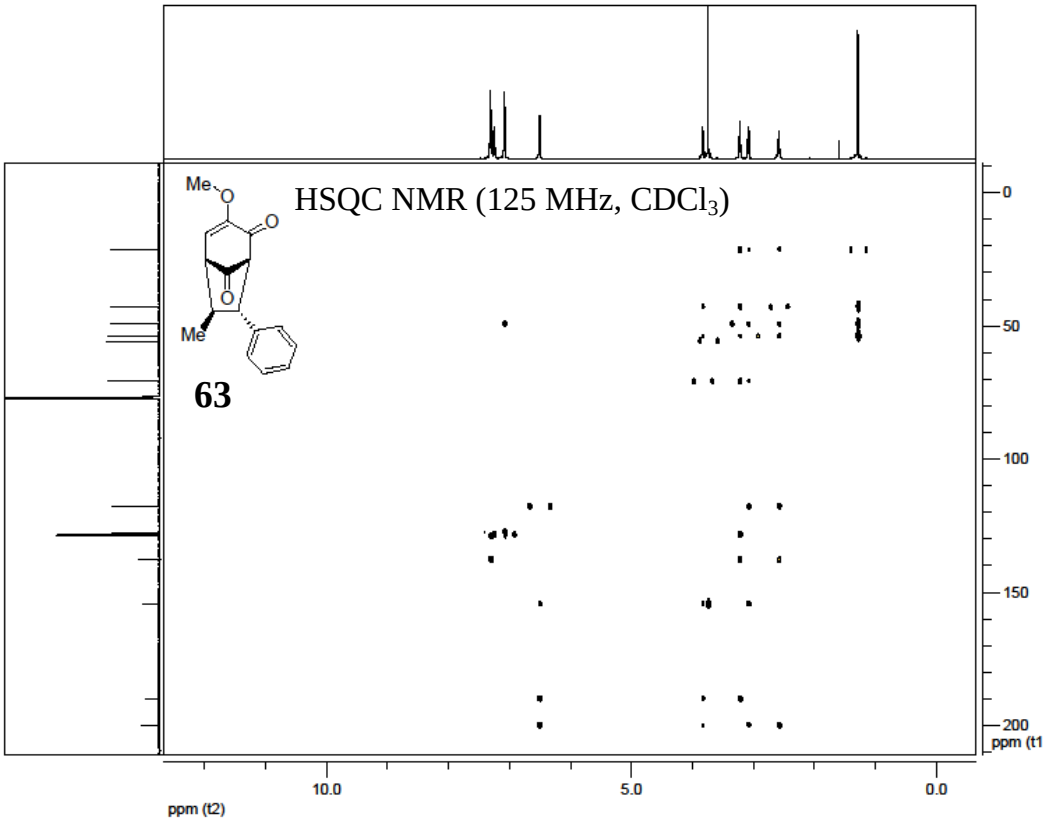
HSQC NMR (125 MHz, CDCl3)
Me
O
O
O
Me
63
0
50
100
150
200
ppm (t1
10.0
5.0
0.0
ppm (t2)

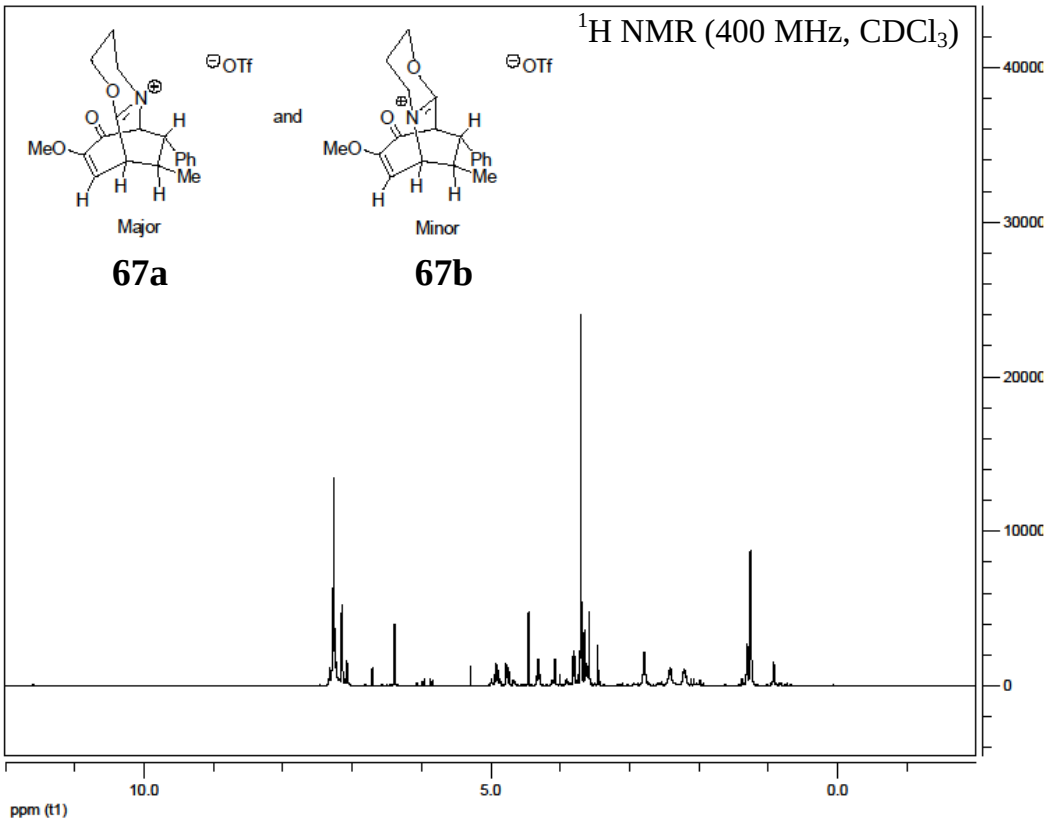
$^{1}$H NMR (400 MHz, $CDCl_3$)
⊖OTf
and
⊖OTf
MeO
Ph
Me
H
Major
Minor
67a
67b
4000
3000
2000
1000
0
10.0
5.0
0.0
ppm (t1)

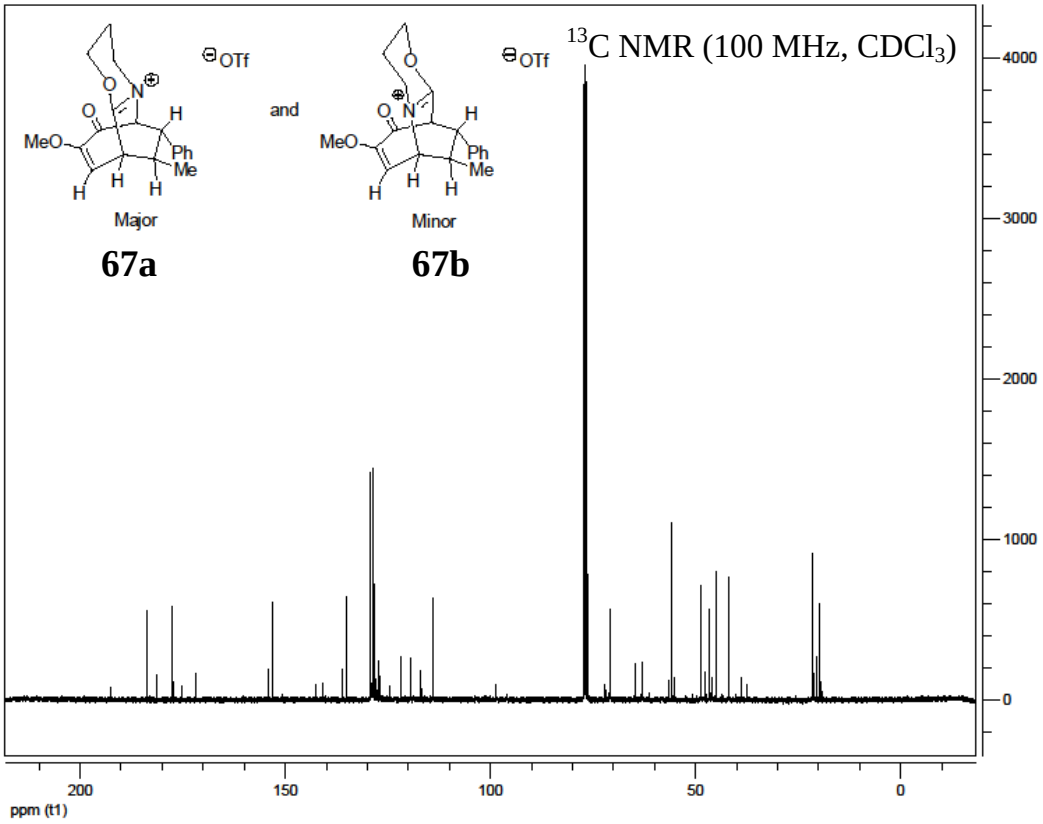
$^{13}$C NMR (100 MHz, $CDCl_3$)
⊖OTf
and
⊖OTf
MeO
Ph
Me
H
Major
Minor
67a
67b
4000
3000
2000
1000
0
200
150
100
50
0
ppm (t1)

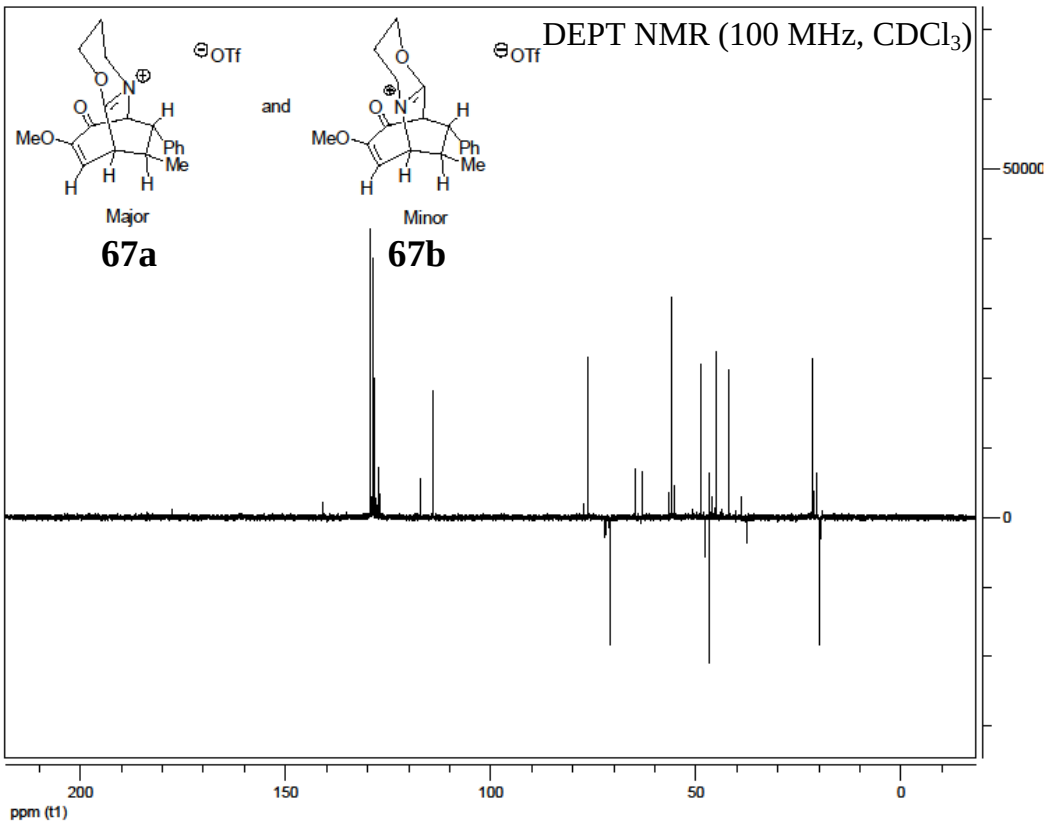
DEPT NMR (100 MHz, CDCl3)
⊖OTf
and
⊖OTf
MeO
Ph
Me
Major
67a
Minor
67b
50000
0
200
150
100
50
0
ppm (t1)

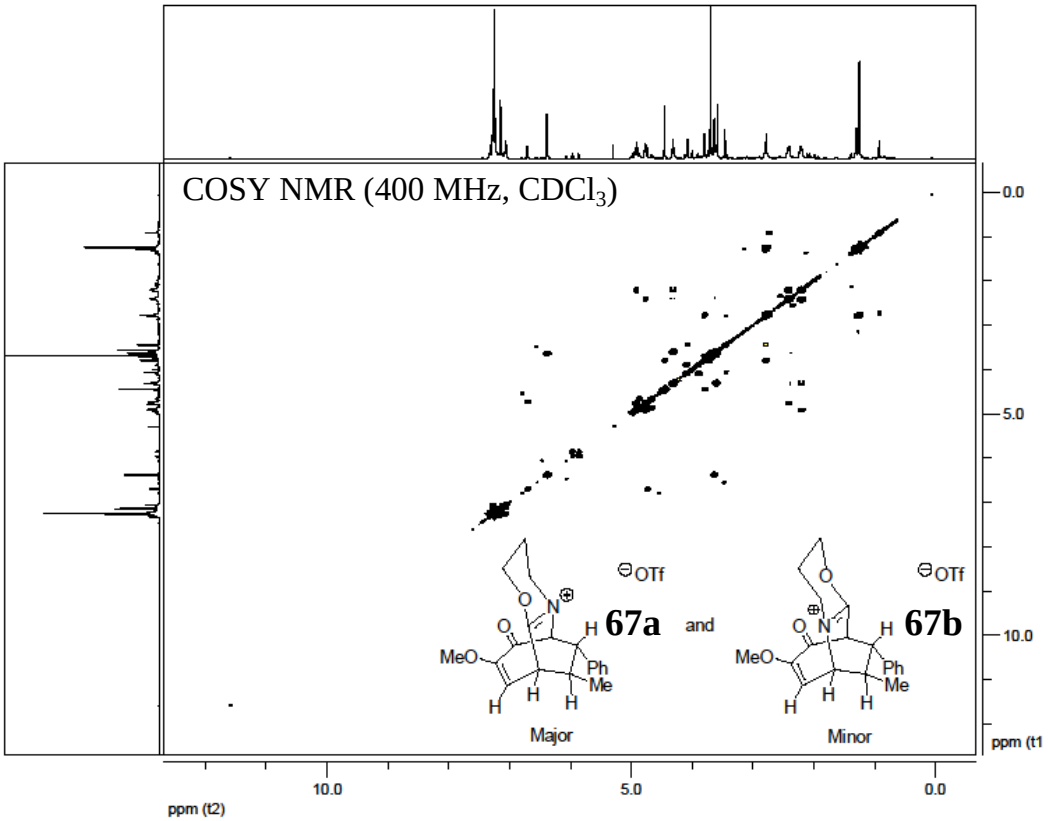
COSY NMR (400 MHz, CDCl3)
⊖OTf
67a
and
⊖OTf
67b
MeO
Ph
Me
Major
Minor
0.0
5.0
10.0
ppm (t1)
10.0
5.0
0.0
ppm (t2)

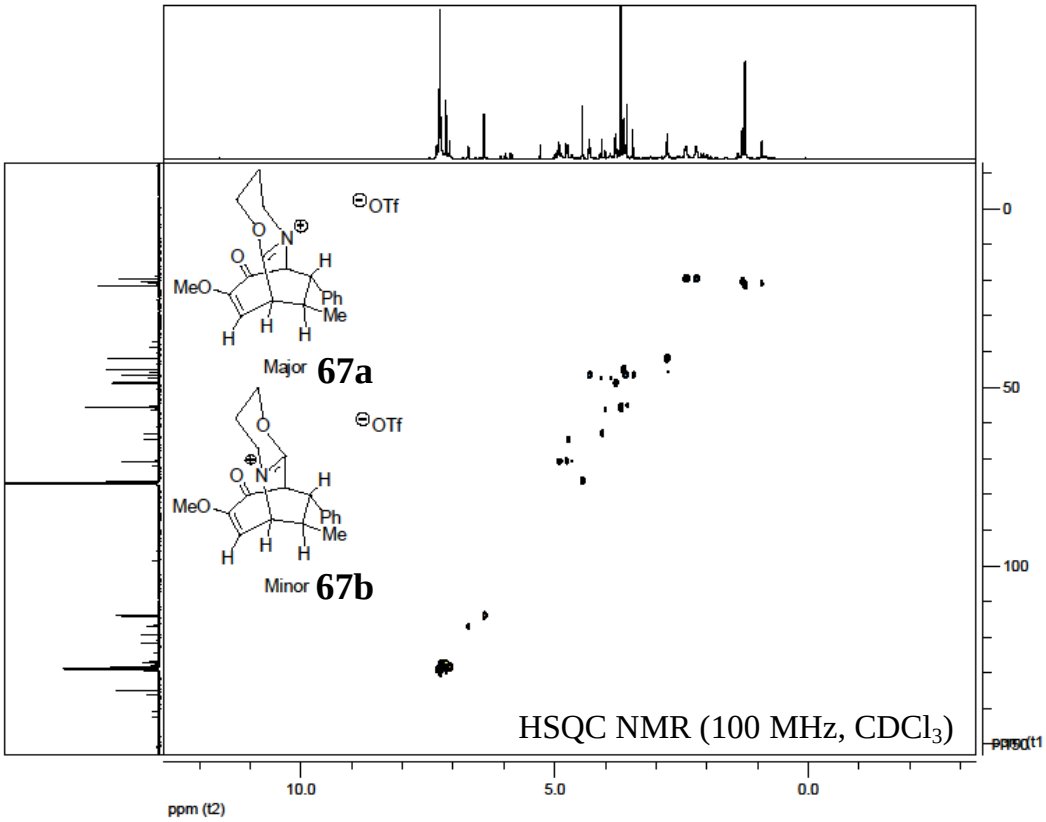
⊖OTf
MeO
Ph
Me
H
Major 67a
⊖OTf
MeO
Ph
Me
H
Minor 67b
HSQC NMR (100 MHz, CDCl3)
10.0
5.0
0.0
ppm (t2)
0
50
100

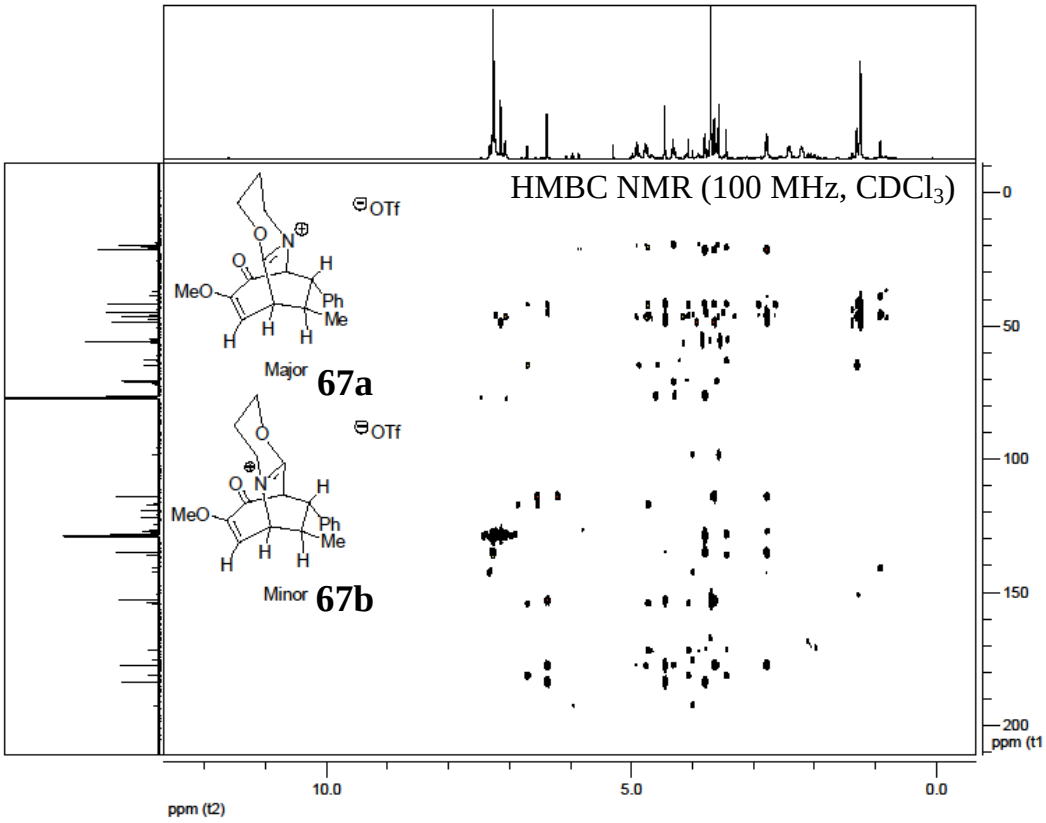
HMBC NMR (100 MHz, CDCl3)
⊖OTf
MeO
Ph
Me
H
Major 67a
⊖OTf
MeO
Ph
Me
H
Minor 67b
10.0
5.0
0.0
ppm (t2)
0
50
100
150
200
ppm (t1

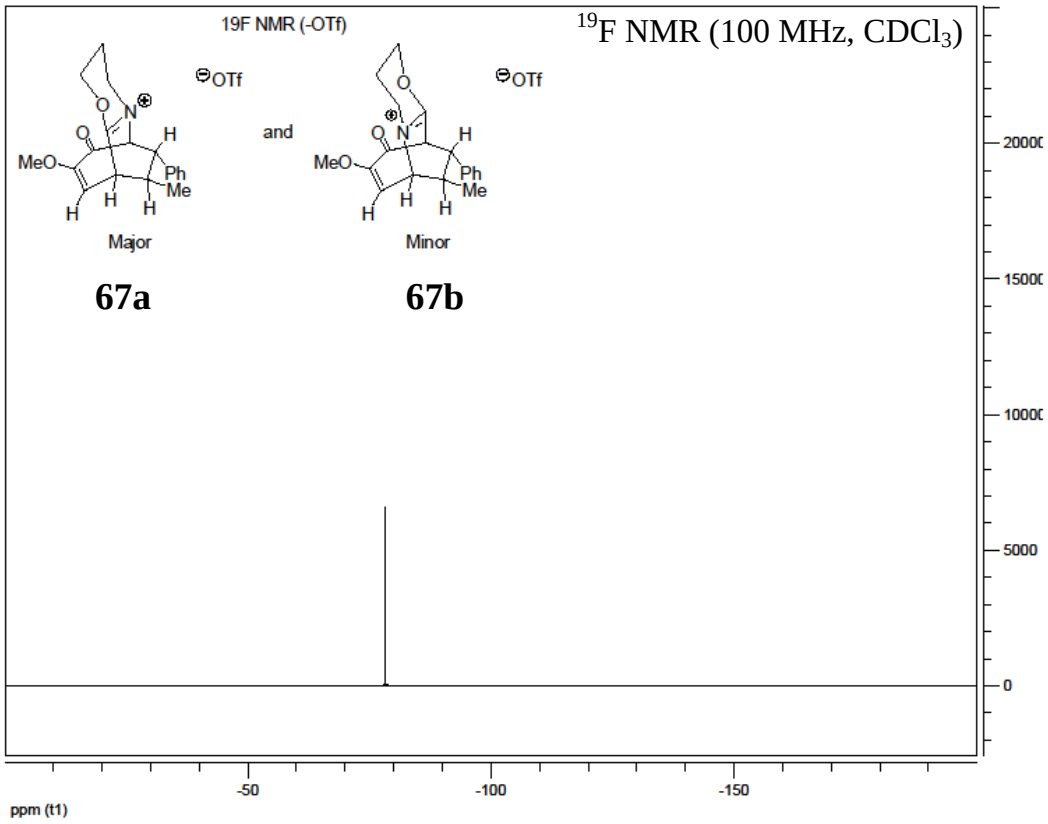
19F NMR (-OTf)
$^{19}$F NMR (100 MHz, $CDCl_3$)
⊖OTf
and
⊖OTf
MeO
Ph
Me
H
Major
Minor
67a
67b
2000
1500
1000
5000
0
-50
-100
-150
ppm (t1)

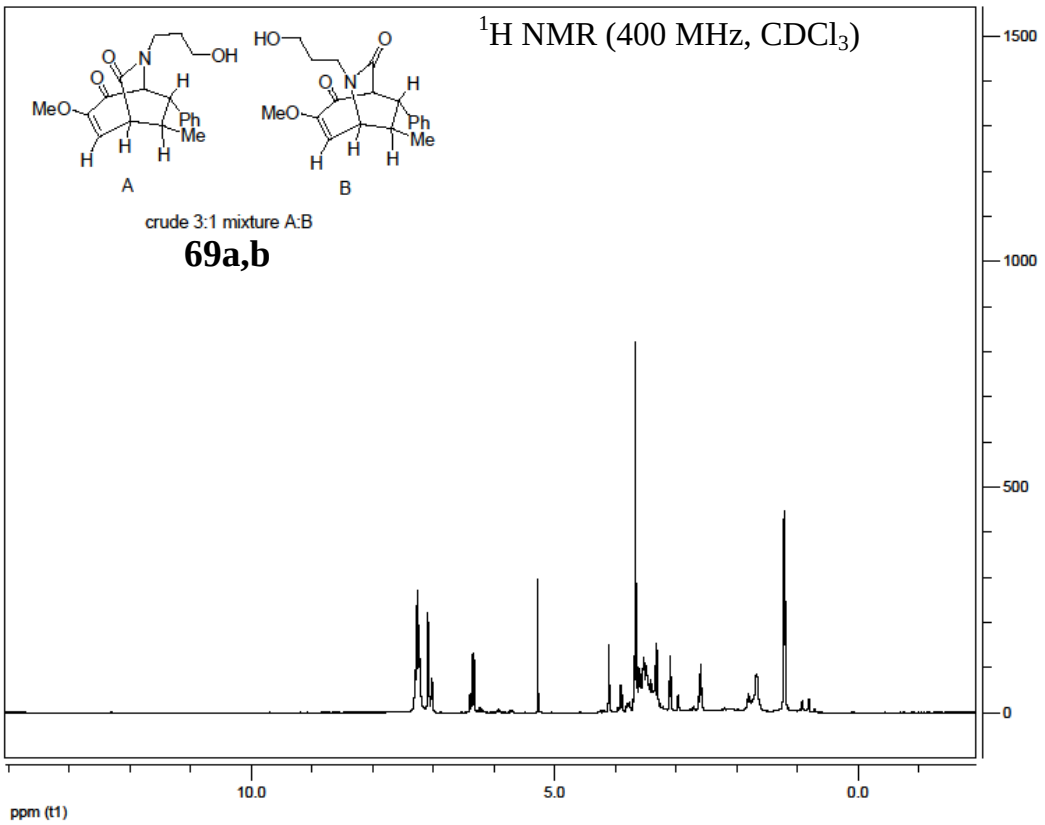
$^{1}$H NMR (400 MHz, $CDCl_3$)
crude 3:1 mixture A:B
69a,b
A
B
1500
1000
500
0
10.0
5.0
0.0
ppm (t1)

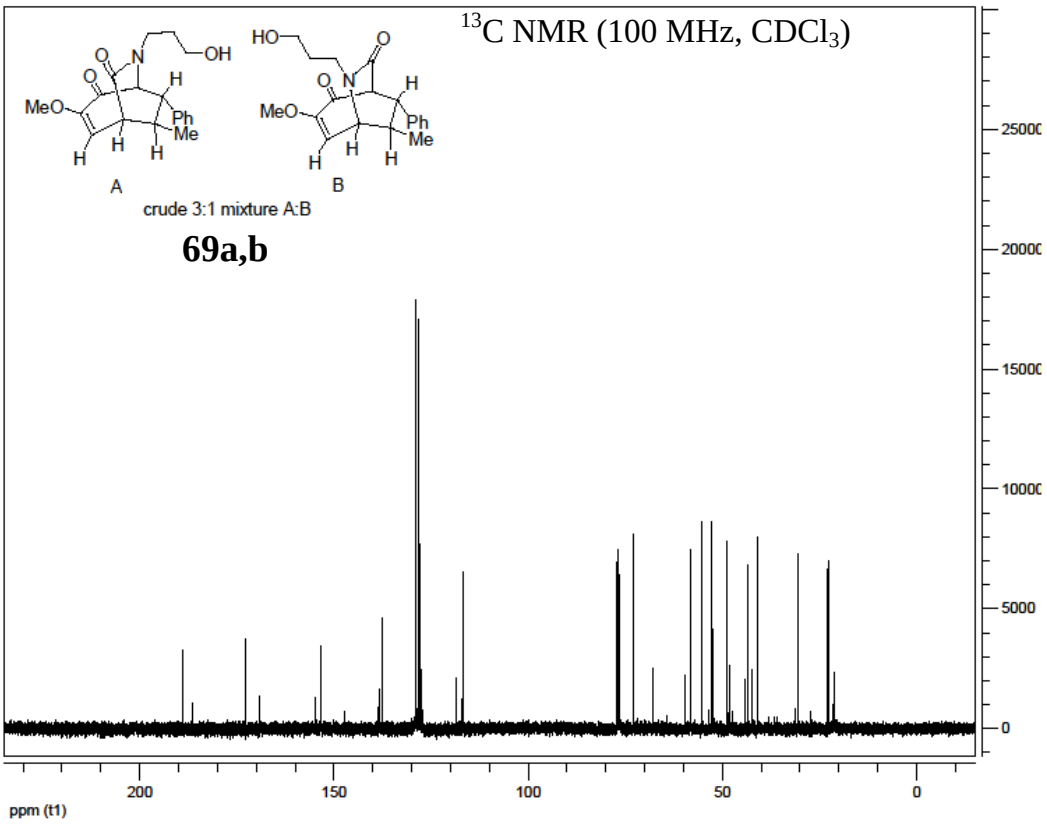
$^{13}$C NMR (100 MHz, $CDCl_3$)
crude 3:1 mixture A:B
69a,b
A
B
25000
20000
15000
10000
5000
0
200
150
100
50
0
ppm (t1)

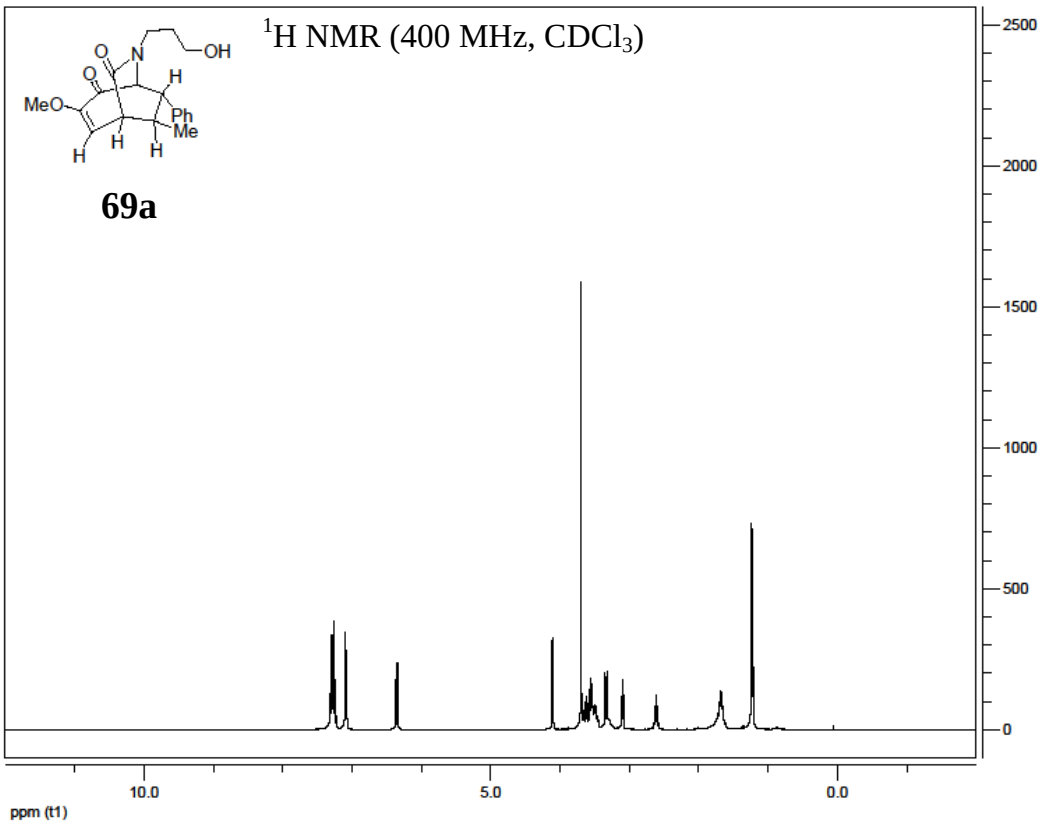


$^{1}$H NMR (400 MHz, $CDCl_3$)

**69a**

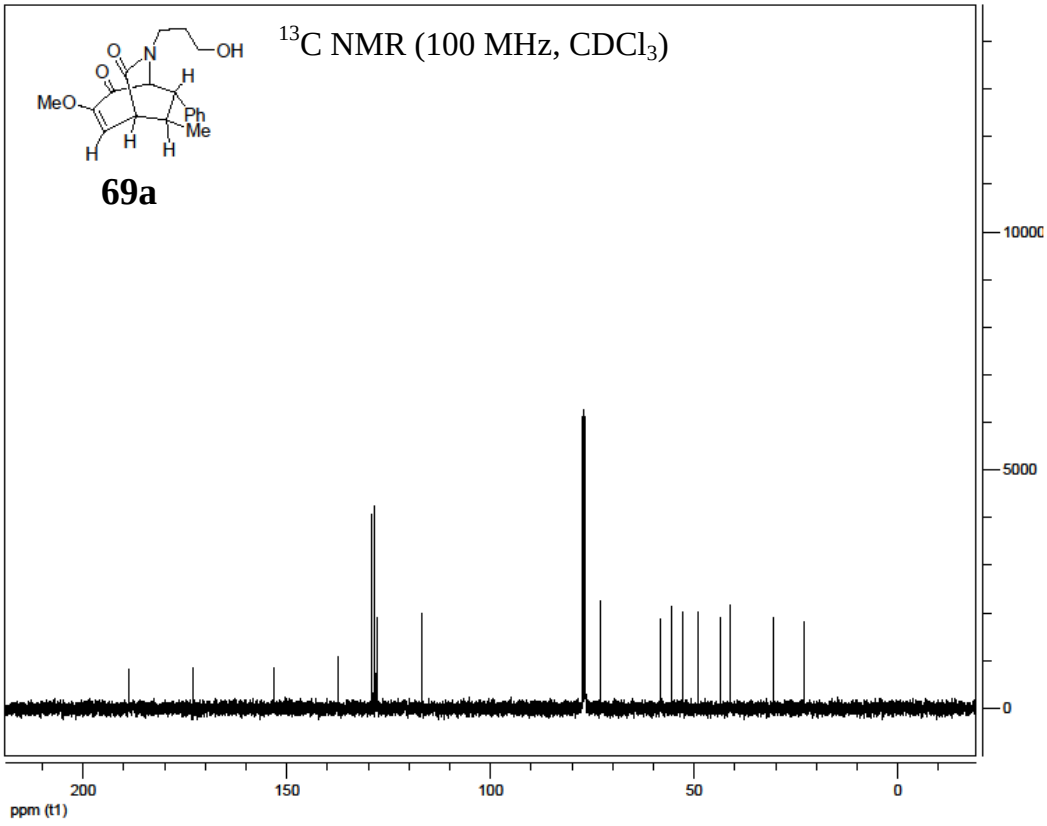


$^{13}$C NMR (100 MHz, $CDCl_3$)

**69a**

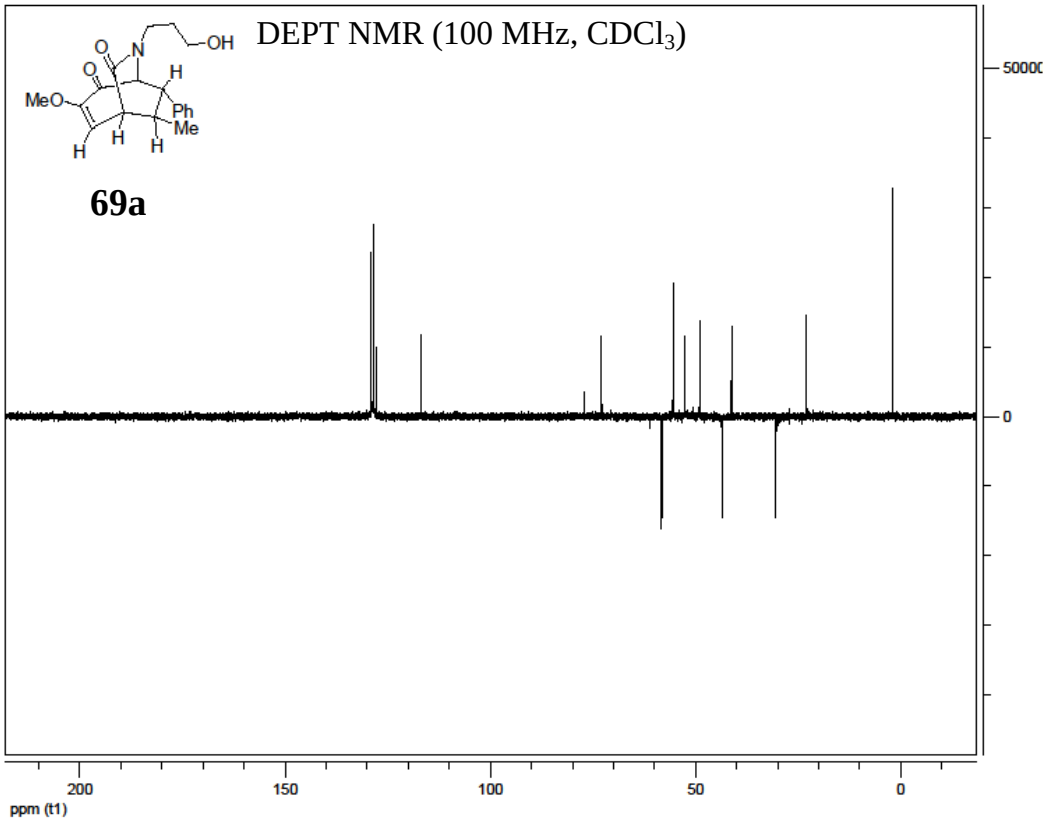
DEPT NMR (100 MHz, CDCl3)
69a
MeO
OH
Ph
Me
50000
0
200
150
100
50
0
ppm (t1)

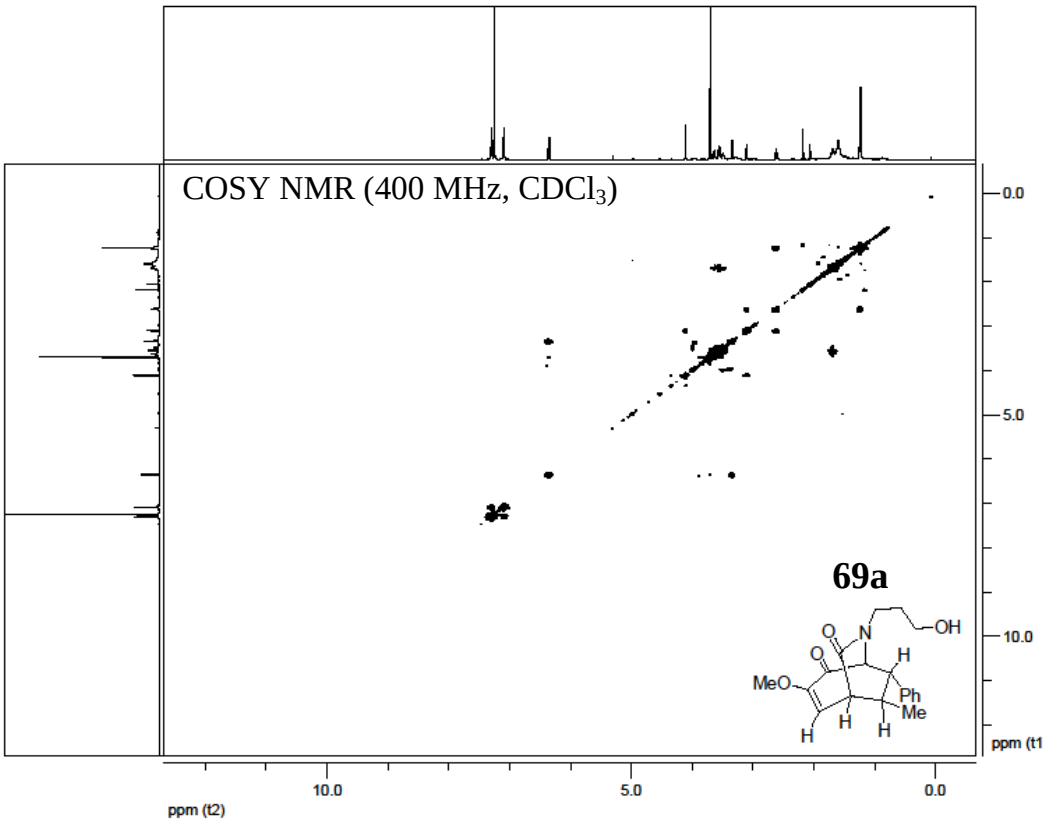
COSY NMR (400 MHz, CDCl3)
69a
MeO
OH
Ph
Me
0.0
5.0
10.0
ppm (t1
10.0
5.0
0.0
ppm (t2)

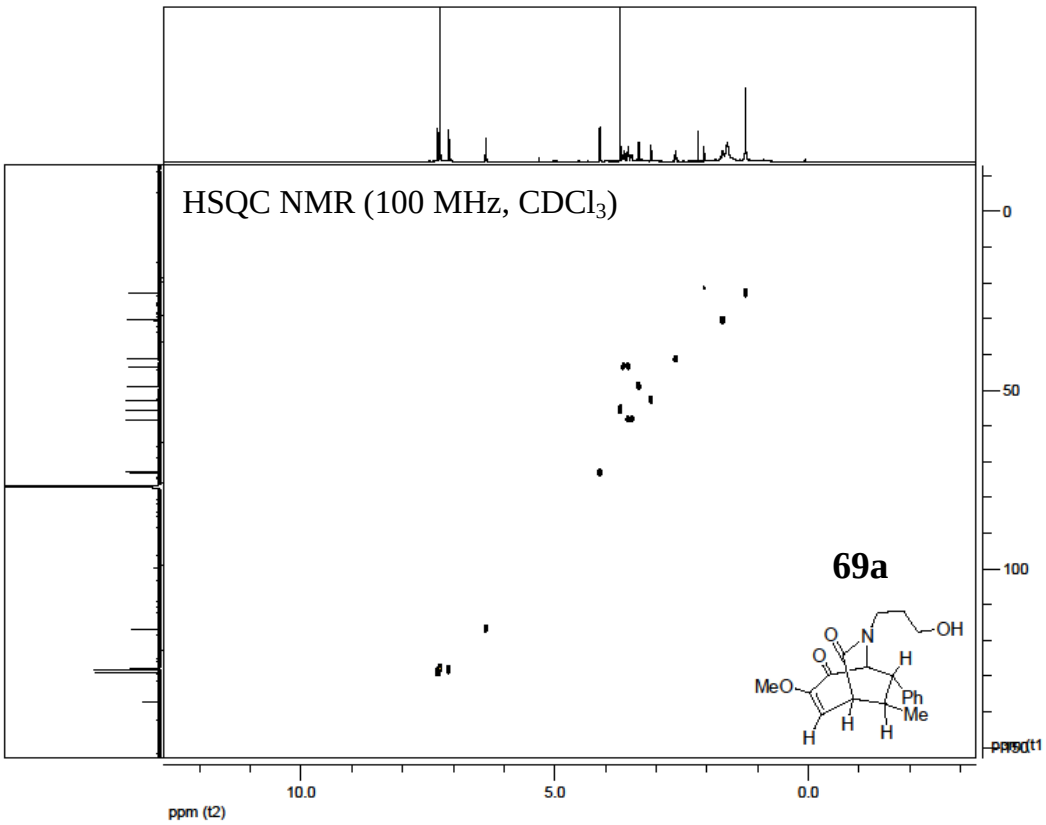
HSQC NMR (100 MHz, CDCl3)
69a
OH
O
N
O
H
MeO
Ph
Me
H
H
H
0
50
100
10.0
5.0
0.0
ppm (t2)

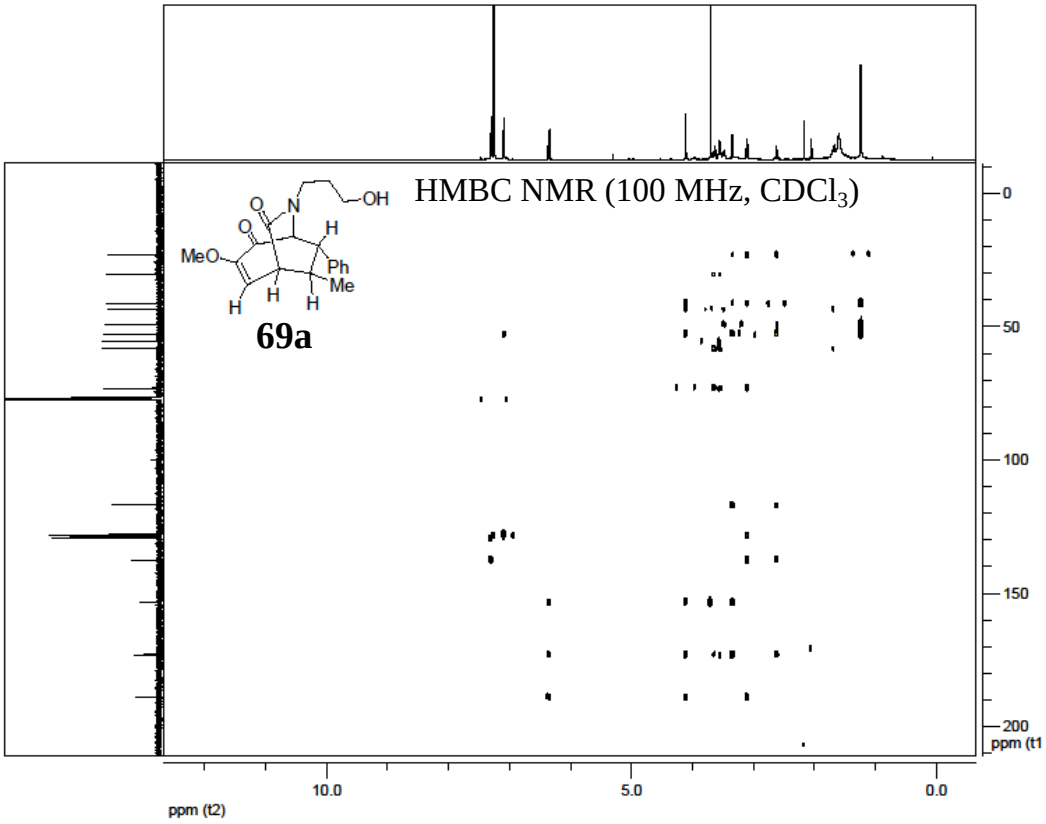
HMBC NMR (100 MHz, CDCl3)
69a
OH
O
N
O
H
MeO
Ph
Me
H
H
H
0
50
100
150
200
10.0
5.0
0.0
ppm (t2)

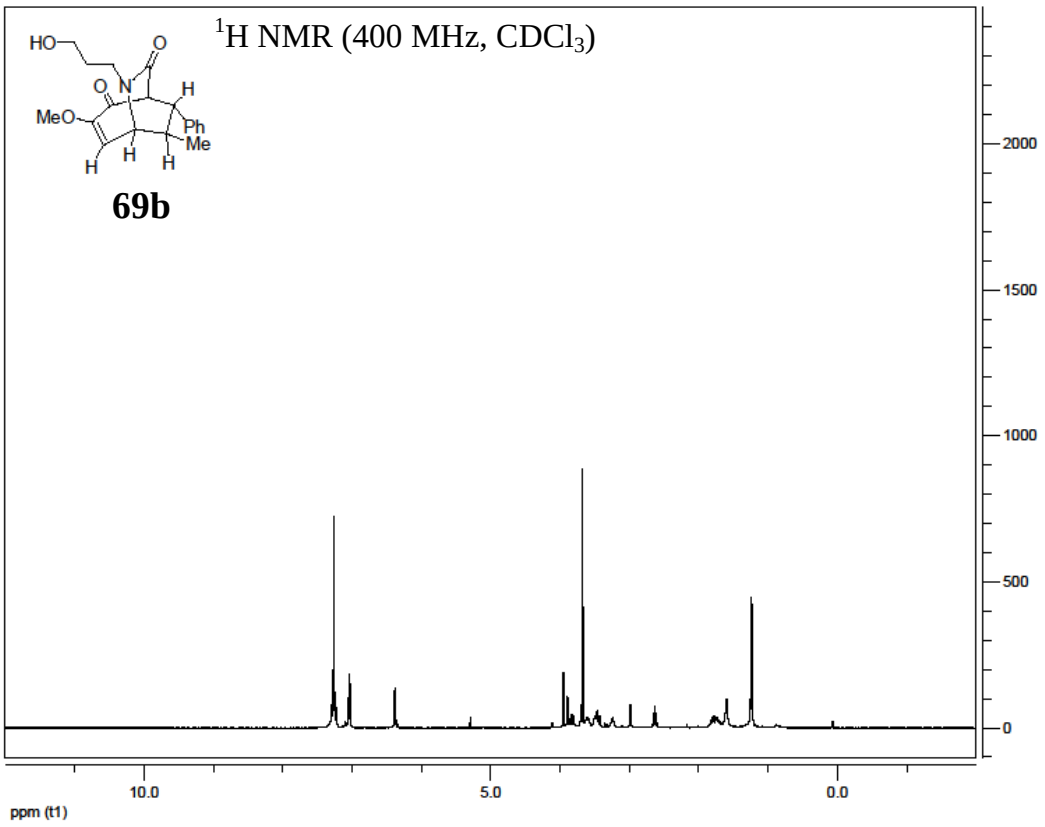
HO
O
O
N
H
MeO
Ph
Me
H
H
H
69b
$^{1}$H NMR (400 MHz, $CDCl_3$)
2000
1500
1000
500
0
10.0
5.0
0.0
ppm (t1)

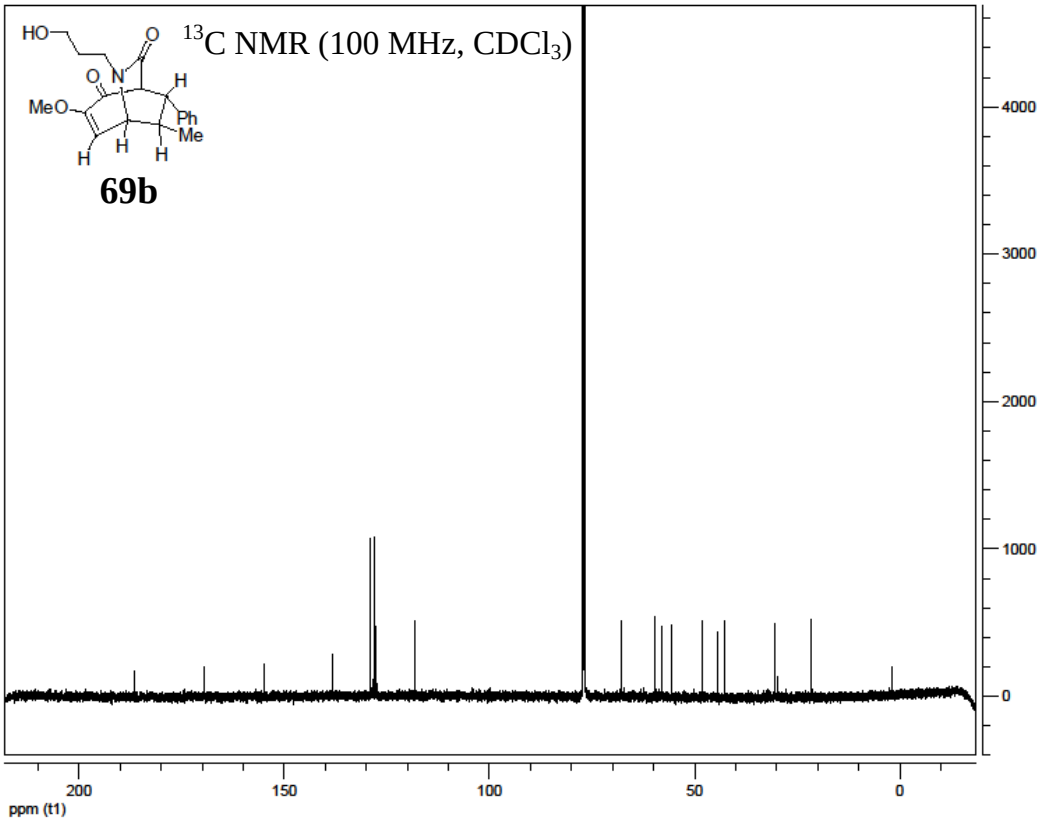
HO
O
O
N
H
MeO
Ph
Me
H
H
H
69b
$^{13}$C NMR (100 MHz, $CDCl_3$)
4000
3000
2000
1000
0
200
150
100
50
0
ppm (t1)

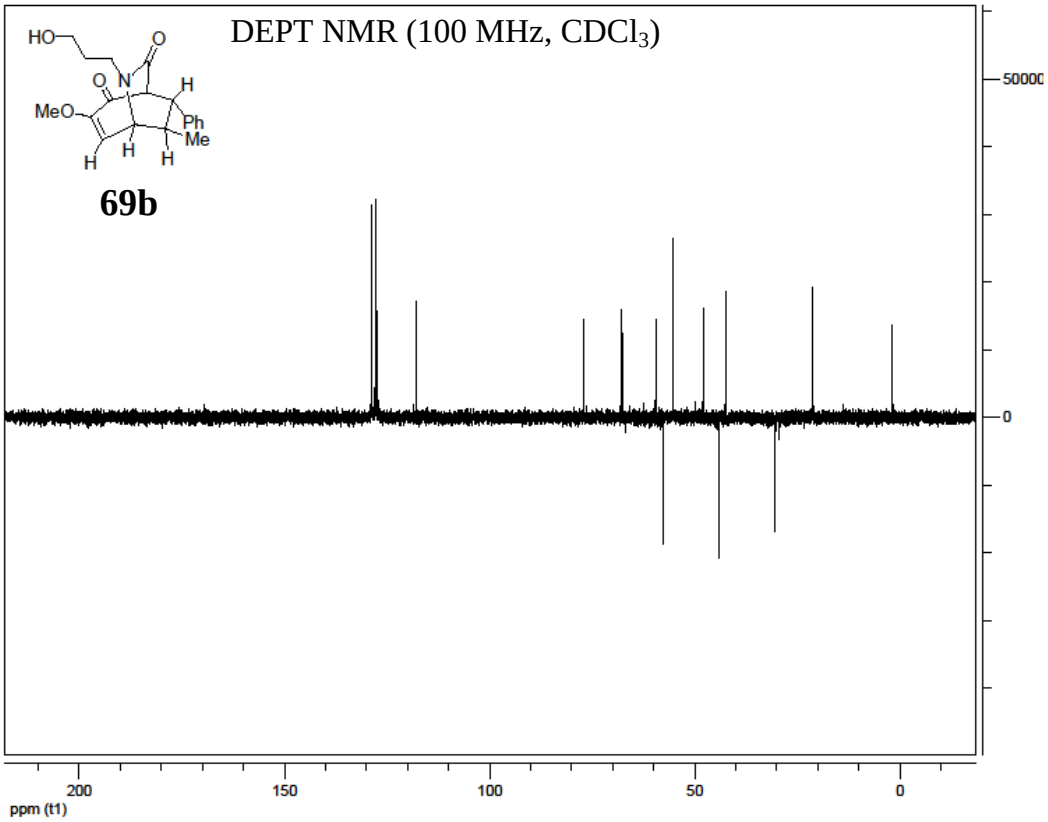
DEPT NMR (100 MHz, CDCl3)
HO
O
O
N
H
MeO
Ph
Me
H
H
H
69b
50000
0
200
150
100
50
0
ppm (t1)

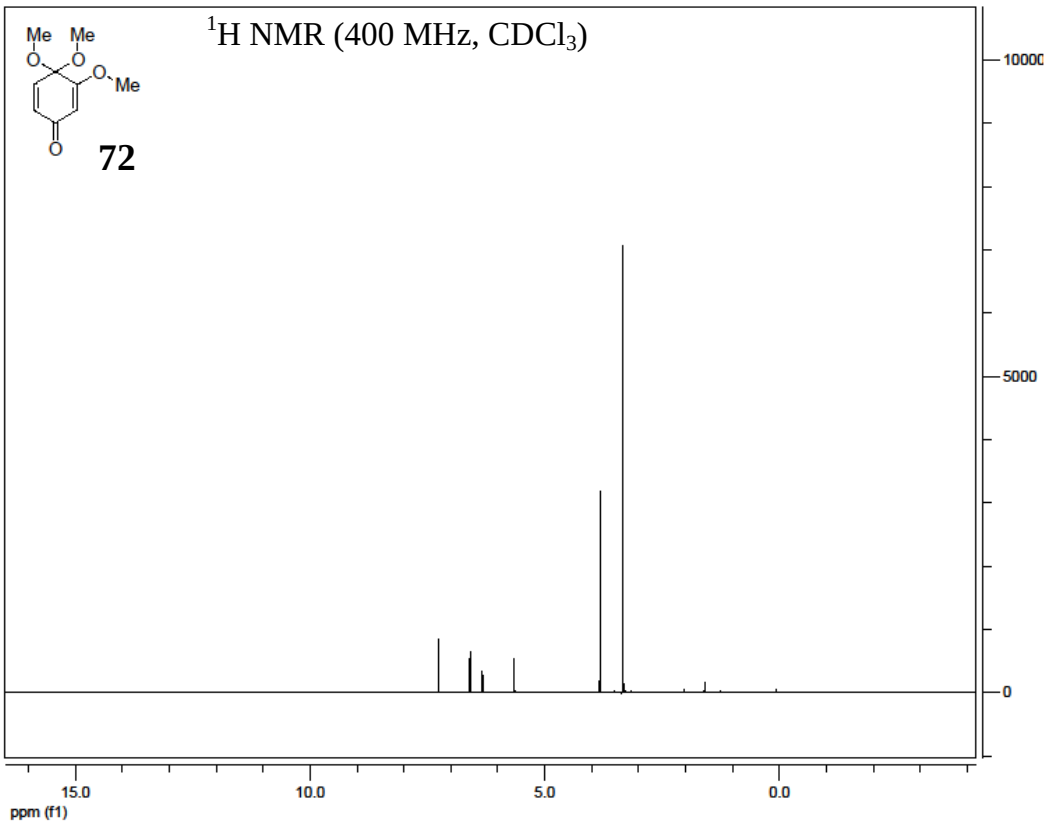
Me
Me
O
O
O
Me
O
72
$^{1}$H NMR (400 MHz, $CDCl_3$)
10000
5000
0
15.0
10.0
5.0
0.0
ppm (f1)

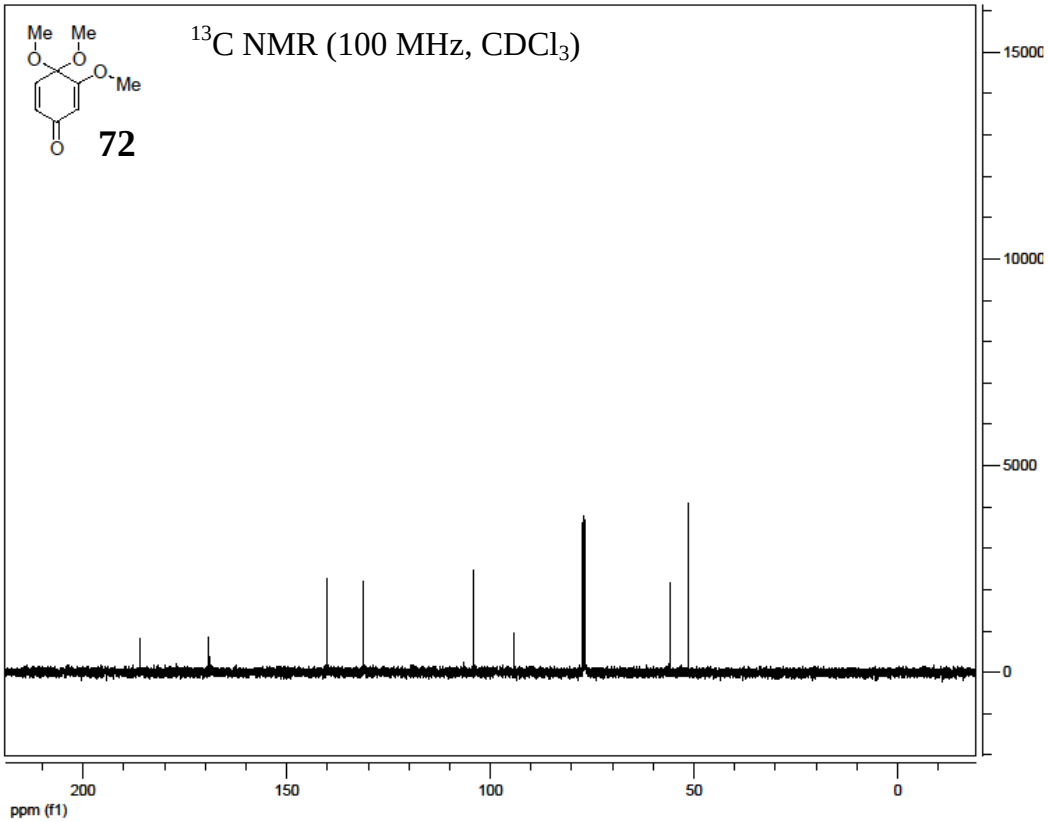
Me
Me
O
O
O
Me
O
72
$^{13}$C NMR (100 MHz, $CDCl_3$)
15000
10000
5000
0
200
150
100
50
0
ppm (f1)

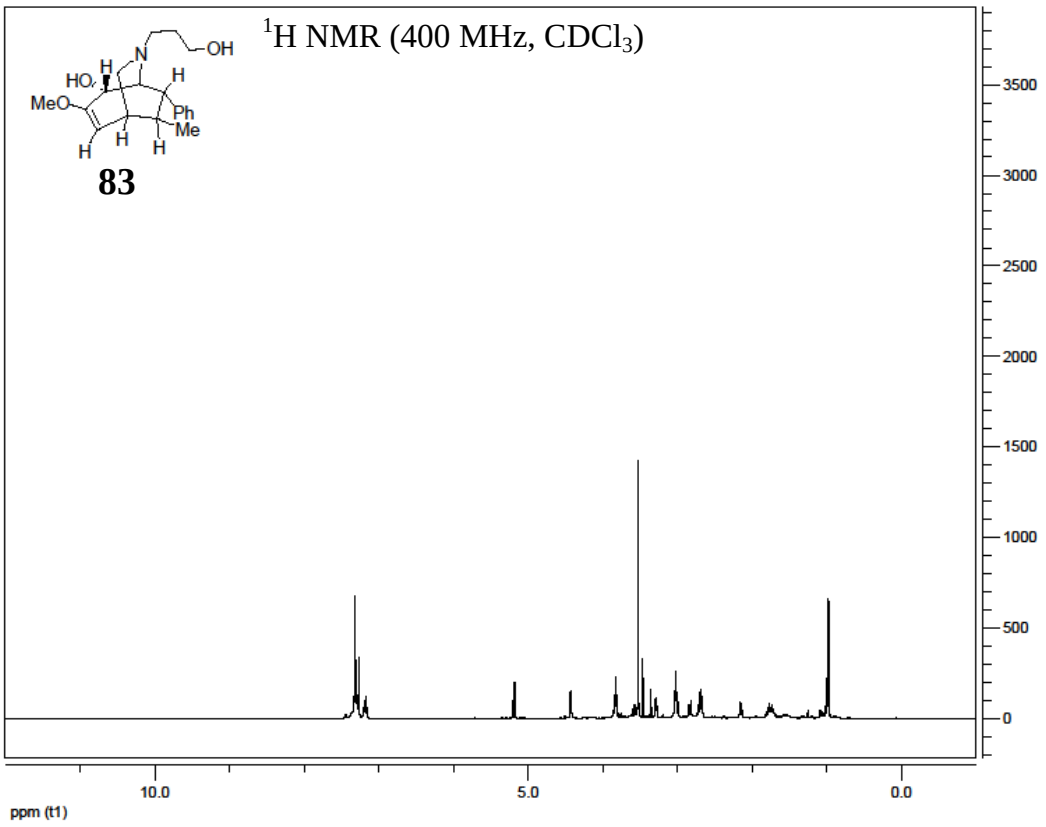
$^{1}$H NMR (400 MHz, $CDCl_3$)
OH
N
H
HO
H
MeO
Ph
Me
H
H
H
83
3500
3000
2500
2000
1500
1000
500
0
10.0
5.0
0.0
ppm (t1)

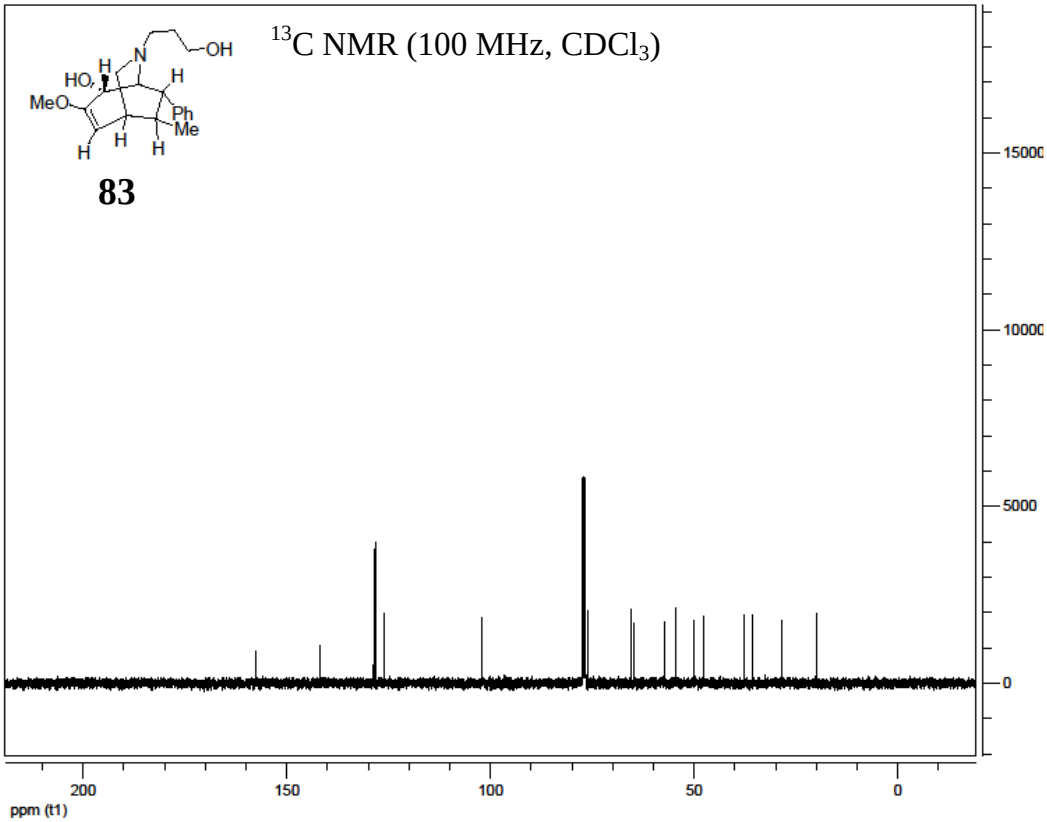
$^{13}$C NMR (100 MHz, $CDCl_3$)
OH
N
H
HO
H
MeO
Ph
Me
H
H
H
83
15000
10000
5000
0
200
150
100
50
0
ppm (t1)

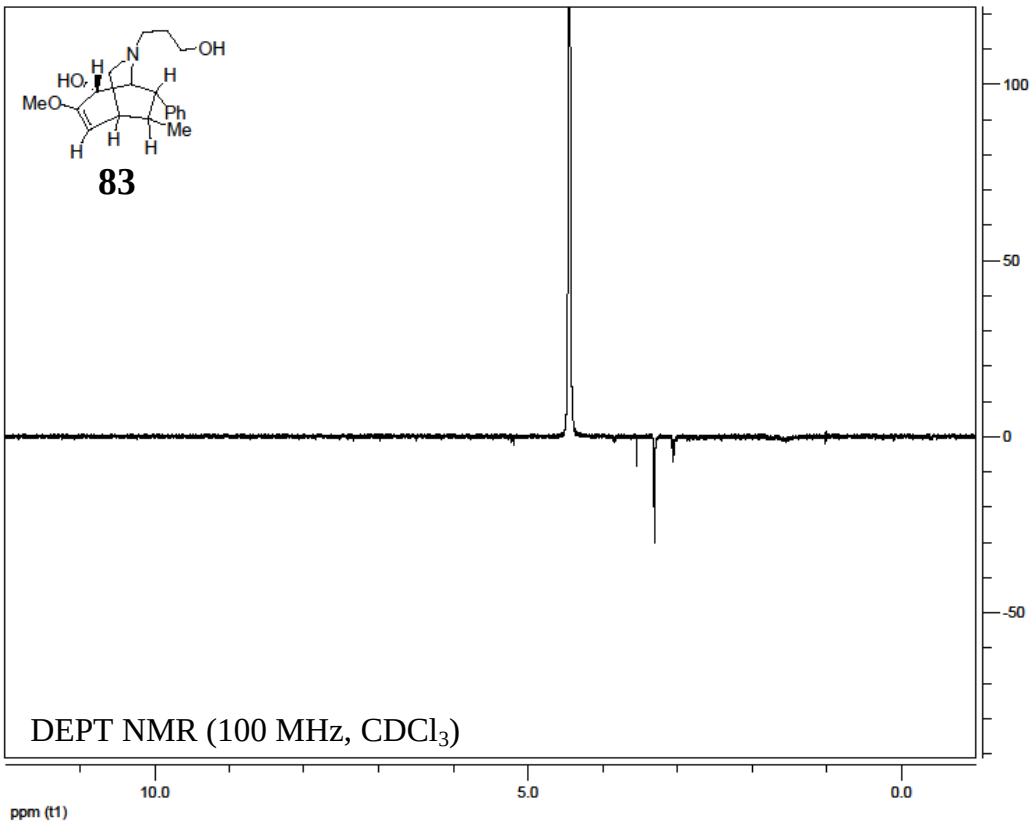
OH
N
H
HO
H
MeO
Ph
Me
H
H
H
83
100
50
0
-50
DEPT NMR (100 MHz, CDCl3)
10.0
5.0
0.0
ppm (t1)

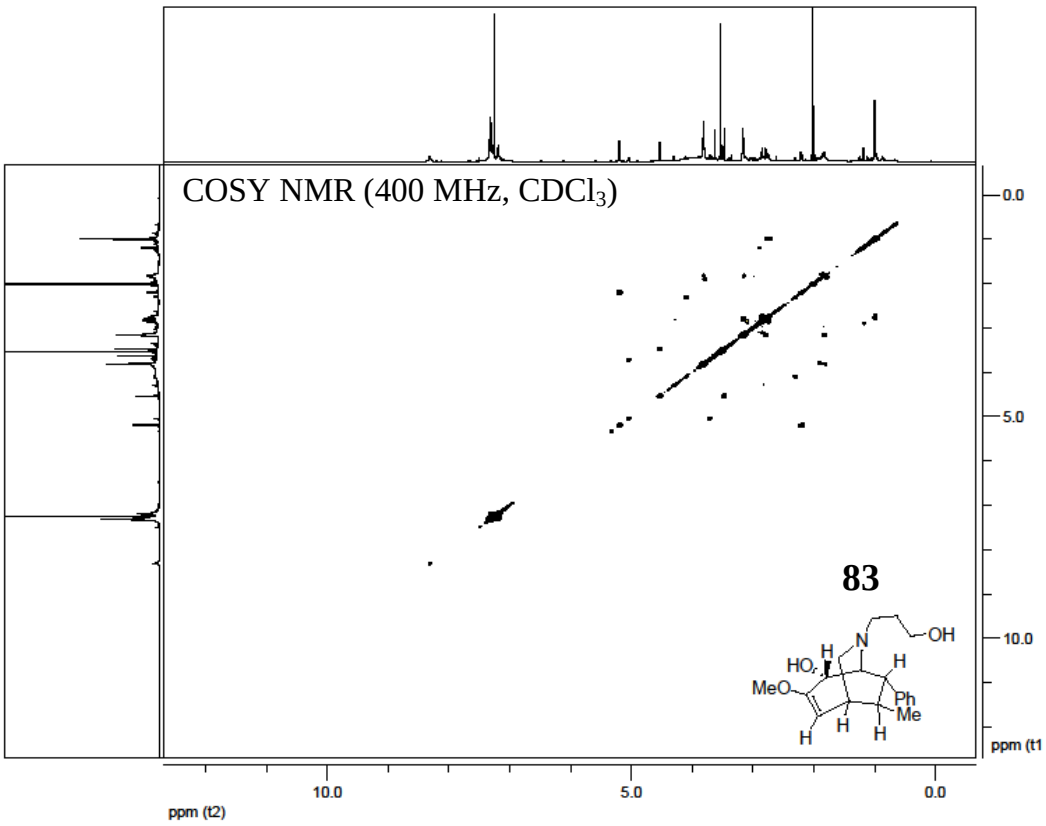
COSY NMR (400 MHz, CDCl3)
83
OH
N
H
HO
H
MeO
Ph
Me
H
H
H
0.0
5.0
10.0
ppm (t1
10.0
5.0
0.0
ppm (t2)

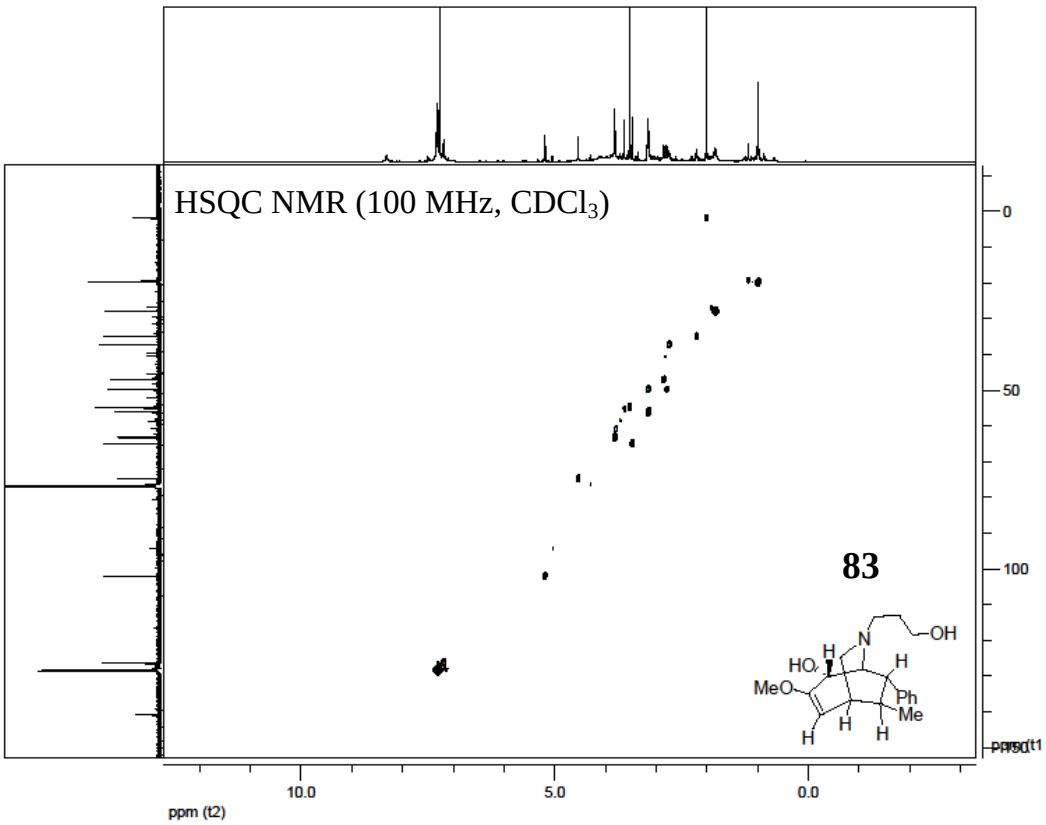
HSQC NMR (100 MHz, CDCl3)
83
OH
N
H
HO
H
MeO
Ph
Me
H
H
H
0
50
100
10.0
5.0
0.0
ppm (t2)

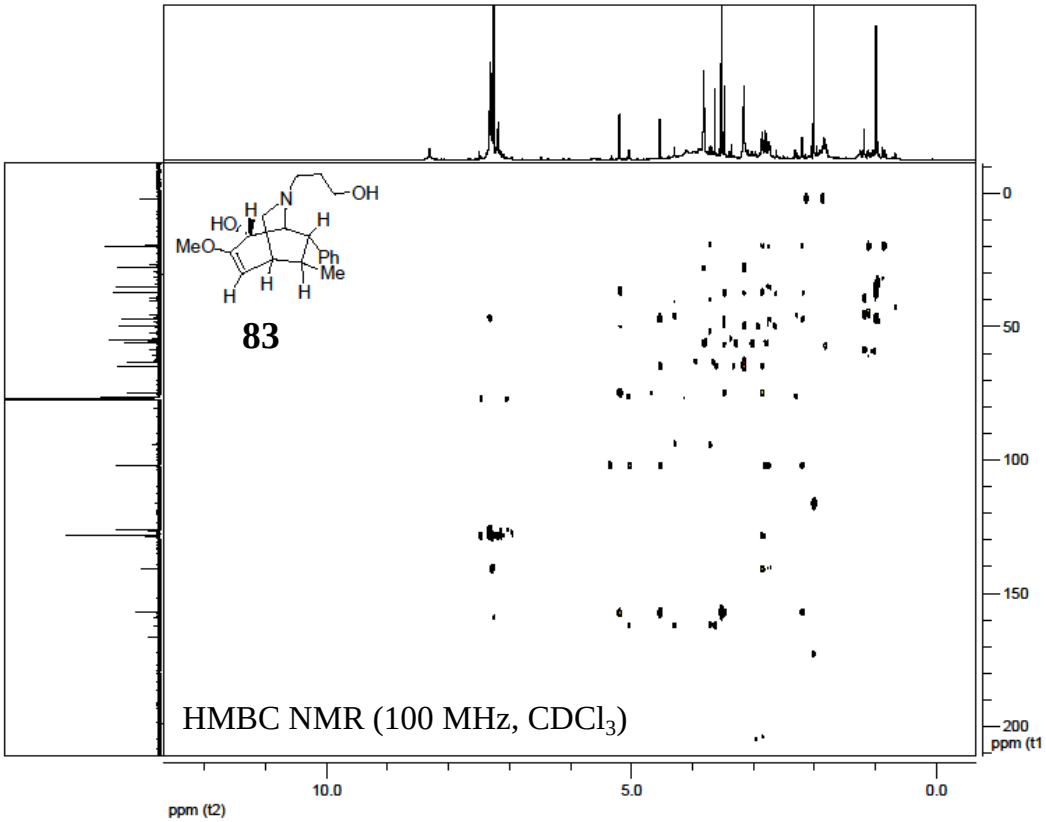
83
OH
N
H
HO
H
MeO
Ph
Me
H
H
H
HMBC NMR (100 MHz, CDCl3)
0
50
100
150
200
10.0
5.0
0.0
ppm (t2)

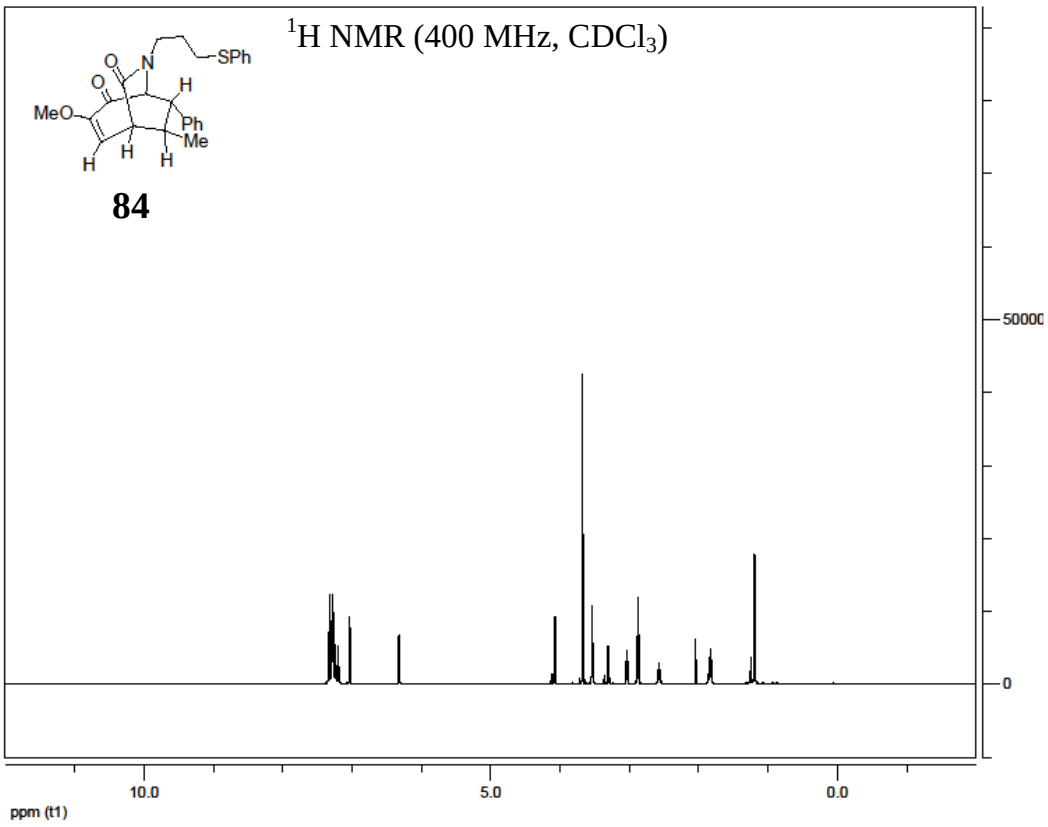
$^{1}$H NMR (400 MHz, $CDCl_3$)
O
N
SPh
O
H
MeO
Ph
Me
H
H
H
84
50000
0
10.0
5.0
0.0
ppm (t1)

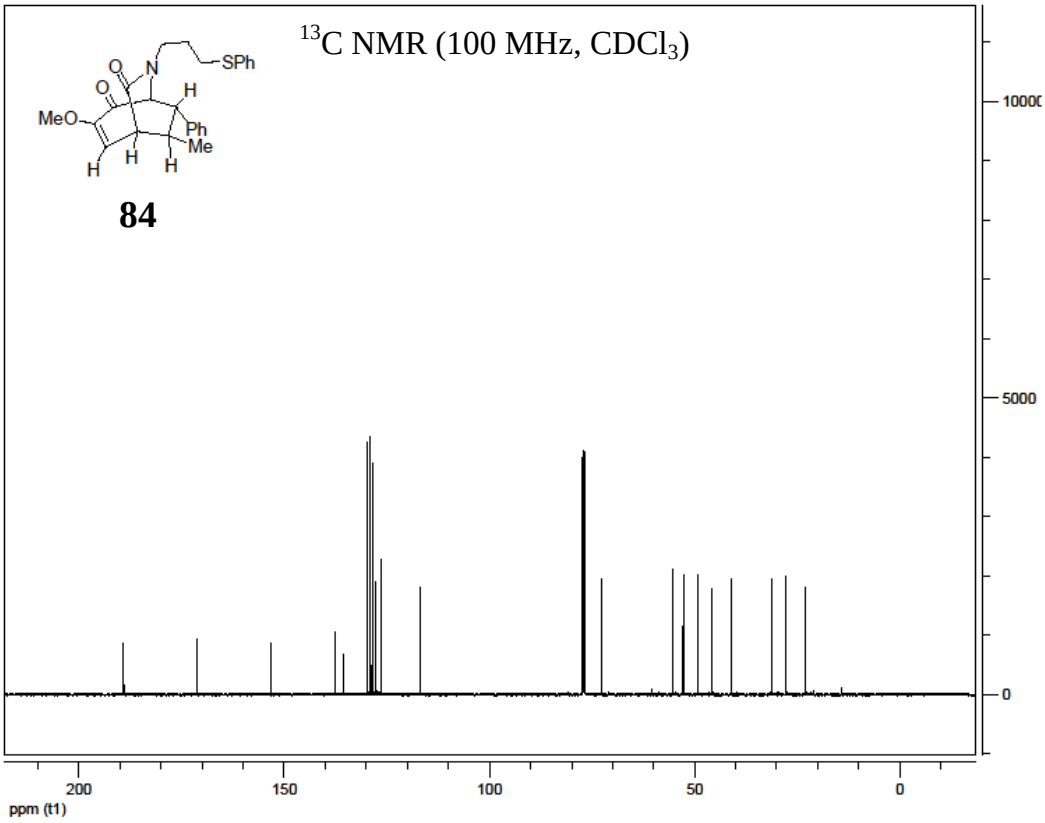
$^{13}$C NMR (100 MHz, $CDCl_3$)
O
N
SPh
O
H
MeO
Ph
Me
H
H
H
84
10000
5000
0
200
150
100
50
0
ppm (t1)

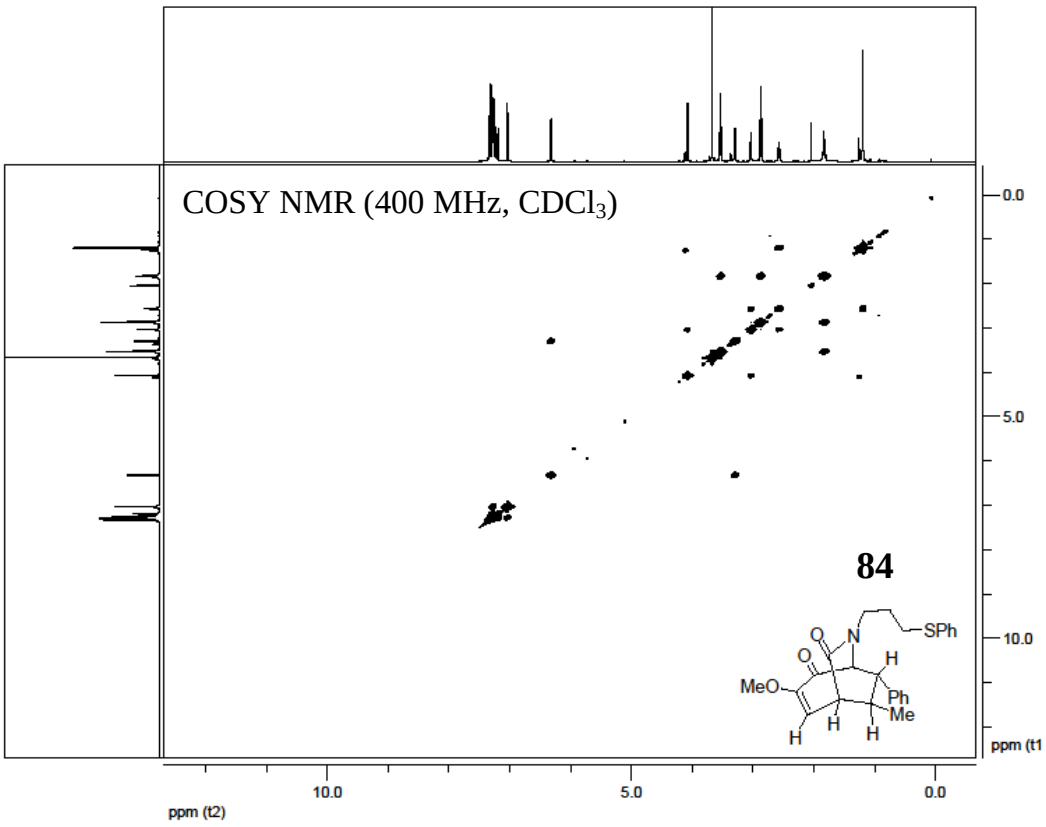
COSY NMR (400 MHz, CDCl3)
84
SPh
O
N
O
H
MeO
Ph
Me
H
H
H
0.0
5.0
10.0
ppm (t1
10.0
5.0
0.0
ppm (t2)

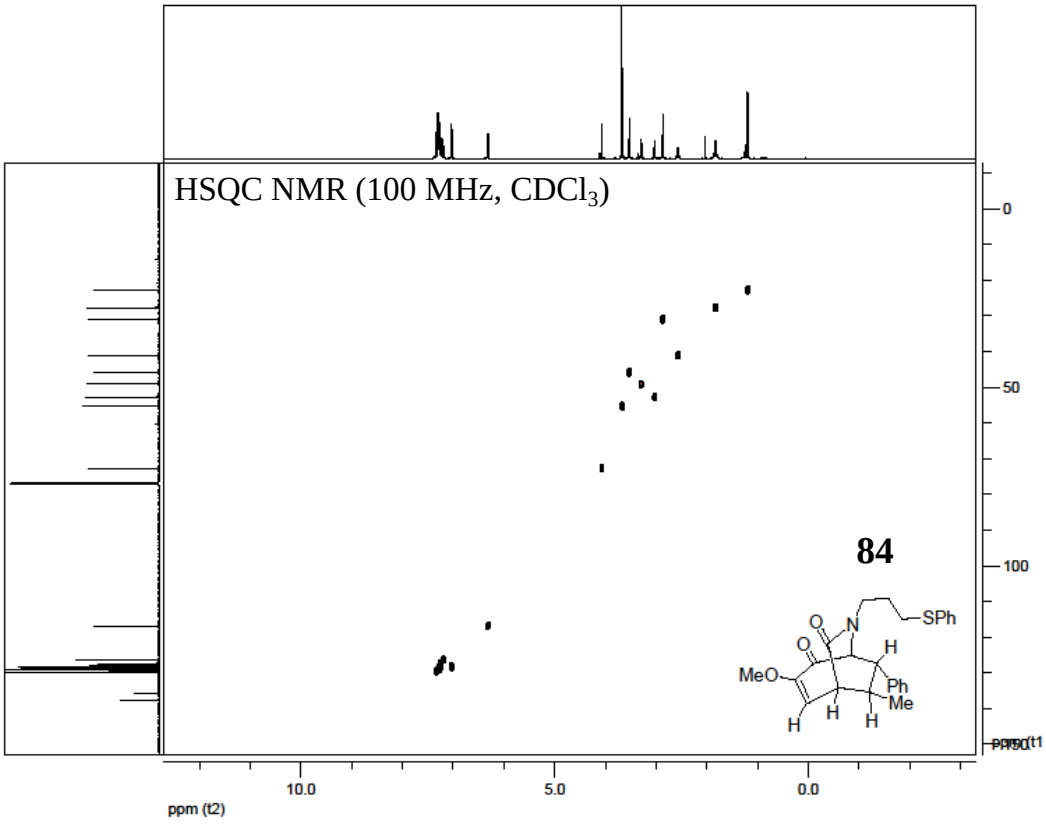
HSQC NMR (100 MHz, CDCl3)
84
SPh
O
N
O
H
MeO
Ph
Me
H
H
H
0
50
100
10.0
5.0
0.0
ppm (t2)

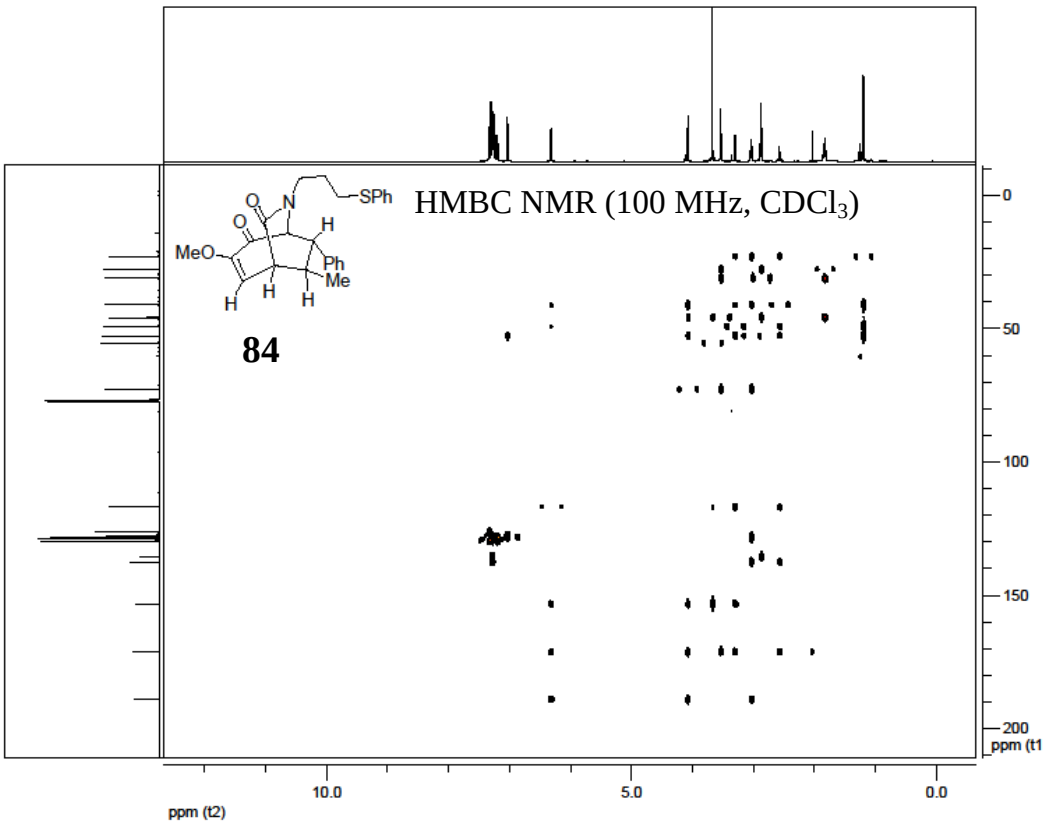
HMBC NMR (100 MHz, CDCl3)
O
N
SPh
O
H
MeO
Ph
Me
H
H
H
84
0
50
100
150
200
ppm (t1
10.0
5.0
0.0
ppm (t2)

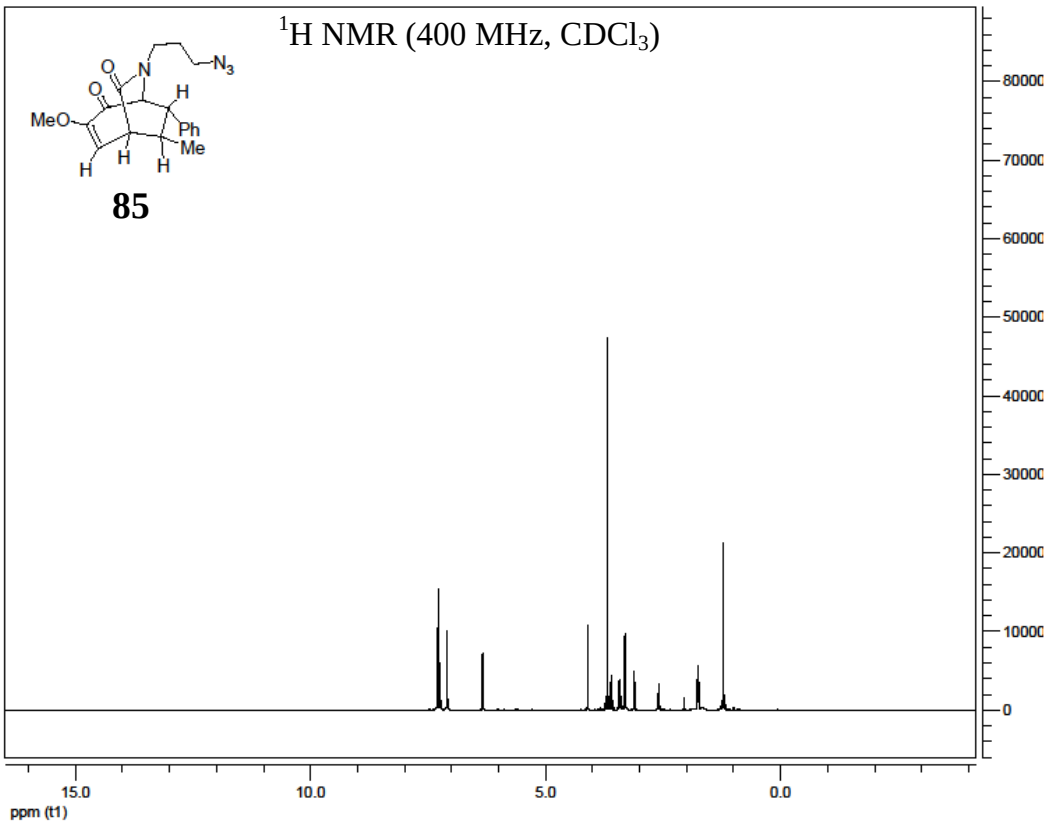
$^1$H NMR (400 MHz, $CDCl_3$)
O
N
$N_3$
O
H
MeO
Ph
Me
H
H
H
85
80000
70000
60000
50000
40000
30000
20000
10000
0
15.0
10.0
5.0
0.0
ppm (t1)

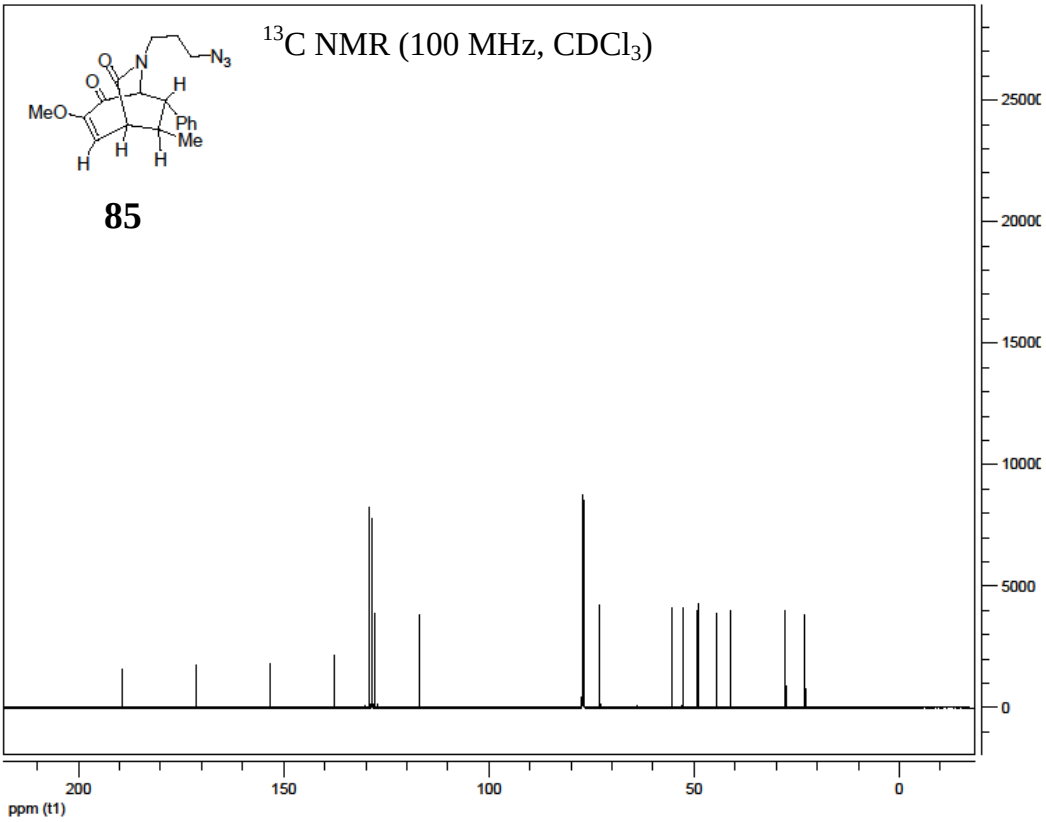
$^{13}$C NMR (100 MHz, $CDCl_3$)
O
N
$N_3$
O
H
MeO
Ph
Me
H
H
H
85
25000
20000
15000
10000
5000
0
200
150
100
50
0
ppm (t1)

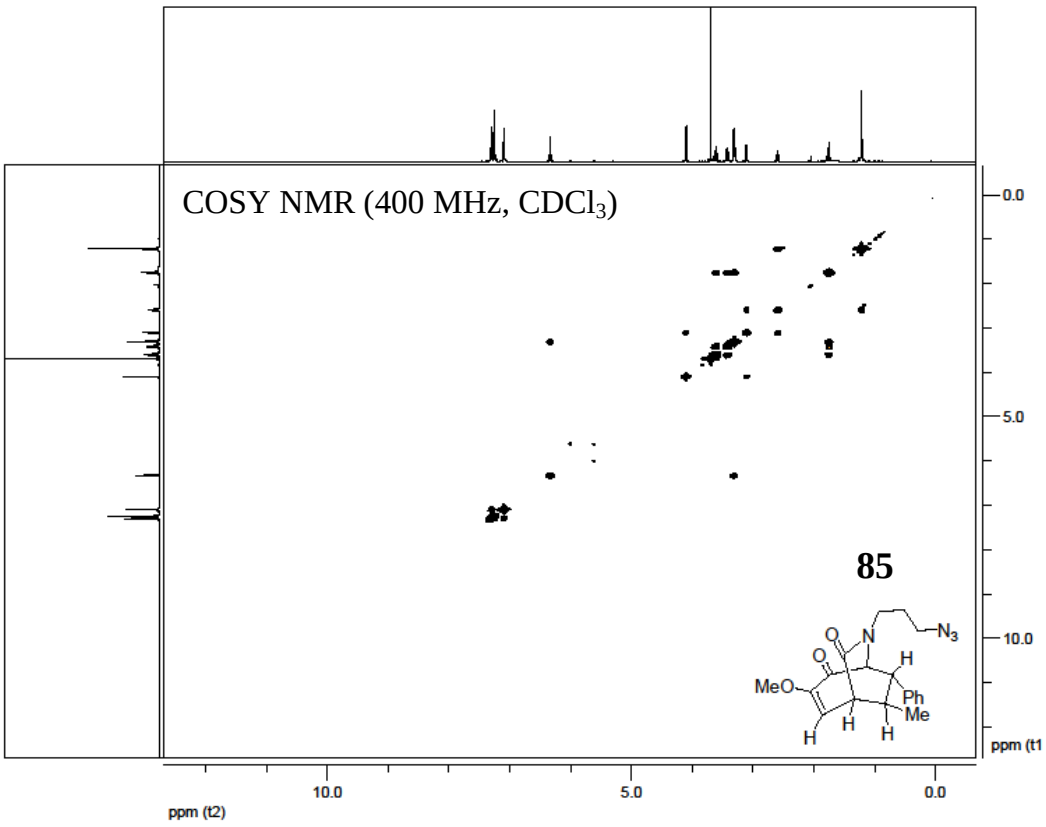
COSY NMR (400 MHz, CDCl3)
85
MeO
Ph
Me
10.0
5.0
0.0
ppm (t2)
ppm (t1

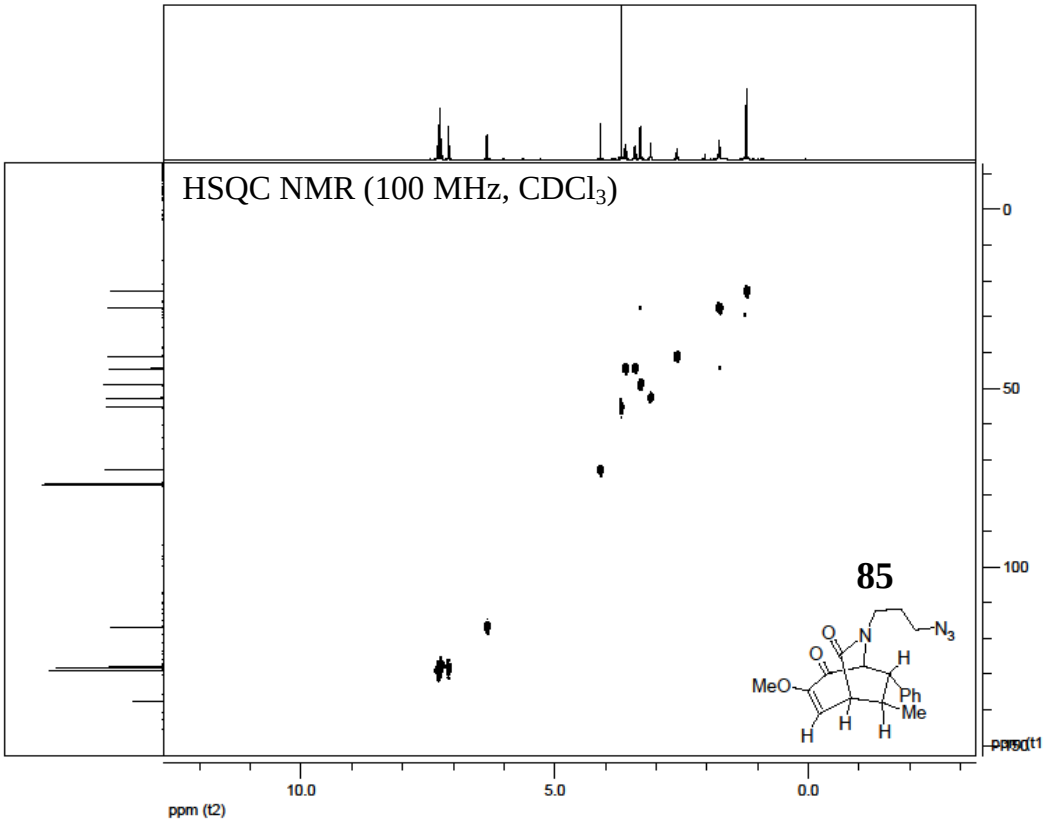
HSQC NMR (100 MHz, CDCl3)
85
MeO
Ph
Me
10.0
5.0
0.0
ppm (t2)
ppm (t1

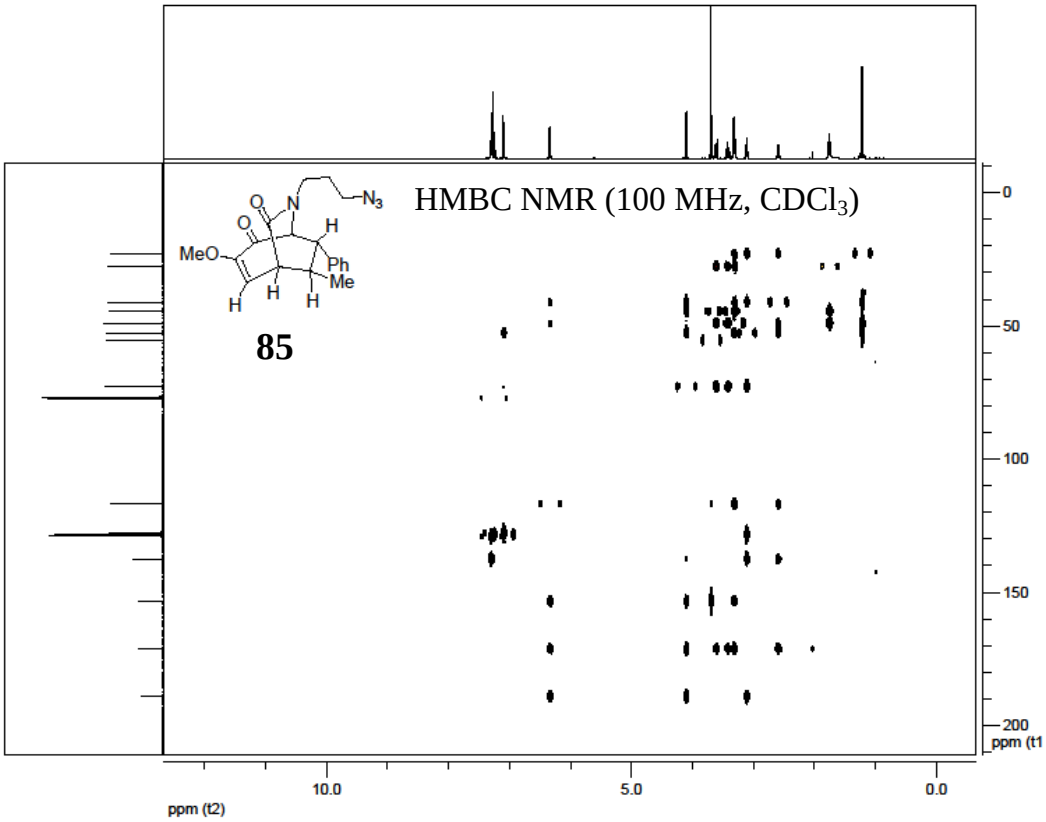
HMBC NMR (100 MHz, CDCl3)
85
MeO
O
O
N
N3
H
Ph
Me
H
H
H
0
50
100
150
200
ppm (t1
10.0
5.0
0.0
ppm (t2)

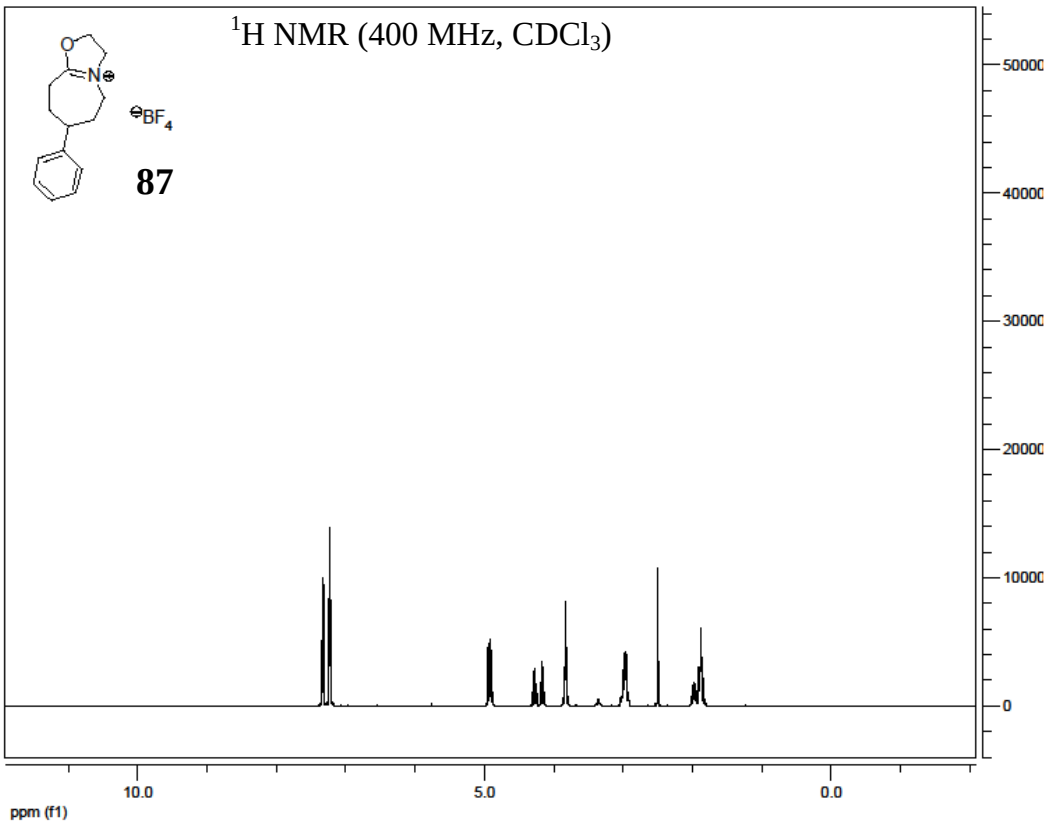
$^{1}$H NMR (400 MHz, $CDCl_3$)
$^{\ominus}BF_4$
87
50000
40000
30000
20000
10000
0
10.0
5.0
0.0
ppm (f1)

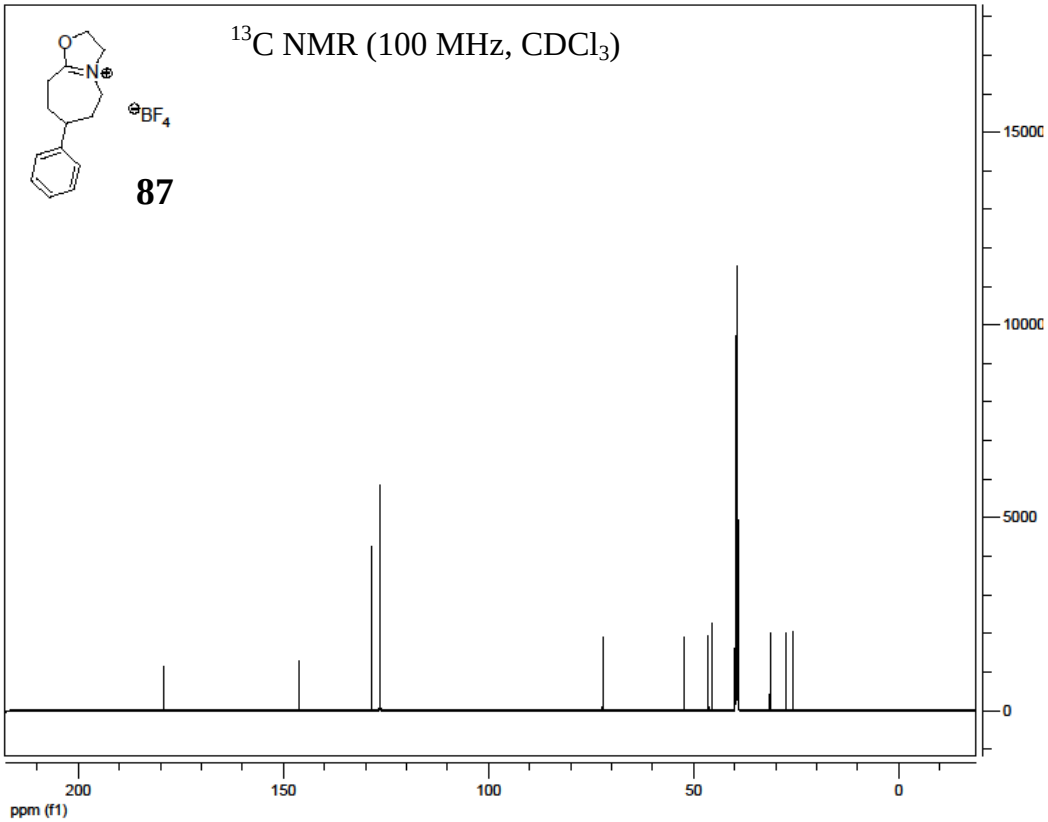
$^{13}$C NMR (100 MHz, $CDCl_3$)
$^{\ominus}BF_4$
87
15000
10000
5000
0
200
150
100
50
0
ppm (f1)

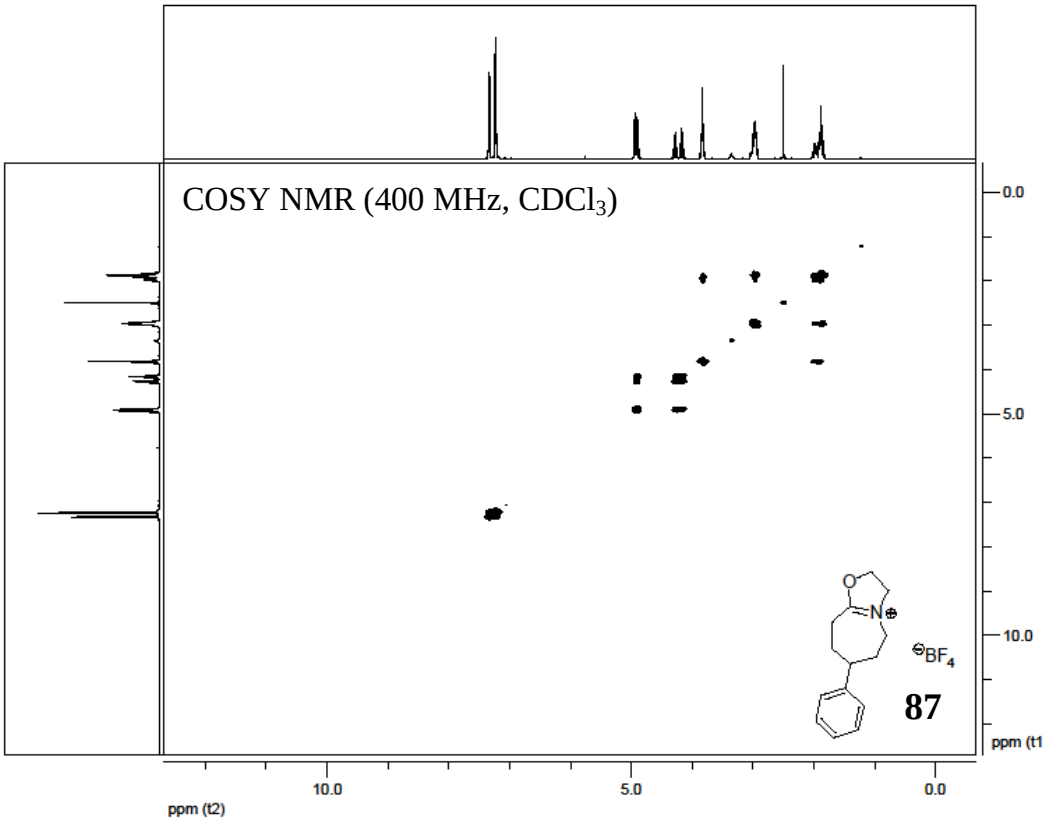
COSY NMR (400 MHz, CDCl3)
0.0
5.0
10.0
ppm (t1
10.0
5.0
0.0
ppm (t2)
O
N⊕
⊖BF4
87

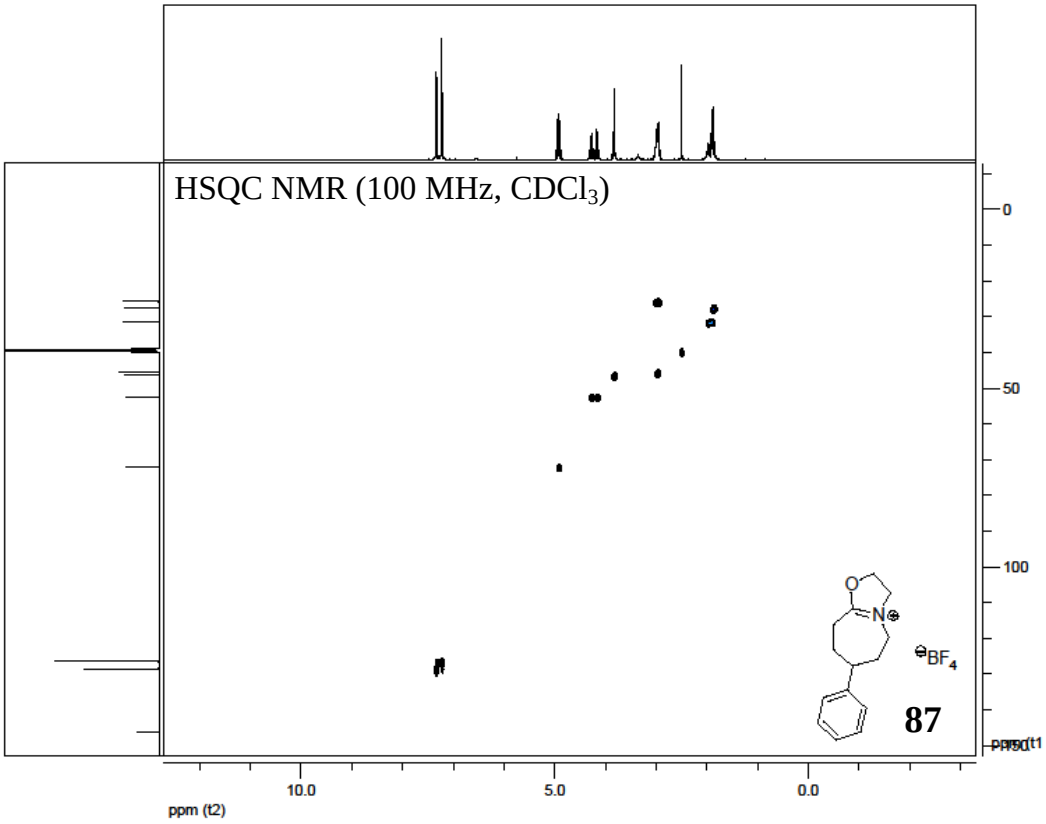
HSQC NMR (100 MHz, CDCl3)
0
50
100
ppm(t1
10.0
5.0
0.0
ppm (t2)
O
N⊕
⊖BF4
87

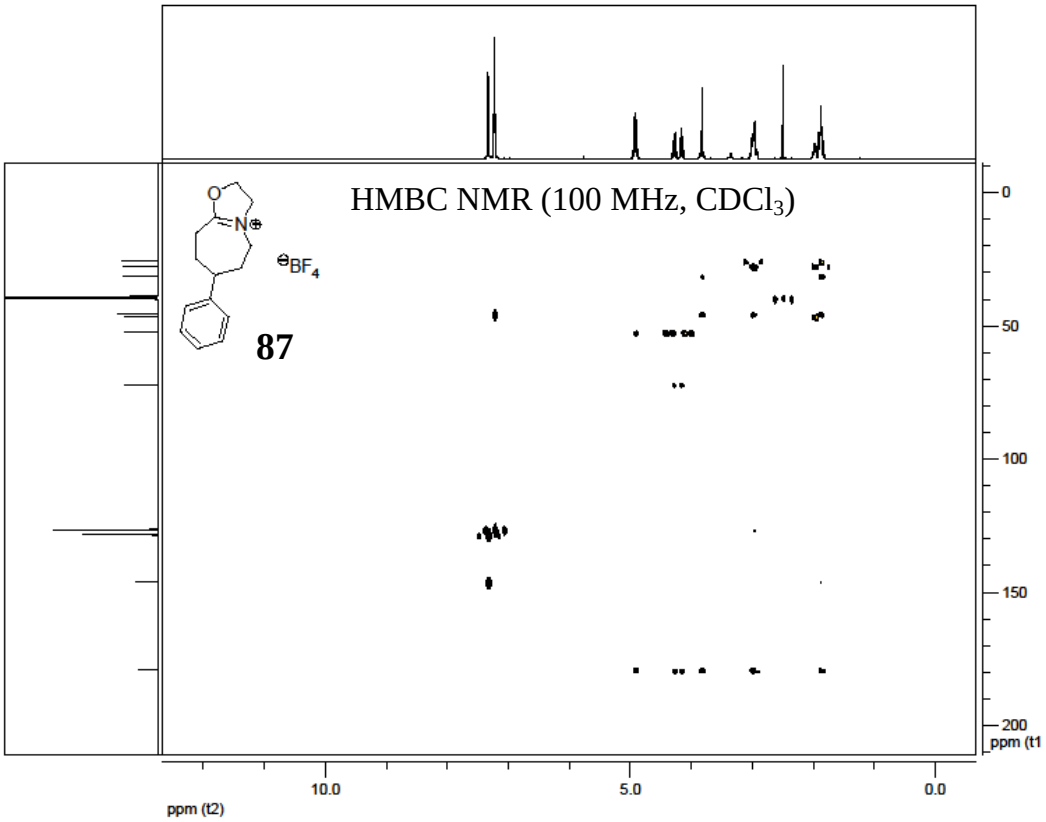
HMBC NMR (100 MHz, $CDCl_3$)
$^{\ominus}BF_4$
87
0
50
100
150
200
ppm (t1
10.0
5.0
0.0
ppm (t2)

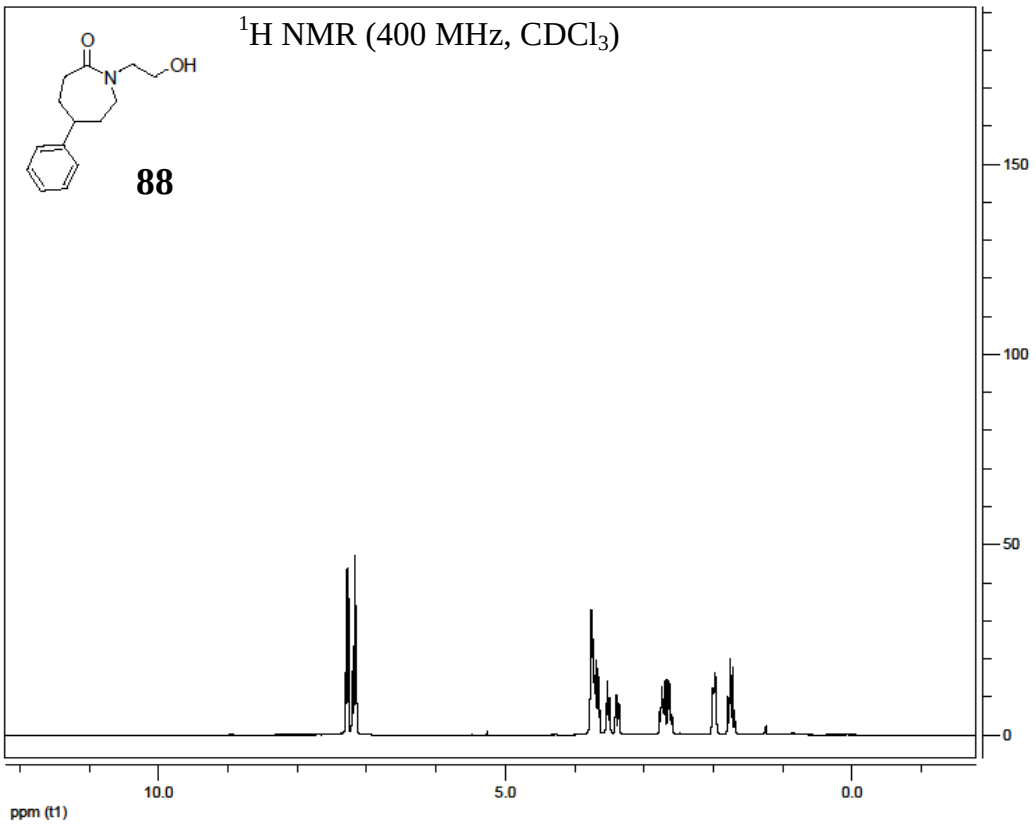


$^{1}$H NMR (400 MHz, $CDCl_3$)

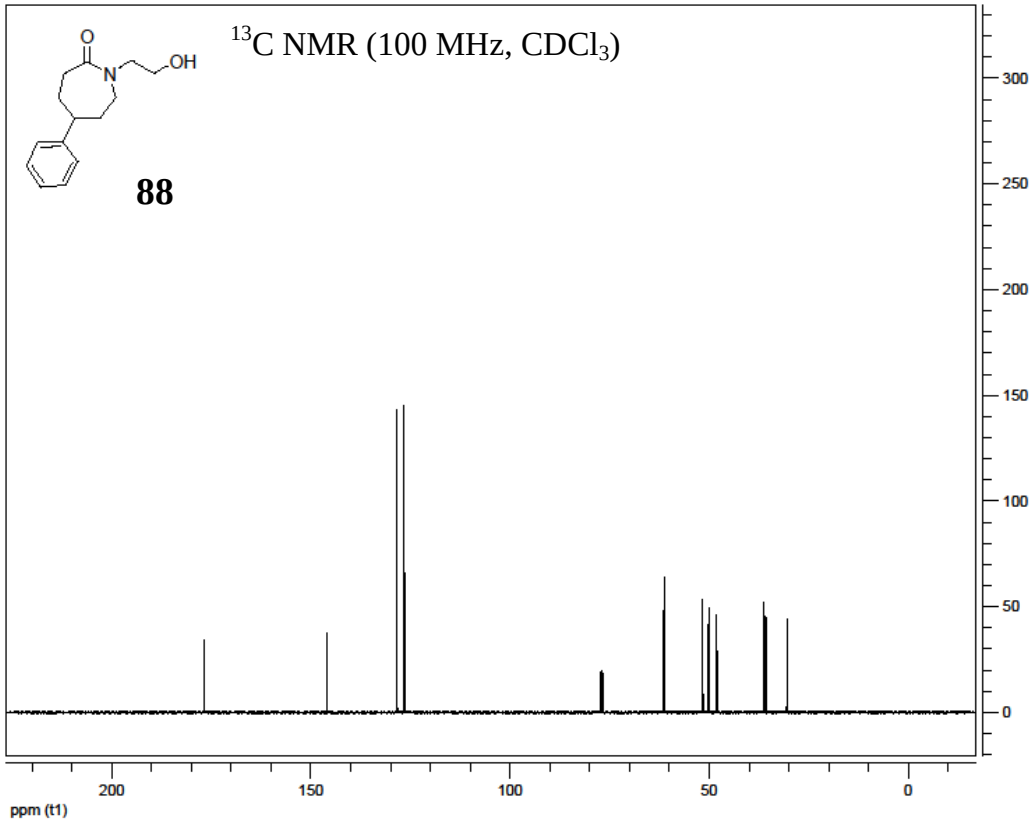


$^{13}$C NMR (100 MHz, $CDCl_3$)

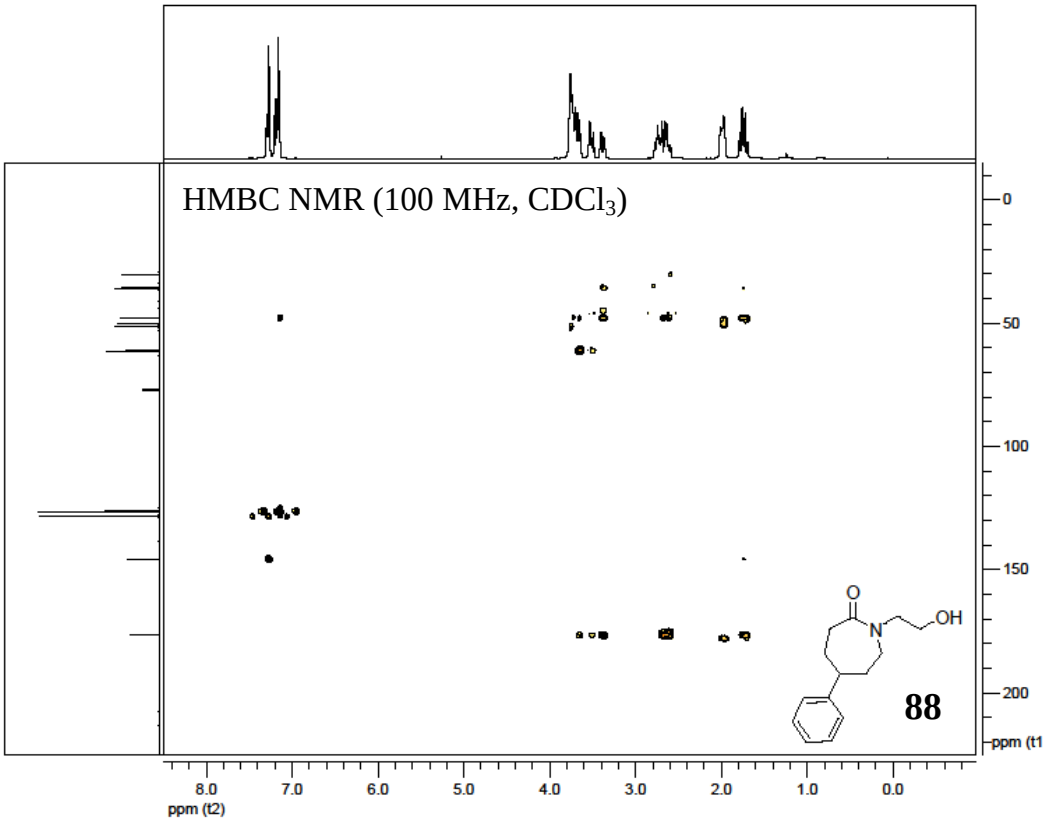
HMBC NMR (100 MHz, CDCl3)
O
N
OH
88
0
50
100
150
200
ppm (t1
8.0
7.0
6.0
5.0
4.0
3.0
2.0
1.0
0.0
ppm (t2)

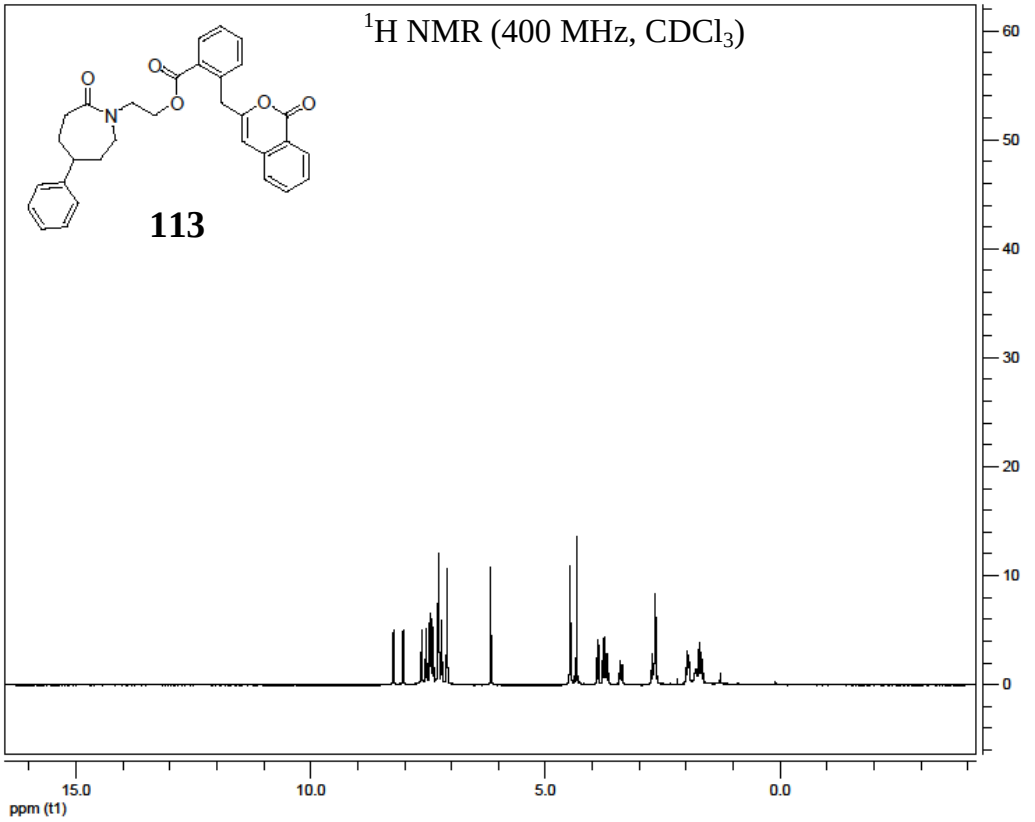
$^{1}$H NMR (400 MHz, $CDCl_3$)
113
60
50
40
30
20
10
0
15.0
10.0
5.0
0.0
ppm (t1)

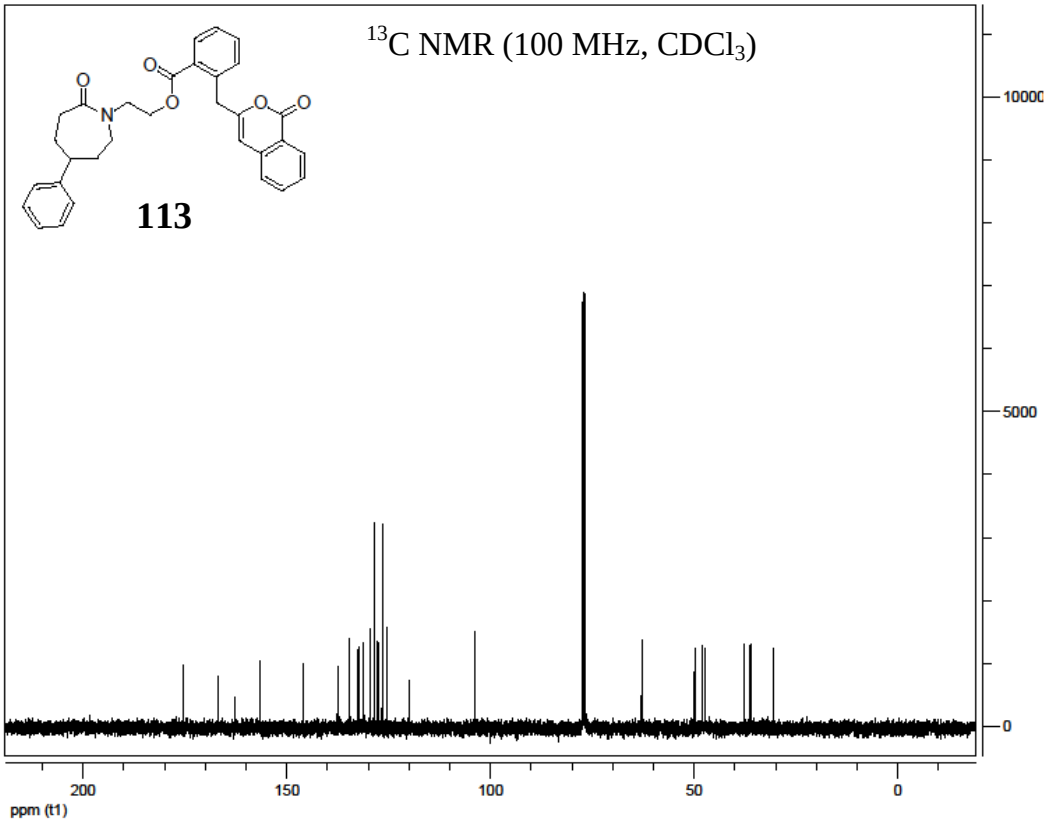
$^{13}$C NMR (100 MHz, $CDCl_3$)
113
10000
5000
0
200
150
100
50
0
ppm (t1)

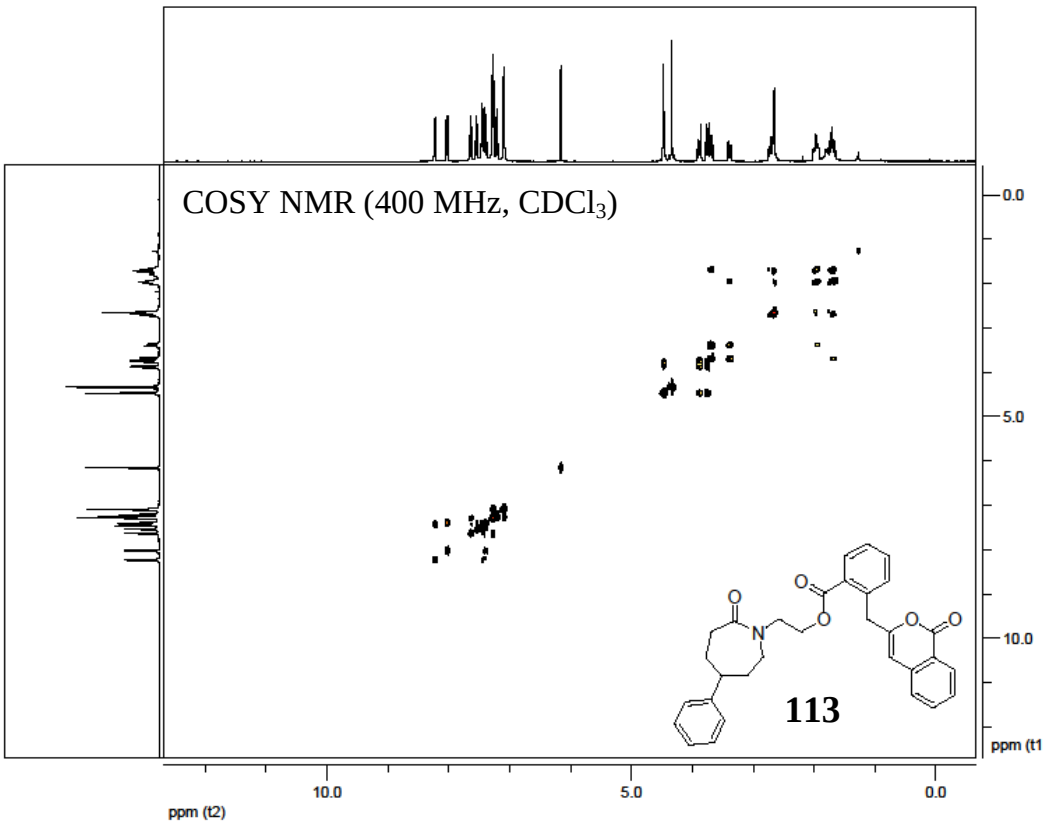
COSY NMR (400 MHz, CDCl3)
113
0.0
5.0
10.0
ppm (t1
10.0
5.0
0.0
ppm (t2)

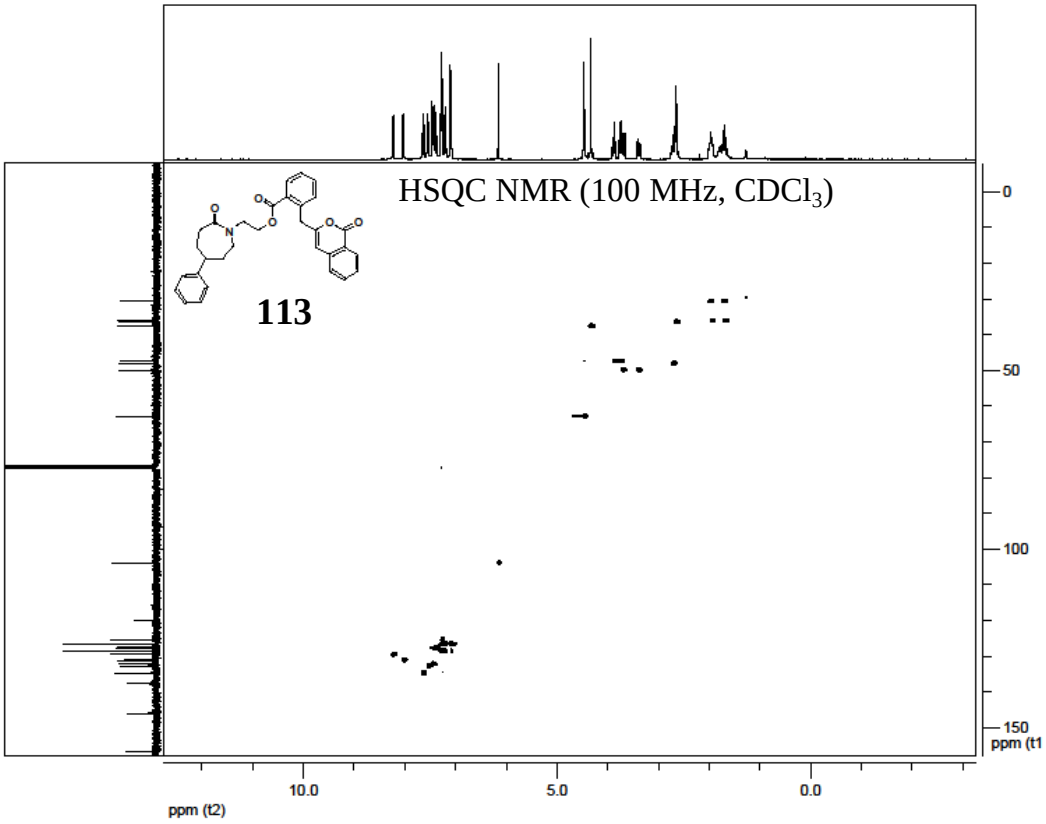
HSQC NMR (100 MHz, CDCl3)
113
0
50
100
150
ppm (t1
10.0
5.0
0.0
ppm (t2)

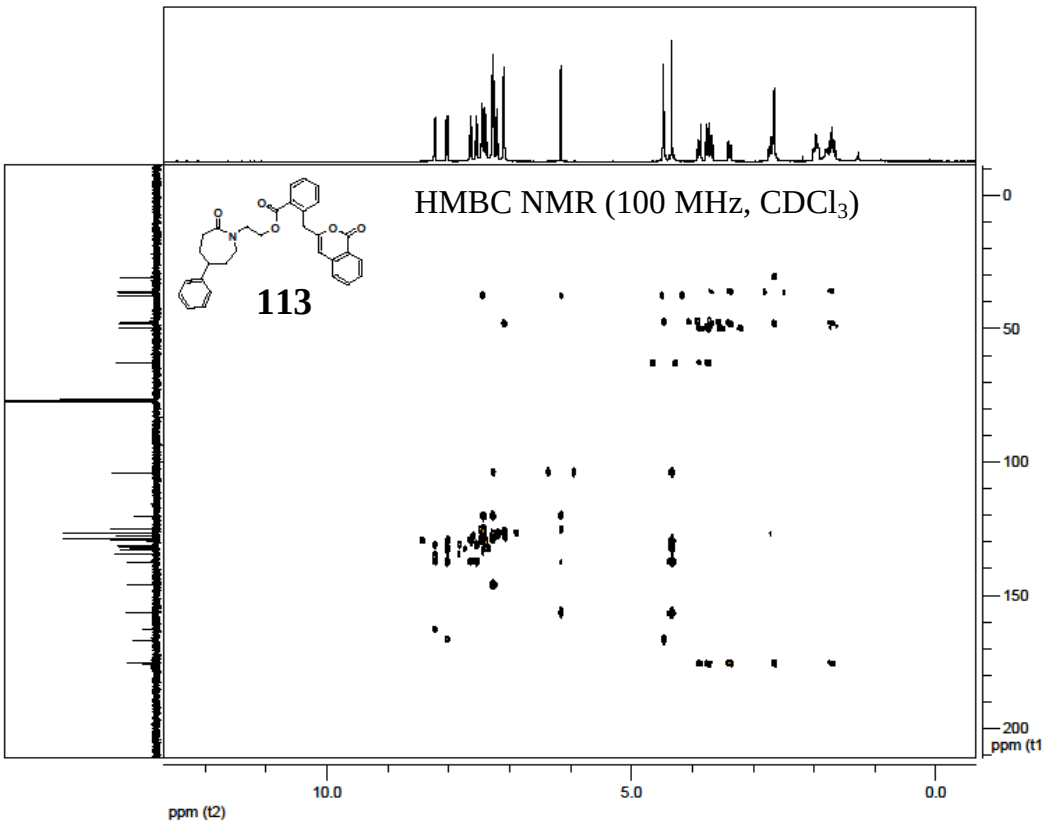
HMBC NMR (100 MHz, $CDCl_3$)
113
0
50
100
150
200
ppm (t1
10.0
5.0
0.0
ppm (t2)

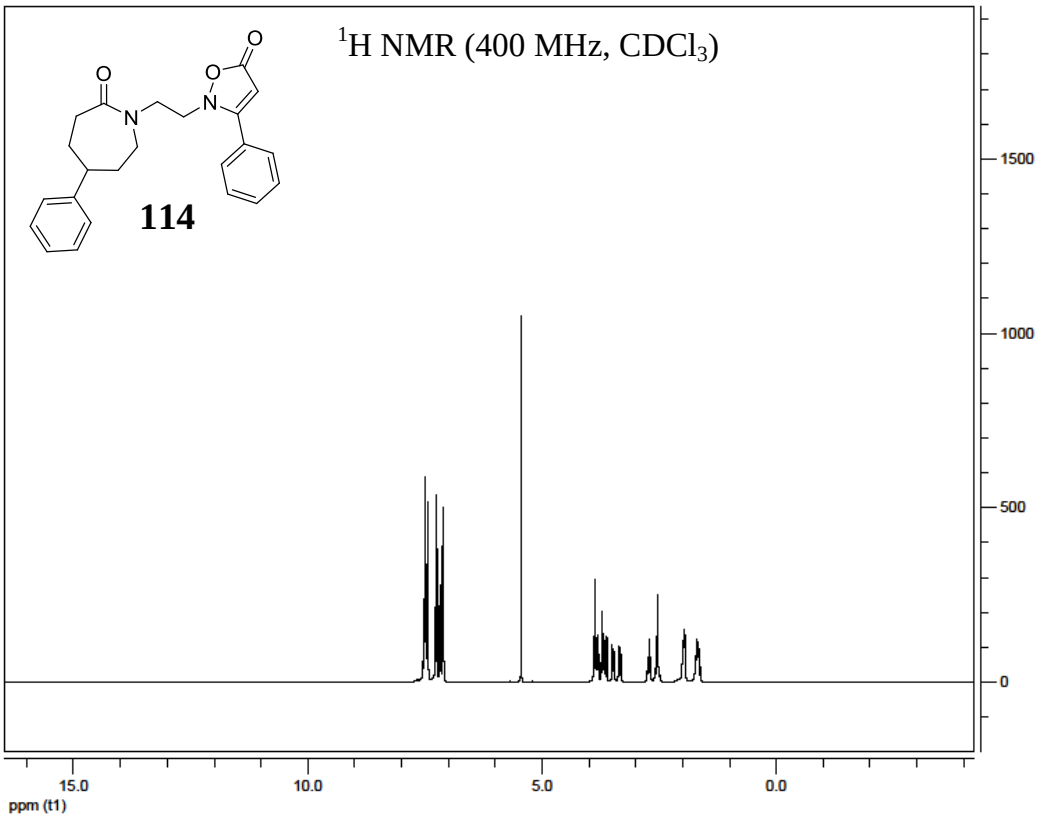
$^{1}$H NMR (400 MHz, $CDCl_3$)
114
1500
1000
500
0
15.0
10.0
5.0
0.0
ppm (t1)

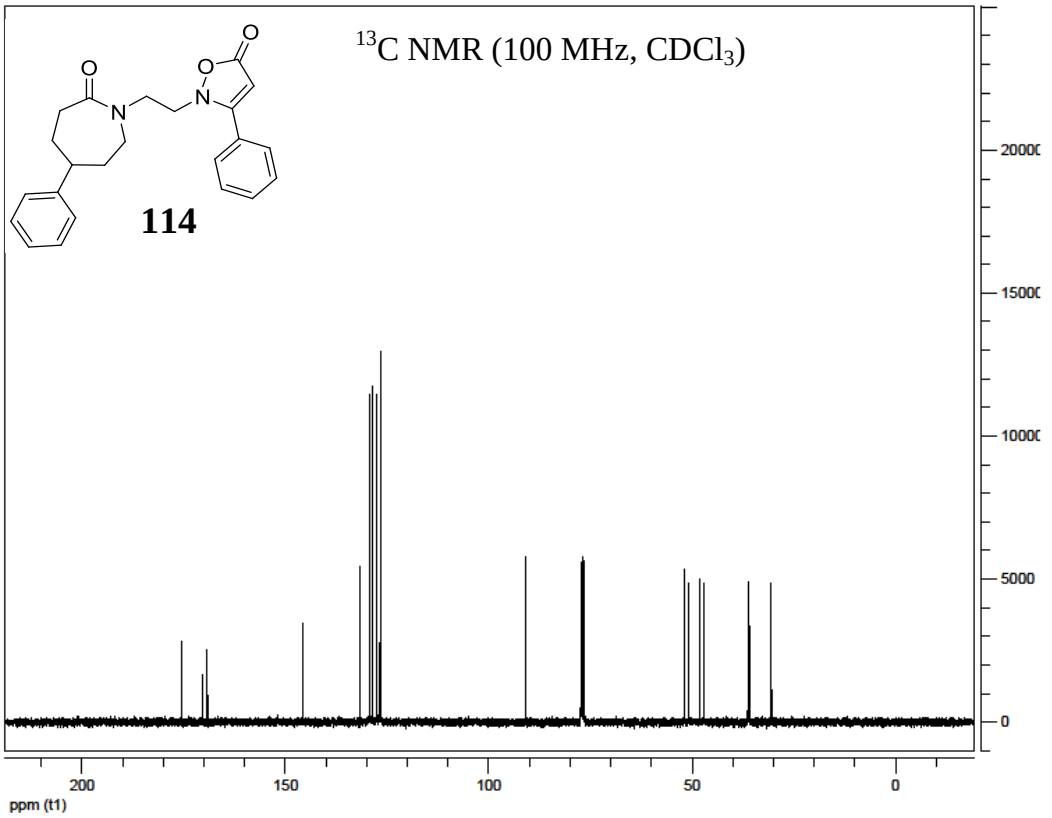
$^{13}$C NMR (100 MHz, $CDCl_3$)
114
20000
15000
10000
5000
0
200
150
100
50
0
ppm (t1)

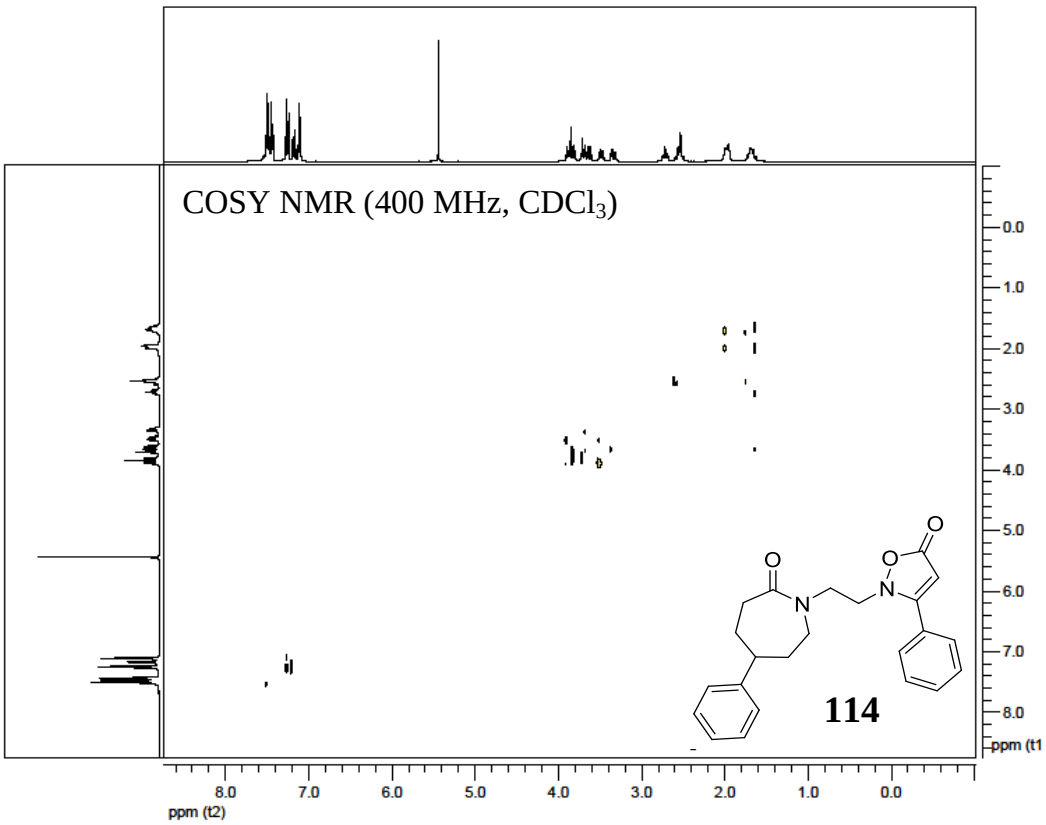
COSY NMR (400 MHz, CDCl3)
114
ppm (t2)
ppm (t1

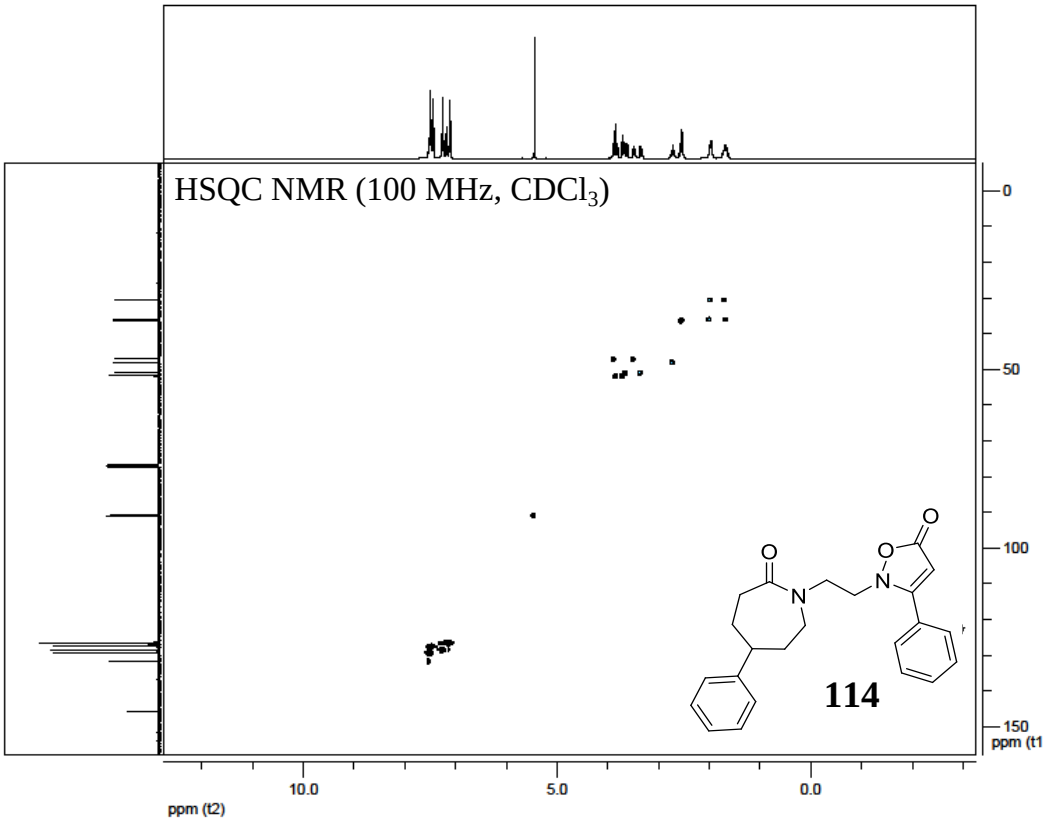
HSQC NMR (100 MHz, CDCl3)
114
ppm (t2)
ppm (t1

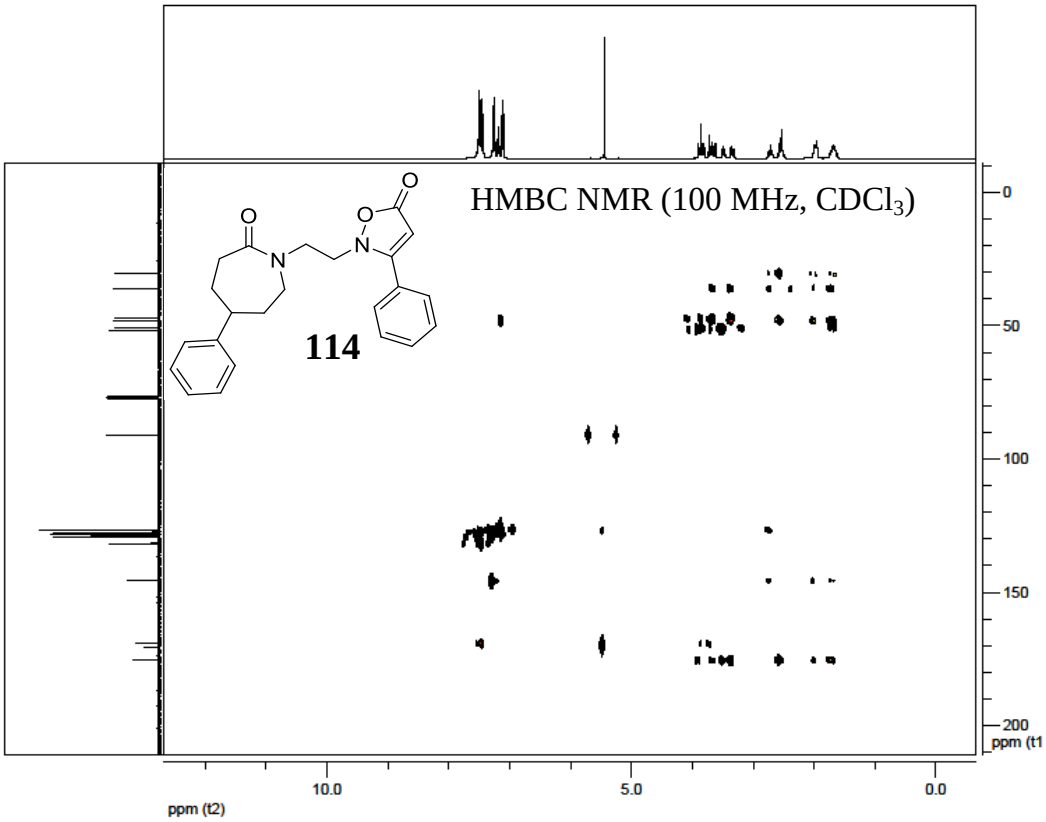
HMBC NMR (100 MHz, $CDCl_3$)
114
0
50
100
150
200
ppm (t1
10.0
5.0
0.0
ppm (t2)

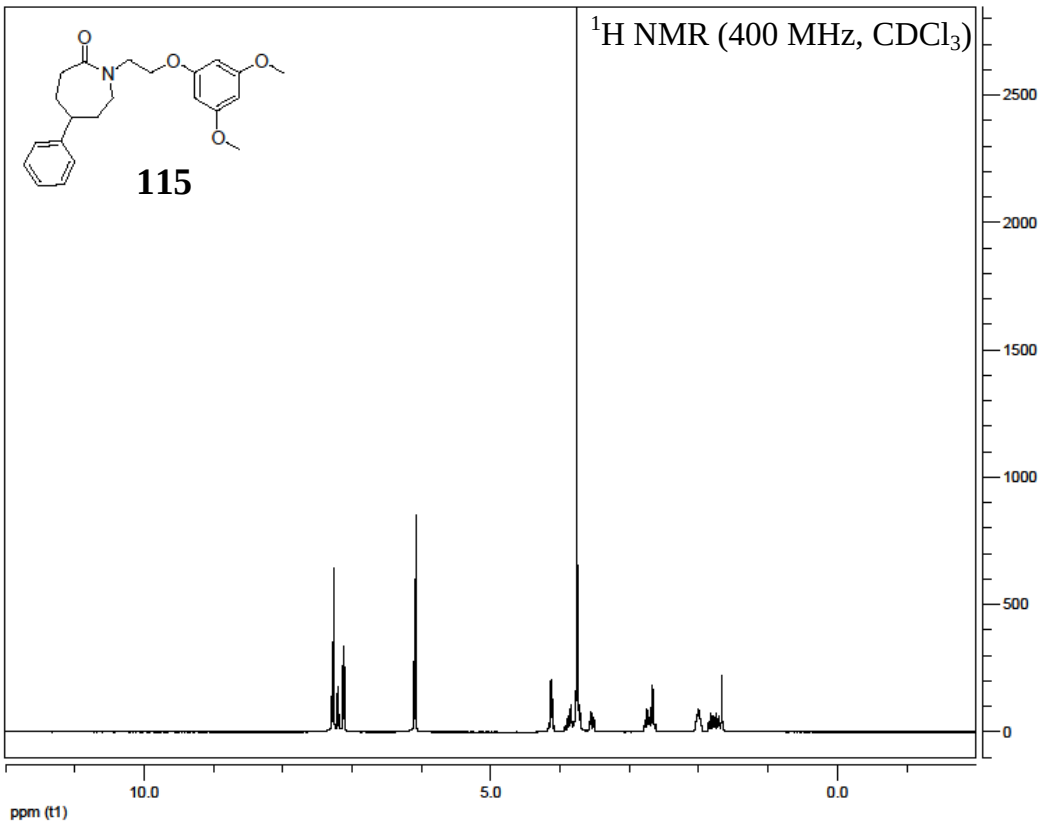
$^{1}$H NMR (400 MHz, $CDCl_3$)
115
2500
2000
1500
1000
500
0
10.0
5.0
0.0
ppm (t1)

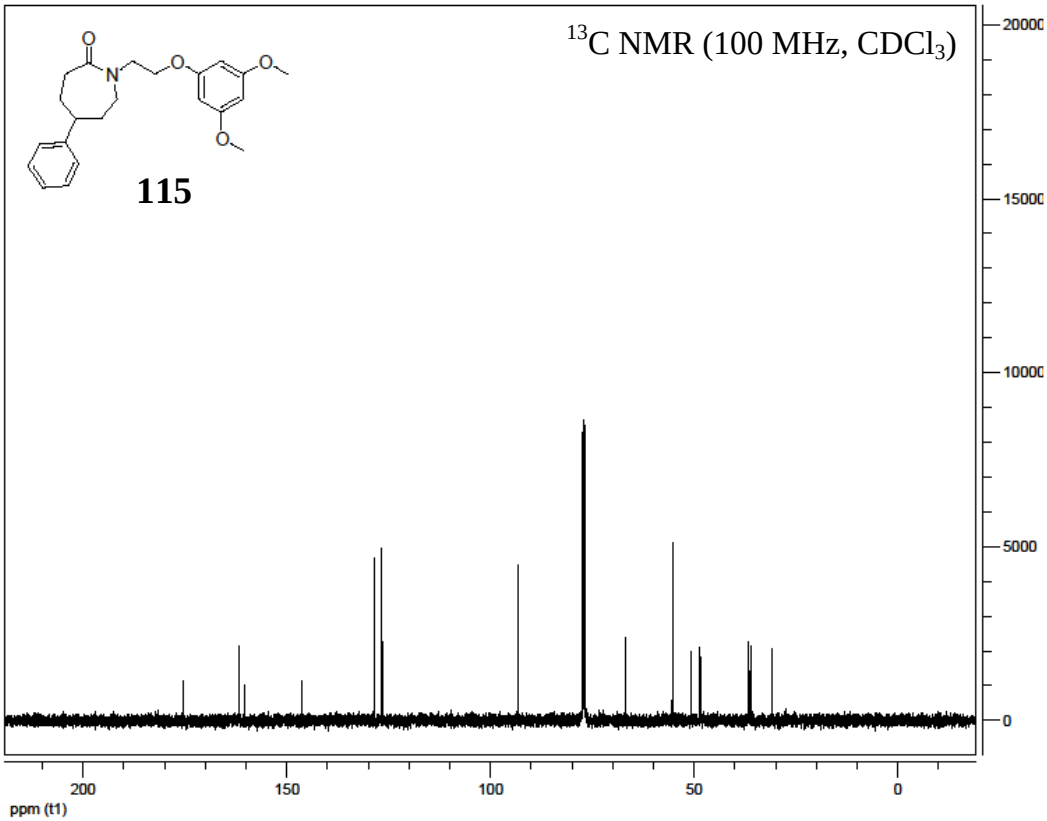
$^{13}$C NMR (100 MHz, $CDCl_3$)
115
20000
15000
10000
5000
0
200
150
100
50
0
ppm (t1)

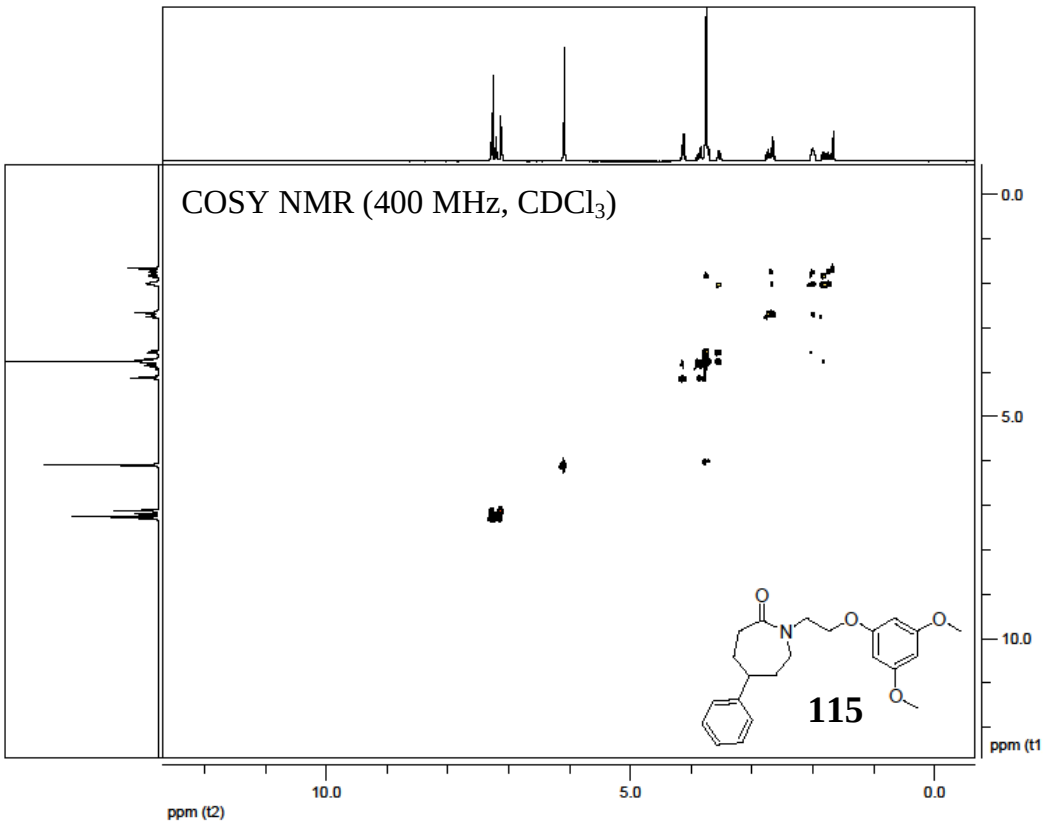
COSY NMR (400 MHz, CDCl3)
115
10.0
5.0
0.0
ppm (t2)
ppm (t1

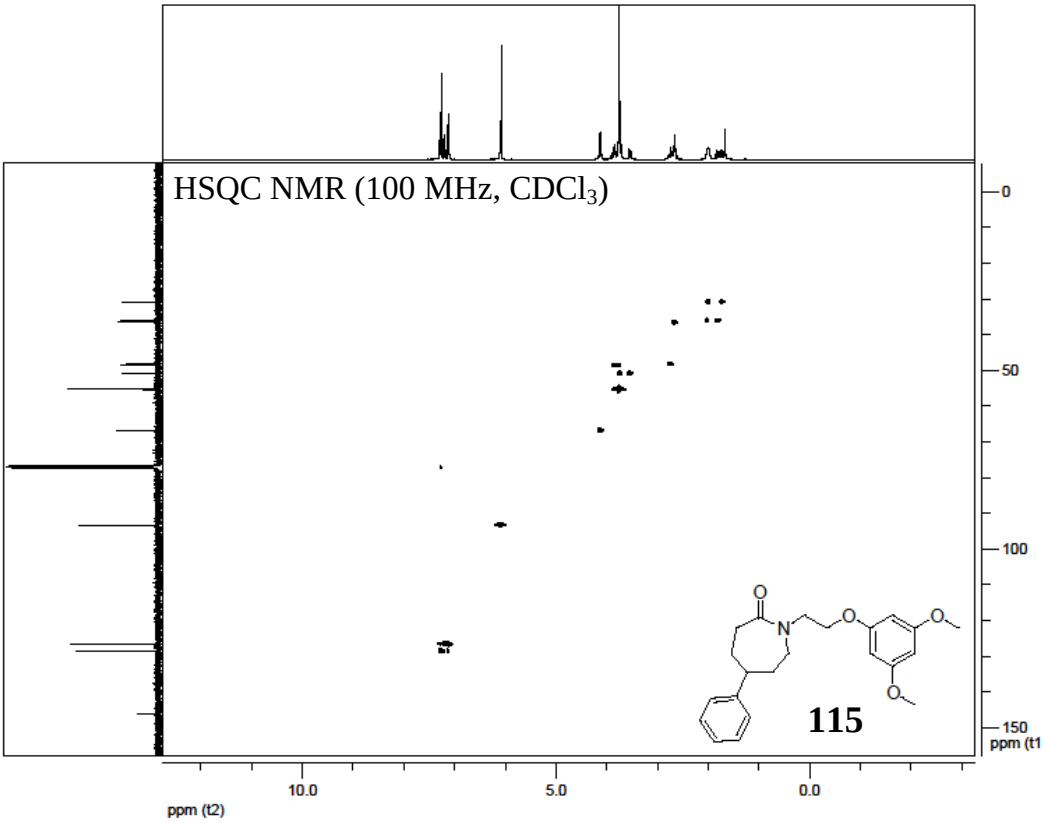
HSQC NMR (100 MHz, CDCl3)
115
10.0
5.0
0.0
ppm (t2)
ppm (t1

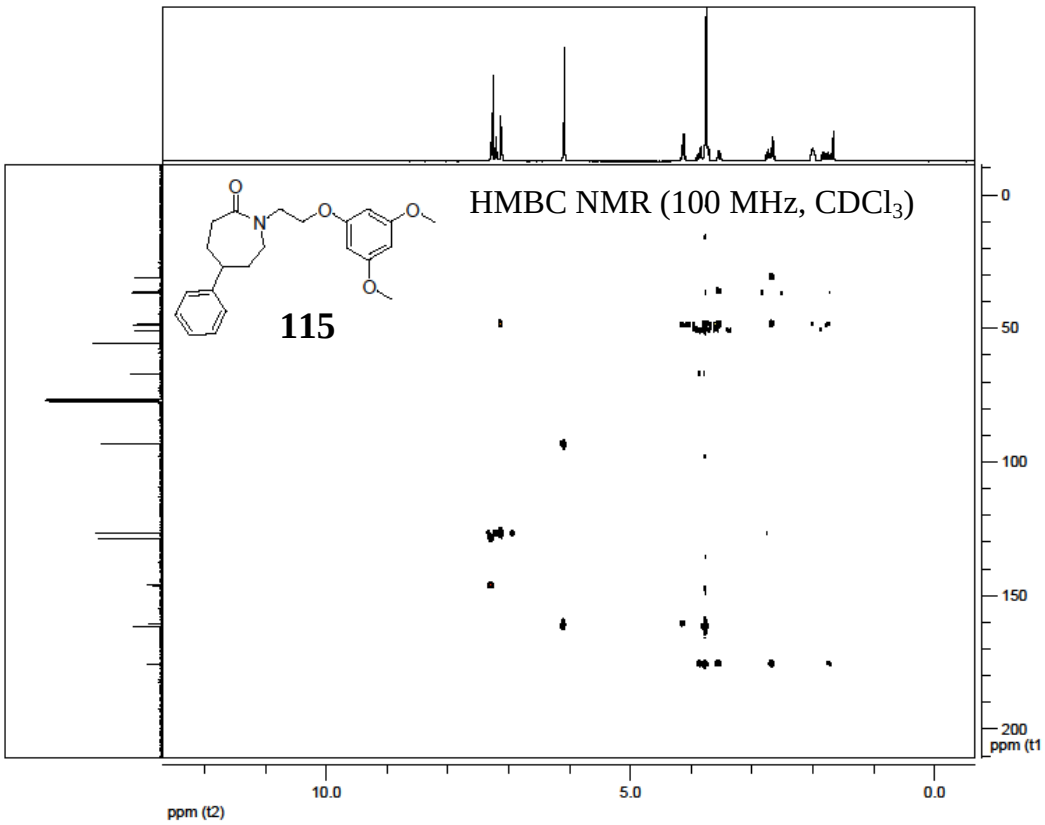
HMBC NMR (100 MHz, $CDCl_3$)
115
O
N
O
O
O
0
50
100
150
200
ppm (t1
10.0
5.0
0.0
ppm (t2)

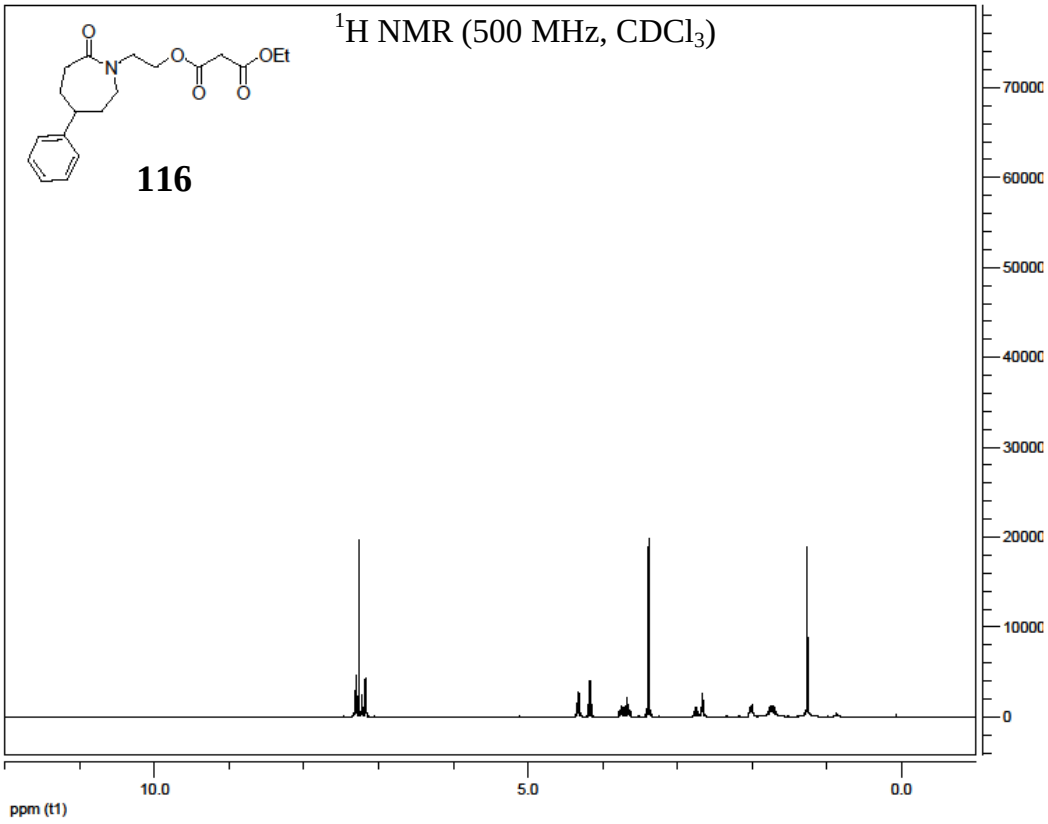
$^{1}$H NMR (500 MHz, $CDCl_3$)
116
70000
60000
50000
40000
30000
20000
10000
0
10.0
5.0
0.0
ppm (t1)

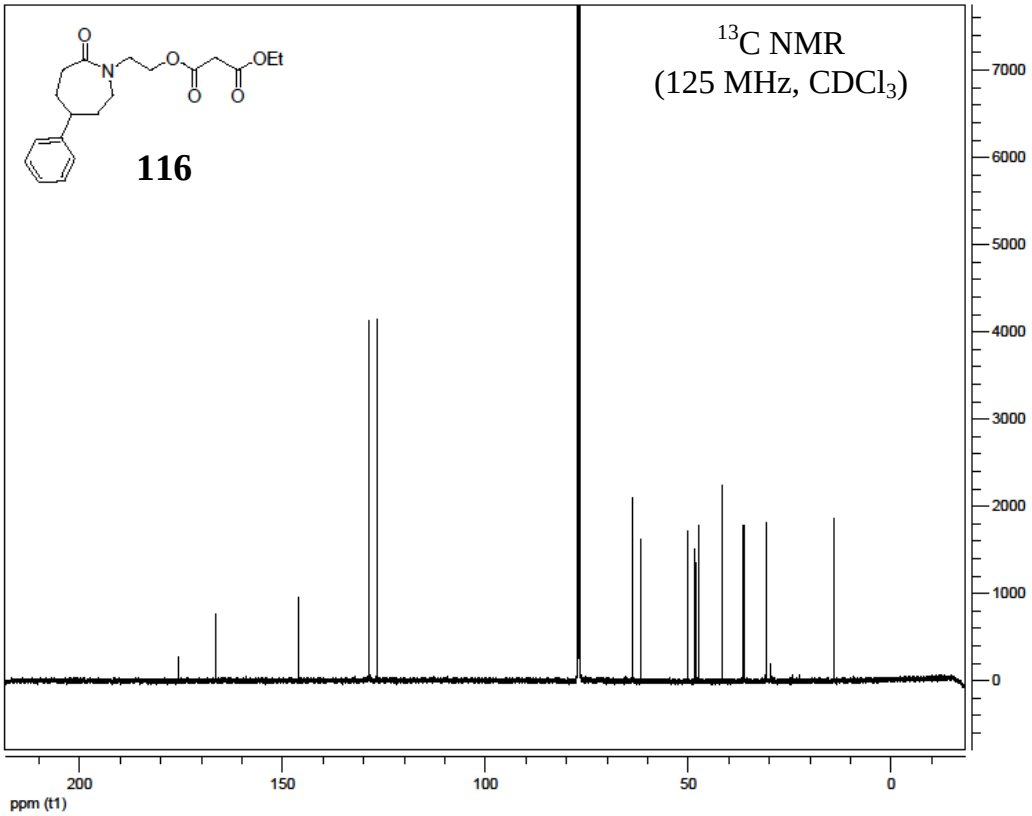
$^{13}$C NMR
(125 MHz, $CDCl_3$)
116
7000
6000
5000
4000
3000
2000
1000
0
200
150
100
50
0
ppm (t1)

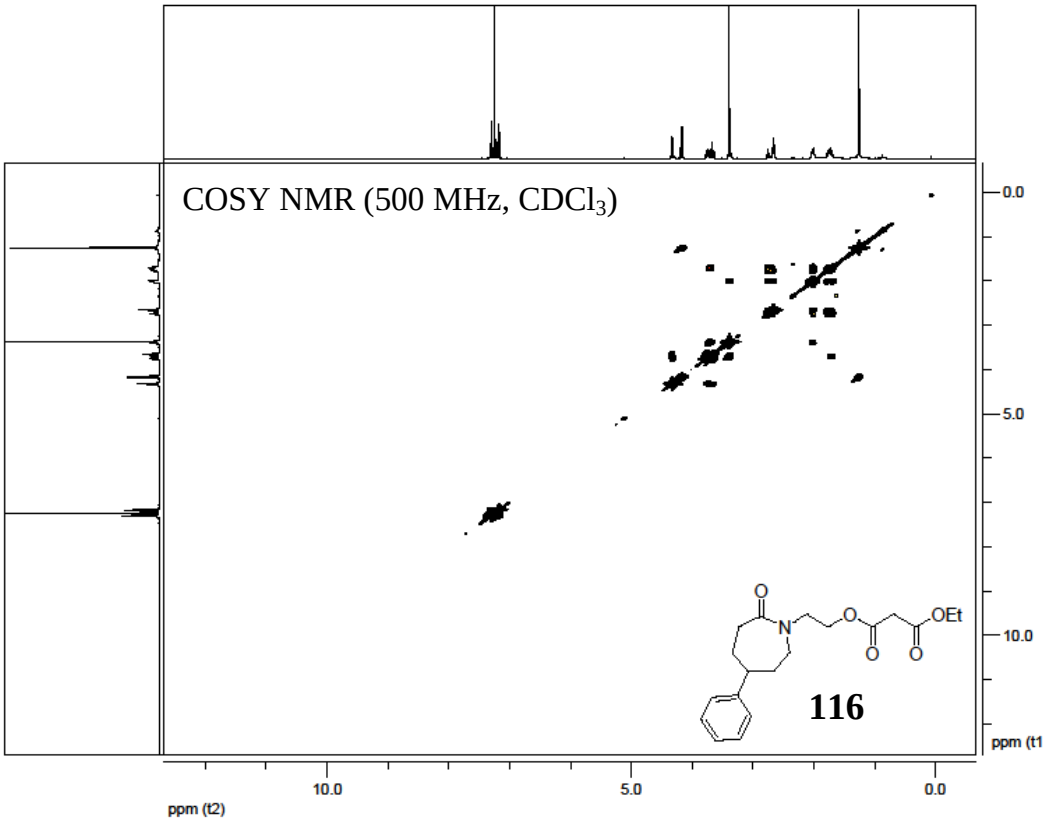
COSY NMR (500 MHz, CDCl3)
0.0
5.0
10.0
ppm (t1
10.0
5.0
0.0
ppm (t2)
O
N
O
OEt
O
O
116

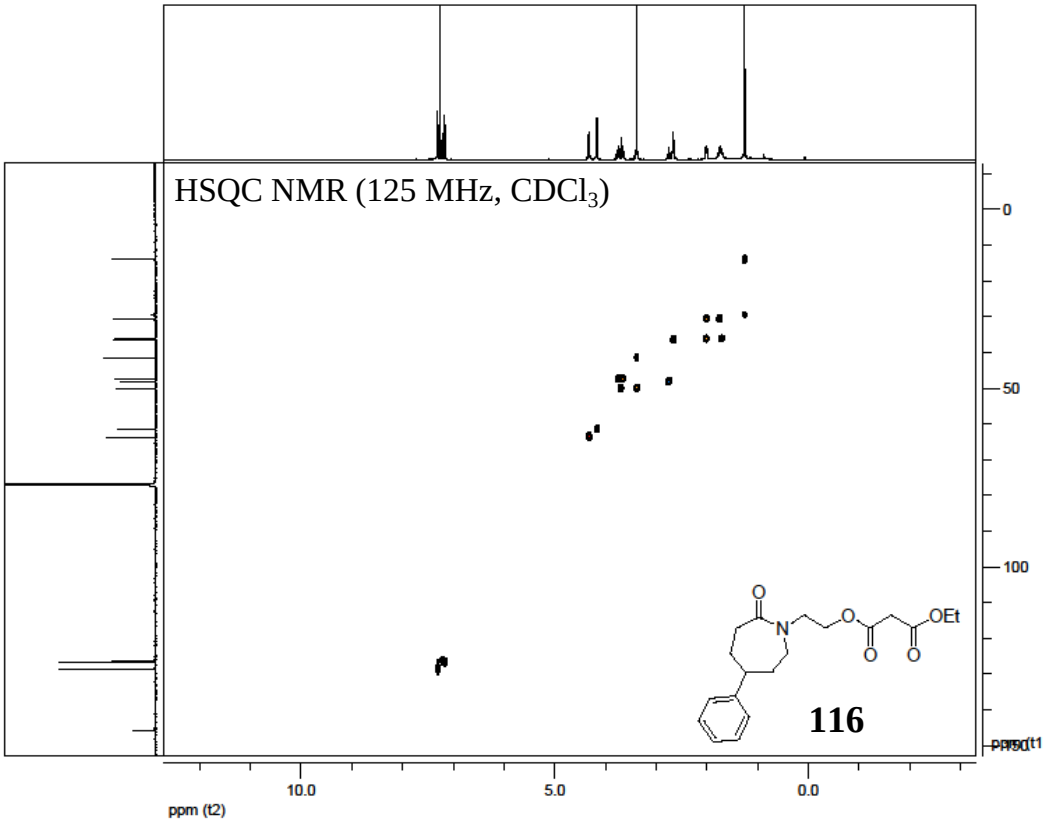
HSQC NMR (125 MHz, CDCl3)
0
50
100
10.0
5.0
0.0
ppm (t2)
O
N
O
OEt
O
O
116

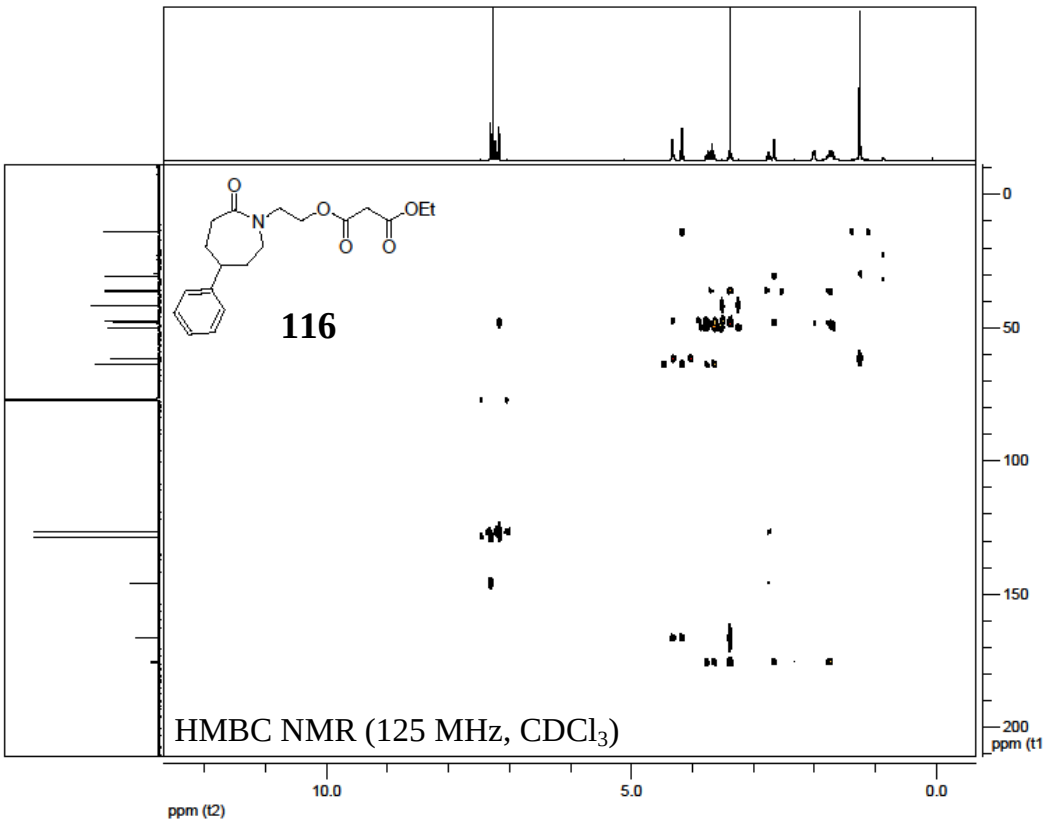


HMBC NMR (125 MHz, $CDCl_3$)

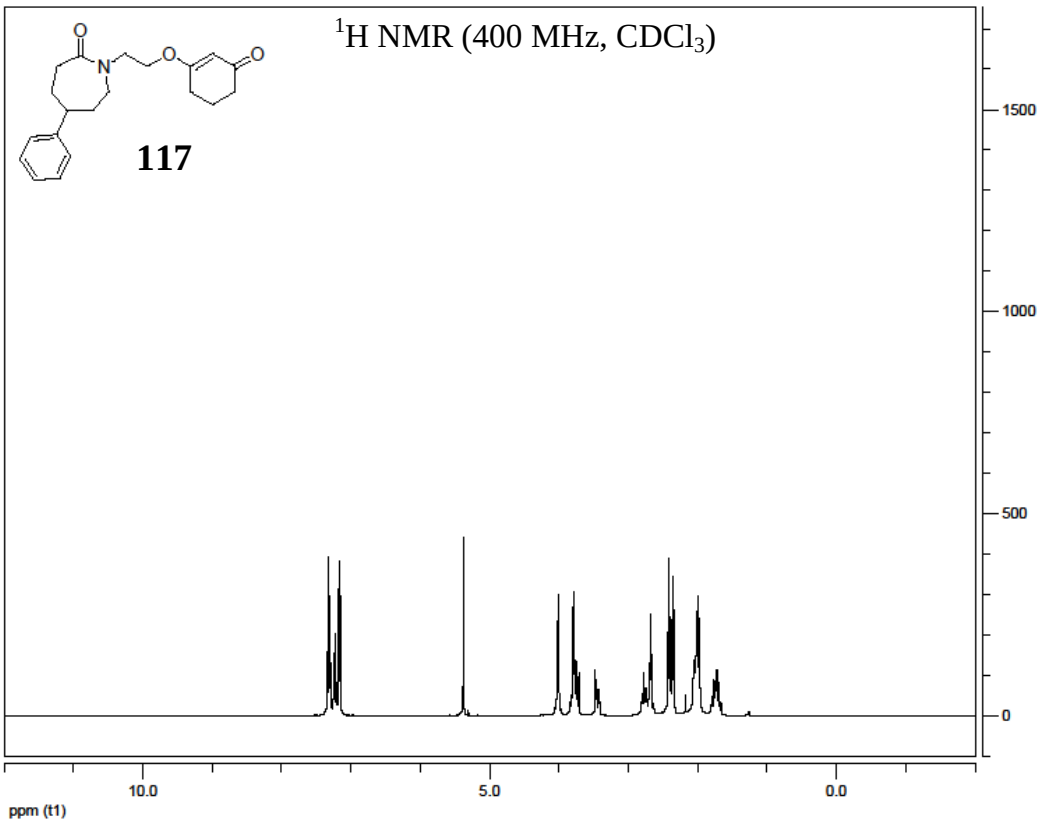
117
$^{1}$H NMR (400 MHz, $CDCl_3$)
1500
1000
500
0
10.0
5.0
0.0
ppm (t1)

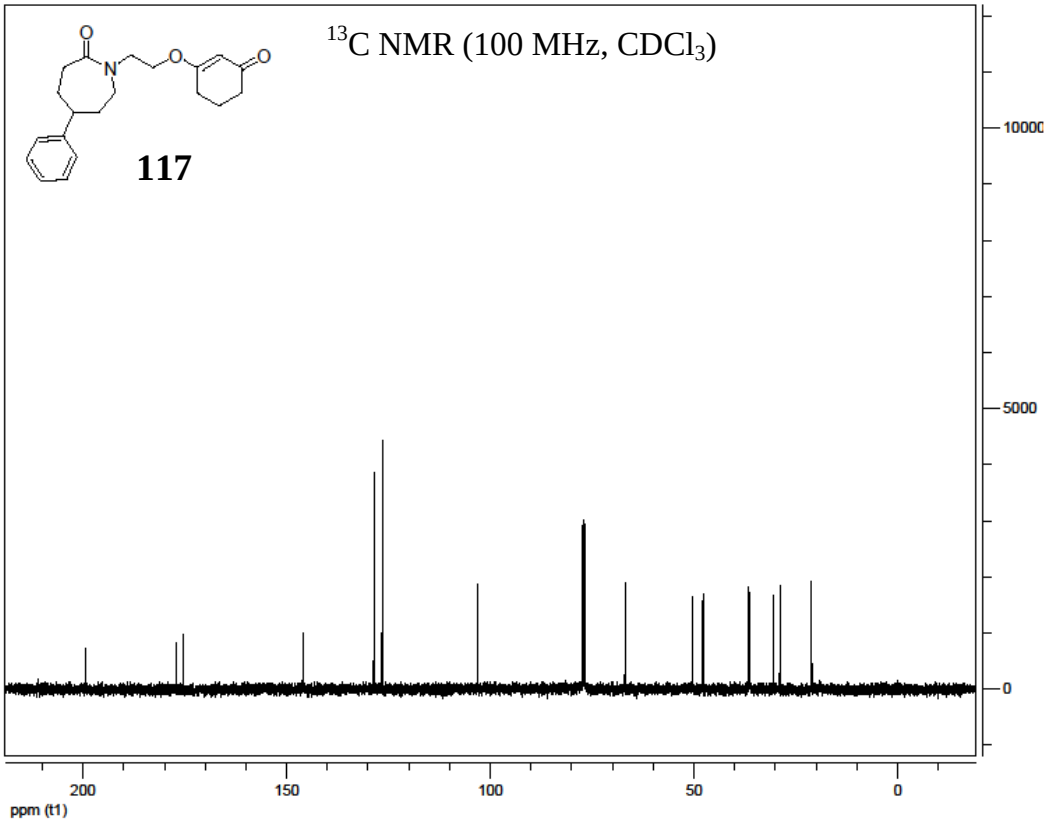
117
$^{13}$C NMR (100 MHz, $CDCl_3$)
10000
5000
0
200
150
100
50
0
ppm (t1)

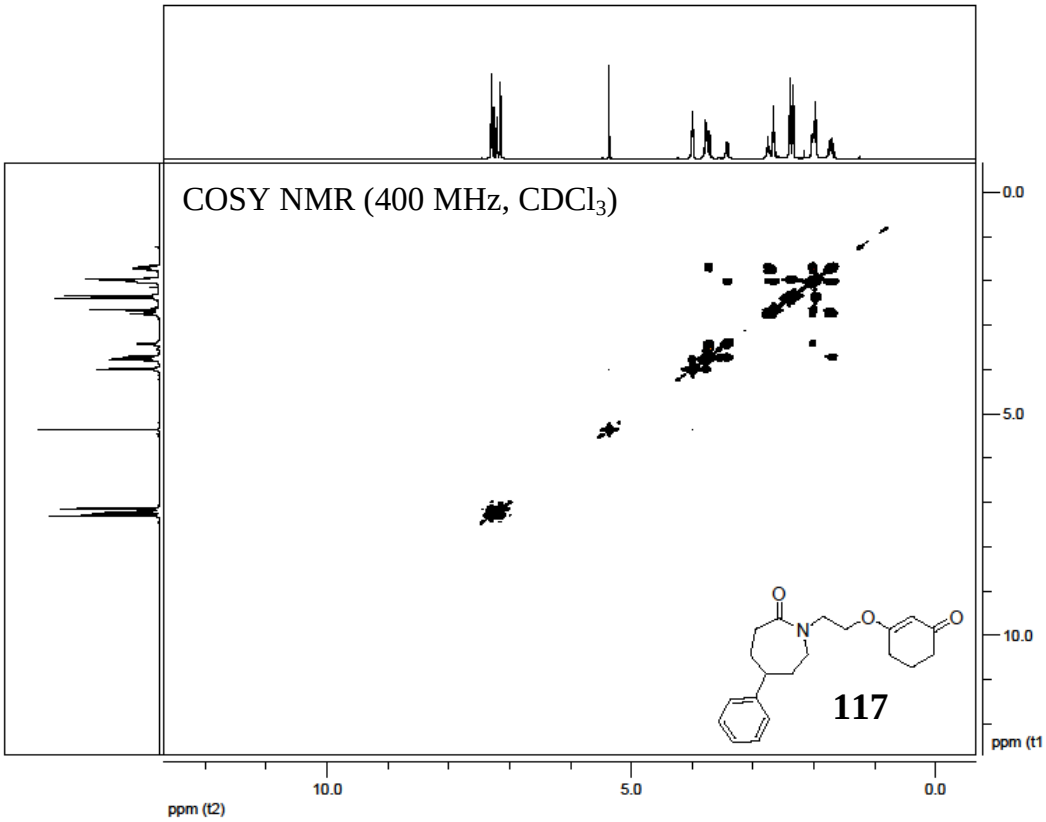
COSY NMR (400 MHz, CDCl3)
117
10.0
5.0
0.0
ppm (t2)
ppm (t1

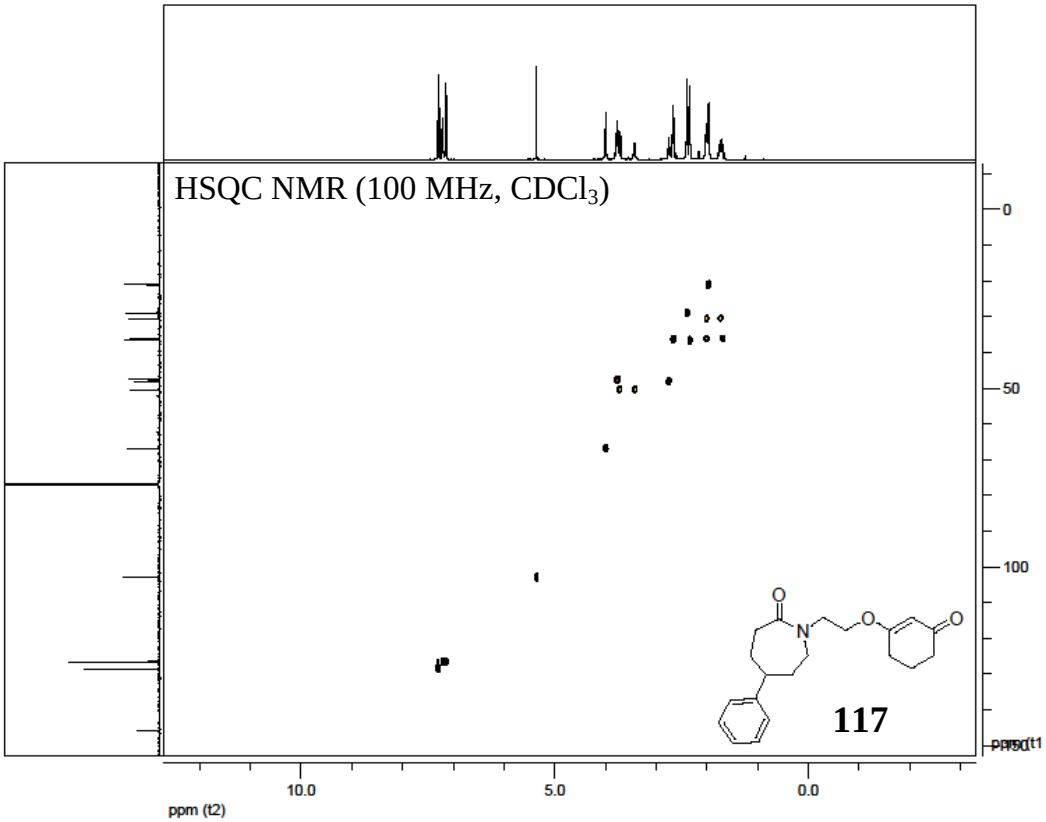
HSQC NMR (100 MHz, CDCl3)
117
10.0
5.0
0.0
ppm (t2)
0
50
100

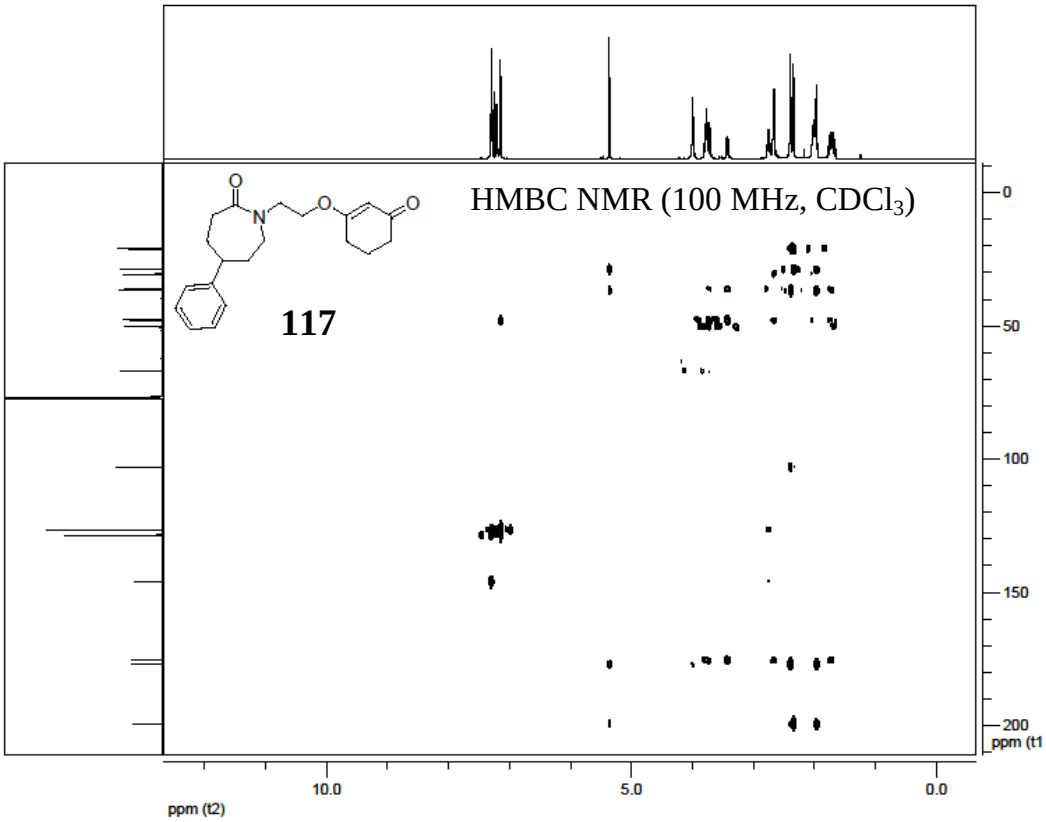
HMBC NMR (100 MHz, CDCl3)
117
0
50
100
150
200
ppm (t1
10.0
5.0
0.0
ppm (t2)

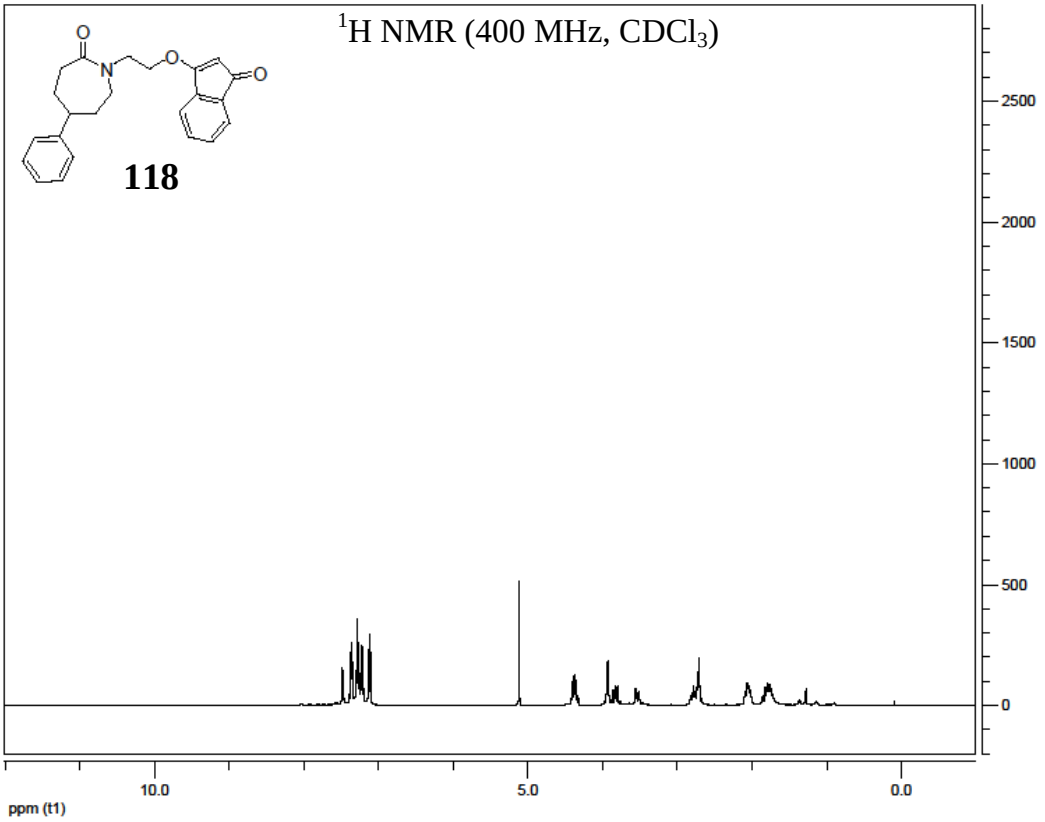
$^{1}$H NMR (400 MHz, $CDCl_3$)
118
2500
2000
1500
1000
500
0
10.0
5.0
0.0
ppm (t1)

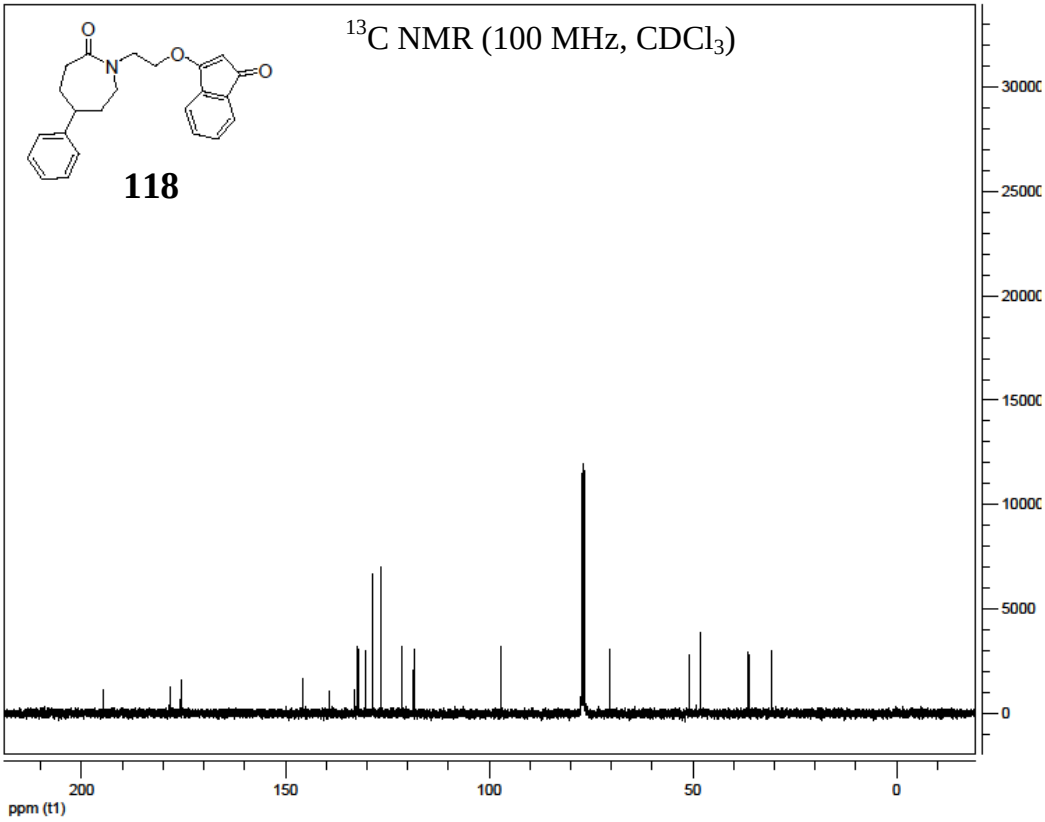
$^{13}$C NMR (100 MHz, $CDCl_3$)
118
30000
25000
20000
15000
10000
5000
0
200
150
100
50
0
ppm (t1)

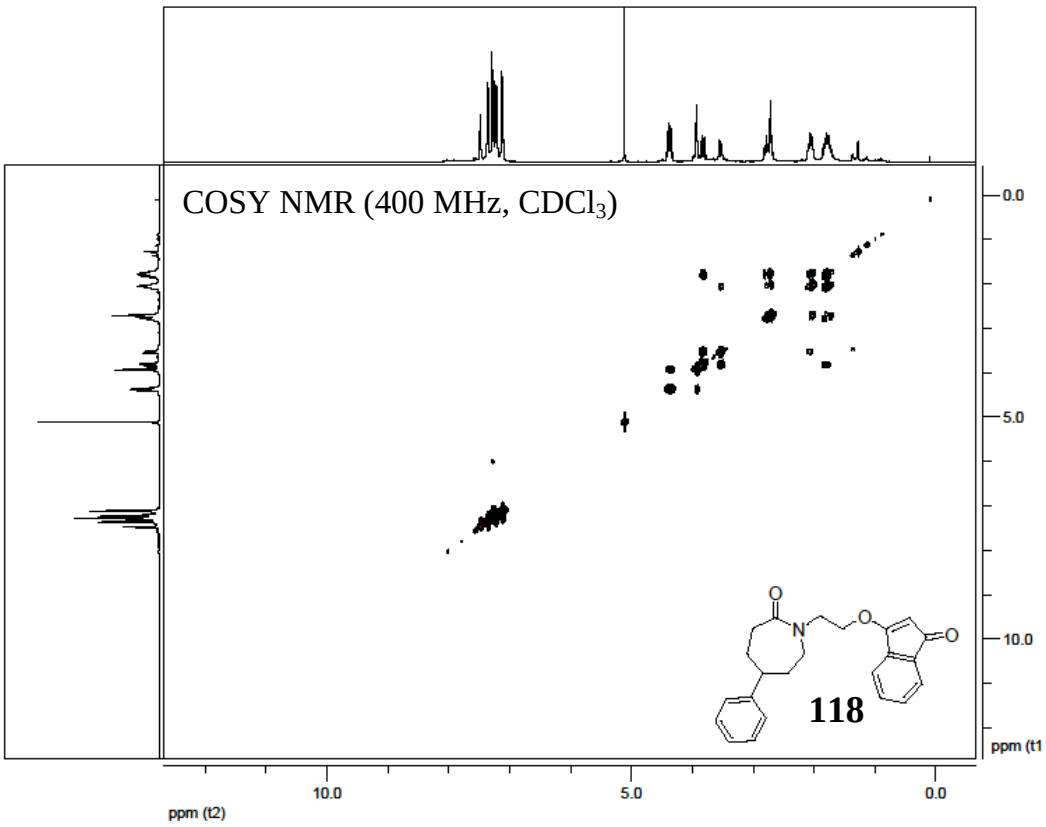
COSY NMR (400 MHz, CDCl3)
118
0.0
5.0
10.0
ppm (t1
10.0
5.0
0.0
ppm (t2)

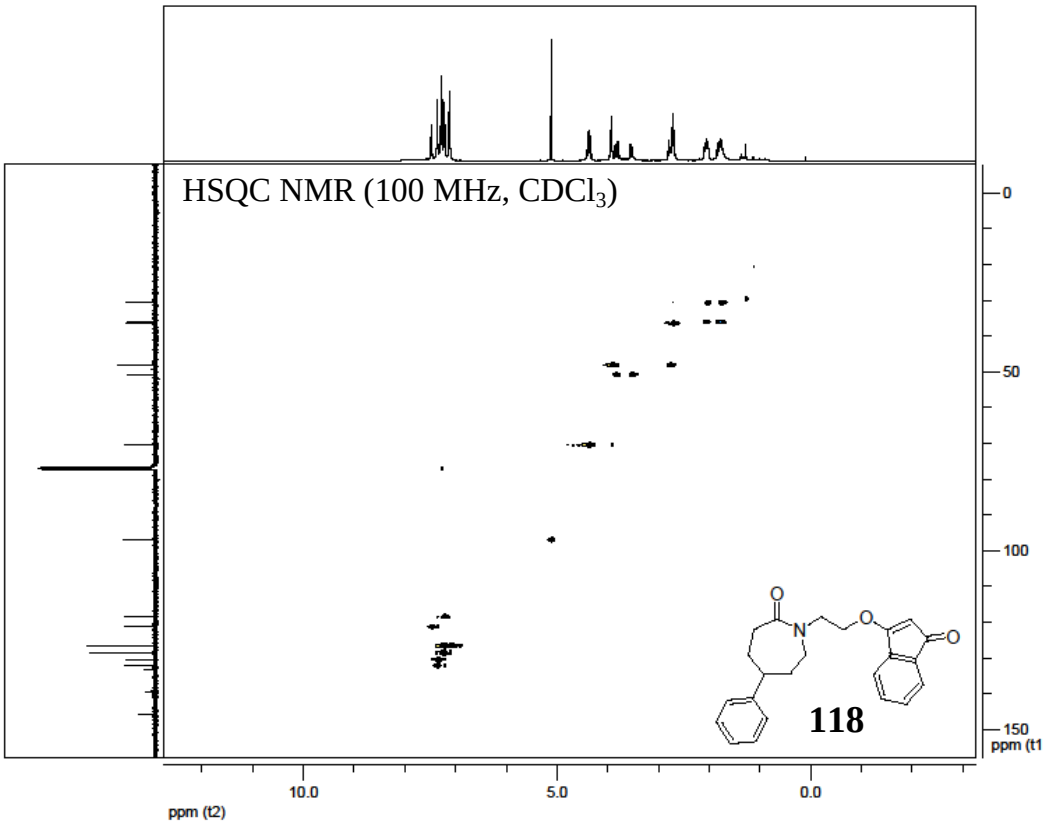
HSQC NMR (100 MHz, CDCl3)
118
0
50
100
150
ppm (t1
10.0
5.0
0.0
ppm (t2)

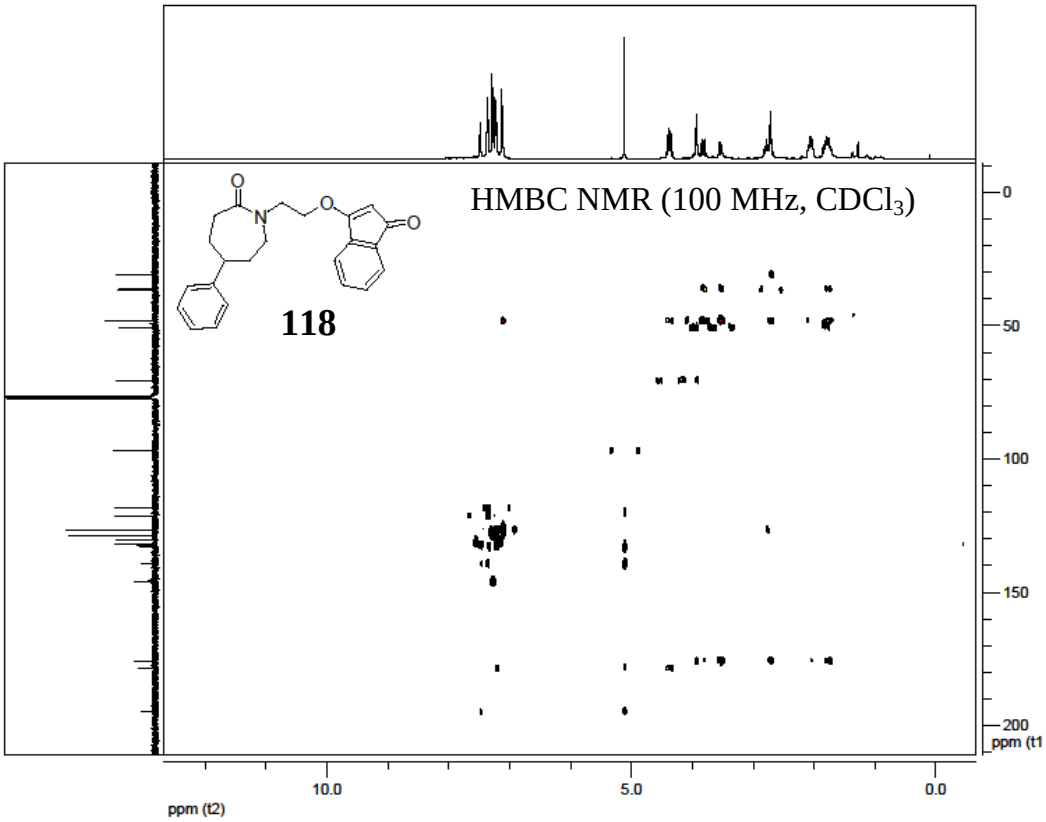
HMBC NMR (100 MHz, CDCl3)
118
O
N
O
O
0
50
100
150
200
ppm (t1
10.0
5.0
0.0
ppm (t2)

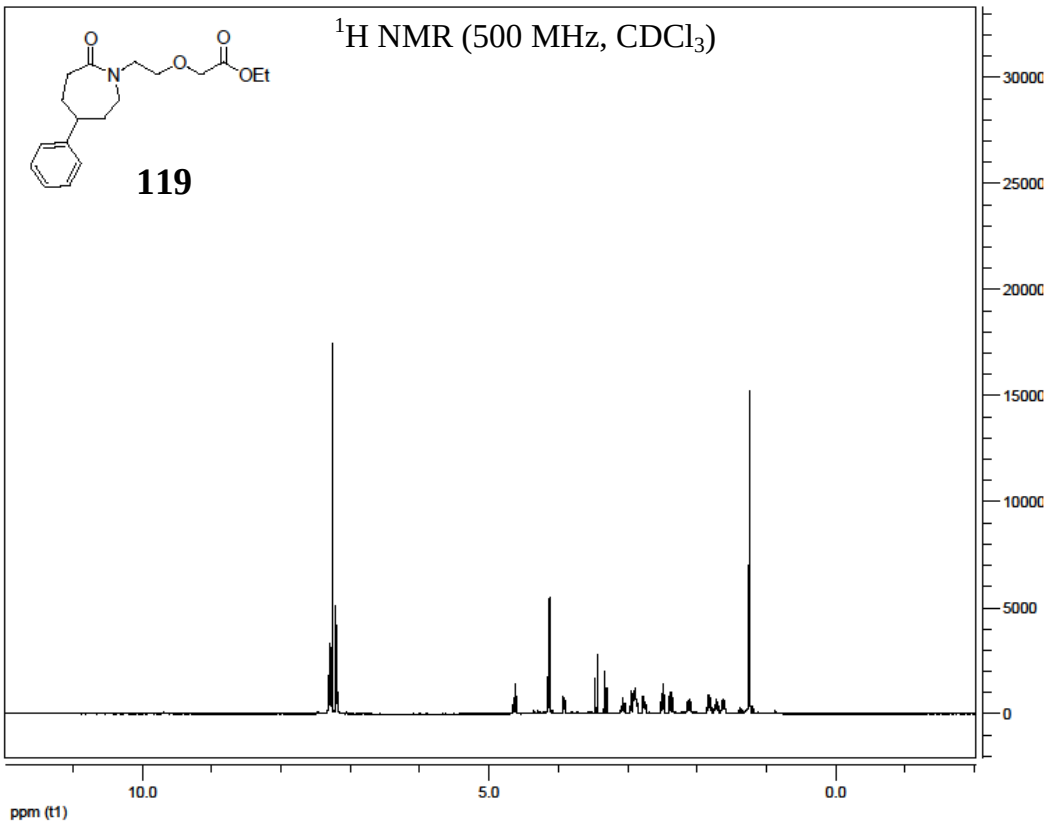
$^{1}$H NMR (500 MHz, $CDCl_3$)
119
30000
25000
20000
15000
10000
5000
0
10.0
5.0
0.0
ppm (t1)

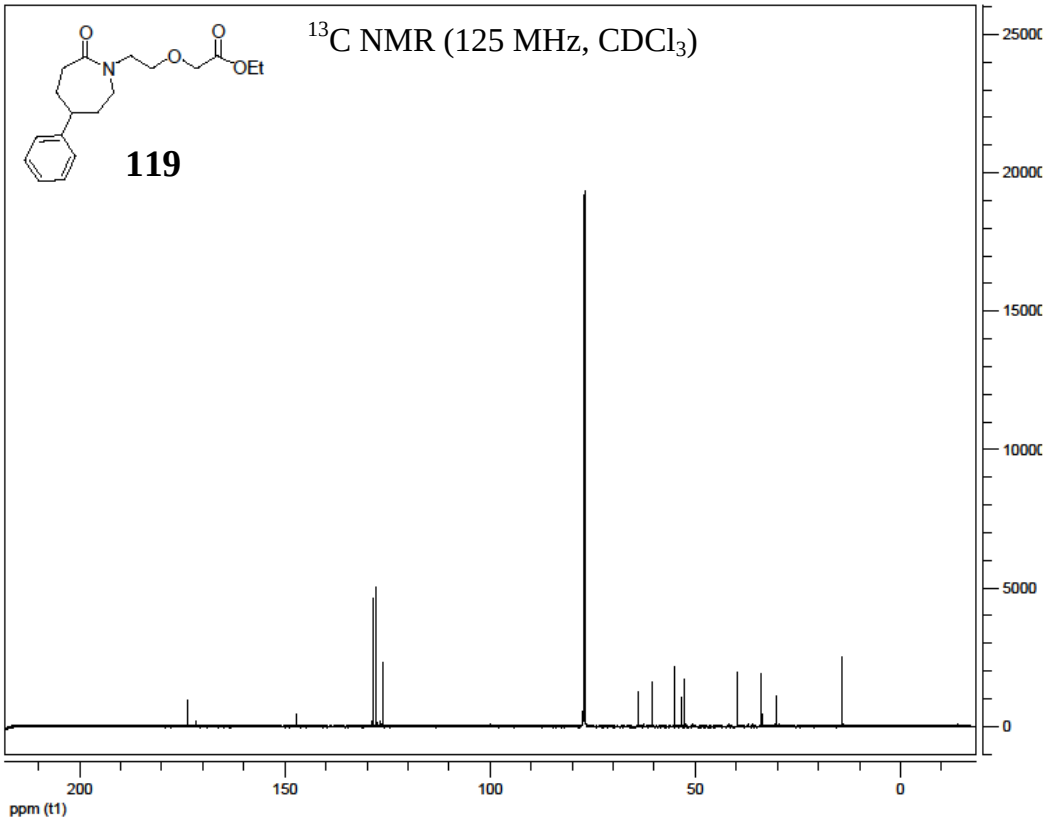
$^{13}$C NMR (125 MHz, $CDCl_3$)
119
25000
20000
15000
10000
5000
0
200
150
100
50
0
ppm (t1)

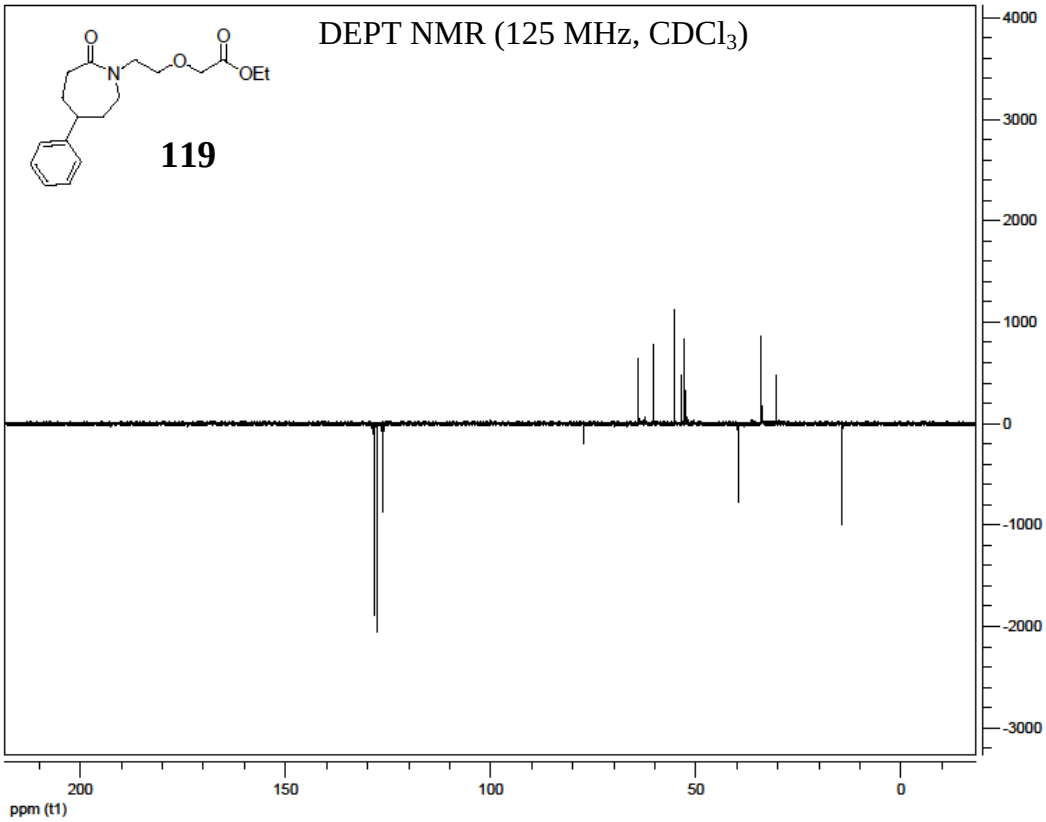
DEPT NMR (125 MHz, CDCl3)
119
4000
3000
2000
1000
0
-1000
-2000
-3000
200
150
100
50
0
ppm (t1)

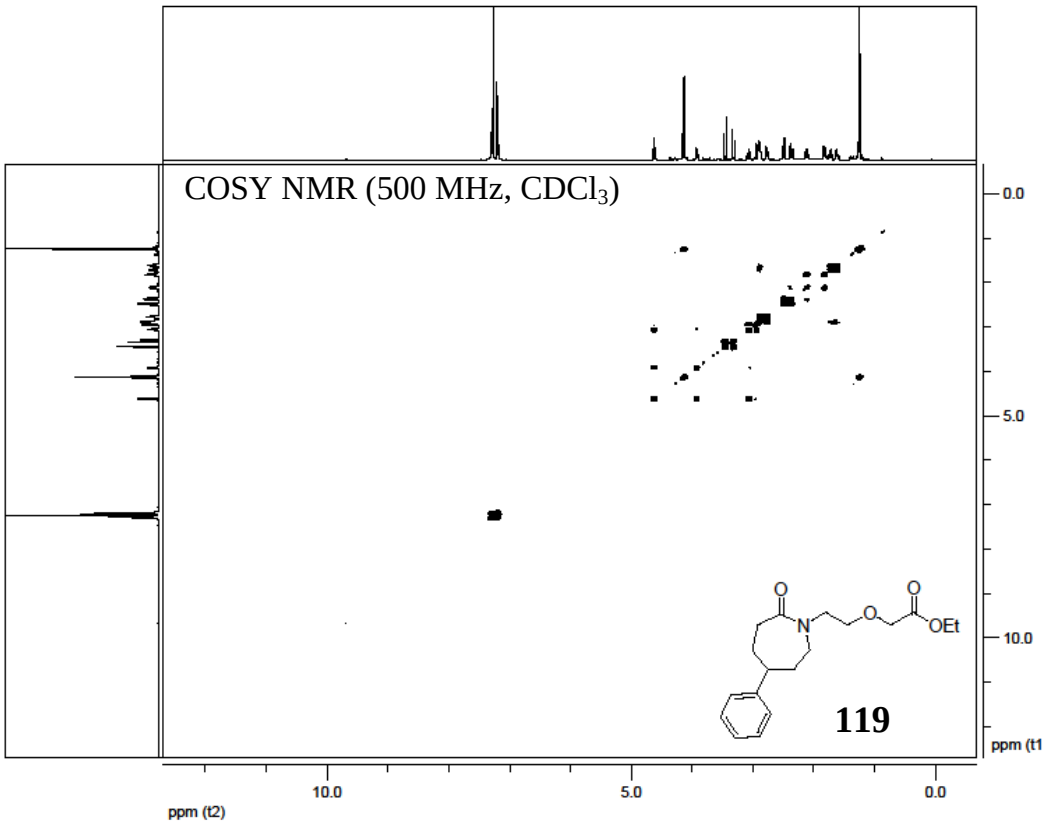
COSY NMR (500 MHz, CDCl3)
119
0.0
5.0
10.0
ppm (t1
10.0
5.0
0.0
ppm (t2)

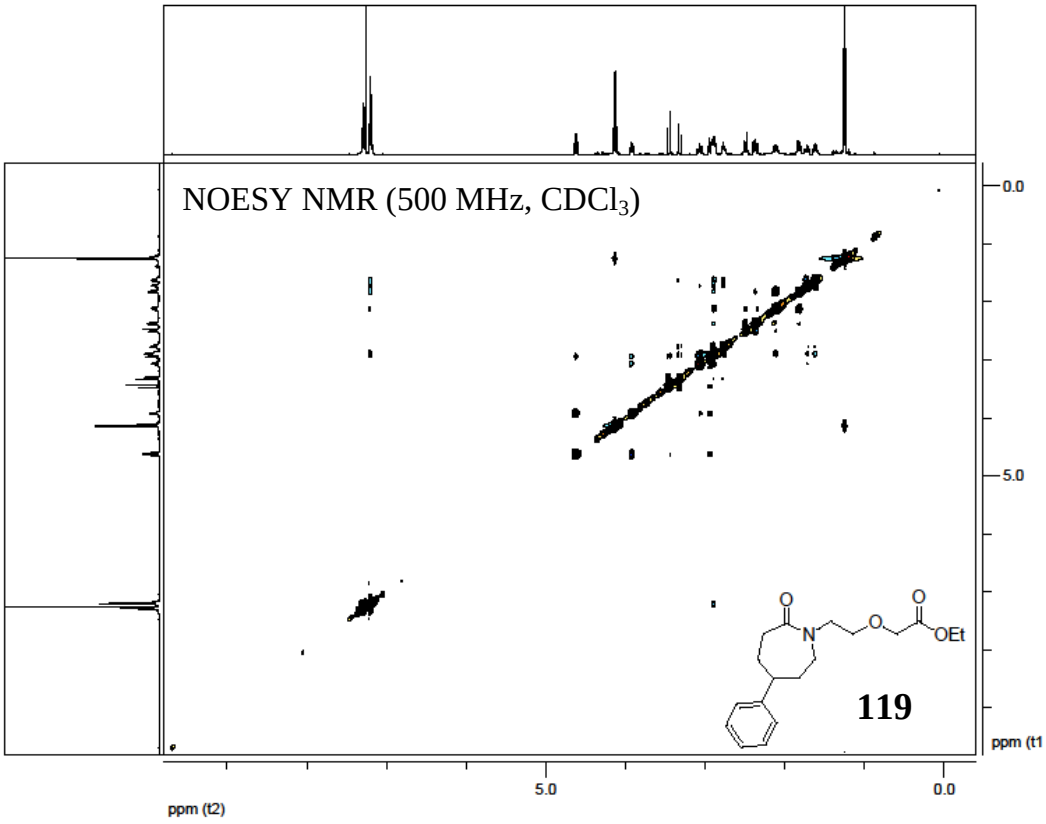
NOESY NMR (500 MHz, CDCl3)
0.0
5.0
O
N
O
O
OEt
119
ppm (t1
5.0
0.0
ppm (t2)

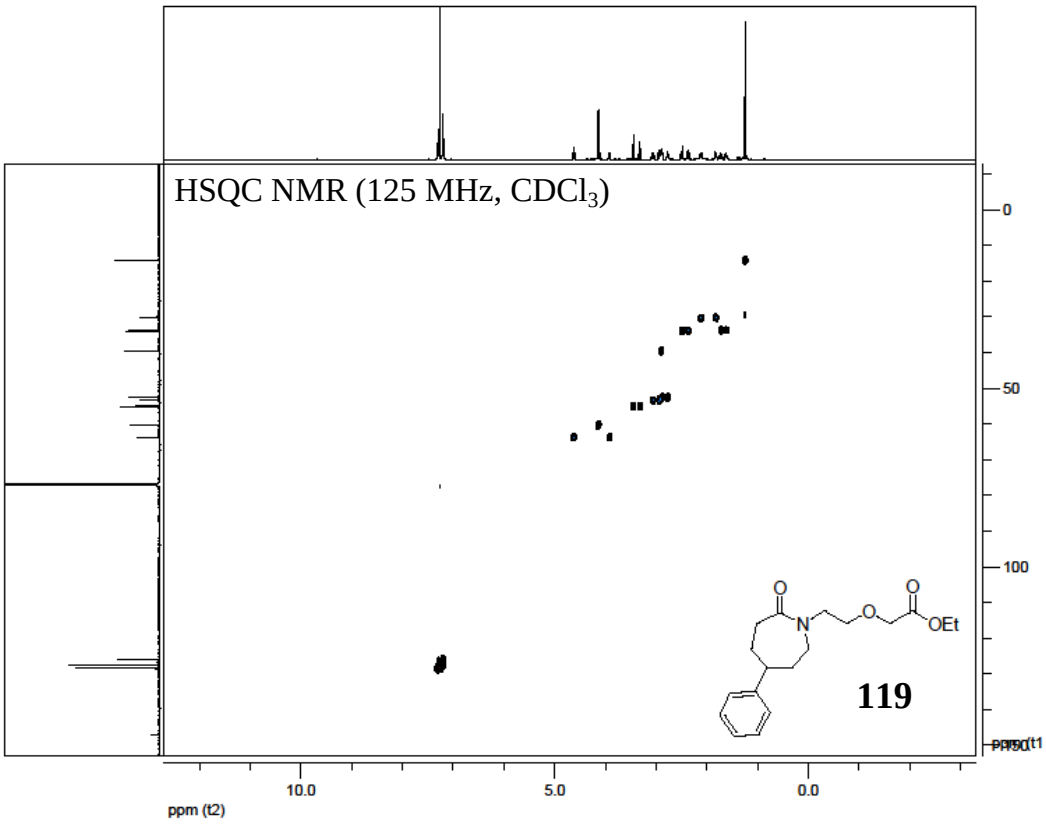
HSQC NMR (125 MHz, CDCl3)
0
50
100
O
N
O
O
OEt
119
ppm (t1
10.0
5.0
0.0
ppm (t2)

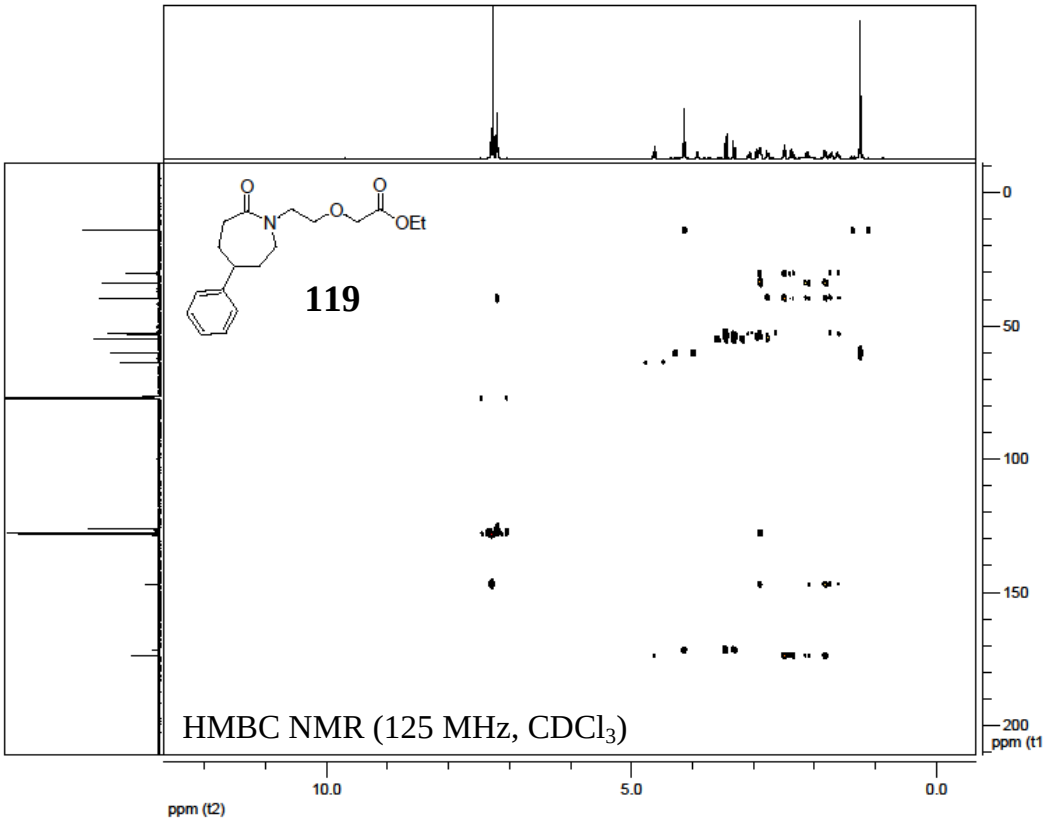


HMBC NMR (125 MHz, $CDCl_3$)

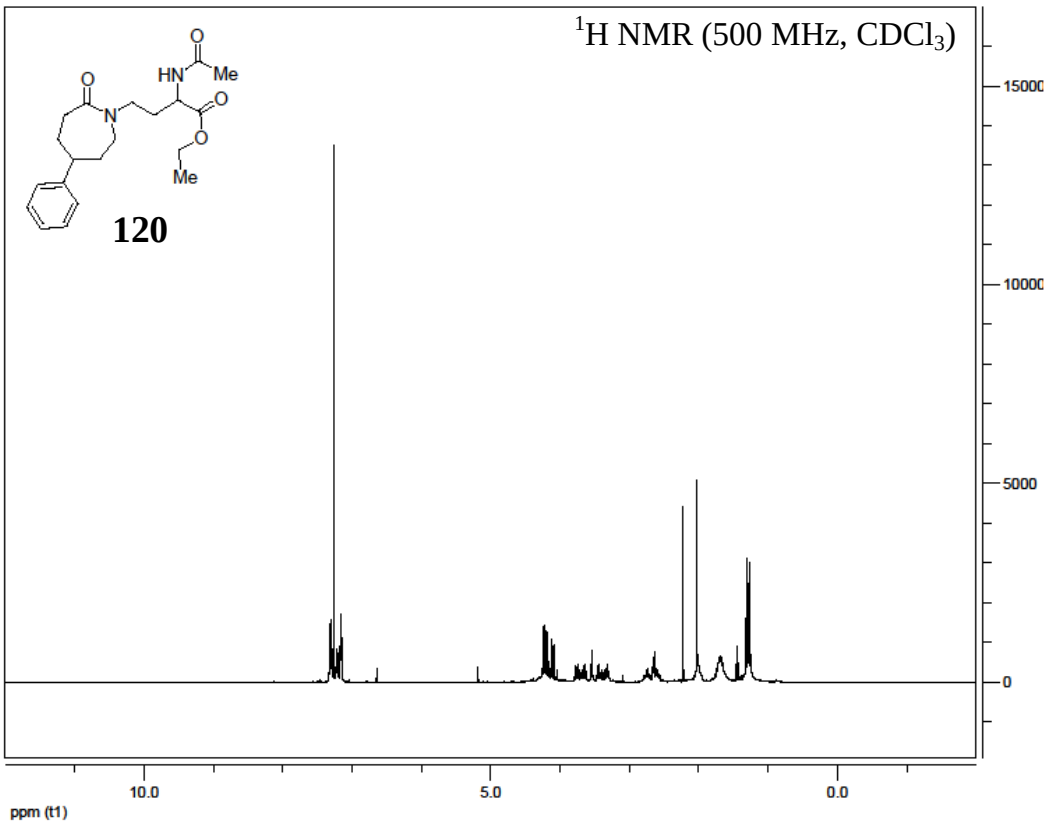
$^{1}$H NMR (500 MHz, $CDCl_3$)
HN
Me
O
N
O
O
Me
120
15000
10000
5000
0
10.0
5.0
0.0
ppm (t1)

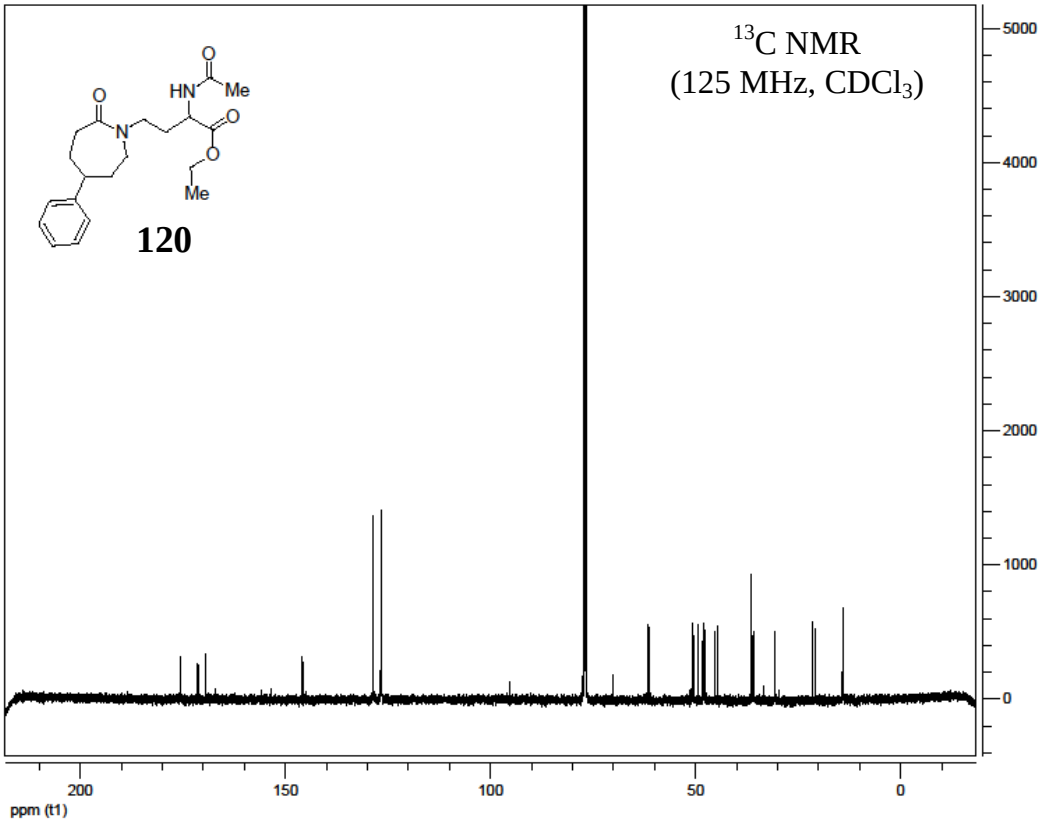
$^{13}$C NMR
(125 MHz, $CDCl_3$)
HN
Me
O
N
O
O
Me
120
5000
4000
3000
2000
1000
0
200
150
100
50
0
ppm (t1)

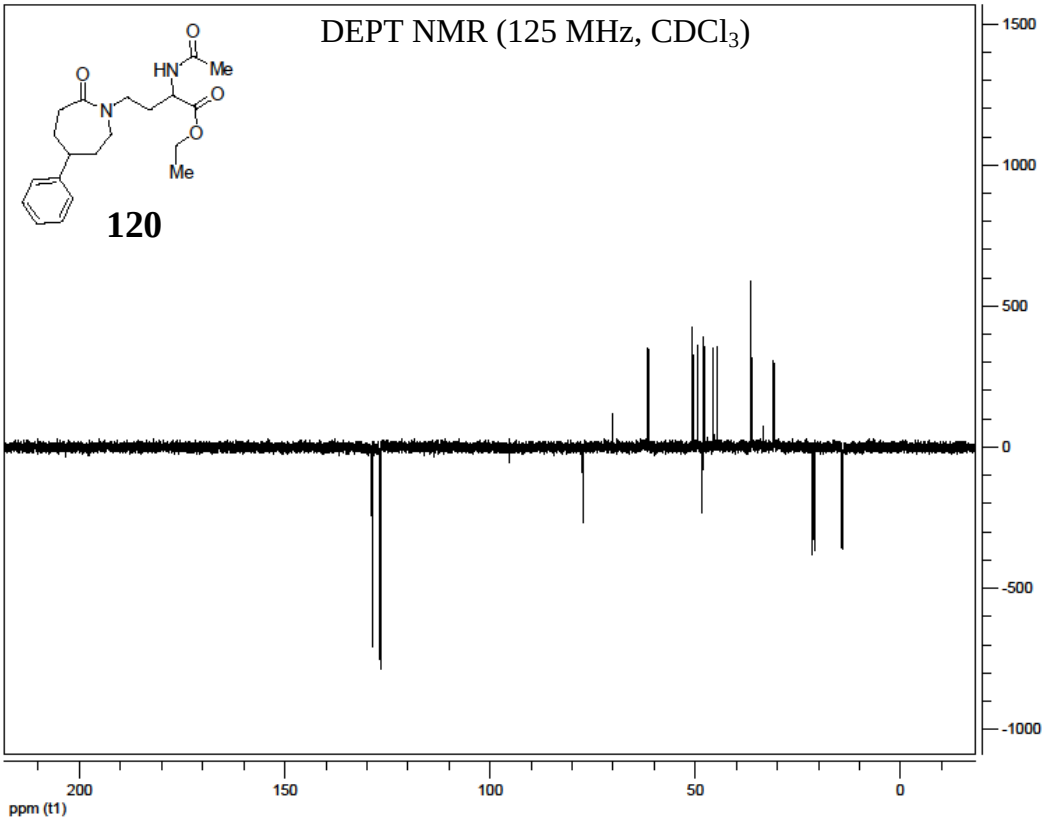
DEPT NMR (125 MHz, CDCl3)
120
1500
1000
500
0
-500
-1000
200
150
100
50
0
ppm (t1)

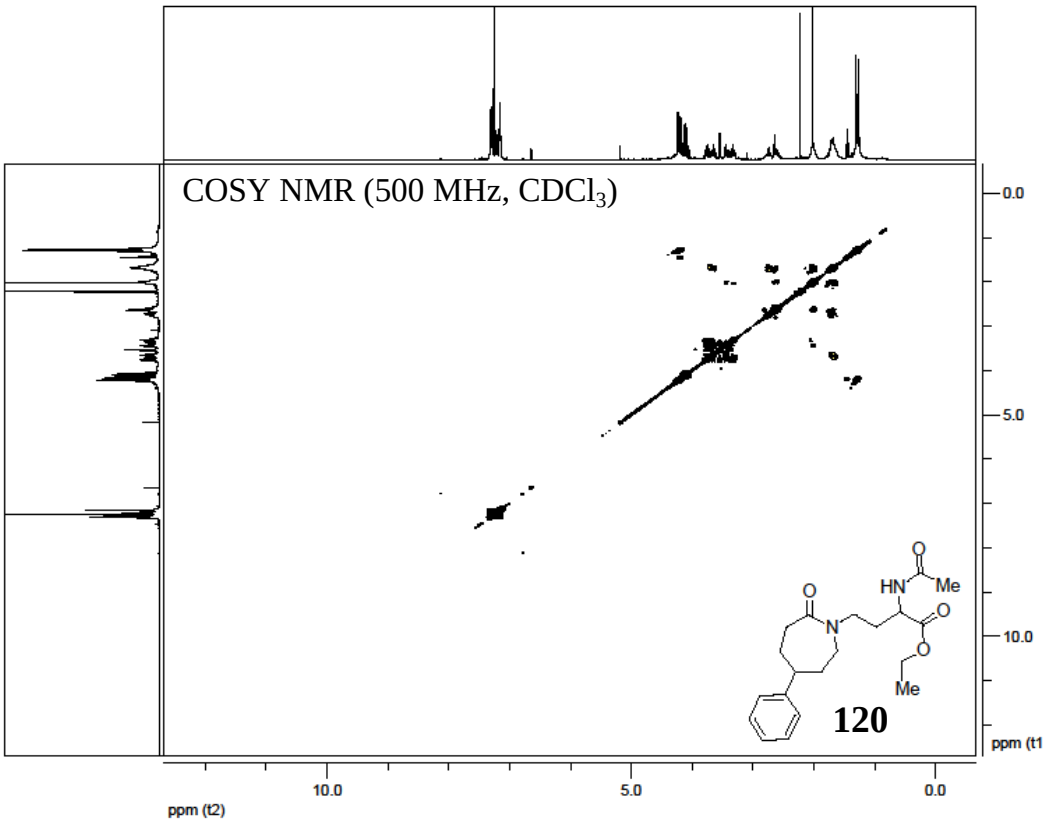
COSY NMR (500 MHz, CDCl3)
120
0.0
5.0
10.0
10.0
5.0
0.0
ppm (t2)
ppm (t1

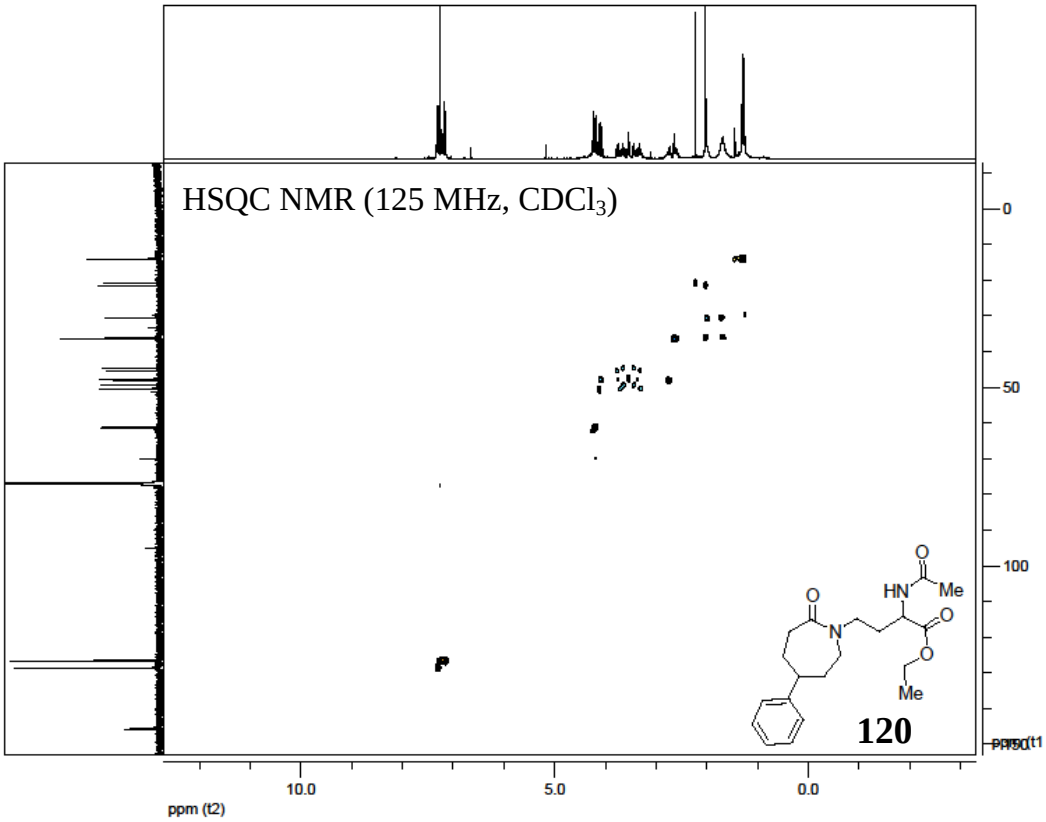
HSQC NMR (125 MHz, CDCl3)
120
10.0
5.0
0.0
ppm (t2)
0
50
100

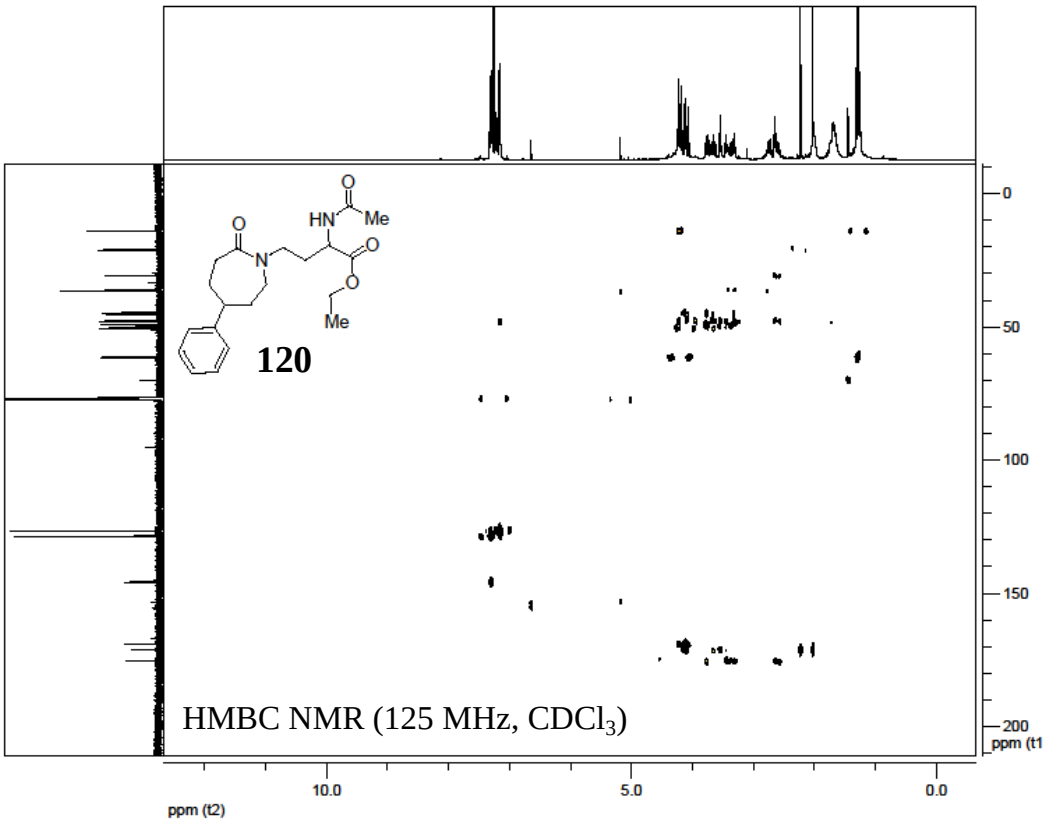
120
HMBC NMR (125 MHz, CDCl3)
10.0
5.0
0.0
ppm (t2)
0
50
100
150
200
ppm (t1

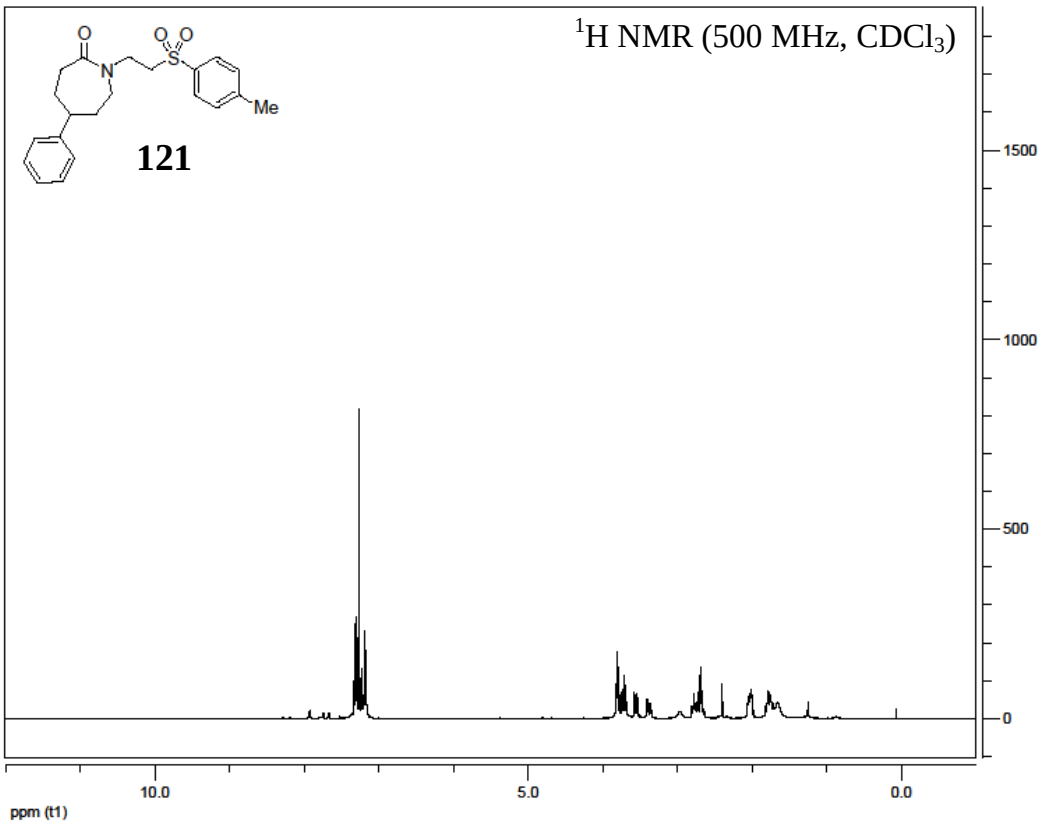
$^{1}$H NMR (500 MHz, $CDCl_3$)
121
Me
1500
1000
500
0
10.0
5.0
0.0
ppm (t1)

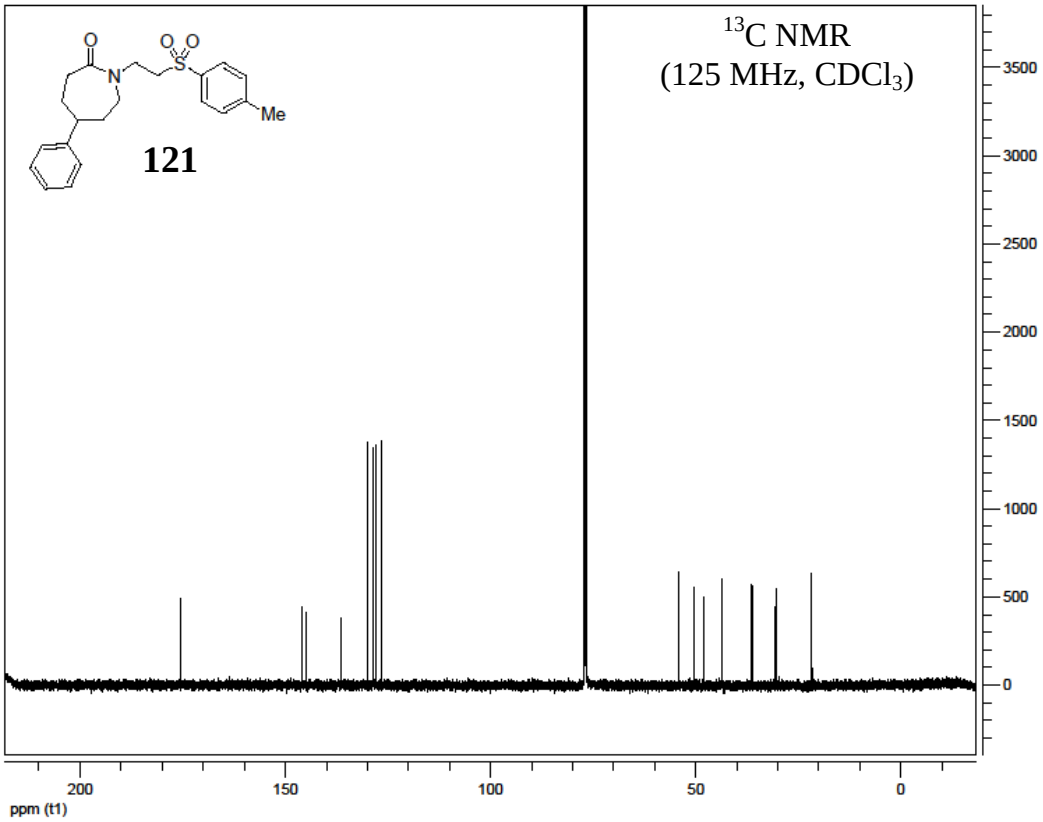
$^{13}$C NMR
(125 MHz, $CDCl_3$)
121
Me
3500
3000
2500
2000
1500
1000
500
0
200
150
100
50
0
ppm (t1)

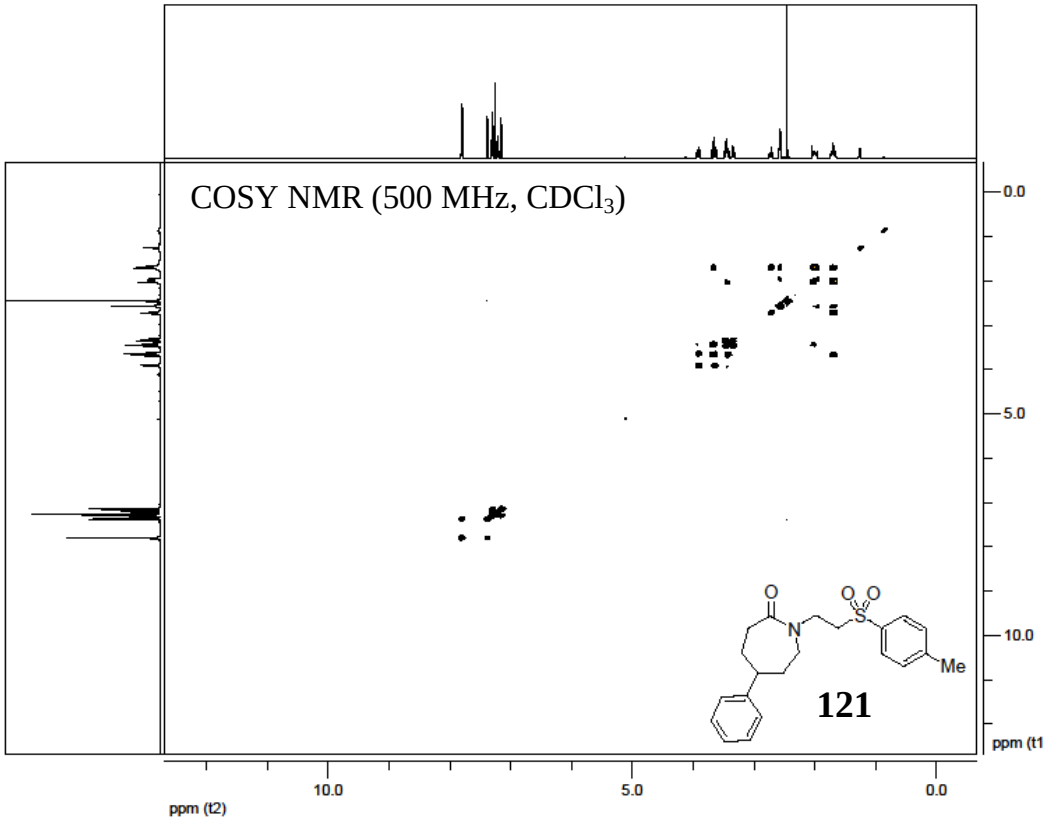
COSY NMR (500 MHz, CDCl3)
O
O O
N
S
Me
121
0.0
5.0
10.0
ppm (t1
10.0
5.0
0.0
ppm (t2)

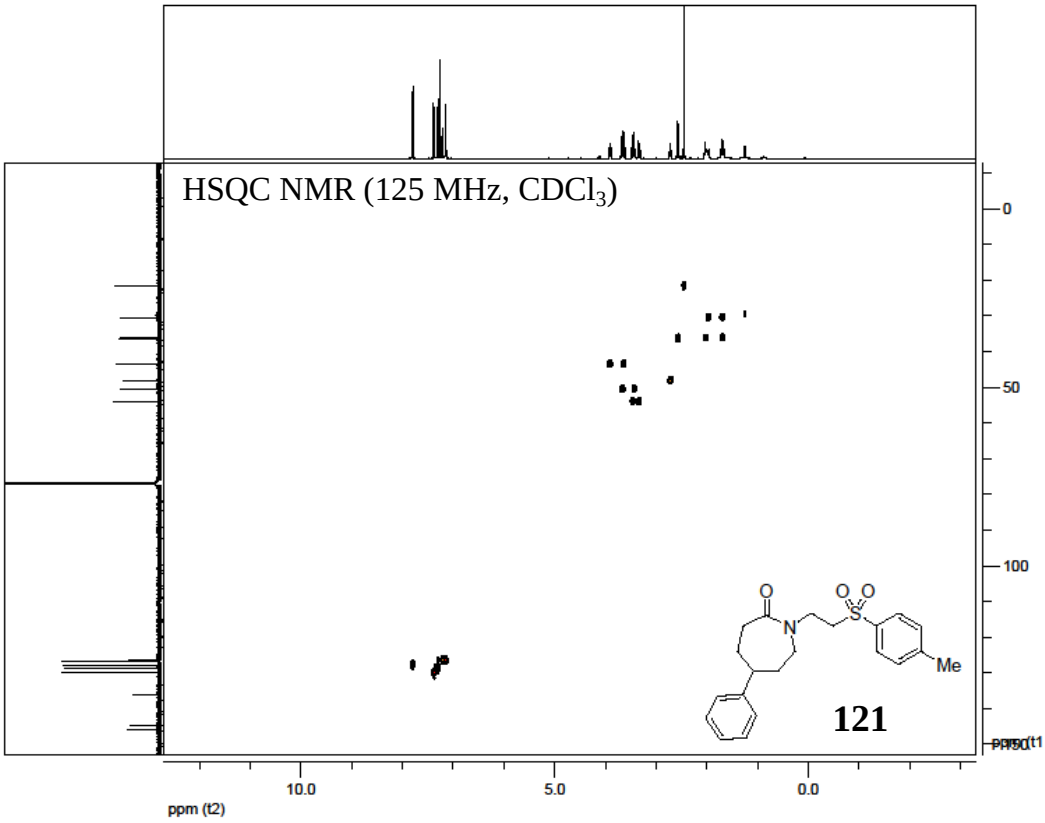
HSQC NMR (125 MHz, CDCl3)
O
O O
N
S
Me
121
0
50
100
10.0
5.0
0.0
ppm (t2)

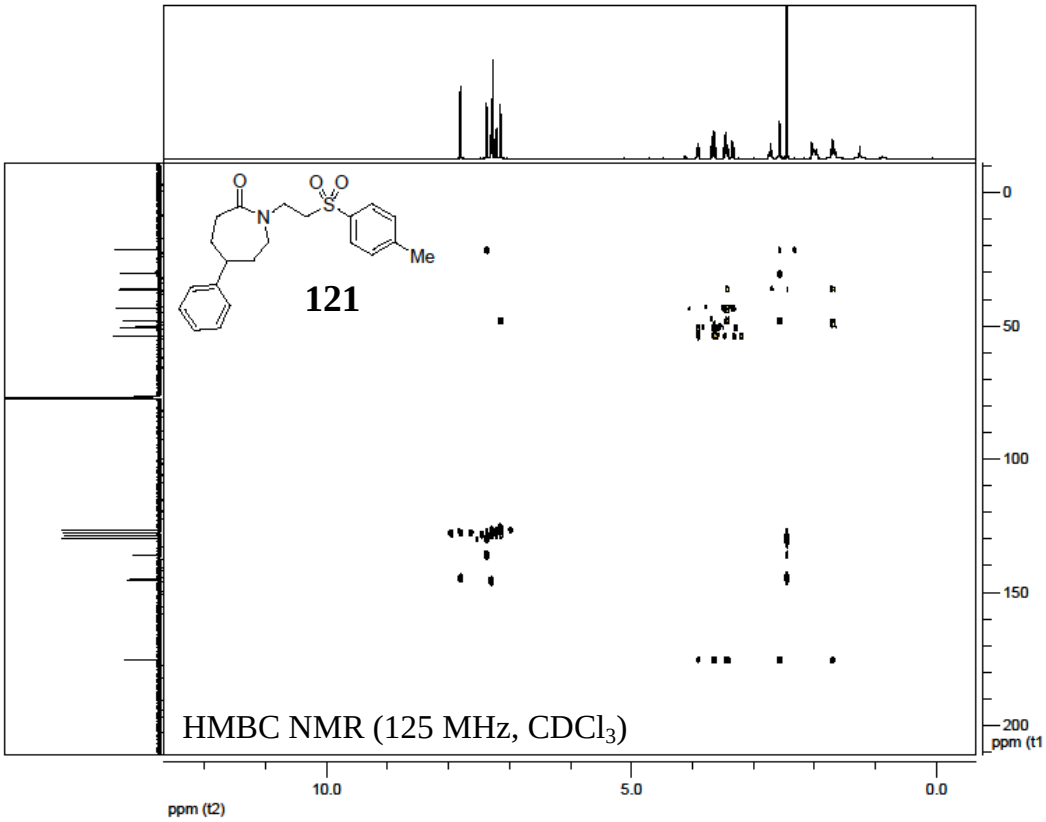


HMBC NMR (125 MHz, $CDCl_3$)

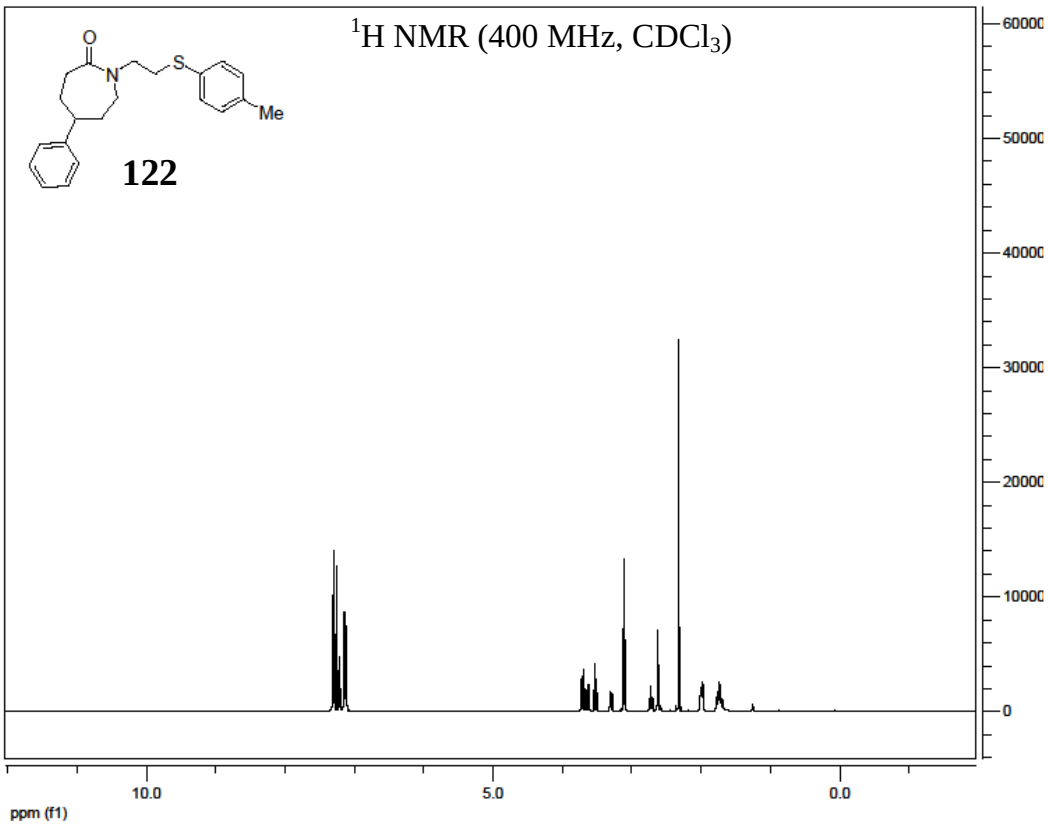
$^{1}$H NMR (400 MHz, $CDCl_3$)
O
N
S
Me
122
60000
50000
40000
30000
20000
10000
0
10.0
5.0
0.0
ppm (f1)

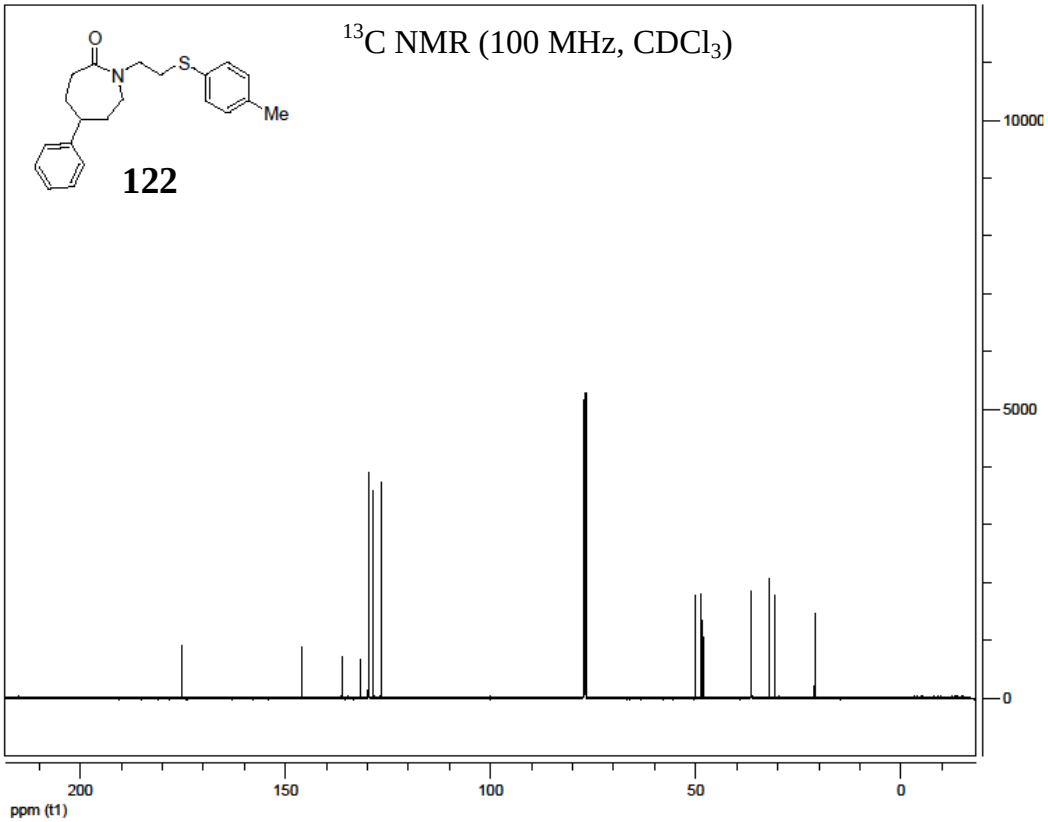
$^{13}$C NMR (100 MHz, $CDCl_3$)
O
N
S
Me
122
10000
5000
0
200
150
100
50
0
ppm (t1)

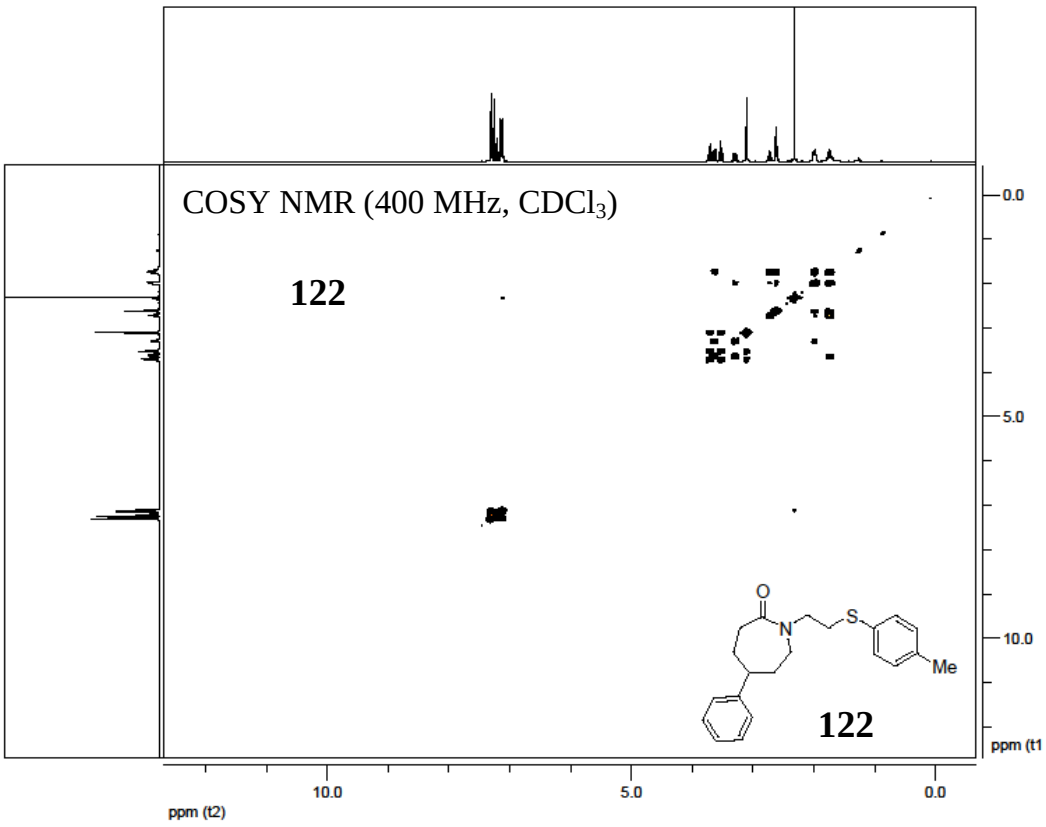
COSY NMR (400 MHz, CDCl3)
122
O
N
S
Me
122
0.0
5.0
10.0
ppm (t1
10.0
5.0
0.0
ppm (t2)

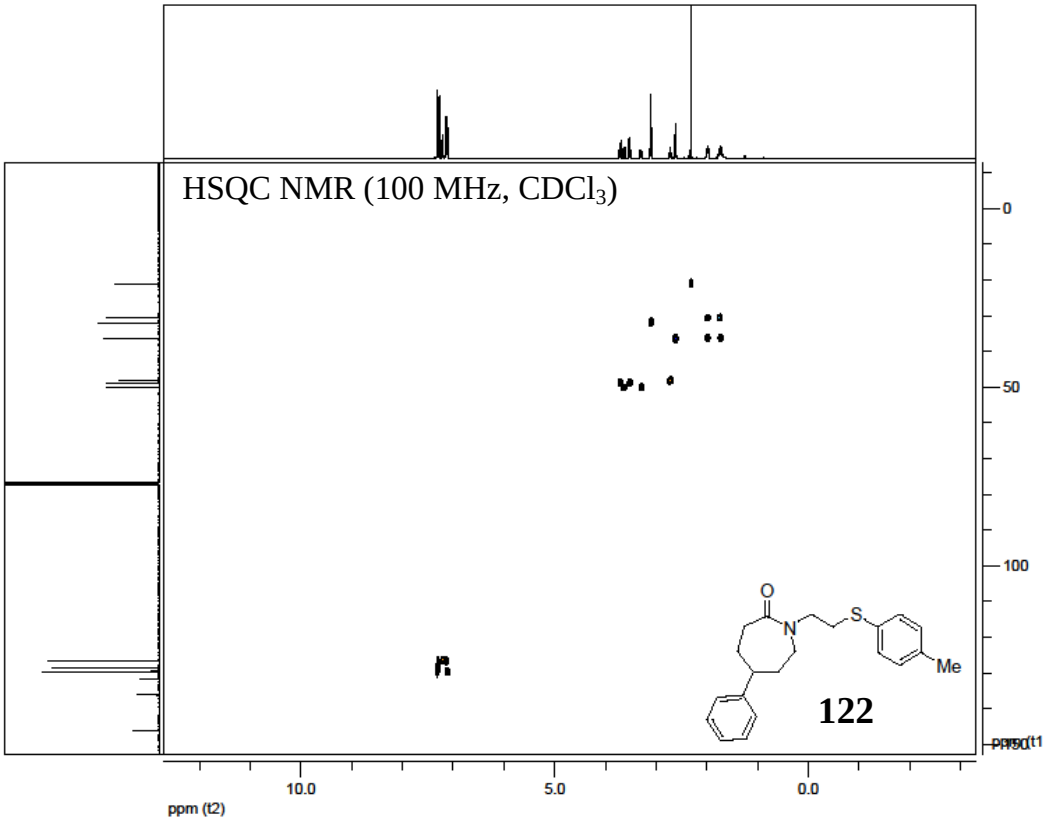
HSQC NMR (100 MHz, CDCl3)
O
N
S
Me
122
0
50
100
10.0
5.0
0.0
ppm (t2)

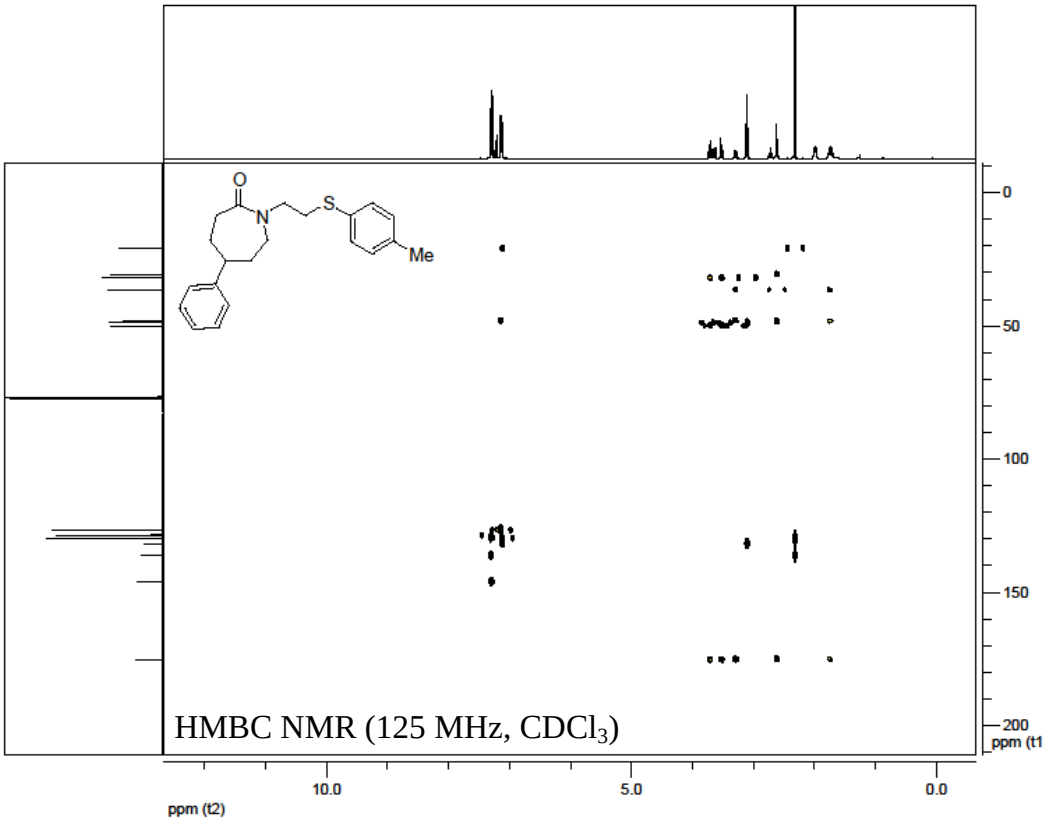


HMBC NMR (125 MHz, $CDCl_3$)

$^{1}$H NMR (400 MHz, $CDCl_3$)

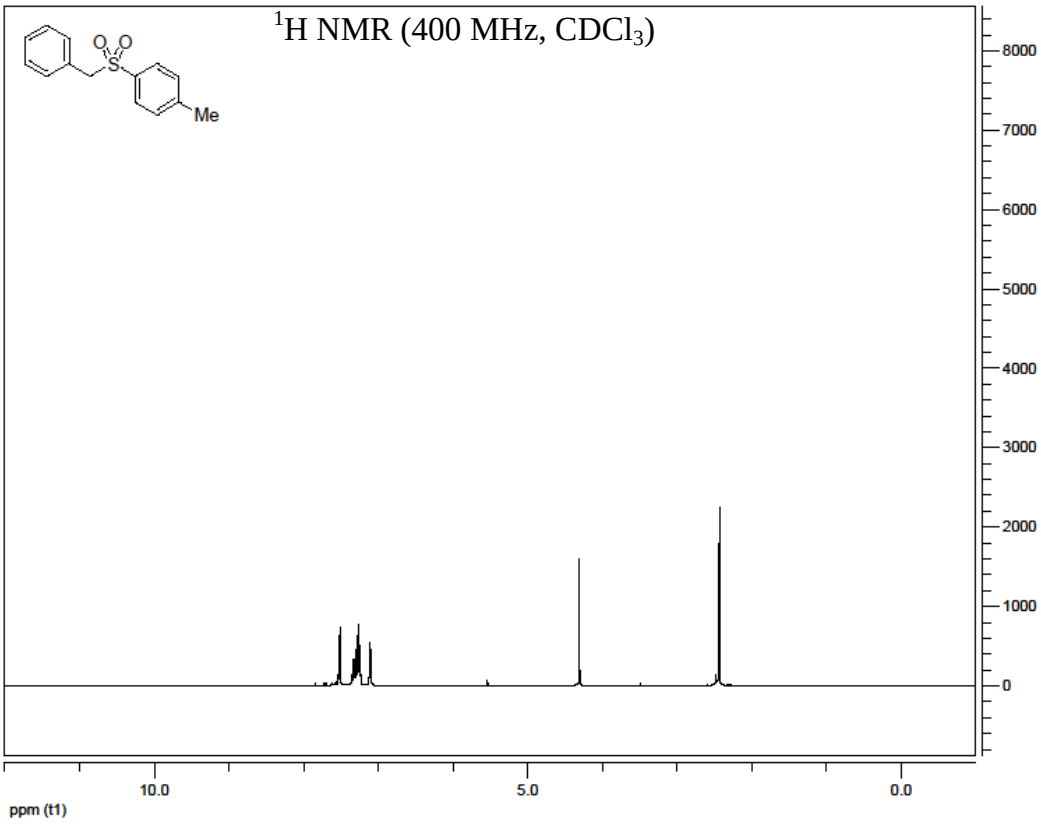


$^{13}$C NMR (100 MHz, $CDCl_3$)

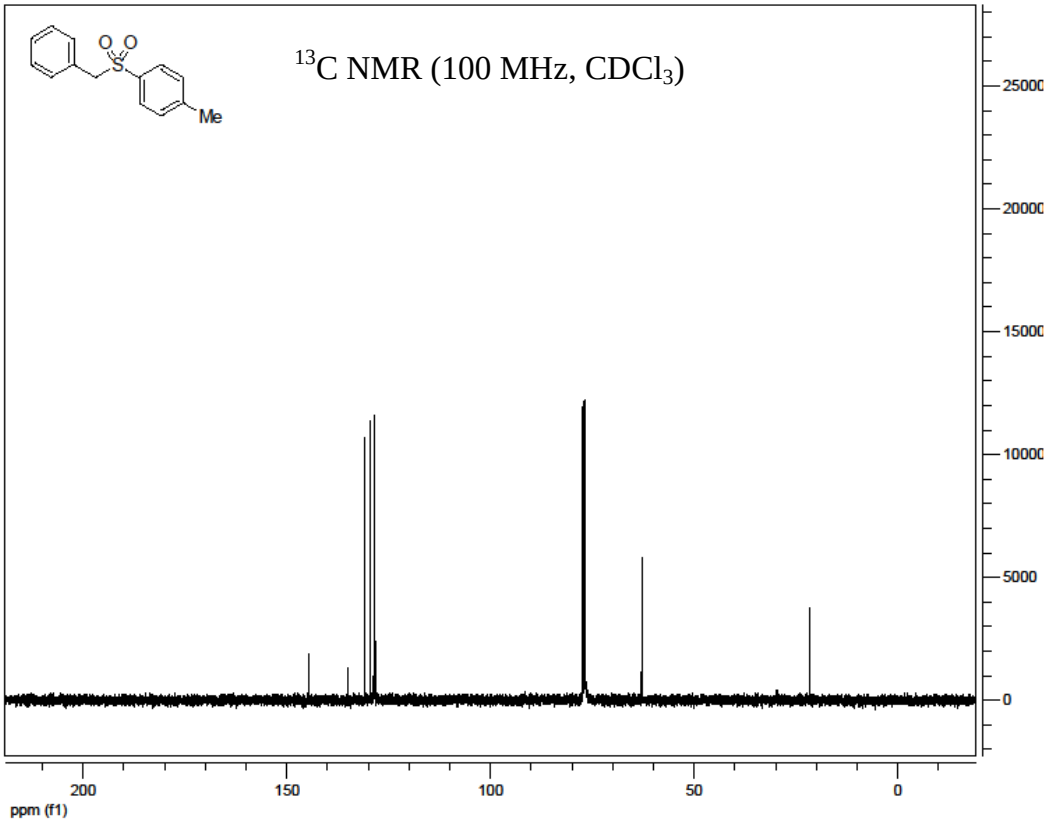

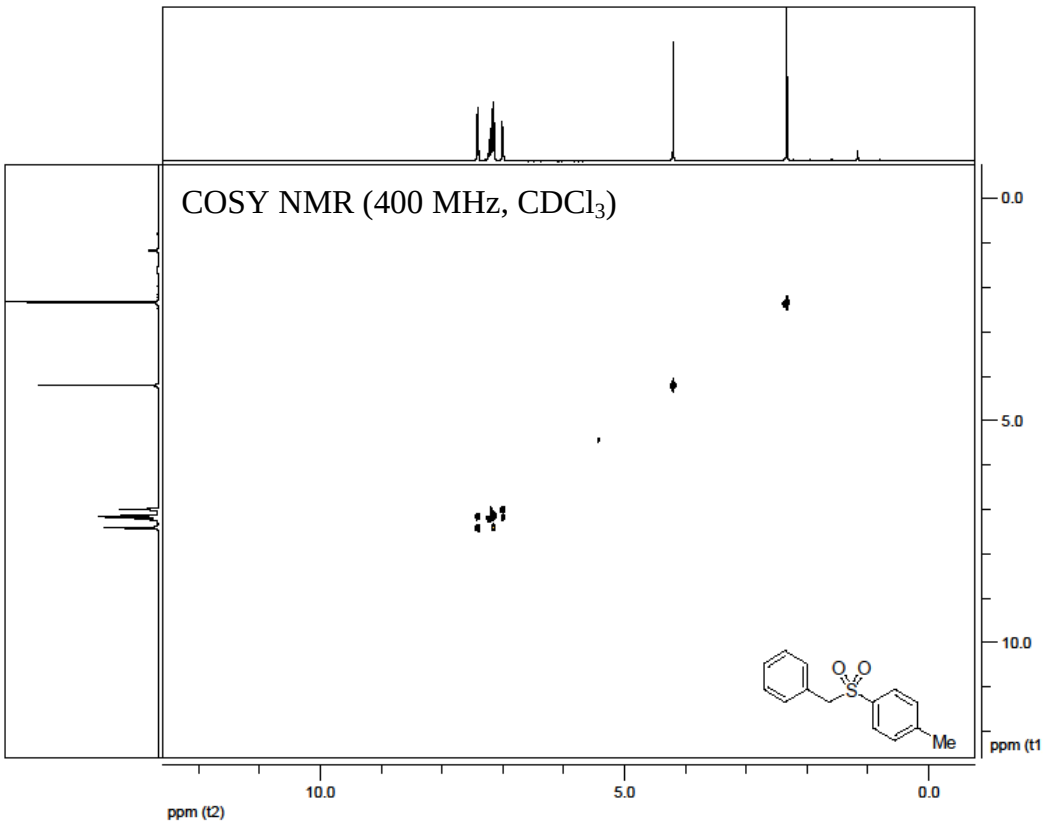
COSY NMR (400 MHz, CDCl3)
0.0
5.0
10.0
ppm (t1
10.0
5.0
0.0
ppm (t2)
O
O
S
Me

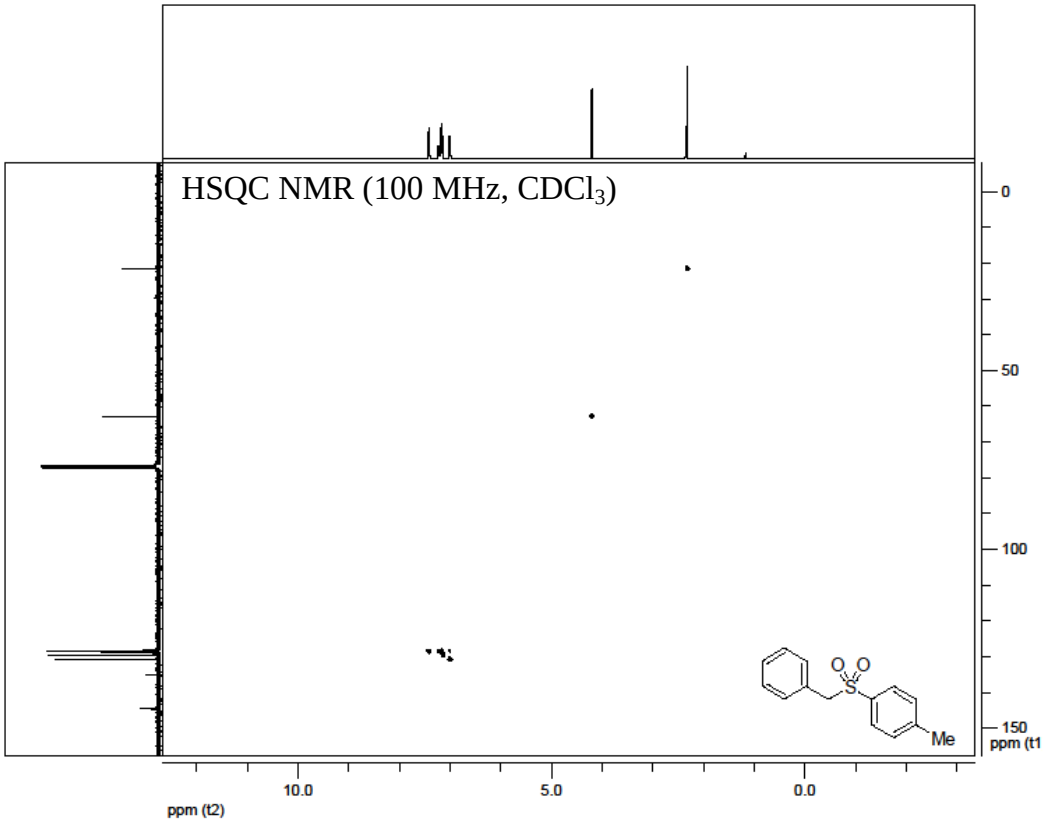
HSQC NMR (100 MHz, CDCl3)
0
50
100
150
ppm (t1
10.0
5.0
0.0
ppm (t2)
O
O
S
Me

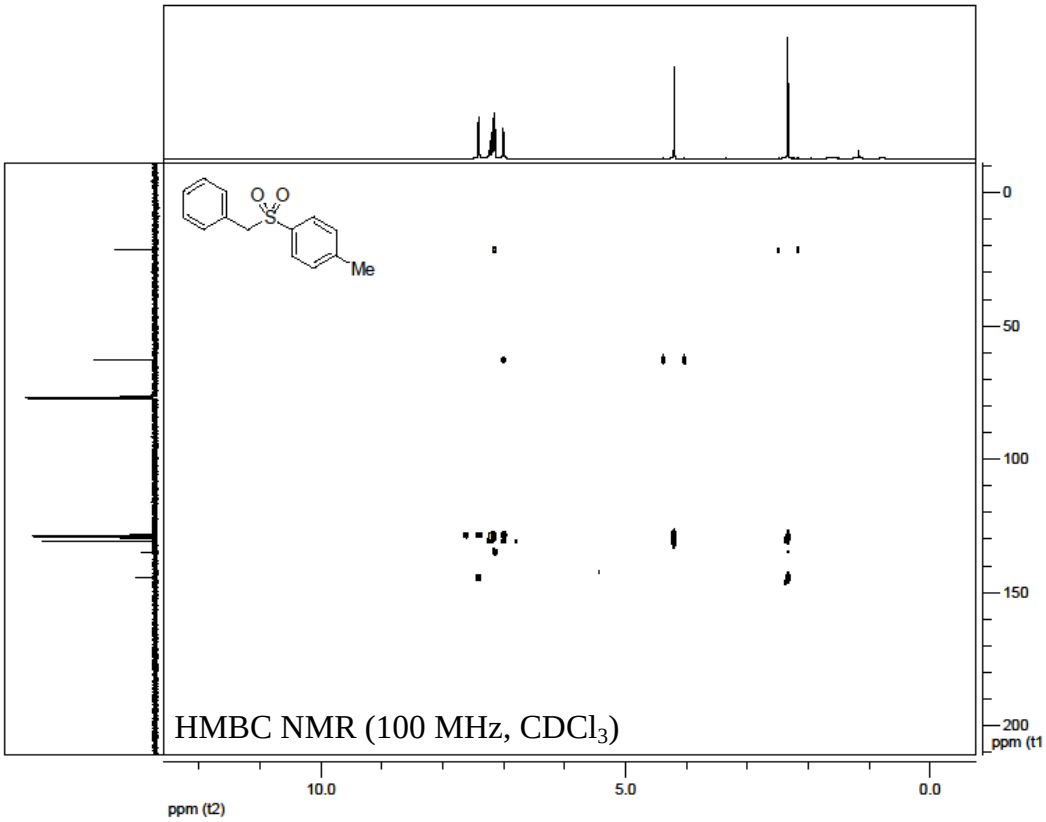


HMBC NMR (100 MHz, $CDCl_3$)

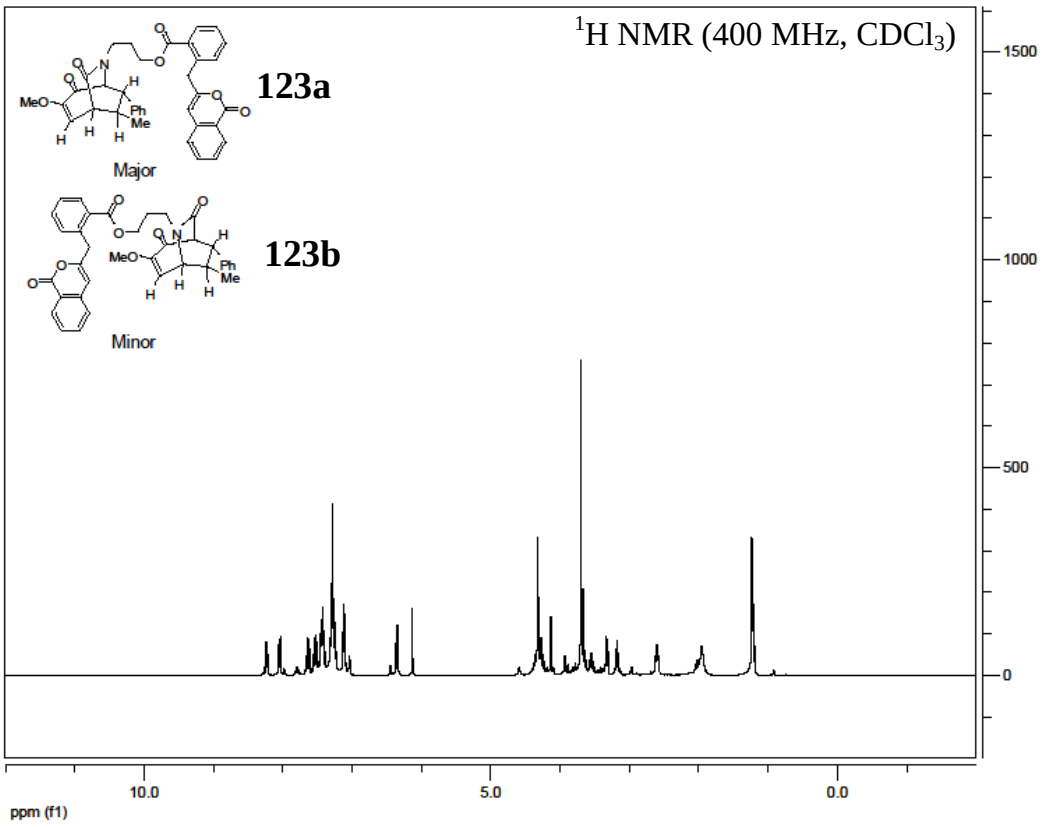
$^1$H NMR (400 MHz, $CDCl_3$)
123a
Major
123b
Minor
1500
1000
500
0
10.0
5.0
0.0
ppm (f1)

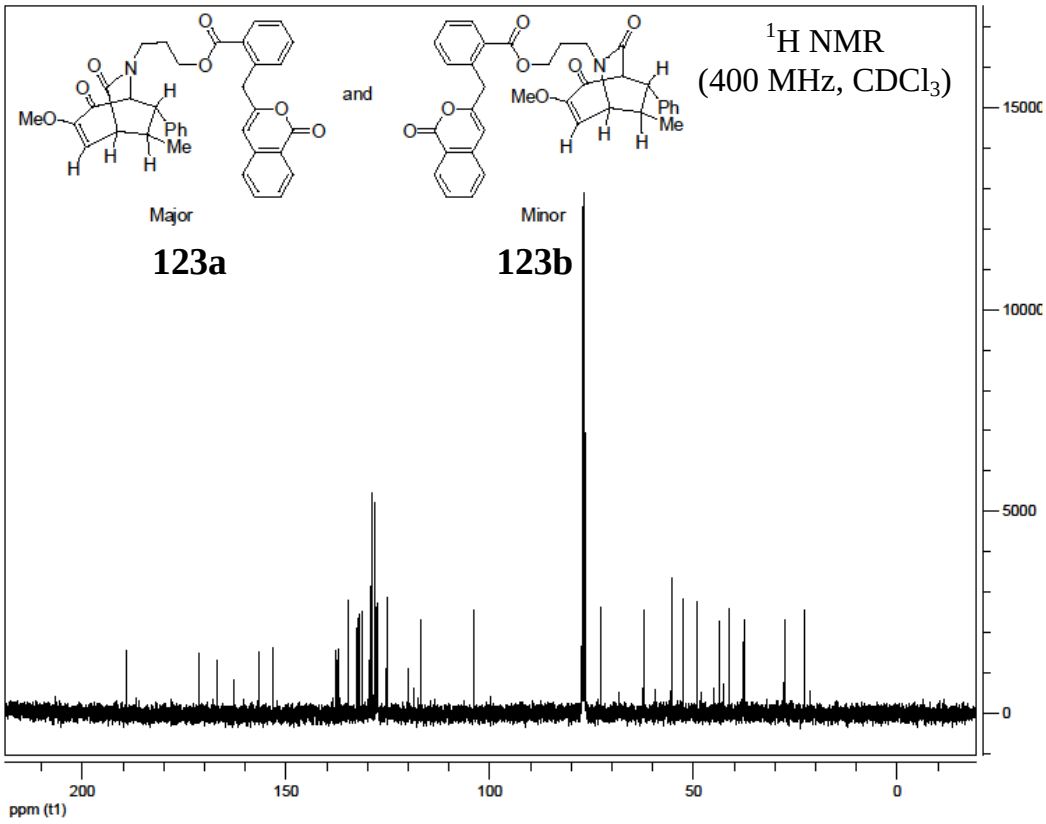
$^1$H NMR
(400 MHz, $CDCl_3$)
and
Major
123a
Minor
123b
15000
10000
5000
0
200
150
100
50
0
ppm (t1)

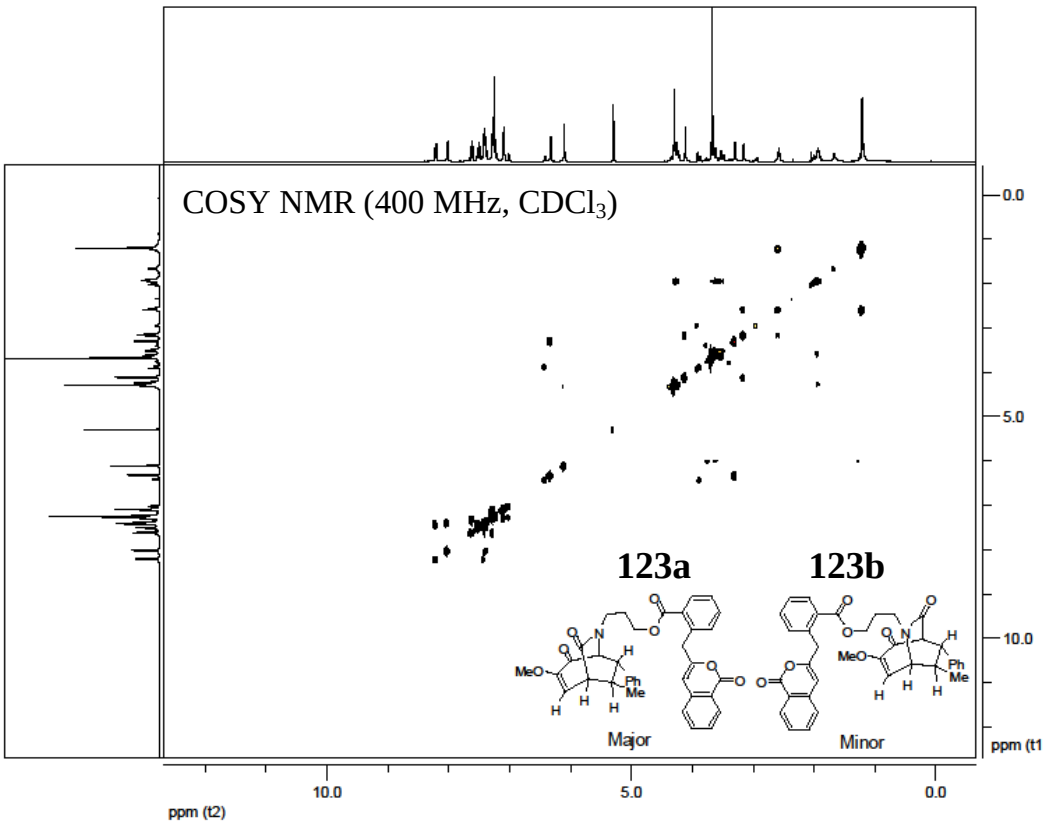
COSY NMR (400 MHz, CDCl3)
123a
123b
Major
Minor
ppm (t2)
ppm (t1

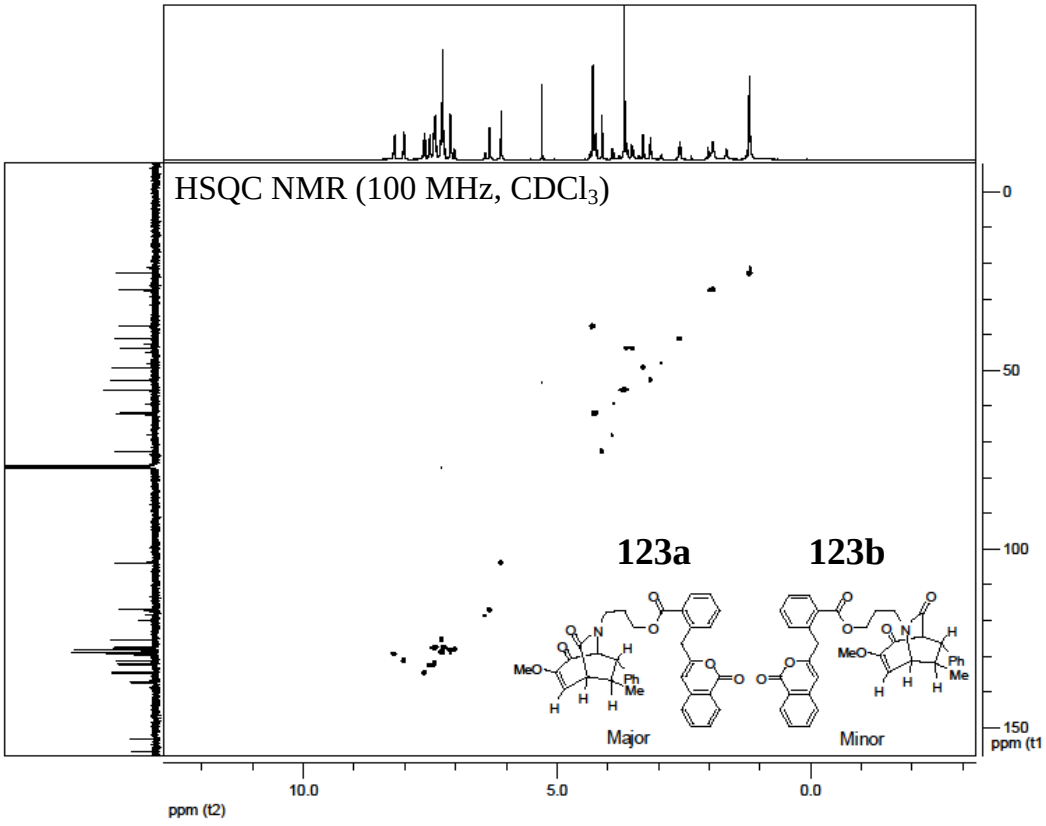
HSQC NMR (100 MHz, CDCl3)
123a
123b
Major
Minor
ppm (t2)
ppm (t1

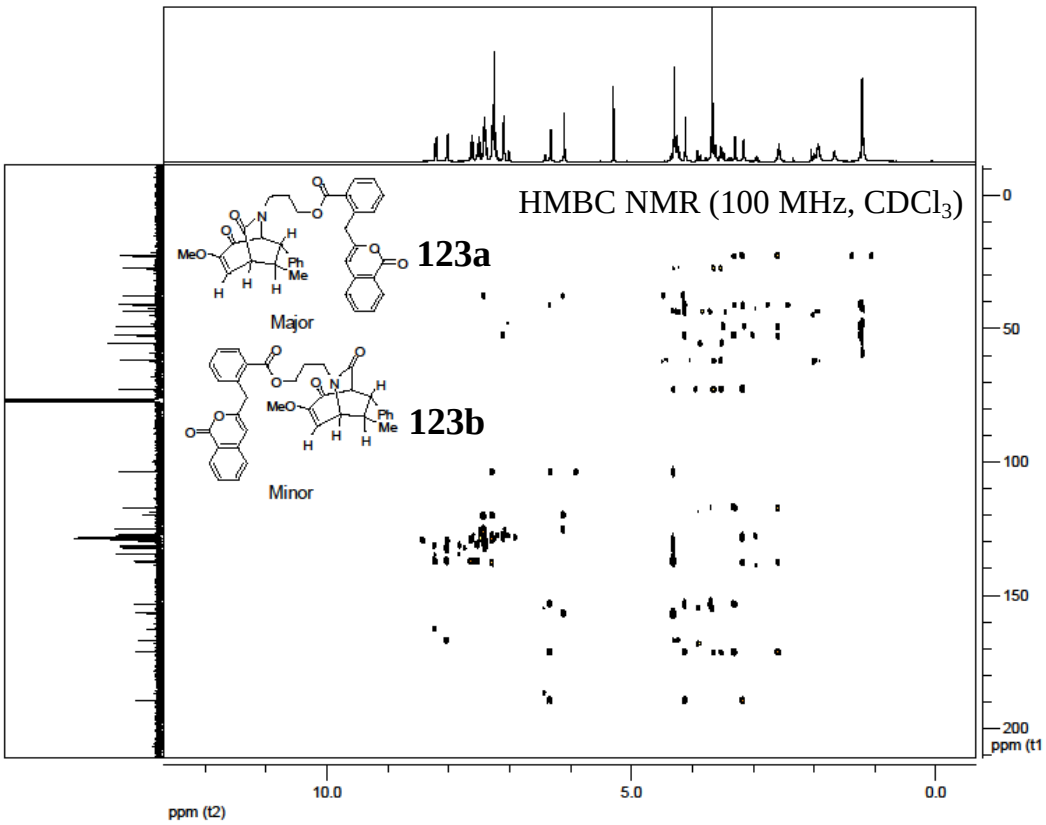
HMBC NMR (100 MHz, CDCl3)
123a
Major
123b
Minor
MeO
Ph
Me
H
O
N
0
50
100
150
200
ppm (t1
10.0
5.0
0.0
ppm (t2)

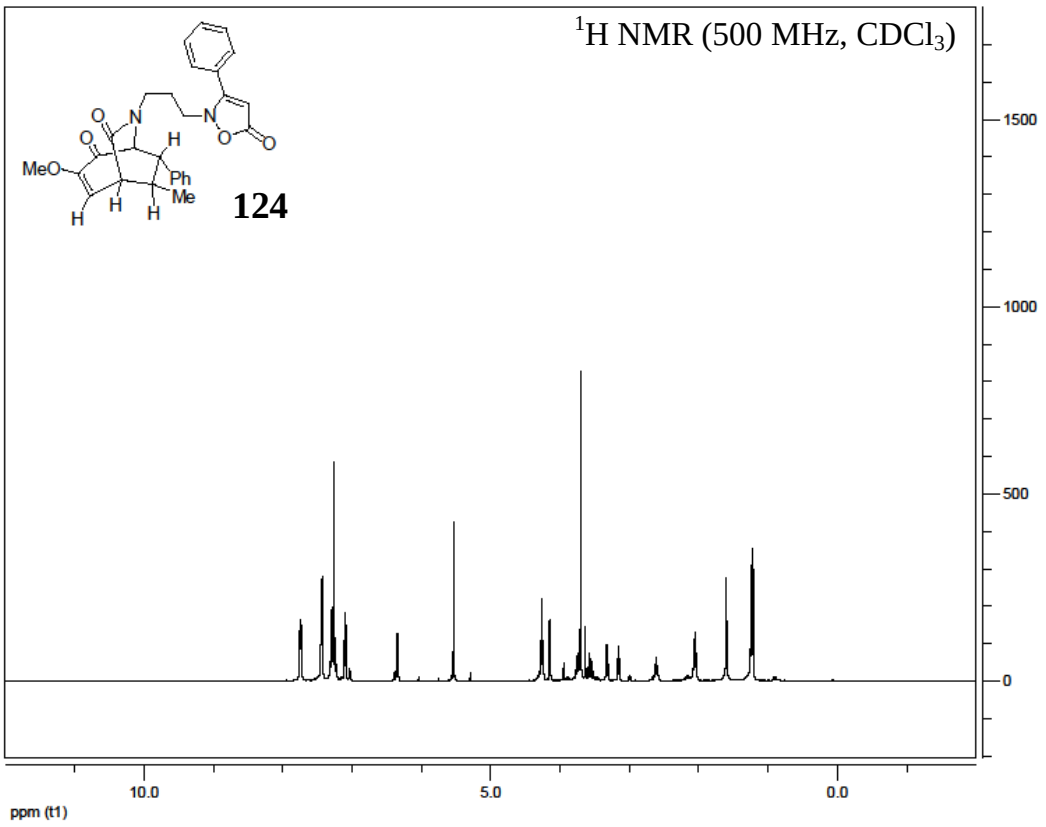
$^{1}$H NMR (500 MHz, $CDCl_3$)
124
1500
1000
500
0
10.0
5.0
0.0
ppm (t1)

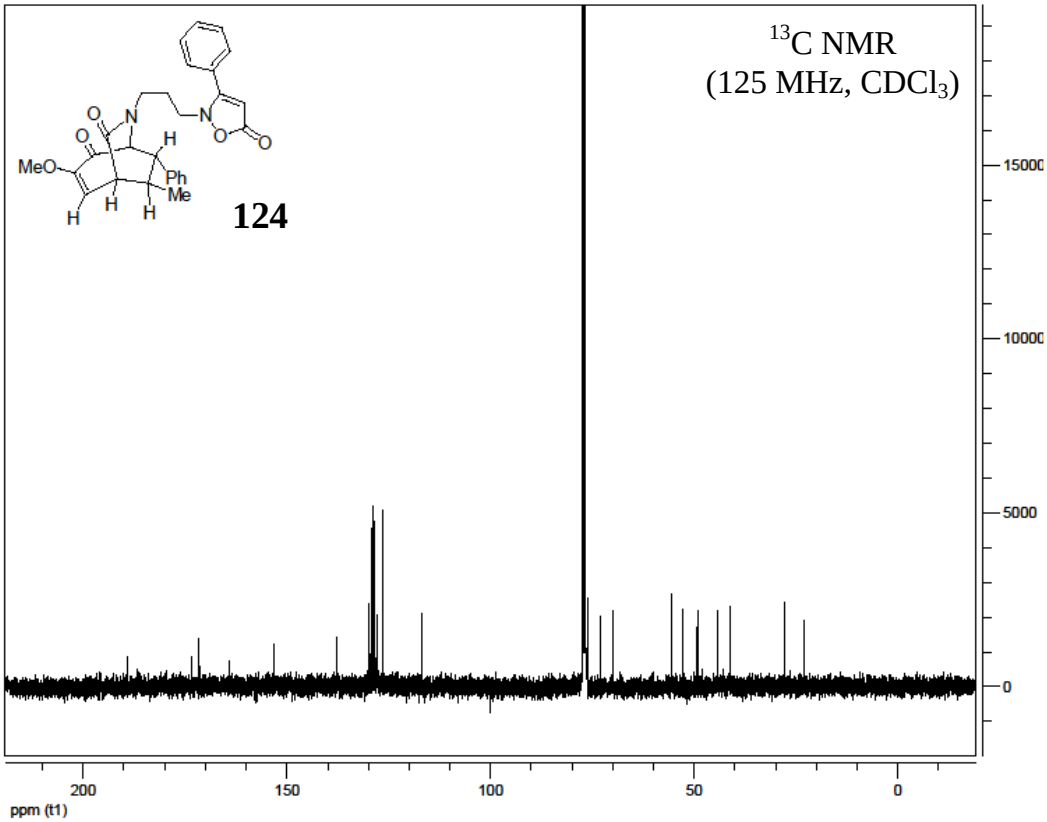
$^{13}$C NMR
(125 MHz, $CDCl_3$)
124
15000
10000
5000
0
200
150
100
50
0
ppm (t1)

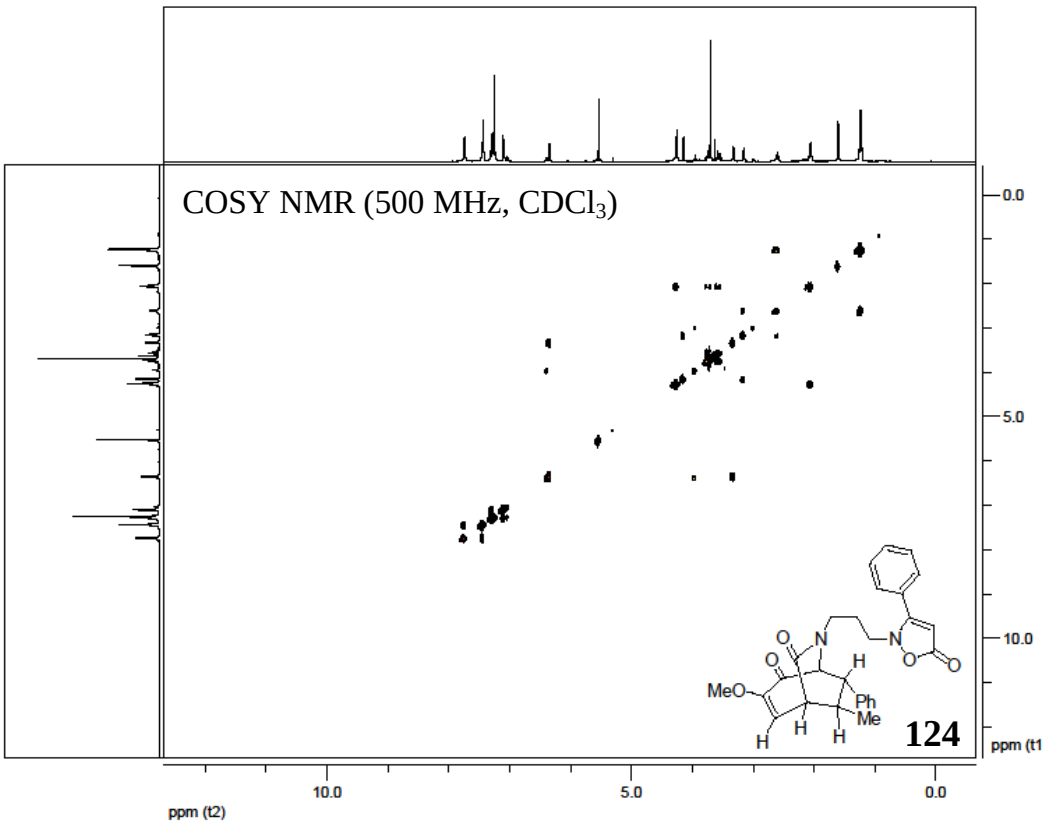
COSY NMR (500 MHz, CDCl3)
MeO
Ph
Me
124
10.0
5.0
0.0
ppm (t2)
ppm (t1

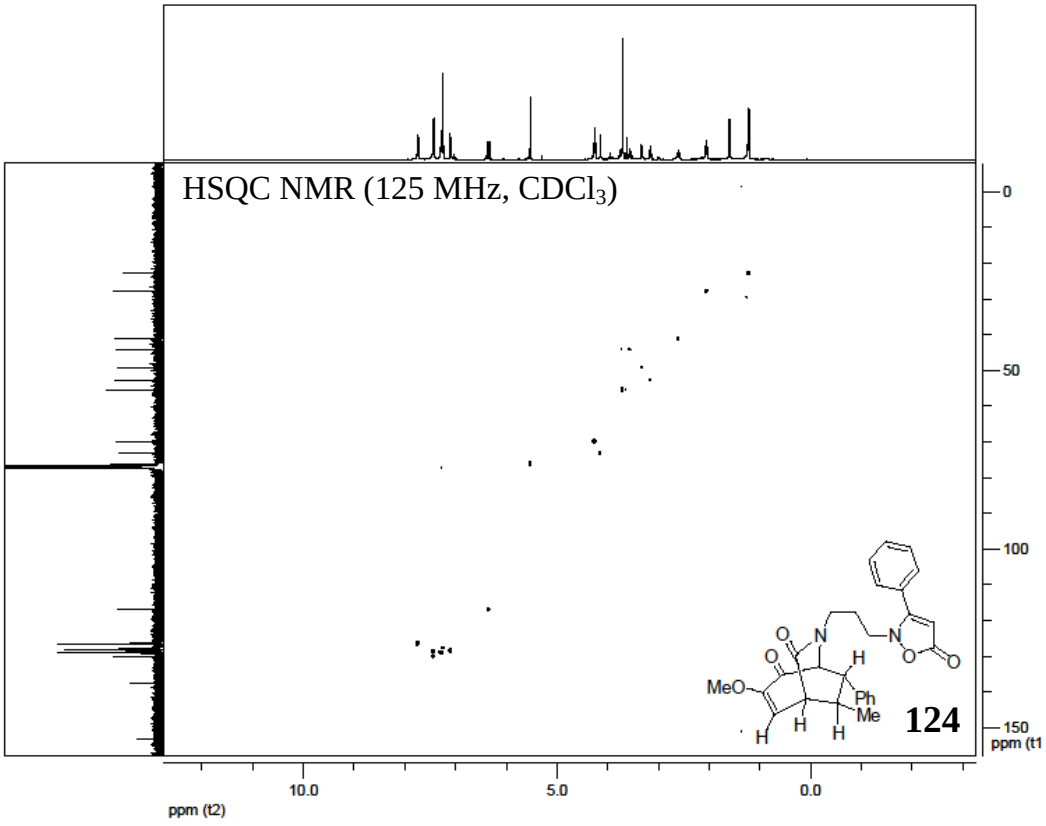
HSQC NMR (125 MHz, CDCl3)
MeO
Ph
Me
124
10.0
5.0
0.0
ppm (t2)
ppm (t1

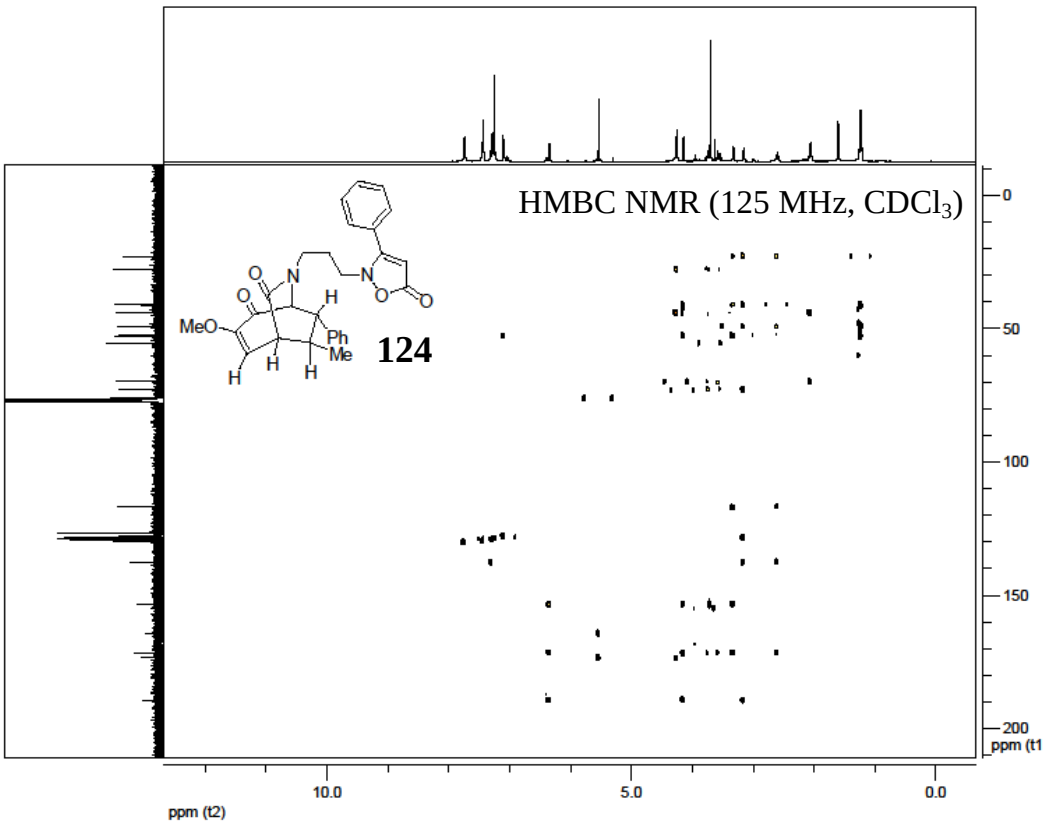
HMBC NMR (125 MHz, CDCl3)
124
MeO
Ph
Me
H
O
N
0
50
100
150
200
ppm (t1
10.0
5.0
0.0
ppm (t2)

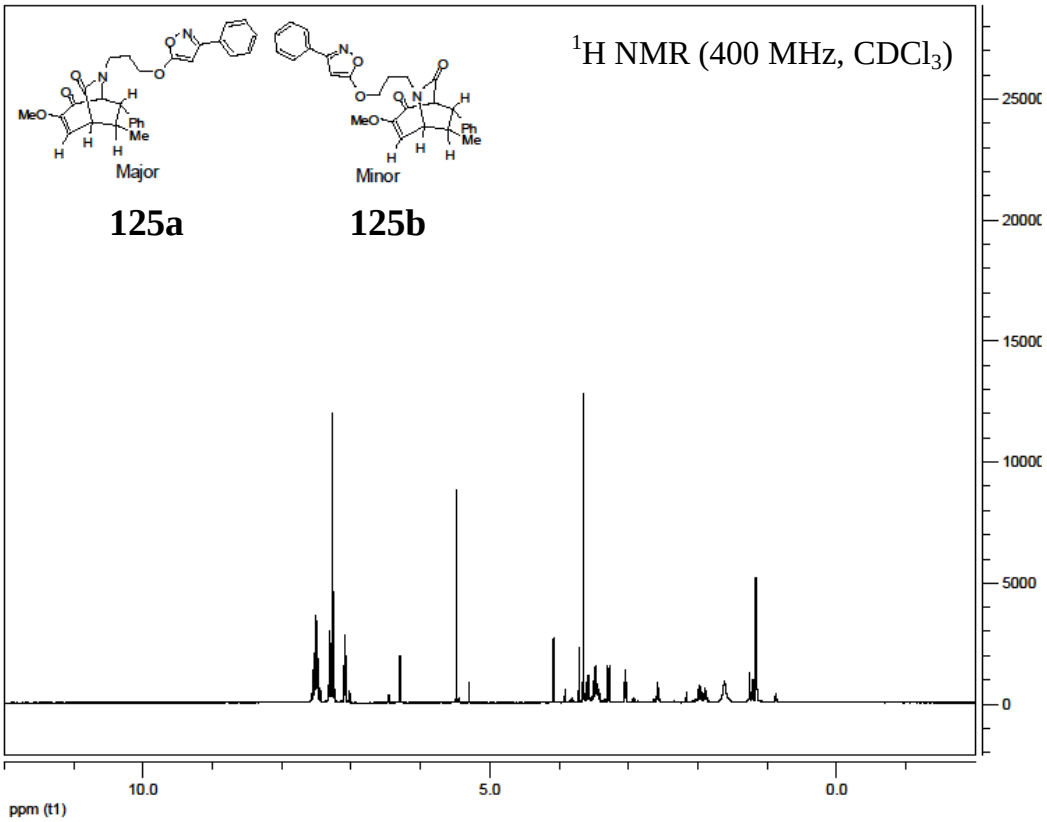
Major
Minor
125a
125b
$^{1}$H NMR (400 MHz, $CDCl_3$)
10.0
5.0
0.0
ppm (t1)

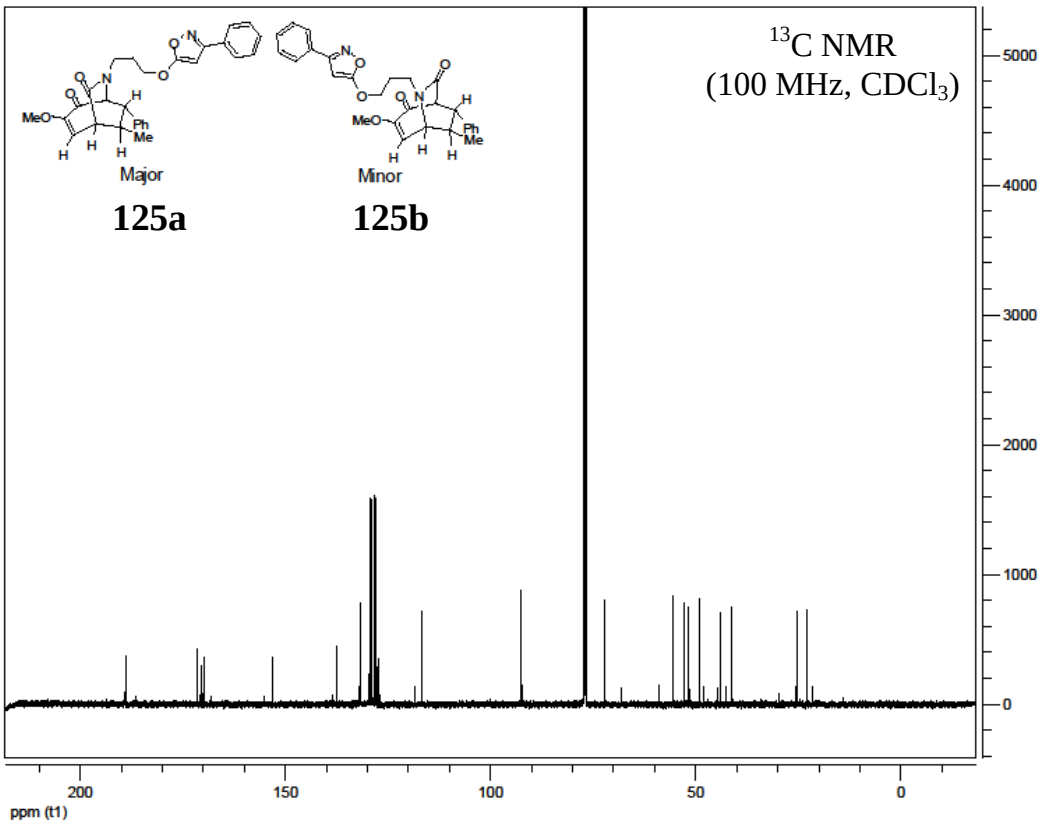
Major
Minor
125a
125b
$^{13}$C NMR
(100 MHz, $CDCl_3$)
200
150
100
50
0
ppm (t1)

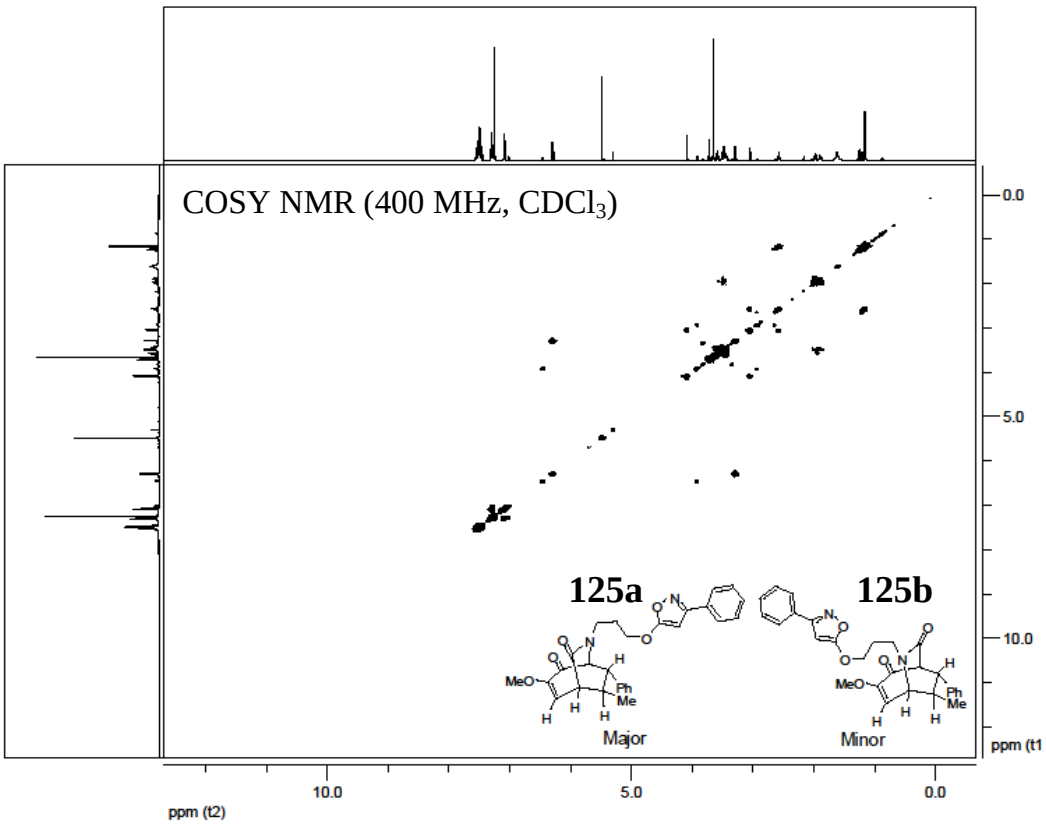
COSY NMR (400 MHz, CDCl3)
125a
125b
Major
Minor
ppm (t2)
ppm (t1)
10.0
5.0
0.0

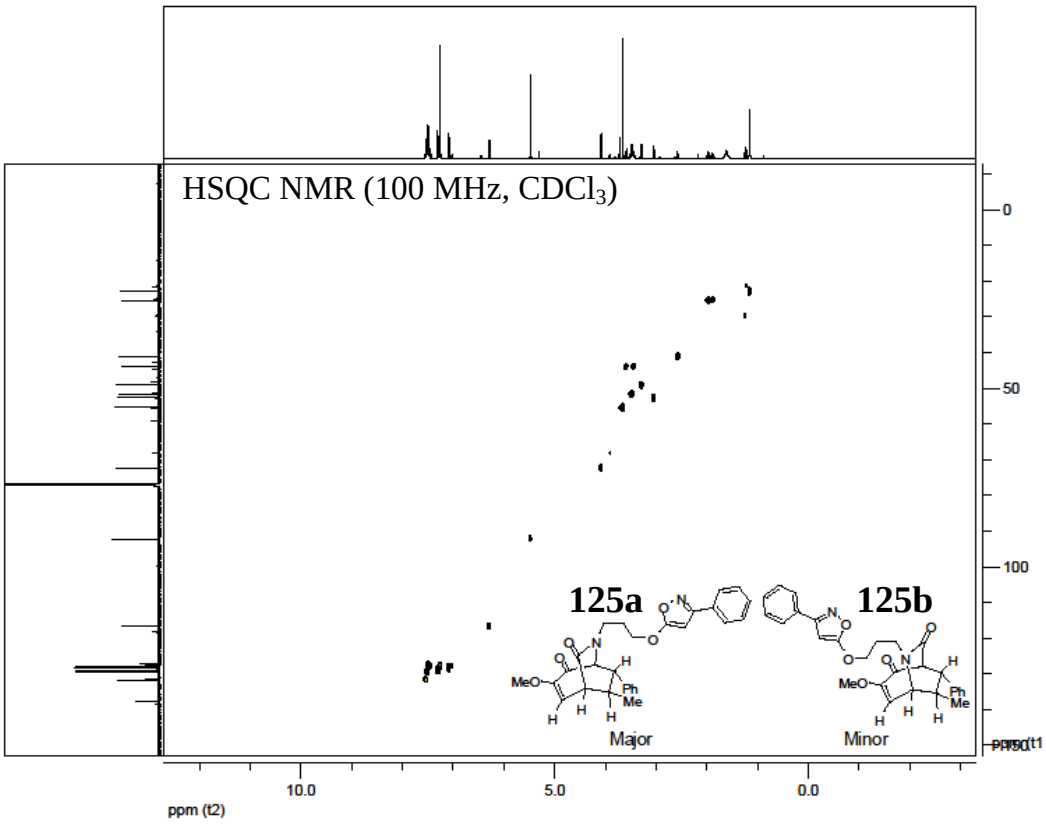
HSQC NMR (100 MHz, CDCl3)
125a
125b
Major
Minor
ppm (t2)
ppm (t1)
10.0
5.0
0.0
0
50
100

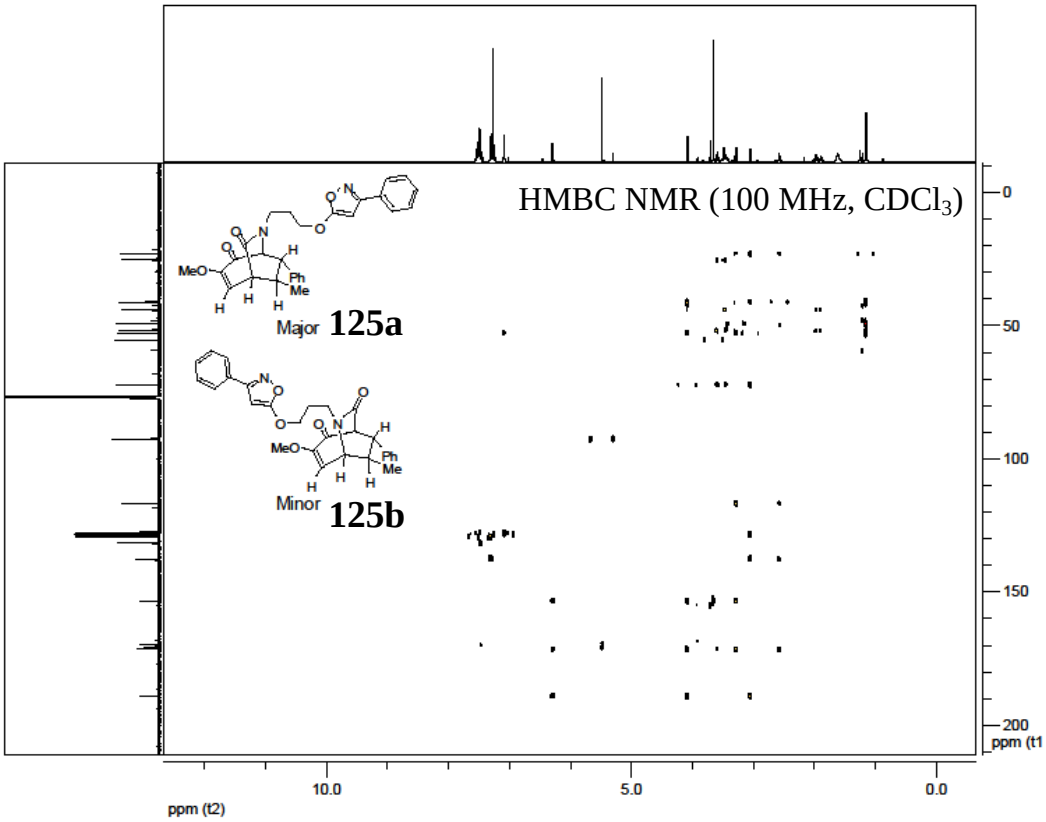
HMBC NMR (100 MHz, CDCl3)
Major 125a
Minor 125b
MeO
Ph
Me
H
O
N
10.0
5.0
0.0
ppm (t2)
0
50
100
150
200
ppm (t1

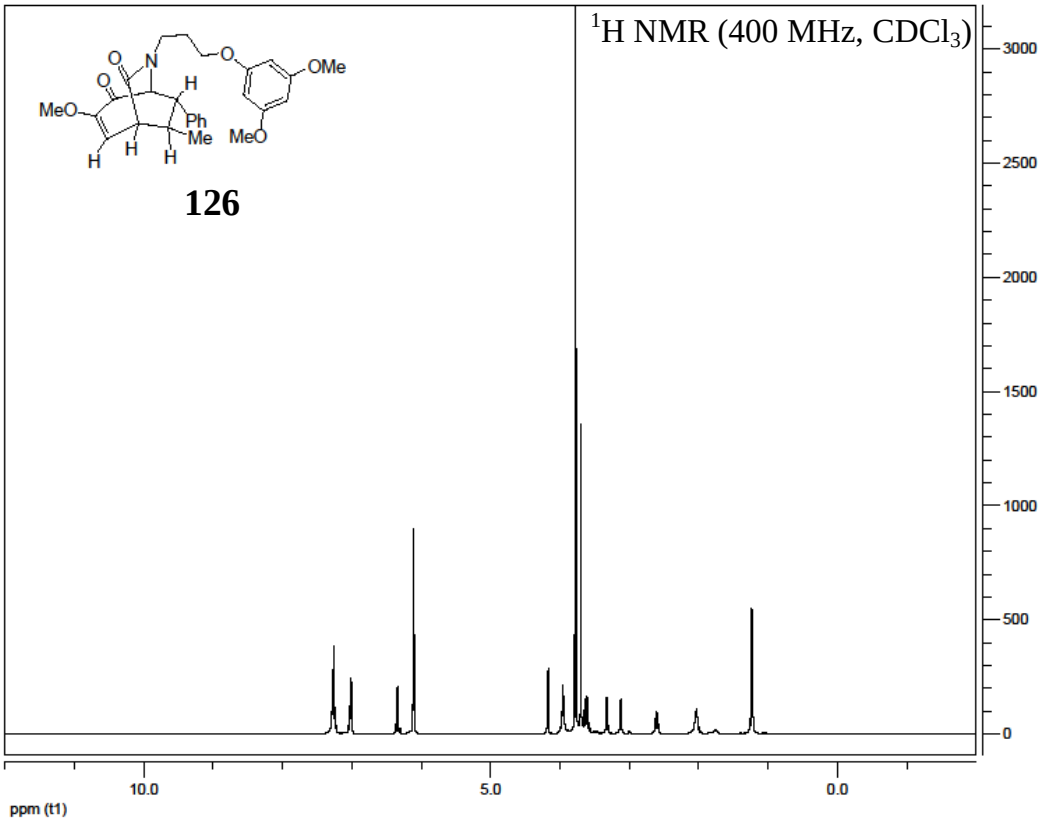
$^1$H NMR (400 MHz, $CDCl_3$)
126
3000
2500
2000
1500
1000
500
0
10.0
5.0
0.0
ppm (t1)

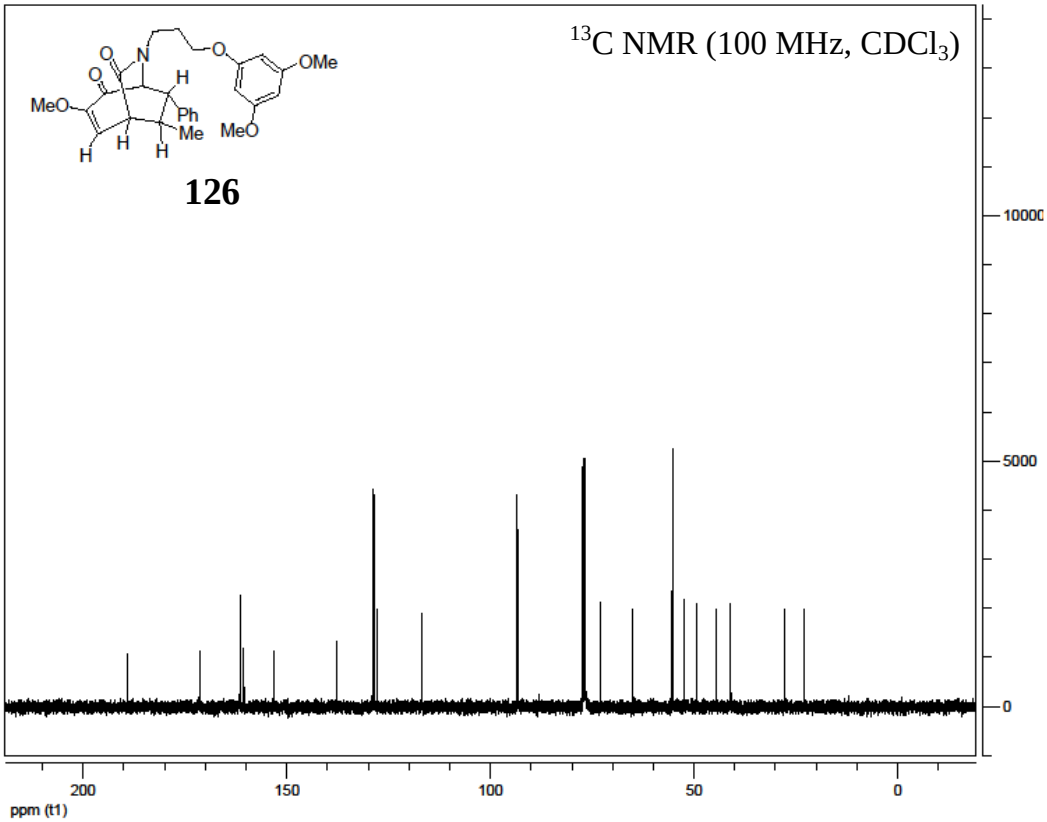
$^{13}$C NMR (100 MHz, $CDCl_3$)
126
10000
5000
0
200
150
100
50
0
ppm (t1)

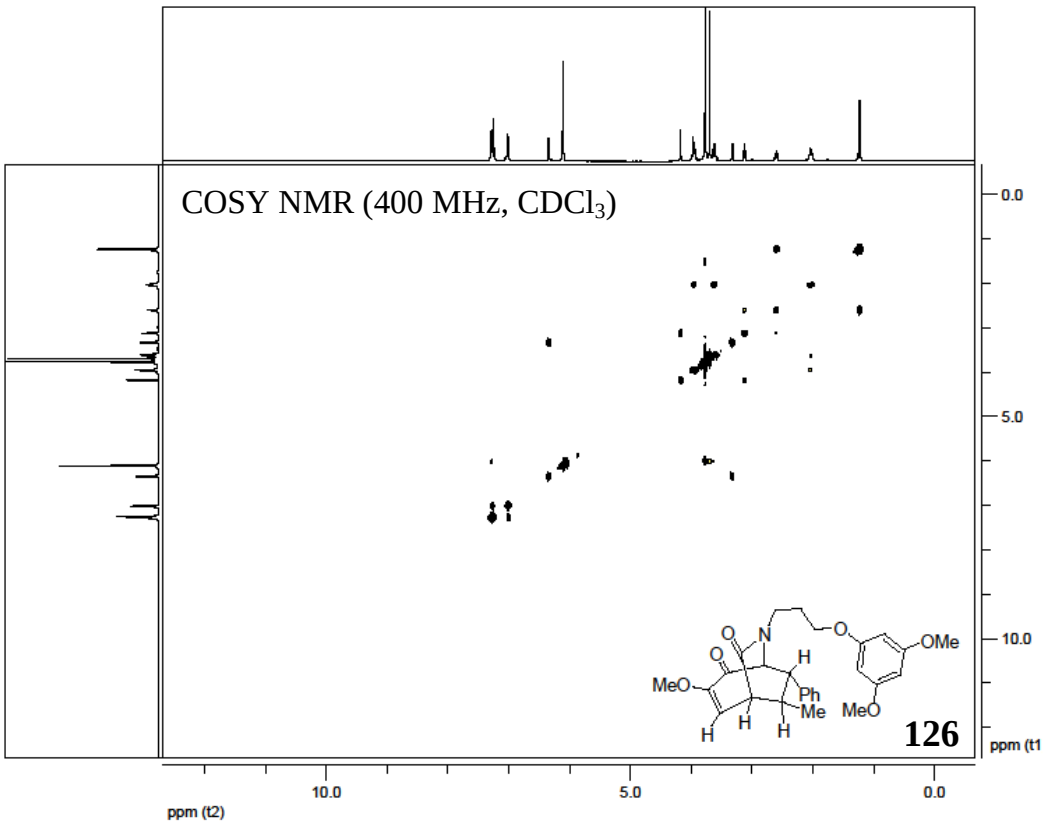
COSY NMR (400 MHz, CDCl3)
126
ppm (t2)
ppm (t1

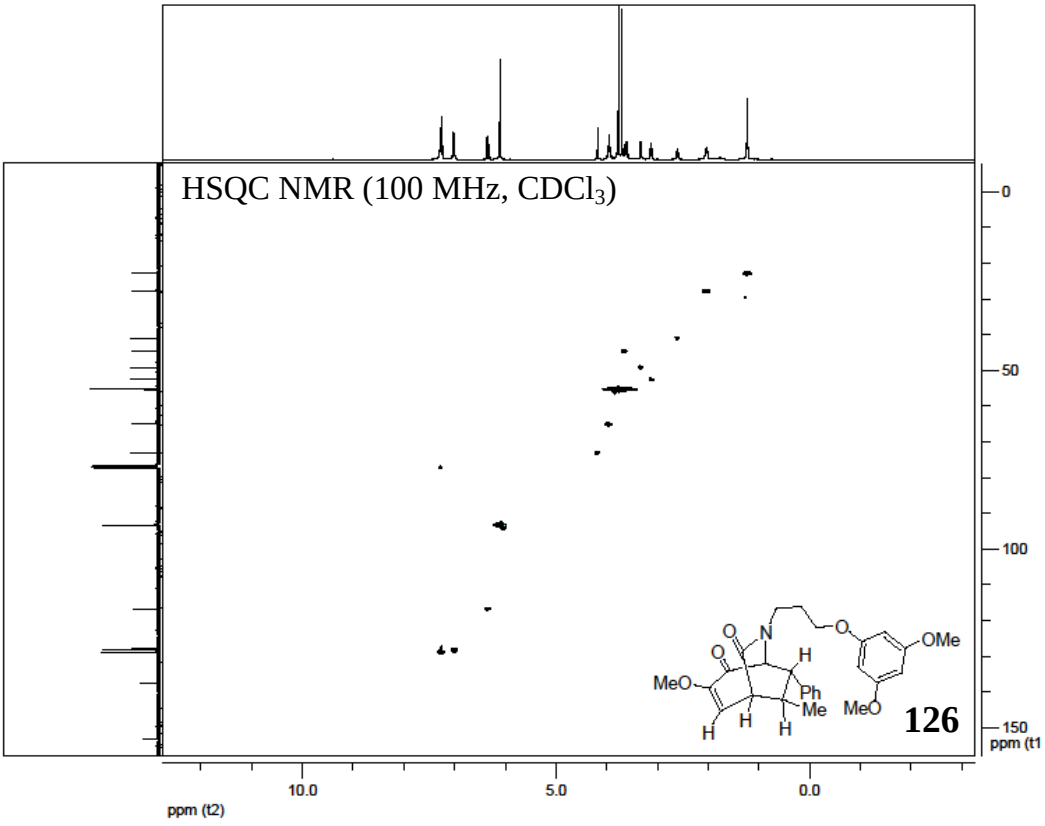
HSQC NMR (100 MHz, CDCl3)
126
ppm (t2)
ppm (t1

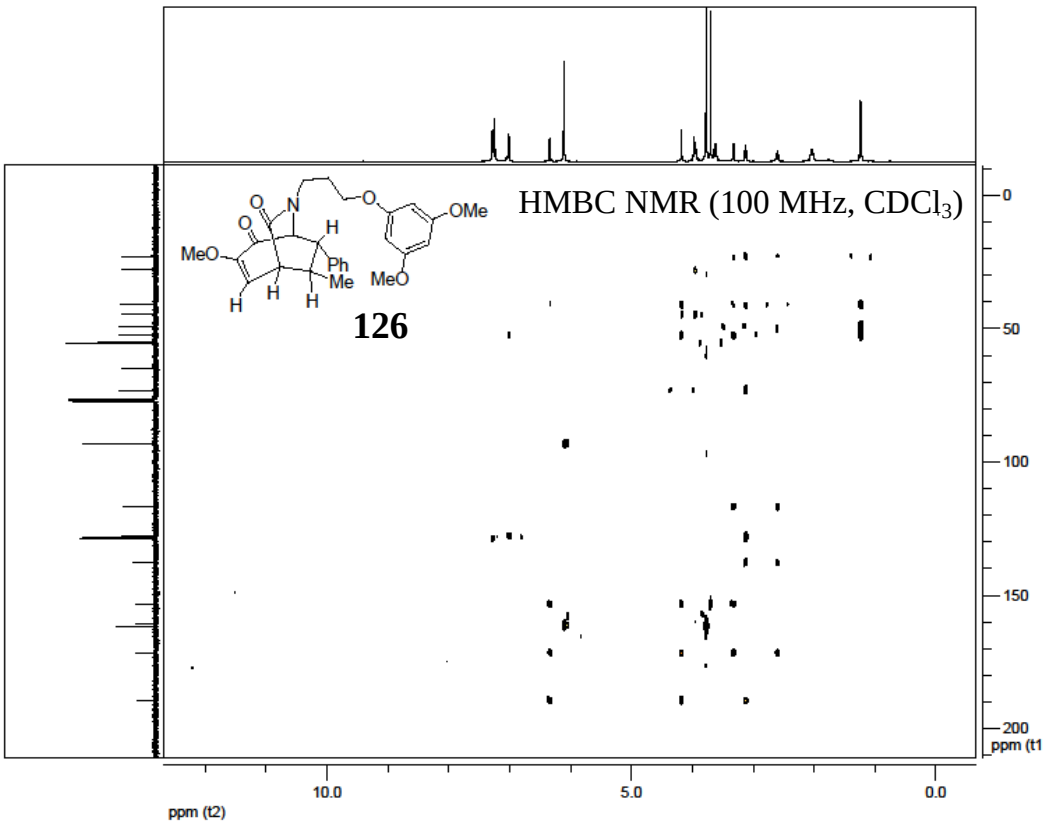
HMBC NMR (100 MHz, CDCl3)
126
MeO
OMe
MeO
Ph
Me
H
H
H
H
O
O
N
O
10.0
5.0
0.0
ppm (t2)
0
50
100
150
200
ppm (t1

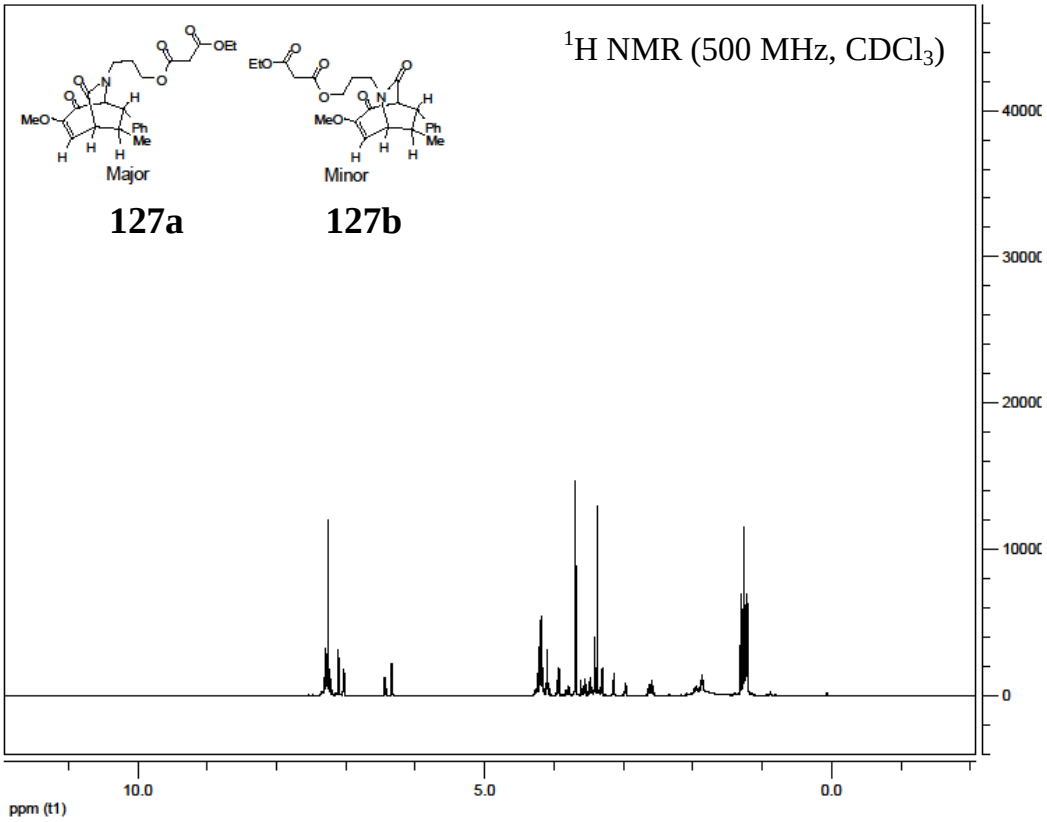
$^{1}$H NMR (500 MHz, $CDCl_3$)
Major
Minor
127a
127b
10.0
5.0
0.0
ppm (t1)

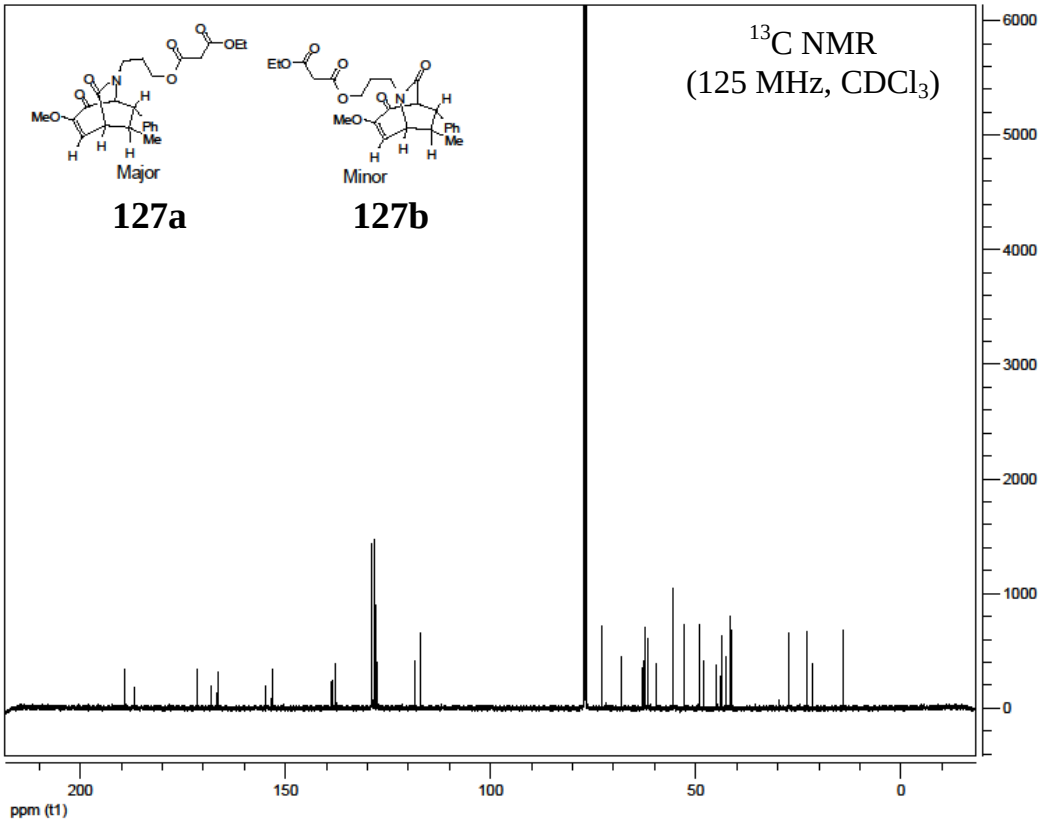
$^{13}$C NMR
(125 MHz, $CDCl_3$)
Major
Minor
127a
127b
200
150
100
50
0
ppm (t1)

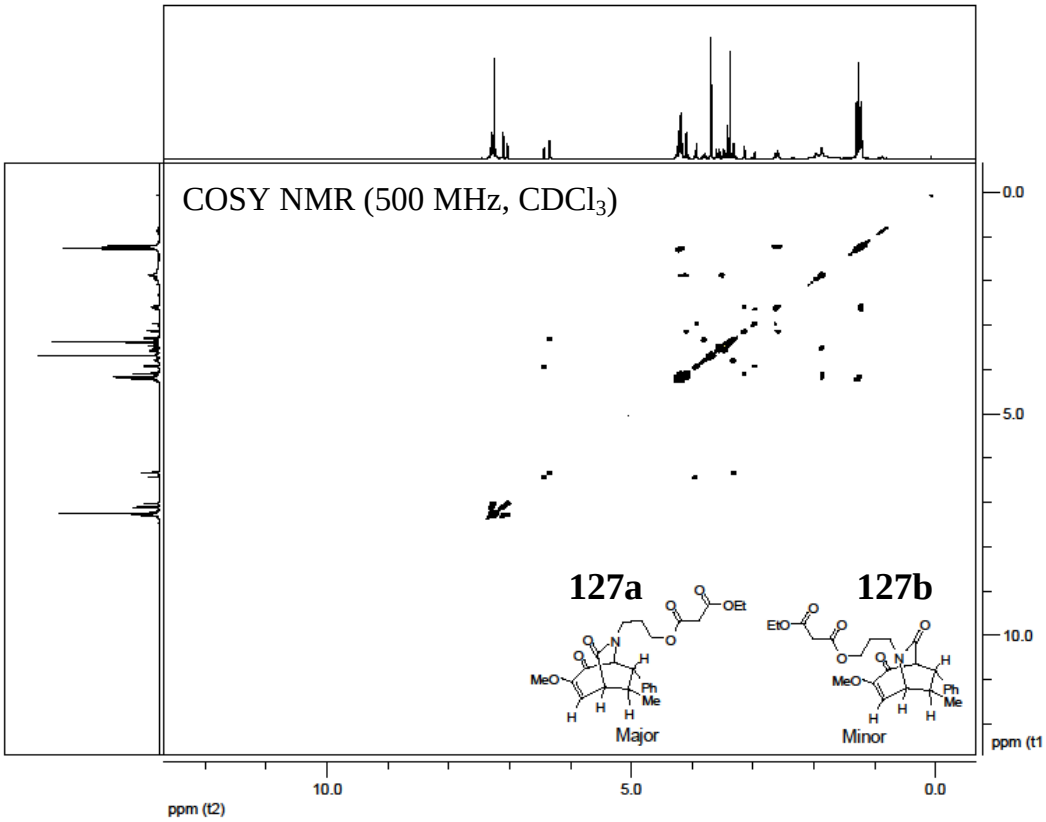
COSY NMR (500 MHz, CDCl3)
127a
127b
Major
Minor
ppm (t2)
ppm (t1)
10.0
5.0
0.0

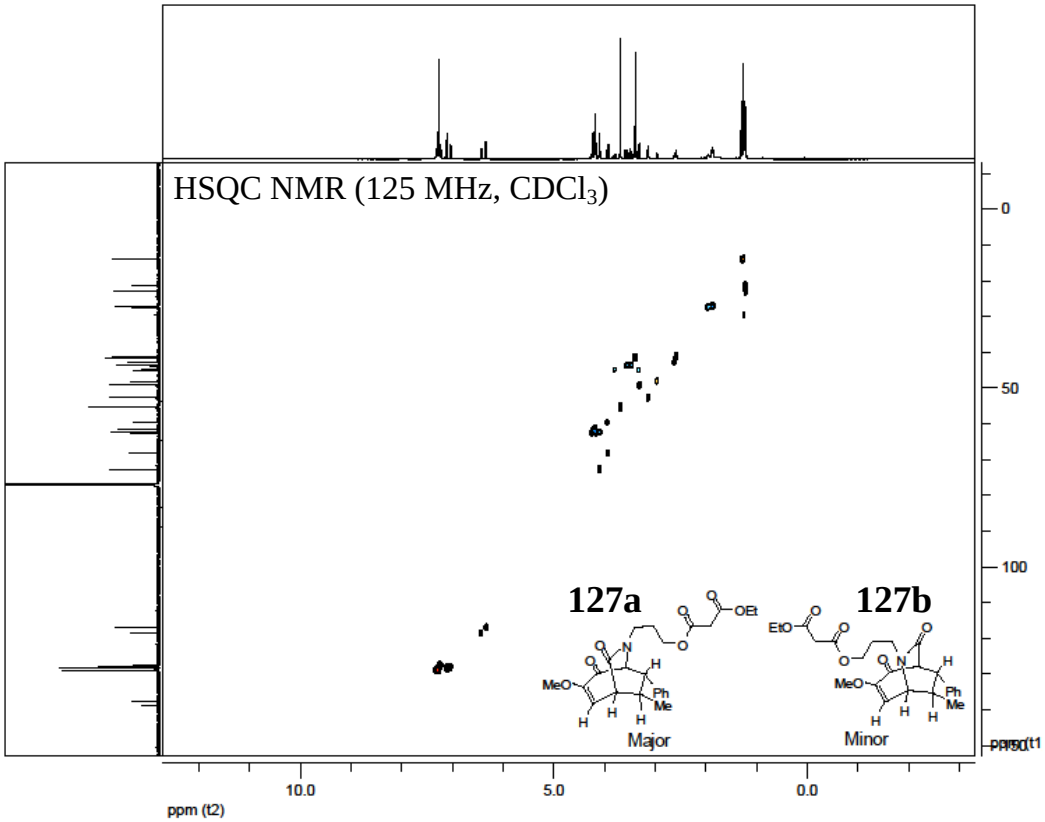
HSQC NMR (125 MHz, CDCl3)
127a
127b
Major
Minor
ppm (t2)
ppm (t1)
10.0
5.0
0.0
0
50
100

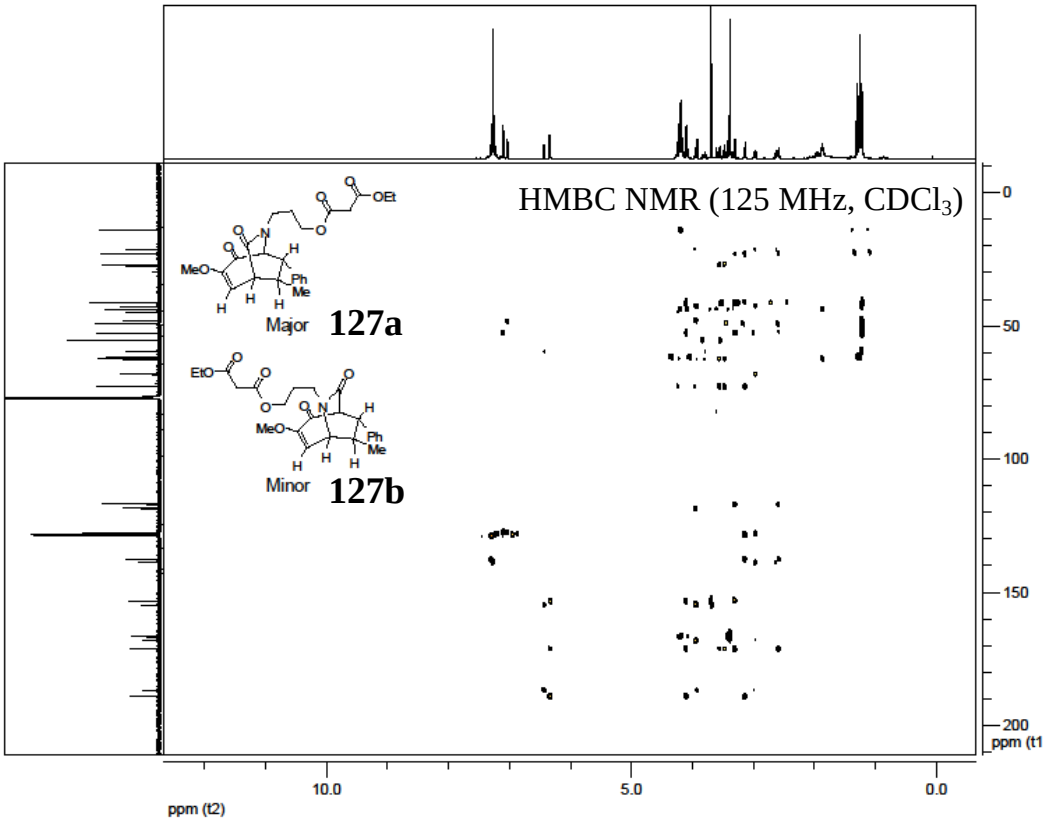
HMBC NMR (125 MHz, CDCl3)
Major
127a
Minor
127b
10.0
5.0
0.0
ppm (t2)
0
50
100
150
200
ppm (t1

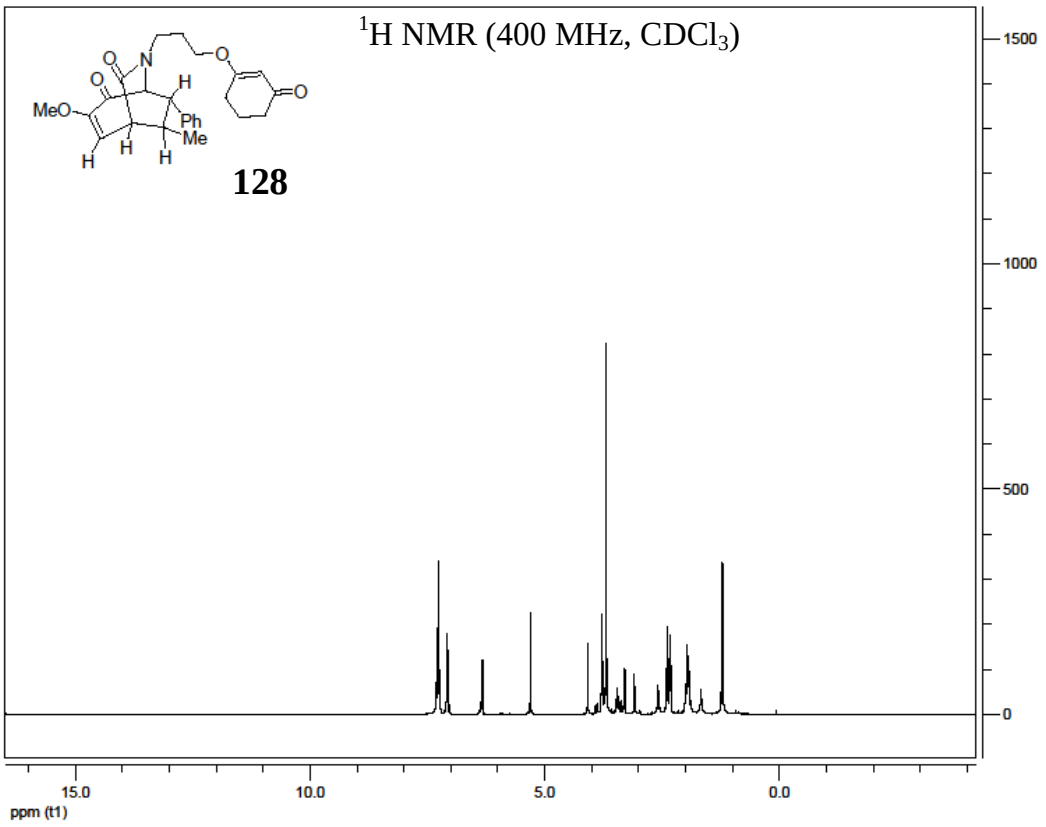
$^{1}$H NMR (400 MHz, $CDCl_3$)
MeO
Ph
Me
H
O
N
1500
1000
500
0
15.0
10.0
5.0
0.0
ppm (t1)

**128**

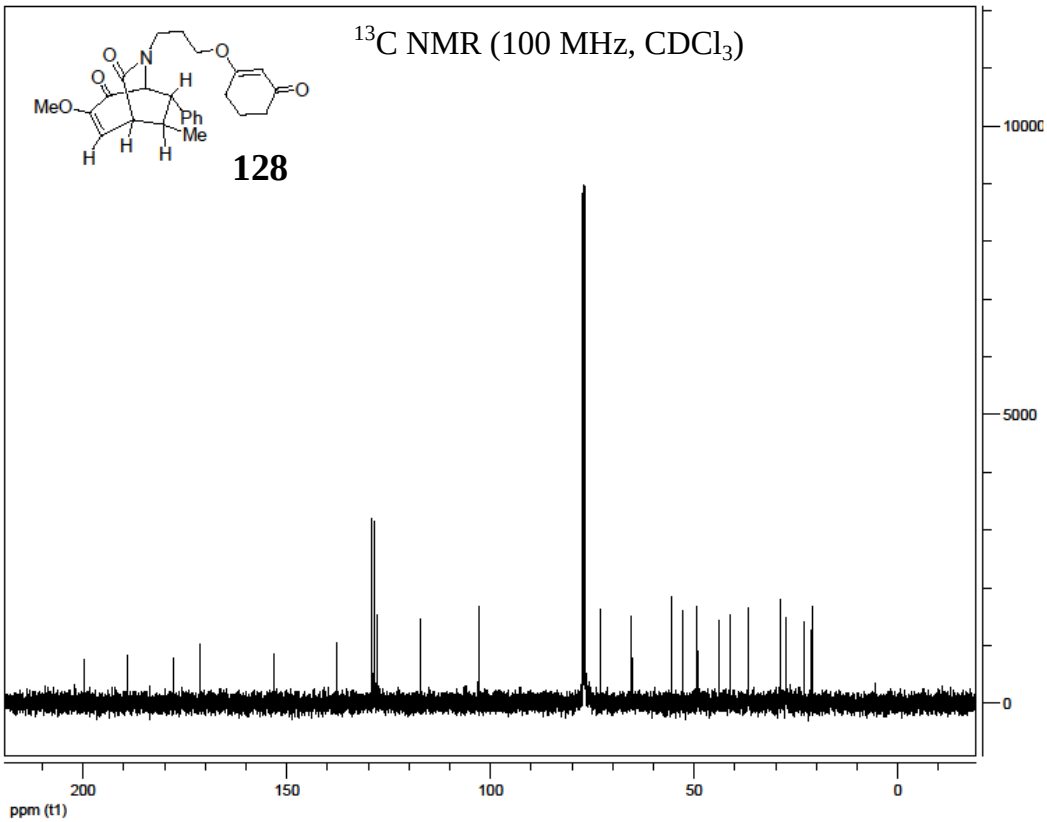
$^{13}$C NMR (100 MHz, $CDCl_3$)
MeO
Ph
Me
H
O
N
10000
5000
0
200
150
100
50
0
ppm (t1)

**128**

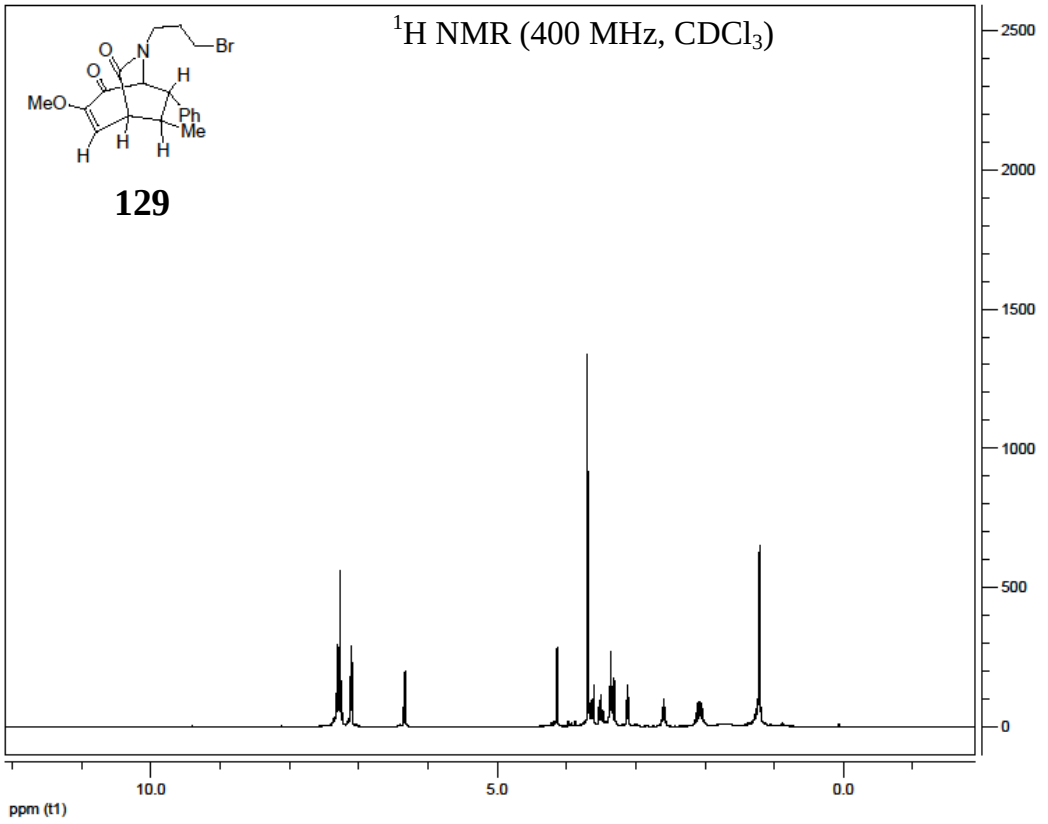
$^{1}$H NMR (400 MHz, $CDCl_3$)
O
N
Br
O
H
MeO
Ph
Me
H
H
H
129
2500
2000
1500
1000
500
0
10.0
5.0
0.0
ppm (t1)

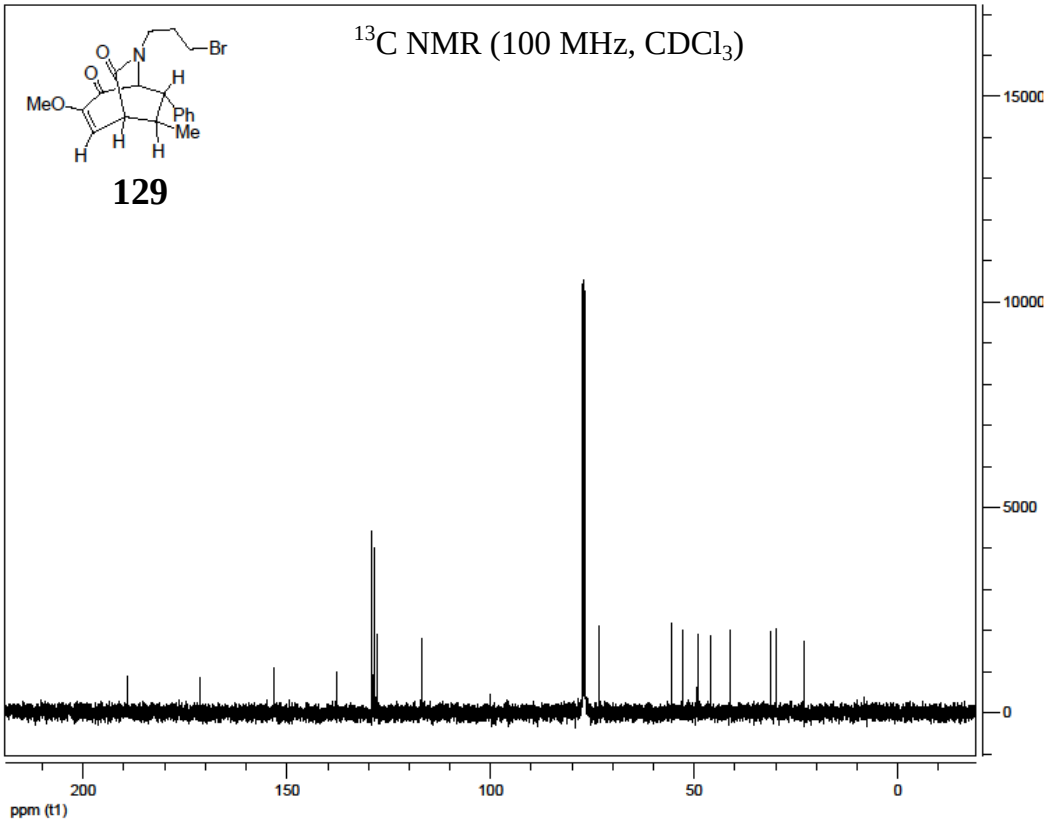
$^{13}$C NMR (100 MHz, $CDCl_3$)
O
N
Br
O
H
MeO
Ph
Me
H
H
H
129
15000
10000
5000
0
200
150
100
50
0
ppm (t1)

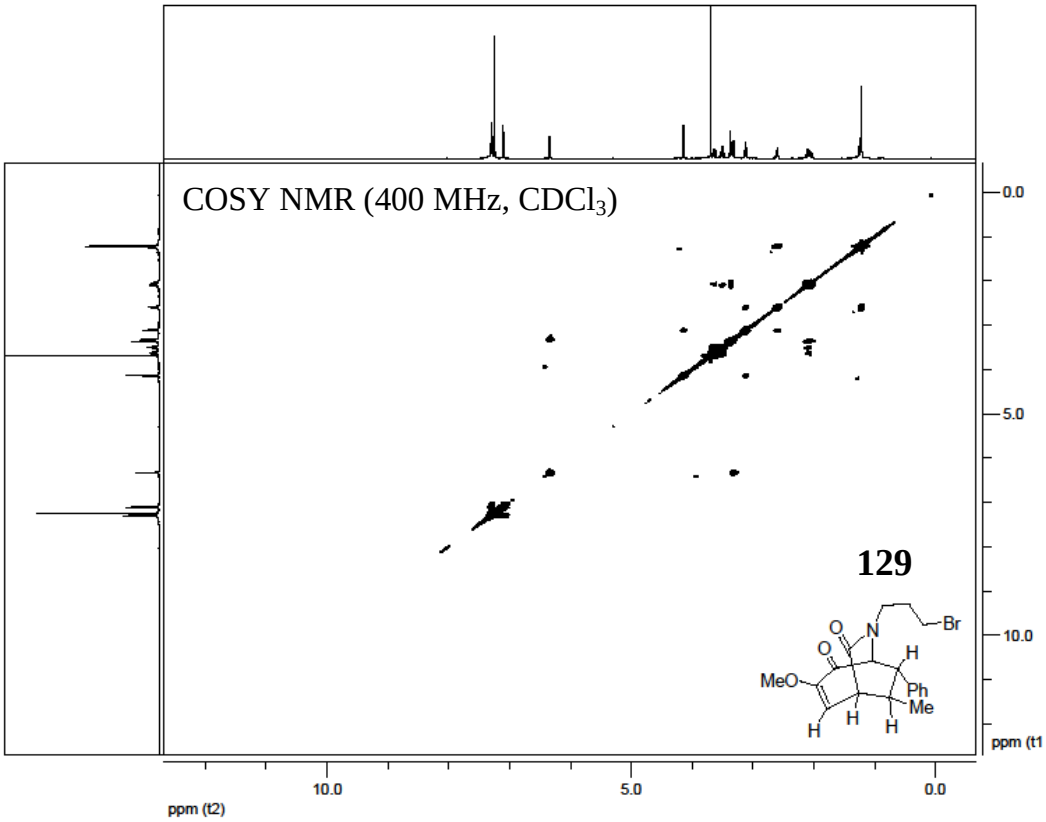
COSY NMR (400 MHz, CDCl3)
129
O
N
Br
O
H
MeO
Ph
Me
H
H
H
0.0
5.0
10.0
ppm (t1
10.0
5.0
0.0
ppm (t2)

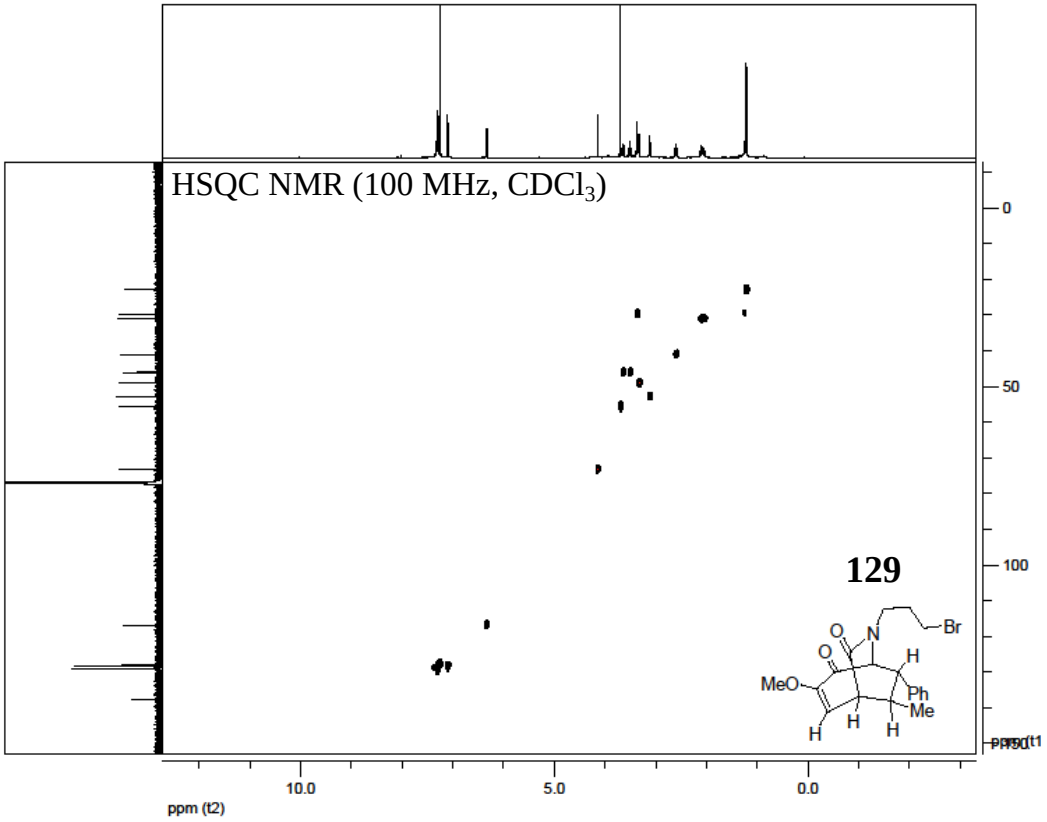
HSQC NMR (100 MHz, CDCl3)
129
O
N
Br
O
H
MeO
Ph
Me
H
H
H
0
50
100
ppm (t1
10.0
5.0
0.0
ppm (t2)

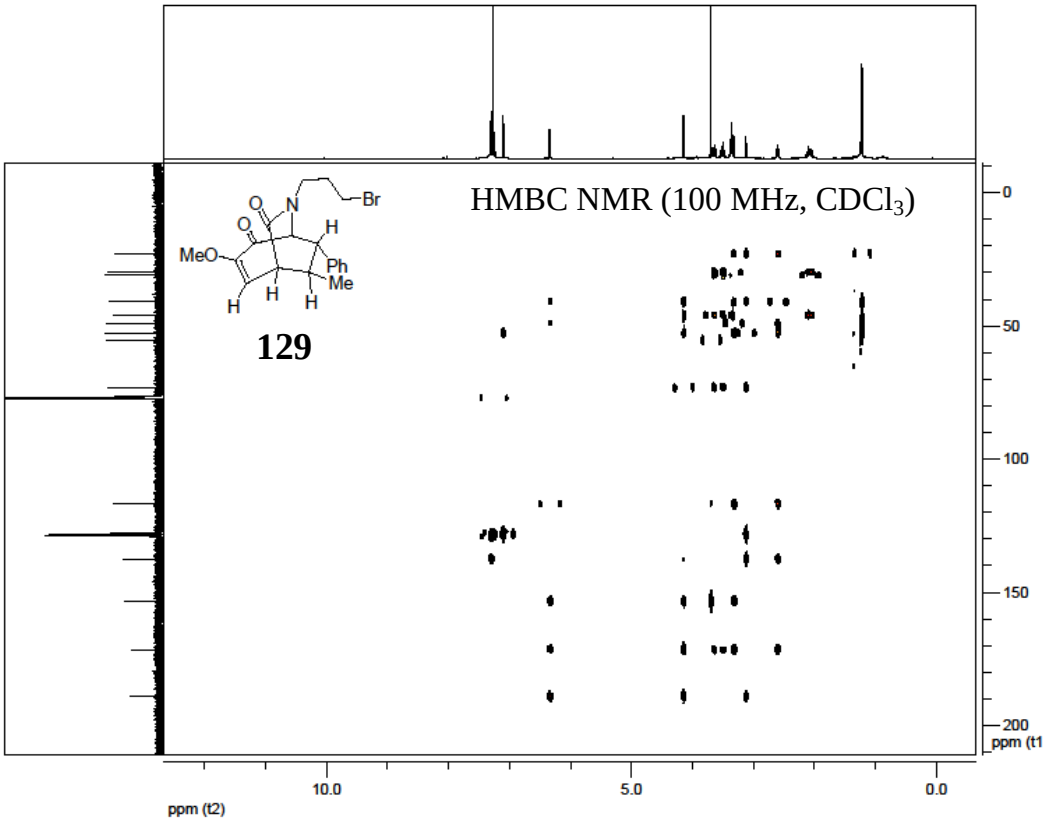
HMBC NMR (100 MHz, CDCl3)
O
N
Br
O
H
MeO
Ph
Me
H
H
H
129
0
50
100
150
200
ppm (t1
10.0
5.0
0.0
ppm (t2)

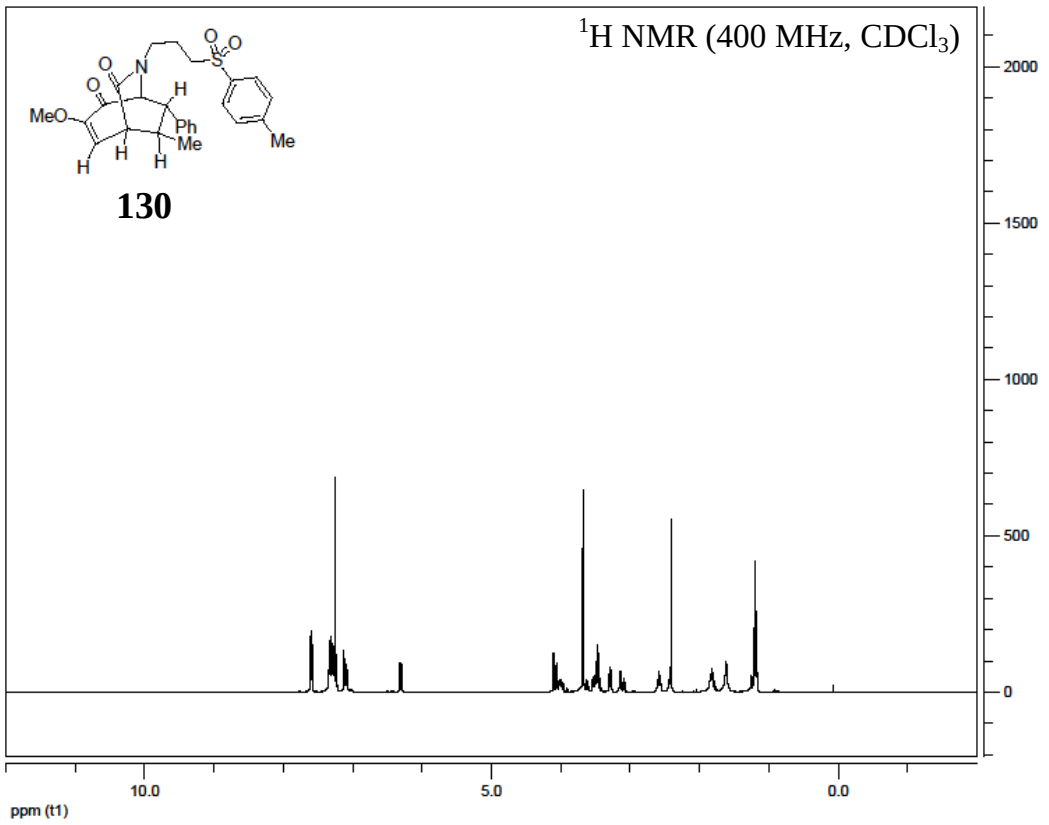
$^{1}$H NMR (400 MHz, $CDCl_3$)
MeO
Ph
Me
Me
H
2000
1500
1000
500
0
10.0
5.0
0.0
ppm (t1)

**130**

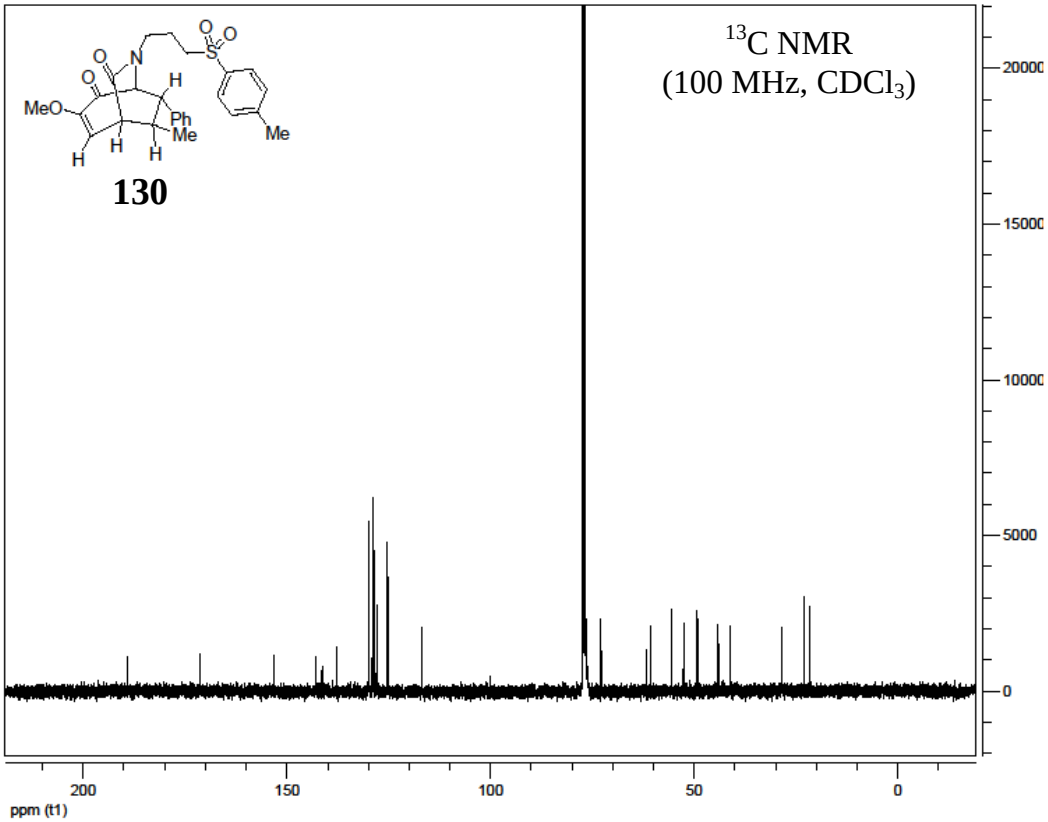
$^{13}$C NMR
(100 MHz, $CDCl_3$)
MeO
Ph
Me
Me
H
20000
15000
10000
5000
0
200
150
100
50
0
ppm (t1)

**130**

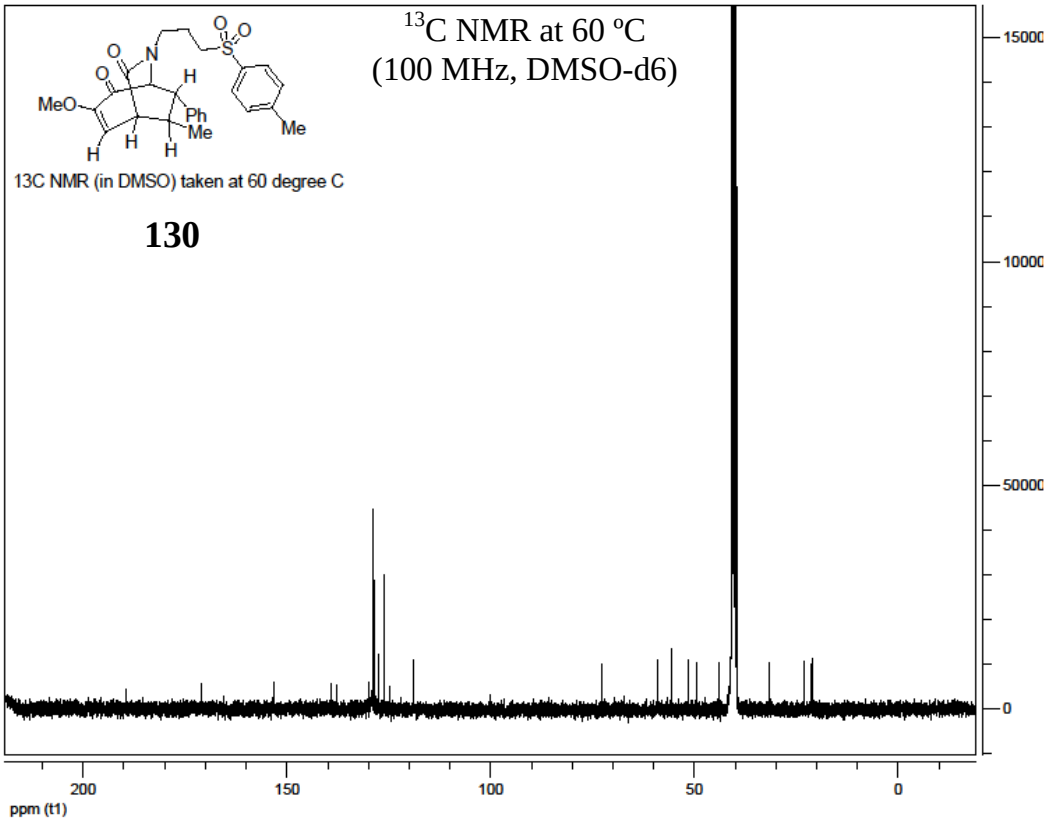
13C NMR (in DMSO) taken at 60 degree C
130
$^{13}$C NMR at 60 ºC
(100 MHz, DMSO-d6)
MeO
Ph
Me
Me
H
H
H
H
O
O
O
O
N
S
150000
100000
50000
0
200
150
100
50
0
ppm (t1)

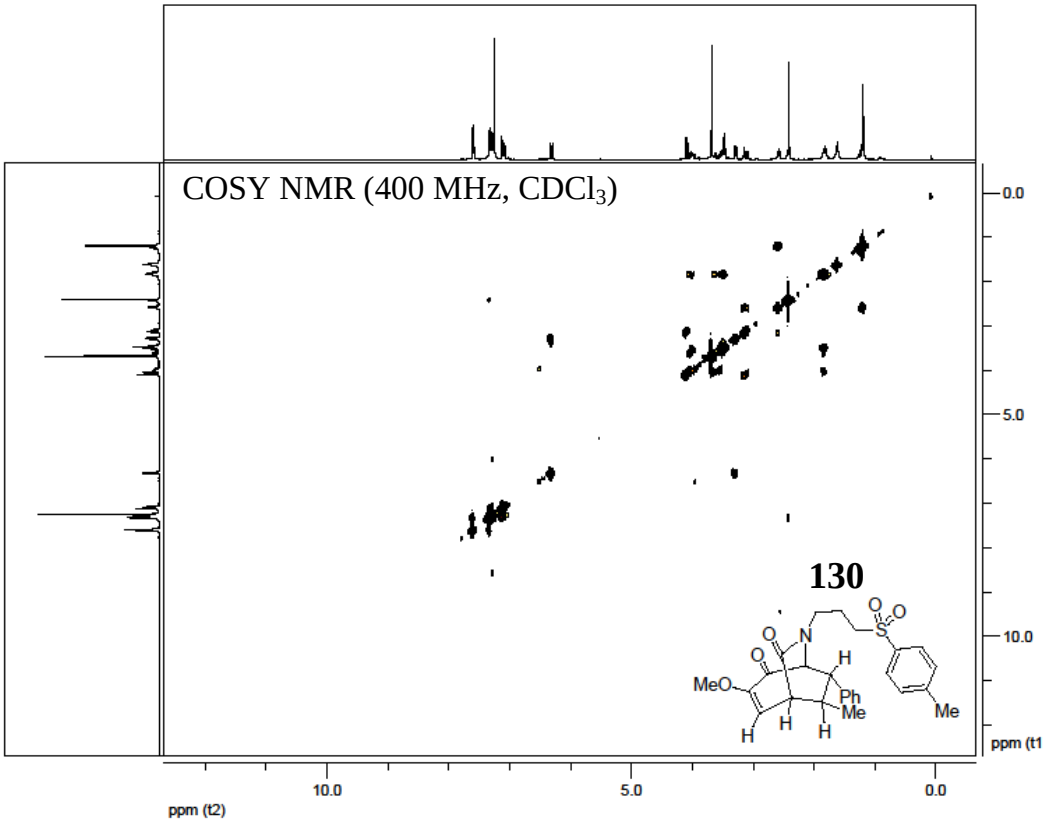
COSY NMR (400 MHz, $CDCl_3$)
130
MeO
Ph
Me
Me
H
H
H
H
O
O
O
O
N
S
0.0
5.0
10.0
ppm (t1
10.0
5.0
0.0
ppm (t2)

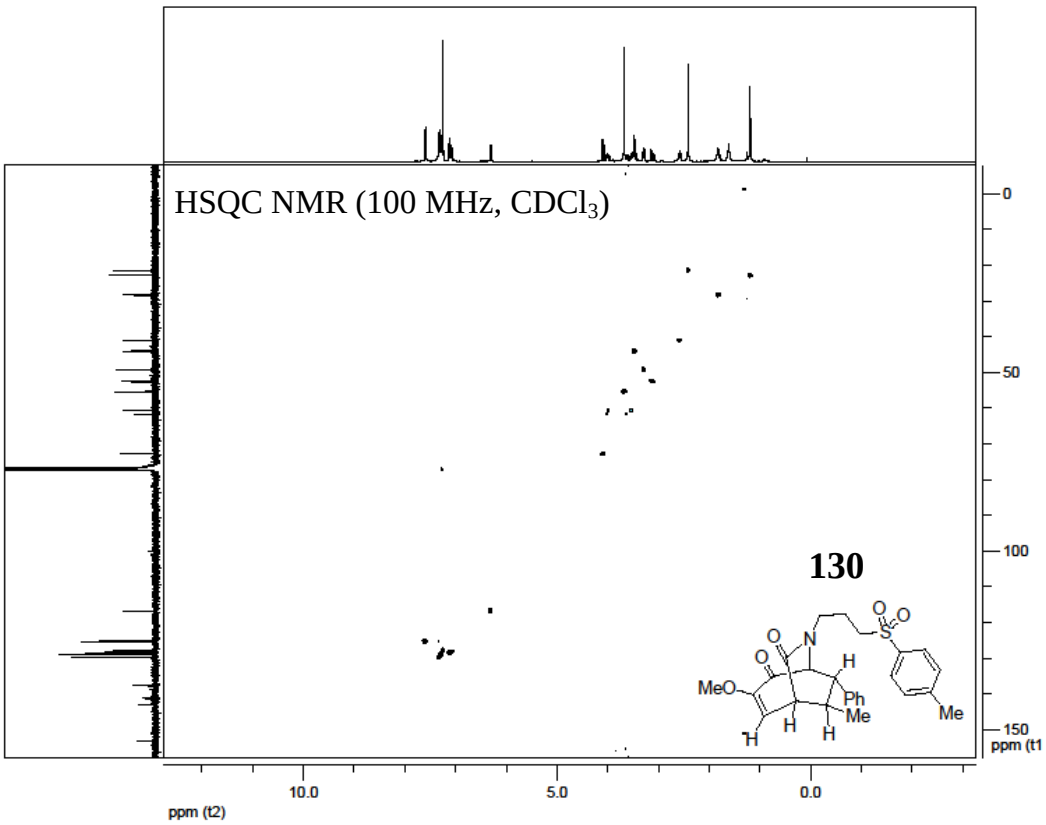
HSQC NMR (100 MHz, $CDCl_3$)
130
MeO
Ph
Me
Me
H
H
H
H
0
50
100
150
ppm (t1
10.0
5.0
0.0
ppm (t2)

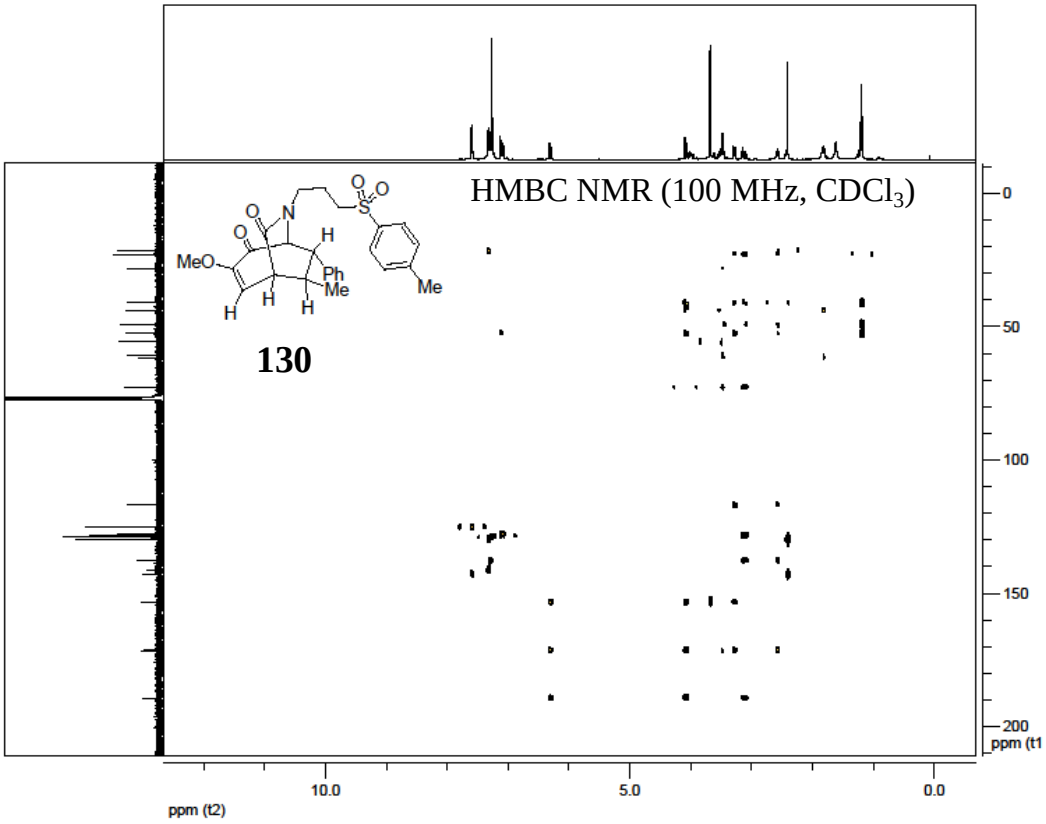
HMBC NMR (100 MHz, $CDCl_3$)
130
MeO
Ph
Me
Me
H
H
H
H
0
50
100
150
200
ppm (t1
10.0
5.0
0.0
ppm (t2)

$^{1}$H NMR (400 MHz, $CDCl_3$)

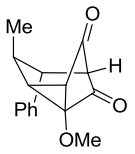


**135**




$^{13}$C NMR (100 MHz, $CDCl_3$)

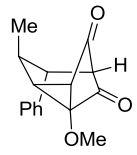


**135**

$^{1}$H NMR (400 MHz, $CDCl_3$)

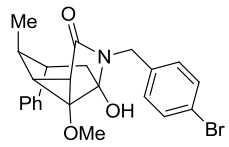


**136**




$^{13}$C NMR (100 MHz, $CDCl_3$)

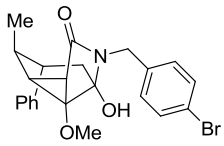


**136**

$^{1}$H NMR (400 MHz, $CDCl_3$)

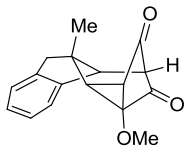


**140**




$^{13}$C NMR (100 MHz, $CDCl_3$)

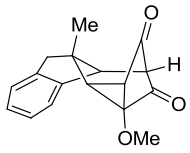


**140**

$^{1}$H NMR (400 MHz, $CDCl_3$)

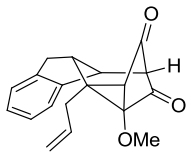


**141**




$^{13}$C NMR (100 MHz, $CDCl_3$)

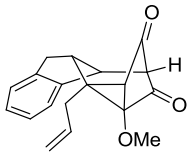


**141**

$^{1}$H NMR (400 MHz, $CDCl_3$)

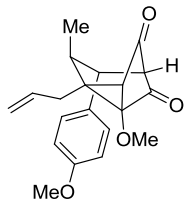


**142**




$^{13}$C NMR (100 MHz, $CDCl_3$)

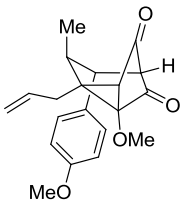


**142**

$^{1}$H NMR (400 MHz, $CDCl_3$)

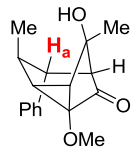


**145**




$^{13}$C NMR (100 MHz, $CDCl_3$)

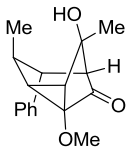


**145**

$^{1}$H NMR (400 MHz, $CDCl_3$)

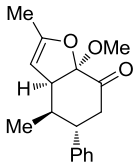


**147**




$^{13}$C NMR (100 MHz, $CDCl_3$)

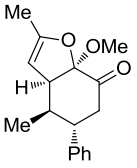


**147**

$^{1}$H NMR (400 MHz, $CDCl_3$)

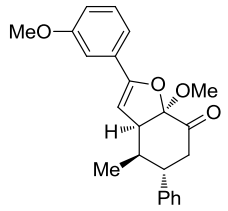


**148**




$^{13}$C NMR (100 MHz, $CDCl_3$)

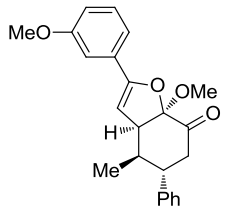


**148**

$^{1}$H NMR (400 MHz, $CDCl_3$)

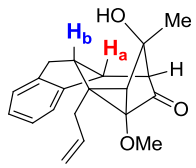


**149**




$^{13}$C NMR (100 MHz, $CDCl_3$)

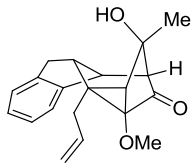


**149**

$^{1}$H NMR (400 MHz, $CDCl_3$)

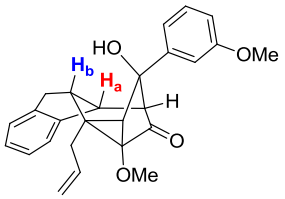


**150**




$^{13}$C NMR (100 MHz, $CDCl_3$)

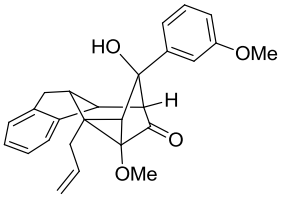


**150**

NOESY for compound **150**
(400 MHz, $CDCl_3$)

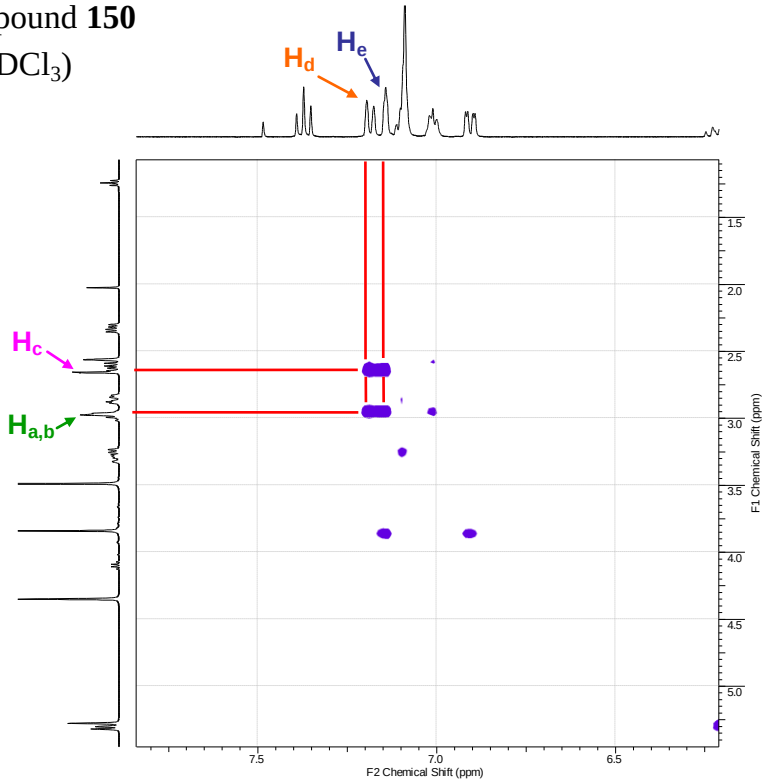


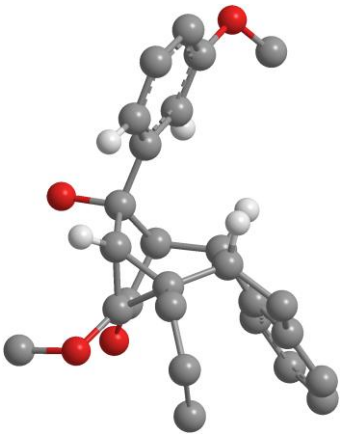

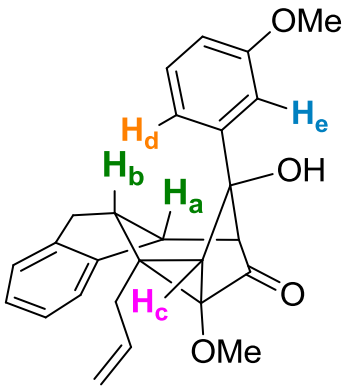

$^{1}$H NMR (400 MHz, $CDCl_3$)

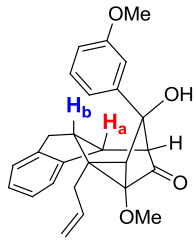


**151**




$^{13}$C NMR (100 MHz, $CDCl_3$)

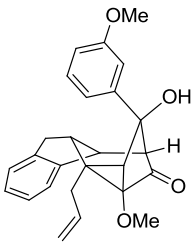


**151**

$^{1}$H NMR (400 MHz, $CDCl_3$)

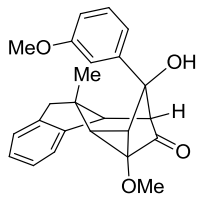





$^{13}$C NMR (100 MHz, $CDCl_3$)

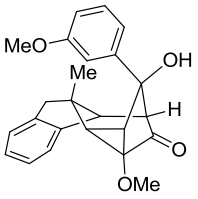

$^{1}$H NMR (400 MHz, $CDCl_3$)

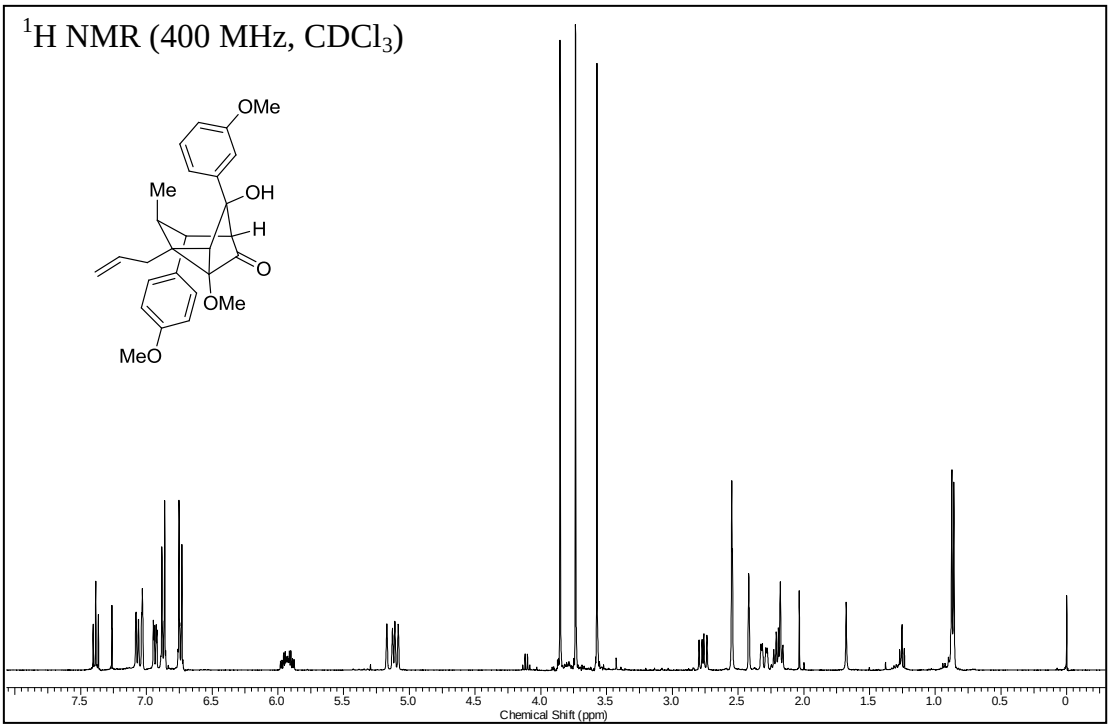


$^{13}$C NMR (100 MHz, $CDCl_3$)

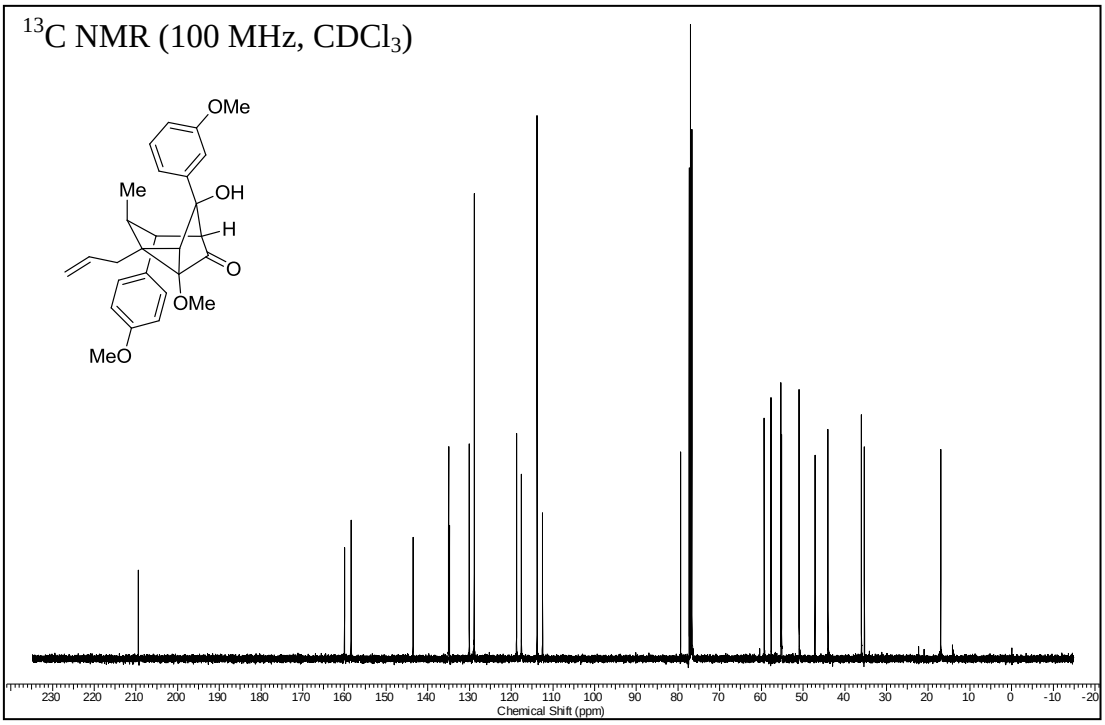

$^{1}$H NMR (500 MHz, $CDCl_3$)

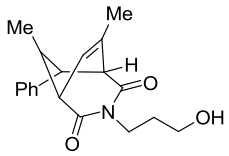


**152**




$^{13}$C NMR (125 MHz, $CDCl_3$)

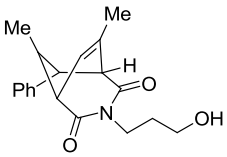


**152**

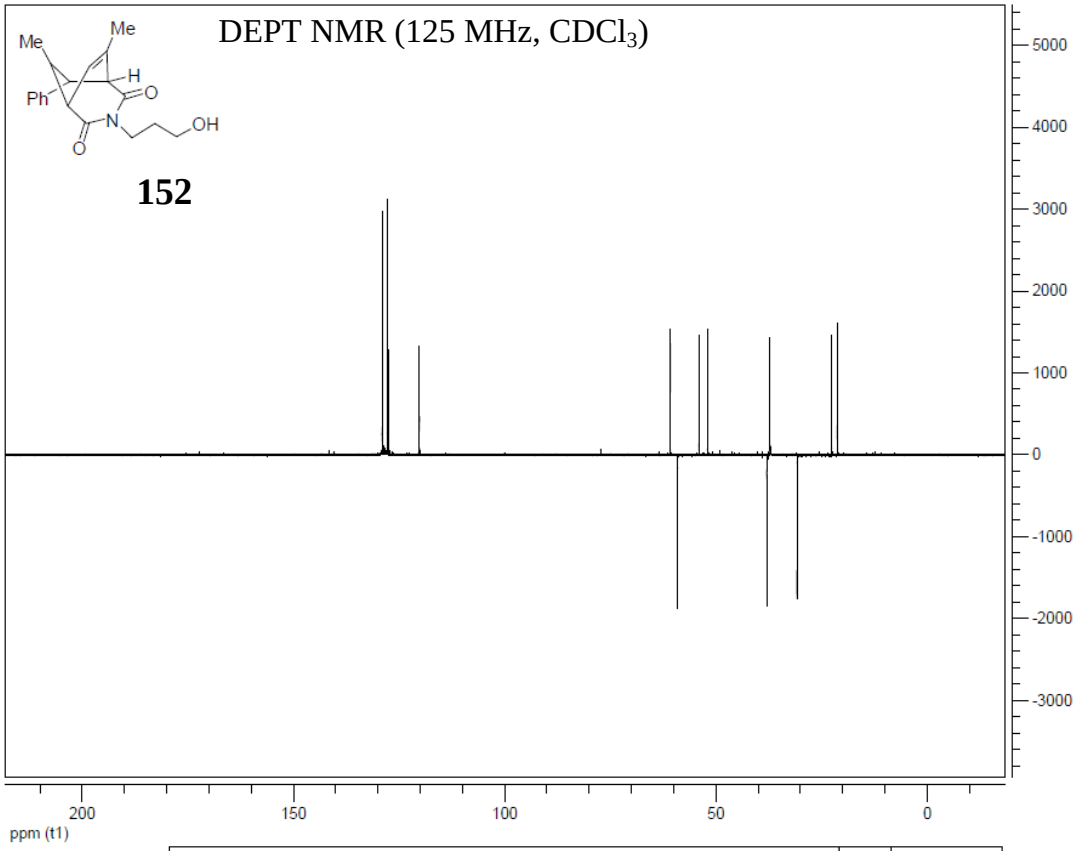
Me
Me
H
O
Ph
N
OH
O
152
DEPT NMR (125 MHz, CDCl3)
5000
4000
3000
2000
1000
0
-1000
-2000
-3000
200
150
100
50
0
ppm (t1)

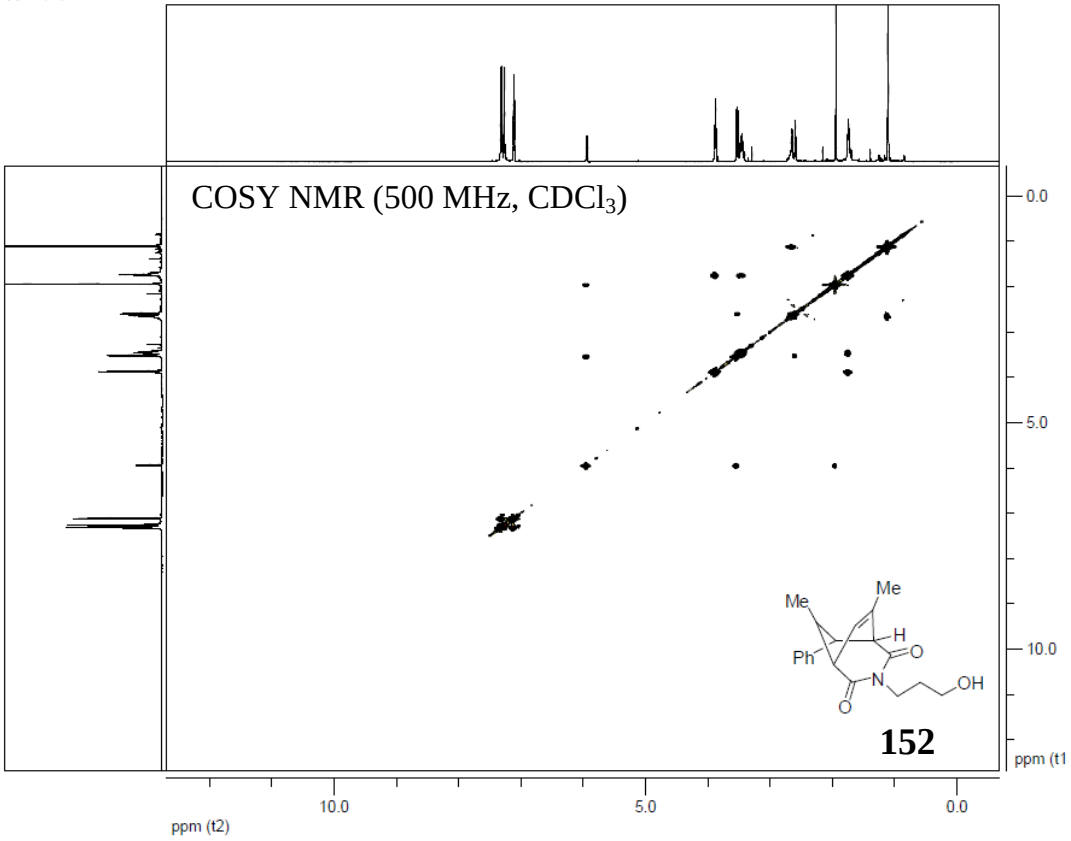
COSY NMR (500 MHz, CDCl3)
0.0
5.0
10.0
ppm (t1
10.0
5.0
0.0
ppm (t2)
Me
Me
H
O
Ph
N
OH
O
152

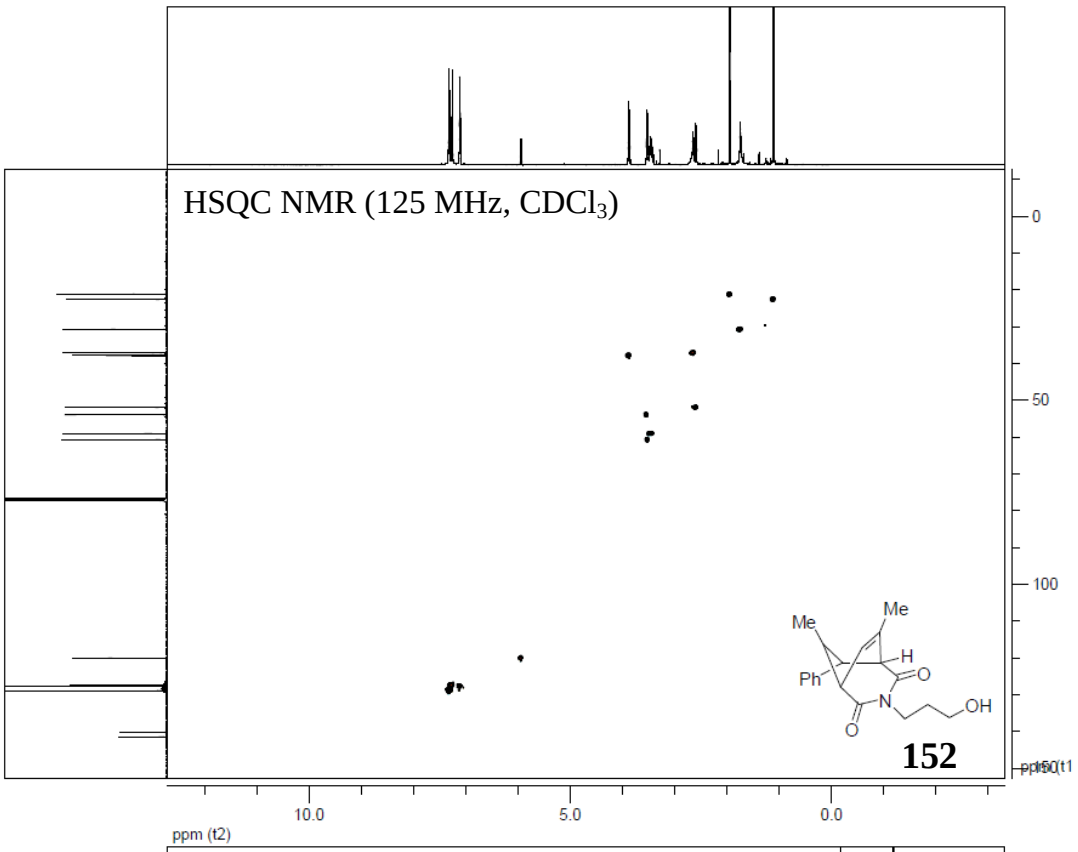
HSQC NMR (125 MHz, CDCl3)
Me
Me
H
Ph
O
N
OH
O
152
0
50
100
10.0
5.0
0.0
ppm (t2)

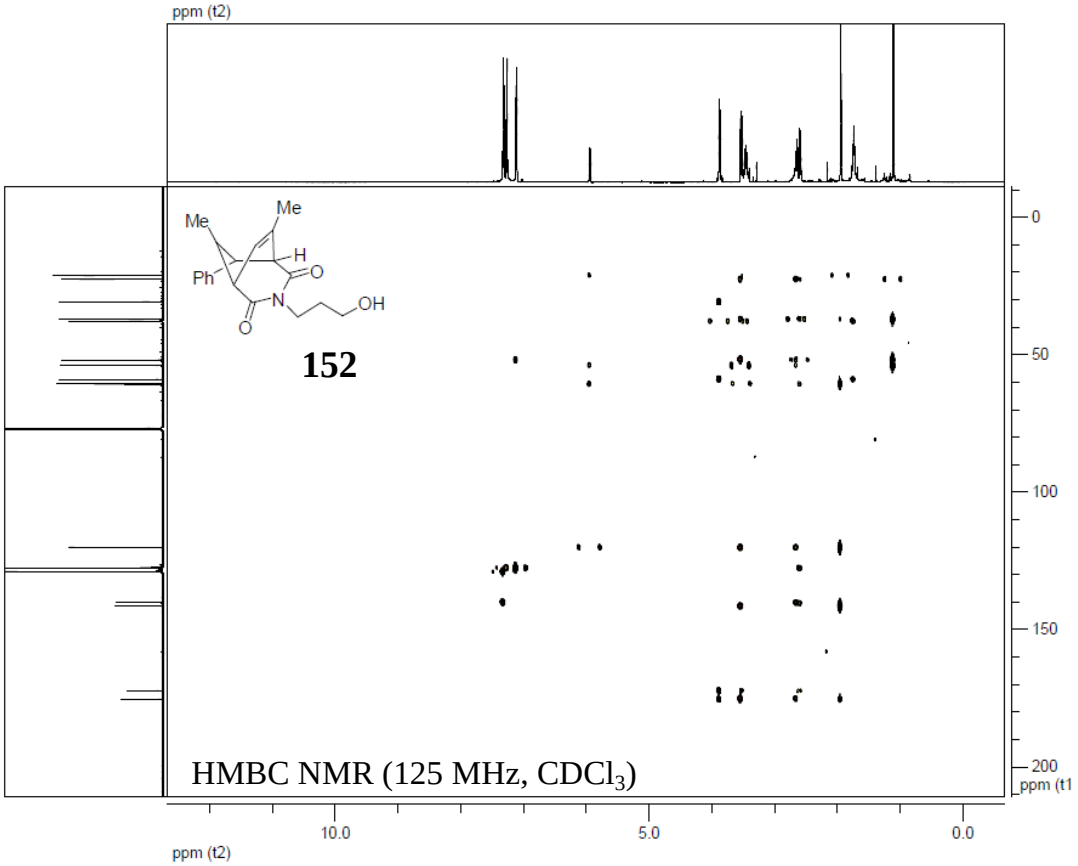
Me
Me
H
Ph
O
N
OH
O
152
HMBC NMR (125 MHz, CDCl3)
0
50
100
150
200
10.0
5.0
0.0
ppm (t2)

$^{1}$H NMR (500 MHz, $CDCl_3$)

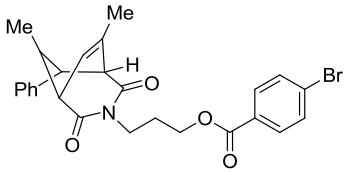


**153**




$^{13}$C NMR (125 MHz, $CDCl_3$)

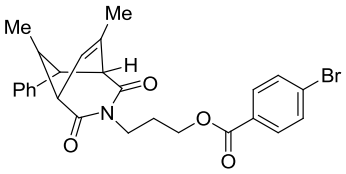


**153**

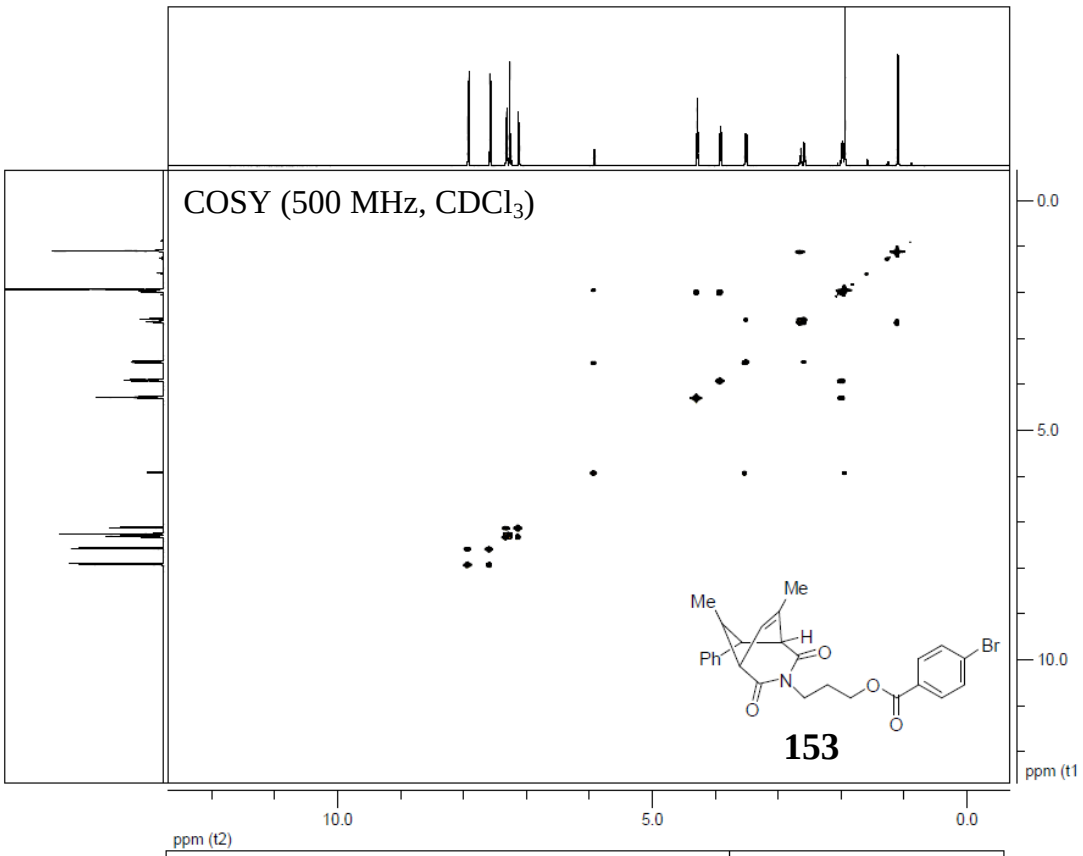
COSY (500 MHz, CDCl3)
Me
Me
H
Ph
O
N
O
O
O
Br
153
0.0
5.0
10.0
ppm (t1
10.0
5.0
0.0
ppm (t2)

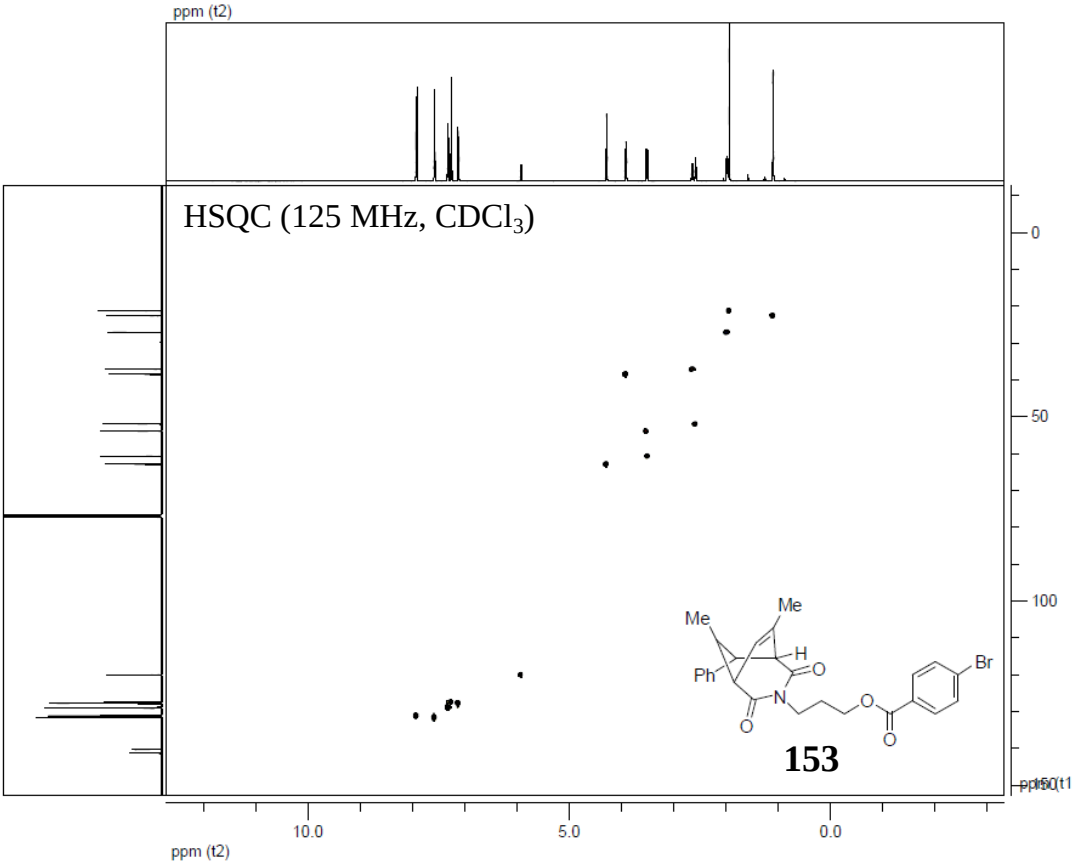
HSQC (125 MHz, CDCl3)
Me
Me
H
Ph
O
N
O
O
O
Br
153
0
50
100
10.0
5.0
0.0
ppm (t2)

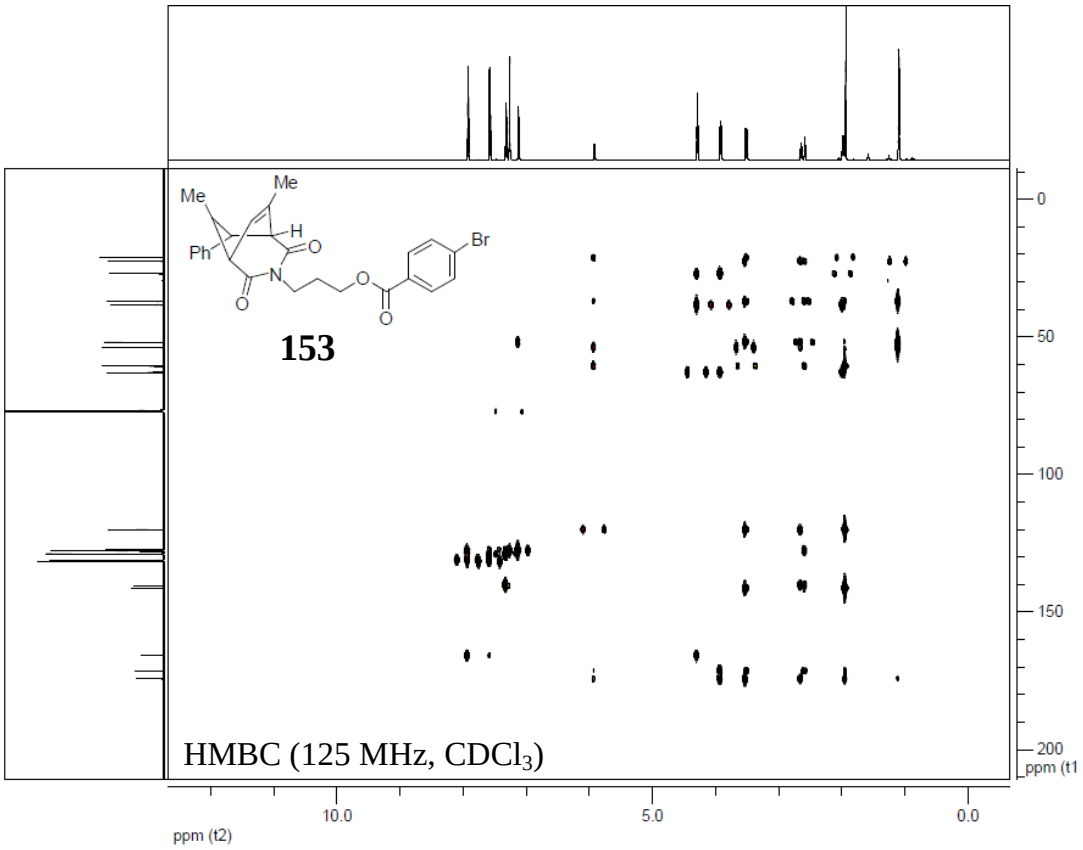
Me
Me
H
Ph
O
N
O
O
O
Br
153
HMBC (125 MHz, CDCl3)
0
50
100
150
200
ppm (t1
10.0
5.0
0.0
ppm (t2)

$^{1}$H NMR (500 MHz, $CDCl_3$)

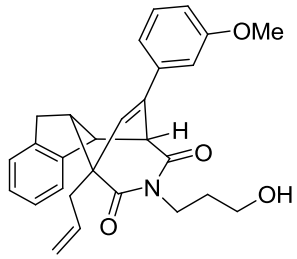


**155**

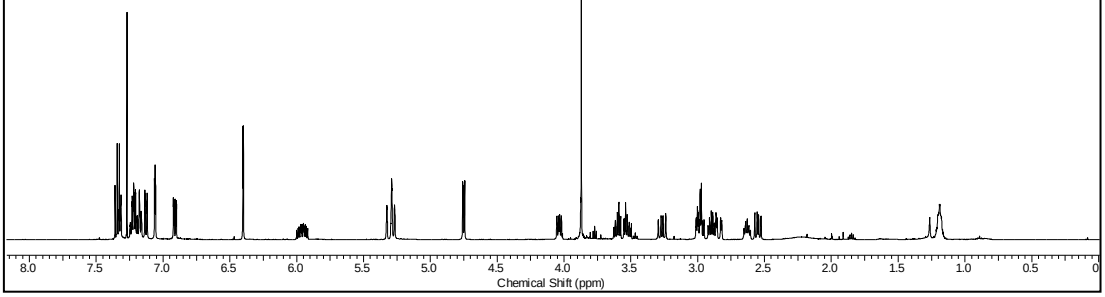


$^{13}$C NMR (125 MHz, $CDCl_3$)

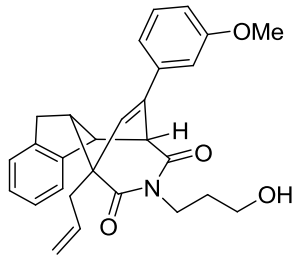


**155**

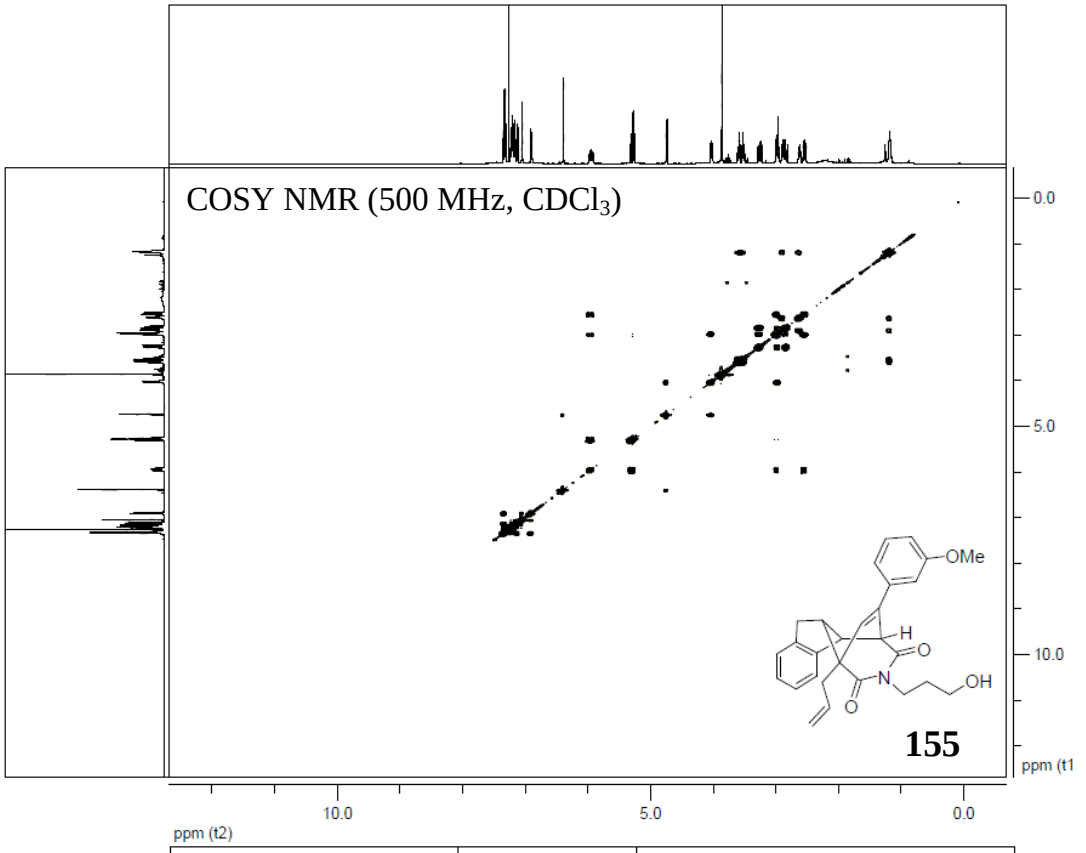
COSY NMR (500 MHz, CDCl3)
OMe
H
O
N
OH
O
155
0.0
5.0
10.0
ppm (t1
10.0
5.0
0.0
ppm (t2)

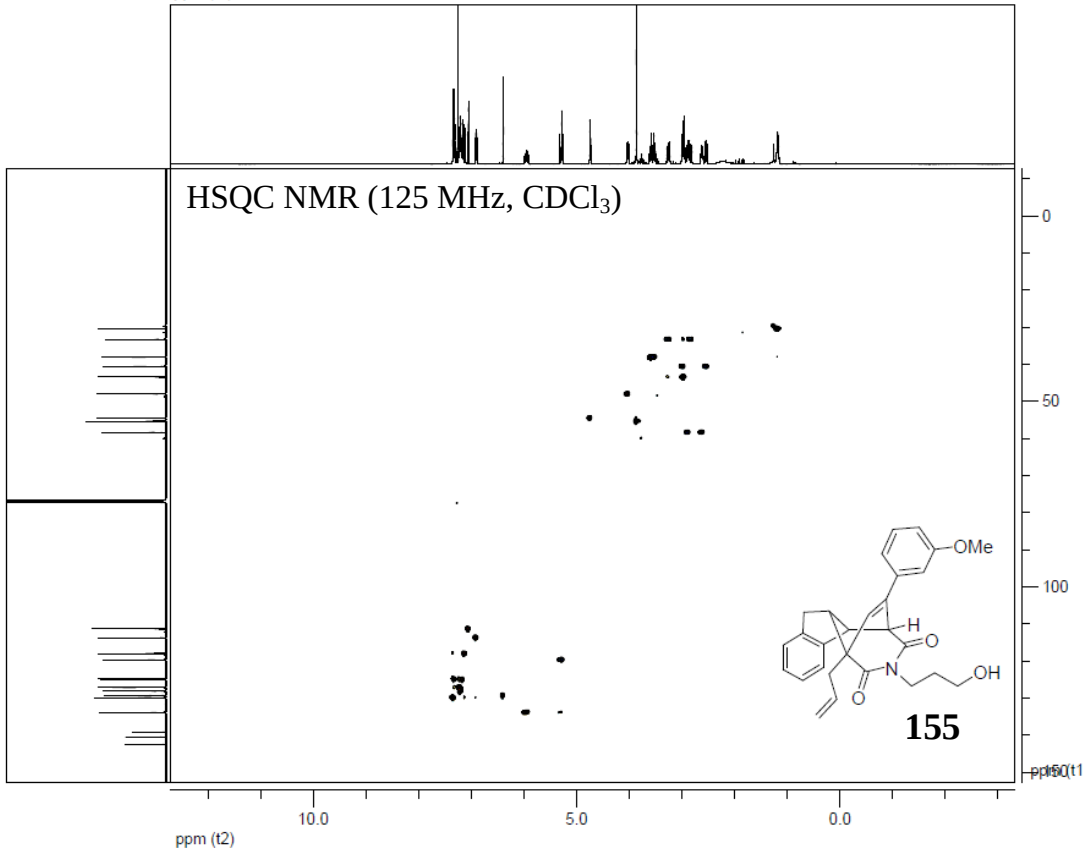
HSQC NMR (125 MHz, CDCl3)
OMe
H
O
N
OH
O
155
0
50
100
10.0
5.0
0.0
ppm (t2)

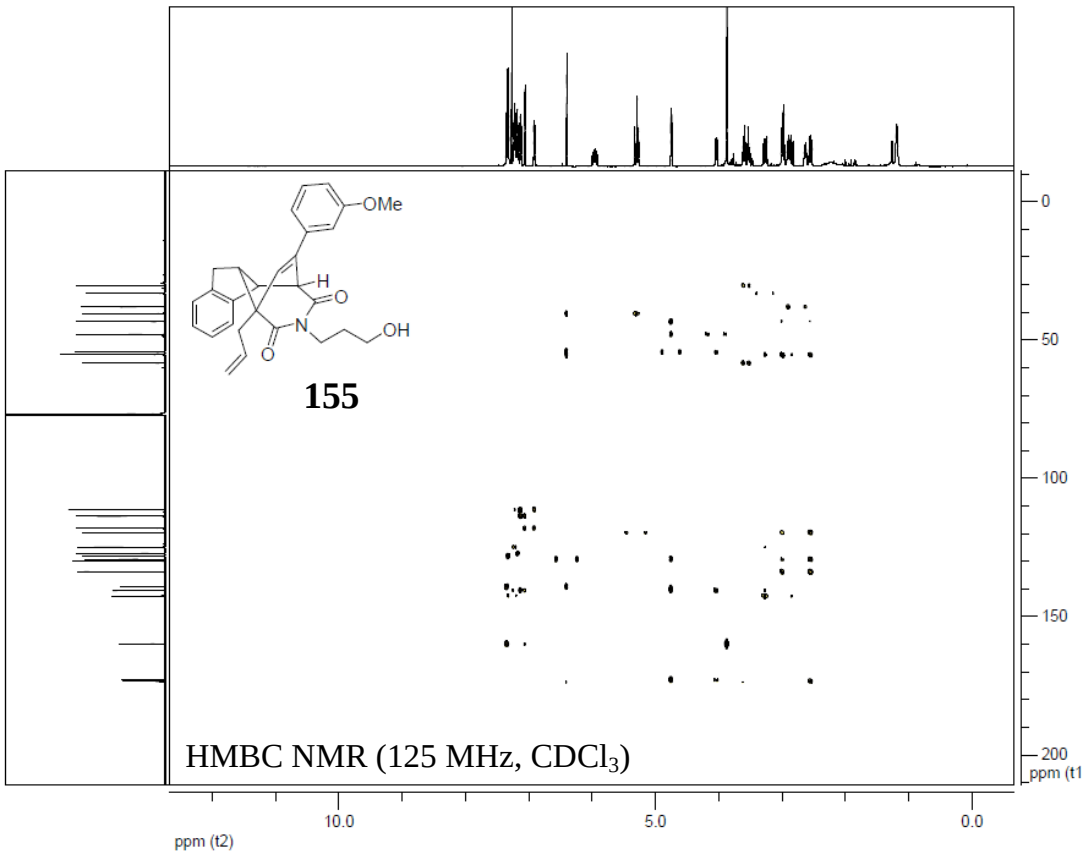
OMe
H
O
N
OH
O
155
HMBC NMR (125 MHz, CDCl3)
0
50
100
150
200
ppm (t1
10.0
5.0
0.0
ppm (t2)

$^{1}$H NMR (500 MHz, $CDCl_3$)

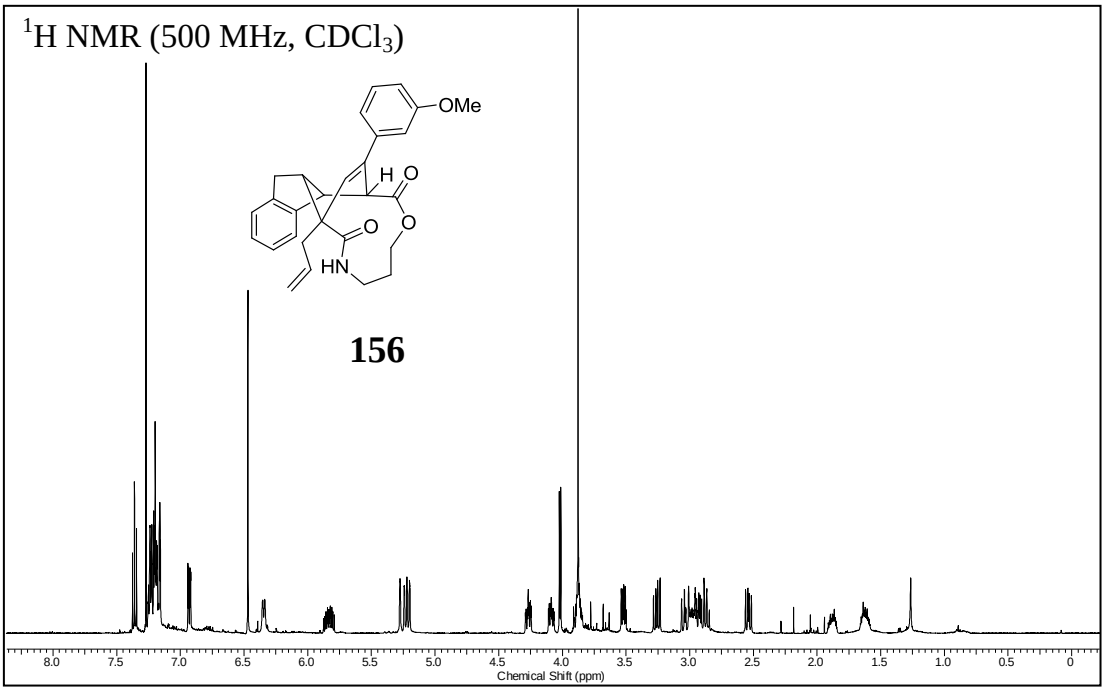


**156**

$^{13}$C NMR (125 MHz, $CDCl_3$)

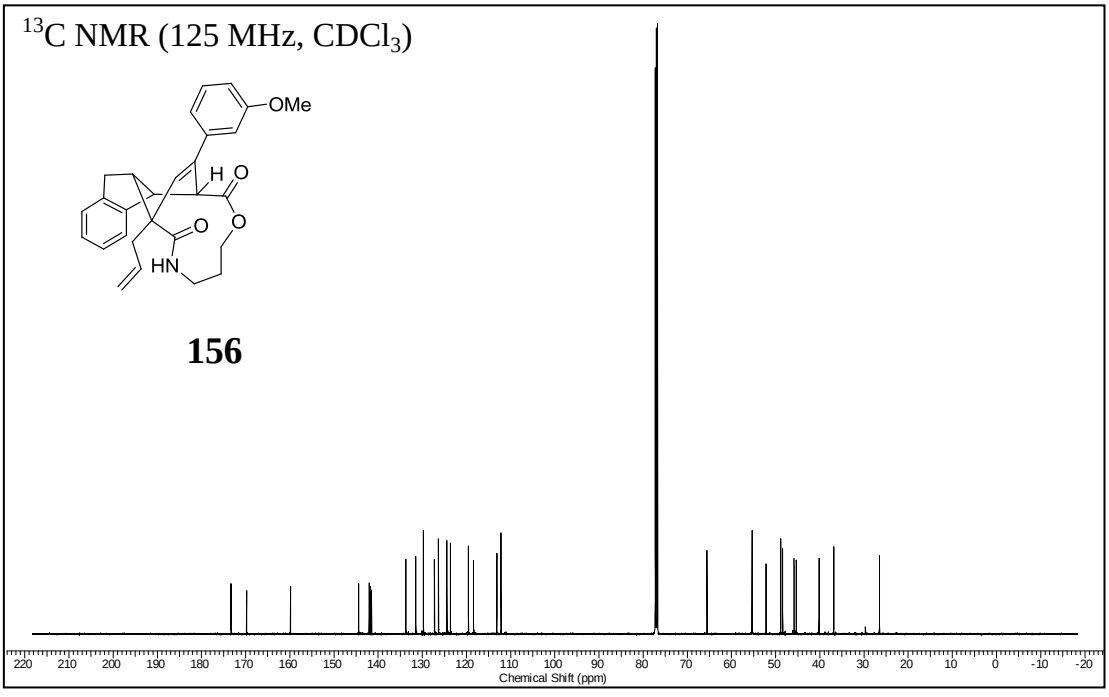


**156**

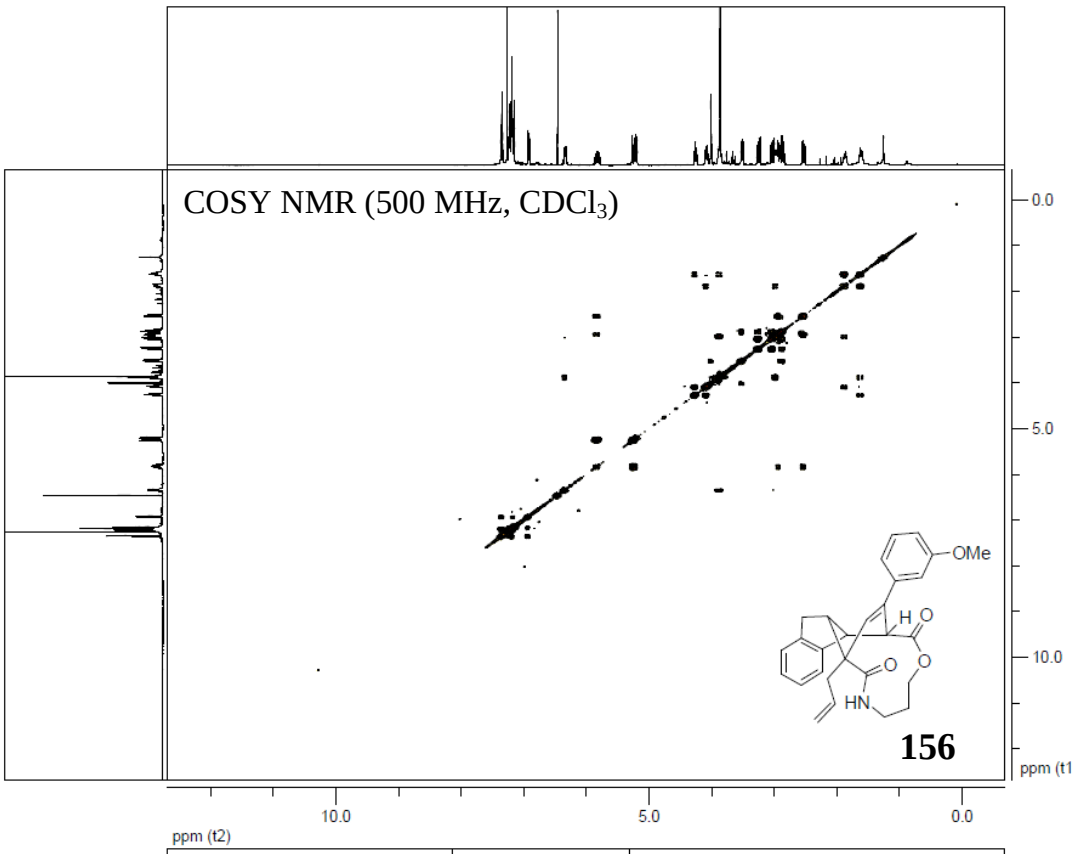
COSY NMR (500 MHz, CDCl3)
OMe
H
O
O
O
HN
156
0.0
5.0
10.0
ppm (t1
10.0
5.0
0.0
ppm (t2)

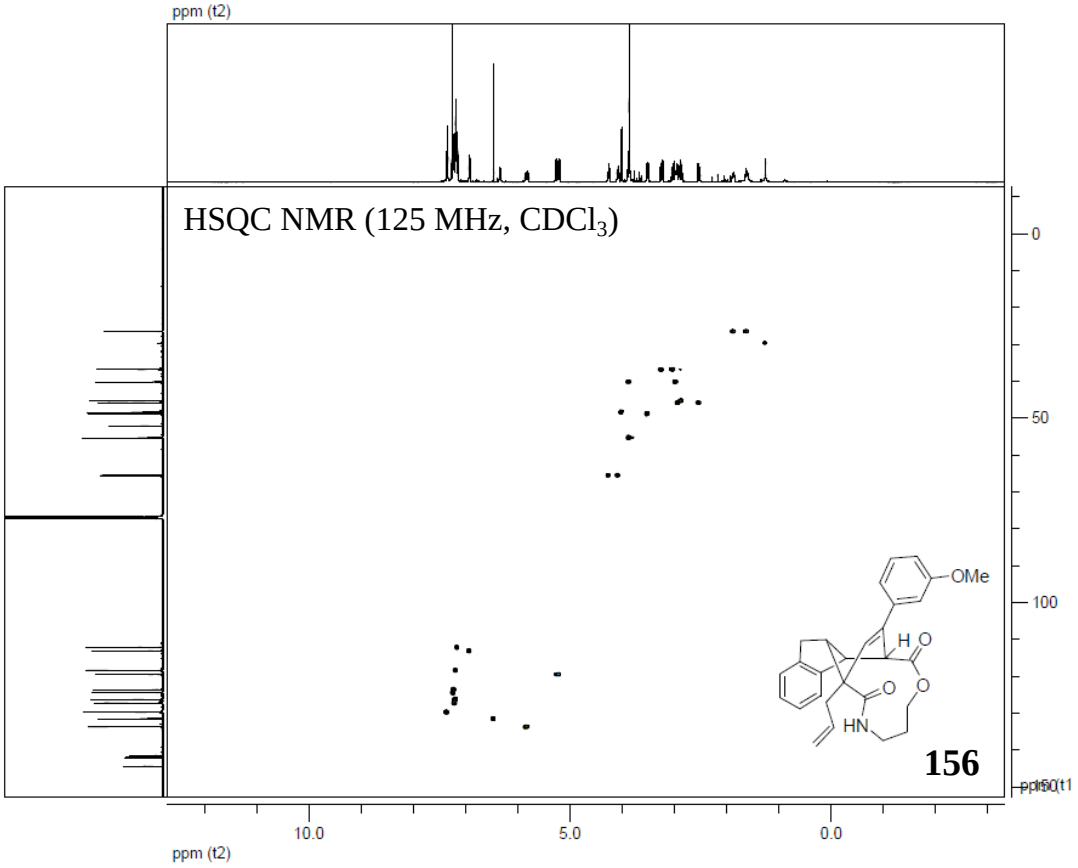
HSQC NMR (125 MHz, CDCl3)
OMe
H
O
O
O
HN
156
0
50
100
10.0
5.0
0.0
ppm (t2)

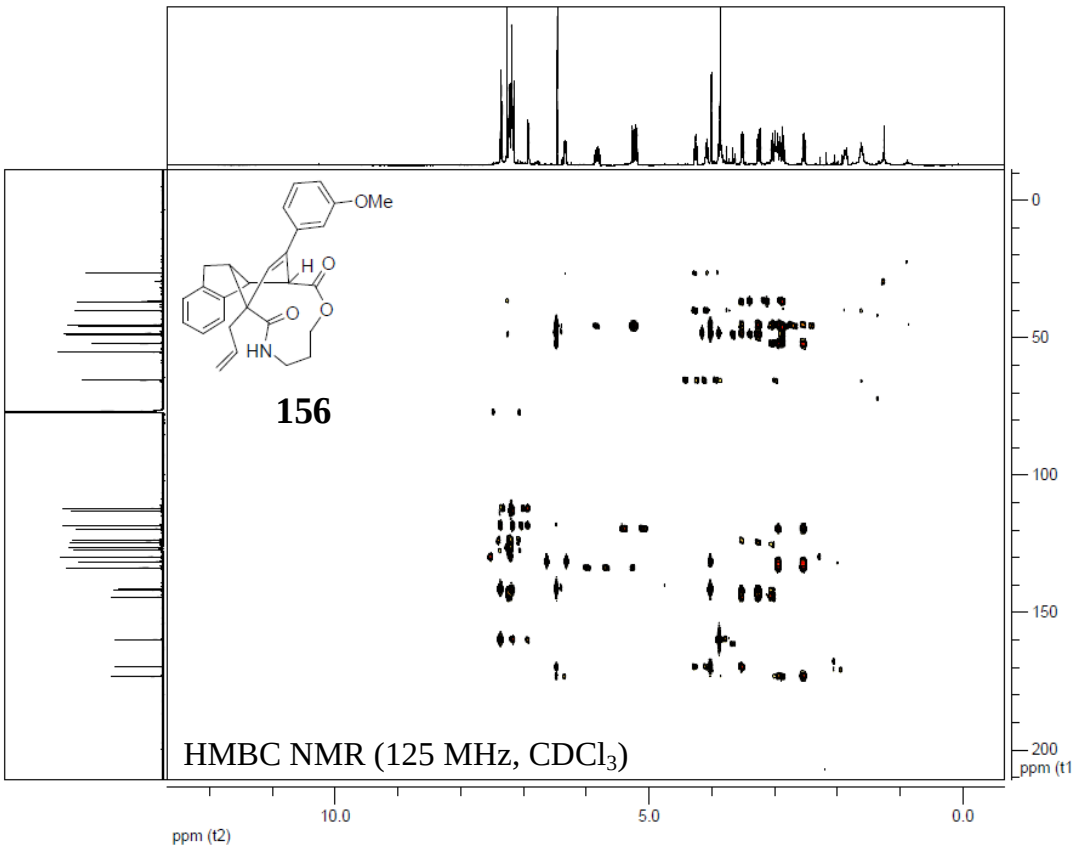
OMe
H
O
O
O
HN
156
HMBC NMR (125 MHz, CDCl3)
0
50
100
150
200
ppm (t1
10.0
5.0
0.0
ppm (t2)

$^{1}$H NMR (400 MHz, $CDCl_3$)

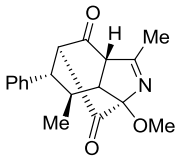


**157**




$^{13}$C NMR (100 MHz, $CDCl_3$)

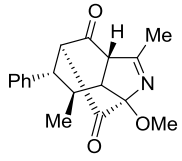


**157**

$^{1}$H NMR (400 MHz, $CDCl_3$)

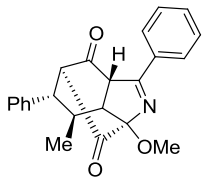


**159**




$^{13}$C NMR (100 MHz, $CDCl_3$)

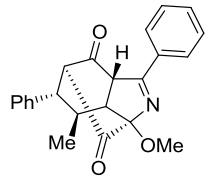


**159**

$^{1}$H NMR (400 MHz, $CDCl_3$)

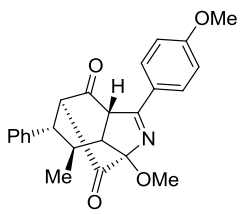


**159**




$^{13}$C NMR (100 MHz, $CDCl_3$)

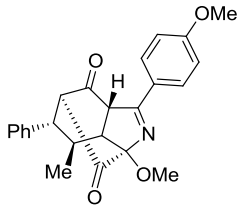


**159**

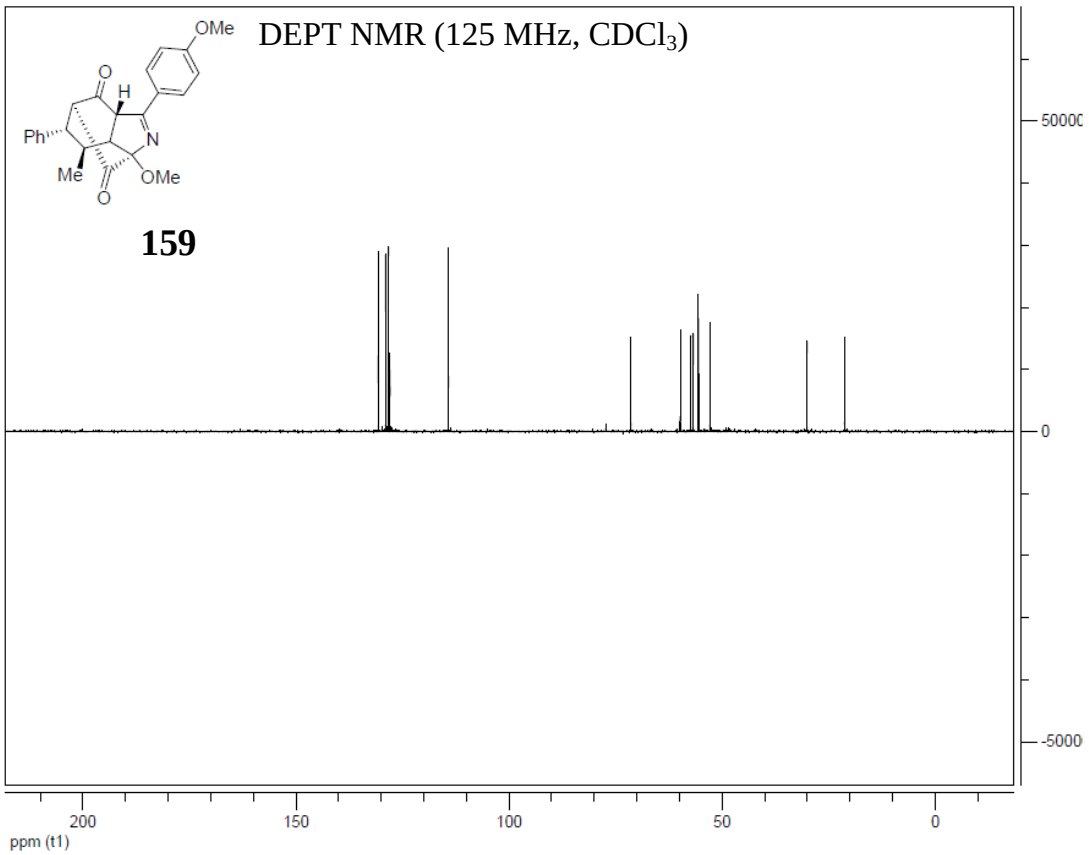
DEPT NMR (125 MHz, CDCl3)
OMe
O
H
Ph
N
Me
OMe
O
159
50000
0
-5000
200
150
100
50
0
ppm (t1)

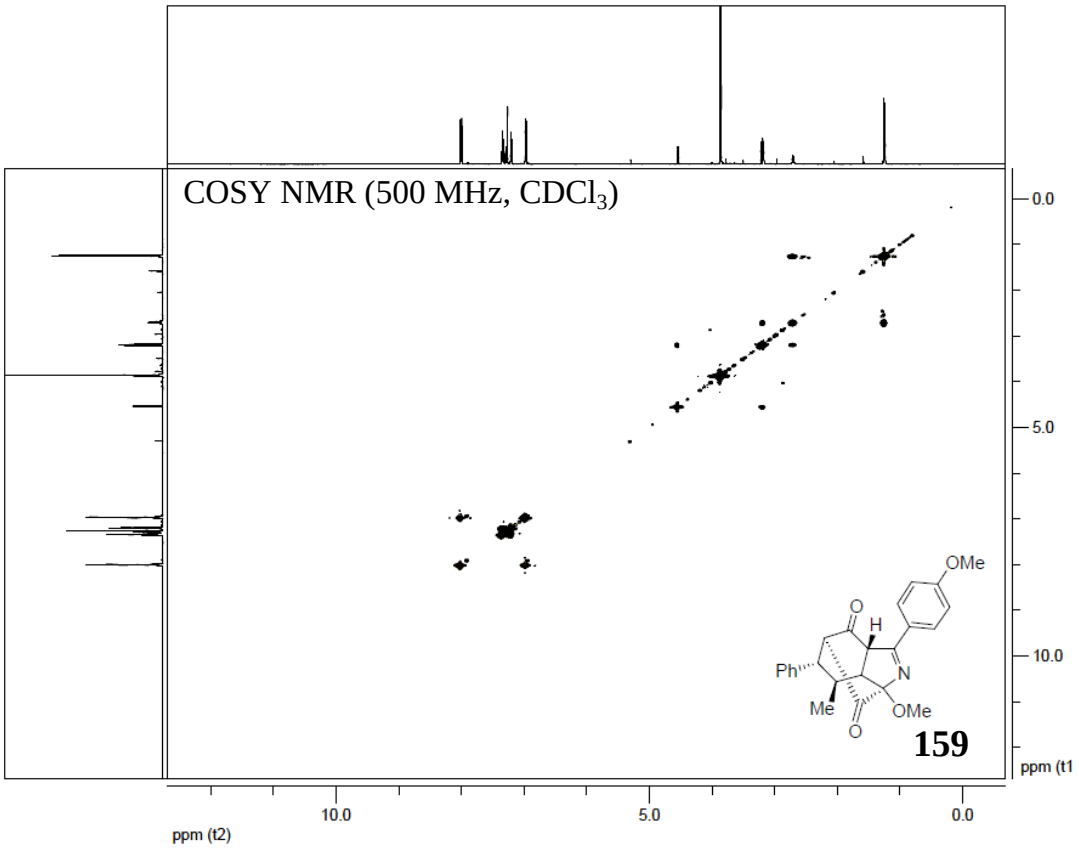
COSY NMR (500 MHz, CDCl3)
0.0
5.0
10.0
OMe
O
H
Ph
N
Me
OMe
O
159
ppm (t1
10.0
5.0
0.0
ppm (t2)

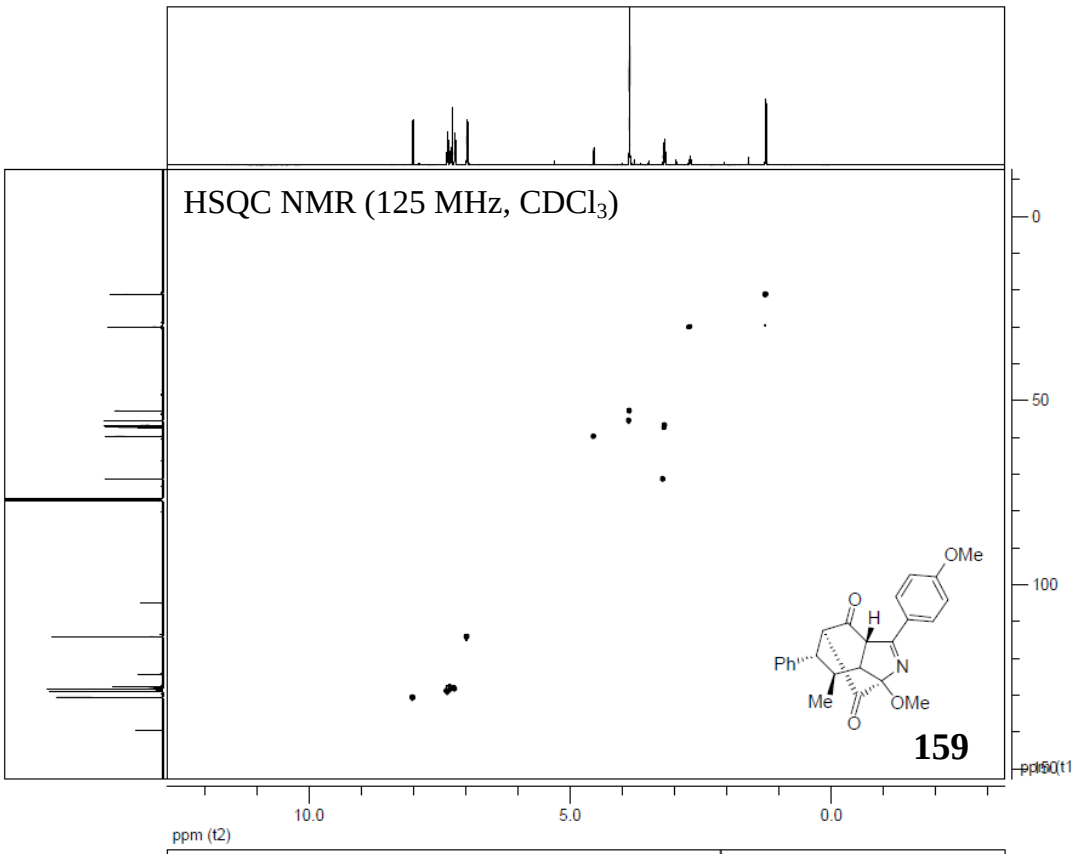
HSQC NMR (125 MHz, CDCl3)
OMe
O
H
Ph
N
Me
OMe
O
159
0
50
100
10.0
5.0
0.0
ppm (t2)
ppm (t1

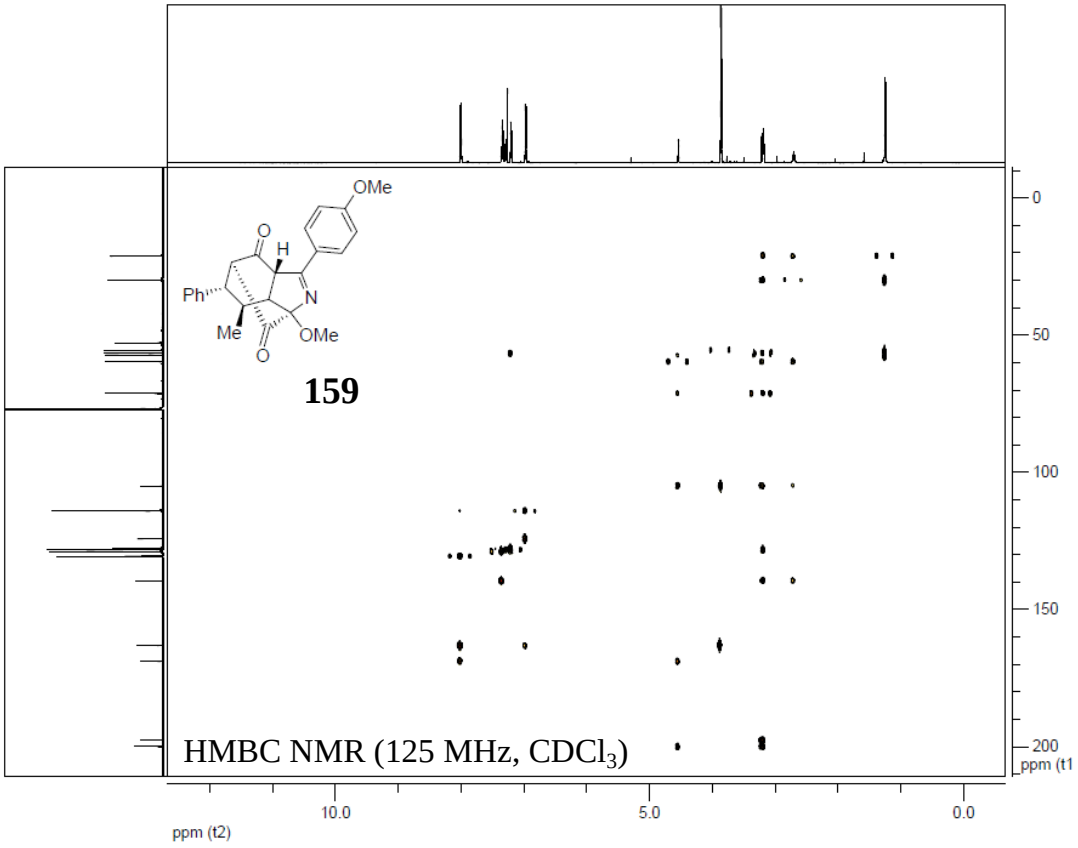
OMe
O
H
Ph
N
Me
OMe
O
159
HMBC NMR (125 MHz, CDCl3)
0
50
100
150
200
10.0
5.0
0.0
ppm (t2)
ppm (t1

$^{1}$H NMR (400 MHz, $CDCl_3$)

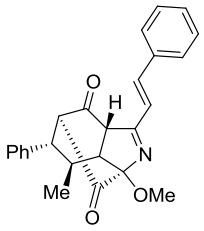


**160**




$^{13}$C NMR (100 MHz, $CDCl_3$)

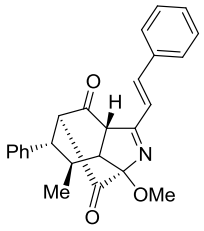


**160**

$^{1}$H NMR (400 MHz, $CDCl_3$)

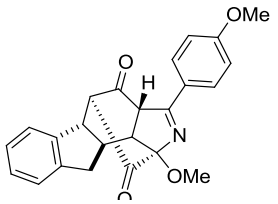


**161**

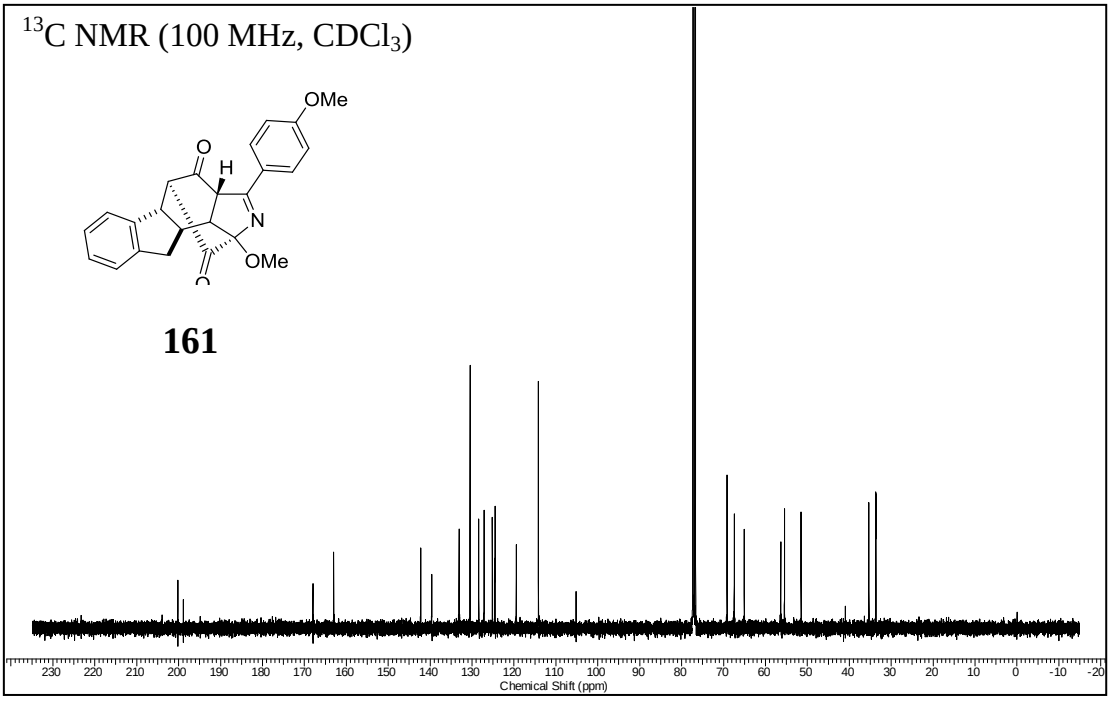


$^{13}$C NMR (100 MHz, $CDCl_3$)




**161**

$^{1}$H NMR (400 MHz, $CDCl_3$)

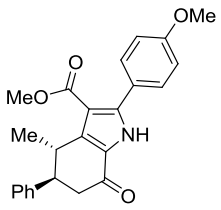


**162**




$^{13}$C NMR (100 MHz, $CDCl_3$)

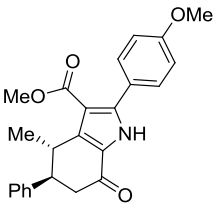


**162**

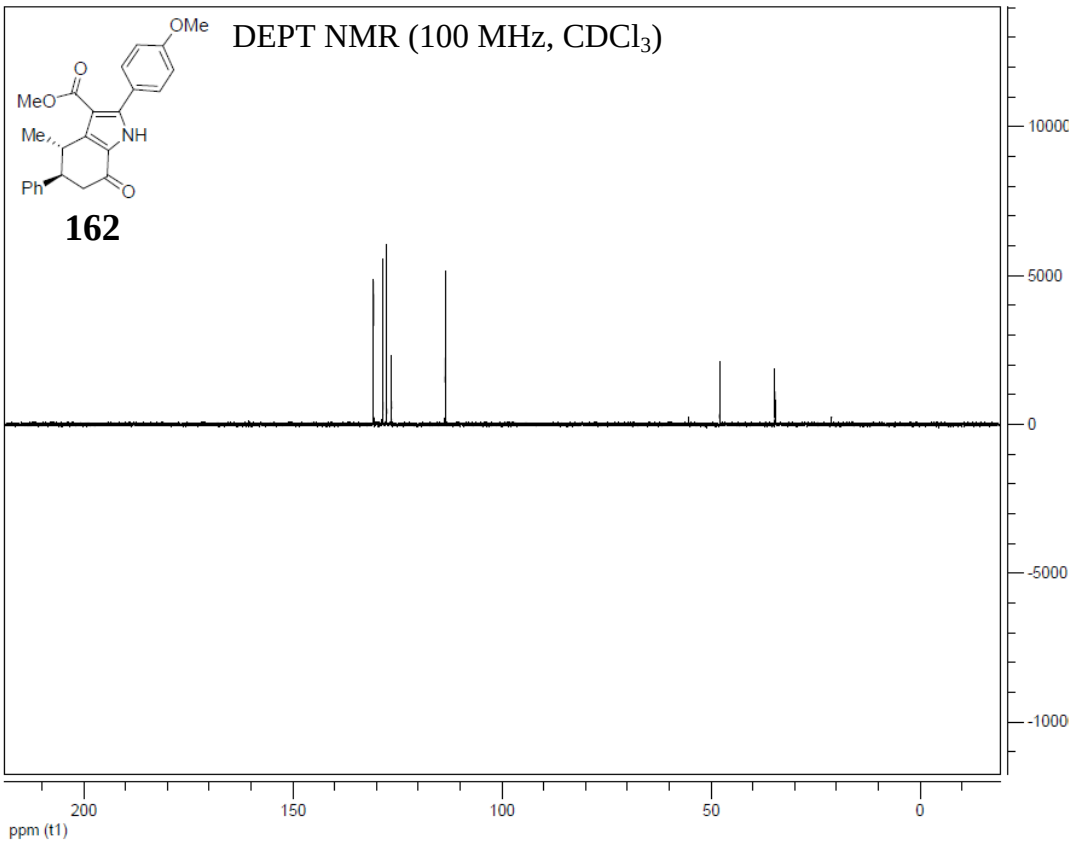
DEPT NMR (100 MHz, CDCl3)
OMe
MeO
O
Me
NH
Ph
O
162
10000
5000
0
-5000
-10000
200
150
100
50
0
ppm (t1)

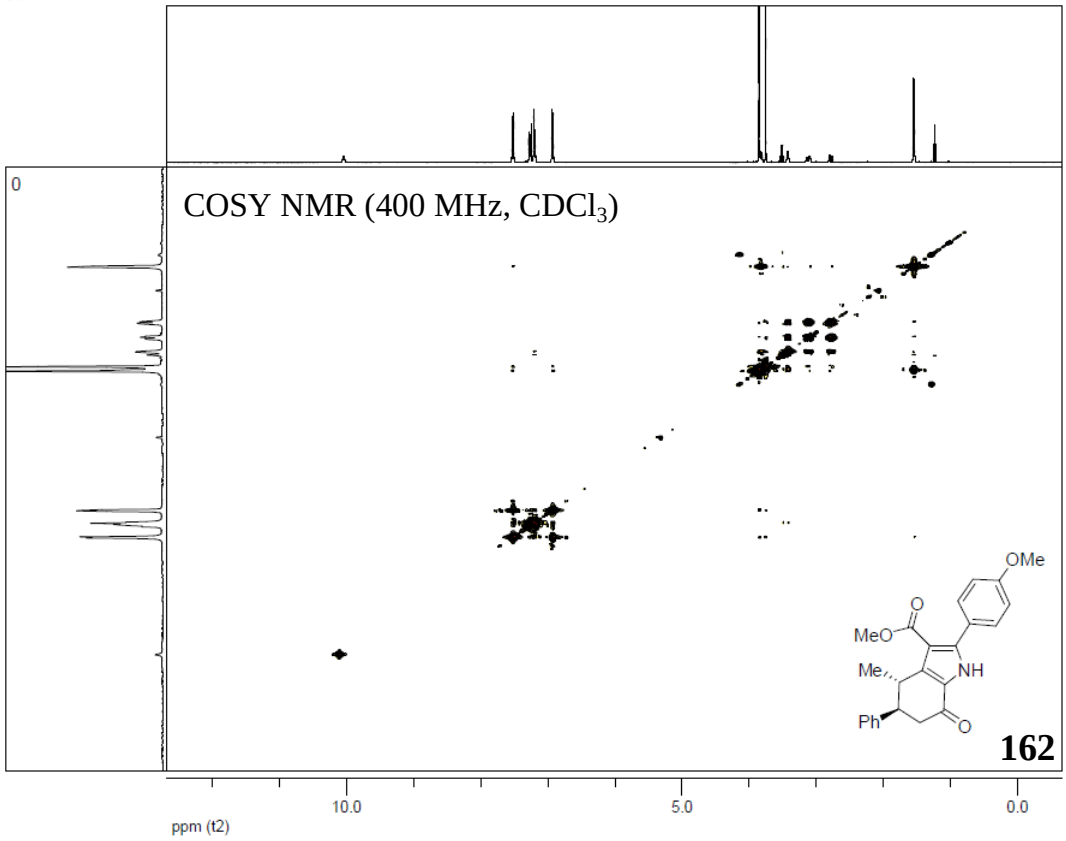
0
COSY NMR (400 MHz, CDCl3)
OMe
MeO
O
Me
NH
Ph
O
162
10.0
5.0
0.0
ppm (t2)

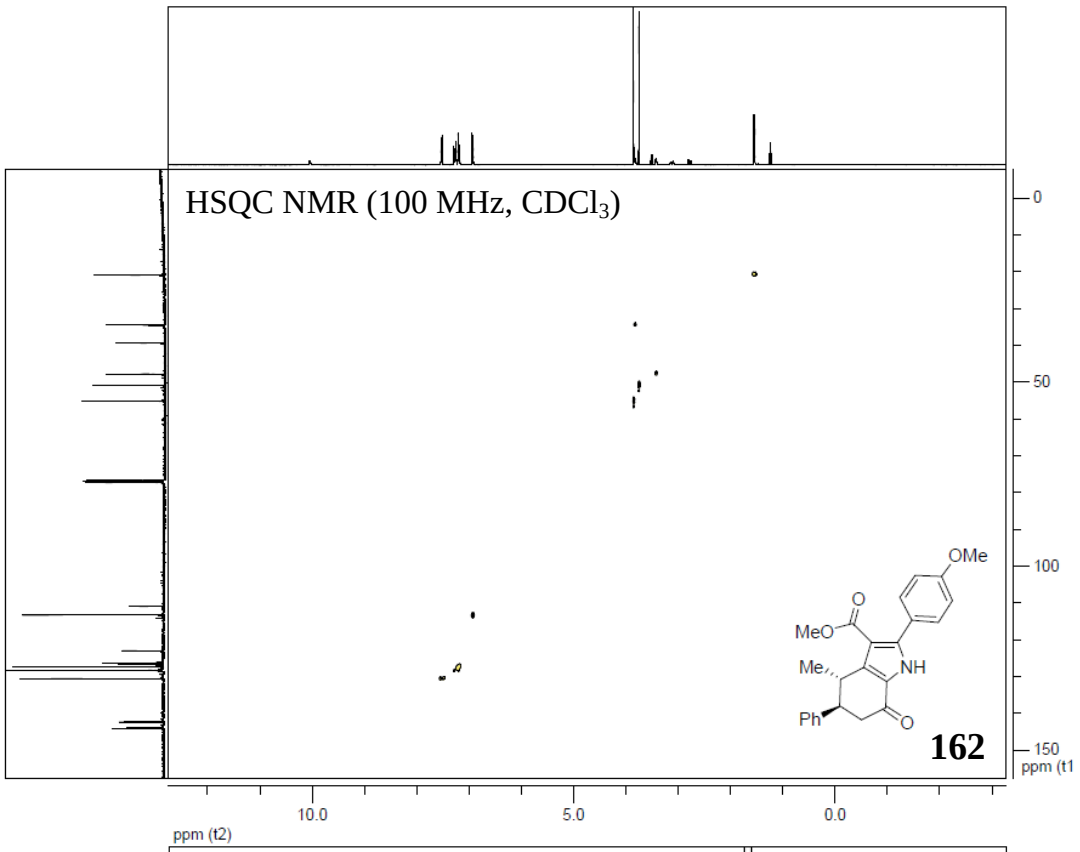
HSQC NMR (100 MHz, CDCl3)
OMe
MeO
O
Me
NH
Ph
O
162
0
50
100
150
ppm (t1
10.0
5.0
0.0
ppm (t2)

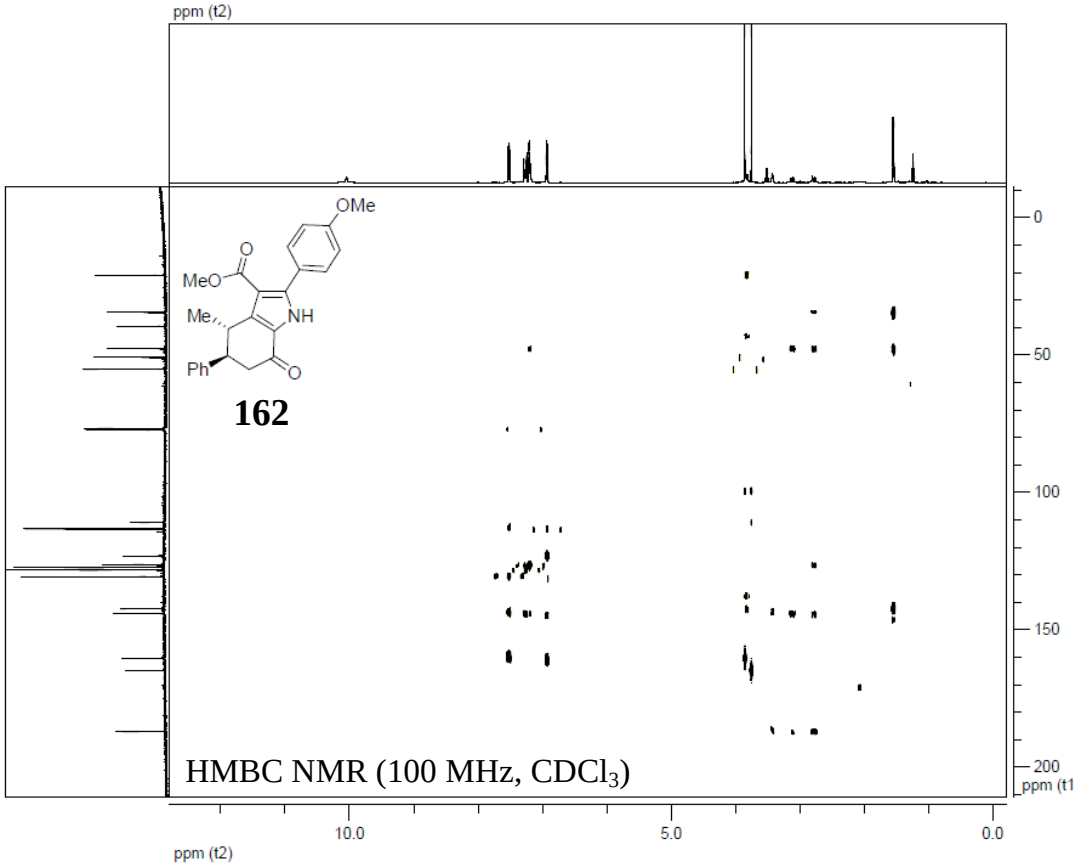
OMe
MeO
O
Me
NH
Ph
O
162
HMBC NMR (100 MHz, CDCl3)
0
50
100
150
200
ppm (t1
10.0
5.0
0.0
ppm (t2)

$^{1}$H NMR (500 MHz, $CDCl_3$)

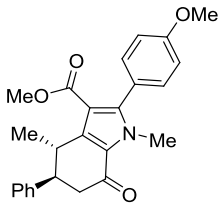


**163**




$^{13}$C NMR (125 MHz, $CDCl_3$)

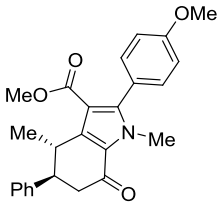


**163**

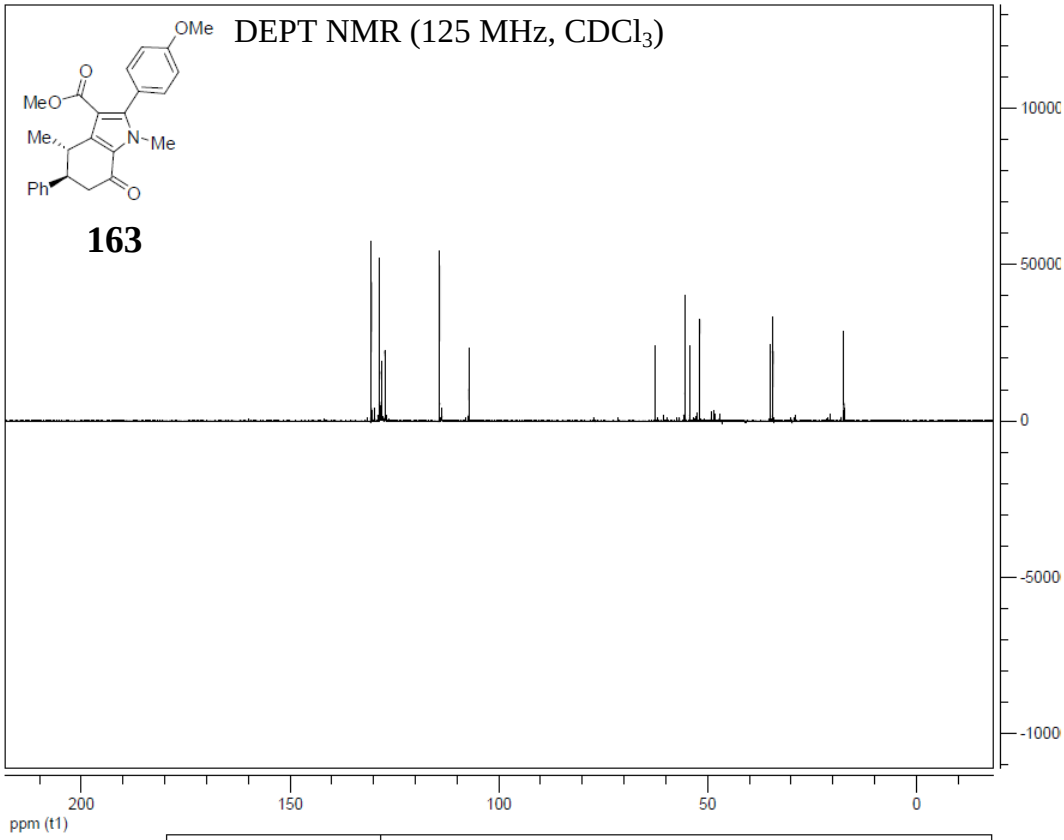
DEPT NMR (125 MHz, CDCl3)
OMe
MeO
O
Me
N
Me
Ph
O
163
10000
50000
0
-5000
-10000
200
150
100
50
0
ppm (t1)

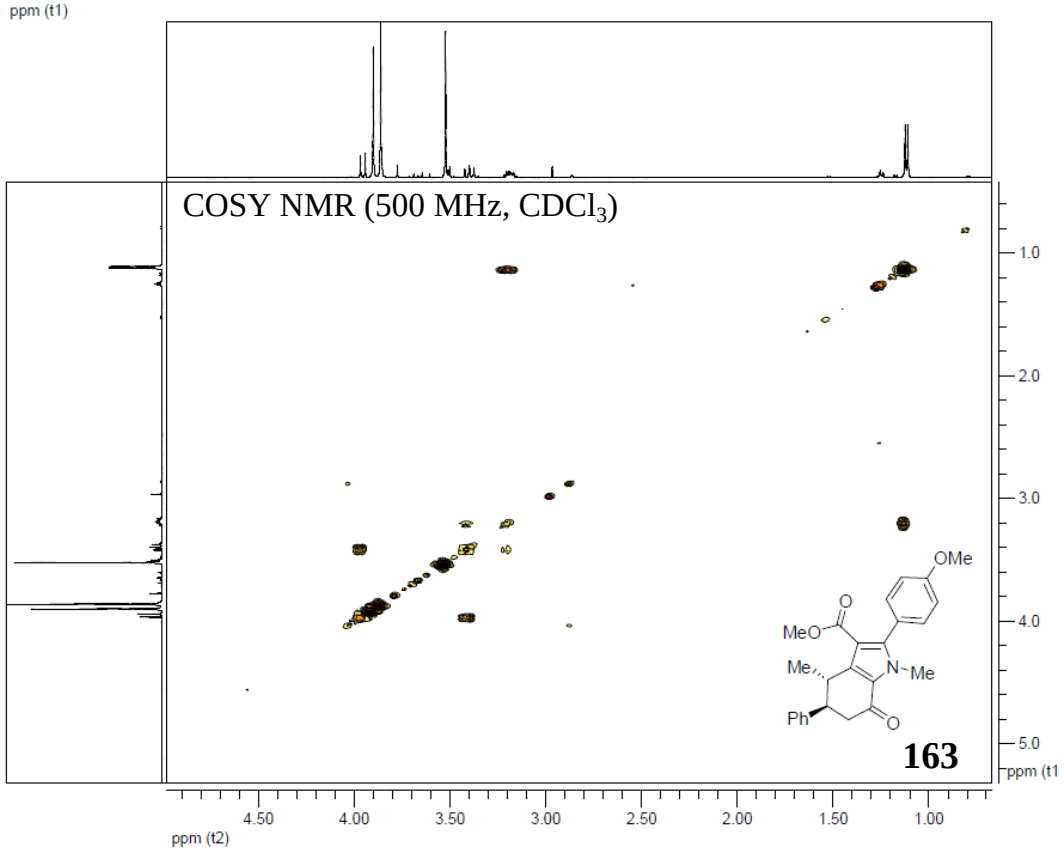
COSY NMR (500 MHz, CDCl3)
OMe
MeO
O
Me
N
Me
Ph
O
163
1.0
2.0
3.0
4.0
5.0
ppm (t1
4.50
4.00
3.50
3.00
2.50
2.00
1.50
1.00
ppm (t2)

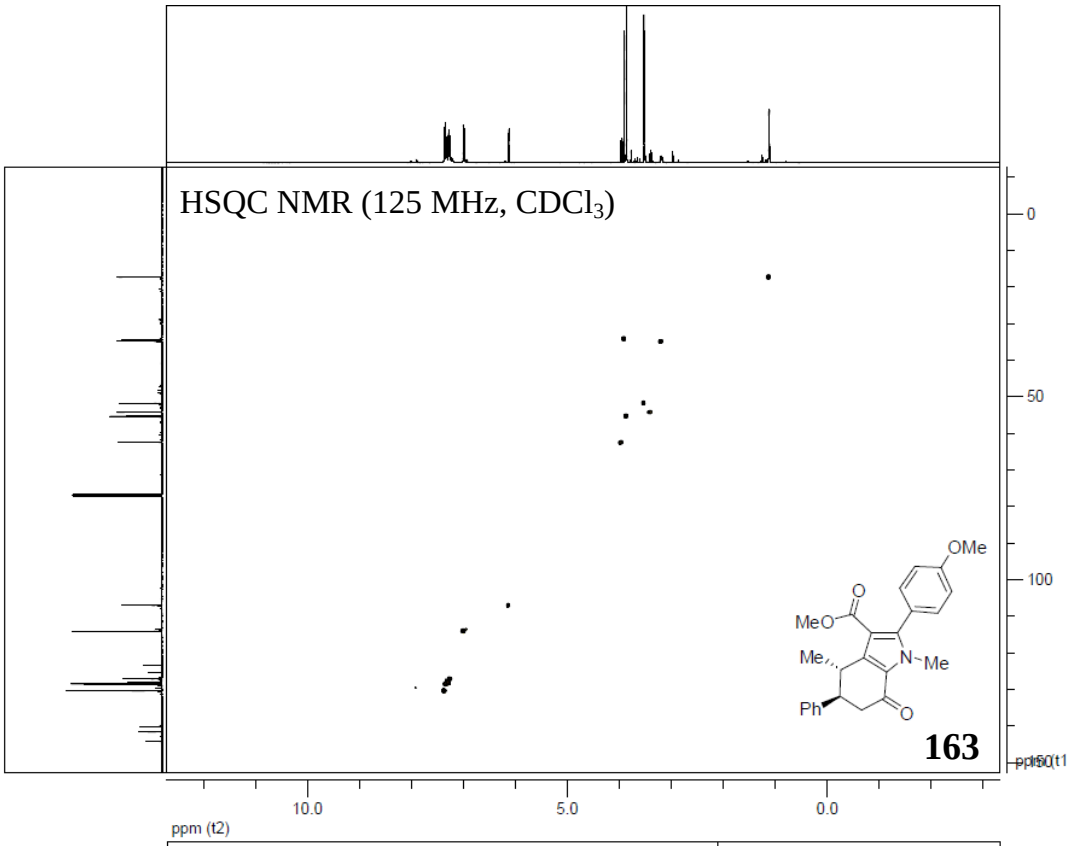
HSQC NMR (125 MHz, CDCl3)
OMe
MeO
Me
N
Me
Ph
O
163
0
50
100
10.0
5.0
0.0
ppm (t2)
ppm (t1

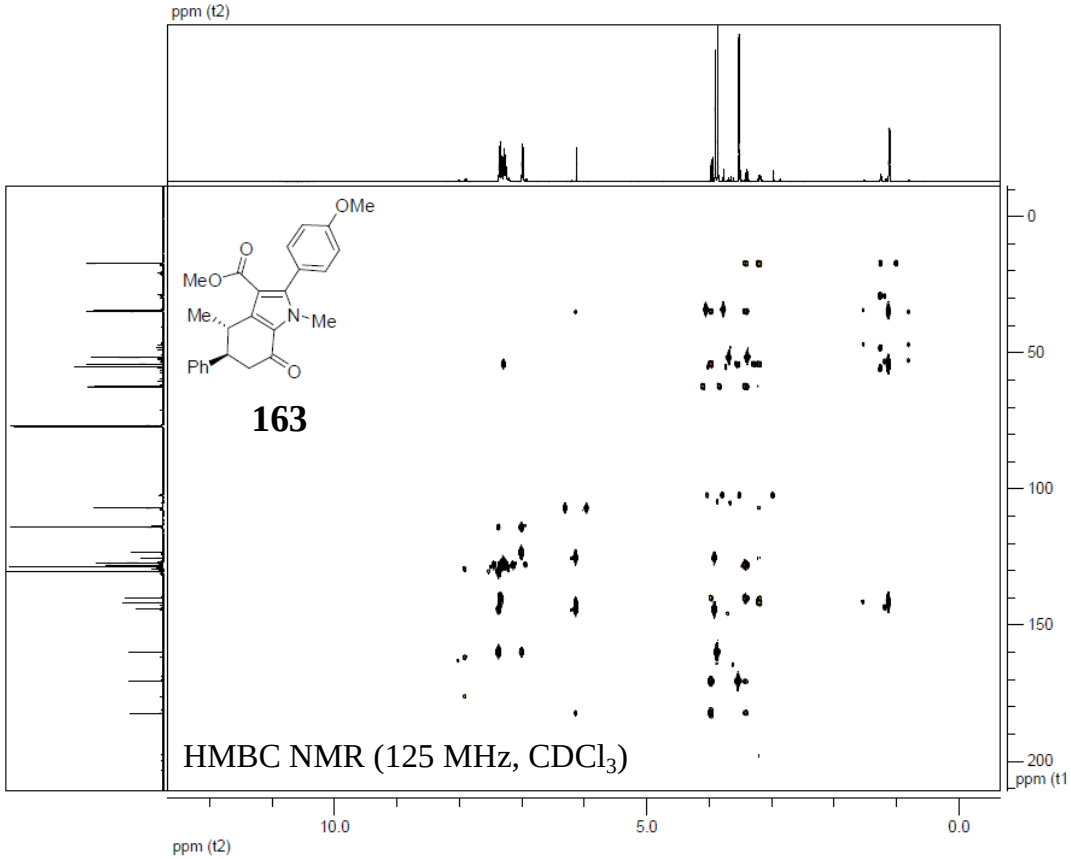
OMe
MeO
Me
N
Me
Ph
O
163
HMBC NMR (125 MHz, CDCl3)
0
50
100
150
200
10.0
5.0
0.0
ppm (t2)
ppm (t1

HMBC for compound **163**
(125 MHz, $CDCl_3$)

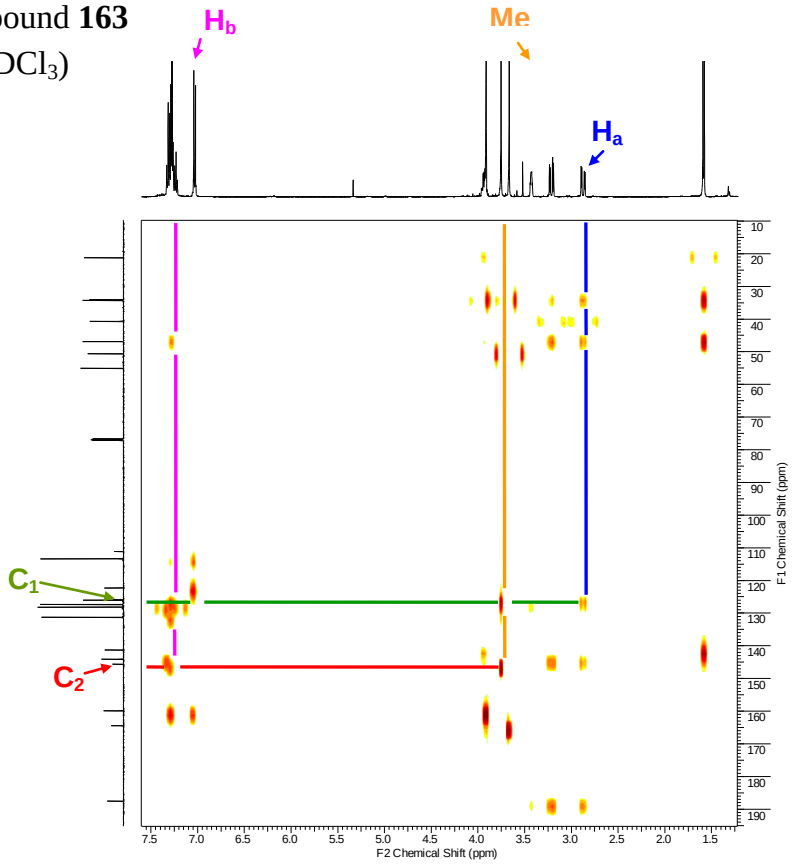


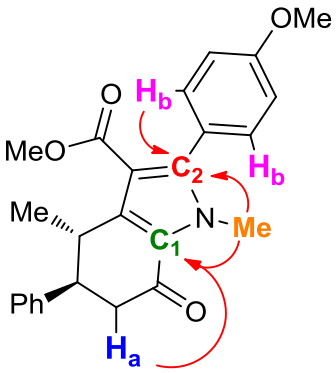

$^{1}$H NMR (500 MHz, Acetone)

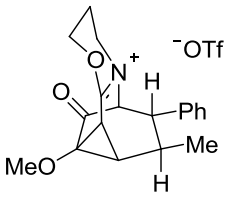


**165**




$^{13}$C NMR (125 MHz, Acetone)

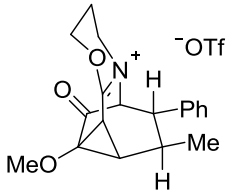


**165**

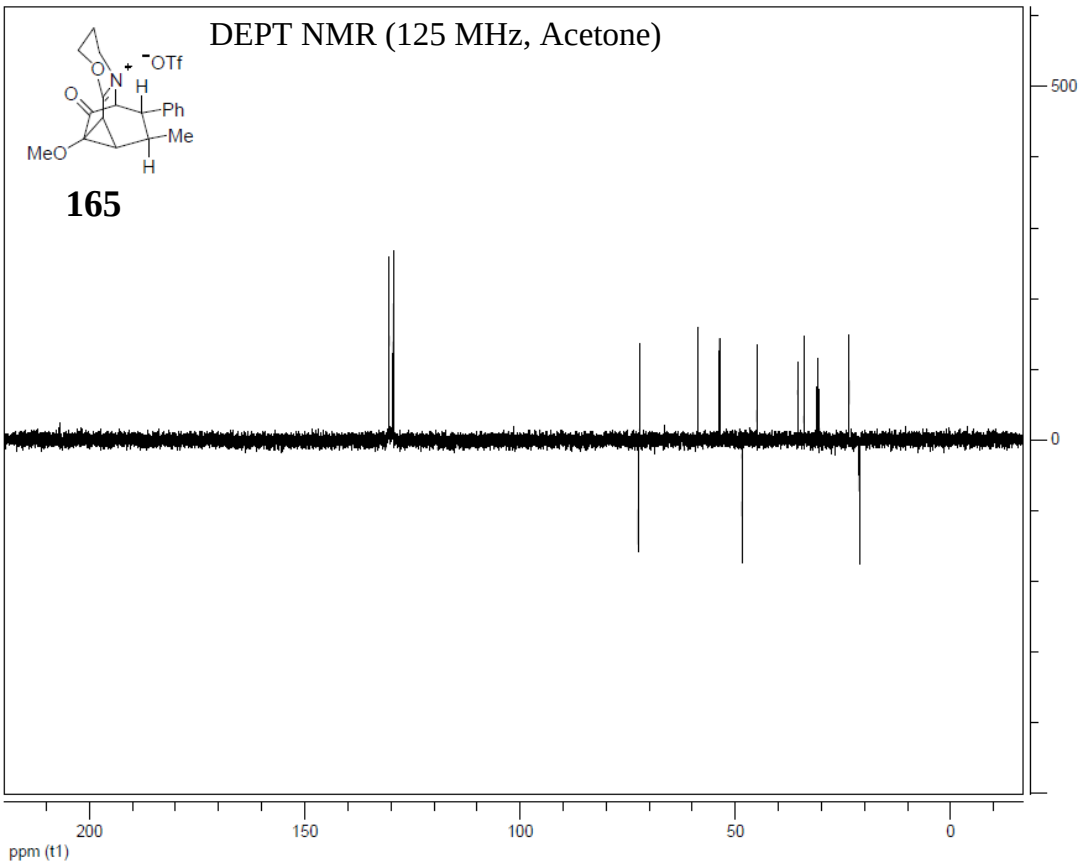
DEPT NMR (125 MHz, Acetone)
OTf
N
H
O
Ph
Me
MeO
H
165
500
0
200
150
100
50
0
ppm (t1)

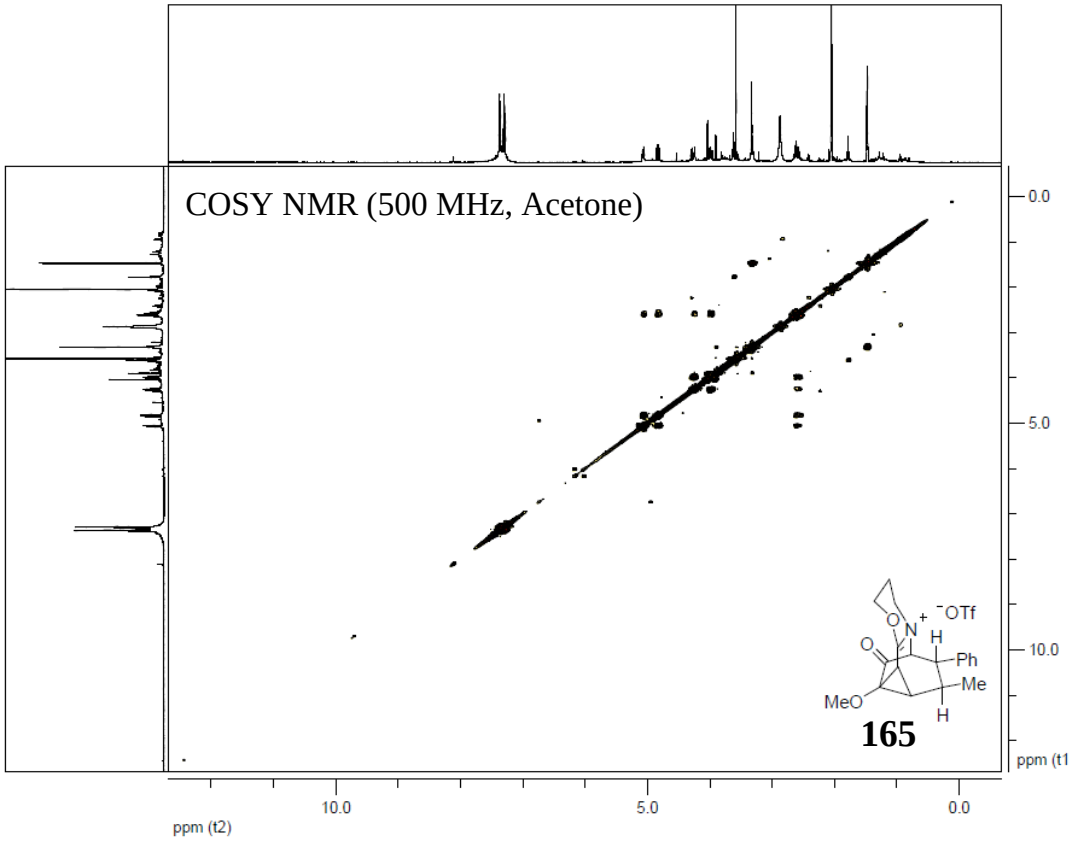
COSY NMR (500 MHz, Acetone)
OTf
N
H
O
Ph
Me
MeO
H
165
0.0
5.0
10.0
ppm (t1
10.0
5.0
0.0
ppm (t2)

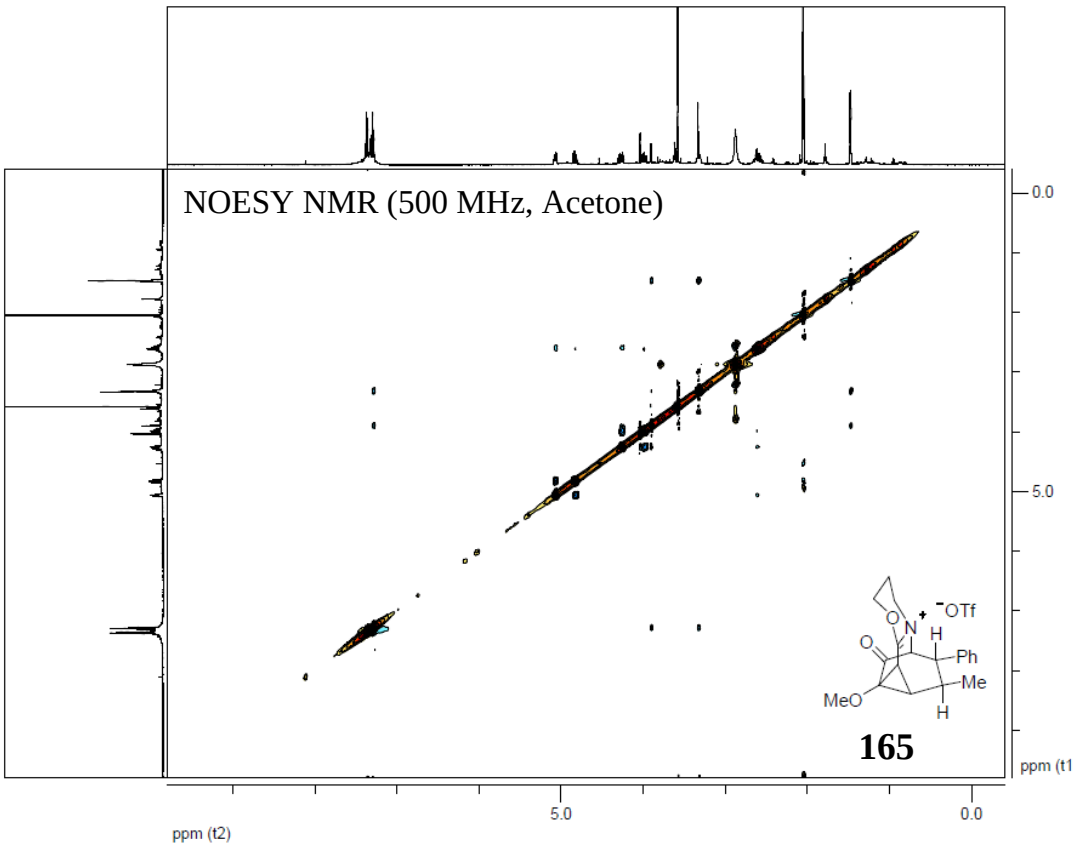
NOESY NMR (500 MHz, Acetone)
0.0
5.0
ppm (t1
5.0
0.0
ppm (t2)
OTf
O
N
H
O
Ph
Me
MeO
H
165

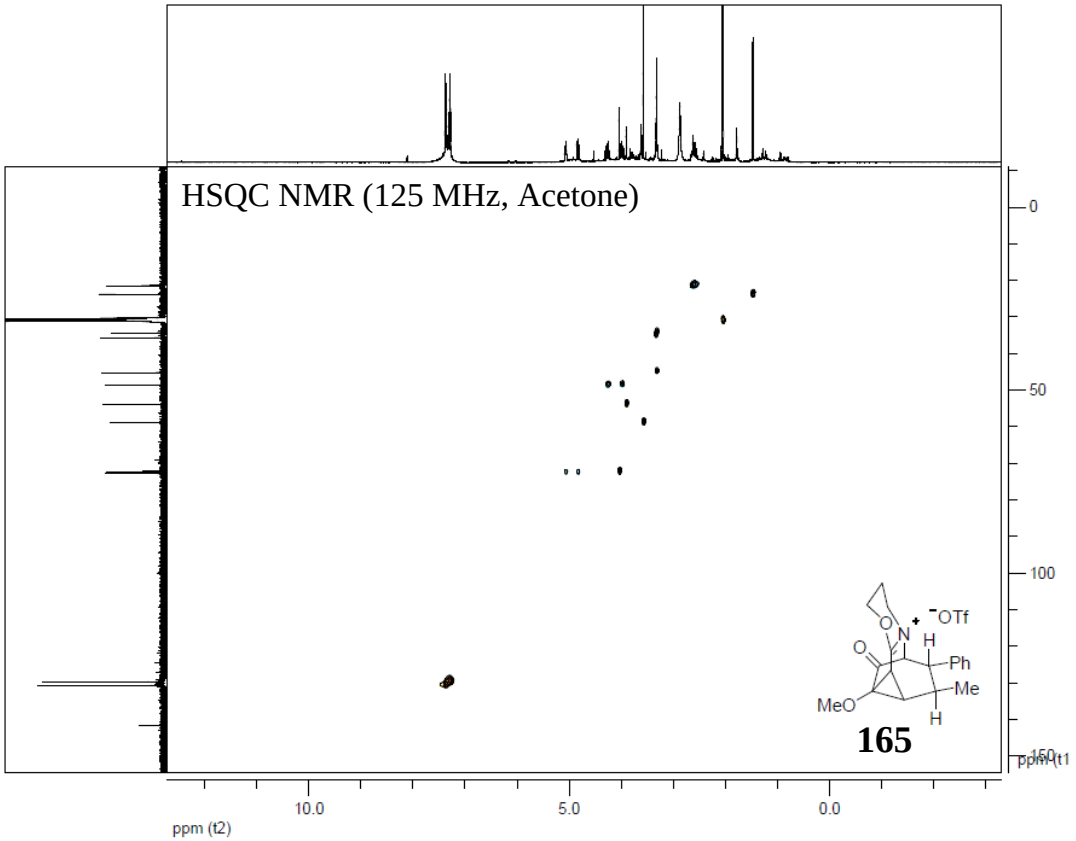
HSQC NMR (125 MHz, Acetone)
0
50
100
150
ppm (t1
10.0
5.0
0.0
ppm (t2)
OTf
O
N
H
O
Ph
Me
MeO
H
165

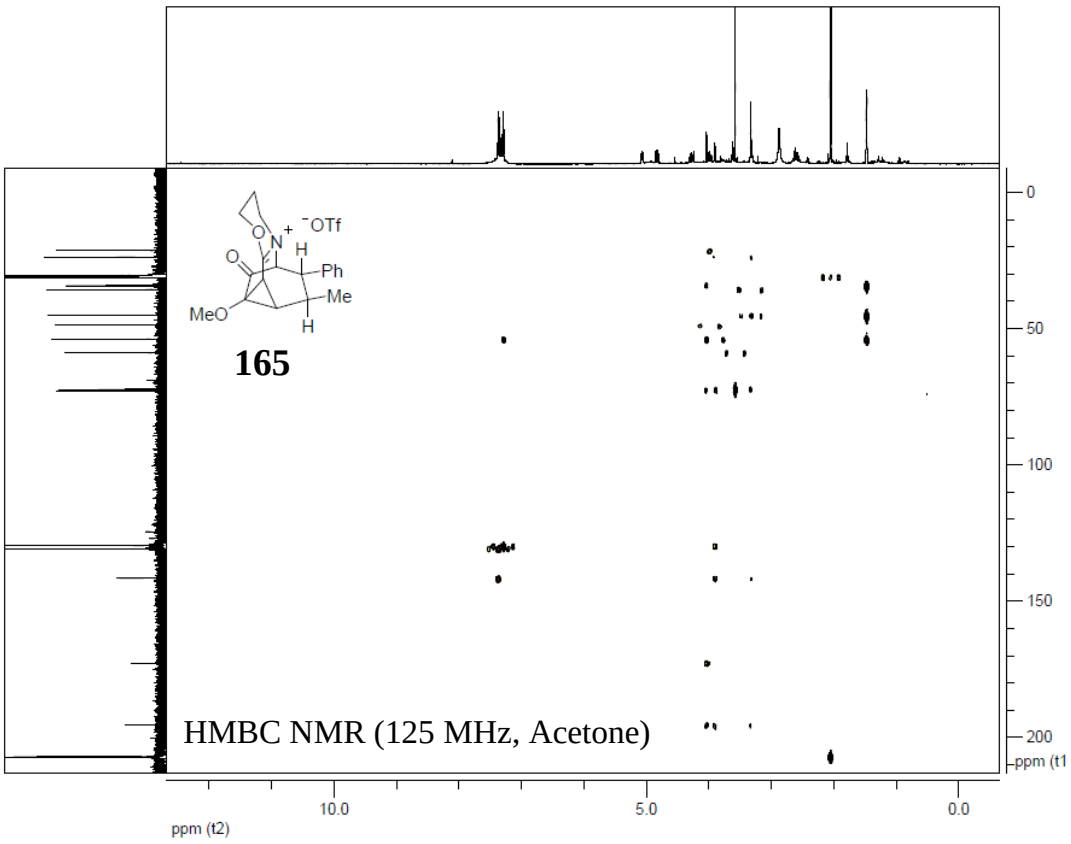
O
N
+
⁻OTf
H
O
Ph
Me
MeO
H
165
HMBC NMR (125 MHz, Acetone)
0
50
100
150
200
ppm (t1
10.0
5.0
0.0
ppm (t2)

$^{1}$H NMR (500 MHz, $CDCl_3$)

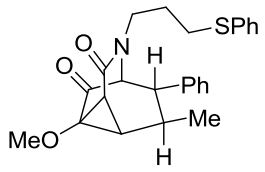


**166**

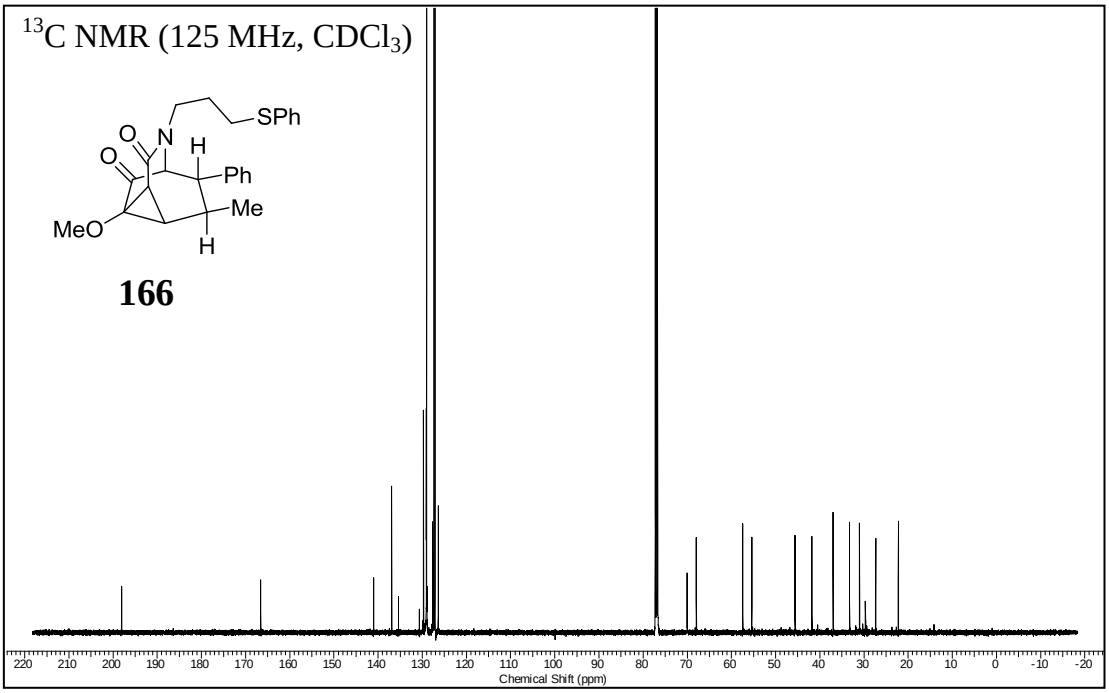


$^{13}$C NMR (125 MHz, $CDCl_3$)




**166**

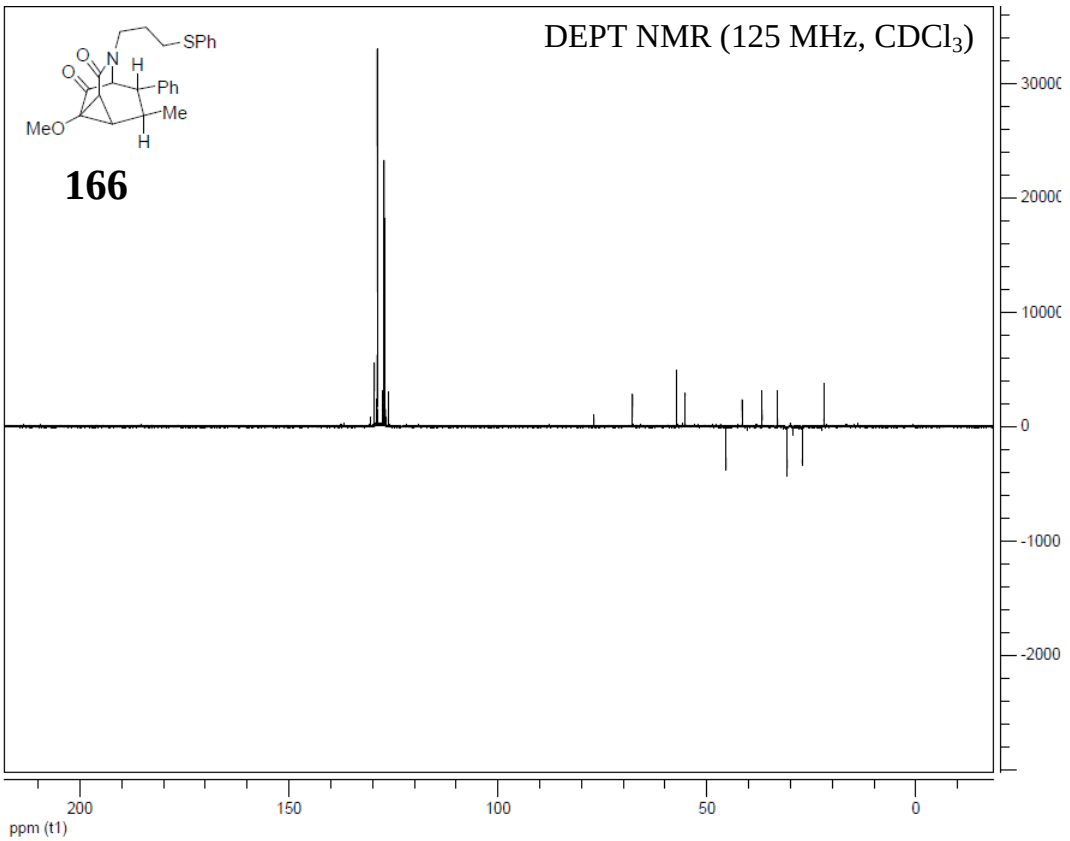
DEPT NMR (125 MHz, CDCl3)
SPh
N
H
O
O
Ph
Me
MeO
H
166
30000
20000
10000
0
-1000
-2000
200
150
100
50
0
ppm (t1)

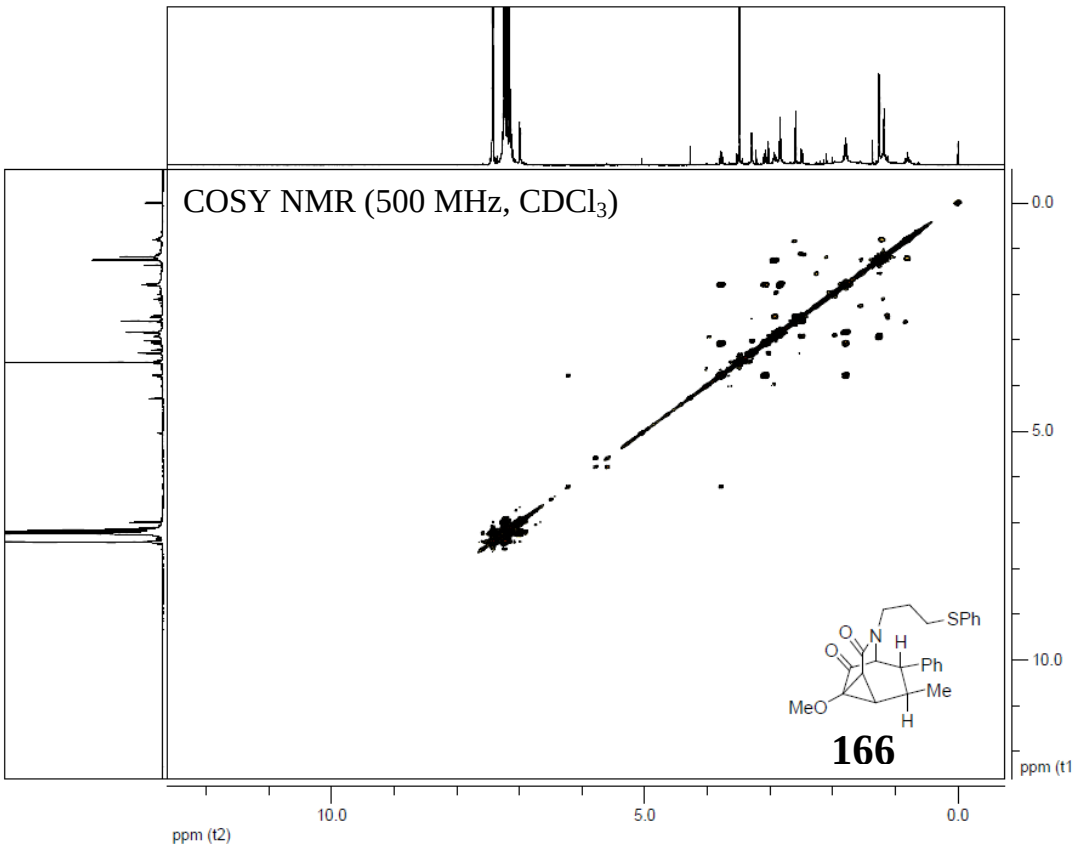
COSY NMR (500 MHz, CDCl3)
SPh
N
H
O
O
Ph
Me
MeO
H
166
0.0
5.0
10.0
ppm (t1
10.0
5.0
0.0
ppm (t2)

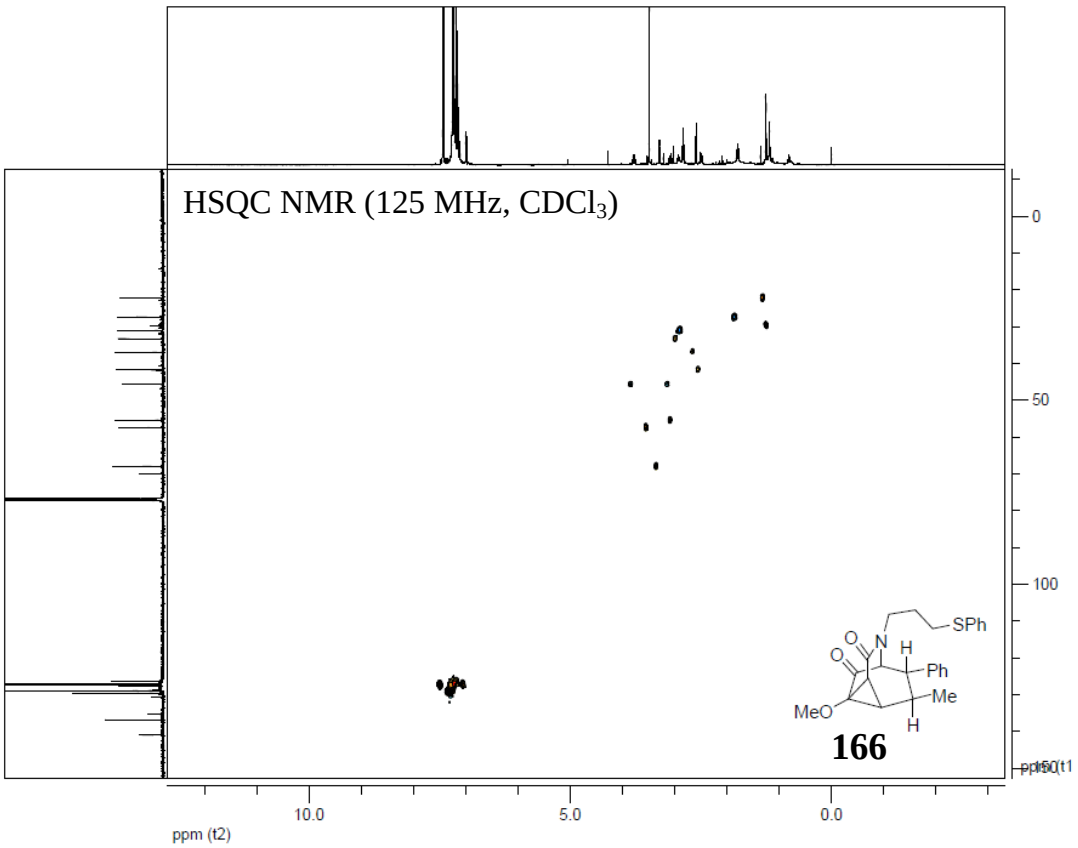
HSQC NMR (125 MHz, CDCl3)
SPh
O
N
H
O
Ph
Me
MeO
H
166
0
50
100
10.0
5.0
0.0
ppm (t2)

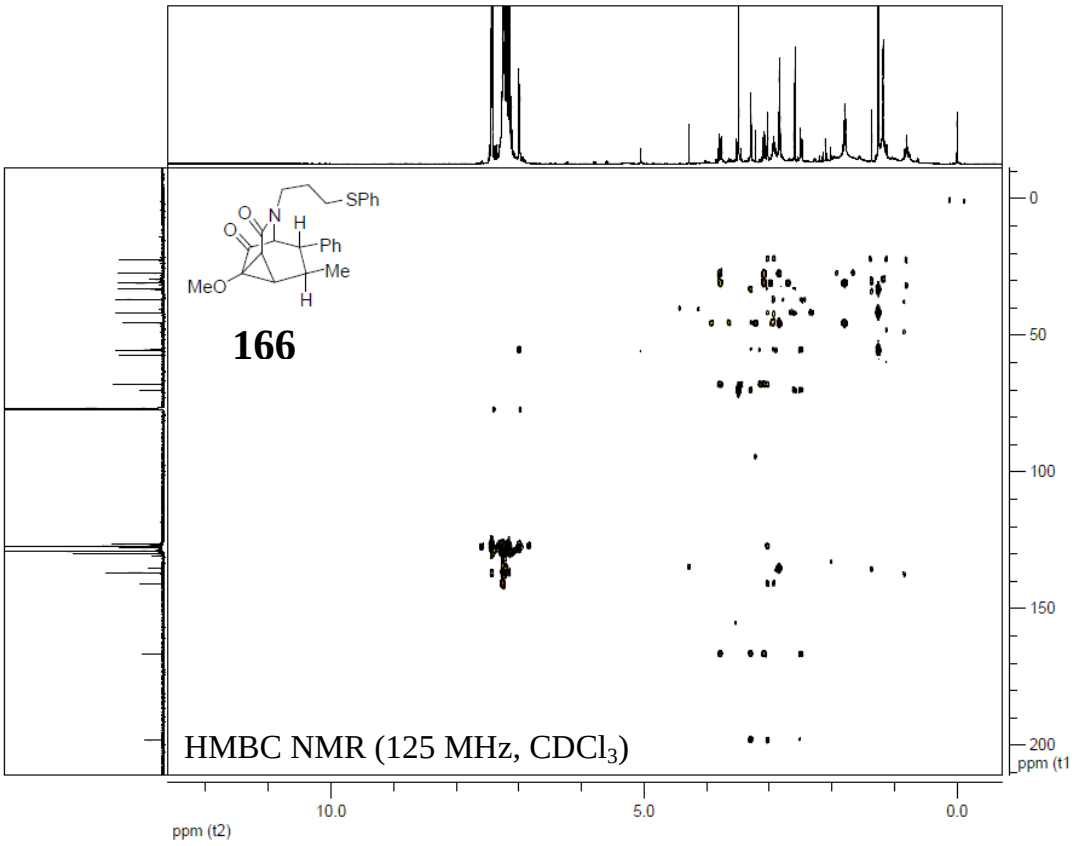
SPh
O
N
H
O
Ph
Me
MeO
H
166
HMBC NMR (125 MHz, CDCl3)
0
50
100
150
200
10.0
5.0
0.0
ppm (t2)

$^{1}$H NMR (500 MHz, $CDCl_3$)

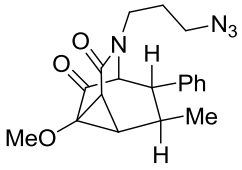


**167**




$^{13}$C NMR (125 MHz, $CDCl_3$)

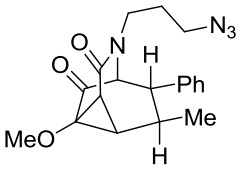


**167**

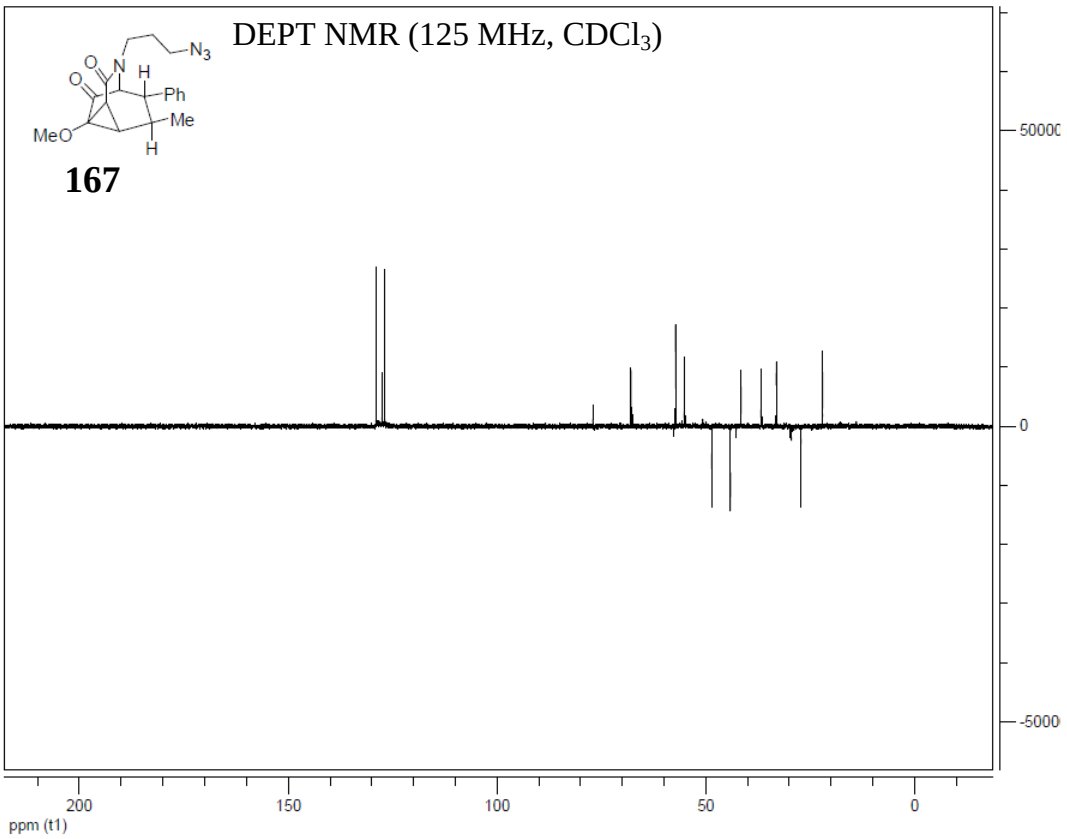
DEPT NMR (125 MHz, CDCl3)
167
50000
0
-5000
200
150
100
50
0
ppm (t1)

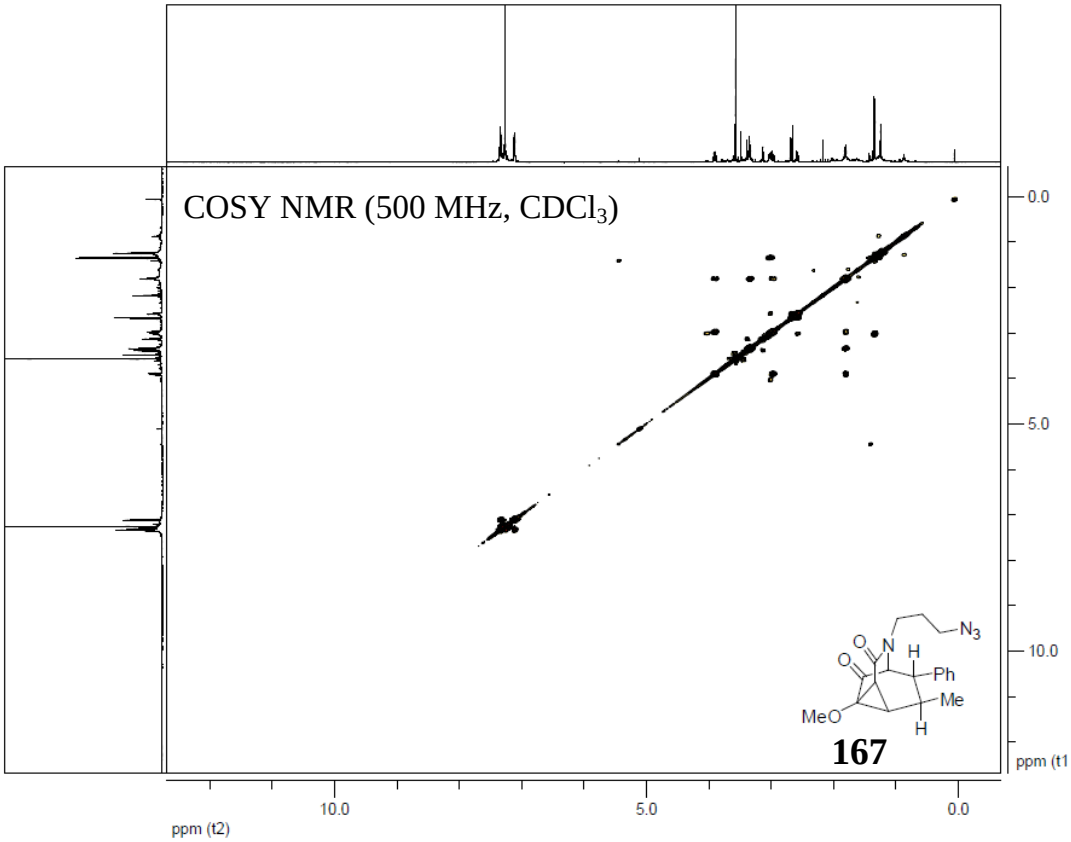
COSY NMR (500 MHz, CDCl3)
167
0.0
5.0
10.0
ppm (t1
10.0
5.0
0.0
ppm (t2)

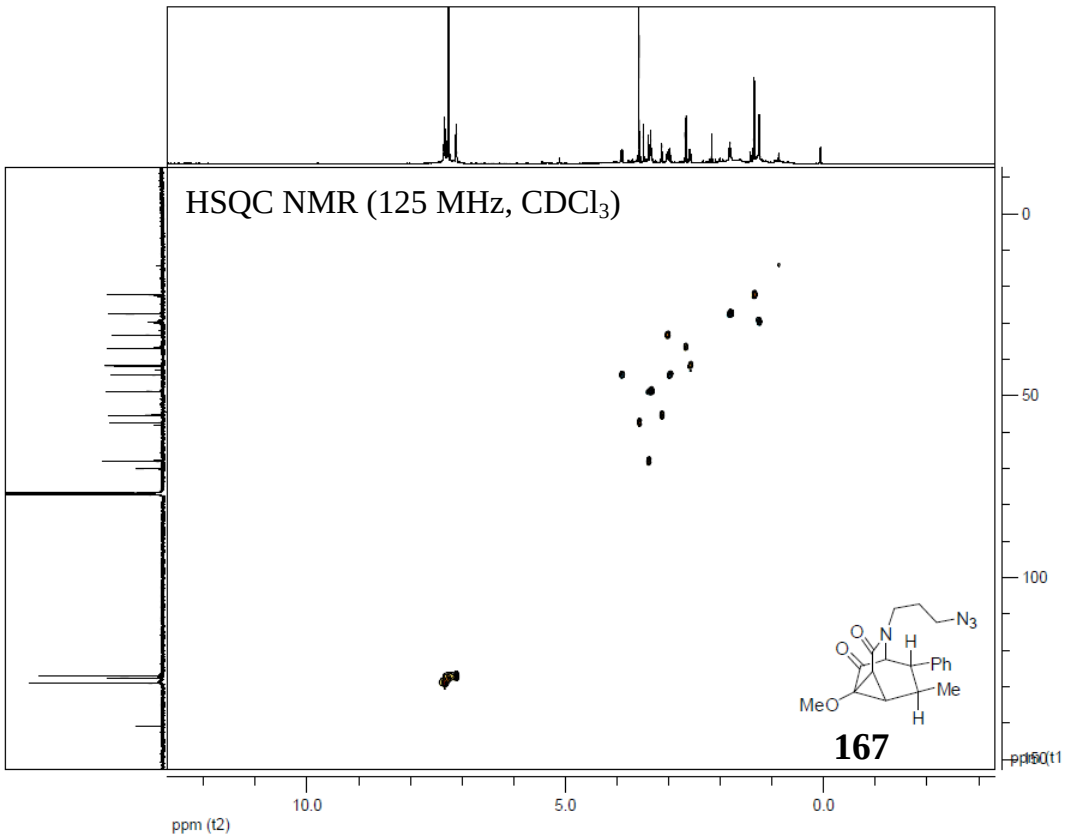
HSQC NMR (125 MHz, CDCl3)
N3
O
N
H
Ph
Me
MeO
H
167
0
50
100
10.0
5.0
0.0
ppm (t2)

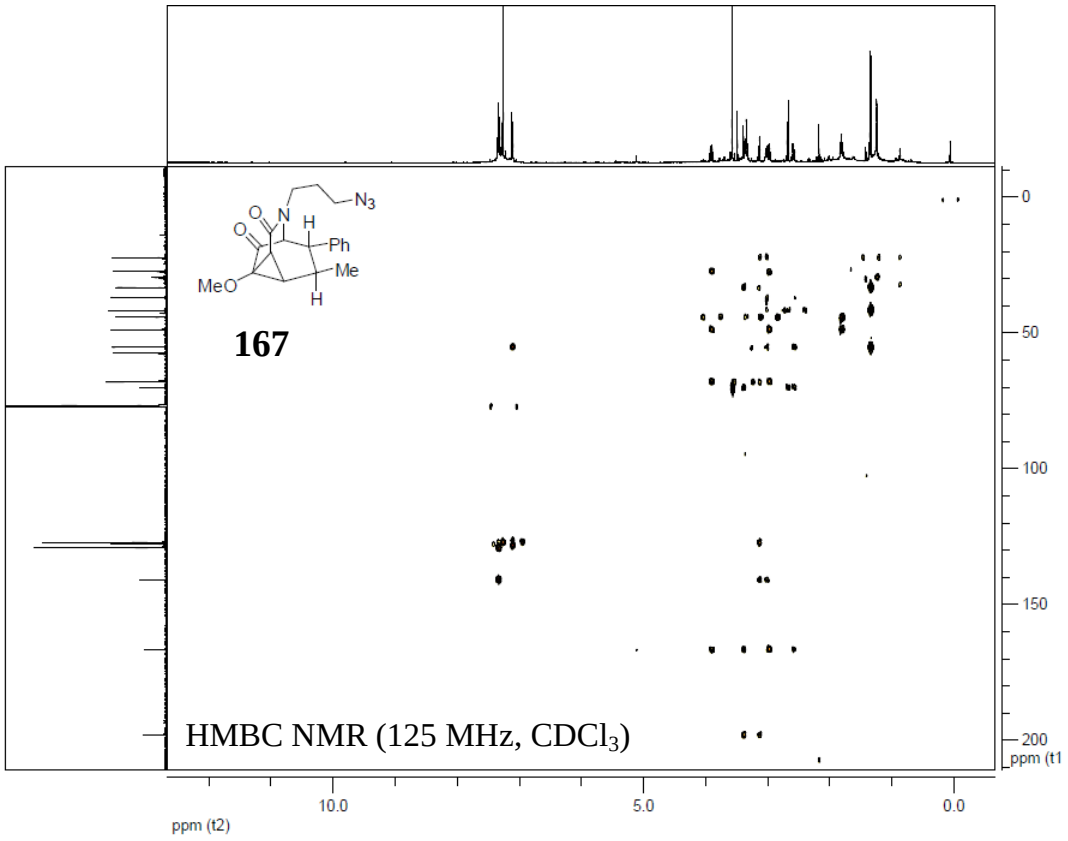
N3
O
N
H
Ph
Me
MeO
H
167
HMBC NMR (125 MHz, CDCl3)
0
50
100
150
200
10.0
5.0
0.0
ppm (t2)

$^{1}$H NMR (500 MHz, $CDCl_3$)

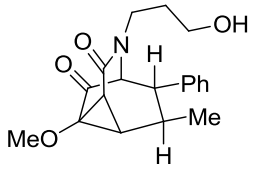


**168**




$^{13}$C NMR (125 MHz, $CDCl_3$)

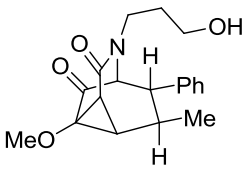


**168**

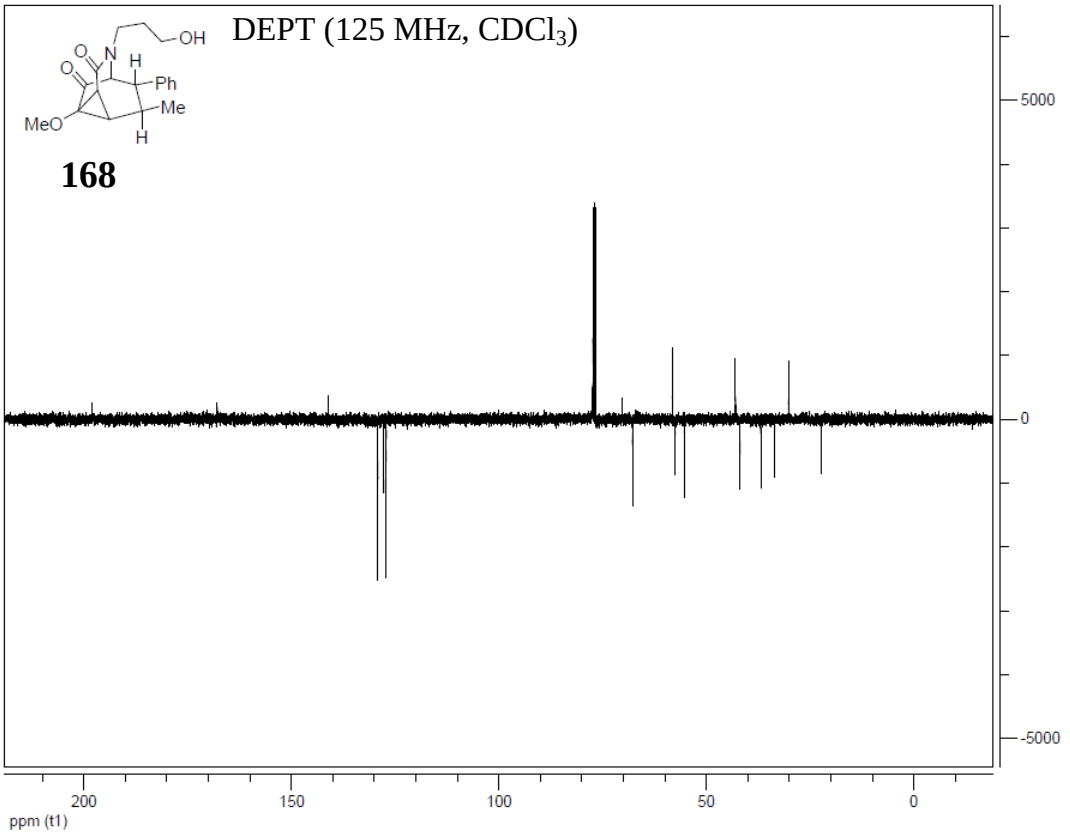
DEPT (125 MHz, CDCl3)
OH
O
N
H
O
Ph
Me
MeO
H
168
5000
0
-5000
200
150
100
50
0
ppm (t1)

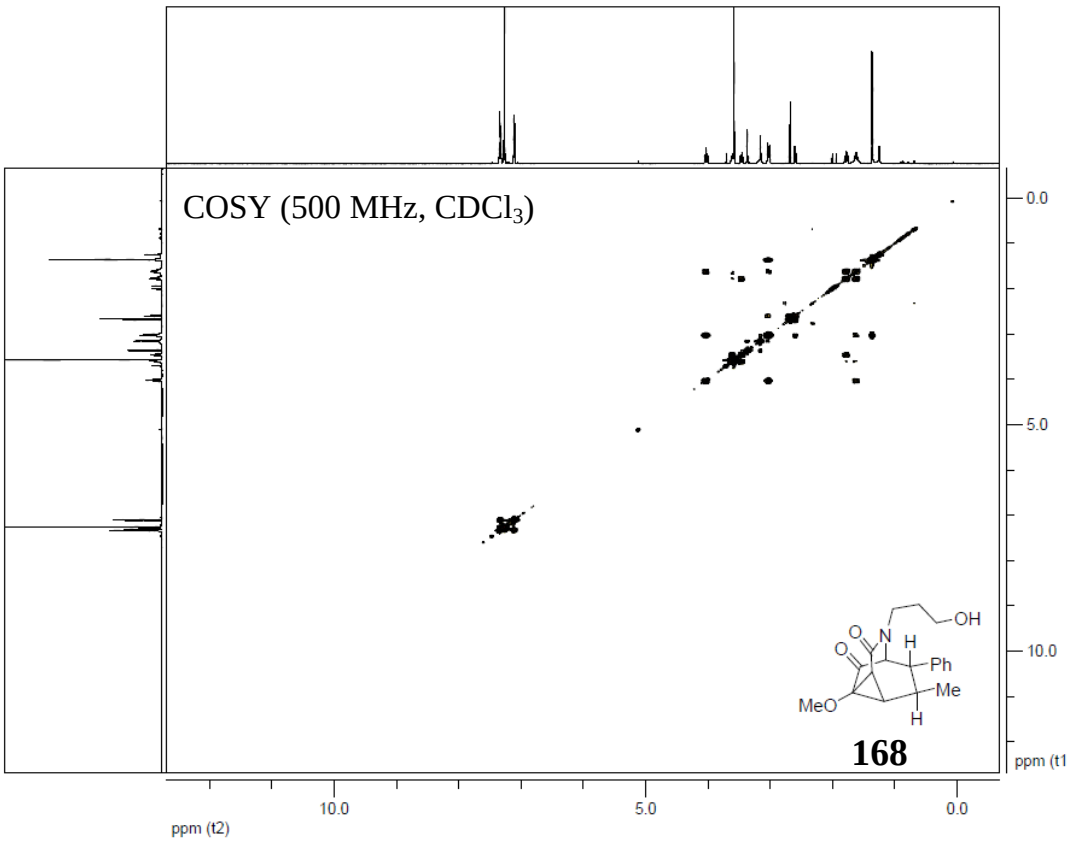
COSY (500 MHz, CDCl3)
0.0
5.0
10.0
OH
O
N
H
O
Ph
Me
MeO
H
168
ppm (t1
10.0
5.0
0.0
ppm (t2)

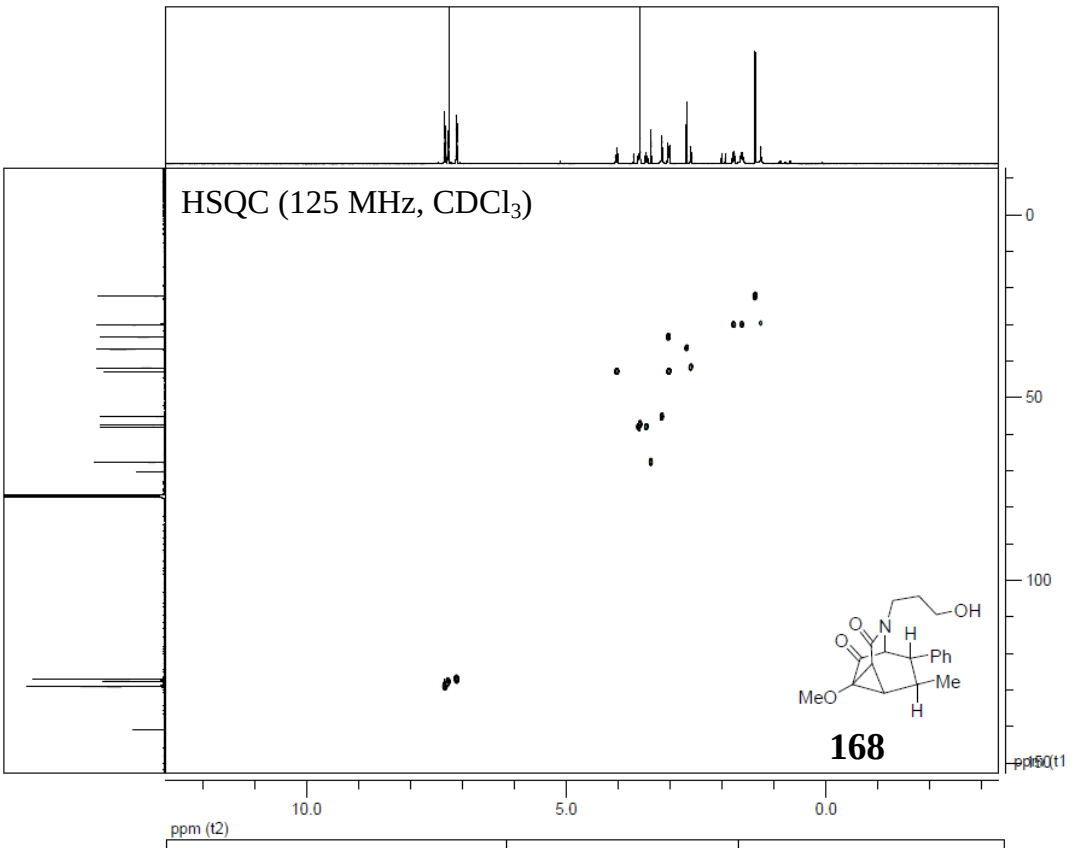
HSQC (125 MHz, CDCl3)
OH
O
N
H
Ph
Me
MeO
O
H
168
0
50
100
150
ppm (t1
10.0
5.0
0.0
ppm (t2)

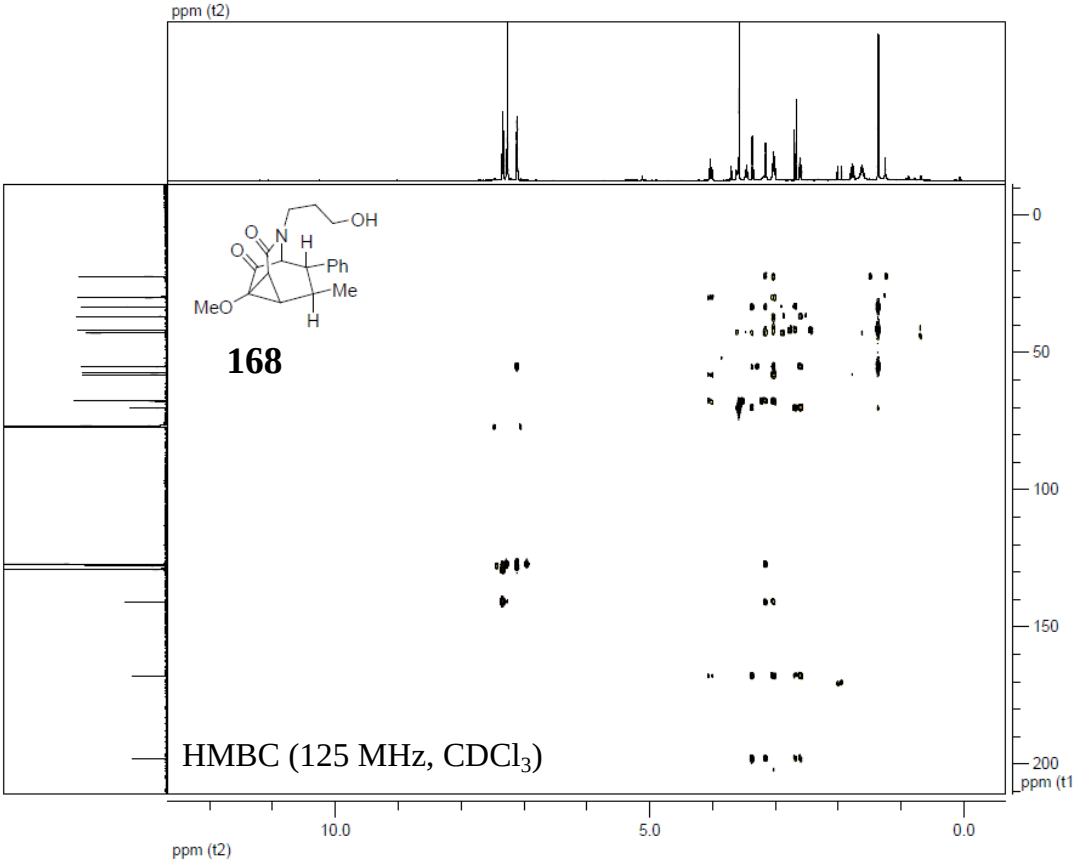
OH
O
O
N
H
Ph
Me
MeO
H
168
HMBC (125 MHz, CDCl3)
0
50
100
150
200
ppm (t1
10.0
5.0
0.0
ppm (t2)

$^{1}$H NMR (400 MHz, $CDCl_3$)

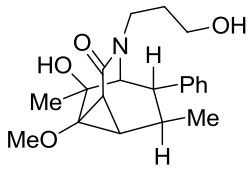


**169**




$^{13}$C NMR (100 MHz, $CDCl_3$)

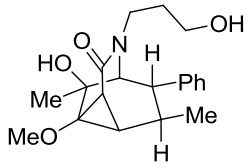


**169**

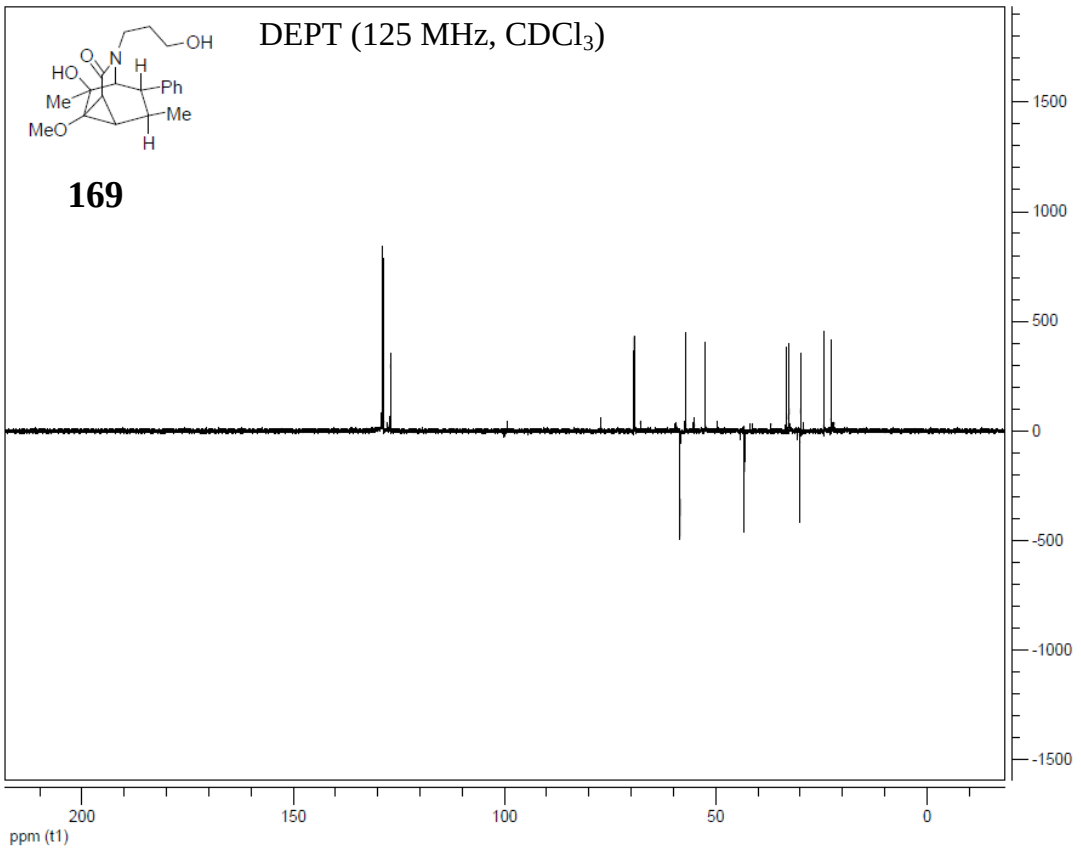
DEPT (125 MHz, CDCl3)
OH
HO
O
N
H
Ph
Me
Me
MeO
H
169
1500
1000
500
0
-500
-1000
-1500
200
150
100
50
0
ppm (t1)

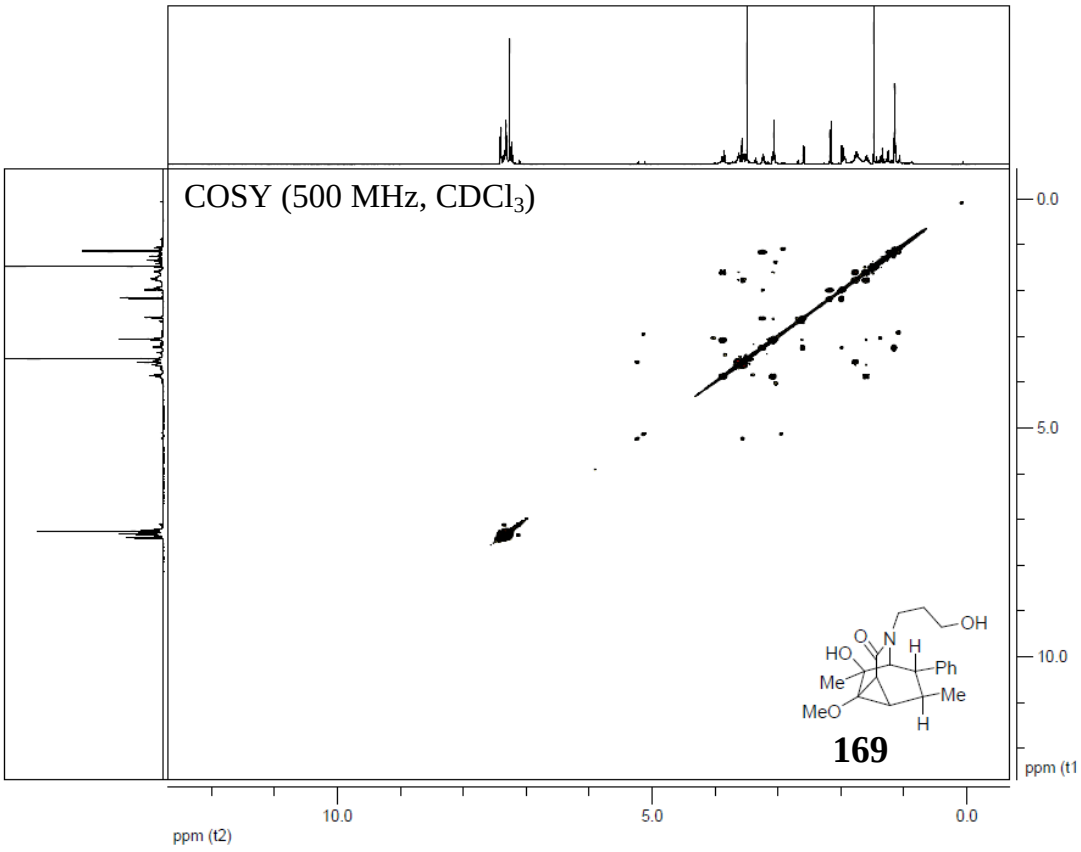
COSY (500 MHz, CDCl3)
OH
HO
O
N
H
Ph
Me
Me
MeO
H
169
0.0
5.0
10.0
ppm (t1
10.0
5.0
0.0
ppm (t2)

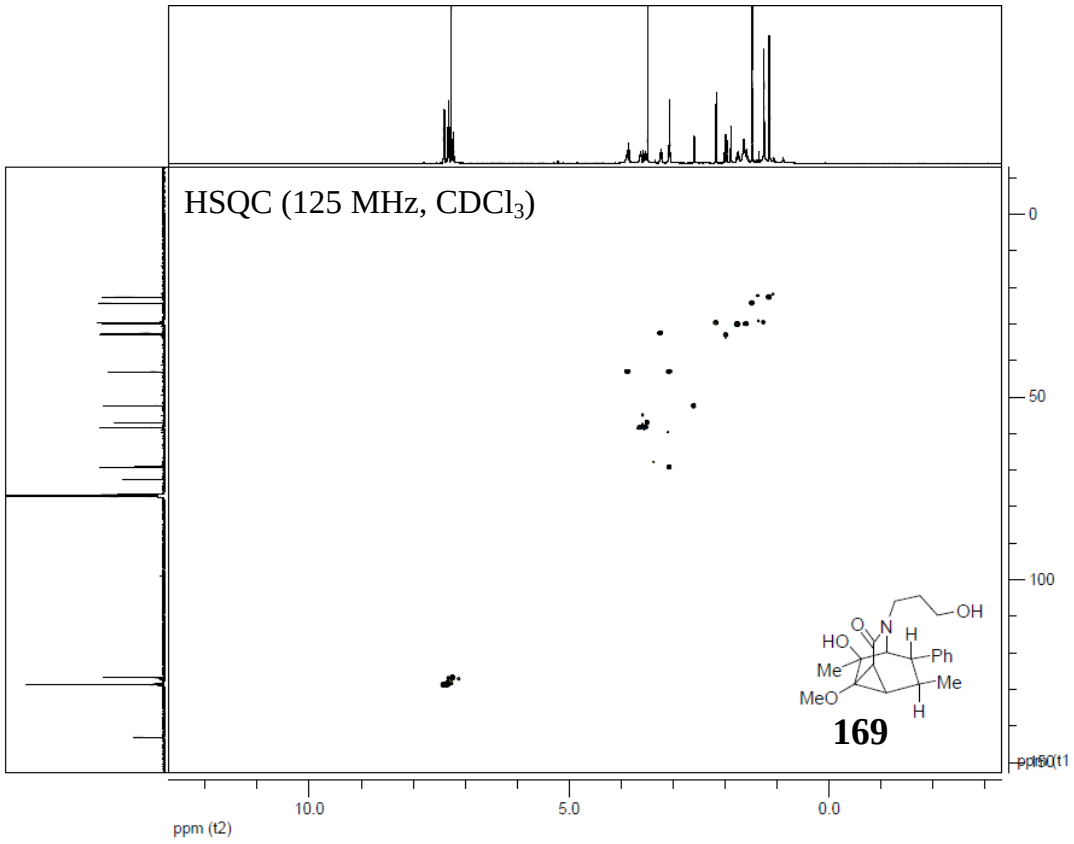
HSQC (125 MHz, CDCl3)
OH
O
N
H
HO
Ph
Me
Me
MeO
H
169
0
50
100
10.0
5.0
0.0
ppm (t2)

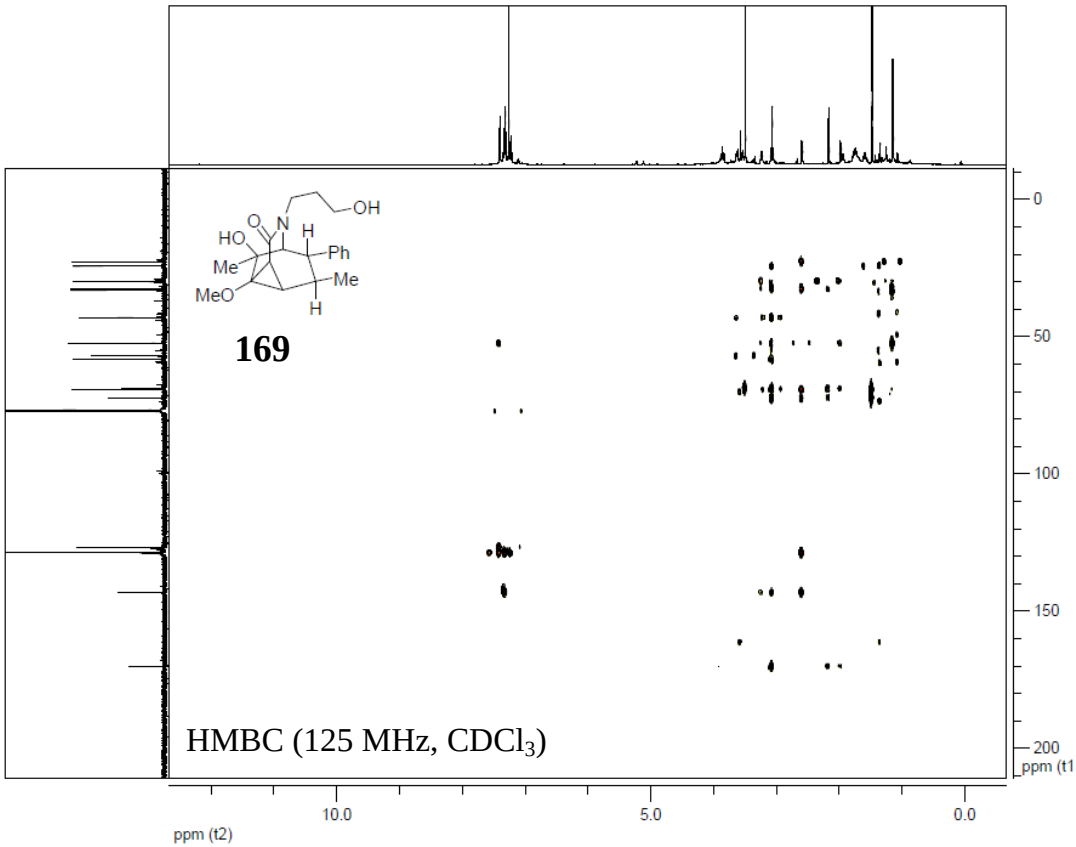
OH
O
N
H
HO
Ph
Me
Me
MeO
H
169
HMBC (125 MHz, CDCl3)
0
50
100
150
200
10.0
5.0
0.0
ppm (t2)